

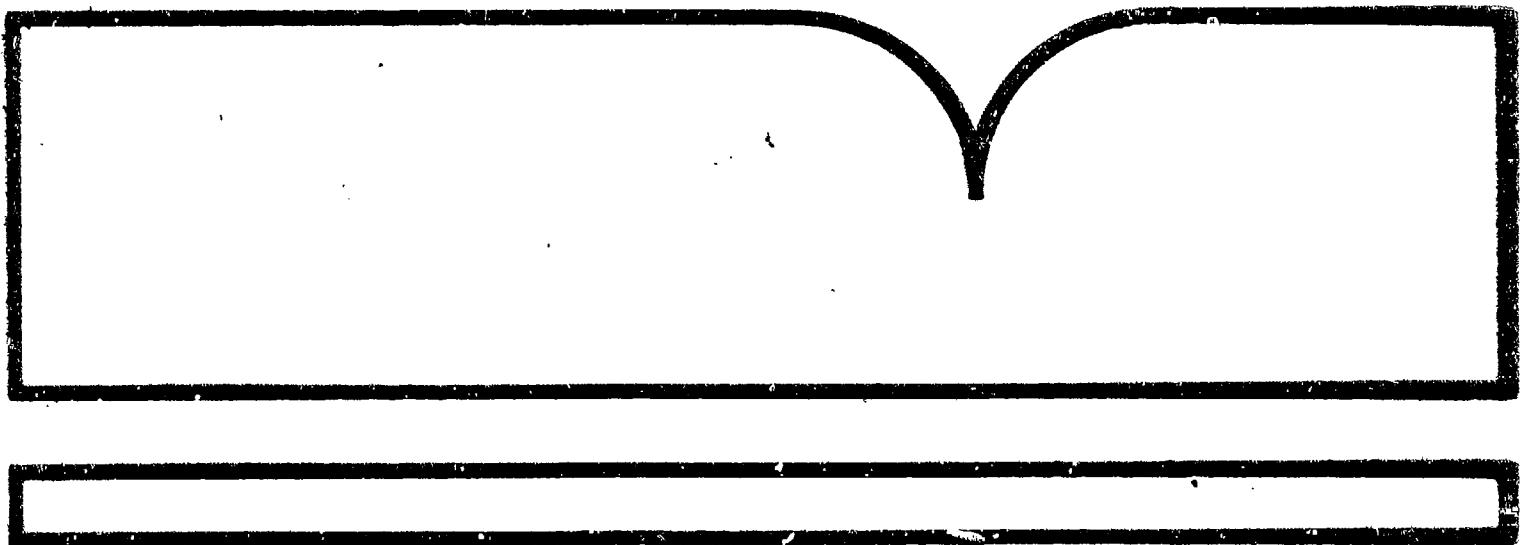
AD-A094 130

PROCEEDINGS OF THE WORKSHOP ON SHIP WAVE-RESISTANCE
COMPUTATIONS VOLUME 2

K. J. Bai, et al

David W Taylor Naval Ship Research and Development Center
Bethesda, MD

1979



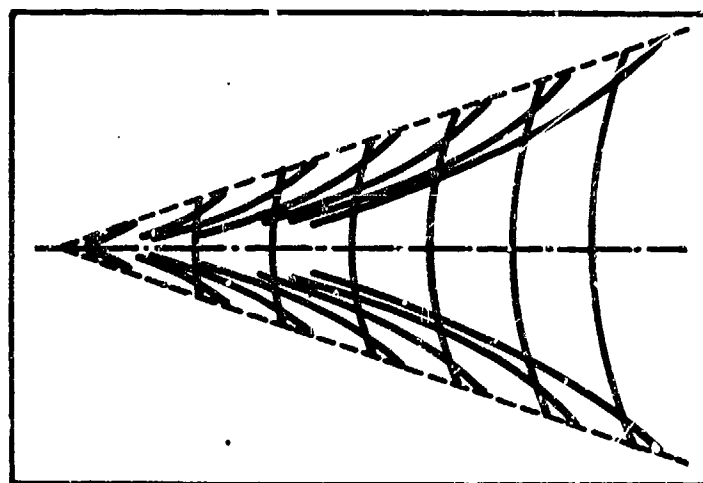
U.S. Department of Commerce
National Technical Information Service

NTIS

AD A094130

**PROCEEDINGS OF THE WORKSHOP ON
SHIP WAVE-RESISTANCE COMPUTATIONS**

VOLUME 2



13-14 November 1979

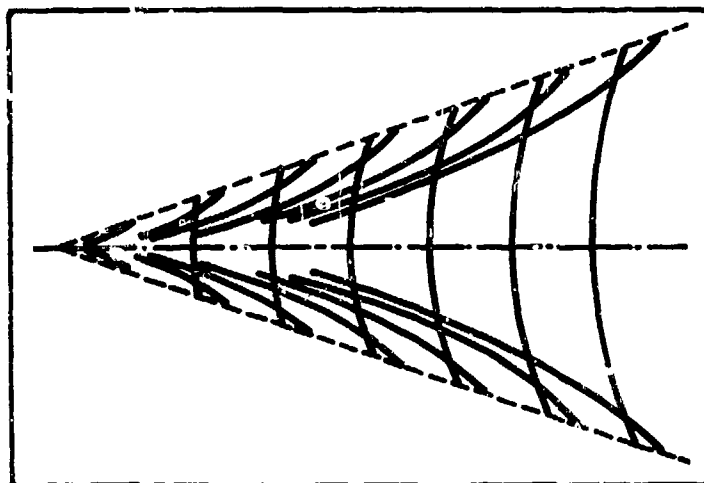
**David W. Taylor Naval Ship Research and Development Center
Bethesda, Maryland 20884
United States of America**

REPRODUCED BY
NATIONAL TECHNICAL
INFORMATION SERVICE
U.S. DEPARTMENT OF COMMERCE
SPRINGFIELD, VA. 22161

Approved for Public Release; Distribution Unlimited

**PROCEEDINGS OF THE WORKSHOP ON
SHIP WAVE-RESISTANCE COMPUTATIONS**

Edited by
Kwang June Bai
Justin H. McCarthy



13-14 November 1979

David W. Taylor Naval Ship Research and Development Center
Bethesda, Maryland 20084
United States of America

PREFACE

The organizers of the Workshop on Ship Wave Resistance Computations trust that these proceedings will be helpful in future years and serve as an impetus for development of improved theories and computational methods. The Workshop has already borne fruit in the form of continuations of workshop discussions held in Japan in May and October of 1980. Contributions from the May meeting form an important appendix to Volume 2 of these Proceedings, and in fact publication of the Proceedings was delayed to permit inclusion of the May contributions.

The Proceedings are divided into two volumes. The first volume contains the workshop introduction, an overview of results, and summaries of the group discussions for each of the five hulls investigated by workshop participants; an appendix contains geometric data and other information on the five hulls. Volume 1 thus constitutes a broad summary of the proceedings of the Workshop. The contributed papers, twenty-three in number, and written discussions, are all contained in Volume 2 of the Proceedings. These papers and discussions form the backbone of the Workshop and deserve continued and careful study.

To all participants, authors, discussion leaders and discussers, the organizers extend sincere thanks for the superb efforts of all in making the Workshop a success.

JHMcC

CONTENTS

VOLUME 1

DEDICATION	v
PREFACE	xii
NOMENCLATURE AND COORDINATE SYSTEM	xvii
INTRODUCTION, Justin H. McCarthy	1
OVERVIEW OF RESULTS, Kwang June Bai	5
WIGLEY PARABOLIC HULL GROUP DISCUSSION, Louis Landweber	51
INUI HULL S-201 GROUP DISCUSSION, Lawrence Ward	66
SERIES 60, BLOCK COEFFICIENT 0.60 GROUP DISCUSSION, John V. Wehausen	69
HSVA TANKER GROUP DISCUSSION, Marshall Tulin	71
ATHENA MODEL GROUP DISCUSSION, Nils Salvesen	75
APPENDIX — SELECTED SHIP HULL GEOMETRIES AND FROUDE NUMBERS	87

VOLUME 2

CONTRIBUTED WORKSHOP PAPERS

SESSION 1: CHAIRMAN: William E. Cummins, DTNSRDC, Bethesda, Maryland, U.S.A.

CONTRIBUTION TO WORKSHOP ON SHIP WAVE RESISTANCE COMPUTATIONS, George E. Gadd	117
CALCULATION OF THE WAVE RESISTANCE OF SHIPS BY THE NUMERICAL SOLUTION OF NEUMANN-KELVIN PROBLEM, Takayuki Tsutsumi	162
WAVE RESISTANCE PREDICTIONS BY USING A SINGULARITY METHOD, Ming Shun Chang	202
WAVE RESISTANCE CALCULATION FOR WIGLEY, INUI HULL S-201 AND SERIES 60 HULLS, Kuniharu Nakatake, Akio Toshima and Ryusuke Yamazaki	215
CALCULATIONS WITH THE XYZ FREE SURFACE PROGRAM FOR FIVE SHIP MODELS, Charles W. Dawson	232

CALCULATION OF SHIP WAVE RESISTANCE WITH SPECIAL REFERENCE TO SINKAGE, Katsuo Suzuki	256
---	-----

SESSION II: CHAIRMAN: Ralph Cooper, Office of Naval Research, Arlington, Virginia,
U.S.A.

CALCULATION OF WAVE-RESISTANCE BY MEANS OF THE LOW SPEED THEORY, Hajime Maruo and K. Suzuki	282
--	-----

COMPUTATIONS OF WAVE-RESISTANCE BY THE LOW SPEED THEORY IMPOSING ACCURATE HULL SURFACE CONDITION, Takamune Kitazawa and Hisashi Kajitani	288
--	-----

WAVE-RESISTANCE COMPUTATIONS BY LOW SPEED THEORY, Eiichi Baba	306
--	-----

SIMPLE CALCULATION OF SHELTERING EFFECT ON WAVE RESISTANCE OF LOW SPEED SHIPS, Bohyun Yim	318
--	-----

SECOND ORDER WAVE RESISTANCE AND RELATED TOPICS, Klaus Eggers (WITH ADDITIONAL CALCULATIONS BY Jurgen Kux)	328
--	-----

WAVE RESISTANCE OF THE WIGLEY AND INUI HULL FORMS PREDICTED BY TWO SIMPLE SLENDER-SHIP WAVE-RESISTANCE FORMULAS, P. Koch and Francis Noblesse	339
---	-----

WAVE-RESISTANCE CALCULATIONS BY THE LOW SPEED THEORY AND GUILLOTON'S METHOD, Hideaki Miyata and Hisashi Kajitani	354
---	-----

NUMERICAL CALCULATION OF SECOND-ORDER WAVE RESISTANCE USING LAGRANGIAN COORDINATES, Young S. Hong	370
---	-----

SESSION III: CHAIRMAN: John P. Breslin, Davidson Laboratory, Hoboken, New Jersey,
U.S.A.

WAVE-RESISTANCE OF DOUBLE MODEL IN FINITE DEPTH AND ITS APPLICATION TO HULL FORM DESIGN, Hyochul Kim and J.C. Seo	383
---	-----

SHIP WAVE-RESISTANCE COMPUTATIONS BY FINITE ELEMENT METHOD, A. C.W.J. Oomen	396
--	-----

WAVE RESISTANCE IN A RESTRICTED WATER BY THE LOCALIZED FINITE ELEMENT METHOD, Kwang June Bai	407
---	-----

NONLINEAR CALCULATIONS OF THREE-DIMENSIONAL POTENTIAL FLOW ABOUT A SHIP, Robert K.-C. Chan and Frank W.-K. Chan	420
---	-----

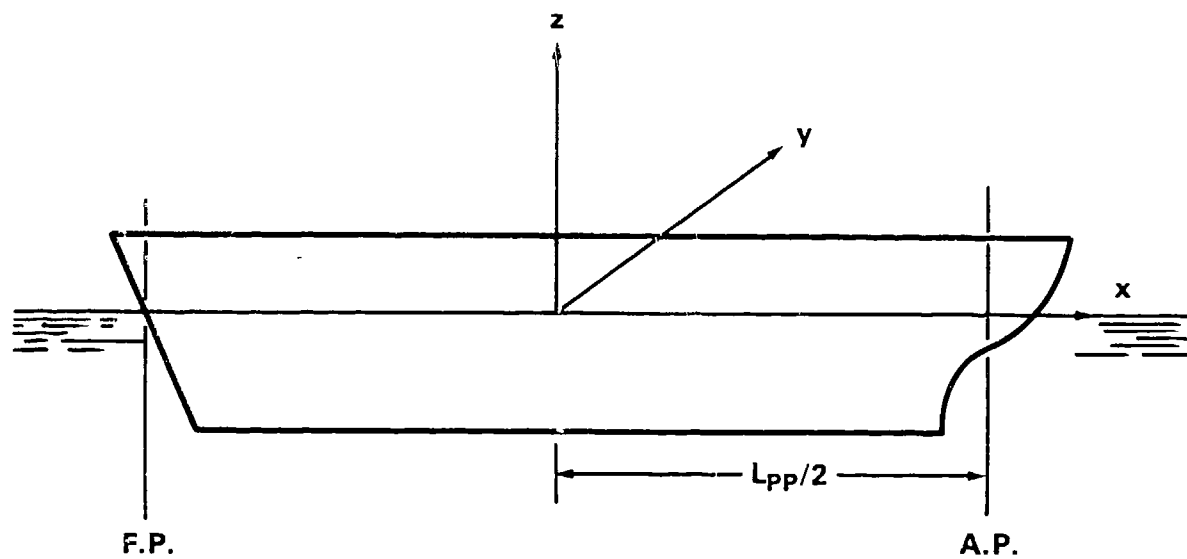
THE GUILLOTON'S METHOD, P. Guevel, G. Delhommeau, and J.P. Cordennier	434
THE CALCULATION OF SHIP WAVE RESISTANCE USING A SURFACE SOURCE DISTRIBUTION, Bruce H. Adee	449
WAVE RESISTANCE COMPUTATION BY NUMERICAL FAR- FIELD WAVE SURVEY DATA, Sander Calisal	457
CALCULATION OF SHIP WAVE RESISTANCE INCLUDING THE EFFECTS OF BOUNDARY LAYER AND WAKE, Kazuhiro Mori	469
ON WAVE MAKING RESISTANCE OF THE MODEL SERIES 60 '4210W' BY REGRESSION ANALYSIS, Masahiro Yamaguchi	484
APPENDIX — SUPPLEMENTARY CONTRIBUTIONS FOLLOWING THE WORKSHOP (MAY 16 — MAY 18, 1980, Shuzenji, Izu, Japan)	491
1. Kitazawa: ON THE LINEARIZATION OF THE FREE SURFACE CONDITION	493
2. Mori: ON THE DOUBLE-HULL LINEARIZED FREE SURFACE CONDITION	501
3. Baba: ON THE FREE-SURFACE CONDITIONS USED BY NAKATAKE ET AL. AND DAWSON	504
4. Suzuki: A NOTE ON THE DOUBLE MODEL APPROXIMATIONS	511
5. Koch & Noblesse: A NOTE ON THE WATERLINE INTEGRAL AND THIN-SHIP APPROXIMATION	515
6. Tsutsumi: COMMENTS ON NUMERICAL SOLUTION OF NEUMANN-KELVIN PROBLEM	523
7. Eggers: A METHOD ASSESSING NUMERICAL SOLUTIONS TO A NEUMANN-KELVIN PROBLEM	526
8. Eggers: MUST THE WATERPLANE AREA BE EXCLUDED WHEN SINGULARITIES ON THE UNDISTURBED FREE SURFACE ARE CONSIDERED?	528
9. Chan & Chan: CONTRIBUTION TO THE DEPTH STUDY ON WAVE RESISTANCE	531
10. Nakatake: DISCUSSION OF PAPERS BY C.W. DAWSON, G.E. GADD, K.J. BAI, A.C.W.J. OOMEN, AND R.C. CHAN AND W.K. CHAN	536
LIST OF WORKSHOP PARTICIPANTS	537

NOMENCLATURE

A_X	Area of midship section
B	Beam at midship
C	Resistance coefficient, $C = R/(\frac{1}{2}\rho U^2 S)$ (with subscripts: pr for pressure resistance, r for residual, s for spray, t for total, vp for viscous pressure, vt for viscous tangential, vw for viscous wake, w for wavemaking, wb for wave breaking, wp for wave pattern)
C_B	Block coefficient, $C_B = V/L_{PP}BH$
C_{PR}	Prismatic coefficient, $C_{PR} = V/A_X L_{PP}$
C_{pr}	Dynamic pressure coefficient, $C_{pr} = (p - p_a + \rho g z)/(\frac{1}{2}\rho U^2)$
C_S	Wetted surface coefficient, $C_S = S/L_{PP}(2H + B)$
C_X	Midship sectional area coefficient, $C_X = A_X/BH$
F_n	Froude number, $F_n = U/\sqrt{gL}$
H	Draft at midship
L	Length at water line
L_{PP}	Length between perpendiculars
R	Resistance (with subscripts: pr for pressure resistance, r for residual, s for spray, t for total, vp for viscous pressure, vt for viscous tangential, vw for viscous wake, w for wavemaking, wb for wave breaking, wp for wave pattern)
R_n	Reynolds number, $R_n = LU/\nu$
S	Wetted surface area at rest
U	Ship or model speed
V	Displaced volume
b	Half beam, $b = B/2$
g	Gravitational acceleration, $g = 32.174 \text{ ft/sec}^2$

$h(x)$	Vertical distance between x -axis and x' -axis (positive above undisturbed free surface); nondimensionalized by $U^2/2g$
k	Wave number, $k = g/U^2$
ℓ	Half length, $\ell = L_{pp}/2$
p	Pressure
p_a	Atmospheric pressure
t	Trim (positive for bow up), $t = h(-\ell) - h(\ell)$; nondimensionalized by $U^2/2g$
s	Sinkage, $s = -(h(-\ell) + h(\ell))/2$, nondimensionalized by $U^2/2g$
$\zeta(x)$	Wave elevation along hull, measured relative to the $x'-y'$ plane; nondimensionalized by $U^2/2g$
$\eta(x)$	Wave elevation along hull, measured relative to the undisturbed free surface plane, $\eta(x) = \zeta(x) + h(x)$; nondimensionalized by $U^2/2g$
ν	Kinematic viscosity, $\nu = 1.059 \times 10^{-5}$ ft ² /sec at $T = 70^\circ\text{F}$
$\xi(x,y)$	Free-surface elevation other than along hull; nondimensionalized by $U^2/2g$
ρ	Mass density, $\rho = 1.935$ slugs/ft ³ (fresh water)

COORDINATE SYSTEM



x, y, z Translating coordinate system with x in the opposite direction of the ship's forward motion, z vertically upward, and the origin at the intersection of the planes of the undisturbed free-surface and the midship section.*

x', y', z' Coordinate system fixed in ship and coinciding with the x - y - z system when ship is at rest.

*Midship section is, by definition, at the midpoint between perpendiculars.

Contribution to Workshop on Ship Wave Resistance

Computations

by G E Gadd, National Maritime Institute, England

1. Introduction

Two methods have been used to obtain the results discussed below. One is a modified version of Guilloton's method,¹ and the other an improved version of my method² using distributions of Rankine sources over the hull surface and the undisturbed free surface. Outlines of these methods are given in the next two sections.

2. Guilloton's method

This method requires isobars (lines of constant pressure) to be traced along the hull. An "equivalent linearized hull" is defined, whose lateral y offsets, at equal x intervals Ut , are equal to the real-hull y offsets on the isobars at x intervals ut , where U is ship speed, u the local x component velocity on the isobar, and t some appropriate time interval (say $L/40$, where L is ship length). The z offsets of the equivalent linearized hull are the depths Z_{01}, Z_{02}, \dots of the isobars when extrapolated far upstream, the top isobar being taken in the water surface, so that $Z_{01} = 0$.

To calculate the isobars in the present method the double-model zero Froude number solution is first found, and 4 isobars for this case are traced along the hull, starting from station 10 (FP) at points equally spaced in the Z direction with spacing $ZK/4$. Here ZK is normally the depth of the keel at station 10, but for a hull form with a curved keel line, like the Inuid form, it is taken to be the maximum draft. The keel line, or the false keel line at maximum draft, is treated as a fifth isobar. (It will not in general be an isobar, but in any case the Guilloton method runs into difficulties

near the keel). The first approximation to the equivalent linearized hull is thus found. Hence, using linearized wavemaking source theory, an approximation to the hull wave profile can be calculated, first for the equivalent linearized hull and then transformed back to the real hull. The original double-model distributions of pressure and flow direction over the hull surface are then altered to become more consistent with this hull wave profile, a new set of isobars is found, and the process is repeated a sufficient number of times to give a converged final solution.

The final solution for the pressure distribution over the hull enables the sinkage and trim to be calculated. The program contains an option to re-calculate the flow round the hull with its offsets modified to represent the hull when sinkage and trim have taken place.

3. Rankine source method

The method is still fundamentally the same as that described in ref 2. The hull and its double model reflection in the free surface are divided into panels, and further panels are situated in the region surrounding the hull in the plane of the undisturbed free surface. Rankine sources are distributed on each panel and the source strengths found so that the hull surface boundary condition is met and a non-linear form of the free surface condition is also satisfied.

In principle the free surface panel distribution should extend over the entire region where there are significant waves. In practice the region of free surface panels has to be severely limited in extent. The neglect of the source distribution outside of this truncated region in the former computations was liable to cause appreciable errors.

In the present modified method these difficulties are partially surmounted as follows. The number of "active" free surface panels is

just as restricted as before, but further "passive" panels are added outside of this region as shown in fig 1. It is assumed that non-linear free surface effects are only important within the active region, and that in the passive region linearized free-surface conditions are obeyed. The waves here are assumed to be those that would be generated by an appropriate distribution of Kelvin wavemaking sources along the axis of the hull at one third of the draft, as shown in fig 1. The strengths of these sources are chosen so that along the line joining the centres of the outer row of active panels the wave profile generated by the Kelvin sources matches that computed from the Rankine source array. This latter array now includes sources on four outer rows of passive panels, where the source strengths accord with the waves predicted by linear theory for the axial Kelvin source distribution. Although there may be significant waves even further outboard, the neglect of the Rankine sources which ought in principle to be considered as acting there will not matter, since they will be too remote from the hull and the active panels to have much effect.

Difficulties remain at the upstream and downstream boundaries. As before the upstream radiation condition is met approximately by forcing the waves here to correspond to the pressures that would be generated by the zero Froude number double model Rankine source distribution on the hull alone. If such a pressure distribution prevailed over the entire free surface (which of course it does not) the Rankine source strengths at the downstream end of the region could easily be calculated. By imposing the condition that the downstream source strengths on the active panels tend to the values so calculated, it is found that acceptable predictions of the flow over most of the hull can be obtained. This procedure "anchors" the downstream end of the Rankine source distribution in such a way that the neglect of the free surface sources which should be considered as acting downstream of the truncated region is not too serious. A modified form of this truncation condition is used where there is a transom stern. Some errors naturally

occur close to the stern. This means that the wave resistance estimated from the calculated pressures on the hull can often be seriously in error, since it is sensitive to the precise values near the stern. The resistance associated with the axial Kelvin source distribution is however usually less unrealistic. This may be because, to ensure reasonable smoothness, this distribution is to some extent biased towards what may be called the equivalent Michell distribution. The latter is calculated from the initial zero Froude number pressures on the outer active panel row with the wavemaking components neglected in the matched pressures generated by the axial source distribution.

Certain further approximations are involved in the results of this method for resistance presented below, which should be regarded as interim ones only. Improvements are clearly needed in the theory with regard to the treatment of the downstream conditions.

4. Results

4.1 Wigley's parabolic hull

Figs 2 and 3 show calculated and measured hull wave profiles, and the calculated profiles are tabulated in tables 1 to 3. It can be seen that the Guilloton profiles are quite realistic except that the bow crest is under-predicted especially at the higher speeds. Inclusion of sinkage and trim effects only makes a significant difference at the higher speeds, when it leads to a better prediction of the waves near the stern.

The Rankine source profiles are moderately realistic, but again under-predict the bow crest. As in all the other cases presented below, only two rows of active panels were used, and it is possible that non-linear effects extend further outboard into the region of passive panels, violating the assumption that the waves behave in a linear fashion there.

Tables 4, 5 and 6 give the predicted values of wave resistance, shown graphically in fig. 4.

4.2 Inuid hull S201

Fig 5 and tables 4 and 6 show the predicted wave resistance values. The corresponding hull wave profiles are presented in tables 7 and 8. Mean sinkage is shown in fig 6 and table 9. The predictions of sinkage agree fairly well with the experimental values.

The Guilloton method became unstable for the top speed attempted, $Fn = 0.65$. This may be a defect, not of the Guilloton method itself, but merely of the present numerical implementation of it.

4.3 Series 60, $C_B = 0.60$

Wave profiles are presented in figs 7 and 8 and tables 10 to 12. Inclusion of sinkage in the Guilloton method appears to make the wave profile prediction better near amidships but worse near the stern. The Rankine source method tends to put the first wave trough too far forward, perhaps because of the limited number of active panels mentioned above. However the wave resistance predictions by this method, shown with those of the Guilloton method in fig 9 and tables 4 to 6, are not unrealistic.

4.4 HSVA tanker

It was not found possible to obtain solutions by the Guilloton method for this case. The numerical procedure adopted for integrating along isobars failed in the bow region where the double model axial velocities are very low. The hull wave profiles predicted by the Rankine source method are shown in table 13, and the wave resistance values in fig 10 and table 6.

4.5 High speed hull, Athena

An ideal inviscid flow calculation would need to consider conditions on the wave surface which smoothly clears the transom stern at sufficiently high speeds. The procedure adopted here is cruder and can best be described with reference to a Michell theory analysis which has been carried out for this case. The usual centreplane source distribution from the bow to the transom stern, which is treated as unclosed, is computed and the associated wave resistance coefficient C_{wu} found. This corresponds, according to the assumptions of Michell theory, to the wave resistance which would be experienced by a hull form with an infinitely long parallel wake of the same cross section as the transom extending downstream. It is assumed that the pressure forces acting on the real hull upstream of the stern are substantially the same as for this infinite wake case. The sinkage of the stern can thus be calculated. The total wave resistance is taken to be the value for the Michell source distribution plus a contribution due to the lowered water level behind the transom. The transom is treated approximately as a rectangle of width w and mean depth d when the ship is at rest. If water filled the cavity behind the stern in motion, the forward force it would exert on the stern due to hydrostatic pressure would be $\rho g w (d+s)^2/2$. It is assumed that this represents the additional drag force due to the transom stern, the component drag coefficient being $C_{ws} = g w (d+s)^2 / U^2 S$. Table 14 presents values of C_{wu} , C_{ws} and total drag coefficient $C_w = C_{wu} + C_{ws}$ for the Michell theory calculation, the Guilloton method, and the Rankine source method, and the three sets of C_w values are shown in fig 11. Both C_{wu} and C_{ws} are smaller for the latter two methods than for the first one. This is because the Michell theory predicts a deeper wave trough near the stern, as can be seen from fig 12 and tables 15 to 17. The Guilloton theory suffers from an instability problem near the stern in this case, similar to that to which it is liable near a flat keel (though the present numerical scheme largely

avoids the latter instability by treating the keel line as an isobar). If the isobars incline upwards under a flat overhanging stern the effective y offsets rapidly increase in the downstream direction, leading to the occurrence of large wavemaking sources. Numerical smoothing schemes incorporated in the present program prevent a complete breakdown of the solution, except for the highest speeds attempted, $F_n = 0.80$ and 1.00 . However they are not entirely successful as can be seen from fig 12, and it is possible that they have suppressed a wave trough which should really be there. Similarly the downstream truncation in the Rankine source method may have led to a significant contribution to the wave resistance being missed.

5. References

1. Guilloton, R. "L'étude théorique du bateau en fluide parfait". Bull. de l'Association Technique Maritime et Aéronautique, Vol 64, 1964, p. 537.
2. Gadd, G E. "A method of computing the flow and surface wave pattern around full forms". Trans. Roy. Inst. Naval Architects, Vol 118, 1976, p. 207.

TABLE 1 WAVE ELEVATIONS WIGLEY HULL

G E Gadd/Guillotton method, no sinkage

Fn	0.266	0.313	0.350	0.402	0.452	0.482	
x/L	$\eta(x)$	$\eta(x)$	$\eta(x)$	$\eta(x)$	$\eta(x)$	$\eta(x)$	
-.4875	.172	.117	.088	.059	.042	.033	
-.4625	.280	.213	.170	.121	.088	.073	
-.4375	.245	.230	.207	.163	.124	.104	
-.4125	.146	.180	.187	.172	.143	.125	
-.3875	.046	.113	.137	.152	.143	.131	
-.3625	-.043	.054	.086	.114	.124	.122	
-.3375	-.112	-.007	.041	.074	.095	.101	
-.3125	-.158	-.063	-.004	.039	.064	.075	
-.275	-.180	-.123	-.067	-.005	.022	.035	
-.225	-.149	-.156	-.124	-.061	-.021	-.008	
-.175	-.093	-.154	-.141	-.105	-.056	-.038	
-.125	-.049	-.128	-.144	-.123	-.088	-.063	
-.075	-.026	-.102	-.133	-.125	-.107	-.085	
-.025	-.028	-.072	-.115	-.125	-.113	-.101	

TABLE 1 CONTD. WAVE ELEVATIONS WIGLEY HULL

G E Gadd/ Guilloton method, no sinkage

Fn	0.266	0.313	0.350	0.402	0.452	0.482
x/L	$\eta(x)$	$\eta(x)$	$\eta(x)$	$\eta(x)$	$\eta(x)$	$\eta(x)$
.025	-.048	-.048	-.097	-.119	-.108	-.103
.075	-.078	-.027	-.073	-.107	-.106	-.100
.125	-.105	-.026	-.073	-.096	-.105	-.098
.175	-.110	-.033	-.044	-.090	-.102	-.098
.225	-.095	-.047	-.031	-.079	-.096	-.099
.275	-.071	-.059	-.026	-.063	-.090	-.097
.325	-.039	-.067	-.022	-.051	-.085	-.091
.375	-.014	-.070	-.017	-.040	-.077	-.083
.4125	.005	-.065	-.022	-.029	-.068	-.078
.4375	.008	-.063	-.024	-.021	-.061	-.074
.4625	.026	-.050	-.018	-.010	-.051	-.069
.4875	.079	-.010	.008	.012	-.034	-.058

TABLE 2 WAVE ELEVATIONS WIGLEY HULL

G F Gadd/Guilloton method, with sinkage

Fn	0.266	0.313	0.350	0.402	0.452	0.482	
x/L	$\eta(x)$	$\eta(x)$	$\eta(x)$	$\eta(x)$	$\eta(x)$	$\eta(x)$	
- 4875	.176	.121	.092	.062	.043	.034	
- .4625	.284	.218	.174	.125	.090	.074	
- .4375	.250	.237	.212	.167	.126	.106	
- .4125	.150	.185	.192	.177	.146	.126	
- .3875	.049	.119	.142	.156	.146	.133	
- .3625	-.041	.058	.091	.118	.129	.125	
- .3375	-.112	-.004	.047	.080	.100	.106	
- .3125	-.160	-.061	.001	.046	.070	.080	
- . 275	-.185	-.122	-.064	.002	.029	.042	
- . 225	-.158	-.161	-.124	-.052	-.011	.001	
- . 175	-.102	-.163	-.147	-.098	-.044	-.027	
- . 125	-.053	-.140	-.155	-.121	-.075	-.050	
- . 075	-.025	-.113	-.147	-.128	-.097	-.072	
- . 025	-.025	-.080	-.130	-.134	-.108	-.092	

TABLE 2 CONTD. WAVE ELEVATIONS WIGLEY HULL

G E Gadd/Guilloton method, with sinkage

Fn	0.266	0.313	0.350	0.402	0.452	0.482
x/L	$\eta(x)$	$\eta(x)$	$\eta(x)$	$\eta(x)$	$\eta(x)$	$\eta(x)$
.025	-.046	-.049	-.108	-.133	-.110	-.097
.075	-.079	-.026	-.081	-.122	-.112	-.098
.125	-.109	-.023	-.060	-.114	-.116	-.101
.175	-.116	-.029	-.045	-.107	-.118	-.107
.225	-.101	-.045	-.029	-.095	-.117	-.116
.275	-.075	-.059	-.022	-.079	-.116	-.123
.325	-.040	-.069	-.016	-.065	-.116	-.127
.375	-.012	-.074	-.014	-.052	-.112	-.129
.4125	.009	-.070	-.020	-.039	-.105	-.127
.4375	.012	-.067	-.021	-.029	-.099	-.124
.4625	.030	-.054	-.014	-.015	-.089	-.117
.4875	.084	-.012	.012	.010	-.068	-.101

TABLE 3 WAVE ELEVATIONS WIGLEY HULL

G E Gadd/Rankine source method

Fn	0.266	0.313	0.350	Fn	0.350	0.402	0.452
x/L	$\eta(x)$	$\eta(x)$	$\eta(x)$	$\eta(x)$	$\eta(x)$	$\eta(x)$	$\eta(x)$
-.43375	.124	.102	.083	-.4875	.083	.065	.042
-.48125	.171	.149	.124	-.4625	.146	.126	.091
-.4625	.179	.175	.153	-.4375	.169	.147	.106
-.4375	.153	.200	.190	-.4125	.181	.168	.134
-.4125	.091	.189	.204	-.3875	.177	.181	.151
-.3875	.021	.137	.182	-.3625	.135	.167	.150
-.3625	-.039	.072	.141	-.3375	.089	.146	.145
-.3375	-.082	.012	.084	-.3125	.032	.093	.118
-.3125	-.116	-.045	.020	-.275	-.031	.025	.072
-.275	-.119	-.095	-.043	-.225	-.090	-.047	.009
-.225	-.097	-.131	-.101	-.175	-.125	-.096	-.039
-.175	-.050	-.127	-.132	-.125	-.140	-.120	-.064
-.125	-.016	-.108	-.144	-.075	-.138	-.126	-.061
-.075	.001	-.081	-.137	-.025	-.118	-.119	-.095
-.025	.002	-.040	-.111				

TABLE 3 CONTD. WAVE ELEVATIONS WIGLEY HULL

G E Gadd/Rankine source method

F_n	0.266	0.313	0.350	0.350	0.402	0.452	
x/L	$\eta(x)$	$\eta(x)$	$\eta(x)$	$\eta(x)$	$\eta(x)$	$\eta(x)$	
.025	-.014	-.018	-.071	-.085	-.100	-.105	
.075	-.038	.003	-.028	-.043	-.077	-.115	
.125	-.056	.006	.003	-.009	-.056	-.122	
.175	-.065	-.007	.011	.005	-.046	-.124	
.225	-.068	-.031	-.001	-.001	-.050	-.120	
.275	-.066	-.056	-.025	-.021	-.060	-.113	
.325	-.062	-.074	-.050	-.045	-.059	-.102	
.375	-.053	-.080	-.068	-.063	-.072	-.085	
.425	-.029	-.057	-.060	-.053	-.049	-.043	
.475	.093	.032	.078	.083	.101	.125	

TABLE 4 WAVE RESISTANCE

G E Gadd/Guilloton method, no sinkage

Wigley		Inuid		Series 60	
Fn	Cw	Fn	Cw	Fn	Cw
.266	.764	.255	2.77	.22	.259
.313	1.434	.270	2.54	.25	.348
.350	1.132	.287	4.11	.28	1.145
.402	1.828	.319	5.19	.30	1.220
.452	2.560	.360	3.34	.32	1.112
.482	2.682	.440	4.81	.35	1.601
		.525	5.08		

TABLE 5 WAVE RESISTANCE

G E Gadd/Guilloton method, with sinkage

Wigley		Series 60				
Fn	Cw	Fn	Cw			
.266	.784	.22	.291			
.313	1.534	.25	.412			
.350	1.186	.28	1.978			
.402	2.189	.30	2.364			
.452	3.347	.32	1.969			
.482	3.657	.35	2.109			

TABLE 6 WAVE RESISTANCE

G E Gadd/Rankine source method

Wigley		Inuid		Series 60		HSVA tanker	
Fn	Cw	Fn	Cw	Fn	Cw	Fn	Cw
.266	.341	.319	4.30	.22	.229	.15	.262
.313	1.110	.360	6.44	.25	.499	.17	.406
.350	1.756	.440	6.81	.28	1.326	.19	1.084
	1.692	.525	13.33	.30	1.886		
.402	2.079			.32	2.359		
.452	3.143						

TABLE 7 WAVE ELEVATIONS INUID HULL

G E Gadd/Guilloton method, no sinkage

Fn	0.255	0.270	0.287	0.319	0.360	0.440	0.525
x/L	$\eta(x)$	$\eta(x)$	$\eta(x)$	$\eta(x)$	$\eta(x)$	$\eta(x)$	$\eta(x)$
-.4875	.376	.328	.277	.207	.153	.083	.051
-.4625	.532	.489	.430	.352	.273	.144	.082
-.4375	.286	.335	.353	.364	.330	.190	.111
-.4125	.033	.128	.194	.255	.279	.208	.132
-.3875	-.160	-.062	.037	.135	.193	.194	.143
-.3625	-.288	-.209	-.105	.015	.112	.159	.141
-.3375	-.358	-.308	-.214	-.094	.038	.117	.130
-.3125	-.380	-.358	-.285	-.179	-.034	.074	.112
-.275	-.347	-.368	-.335	-.258	-.133	.017	.076
-.225	-.246	-.306	-.325	-.298	-.222	-.047	.025
-.175	-.111	-.197	-.262	-.295	-.260	-.102	-.020
-.125	.014	-.068	-.161	-.255	-.269	-.140	-.057
-.075	.062	.030	-.052	-.193	-.253	-.162	-.083
-.025	-.017	.058	.034	-.108	-.218	-.171	-.106

TABLE 7 CONTD. WAVE ELEVATIONS INUID HILL

G E Gadd/Guilloton method, no sinkage

Fn	0.255	0.270	0.287	0.319	0.360	0.440	0.525
x/L	$\eta(x)$	$\eta(x)$	$\eta(x)$	$\eta(x)$	$\eta(x)$	$\eta(x)$	$\eta(x)$
.025	-.112	.007	.058	-.008	-.172	-.168	-.115
.075	-.199	-.095	.021	.045	-.116	-.161	-.121
.125	-.230	-.190	-.067	.056	-.063	-.150	-.125
.175	-.197	-.238	-.155	.026	-.027	-.139	-.130
.225	-.123	-.233	-.214	-.033	-.003	-.132	-.135
.275	-.047	-.182	-.236	-.095	.007	-.129	-.140
.325	.010	-.095	-.210	-.146	-.002	-.123	-.145
.375	-.025	-.020	-.163	-.202	-.026	-.116	-.153
.425	-.129	-.011	-.126	-.254	-.076	-.116	-.163
.475	-.149	-.010	-.046	-.249	-.123	-.110	-.159

TABLE 8 WAVE ELEVATIONS INUID HULL

G E Gadd/Rankine source method

Fn	0.319	0.360	0.440	0.525		
x/L	$\eta(x)$	$\eta(x)$	$\eta(x)$	$\eta(x)$		
-.4875	.198	.122	.086	.073		
-.4625	.442	.365	.232	.193		
-.4375	.452	.476	.256	.195		
-.4125	.303	.432	.362	.264		
-.3875	.185	.282	.381	.286		
-.3625	.079	.144	.307	.296		
-.3375	-.005	.069	.233	.298		
-.3125	-.088	.013	.132	.256		
-.275	-.202	-.072	.046	.200		
-.225	-.286	-.185	-.023	.118		
-.175	-.282	-.256	-.075	.034		
-.125	-.231	-.284	-.120	-.029		
-.075	-.135	-.278	-.155	-.085		
-.025	-.018	-.226	-.180	-.132		

TABLE 8 CONTD. WAVE ELEVATIONS INUID HULL

G E Gadd/Rankine source method

Fn	0.319	0.360	0.440	0.525		
x/L	$\eta(x)$	$\eta(x)$	$\eta(x)$	$\eta(x)$		
.025	.061	-.133	-.203	-.173		
.075	.088	-.021	-.226	-.214		
.125	.069	.061	-.238	-.248		
.175	.007	.073	-.238	-.277		
.225	-.072	.026	-.224	-.289		
.275	-.131	-.034	-.193	-.265		
.325	-.174	-.102	-.170	-.224		
.375	-.192	-.157	-.148	-.169		
.425	-.151	-.149	-.088	-.061		
.475	.117	.108	.186	.260		

G E Gadd

137

TABLE 10 WAVE ELEVATIONS SERIES 60 HULL

G E Gadd/Guillcton method, no sinkage

Fn	0.22	0.25	0.28	0.30	0.32	0.35
x/L_{PP}	$\eta(x)$	$\eta(x)$	$\eta(x)$	$\eta(x)$	$\eta(x)$	$\eta(x)$
-.4875	.209	.167	.132	.116	.098	.079
-.4625	.296	.262	.224	.202	.177	.148
-.4375	.244	.250	.238	.228	.212	.191
-.4125	.167	.207	.214	.213	.204	.200
-.3875	.099	.156	.187	.194	.192	.190
-.3625	.038	.097	.143	.163	.172	.173
-.3375	-.015	.036	.087	.114	.135	.150
-.3125	-.053	-.026	.029	.058	.084	.113
-.275	-.079	-.097	-.058	-.023	.006	.047
-.225	-.097	-.155	-.147	-.125	-.091	-.050
-.175	-.128	-.178	-.202	-.194	-.171	-.128
-.125	-.169	-.185	-.227	-.236	-.224	-.198
-.075	-.195	-.174	-.228	-.248	-.259	-.247
-.025	-.179	-.137	-.193	-.227	-.252	-.266

TABLE 13 CONTD. WAVE ELEVATIONS SERIES 60 HULL

G E Gadd/Guilloton method, no sinkage

Fn	0.22	0.25	0.28	0.30	0.32	0.35
x/L_{PP}	$\eta(x)$	$\eta(x)$	$\eta(x)$	$\eta(x)$	$\eta(x)$	$\eta(x)$
.025	-.098	-.067	-.098	-.149	-.179	-.236
.075	-.066	-.054	-.028	-.080	-.112	-.177
.125	-.115	-.109	-.026	-.043	-.075	-.131
.175	-.189	-.185	-.093	-.059	-.081	-.115
.225	-.198	-.208	-.165	-.100	-.096	-.110
.275	-.132	-.152	-.179	-.122	-.098	-.095
.325	-.043	-.053	-.125	-.105	-.071	-.060
.375	.030	.020	-.037	-.048	-.012	.005
.4125	.078	.079	.034	.011	.037	.052
.4375	.110	.110	.071	.050	.062	.078
.4625	.150	.152	.104	.081	.085	.103
.4875	.181	.186	.147	.109	.110	.128
.5125	.231	.220	.207	.151	.143	.159

TABLE 11 WAVE ELEVATIONS SERIES 60 HULL

G E Gadd / Guilloton method, with sinkage

Fn	0.22	0.25	0.28	0.30	0.32	0.35
x/L_{PP}	$\eta(x)$	$\eta(x)$	$\eta(x)$	$\eta(x)$	$\eta(x)$	$\eta(x)$
-.4875	.220	.179	.143	.128	.109	.089
-.4625	.307	.276	.238	.218	.195	.164
-.4375	.248	.252	.243	.236	.223	.203
-.4125	.163	.204	.212	.212	.208	.204
-.3875	.096	.153	.186	.191	.189	.189
-.3625	.033	.094	.140	.159	.169	.172
-.3375	-.019	.033	.083	.109	.130	.148
-.3125	-.056	-.028	.028	.054	.080	.112
-.275	-.087	-.100	-.056	-.023	.007	.044
-.225	-.109	-.166	-.152	-.127	-.089	-.045
-.175	-.134	-.195	-.218	-.204	-.178	-.127
-.125	-.165	-.197	-.250	-.256	-.238	-.200
-.075	-.186	-.176	-.248	-.274	-.276	-.250
-.025	-.169	-.127	-.199	-.250	-.272	-.270

TABLE 11 CONTD. WAVE ELEVATIONS SERIES 60 HULL

G E Gadd /Guilloton method, with sinkage

Fn	0.22	0.25	0.28	0.30	0.32	0.35
x/l_{PP}	$\eta(x)$	$\eta(x)$	$\eta(x)$	$\eta(x)$	$\eta(x)$	$\eta(x)$
.025	-.088	-.043	-.075	-.138	-.196	-.239
.075	-.055	-.023	.013	-.042	-.112	-.186
.125	-.098	-.085	.032	.020	-.038	-.126
.175	-.133	-.188	-.037	.017	-.003	-.083
.225	-.224	-.252	-.159	-.047	-.006	-.051
.275	-.166	-.219	-.250	-.148	-.057	-.047
.325	-.055	-.093	-.238	-.198	-.108	-.058
.375	.023	.022	-.132	-.158	-.110	-.057
.4125	.072	.097	-.016	-.087	-.076	-.045
.4375	.106	.127	.053	-.029	-.039	-.024
.4625	.144	.156	.098	.027	0	-.008
.4875	.166	.170	.131	.067	.031	.006
.5125	.213	.191	.181	.108	.063	.032

TABLE 12 WAVE ELEVATIONS SERIES 60 HULL

G E Gadd/Rankine source method

Fn	0.22	Fn	0.25	0.28	0.30	0.32
x/L_{pp}	$\eta(x)$	x/L_{pp}	$\eta(x)$	$\eta(x)$	$\eta(x)$	$\eta(x)$
-.49375	.208	-.4875	.200	.170	.152	.144
-.48125	.216	-.4625	.201	.203	.202	.196
-.4625	.216	-.4375	.204	.224	.232	.228
-.4375	.185	-.4125	.170	.207	.232	.239
-.4125	.128	-.3875	.128	.178	.218	.238
-.3875	.084	-.3625	.085	.139	.182	.210
-.3625	.052	-.3375	.044	.092	.134	.169
-.3375	.026	-.3125	-.002	.032	.071	.110
-.3125	-.002	-.275	-.034	-.036	-.015	.023
-.275	-.016	-.225	-.076	-.113	-.116	-.088
-.225	-.051	-.175	-.101	-.153	-.176	-.170
-.175	-.082	-.125	-.105	-.155	-.184	-.198
-.125	-.095	-.075	-.086	-.127	-.154	-.187
-.075	-.094	-.025	-.050	-.075	-.098	-.142
-.025	-.077					

TABLE 12 CONTD. WAVE ELEVATIONS SERIES 60 HULL

G E Gadd/Rankine source method

F_n	0.22	0.25	0.28	0.30	0.32		
x/L_{PP}	$\eta(x)$	$\eta(x)$	$\eta(x)$	$\eta(x)$	$\eta(x)$		
.025	-.072	-.027	-.036	-.052	-.093		
.075	-.088	-.033	-.030	-.038	-.062		
.125	-.111	-.058	-.054	-.054	-.053		
.175	-.117	-.083	-.079	-.080	-.056		
.225	-.093	-.087	-.086	-.091	-.060		
.275	-.050	-.069	-.076	-.082	-.056		
.325	.010	-.028	-.043	-.047	-.033		
.375	.067	.021	.003	.005	.005		
.425	.096	.063	.055	.059	.050		
.475	.164	.156	.169	.179	.171		

TABLE 13 WAVE ELEVATIONS HSVA HULL

G E Gadd/Rankine source method

Fn	0.15	0.17	0.19	Fn	0.15	0.17	0.19
x/L	$\eta(x)$	$\eta(x)$	$\eta(x)$	x/L	$\eta(x)$	$\eta(x)$	$\eta(x)$
-.49375	.752	.780	.810	.025	.037	-.043	0
-.48125	.202	.226	.258	.075	-.062	-.046	-.013
-.4625	-.089	-.095	-.084	.125	-.140	-.079	-.016
-.4375	-.321	-.348	-.349	.175	-.108	-.132	-.027
-.4125	-.416	-.442	-.448	.225	-.062	-.156	-.069
-.3875	-.416	-.433	-.450	.275	-.083	-.132	-.132
-.3625	-.326	-.335	-.366	.325	-.124	-.097	-.174
-.3375	-.192	-.189	-.224	.375	-.089	-.051	-.145
-.3125	-.090	-.076	-.090	.425	.034	.041	-.025
-.275	-.044	-.028	-.001	.475	.204	.192	.156
-.225	-.027	-.019	.033	.525	.320	.336	.304
-.175	-.042	-.025	.016				
-.125	-.052	-.031	.017				
-.075	-.016	-.048	.012				
-.025	.042	-.052	-.006				

TABLE 14 RESISTANCE RESULTS ATHENA HULL

G E Gadd

Method	Midhell		Guilloton			
	Cwu	Cws	Cw	Cwu	Cws	Cw
Fn						
.28	.85	1.42	2.27	.46	1.58	2.04
.35	.79	1.18	2.97	.43	1.20	1.63
.41	1.73	2.05	3.78	.67	1.06	1.73
.48	2.00	2.67	4.67	1.06	1.35	2.41
.65	1.37	2.17	3.54	.81	1.08	1.89
.80	.61	1.60	2.24			
1.00	.17	.81	0.98			
	RANKINE					
.28	.38	1.40	1.78			
.48	1.35	1.02	2.37			

TABLE 15 WAVE ELEVATIONS ATHENA HULL

G E Gadd/Michell method

Fn	0.28	0.48	Fn	0.28	0.48	
x/L	$\eta(x)$	$\eta(x)$	x/L	$\eta(x)$	$\eta(x)$	
-.4875	.097	.025	.025	-.029	-.053	
-.4625	.171	.054	.075	-.022	-.063	
-.4375	.167	.077	.125	-.029	-.069	
-.4125	.131	.092	.175	-.066	-.085	
-.3875	.102	.094	.225	-.125	-.114	
-.3625	.073	.095	.275	-.160	-.142	
-.3375	.051	.086	.325	-.127	-.146	
-.3125	.018	.072	.375	-.023	-.122	
-.275	-.035	.049	.425	.094	-.087	
-.225	-.087	.023	.475	.145	-.071	
-.175	-.094	.011				
-.125	-.073	.002				
-.075	-.049	-.013				
-.025	-.036	-.035				

TABLE 16 WAVE ELEVATIONS ATHENA HULL

G E Gadd/Guilloton method, no sinkage

Fn	0.23	0.48	Fn	0.28	0.48	
x/L	$\eta(x)$	$\eta(x)$	$\eta(x)$	$\eta(x)$	$\eta(x)$	
-.175	.101	.022	.025	-.043	-.067	
-.4625	.176	.052	.075	-.051	-.070	
-.4375	.148	.078	.125	-.084	-.078	
-.4125	.095	.096	.175	-.100	-.087	
-.3875	.062	.103	.225	-.059	-.082	
-.3625	.023	.093	.275	-.017	-.078	
-.3375	-.011	.073	.325	.008	-.066	
-.3125	-.024	.050	.375	-.025	-.024	
-.275	-.036	.020	.425	-.085	-.024	
-.225	-.057	-.003	.475	-.003	-.006	
-.175	-.053	-.010				
-.125	-.043	-.021				
-.075	-.044	-.040				
-.025	-.032	-.057				

TABLE 17 WAVE ELEVATIONS ATHENA HULL

G E Gadd / Rankine source method

Fn		0.28		Fn		0.48		Fn		0.28		0.48	
x/L		$\eta(x)$		x/L		$\eta(x)$		x/L		$\eta(x)$		$\eta(x)$	
-.49375		.054		-.4875		.021		.025		-.024		-.075	
-.48125		.127		-.4625		.046		.075		-.033		-.090	
-.4625		.145		-.4375		.053		.125		-.043		-.098	
-.4375		.154		-.4125		.068		.175		-.047		-.098	
-.425		.123		-.3875		.076		.225		-.036		-.083	
-.3875		.067		-.3625		.085		.275		-.023		-.061	
-.3625		.023		-.3375		.090		.325		-.019		-.038	
-.3375		-.011		-.3125		.090		.375		-.003		0	
-.3125		-.032		-.2875		.090		.425		.007		.024	
-.2875		-.040		-.2625		.082		.475		.007		.025	
-.2625		-.044		-.225		.072							
-.225		-.021		-.175		.046							
-.175		-.002		-.125		.014							
-.125		-.001		-.075		-.019							
-.075		-.009		-.025		-.047							
-.025		-.014											

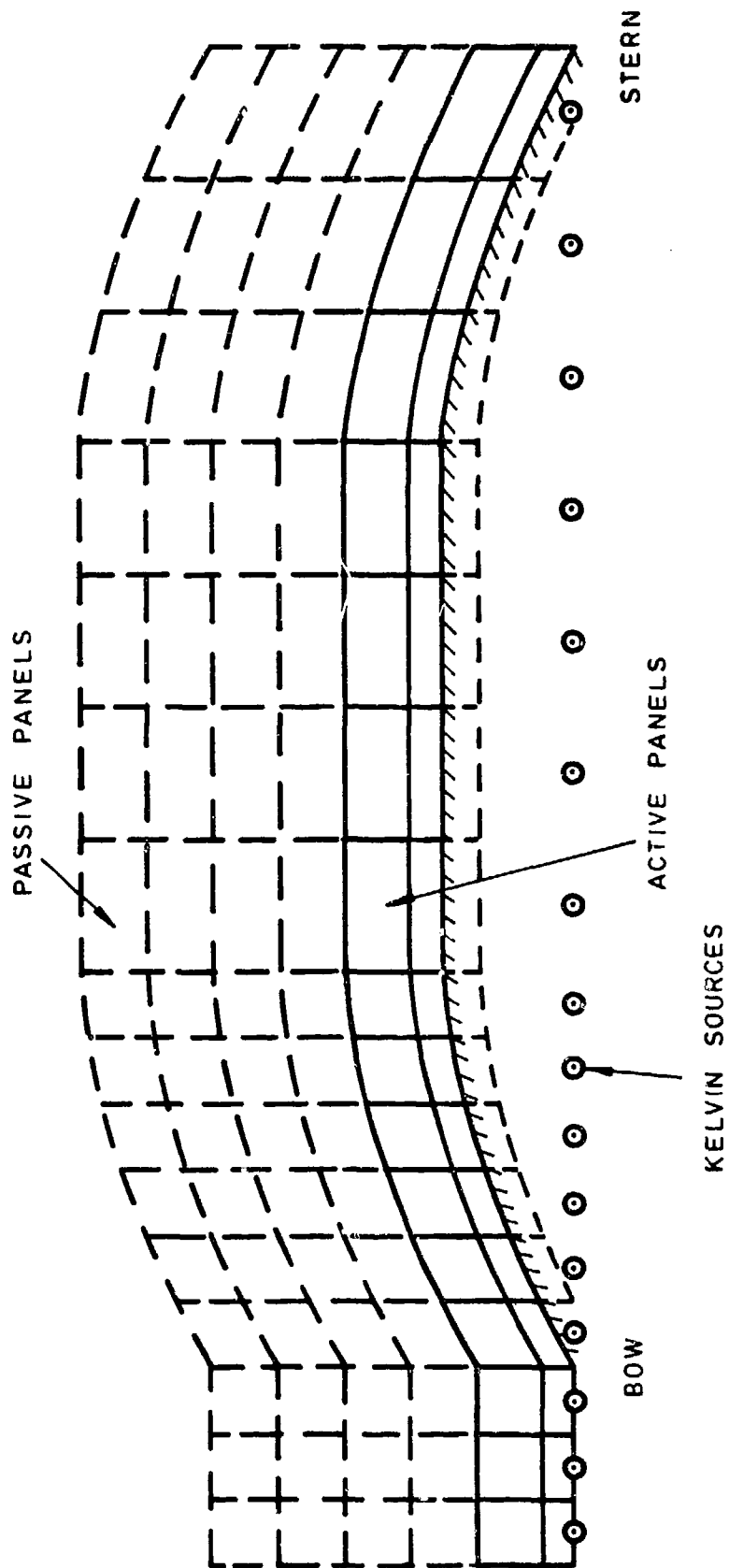
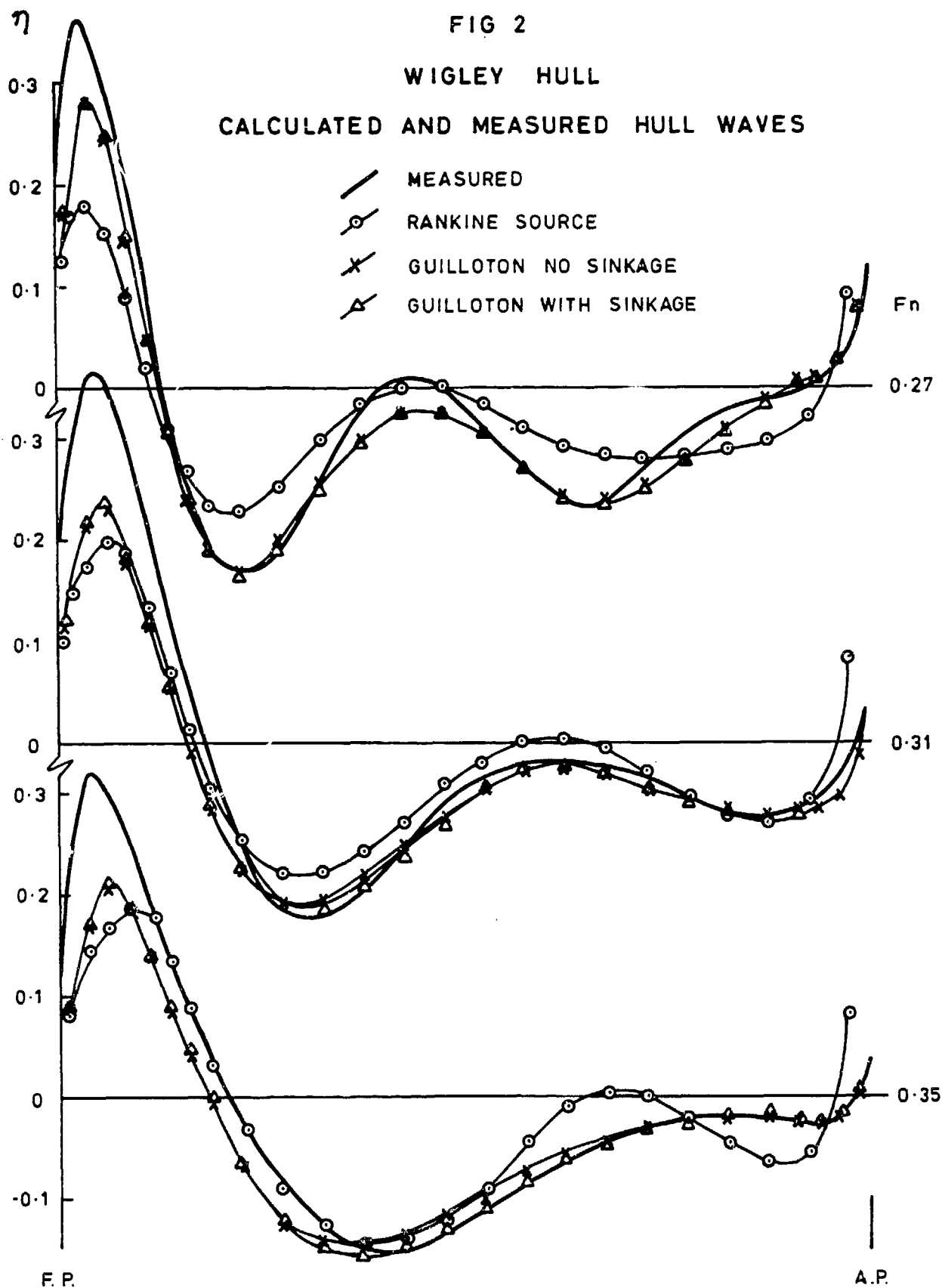


FIG.1 BASIS OF IMPROVED RANKINE SOURCE METHOD

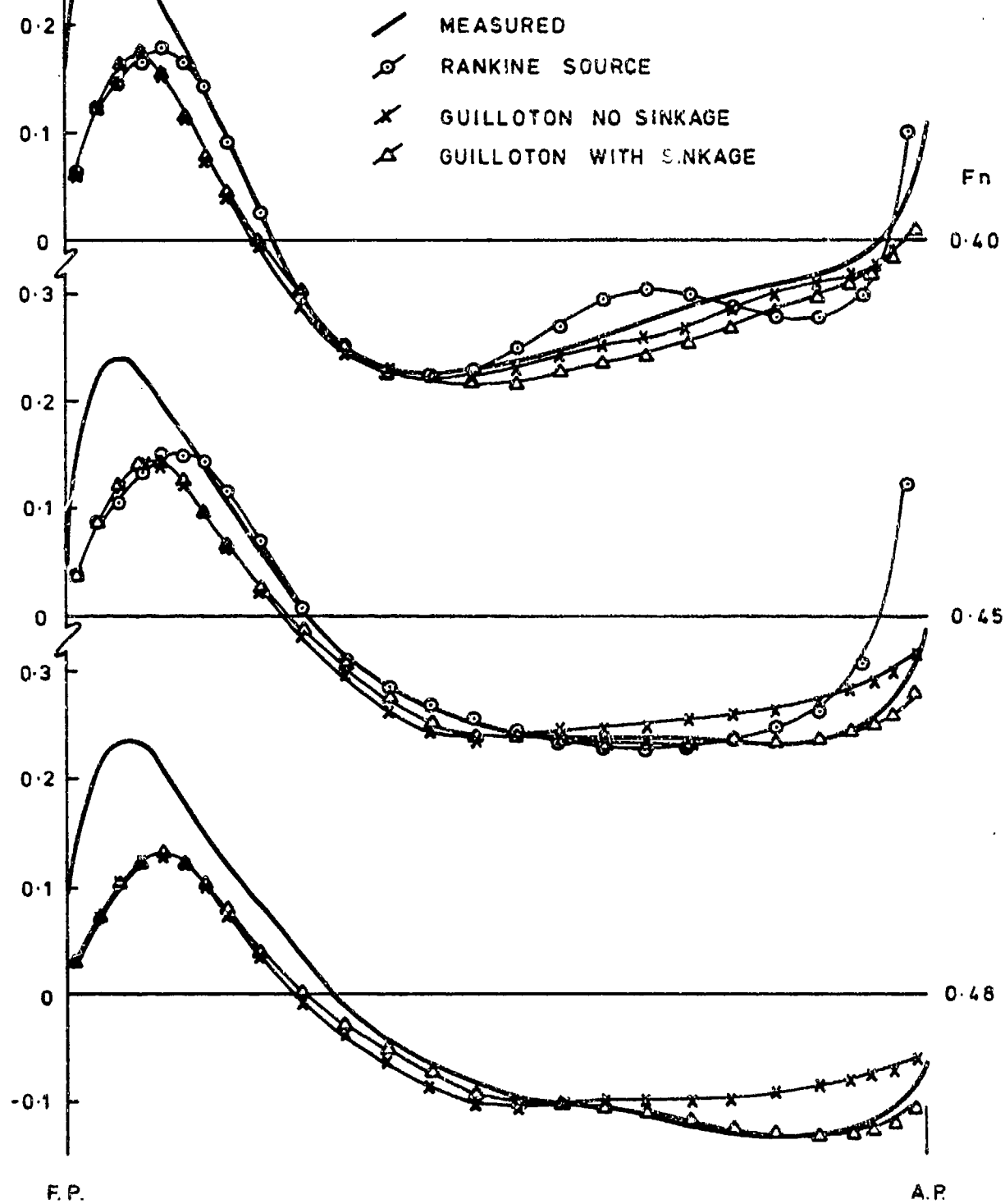


η

FIG. 3

WIGLEY HULL

CALCULATED AND MEASURED HULL WAVES



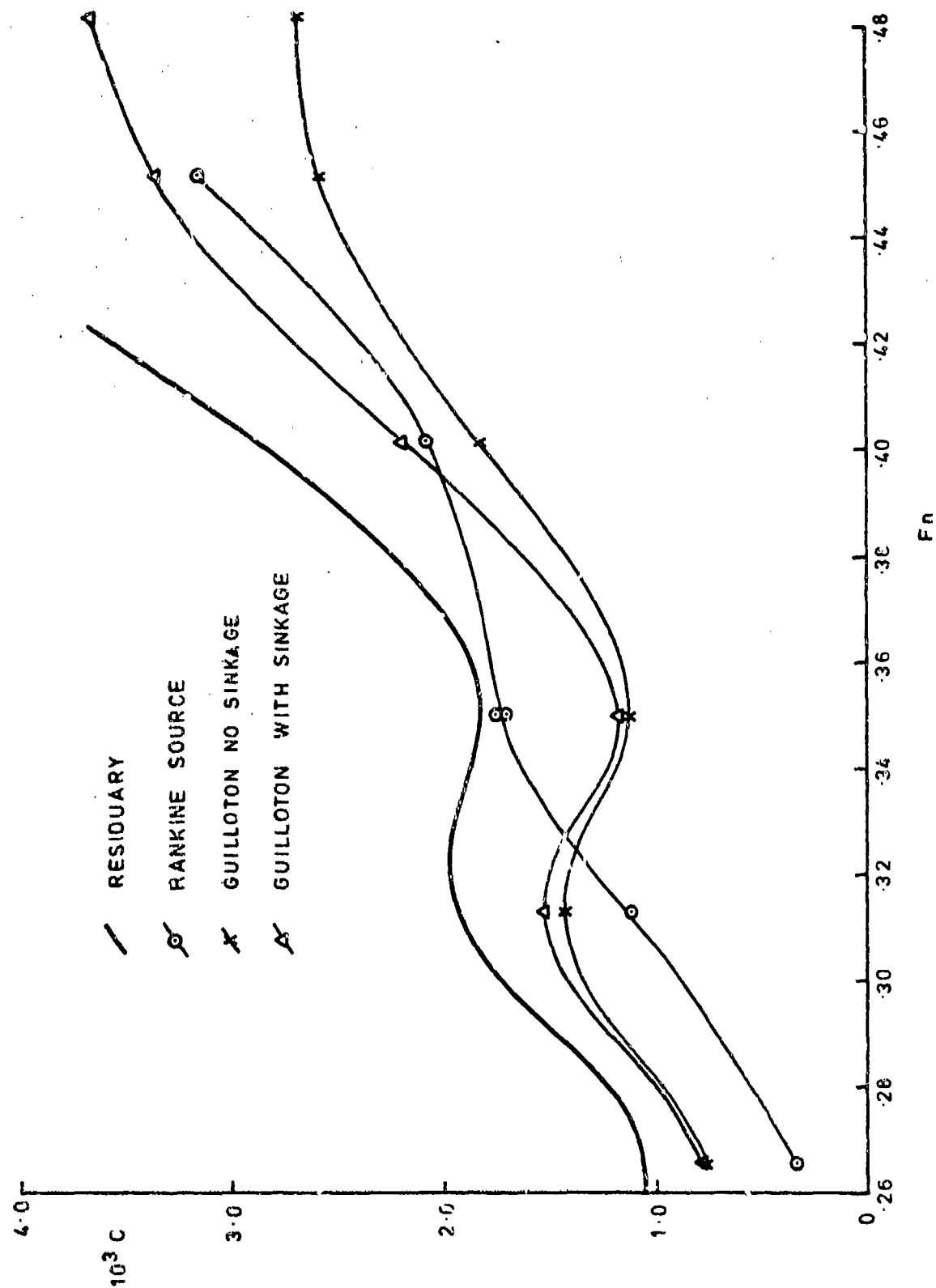


FIG. 4 RESISTANCE CURVES, WIGLEY HULL

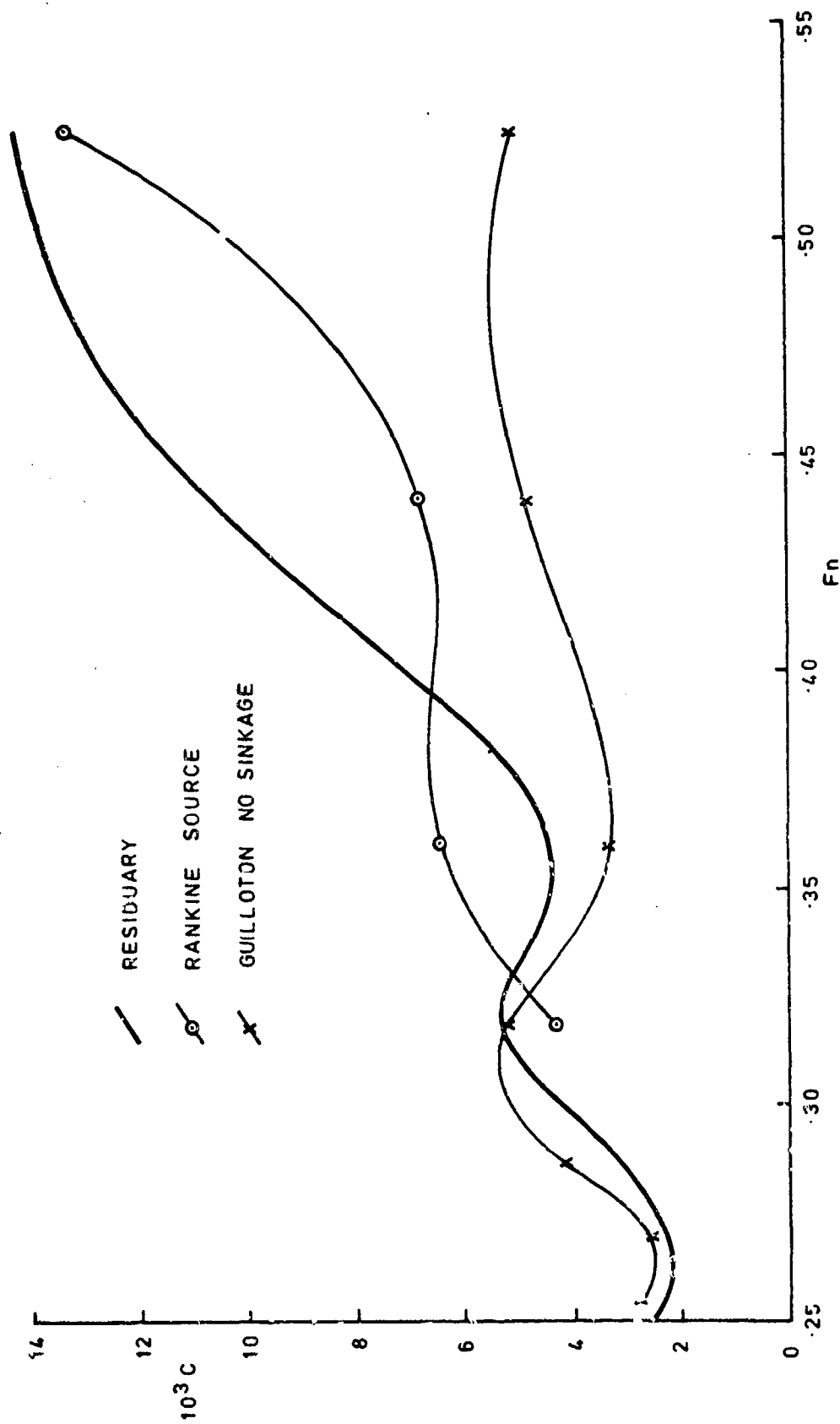


FIG 5 RESISTANCE CURVES, INUID HULL

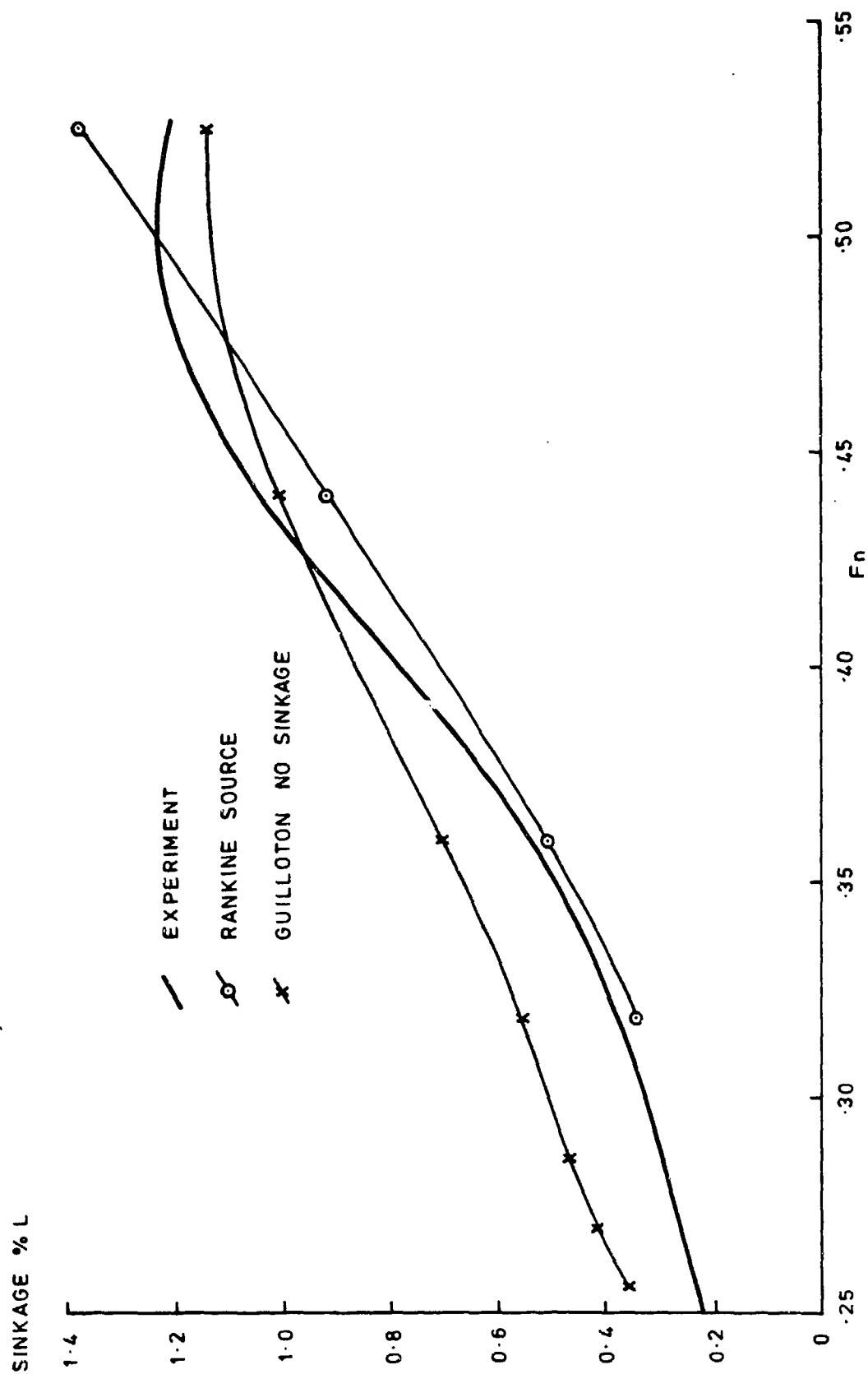
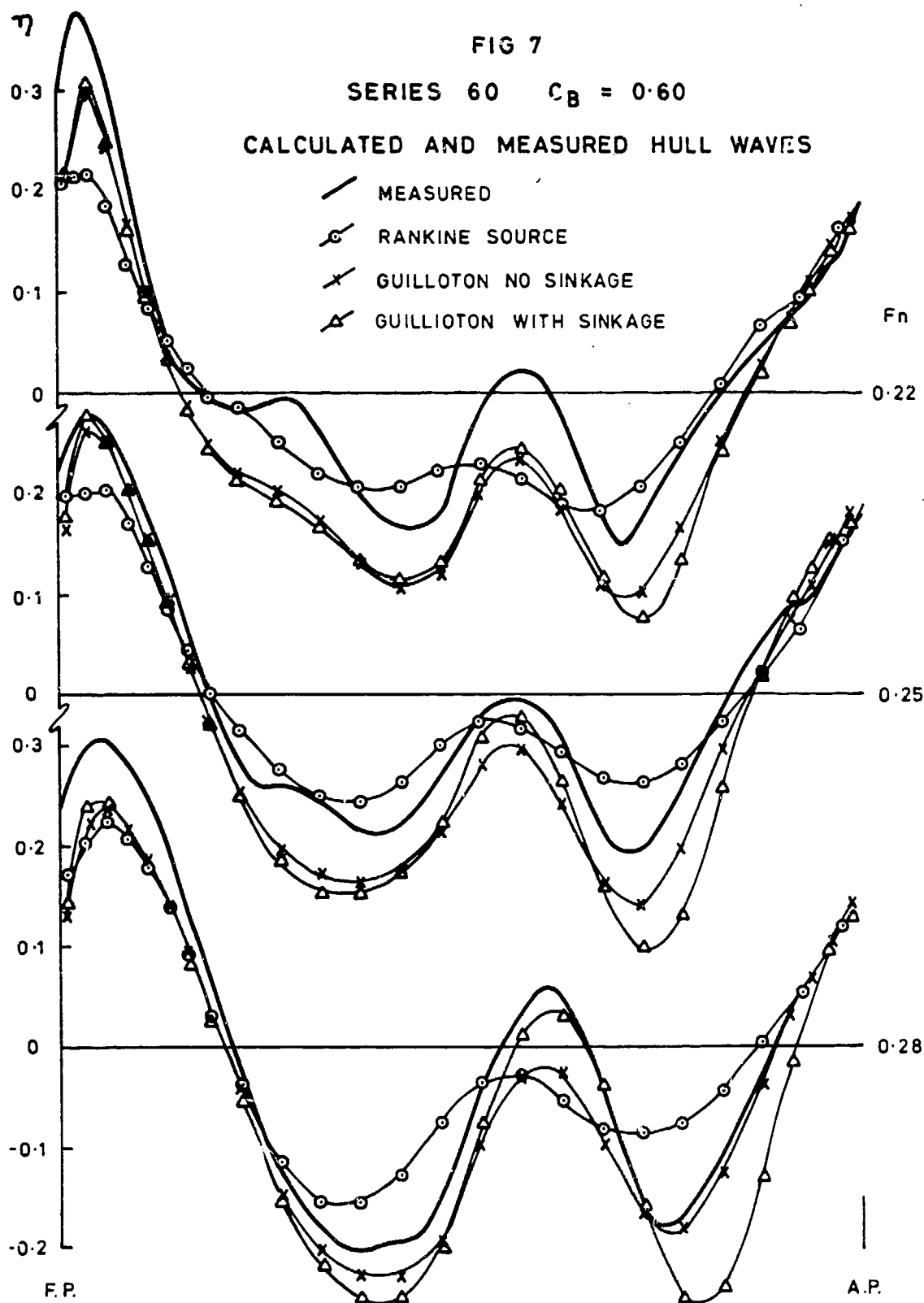
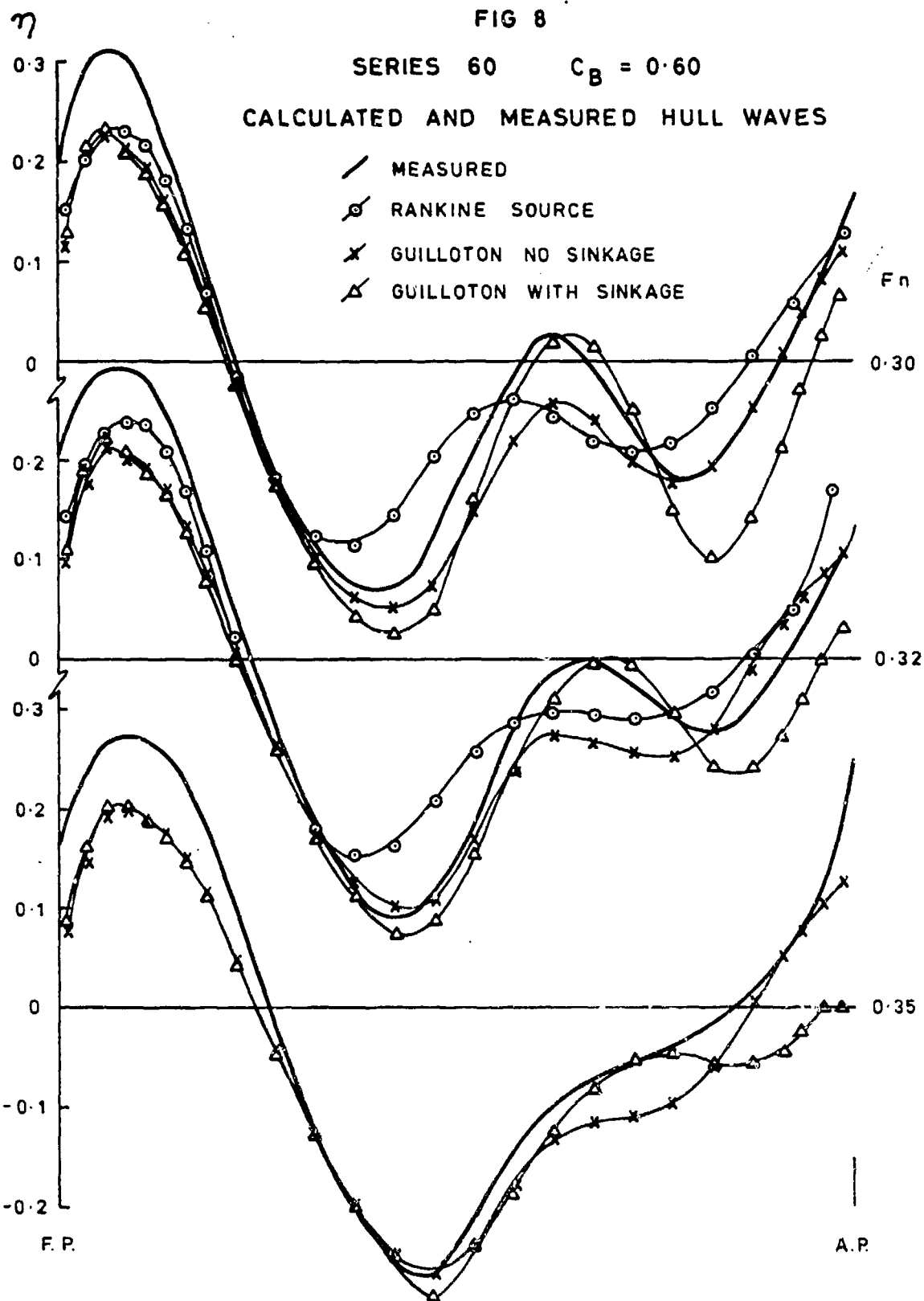


FIG 6 SINKAGE CURVES, INITIAL HULL





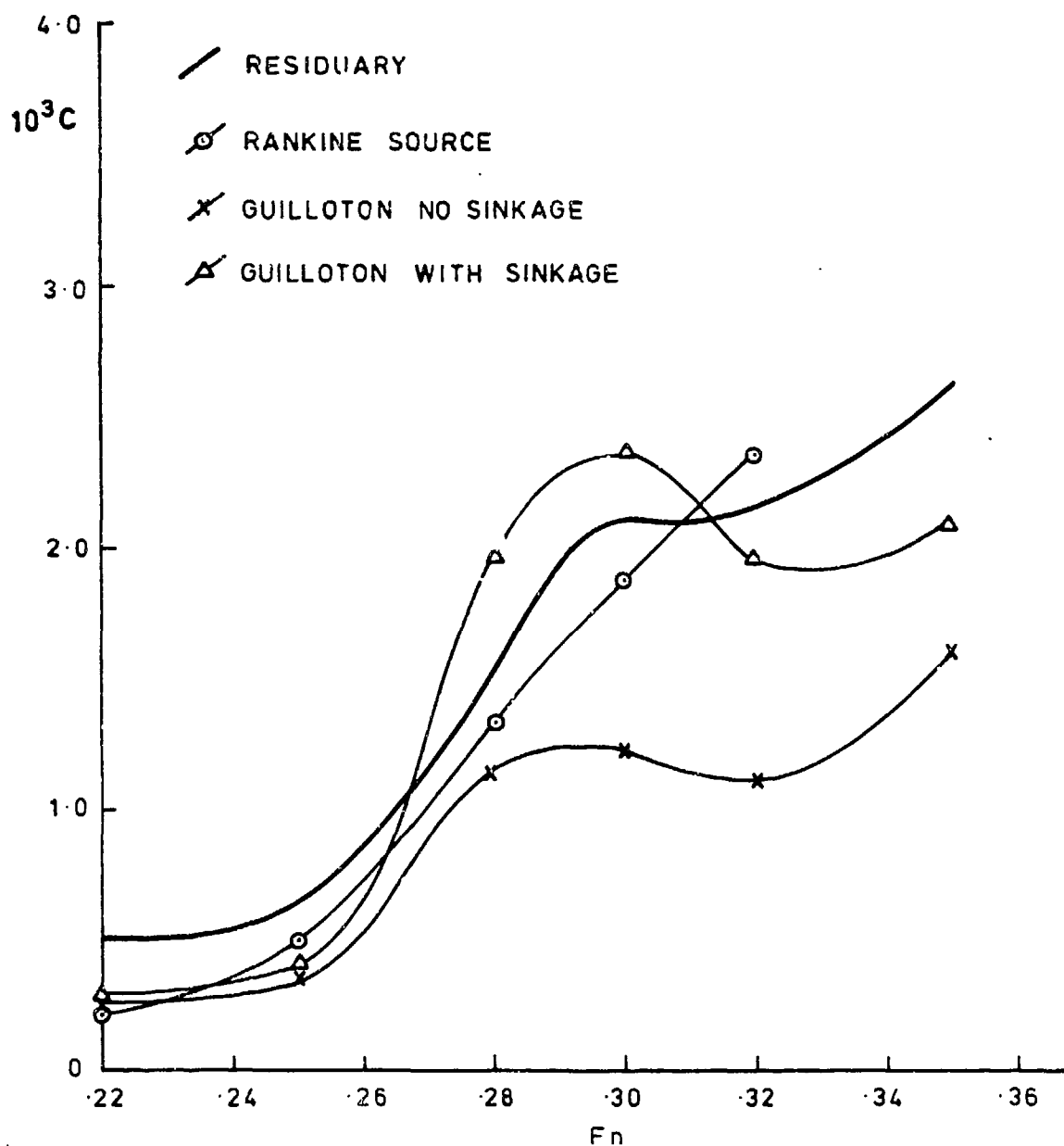


FIG. 9 RESISTANCE CURVES, SERIES 60 HULL

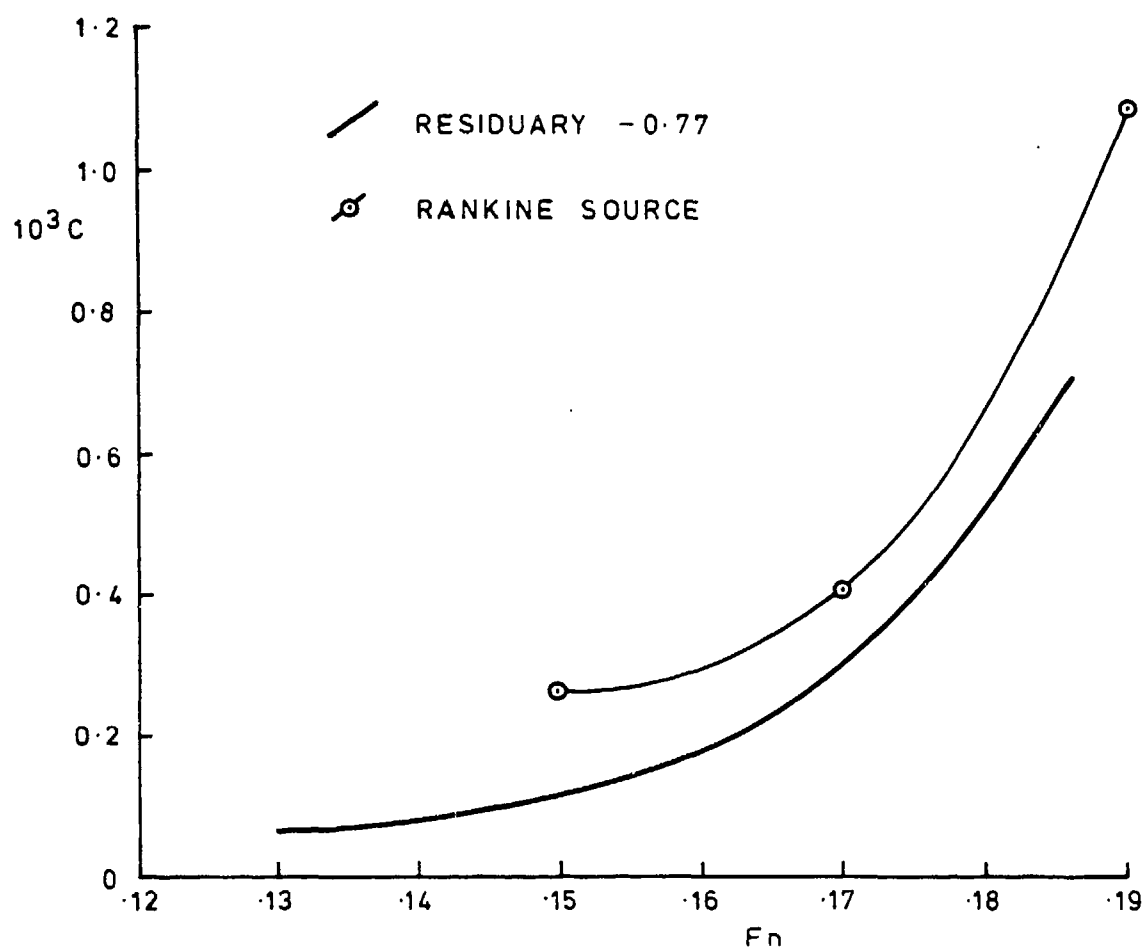


FIG 10 RESISTANCE CURVES, HSVA HULL

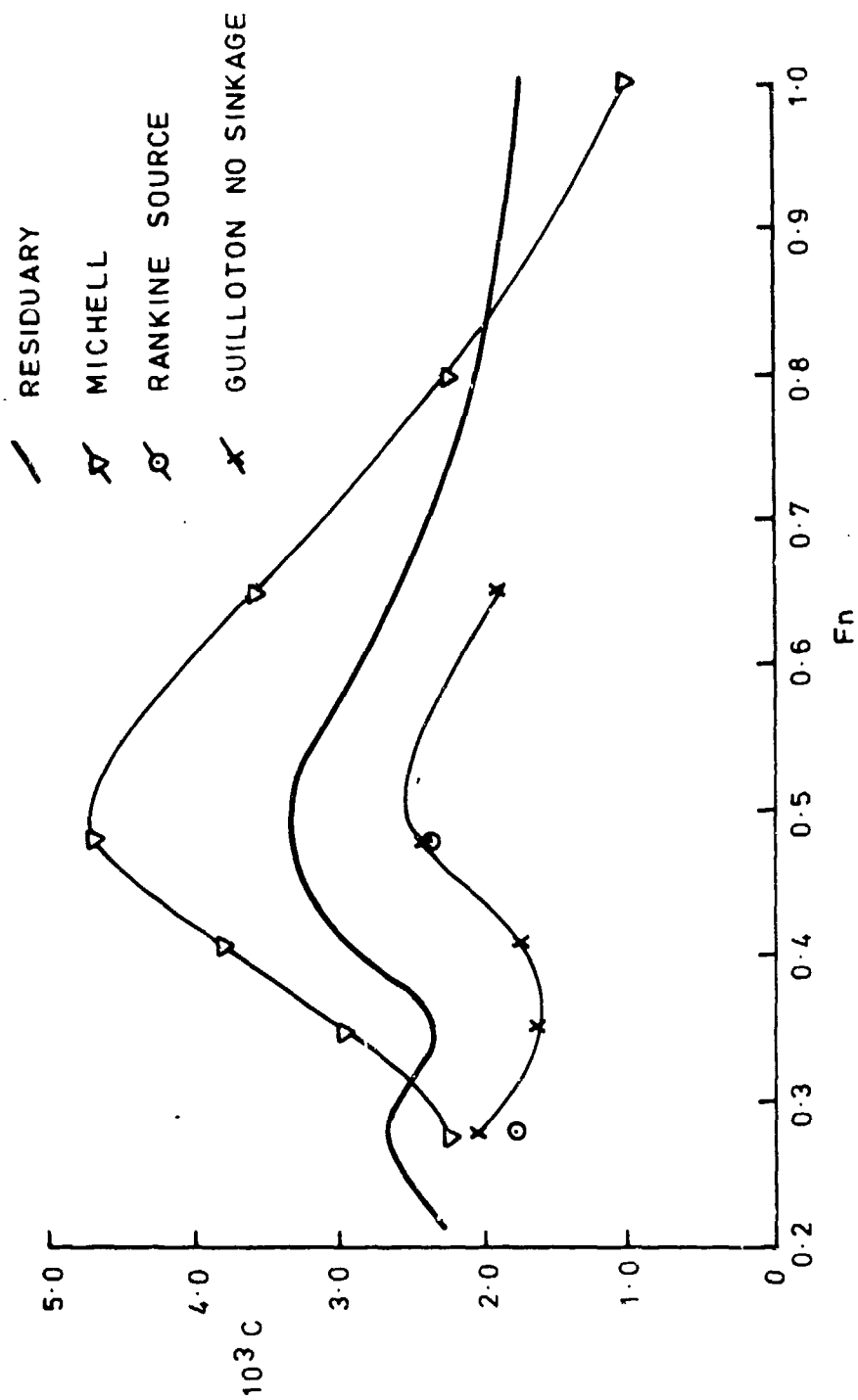
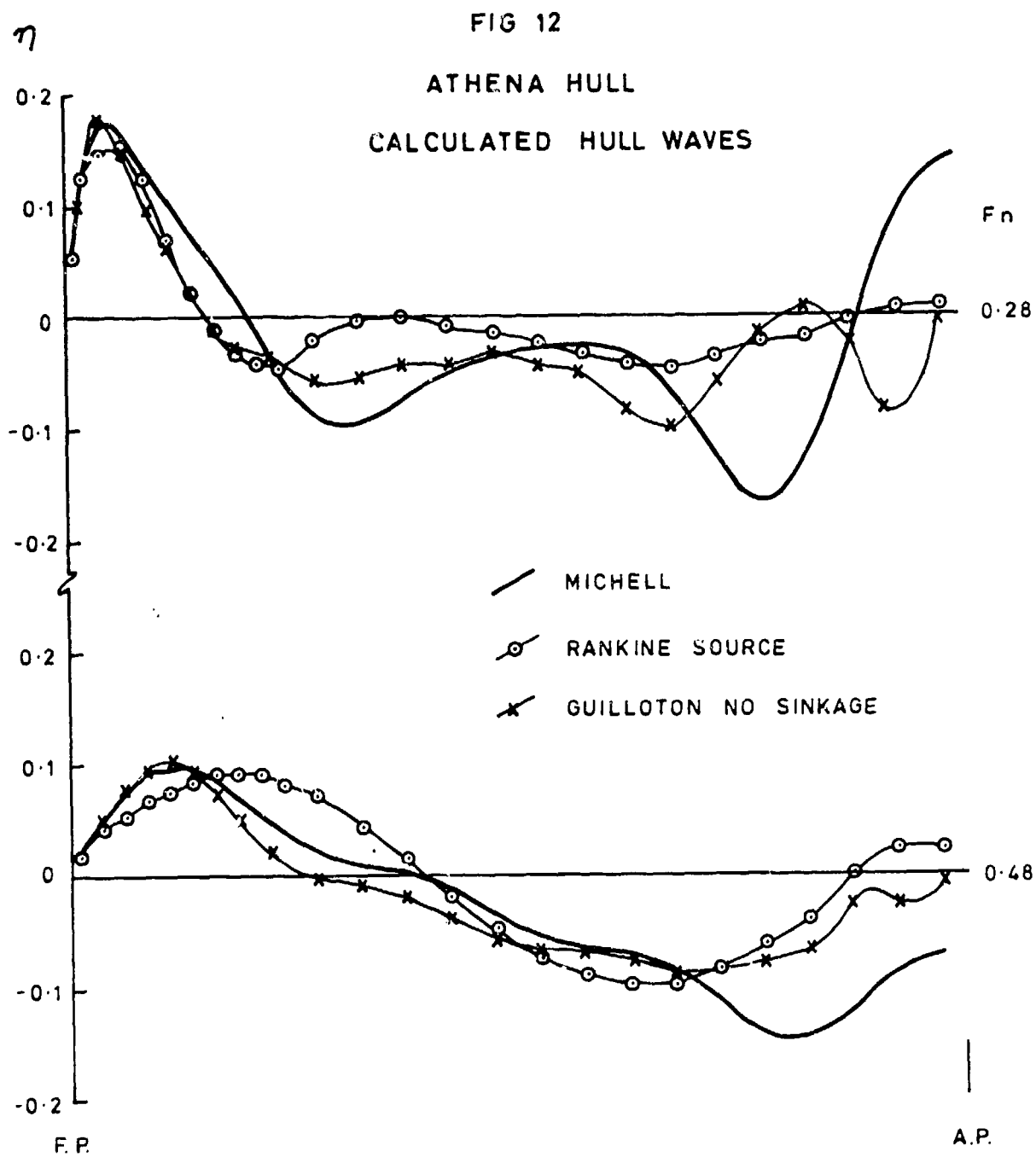


FIG 11 RESISTANCE CURVES, ATHENA HULL



Discussion*

by G. E. Gadd

An improved version of the Rankine source method has been developed. The downstream truncation condition now relates the source strengths on the downstream panels to the wave system generated by the Kelvin source array. Further, the numerical evaluation of the waves due to the Kelvin sources has been improved for low Froude numbers. Results are as follows:

1. Wigley's parabolic hull

	Fn	.313	.350	.402	.452	.482
10^3	Cw	1.52	1.32	2.19	3.15	4.05

2. Inuid hull 5201

	Fn	.255	.287	.319	.360
10^3	Cw	2.22	3.58	5.10	2.82

3. Series 60, $C_B = 0.60$

	Fn	.27	.28	.30	.32	.35
10^3	Cw	.71	1.22	1.82	2.37	2.27

4. Forebody of HSV A tanker

	Fn	.13	.15	.17	.19
10^3	Cw	.012	.023	.225	.313

5. High speed hull, Athena

	Fn	.35	.41	.48	.65
<u>Stern sinkage</u>		.0004	.0027	.0034	.0138
<u>Ship length</u>					
	Cwu	0.95	1.50	1.95	1.42
	Cwu	0.88	0.94	1.42	1.29
	Cw	1.83	2.44	3.37	2.71

*Editor's Note: Dr. G. E. Gadd has submitted this improved version after the Workshop.

CALCULATION OF THE WAVE RESISTANCE OF
SHIPS BY THE NUMERICAL SOLUTION OF
NEUMANN-KELVIN PROBLEM

T. Tsutsumi

Ishikawajima-Harima Heavy Industries Co., Ltd. Japan

ABSTRACT

The Solution of the Neumann-Kelvin problem, which Brard (1972) dealt with, is computed numerically for Wigley's hull and Series 60. Wave resistances, wave spectra, wave elevations and dynamic pressure coefficients are calculated by the numerical solution of Neumann-Kelvin problem. The results are compared with the results obtained from double model sources.

1. BASIC EQUATIONS

We consider a unit source at a point $Q(x'', y'', z'')$ on the hull surface. The Green's function satisfying the Laplace equation, the radiation condition and the linearized free surface condition, is expressed as:

$$G(P, Q) = G_1 + G_2 + G_3 \quad \text{at } P(x, y, z), \quad (1)$$

where

$$G_1 = \frac{1}{r} + \frac{1}{r'}, \quad (2)$$

$$G_2 = -\frac{2}{\pi} \int_{-\pi/2}^{\pi/2} d\theta \int_0^{\infty} e^{-\kappa(z+z'')} \frac{\kappa}{\kappa - \kappa \sec^2 \theta} \cos\{\kappa(x-x'') \cos \theta\} \\ \times \cos\{\kappa(y-y'') \sin \theta\} d\kappa, \quad (3)$$

$$G_3 = 2 \int_{-\pi/2}^{\pi/2} e^{-\kappa(z+z'') \sec^2 \theta} \cdot \kappa \sec^2 \theta \sin\{\kappa(x-x'') \sec \theta\} \\ \times \cos\{\kappa(y-y'') \sin \theta \sec^2 \theta\} d\theta, \quad (4)$$

$$r^2 = (x - x'')^2 + (y - y'')^2 + (z - z'')^2, \quad (5)$$

$$r'^2 = (x - x'')^2 + (y - y'')^2 + (z + z'')^2. \quad (6)$$

The perturbation velocity potential $\phi(P)$ may be expressed as a function of sources $m(Q)$.

$$\phi(P) = - \int_S m(Q) G(P, Q) dS - \frac{1}{K} \oint_{C_0} m(Q) G(P, Q) n_x(Q) dy'', \quad (7)$$

where C_0 represents the still water line of the ship, n_x is the x-direction cosine of a normal outward unit vector on the body.

The integral equation for $m(P)$ is obtained from the hull surface condition.

$$2\pi m(P) - \int_S m(Q) G_n(P, Q) dS - \frac{1}{K} \oint_{C_0} m(Q) G_n(P, Q) n_x(Q) dy'' + U n_y(P) = 0 \quad \text{for the point } P \text{ on } S, \quad (8)$$

where

$$G_n(P, Q) = \left(n_x(P) \frac{\partial}{\partial x} + n_y(P) \frac{\partial}{\partial y} + n_z(P) \frac{\partial}{\partial z} \right) G(P, Q). \quad (9)$$

In the case of double body sources, the following equation is used for $m(P)$.

$$2\pi m(P) - \int_S m(Q) G_{lm}(P, Q) dS + U n_y(P) = 0 \quad \text{for the point } P \text{ on } S, \quad (10)$$

where

$$G_{im}(P, \theta) = \left(\eta_x(P) \frac{\partial}{\partial x} + \eta_y(P) \frac{\partial}{\partial y} + \eta_z(P) \frac{\partial}{\partial z} \right) G_i.$$

The wave-resistance coefficient C_w is expressed as:

$$C_w = \frac{R_w}{\frac{1}{2} \rho U^2 S} = \frac{2\pi}{S} \int_0^{\pi/2} A^*(\theta) d\theta. \quad (12)$$

where the wave spectrum A^* is

$$A^*(\theta) = \{ C^*(\theta) \}^2 + \{ S^*(\theta) \}^2. \quad (13)$$

$$\begin{aligned} \left. \begin{matrix} C^*(\theta) \\ S^*(\theta) \end{matrix} \right\} &= \frac{4K}{U} \left\{ \sec \theta \right\}^{\frac{3}{2}} \left[\int_S m(Q) e^{Kz'' \sec^2 \theta} \left\{ \begin{matrix} \cos \\ \sin \end{matrix} \right\} (Kp'' \sec^2 \theta) dS \right. \\ &\quad \left. + \frac{1}{K} \int_{c_0} m(Q; \eta_x(Q)) \left\{ \begin{matrix} \cos \\ \sin \end{matrix} \right\} (Kp'' \sec^2 \theta) dy'' \right], \quad (14) \end{aligned}$$

$$p'' = x'' \cos \theta + y'' \sin \theta. \quad (15)$$

The wave elevation along hull, $\eta(x)$, and the dynamic pressure coefficient on hull surface, C_{pr} , are obtained from the linearized equations.

$$\eta(x) = -\frac{2}{U} \phi_x(P) \quad \text{on } Z=0, \quad (16)$$

$$C_{pr} = -\frac{2}{U} \phi_x(P) \quad \text{on } S. \quad (17)$$

2. METHOD OF NUMERICAL CALCULATION

Firstly, we approximate the hull surface on the starboard side by a large number of small elemental planes $S_{i,j}$ ($i = 1, 2, \dots, M$; $j = 1, 2, \dots, N$), where M and N are the numbers of elements numbered in the positive x and negative z directions, respectively. As a result of symmetry with respect to the vertical centerplane of the body, small elemental planes on the portside are specified. Secondly, we assume that $m(Q)$ is

constant on each elemental plane. Finally we choose the mean point of the plane as the point at which Equation (8) is satisfied. Thus Equation (8) becomes the $M \times N$ linear simultaneous equations for $m(Q)$ and be calculated numerically. Double body sources in Equation (10) are calculated in the same way.

3. RESULTS OF CALCULATION

3.1 Wigley's hull

The number of elements on Wigley's hull was chosen as $M \times N = 24 \times 10$. The calculations of wave spectra, wave profiles and dynamic pressure coefficients were carried out for $F_n = 0.266$, $F_n = 0.313$, $F_n = 0.350$ and $F_n = 0.452$.

- | | |
|---------|--|
| Fig. 1 | Shapes of the elements on Wigley's hull surface.
(Arrows on the elements show the stream directions by double body sources in the infinite flow.) |
| Fig. 2 | Comparison of wave resistance of Wigley's hull |
| Fig. 3 | Comparison of wave spectra of Wigley's hull |
| Fig. 4 | Wave profiles along Wigley's hull |
| Fig. 5 | Dynamic pressure coefficients on Wigley's hull surface |
| Table 1 | Calculated wave resistance by the numerical solution of Neumann-Kelvin problem |
| Table 2 | Calculated wave resistance by double model sources |
| Table 3 | Calculated wave spectra by the numerical solution of Neumann-Kelvin problem |
| Table 4 | Calculated wave spectra by double body sources |
| Table 5 | Calculated wave elevations along Wigley's hull |
| Table 6 | Calculated dynamic pressure coefficients on Wigley's hull surface |

3.2 Series 60, $C_B = 0.60$

The number of elements on the hull surface of Series 60, $C_B = 0.60$ was chosen as $M \times N = 24 \times 9$. The calculations of wave spectra, wave profiles and dynamic pressure coefficients were carried out for $F_n = 0.28$, $F_n = 0.30$, $F_n = 0.32$ and $F_n = 0.35$.

Fig. 6 Shapes of the elements on the hull surface of Series 60, $C_B = 0.60$. (Arrows on the elements show the stream directions by double body sources in the infinite flow.)

Fig. 7 Comparison of wave resistance of Series 60, $C_B = 0.60$

Fig. 8 Comparison of wave spectra of Series 60, $C_B = 0.60$

Fig. 9 Wave profiles along the hull of Series 60, $C_B = 0.60$

Fig. 10 Dynamic pressure coefficients on the hull surface of Series 60, $C_B = 0.60$

Table 1 Calculated wave resistance by the numerical solution of Neumann-Kelvin problem

Table 2 Calculated wave resistance by double model sources

Table 7 Calculated wave spectra by the numerical solution of Neumann-Kelvin problem

Table 8 Calculated wave spectra by double body sources

Table 9 Calculated wave elevations along the hull of Series 60, $C_B = 0.6$

Table 10 Calculated dynamic pressure coefficients on the hull surface of Series 60, $C_B = 0.6$

REFERENCE

- (1) Brard, R. "The Representation of a Given Ship Form by Singularity Distributions When the Boundary Condition on the Free

Surface Is Linearized", J. Ship Res., Vol. 16 (1972).

- (2) Tsutsumi, T. "On the Wave Resistance of Ships Represented by Sources Distributed over the Hull Surface", Trans. of the West-Japan Soc. Nav. Arch., No. 51 (1976).
- (3) Tsutsumi, T. "Calculation of the Source Distributions over the Hull Surface When the Free Surface Condition Is Linearized", Dept. Nav. Arch. Mar. Eng., Univ. of Michigan, Report No. 197, Ann Arbor (1978).

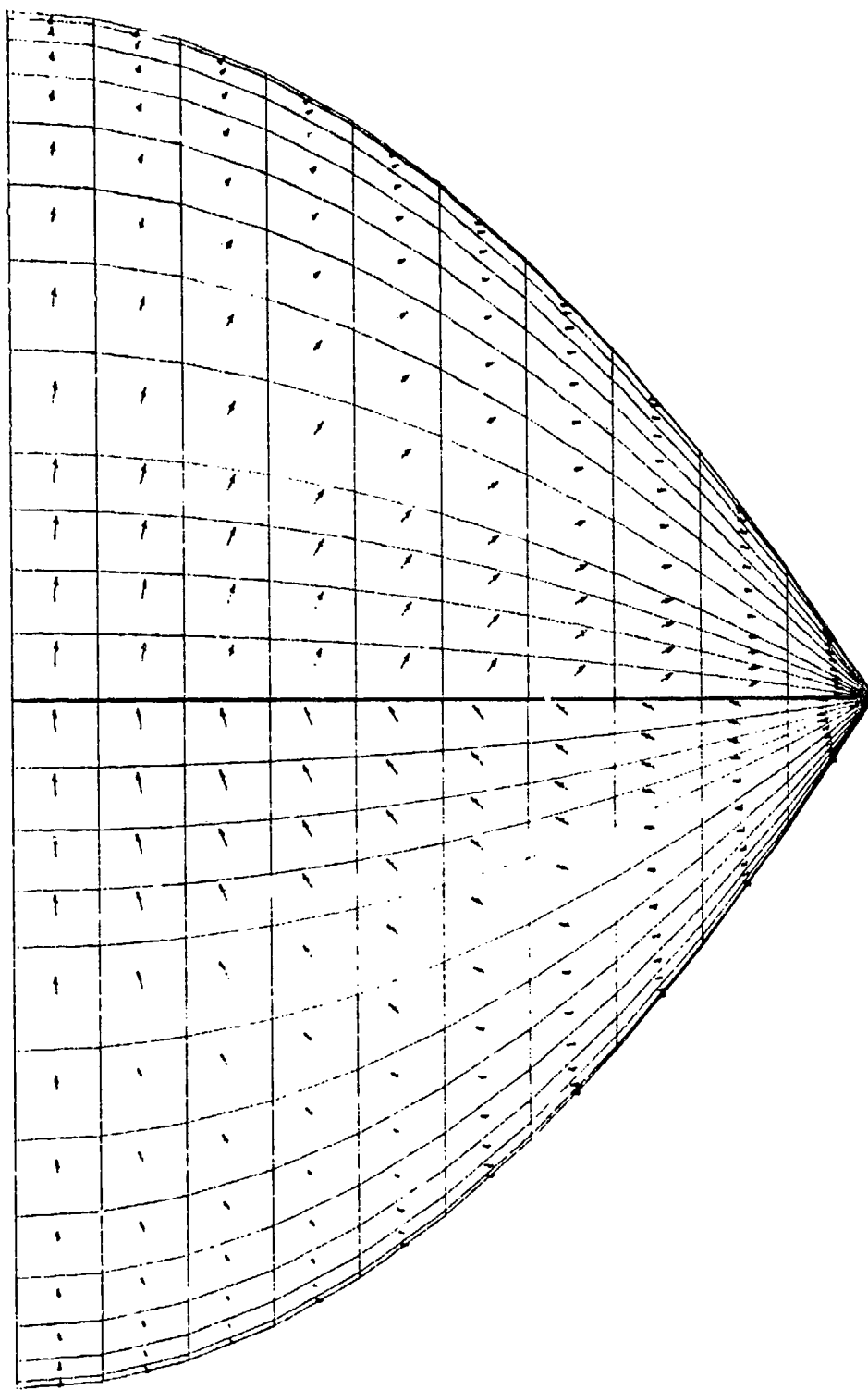


Fig. 1 Shapes of the elements on Wigley's hull surface

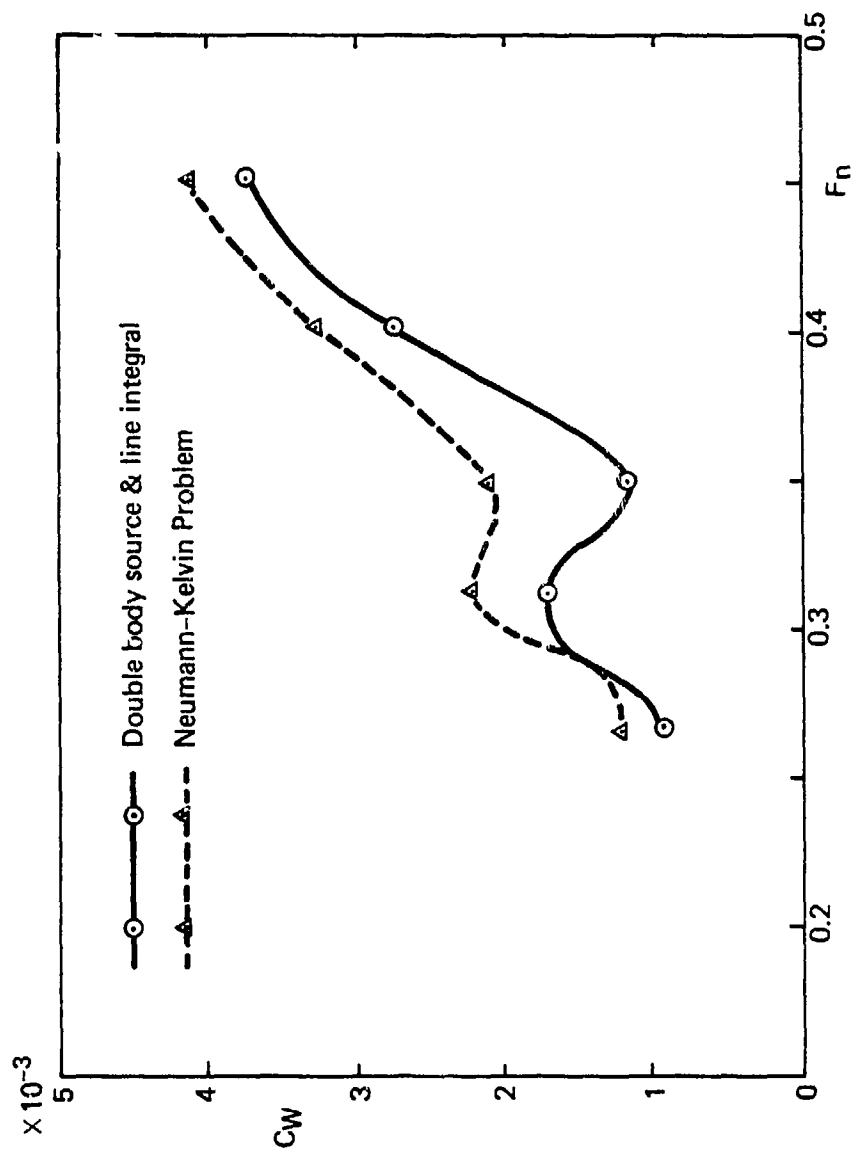


Fig. 2 Comparison of wave resistance of Wigley's hull

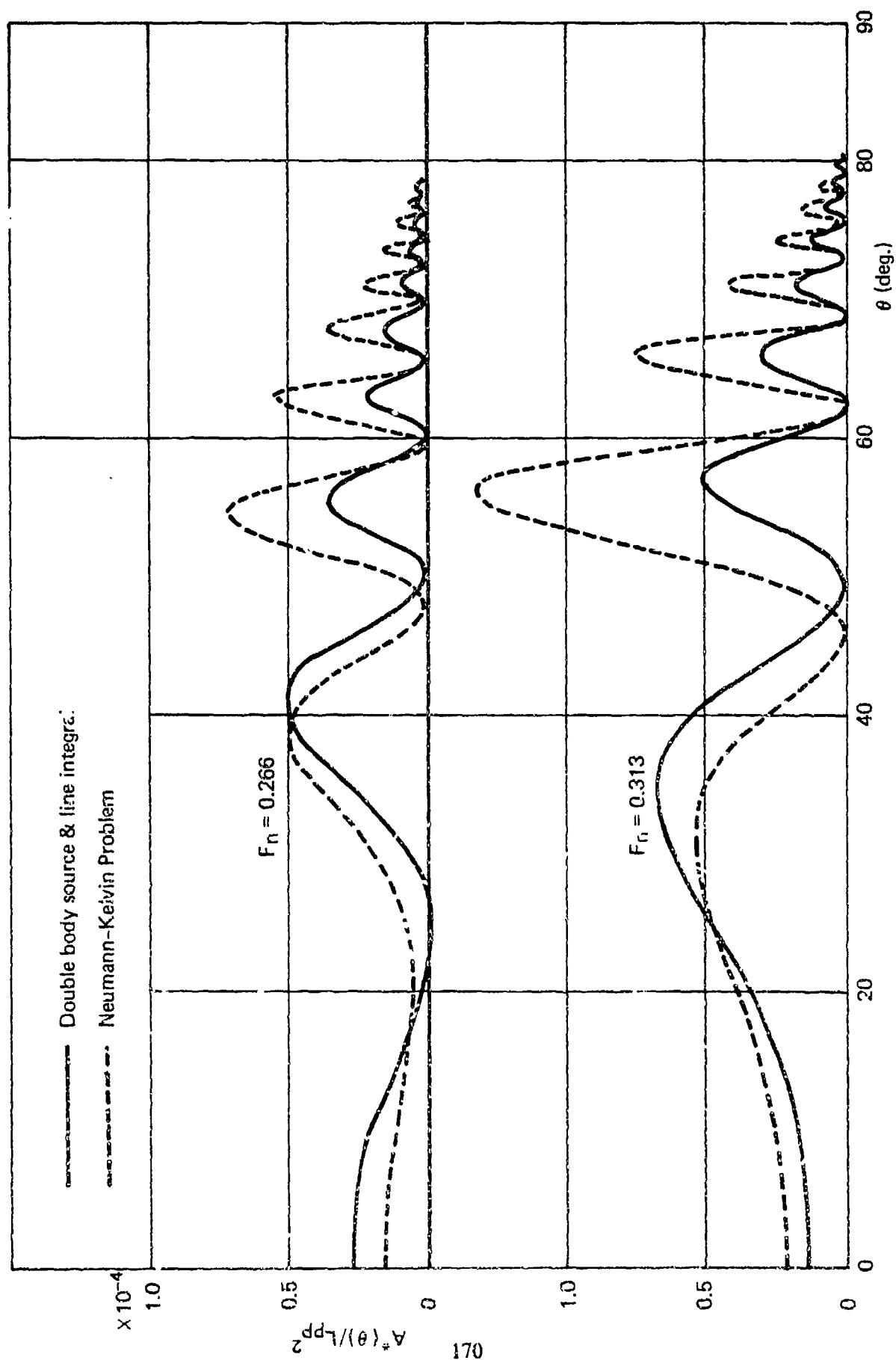


Fig. 3 Comparison of wave spectra of Wigley's hull

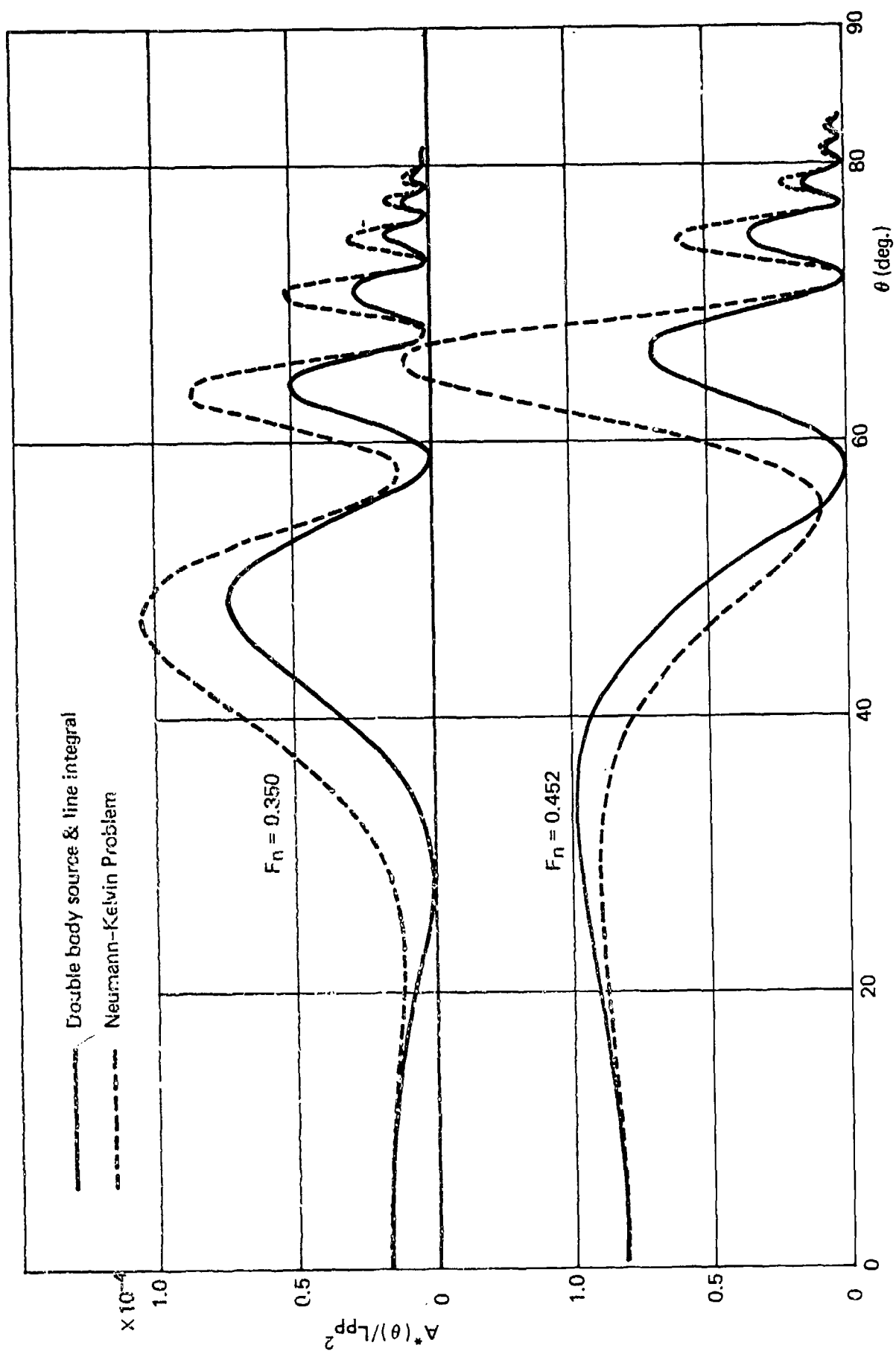


Fig. 3 (Continued)

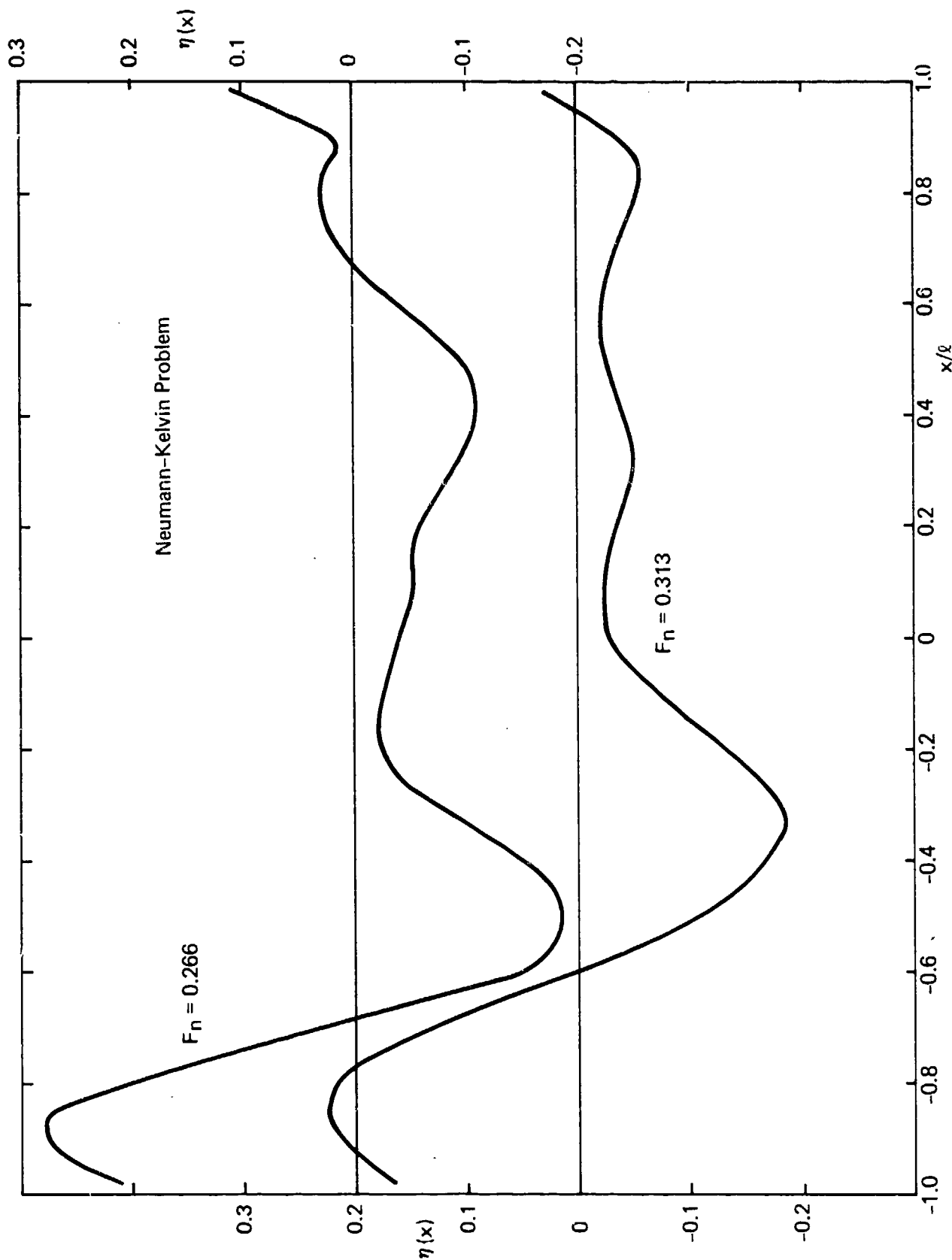


Fig. 4 Wave profiles along Wigley's hull

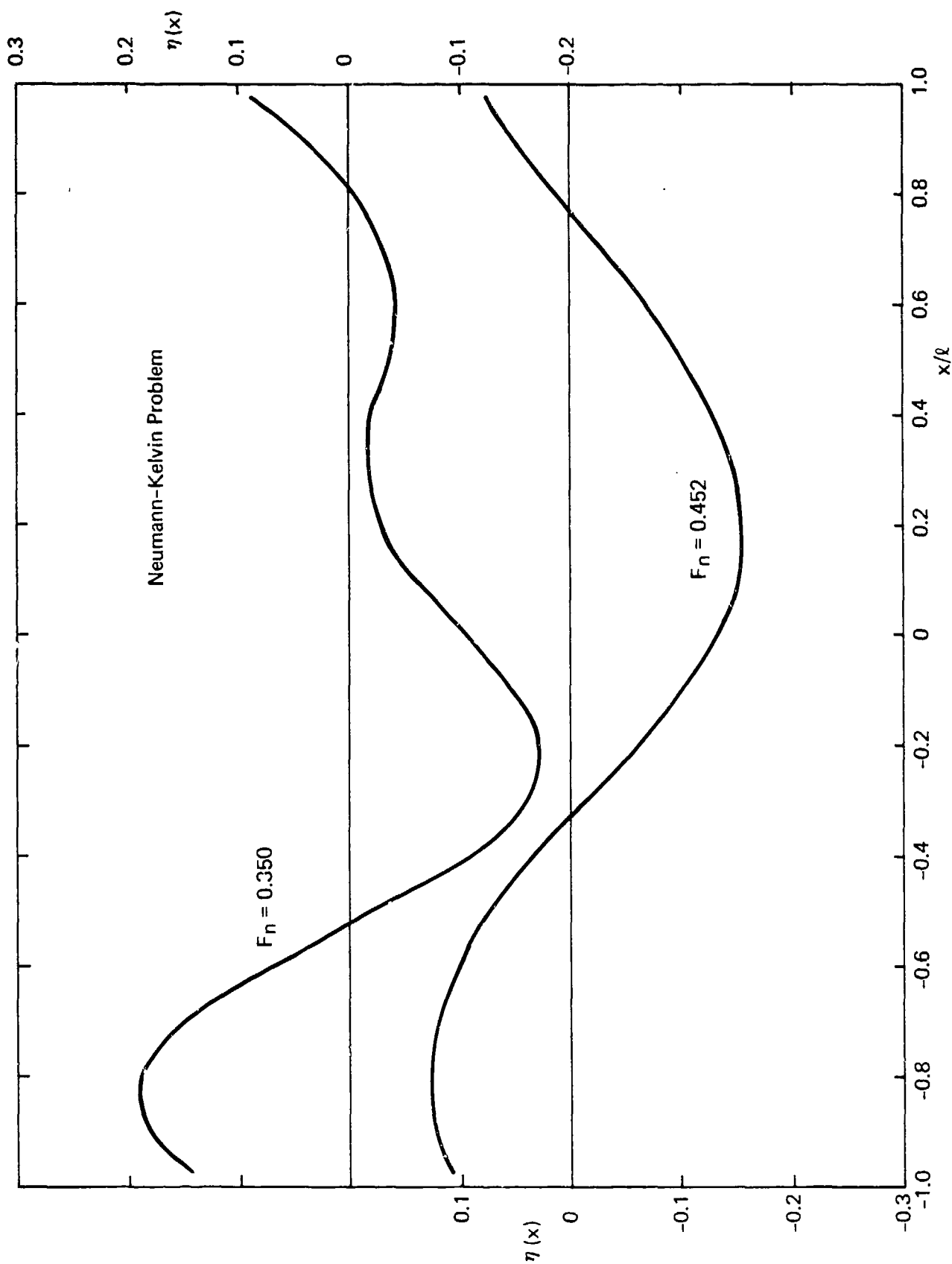


Fig. 4 (Continued)

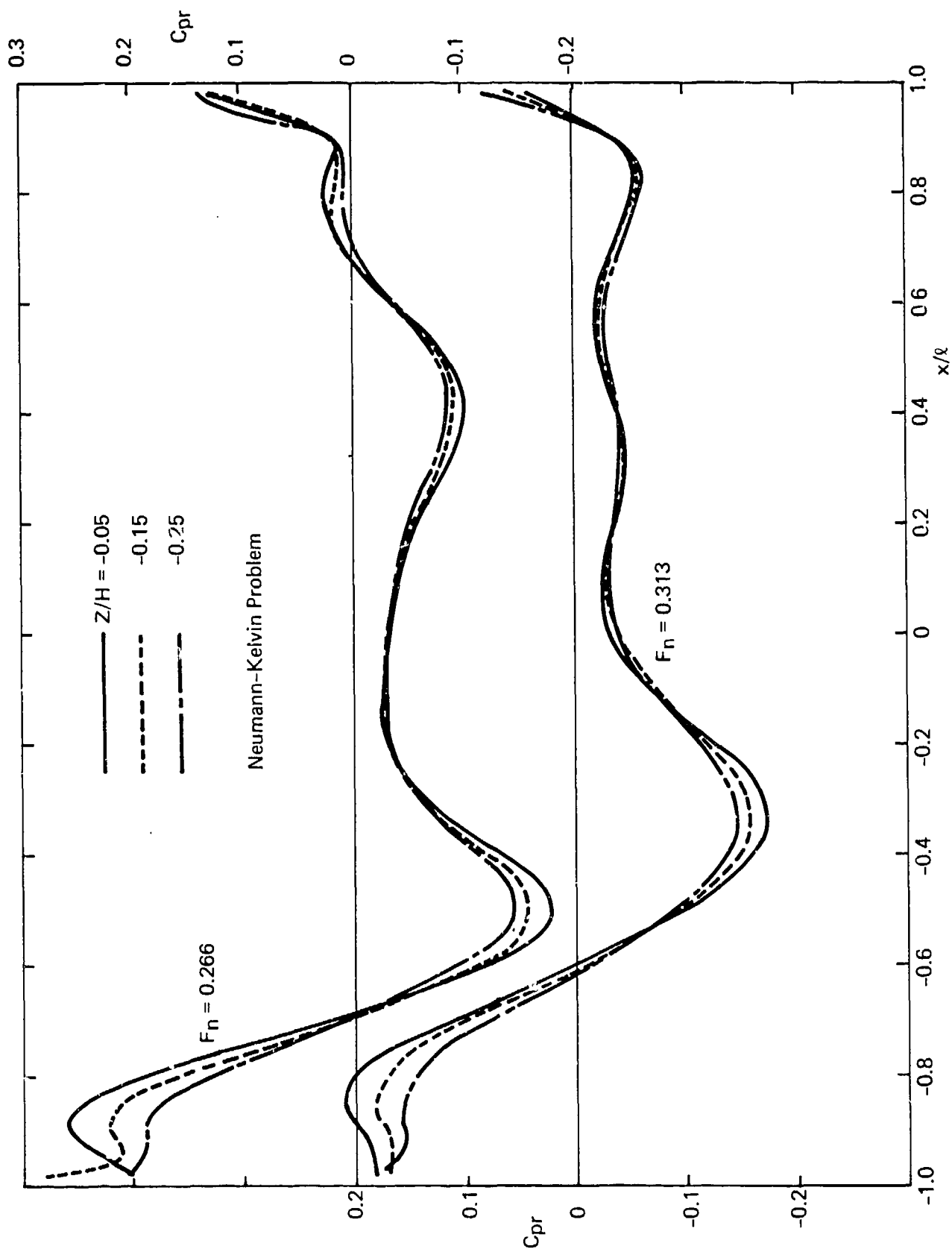


Fig. 5 Dynamic pressure coefficients on Wigley's hull surface

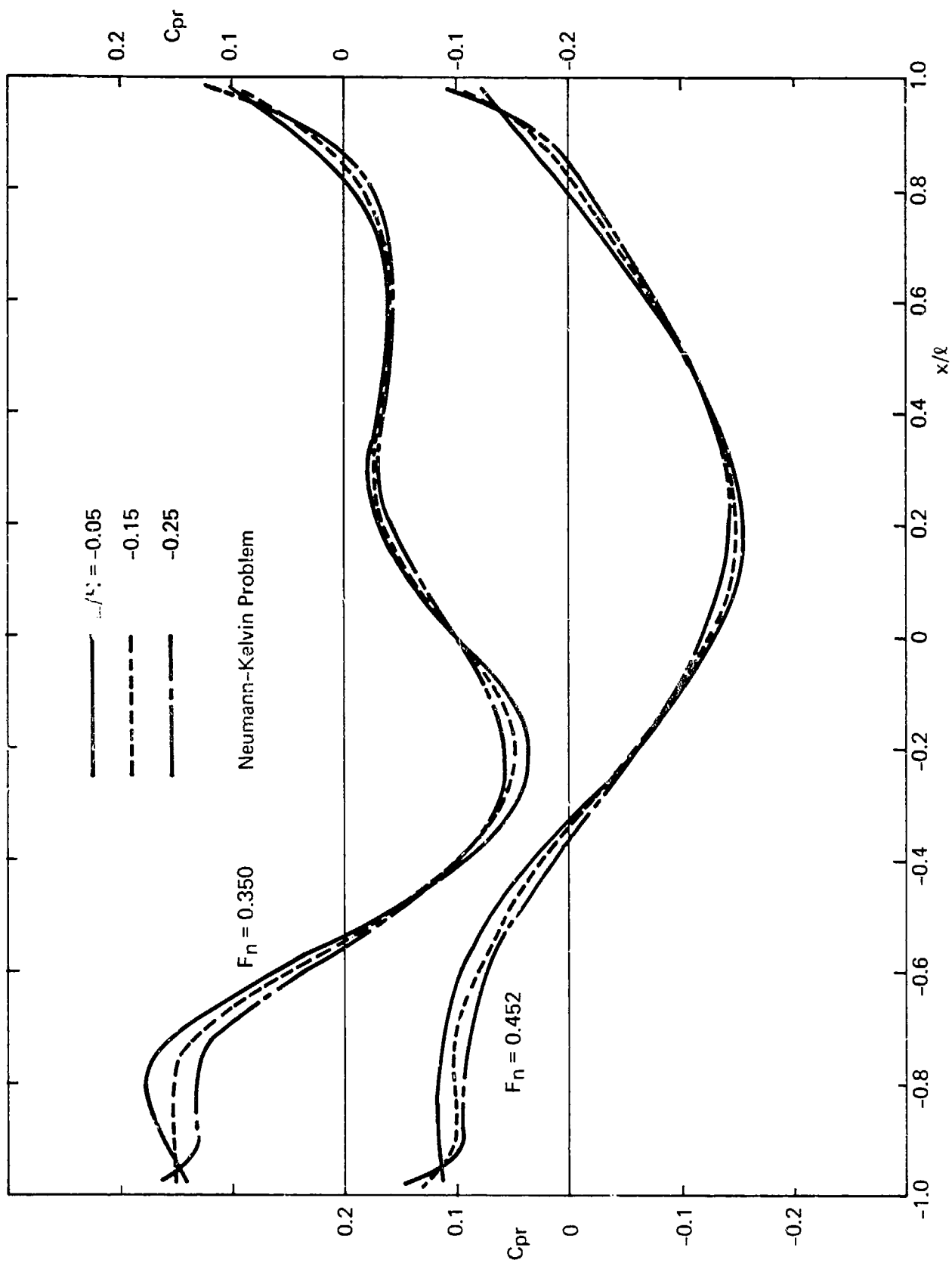
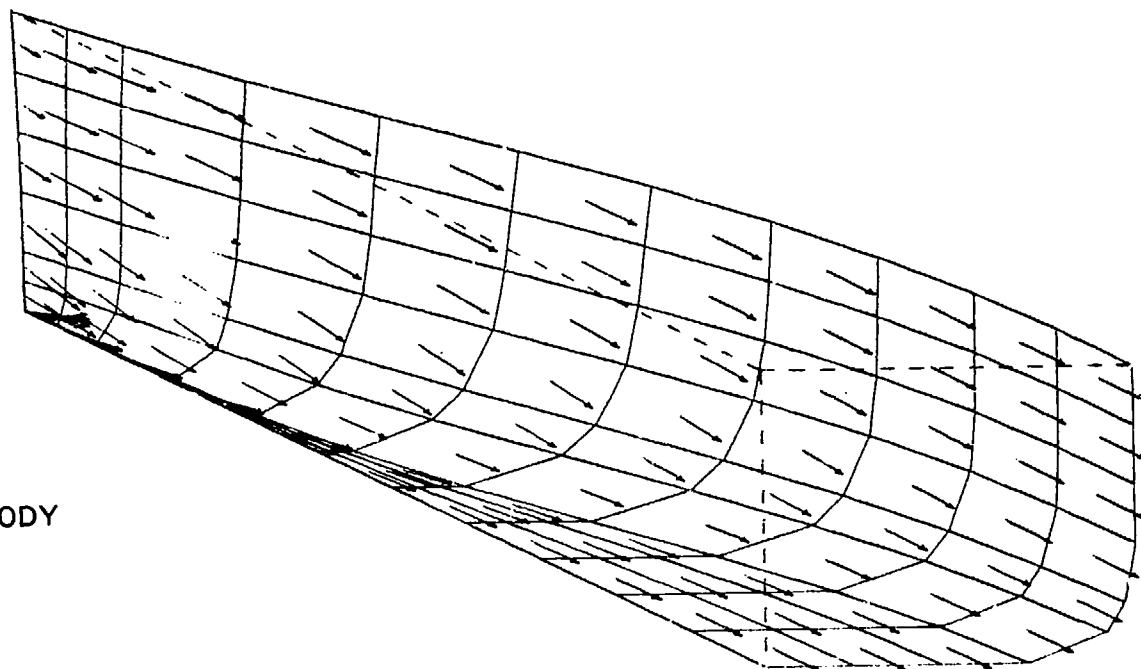


Fig. 5 (Continued)

FORE BODY



AFT BODY

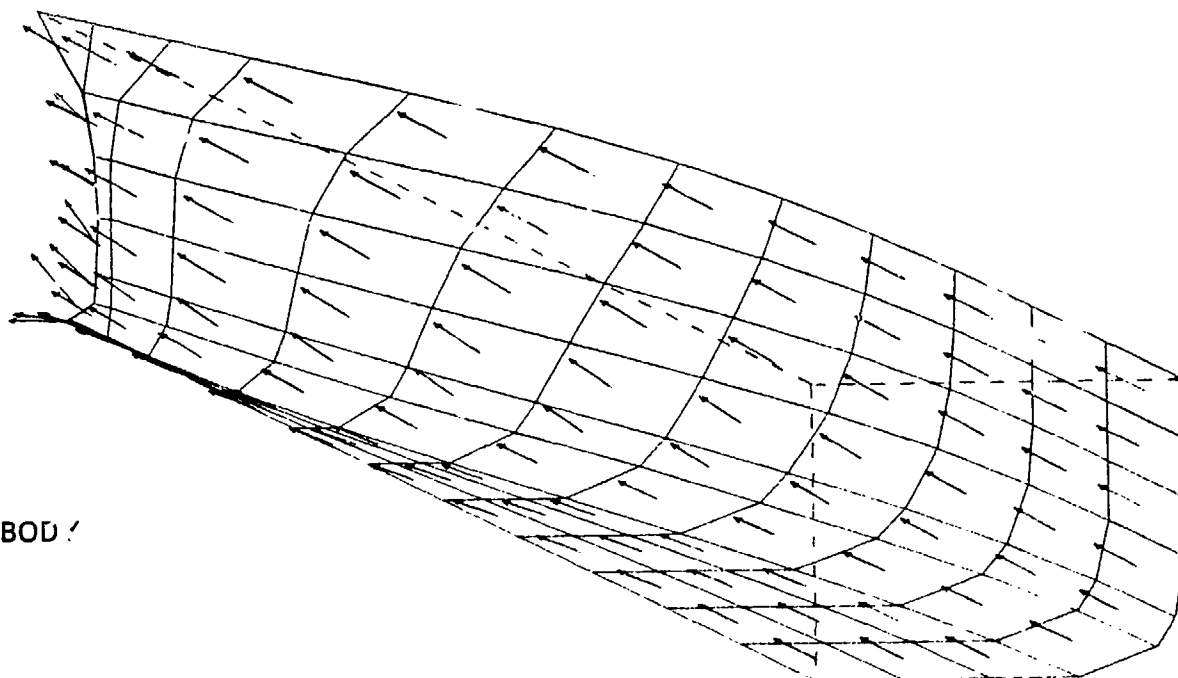


Fig. 6 Shapes of the elements on the hull surface of Series 60, $C_B = 0.60$

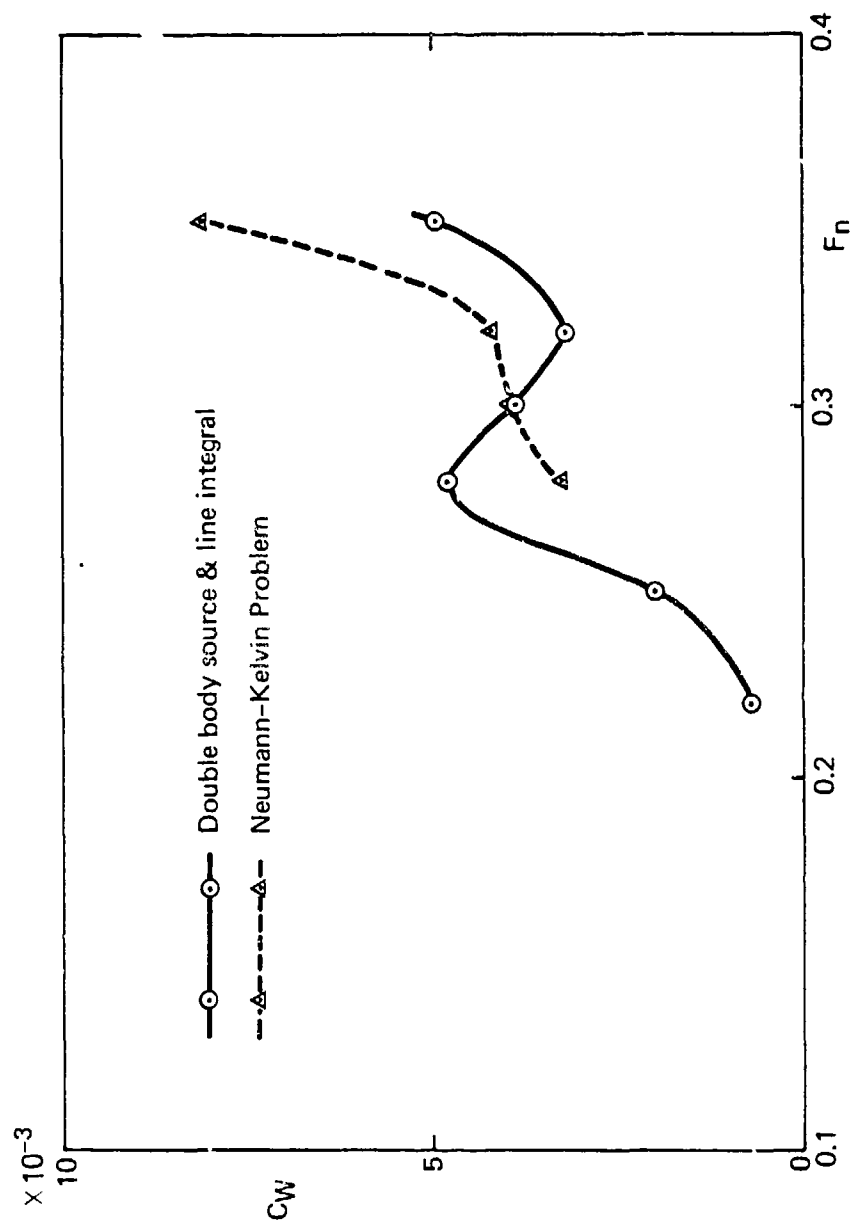


Fig. 7 Comparison of wave resistance of Series 60, $C_B = 0.60$

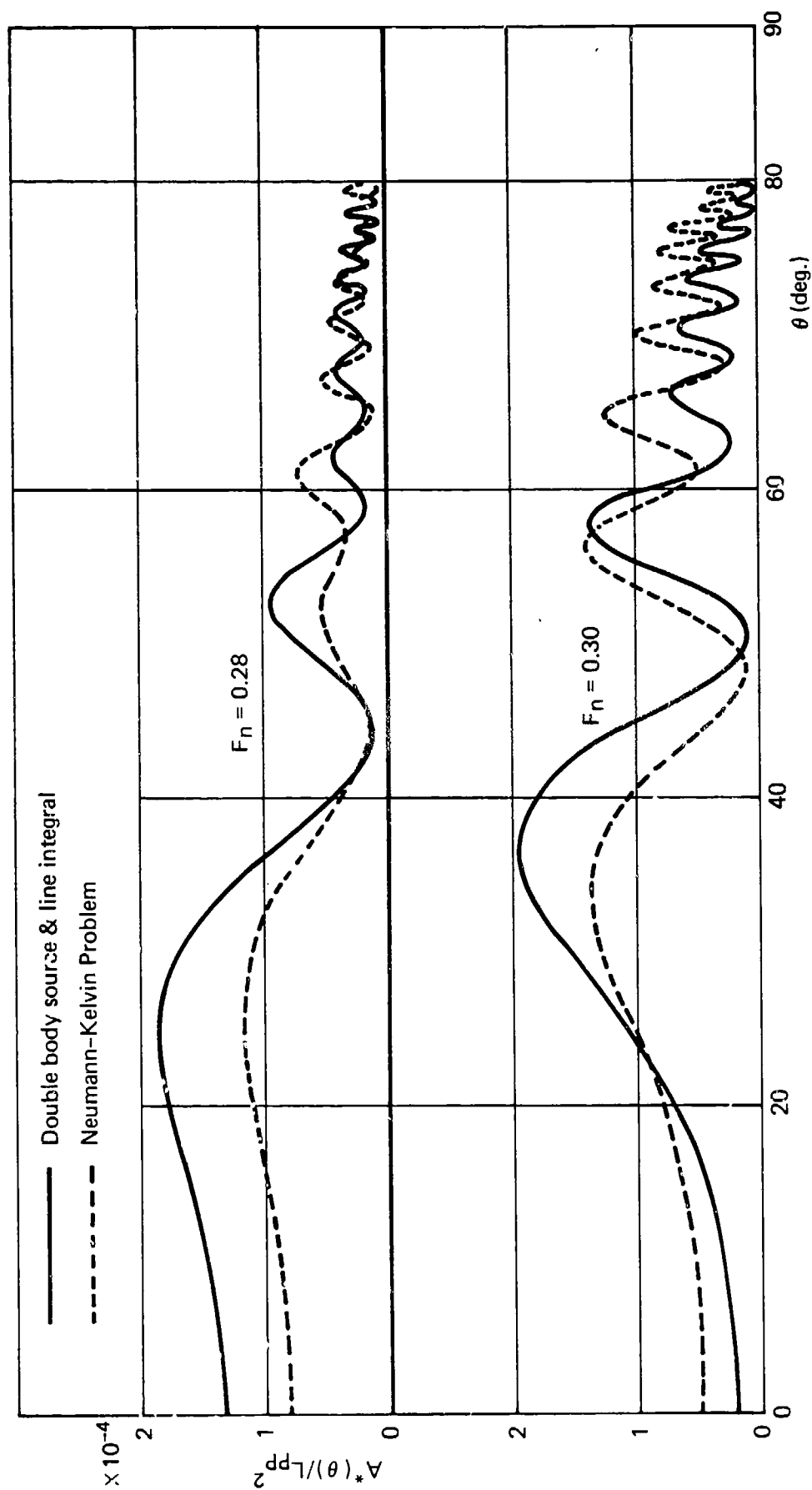


Fig. 8 Comparison of wave spectra of Series 60, $C_B = 0.60$

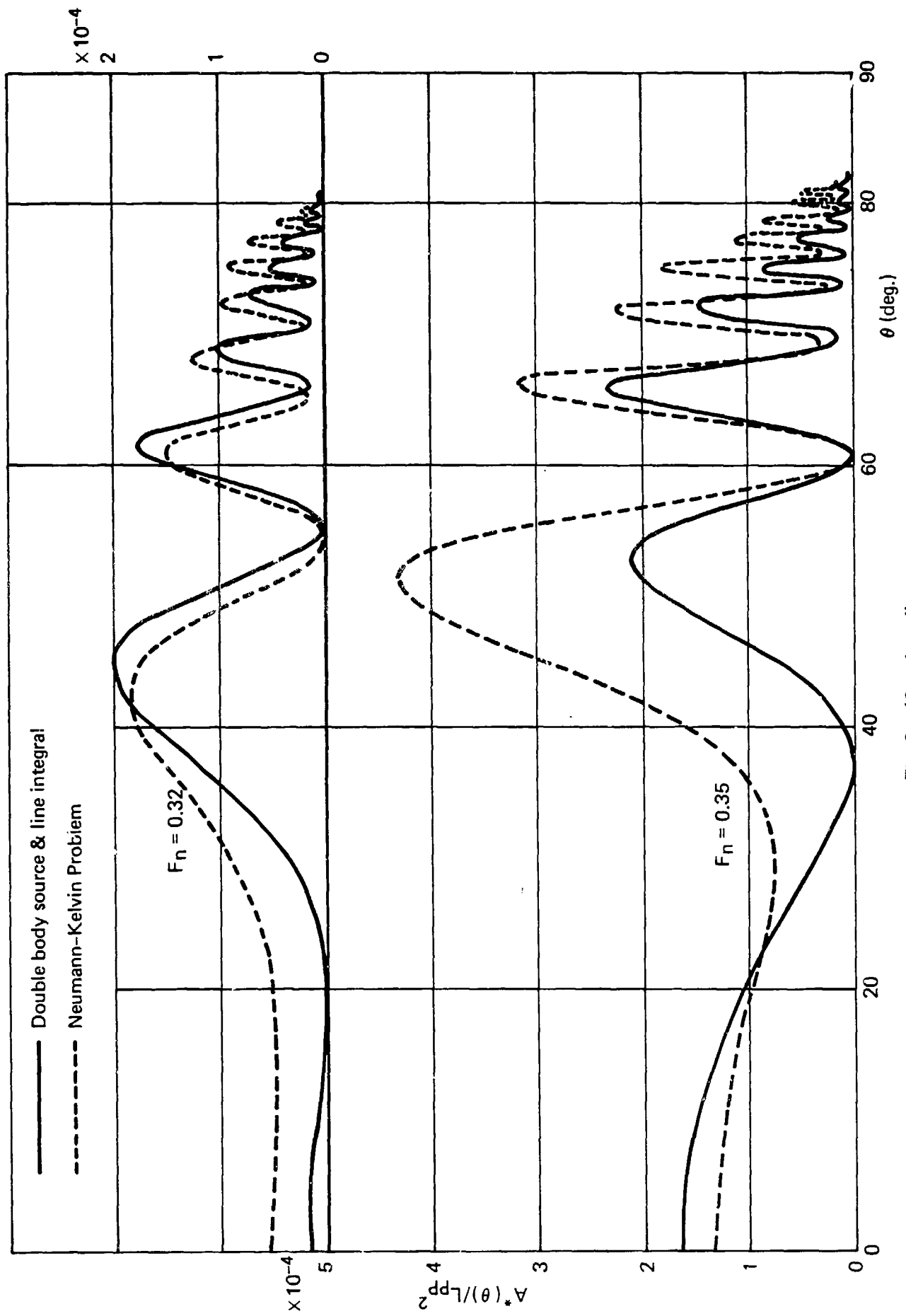


Fig. 8 (Continued)

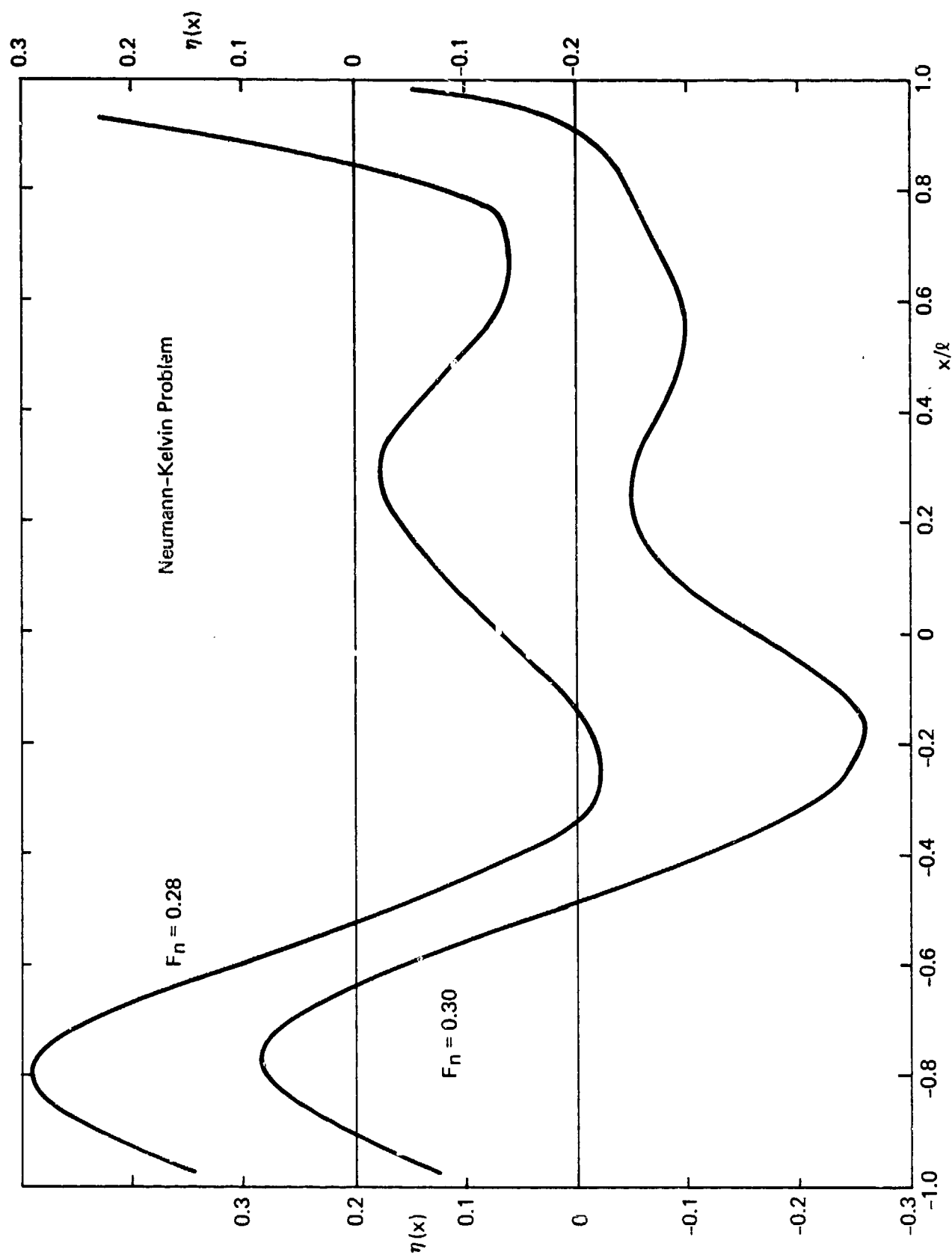


Fig. 9 Wave profiles along the hull of Series 60, $C_B = 0.60$

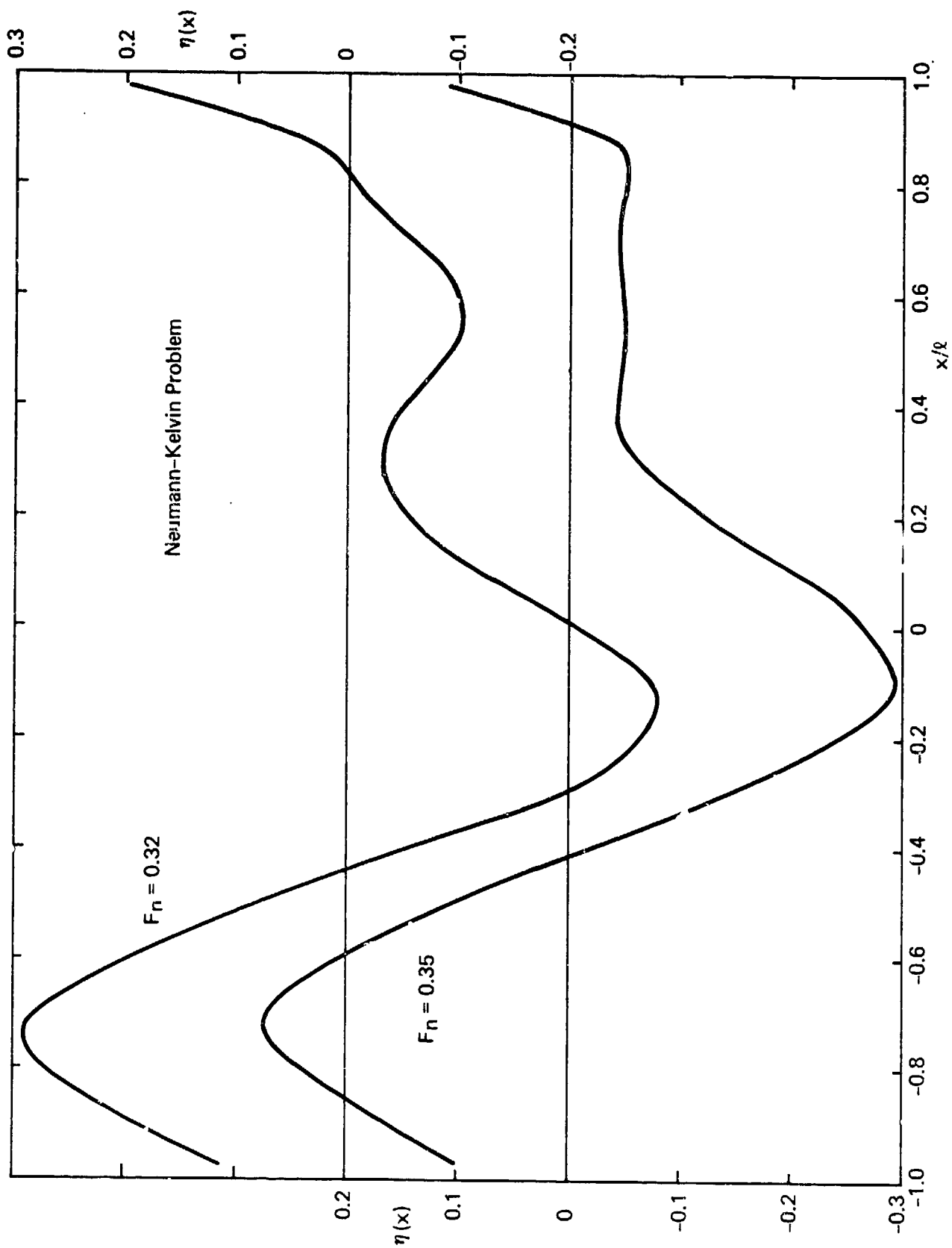


Fig. 9 (Continued)

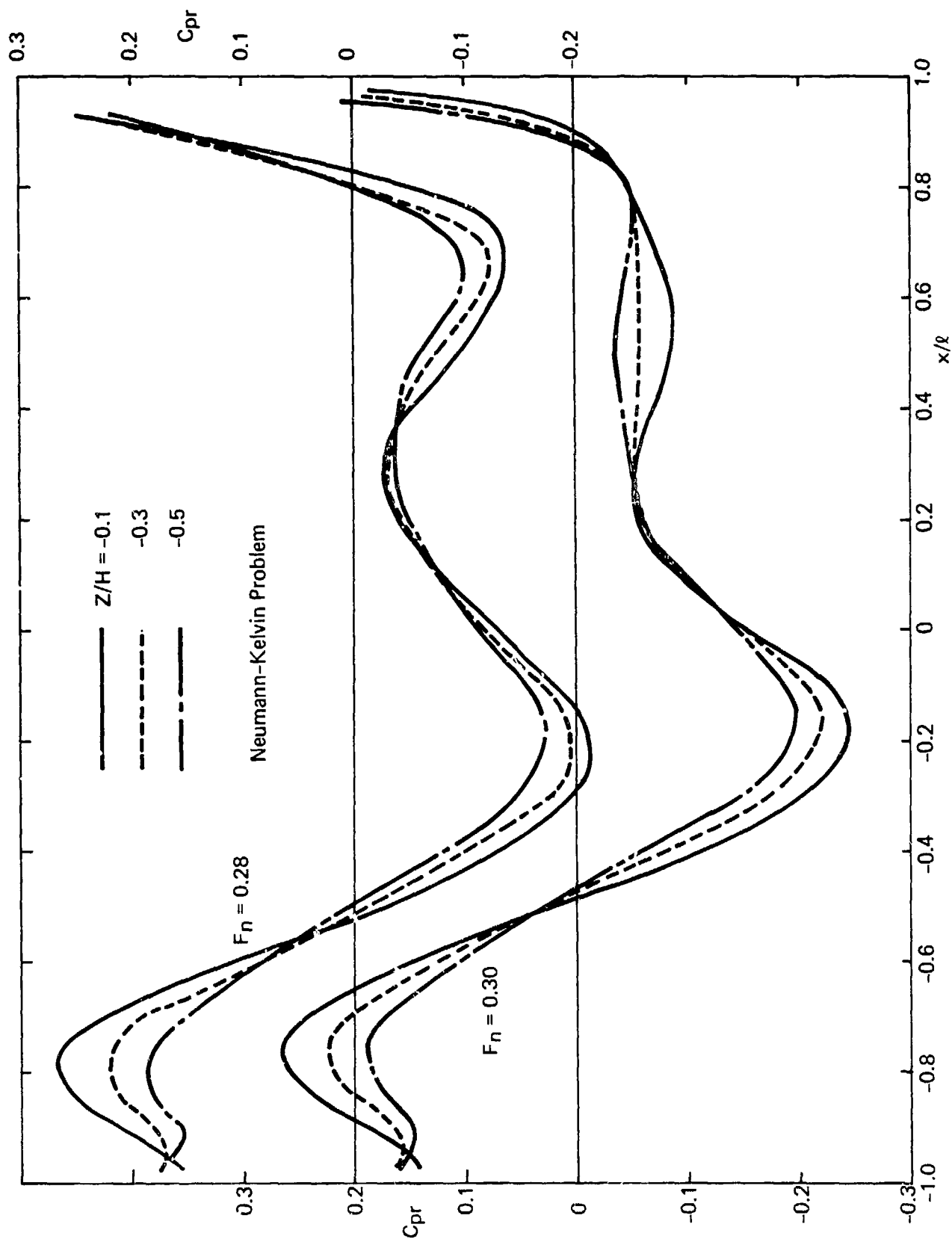


Fig. 10 Dynamic pressure coefficients on the hull surface of Series 60, $CB = 0.60$

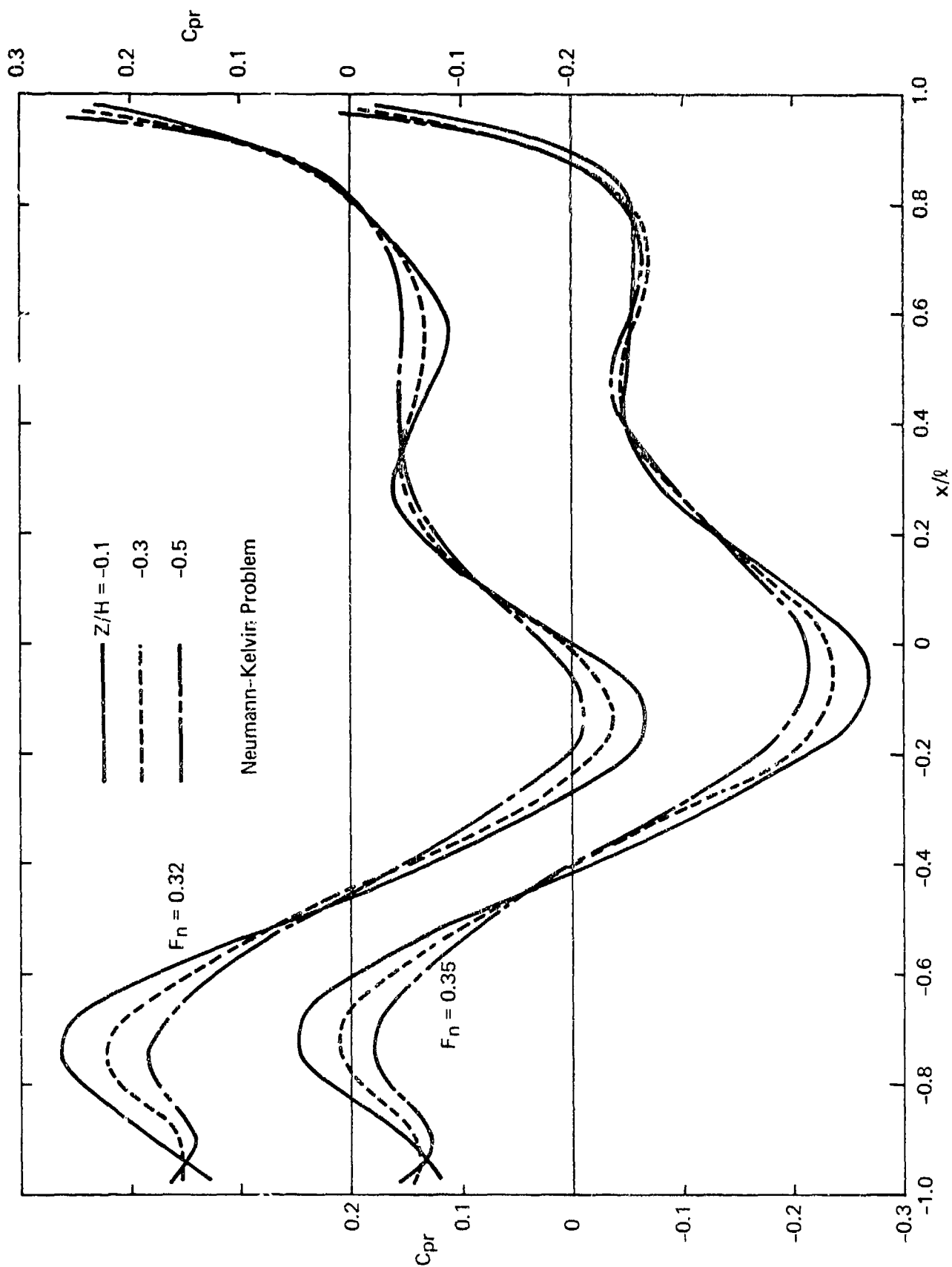


Fig. 10 (Continued)

Table 1 Calculated wave resistance

T. Tsutsumi/Neumann-Kelvin Problem

Wigley		Series 60				
F _n	C _w	F _n	C _w			
0.266	1.21x10 ⁻³	0.28	3.29x10 ⁻³			
0.313	2.20	0.30	3.95			
0.350	2.10	0.32	4.18			
0.402	3.25	0.35	8.11			
0.452	4.12					

Table 2 Calculated wave resistance

T. Tsutsumi/Double body source & line integral					
Wigley		Series 60			
F _n	C _w	F _n	C _w		
0.266	0.95	0.22	0.69		
0.313	1.69	0.25	1.92		
0.350	1.18	0.28	4.76		
0.402	2.74	0.30	3.89		
0.452	3.71	0.32	3.17		
		0.35	4.91		

Table 3 Calculated wave spectra

T. Tsutsumi/Neumann-Kelvin Problem

Wigley/F _n = 0.266				Wigley/F _n = 0.313			
θ (deg.)	$A^*(\theta)/L_{pp}^2$	θ (deg.)	$A^*(\theta)/L_{pp}^2$	θ (deg.)	$A^*(\theta)/L_{pp}^2$	θ (deg.)	$A^*(\theta)/L_{pp}^2$
0	0.160x10 ⁻⁴	40	0.482x10 ⁻⁴	0	0.218x10 ⁻⁴	40	0.283x10 ⁻⁴
2	0.158	42	0.400	2	0.219	42	0.163
4	0.154	44	0.252	4	0.224	44	0.058
6	0.146	46	0.088	6	0.232	46	0.014
8	0.136	48	0.007	8	0.243	48	0.087
10	0.123	50	0.115	10	0.258	50	0.320
12	0.109	52	0.413	12	0.277	52	0.703
14	0.094	54	0.693	14	0.299	54	1.118
16	0.079	56	0.622	16	0.325	56	1.323
18	0.067	58	0.192	18	0.355	58	1.074
20	0.059	60	0.035	20	0.388	60	0.432
22	0.059	62	0.458	22	0.424	62	0.002
24	0.071	64	0.372	24	0.459	64	0.362
26	0.097	66	0.023	26	0.493	66	0.753
28	0.140	68	0.354	28	0.521	68	0.156
30	0.202	70	0.031	30	0.538	70	0.237
32	0.280	72	0.070	32	0.539	72	0.175
34	0.365	74	0.092	34	0.518	74	0.246
36	0.443	76	0.015	36	0.469	76	0.092
38	0.490	78	0.047	38	0.390	78	0.088
		80	0.015			80	0.005
		82	0.020			82	0.005
		84	0.000			84	0.001

Table 3 (Continued)

T. Tsutsumi/Neumann-Kelvin Problem

Wigley/F _n = 0.350				Wigley/F _n = 0.452			
θ(deg.)	A* (θ)/L _{pp} ²	θ(deg.)	A* (θ)/L _{pp} ²	θ(deg.)	A* (θ)/L _{pp} ²	θ(deg.)	A* (θ)/L _{pp} ²
0	0.176x10 ⁻⁴	40	0.677x10 ⁻⁴	0	0.813x10 ⁻⁴	40	0.774x10 ⁻⁴
2	0.175	42	0.815	2	0.814	42	0.707
4	0.172	44	0.940	4	0.816	44	0.623
6	0.168	46	1.027	6	0.820	46	0.521
8	0.161	48	1.043	8	0.825	48	0.405
10	0.154	50	0.958	10	0.831	50	0.283
12	0.145	52	0.760	12	0.838	52	0.173
14	0.137	54	0.478	14	0.847	54	0.103
16	0.128	56	0.211	16	0.856	56	0.112
18	0.121	58	0.116	18	0.865	58	0.244
20	0.116	60	0.314	20	0.875	60	0.535
22	0.116	62	0.703	22	0.884	62	0.967
24	0.121	64	0.847	24	0.892	64	1.410
26	0.135	66	0.405	26	0.899	66	1.588
28	0.160	68	0.022	28	0.902	68	1.200
30	0.199	70	0.451	30	0.902	70	0.373
32	0.255	72	0.243	32	0.896	72	0.025
34	0.331	74	0.176	34	0.882	74	0.570
36	0.428	76	0.015	36	0.859	76	0.240
38	0.545	78	0.037	38	0.823	78	0.174
		80	0.000			80	0.000
		82	0.065			82	0.013
		84	0.000			84	0.015

Table 4 Calculated wave spectra

T. Tsutsumi/Double body source & line integral					Wigley/F _n = 0.313				
Wigley/F _n = 0.266					Wigley/F _n = 0.266				
θ (deg.)	$A^*(\theta)/L_{pp}^2$	θ (deg.)	$A^*(\theta)/L_{pp}^2$	θ (deg.)	$A^*(\theta)/L_{pp}^2$	θ (deg.)	$A^*(\theta)/L_{pp}^2$	θ (deg.)	$A^*(\theta)/L_{pp}^2$
0	0.269x10 ⁻⁴	40	0.502x10 ⁻⁴	0	0.151x10 ⁻⁴	40	0.556x10 ⁻⁴		
2	0.266	42	0.506	2	0.153	42	0.430		
4	0.259	44	0.423	4	0.158	44	0.282		
6	0.246	46	0.263	6	0.167	46	0.133		
8	0.229	48	0.088	8	0.180	48	0.025		
10	0.207	50	0.000	10	0.197	50	0.007		
12	0.180	52	0.079	12	0.218	52	0.109		
14	0.150	54	0.269	14	0.245	54	0.305		
16	0.117	56	0.354	16	0.277	56	0.481		
18	0.082	58	0.182	18	0.315	58	0.474		
20	0.050	60	0.001	20	0.358	50	0.237		
22	0.023	62	0.145	22	0.406	62	0.009		
24	0.004	64	0.191	24	0.459	64	0.122		
26	0.001	66	0.000	26	0.514	66	0.314		
28	0.017	68	0.148	28	0.568	68	0.073		
30	0.059	70	0.004	30	0.617	70	0.098		
32	0.127	72	0.042	32	0.656	72	0.085		
34	0.221	74	0.054	34	0.677	74	0.111		
36	0.329	76	0.017	36	0.671	76	0.036		
38	0.432	78	0.026	38	0.630	78	0.042		
		80	0.017			80	0.002		
		82	0.008			82	0.004		
		84	0.000			84	0.000		

Table 4 (Continued)

Wigley/Fn = 0.350				Wigley/Fn = 0.452			
θ (deg.)	$A^*(\theta)/L_{pp}^2$	θ (deg.)	$A(\theta)/L_{pp}^2$	θ (deg.)	$A^*(\theta)/L_{pp}^2$	θ (deg.)	$A^*(\theta)/L_{pp}^2$
0	0.173×10^{-4}	40	0.312×10^{-4}	0	0.819×10^{-4}	40	0.906×10^{-4}
2	0.171	42	0.428	2	0.820	42	0.856
4	0.167	44	0.547	4	0.823	44	0.785
6	0.159	46	0.651	6	0.827	46	0.692
8	0.149	48	0.711	8	0.833	48	0.576
10	0.136	50	0.698	10	0.841	50	0.440
12	0.121	52	0.590	12	0.850	52	0.292
14	0.104	54	0.392	14	0.861	53	0.150
16	0.085	56	0.161	16	0.874	56	0.040
18	0.065	58	0.010	18	0.887	58	0.000
20	0.046	60	0.060	20	0.901	60	0.068
22	0.028	62	0.303	22	0.916	62	0.258
24	0.013	64	0.482	24	0.930	64	0.518
26	0.003	66	0.293	26	0.944	66	0.696
28	0.000	68	0.005	28	0.956	68	0.589
30	0.009	70	0.196	30	0.965	70	0.200
32	0.031	72	0.159	32	0.970	72	0.009
34	0.070	74	0.072	34	0.969	74	0.313
36	0.130	76	0.017	36	0.960	76	0.141
38	0.211	78	0.035	38	0.940	78	0.112
		80	0.000			80	0.002
		82	0.015			82	0.000
		84	0.001			84	0.008

Table 5 Calculated wave elevations along Wigley's hull

T. Tsutsumi/Neumann-Kelvin Problem

Wigley/ $F_n=0.266$		Wigley/ $F_n=0.313$		Wigley/ $F_n=0.350$		Wigley/ $F_n=0.452$	
x/λ	$\eta(x)$	x/λ	$\eta(x)$	x/λ	$\eta(x)$	x/λ	$\eta(x)$
-0.975	0.202	-0.075	0.162	-0.975	0.138	-0.975	0.104
-0.925	0.256	-0.925	0.194	-0.925	0.166	-0.925	0.118
-0.875	0.274	-0.875	0.216	-0.875	0.180	-0.875	0.123
-0.825	0.244	-0.825	0.220	-0.825	0.190	-0.875	0.126
-0.75	0.122	-0.75	0.182	-0.75	0.178	-0.75	0.124
-0.65	-0.062	-0.65	0.062	-0.65	0.114	-0.65	0.112
-0.55	-0.176	-0.55	-0.054	-0.55	0.018	-0.55	0.090
-0.45	-0.174	-0.45	-0.144	-0.45	-0.068	-0.45	0.057
-0.35	-0.106	-0.35	-0.180	-0.35	-0.140	-0.35	0.011
-0.25	-0.040	-0.25	-0.158	-0.25	-0.166	-0.25	-0.035
-0.15	-0.022	-0.15	-0.100	-0.15	-0.162	-0.15	-0.079
-0.05	-0.032	-0.05	-0.046	-0.05	-0.128	-0.05	-0.116
0.05	-0.050	0.05	-0.024	0.05	-0.084	0.05	-0.143
0.15	-0.054	0.15	-0.030	0.15	-0.040	0.15	-0.155
0.25	-0.074	0.25	-0.046	0.25	-0.022	0.25	-0.152
0.35	-0.102	0.35	-0.048	0.35	-0.018	0.35	-0.139
0.45	-0.106	0.45	-0.034	0.45	-0.028	0.45	-0.115
0.55	-0.064	0.55	-0.020	0.55	-0.040	0.55	-0.086
0.65	-0.008	0.65	-0.028	0.65	-0.038	0.65	-0.050
0.75	0.022	0.75	-0.046	0.75	-0.022	0.75	-0.010
0.825	0.026	0.825	-0.056	0.825	0.008	0.825	0.022
0.875	0.014	0.875	-0.048	0.875	0.032	0.875	0.038
0.925	0.056	0.925	-0.014	0.925	0.060	0.925	0.062
0.975	0.106	0.975	0.032	0.975	0.088	0.975	0.072

Table 6 Calculated dynamic pressure coefficients on Wigley's hull surface

T. Tsutsumi/Neumann-Kelvin Problem/Wigley, $Z/H = -0.05$

$F_n=0.266$		$F_n=0.313$		$F_n=0.350$		$F_n=0.452$	
x/ℓ	C_{pr}	x/ℓ	C_{pr}	x/ℓ	C_{pr}	x/ℓ	C_{pr}
-0.975	0.202	-0.975	0.184	-0.975	0.142	-0.975	0.112
-0.925	0.242	-0.925	0.186	-0.925	0.158	-0.925	0.114
-0.875	0.258	-0.875	0.204	-0.875	0.170	-0.875	0.118
-0.825	0.228	-0.825	0.206	-0.825	0.178	-0.825	0.120
-0.75	0.112	-0.75	0.170	-0.75	0.168	-0.75	0.118
-0.65	-0.058	-0.65	0.056	-0.65	0.106	-0.65	0.106
-0.55	-0.166	-0.55	-0.054	-0.55	0.016	-0.55	0.086
-0.45	-0.166	-0.45	-0.138	-0.45	-0.068	-0.45	0.052
-0.35	-0.102	-0.35	-0.172	-0.35	-0.132	-0.35	0.008
-0.25	-0.042	-0.25	-0.152	-0.25	-0.160	-0.25	-0.036
-0.15	-0.024	-0.15	-0.100	-0.15	-0.158	-0.15	-0.078
-0.05	-0.032	-0.05	-0.048	-0.05	-0.126	-0.05	-0.114
0.05	-0.040	0.05	-0.026	0.05	-0.084	0.05	-0.140
0.15	-0.050	0.15	-0.030	0.15	-0.042	0.15	-0.152
0.25	-0.070	0.25	-0.044	0.25	-0.022	0.25	-0.150
0.35	-0.096	0.35	-0.046	0.35	-0.020	0.35	-0.138
0.45	-0.100	0.45	-0.034	0.45	-0.030	0.45	-0.116
0.55	-0.062	0.55	-0.022	0.55	-0.040	0.55	-0.086
0.65	-0.010	0.64	-0.028	0.65	-0.038	0.65	-0.052
0.75	0.020	0.75	-0.046	0.75	-0.024	0.75	-0.014
0.825	0.022	0.825	-0.058	0.825	0.004	0.825	0.016
0.875	0.012	0.875	-0.048	0.875	0.028	0.875	0.034
0.925	0.052	0.925	-0.016	0.925	0.056	0.925	0.056
0.975	0.112	0.975	0.042	0.975	0.092	0.975	0.078

Table 6 (Continued)

T. Tsutsumi/Neumann-Kelvin Problem/Wigley, $Z/H = -0.15$

$F_n=0.266$		$F_n=0.313$		$F_n=0.350$		$F_n=0.452$	
x/λ	C_{pr}	x/λ	C_{pr}	x/λ	C_{pr}	x/λ	C_{pr}
-0.975	0.202	-0.975	0.170	-0.975	0.152	-0.975	0.126
-0.925	0.212	-0.925	0.168	-0.925	0.144	-0.925	0.106
-0.875	0.222	-0.875	0.180	-0.875	0.152	-0.875	0.106
-0.825	0.192	-0.825	0.176	-0.825	0.154	-0.825	0.106
-0.75	0.094	-0.75	0.146	-0.75	0.148	-0.75	0.106
-0.65	-0.052	-0.65	0.044	-0.65	0.090	-0.65	0.094
-0.55	-0.146	-0.55	-0.054	-0.55	0.010	-0.55	0.076
-0.45	-0.150	-0.45	-0.126	-0.45	-0.066	-0.45	0.042
-0.35	-0.096	-0.35	-0.156	-0.35	-0.122	-0.35	0.002
-0.25	-0.044	-0.25	-0.140	-0.25	-0.148	-0.25	-0.038
-0.15	-0.026	-0.15	-0.098	-0.15	-0.148	-0.15	-0.078
-0.05	-0.030	-0.05	-0.052	-0.05	-0.120	-0.05	-0.110
0.05	-0.036	0.05	-0.030	0.05	-0.084	0.05	-0.134
0.15	-0.046	0.15	-0.030	0.15	-0.048	0.15	-0.146
0.25	-0.066	0.25	-0.040	0.25	-0.026	0.25	-0.146
0.35	-0.088	0.35	-0.044	0.35	-0.024	0.35	-0.136
0.45	-0.092	0.45	-0.034	0.45	-0.032	0.45	-0.116
0.55	-0.060	0.55	-0.026	0.55	-0.040	0.55	-0.088
0.65	-0.014	0.65	-0.030	0.65	-0.040	0.64	-0.058
0.75	0.014	0.75	-0.046	0.75	-0.028	0.75	-0.022
0.825	0.014	0.825	-0.062	0.825	-0.006	0.825	0.004
0.875	0.008	0.875	-0.048	0.875	0.018	0.875	0.024
0.925	0.046	0.925	-0.018	0.925	0.048	0.925	0.046
0.975	0.124	0.975	0.058	0.975	0.104	0.975	0.092

Table 6 (Continued)

T. Tsutsumi/Neumann-Kelvin Problem/Wigley, $z/H = -0.25$

$F_n=0.266$		$F_n=0.313$		$F_n=0.350$		$F_n=0.452$	
x/l	Cpr	x/l	Cpr	x/l	Cpr	x/l	Cpr
-0.975	0.206	-0.975	0.182	-0.975	0.166	-0.975	0.142
-0.925	0.186	-0.925	0.152	-0.925	0.132	-0.925	0.100
-0.875	0.188	-0.875	0.156	-0.875	0.134	-0.875	0.096
-0.825	0.158	-0.825	0.150	-0.825	0.132	-0.825	0.092
-0.75	0.078	-0.75	0.124	-0.75	0.128	-0.75	0.092
-0.65	-0.050	-0.65	0.032	-0.65	0.074	-0.65	0.082
-0.55	-0.132	-0.55	-0.054	-0.55	0	-0.55	0.062
-0.45	-0.136	-0.45	-0.116	-0.45	-0.068	-0.45	0.032
-0.35	-0.090	-0.35	-0.144	-0.35	-0.116	-0.35	-0.004
-0.25	-0.044	-0.25	-0.130	-0.25	-0.138	-0.25	-0.042
-0.15	-0.028	-0.15	-0.094	-0.15	-0.136	-0.15	-0.076
-0.05	-0.032	-0.05	-0.054	-0.05	-0.114	-0.05	-0.106
0.05	-0.034	0.05	-0.034	0.05	-0.082	0.05	-0.128
0.15	-0.042	0.15	-0.032	0.15	-0.052	0.15	-0.140
0.25	-0.060	0.25	-0.040	0.25	-0.032	0.25	-0.142
0.35	-0.082	0.35	-0.042	0.35	-0.028	0.35	-0.134
0.45	-0.086	0.45	-0.036	0.45	-0.036	0.45	-0.118
0.55	-0.060	0.55	-0.030	0.55	-0.042	0.55	-0.094
0.65	-0.020	0.65	-0.036	0.65	-0.042	0.65	-0.064
0.75	0.006	0.75	-0.050	0.75	-0.032	0.75	-0.032
0.825	0.006	0.825	-0.064	0.825	-0.016	0.825	-0.010
0.875	0.006	0.875	-0.050	0.875	-0.010	0.875	0.012
0.925	0.044	0.925	-0.018	0.925	0.042	0.925	0.040
0.975	0.138	0.975	0.078	0.975	0.120	0.975	0.108

Table 7 Calculated wave spectra

T. Tsutsumi/Neumann-Kelvin Problem

Series $60/F_n = 0.28$				Series $60/F_n = 0.30$			
θ (deg.)	$A^*(\theta)/L_{pp}^2$	θ (deg.)	$A^*(\theta)/L_{pp}^2$	θ (deg.)	$A^*(\theta)/L_{pp}^2$	θ (deg.)	$A^*(\theta)/L_{pp}^2$
0	0.807×10^{-4}	40	0.383×10^{-4}	0	0.474×10^{-4}	40	1.063×10^{-4}
2	0.811	42	0.237	2	0.477	42	0.818
4	0.821	44	0.162	4	0.484	44	0.533
6	0.838	46	0.184	6	0.496	46	0.273
8	0.861	48	0.297	8	0.514	48	0.135
10	0.891	50	0.443	10	0.539	50	0.220
12	0.926	52	0.521	12	0.571	52	0.564
14	0.966	54	0.462	14	0.612	54	1.049
16	1.009	56	0.339	16	0.663	56	1.371
18	1.053	58	0.380	18	0.725	58	1.208
20	1.096	60	0.644	20	0.797	60	0.675
22	1.132	62	0.643	22	0.880	62	0.540
24	1.158	64	0.161	24	0.972	64	1.118
26	1.166	66	0.300	26	1.069	66	0.971
28	1.150	68	0.383	28	1.166	68	0.287
30	1.104	70	0.273	30	1.254	70	0.971
32	1.021	72	0.229	32	1.321	72	0.334
34	0.900	74	0.299	34	1.351	74	0.476
36	0.742	76	0.169	36	1.328	76	0.486
38	0.562	78	0.307	38	1.234	78	0.291
		80	0.173			80	0.242
		82	0.069			82	0.095
		84	0.020			84	0.036

Table 7 (Continued)

T. Tsutsumi/Neumann-Kelvin Problem

Series 60/F _n = 0.32			Series 60/F _n = 0.35		
θ (deg.)	$A^*(\theta)/L_{pp}^2$	θ (deg.)	$A^*(\theta)/L_{pp}^2$	θ (deg.)	$A^*(\theta)/L_{pp}^2$
0	0.531×10^{-4}	40	1.781×10^{-4}	0	1.345×10^{-4}
2	0.530	42	1.865	2	1.341
4	0.526	44	1.832	4	1.330
6	0.520	46	1.640	6	1.312
8	0.513	48	1.275	8	1.286
10	0.505	50	0.778	10	1.252
12	0.498	52	0.281	12	1.212
14	0.493	54	0.007	14	1.164
16	0.494	56	0.182	16	1.111
18	0.502	58	0.821	18	1.052
20	0.521	60	1.473	20	0.996
22	0.554	62	1.359	22	0.928
24	0.605	64	0.446	24	0.868
26	0.678	66	0.324	26	0.816
28	0.778	68	1.278	28	0.780
30	0.906	70	0.404	30	0.768
32	1.061	72	0.953	32	0.794
34	1.241	74	0.216	34	0.871
36	1.435	76	0.251	36	1.016
38	1.625	78	0.228	38	1.248
		80	0.307		
		82	0.097		
		84	0.008		
				40	1.582×10^{-4}
				42	2.026
				44	2.571
				46	3.180
				48	3.771
				50	4.207
				52	4.298
				54	3.846
				56	2.768
				58	1.294
				60	0.145
				62	0.326
				63	2.024
				66	3.154
				68	1.339
				70	0.541
				72	2.206
				74	0.527
				76	0.477
				78	0.290
				80	0.583
				82	0.131
				84	0.017

Table 8 Calculated wave spectra

T. Tsutsumi/Double body source & line integral					
Series 60/F _n = 0.28			Series 60/F _n = 0.30		
θ (deg.)	A* (θ)/L _{PP} ²	θ (deg.)	A* (θ)/L _{PP} ²	θ (deg.)	A* (θ)/L _{PP} ²
0	1.336x10 ⁻⁴	40	0.458x10 ⁻⁴	0	0.204x10 ⁻⁴
2	1.342	42	0.226	2	0.207
4	1.359	44	0.118	4	0.218
6	1.386	46	0.180	6	0.236
8	1.424	48	0.407	8	0.264
10	1.471	50	0.712	10	0.301
12	1.527	52	0.923	12	0.350
14	1.589	54	0.865	14	0.413
16	1.654	56	0.529	16	0.491
18	1.718	58	0.196	18	0.587
20	1.777	60	0.211	20	0.702
22	1.823	62	0.422	22	0.837
24	1.848	63	0.278	24	0.992
26	1.843	66	0.176	26	1.164
28	1.796	68	0.428	28	1.347
30	1.698	70	0.165	30	1.533
32	1.542	72	0.342	32	1.707
34	1.325	74	0.439	34	1.848
36	1.054	76	0.219	36	1.932
38	0.752	78	0.150	38	1.928
		80	0.019		
		82	0.027		
		84	0.006		
				40	1.812x10 ⁻⁴
				42	1.565
				44	1.196
				46	0.756
				48	0.344
				50	0.106
				52	0.179
				54	0.590
				56	1.129
				58	1.358
				60	0.943
				62	0.262
				63	0.265
				66	0.696
				68	0.223
				70	0.488
				72	0.136
				74	0.442
				76	0.344
				78	0.058
				80	0.134
				82	0.031
				84	0.007

Table 8 (Continued)

Series 60/F _n = 0.32					Series 60/F _n = 0.35				
θ (deg.)	$A^*(\theta)/L_{pp}^2$	θ (deg.)	$A^*(\theta)/L_{pp}^2$	θ (deg.)	$A^*(\theta)/L_{pp}^2$	θ (deg.)	$A^*(\theta)/L_{pp}^2$	θ (deg.)	$A^*(\theta)/L_{pp}^2$
0	0.170x10 ⁻⁴	40	1.616x10 ⁻⁴	0	1.650x10 ⁻⁴	40	0.099x10 ⁻⁴		
2	0.167	42	1.860	2	1.645	42	0.267		
4	0.159	44	2.003	4	1.629	44	0.543		
6	0.145	46	1.981	6	1.601	46	0.921		
8	0.126	48	1.742	8	1.562	48	1.362		
10	0.104	50	1.285	10	1.511	50	1.786		
12	0.080	52	0.698	12	1.448	52	2.064		
14	0.057	54	0.199	14	1.372	54	2.041		
16	0.037	56	0.091	16	1.282	56	1.605		
18	0.023	58	0.577	18	1.180	58	0.832		
20	0.020	60	1.418	20	1.064	60	0.136		
22	0.032	62	1.771	22	0.935	62	0.206		
24	0.067	64	0.973	24	0.796	64	1.335		
26	0.128	66	0.120	26	0.649	66	2.297		
28	0.225	68	0.808	28	0.499	68	1.180		
30	0.361	70	0.580	30	0.351	70	0.137		
32	0.543	72	0.476	32	0.217	72	1.457		
34	0.769	74	0.102	34	0.107	74	0.081		
36	1.036	76	0.172	36	0.038	76	0.323		
38	1.327	78	0.037	38	0.029	78	0.091		
		80	0.029		0.019	80	0.127		
		82	0.019		0.008	82	0.008		
		84	0.008			84	0.020		

Table 9 Calculated wave elevations along the hull of Series 60, $C_B = 0.6$

T. Tsutsumi/Neumann-Kelvin Problem

Series 60/ $F_n=0.28$		Series 60/ $F_n=0.30$		Series 60/ $F_n=0.32$		Series 60/ $F_n=0.35$	
x/l	$\eta(x)$	x/l	$\eta(x)$	x/l	$\eta(x)$	x/l	$\eta(x)$
-0.975	0.145	-0.975	0.123	-0.975	0.114	-0.975	0.102
-0.925	0.196	-0.925	0.172	-0.925	0.163	-0.925	0.141
-0.85	0.275	-0.85	0.249	-0.85	0.225	-0.85	0.198
-0.75	0.280	-0.75	0.282	-0.75	0.286	-0.75	0.264
-0.65	0.175	-0.65	0.212	-0.65	0.234	-0.65	0.246
-0.55	0.038	-0.55	0.089	-0.55	0.130	-0.55	0.162
-0.45	-0.098	-0.45	-0.052	-0.45	-0.006	-0.45	0.048
-0.35	-0.192	-0.35	-0.170	-0.35	-0.138	-0.35	-0.073
-0.25	-0.220	-0.25	-0.241	-0.25	-0.236	-0.25	-0.185
-0.15	-0.206	-0.15	-0.255	-0.15	-0.279	-0.15	-0.281
-0.05	-0.157	-0.05	-0.198	-0.05	-0.248	-0.05	-0.281
0.05	-0.107	0.05	-0.121	0.05	-0.166	0.05	-0.238
0.15	-0.063	0.15	-0.066	0.15	-0.082	0.15	-0.163
0.25	-0.026	0.25	-0.046	0.25	-0.036	0.25	-0.090
0.35	-0.032	0.35	-0.061	0.35	-0.039	0.35	-0.045
0.45	-0.078	0.45	-0.089	0.45	-0.072	0.45	-0.046
0.55	-0.122	0.55	-0.096	0.55	-0.103	0.55	-0.050
0.65	-0.139	0.65	-0.086	0.65	-0.070	0.65	-0.045
0.75	-0.132	0.75	-0.057	0.75	-0.026	0.75	-0.046
0.85	0.013	0.85	-0.033	0.85	0.013	0.85	-0.051
0.925	0.226	0.925	0.022	0.925	0.104	0.925	0.030
0.975	0.420	0.975	0.144	0.975	0.204	0.975	0.104

Table 10 Calculated dynamic pressure coefficients on the hull surface of Series 60, $C_B = 0.6$

T. Tsutsumi/Neumann-Kelvin Problem/Series 60, $z/H = -0.1$

$F_n = 0.28$		$F_n = 0.30$		$F_n = 0.32$		$F_n = 0.35$	
x/ℓ	C_{pr}	x'/ℓ	C_{pr}	x/ℓ	C_{pr}	x/ℓ	C_{pr}
-0.975	0.156	-0.975	0.142	-0.975	0.132	-0.975	0.120
-0.925	0.188	-0.925	0.168	-0.925	0.160	-0.925	0.140
-0.85	0.250	-0.85	0.232	-0.85	0.210	-0.85	0.184
-0.75	0.258	-0.75	0.264	-0.75	0.264	-0.75	0.246
-0.65	0.166	-0.65	0.198	-0.65	0.218	-0.65	0.230
-0.55	0.040	-0.55	0.088	-0.55	0.124	-0.55	0.152
-0.45	0.080	-0.45	-0.040	-0.45	-0.002	-0.45	0.048
-0.35	-0.174	-0.35	-0.156	-0.35	-0.126	-0.35	-0.068
-0.25	-0.210	-0.25	-0.228	-0.25	-0.220	-0.25	-0.172
-0.15	-0.200	-0.15	-0.242	-0.15	-0.266	-0.15	-0.248
-0.05	-0.152	-0.05	-0.192	-0.05	-0.238	-0.05	-0.266
0.05	-0.102	0.05	-0.120	0.05	-0.164	0.05	-0.230
0.15	-0.060	0.15	-0.068	0.15	-0.088	0.15	-0.162
0.25	-0.028	0.25	-0.050	0.25	-0.044	0.25	-0.096
0.35	-0.034	0.35	-0.060	0.35	-0.042	0.35	-0.054
0.45	-0.070	0.45	-0.078	0.45	-0.068	0.45	-0.044
0.55	-0.112	0.55	-0.084	0.55	-0.088	0.55	-0.05
0.65	-0.136	0.65	-0.076	0.65	-0.068	0.65	-0.054
0.75	-0.112	0.75	-0.056	0.75	-0.026	0.75	-0.056
0.85	0.036	0.85	0.032	0.85	0.026	0.85	-0.036
0.925	0.236	0.925	0.044	0.925	0.114	0.925	0.050
0.975	0.424	0.975	0.184	0.975	0.232	0.975	0.170

Table 10 (Continued)

T. Tsutsumi/Neumann-Kelvin Problem/Series 60, $z/H = -0.3$

$F_n=0.28$		$F_n=0.30$		$F_n=0.32$		$F_n=0.35$	
x/l	Cpr	x/l	Cpr	x/l	Cpr	x/l	Cpr
-0.975	0.174	-0.975	0.164	-0.975	0.156	-0.975	0.148
-0.925	0.170	-0.925	0.158	-0.925	0.152	-0.925	0.136
-0.85	0.210	-0.85	0.196	-0.85	0.180	-0.85	0.160
-0.75	0.216	-0.75	0.224	-0.75	0.224	-0.75	0.210
-0.65	0.142	-0.65	0.168	-0.65	0.184	-0.65	0.196
-0.55	0.044	-0.55	0.082	-0.55	0.108	-0.55	0.130
-0.45	-0.054	-0.45	-0.022	-0.45	0.006	-0.45	0.046
-0.35	-0.142	-0.35	-0.126	-0.35	-0.104	-0.35	-0.058
-0.25	-0.188	-0.25	-0.198	-0.25	-0.190	-0.25	-0.150
-0.15	-0.186	-0.15	-0.220	-0.15	-0.238	-0.15	-0.220
-0.05	-0.142	-0.05	-0.180	-0.05	-0.218	-0.05	-0.238
0.05	-0.094	0.05	-0.118	0.05	-0.160	0.05	-0.212
0.15	-0.056	0.15	-0.072	0.15	-0.096	0.15	-0.160
0.25	-0.034	0.25	-0.054	0.25	-0.056	0.25	-0.106
0.35	-0.038	0.35	-0.056	0.35	-0.046	0.35	-0.064
0.45	-0.056	0.45	-0.056	0.45	-0.058	0.45	-0.040
0.55	-0.094	0.55	-0.060	0.55	-0.066	0.55	-0.050
0.65	-0.124	0.65	-0.058	0.65	-0.060	0.65	-0.066
0.75	-0.078	0.75	-0.056	0.75	-0.026	0.75	-0.066
0.85	0.074	0.85	-0.030	0.85	0.026	0.85	-0.020
0.925	0.244	0.925	0.082	0.925	0.126	0.925	0.086
0.975	0.456	0.975	0.278	0.975	0.314	0.975	0.278

Table 10 (Continued)

T. Tsutsumi/Neumann-Kelvin Problem/Series 60, $Z/H = -0.5$

$F_n=0.28$		$F_n=0.30$		$F_n=0.32$		$F_n=0.35$	
x/λ	C_{pr}	x/λ	C_{pr}	x/λ	C_{pr}	x/λ	C_{pr}
-0.975	0.176	-0.975	0.170	-0.975	0.164	-0.975	0.156
-0.925	0.154	-0.925	0.146	-0.925	0.142	-0.925	0.130
-0.85	0.178	-0.85	0.170	-0.85	0.158	-0.85	0.144
-0.75	0.178	-0.75	0.186	-0.75	0.188	-0.75	0.178
-0.65	0.116	-0.65	0.138	-0.65	0.152	-0.65	0.162
-0.55	0.042	-0.55	0.070	-0.55	0.090	-0.55	0.108
-0.45	-0.040	-0.45	-0.016	-0.45	0.006	-0.45	0.036
-0.35	-0.114	-0.35	-0.102	-0.35	-0.086	-0.35	-0.050
-0.25	-0.164	-0.25	-0.170	-0.25	-0.162	-0.25	-0.132
-0.15	-0.170	-0.15	-0.196	-0.15	-0.208	-0.15	-0.194
-0.05	-0.132	-0.05	-0.168	-0.05	-0.198	-0.05	-0.212
-0.05	-0.088	0.05	-0.116	0.05	-0.152	0.05	-0.196
0.15	-0.054	0.15	-0.074	0.15	-0.098	0.15	-0.156
0.25	-0.040	0.25	-0.054	0.25	-0.062	0.25	-0.110
0.35	-0.036	0.35	-0.046	0.35	-0.046	0.35	-0.066
0.45	-0.044	0.45	-0.036	0.45	-0.042	0.45	-0.036
0.55	-0.078	0.55	-0.038	0.55	-0.048	0.55	-0.042
0.65	-0.100	0.65	-0.048	0.65	-0.046	0.65	-0.060
0.75	-0.062	0.75	-0.052	0.75	-0.026	0.75	-0.060
0.85	0.064	0.85	-0.028	0.85	0.016	0.85	-0.022
0.925	0.218	0.925	0.080	0.925	0.120	0.925	0.084
0.975	0.526	0.975	0.032	0.975	0.408	0.975	0.384

WAVE RESISTANCE PREDICTIONS USING A SINGULARITY METHOD

by

MING-SHUN CHANG

David W. Taylor Naval Ship Research and Development Center

Bethesda, MD 20084

The singularity method of Chang and Pien(1,2) was used to calculate the wave resistances of all the ship hulls specified by the Workshop, but the HSVA Tanker. The calculated wave resistances from the linearized theory are in fairly good agreement with the experimental data supplied by the Workshop.

In brief, the present singularity method distributes the sources on the hull to form a stream surface for the wetted ship surface. The distribution of sources on the hull and the velocity potential on the wetted surface are calculated satisfying the linearized free surface condition and the exact hull boundary condition. From the resulting velocity potential, calculations are made of the pressure distribution, wave profile, velocity field and the sinkage and trim. Within the constraints of the linear theory, the effects of the sinkage and trim of a ship on the flow field are considered to be of higher order. Hence, the numerical results presented in this paper are calculated from the velocity potential generated by only the hull surfaces below the design waterline, in the absence of trim and sinkage.

Overall, computed values of wave resistance are in fairly good agreement with the experimental data. However, the details of the comparisons depend upon the individual ship and the value of Froude number. For the Wigley hull, the calculated values of wave resistance, Figure 1, are in good agreement with the measured values at moderate values of Froude number, ie. below 0.4. At higher values of Froude number, the calculated values of wave resistance are lower than those obtained from measurement. This result is consistent with the results obtained previously by the present method for the other Wigley type of ship hulls(2).

The wave resistance calculated for the Inui hull, Figure 2, is in very good agreement with the residual resistance derived from the measurements, except at values of Froude number of 0.36 and 0.65. At Froude number 0.36 the calculated wave resistance is too high in comparison with the measurement, while at Froude number 0.65 the calculated result is too low. The discrepancy in the low speed range could result from an insufficient number of panels used in representing the ship geometry (96 panels were used).

The calculated values of the Series 60 wave resistance, Figure 3, have a much more pronounced local maximum near a Froude number of 0.3 than the residual resistance derived from measurements. The cause of this discrepancy at a Froude number near 0.3 may be attributable to the effect of viscosity, the hull shape whose design speed is much lower than that of the other ships under investigation and errors in the method used to estimate the pressure resistance.

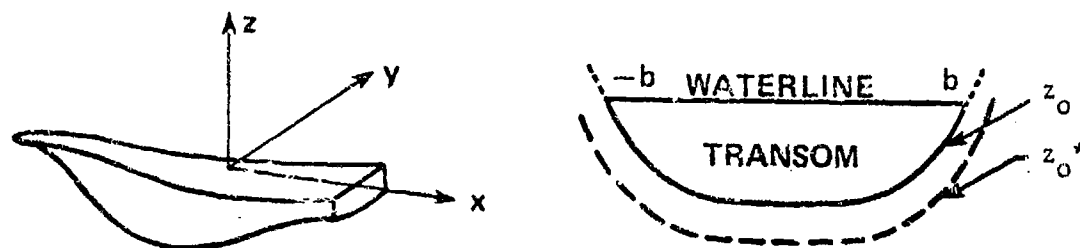
For ATHENA it will be observed that the residual resistance curve does not have the same characteristics as for the other ships. In comparison with the residual resistance of the other ships, the residual resistance of ATHENA at Froude numbers lower than 0.5 does not decrease as fast. This is because at low values of Froude number a significant portion of the residual resistance of ATHENA is due to the hydrostatic part of the pressure force, which is of more importance than for the other ships. ATHENA is a high speed ship with a transom stern. When it is operated at a Froude number higher than 0.3 the free surface behind the stern separates cleanly from the stern. The pressure, everywhere on the transom, then becomes equal to the atmospheric pressure. Because of this flow separation at the stern, the resistance from the hydrostatic part of the pressure is no longer a higher order quantity, as it is for a ship with a non-transom stern. In linearized theory the hydrostatic part of the resistance, R_H , can be evaluated easily, for both a fixed model and a model free to sink and trim:

$$R_H = \iint_{\text{WETTED HULL SURFACE}} \rho g z dS = - \iint_{\text{TRANSOM}} \rho g z dS$$

$$z = \begin{cases} \frac{1}{2} \int_{-b}^b \rho g z_0^2(y) dy & \text{FIXED MODEL} \\ \frac{1}{2} \int_{-b}^b \rho g z_0^{*2}(y) dy & \text{FREE MODEL} \end{cases} \quad (1)$$

$$(2)$$

Where ρ is the density of the water and g is the gravitational acceleration. The (x,y,z) coordinate system is shown schematically in the inserted figure, b is the width of the stern at waterline, z_0 is the design transom depth and z_0^* is the transom depth predicted from the linear theory.



For a model towed with a fixed trim and sinkage this hydrostatic force is a constant, and its contribution to the resistance coefficient is inversely proportional to the square of the Froude number, since the resistance is nondimensionalized by the velocity squared. This characteristic of the resistance curve differs from that of a ship with a regular stern. It becomes especially pronounced at low and moderate values of Froude number as mentioned previously. The experimentally determined hydrostatic resistances of ATHENA fixed and free to trim and sink are shown as Figures 4 and 5, respectively; the experimental hydrostatic resistances are derived from the measured values of stern submergences. It is seen in the figures that, for ATHENA fixed in trim and sinkage, the hydrostatic resistance is significant at Froude numbers below 0.5; above a Froude number of 0.5 the hydrostatic resistance is reduced to approximately 25 percent of the total residual resistance. In contrast, for ATHENA free to trim and sink the hydrostatic resistance is important

at all Froude numbers investigated; the ratio of the hydrostatic resistance to the total residual resistances varies from 75-percent at Froude number 0.28 to 30-percent at Froude number 0.8. The difference in the hydrostatic resistance between the fixed model and the free model is approximately the same as the difference between the total residual resistances for the two model conditions.

The total pressure resistance of ATHENA free to trim and sink is the sum of the dynamic resistance and the hydrostatic resistance of Equation (2). In the linearized theory, the dynamic wave resistance is the same as that of the fixed model. Thus the pressure resistance of ATHENA can be predicted from the design waterline of the ship. The calculated values of the dynamic wave resistance plus the hydrostatic force of Equation (2), Figure 6, are lower everywhere than the experimental residual resistance data. The discrepancies between the present numerical results and the experimental data at high Froude numbers are consistent with the comparisons given for the other ships; calculated values are somewhat lower than the measurements. This could be due to the more complex flow field at the bow at high speeds. The discrepancies at the lower Froude numbers could be due to the inaccuracies associated with the estimated hydrostatic resistance. Figure 7 shows the measured and calculated submergences of the stern when ATHENA is free to trim and sink. It is seen that the calculated values are somewhat lower than the measured values at lower Froude numbers. The predictions of the residual resistance at lower Froude numbers will probably be improved if the predictions on the stern submergences are improved.

REFERENCES

1. Chang, M-S and P.C. Pien, "Hydrodynamic Forces on a Body Moving Beneath a Free Surface", First Int'l. Conference on Computational Ship Hydrodynamics, Gaithersburg, 1975.
2. Chang, M-S, "Computations of Three-Dimensional Ship-Motions with Forward Speed", Second Int'l. Conference on Computational Ship Hydrodynamics, Berkeley, 1977.

TABLE 1 Calculated Wave Resistance Coefficient

Wigley		Inui		Series 60 , $C_B = 0.60$		ATHENA	
F_n	$C_W \times 10^3$	F_n	$C_W \times 10^3$	F_n	$C_W \times 10^3$	F_n	$C_W \times 10^3$
.276	1.20	.30	5.29	.28	1.06	.35	1.90
.313	1.93	.32	5.29	.32	3.20	.41	2.22
.350	1.38	.36	6.13	.35	2.90	.48	2.45
.450	3.60	.40	7.32			.65	2.05
.550	4.10	.44	10.50			.80	1.50
		.50	13.47				
		.55	14.13				
		.65	9.85				

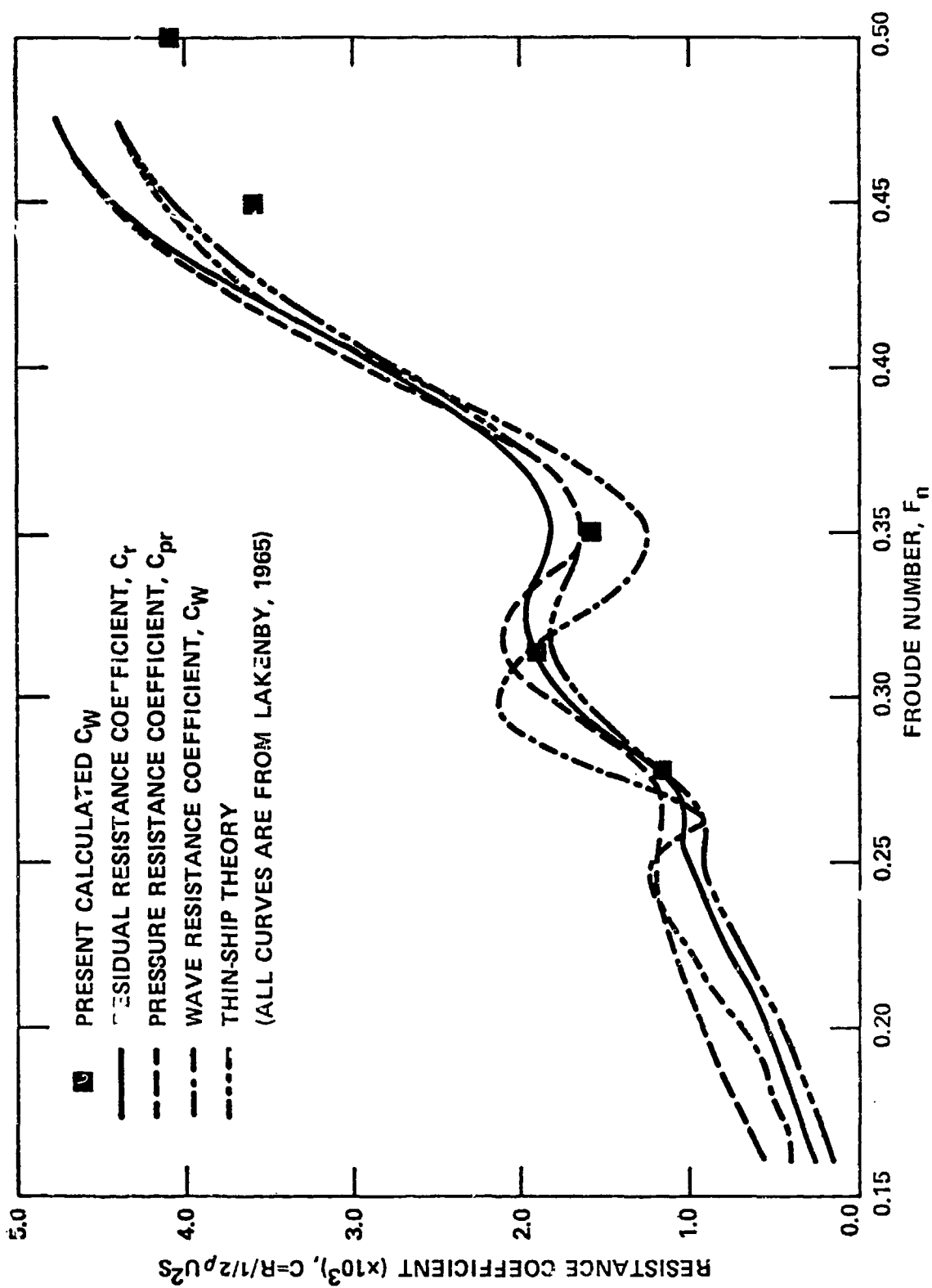


FIGURE 1 Resistance Coefficient for Wigley Hull

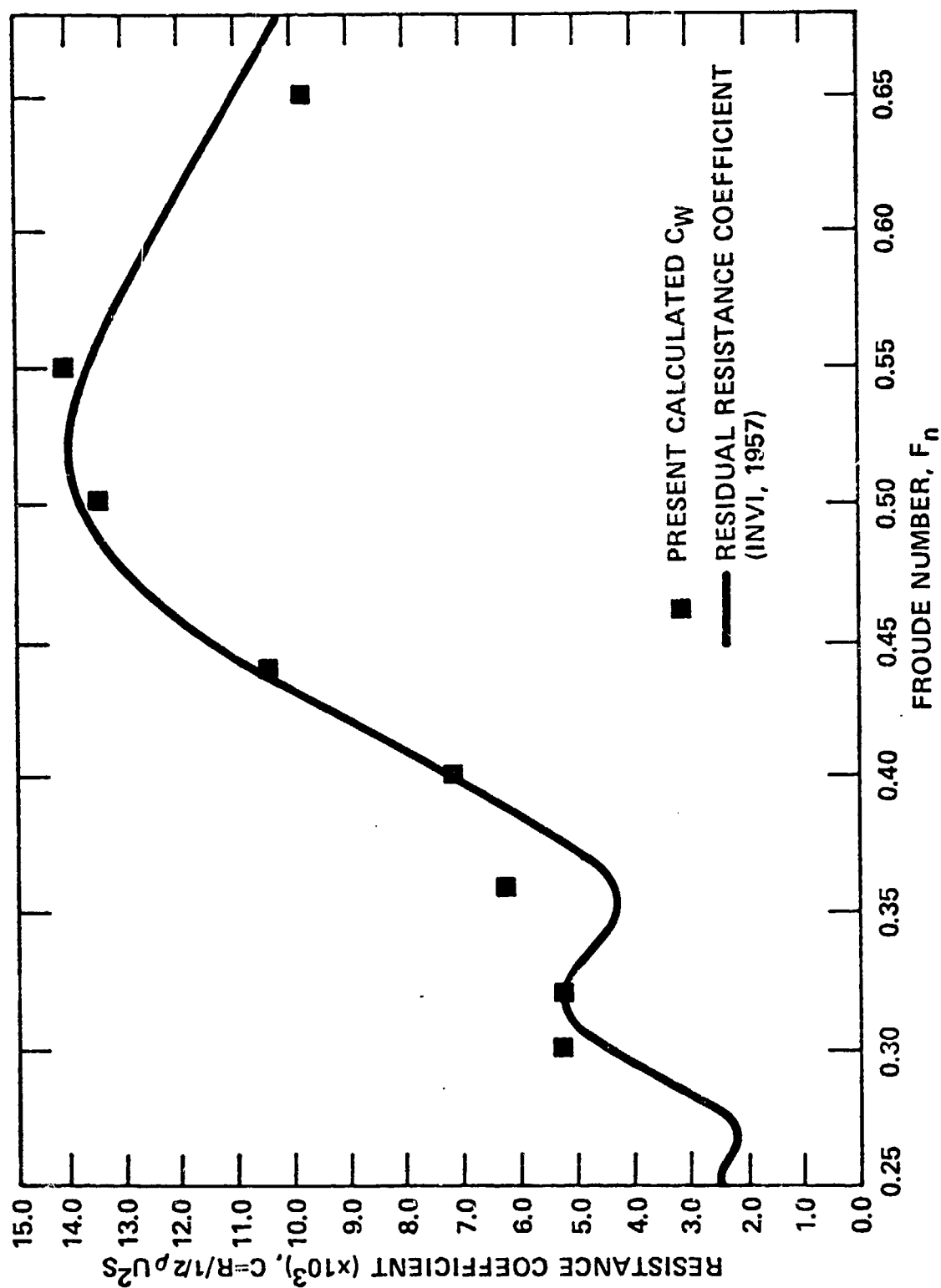


FIGURE 2 Resistance Coefficient for Inuid Hull

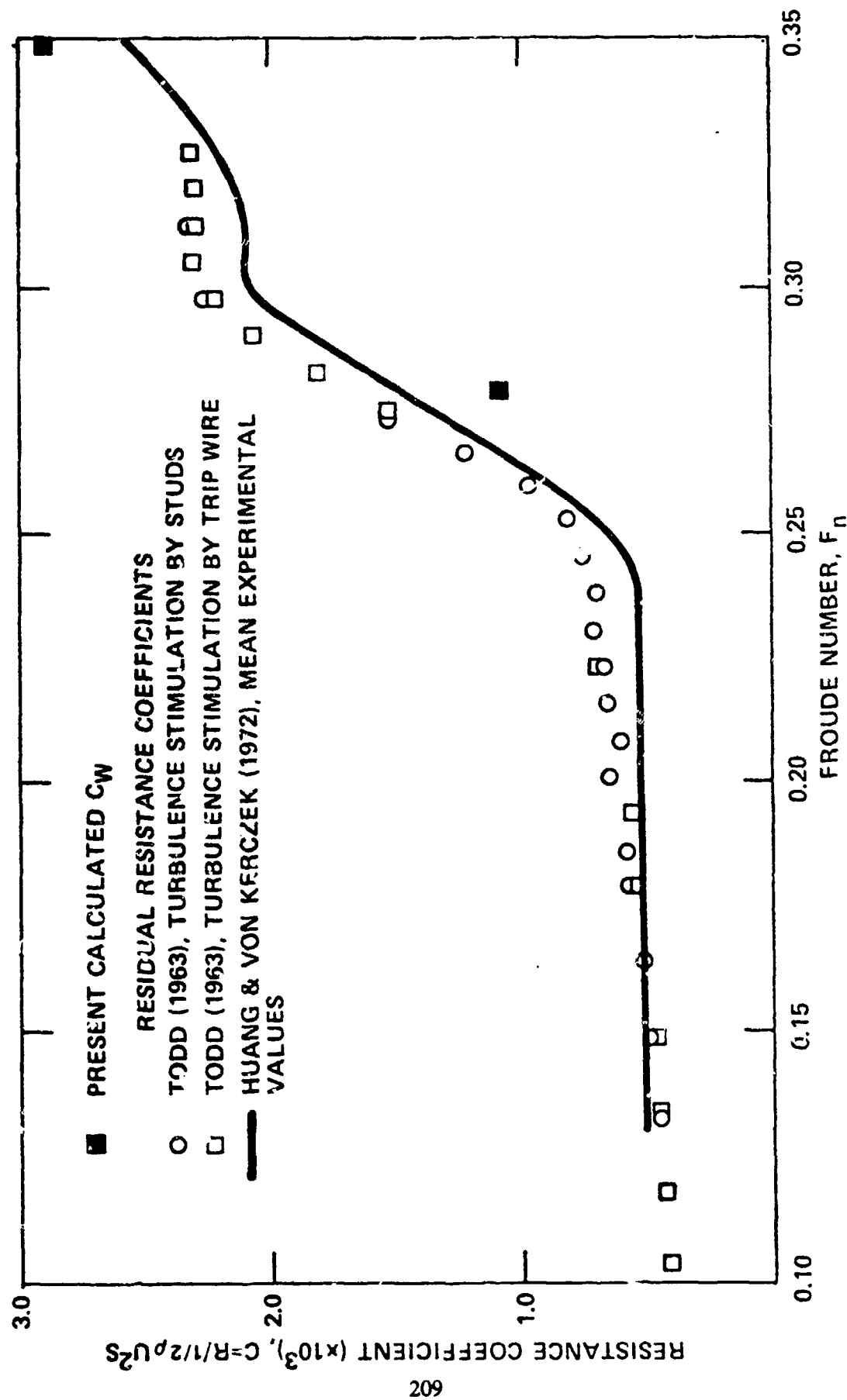


FIGURE 5 Resistance Coefficient for Series 60, $C_g = 0.60$

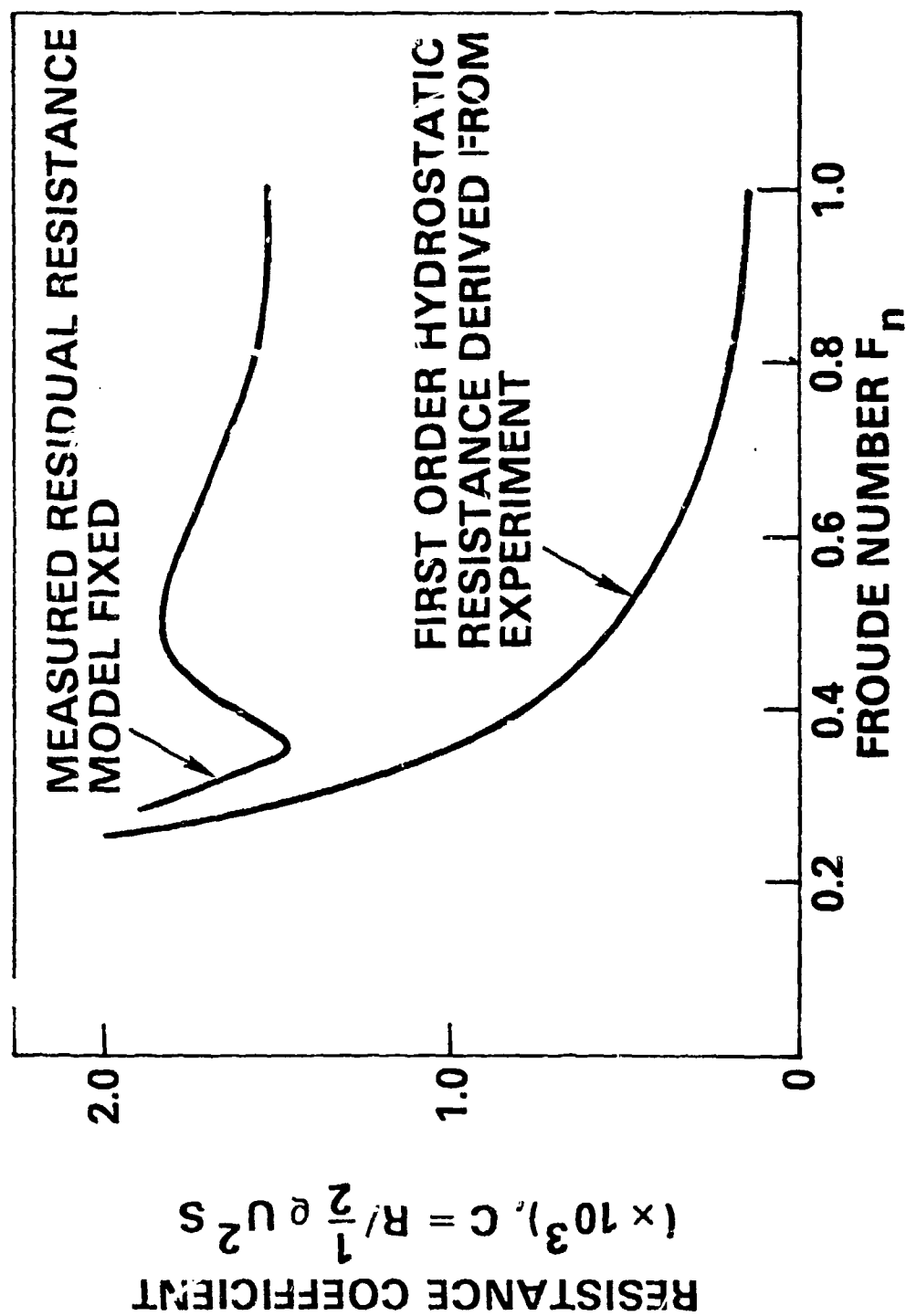


FIGURE 4 Measured Residual Resistance and Hydrostatic Resistance for ATHENA Fixed

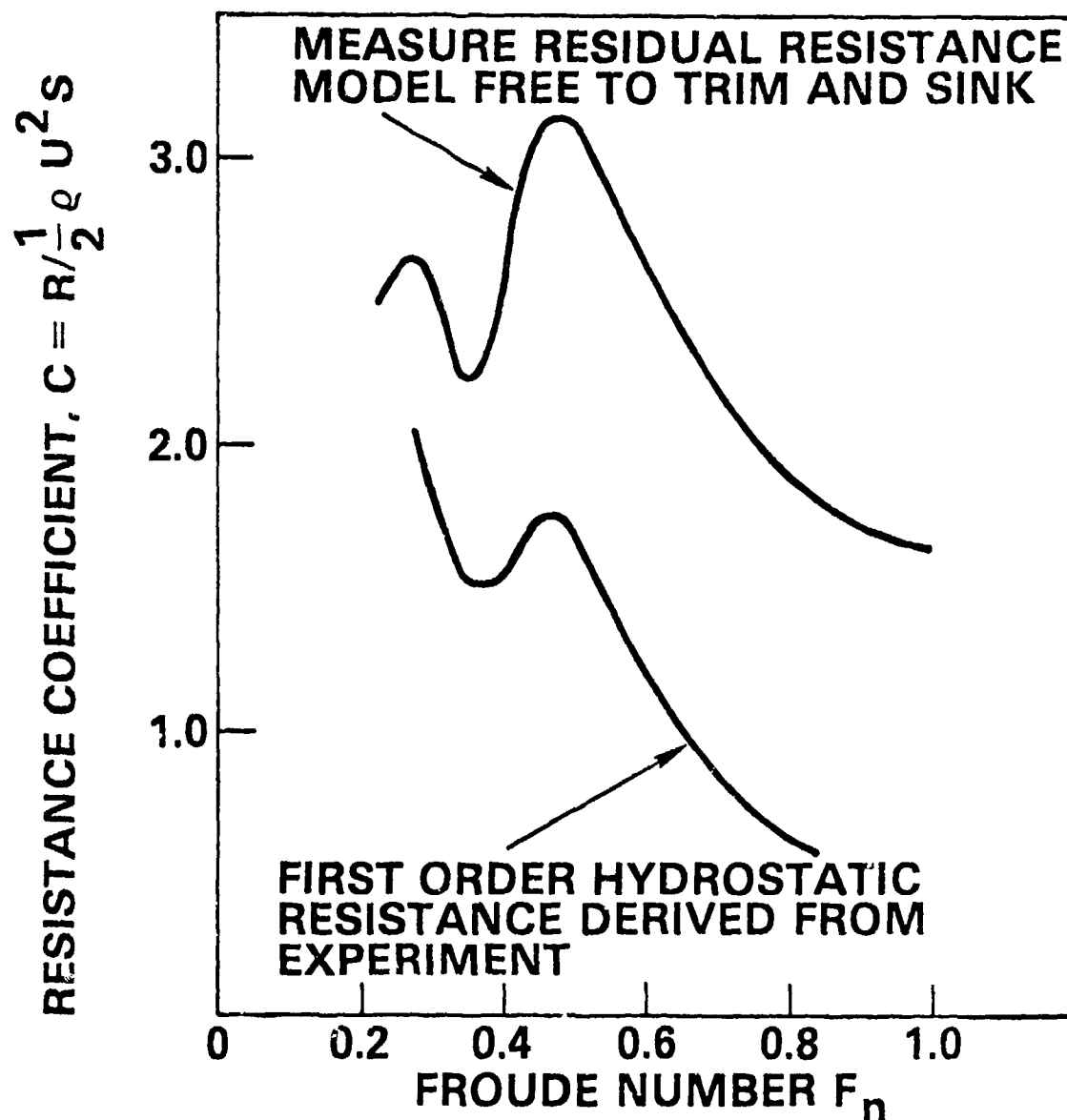


FIGURE 5 Measured Residual Resistance and Hydrostatic Resistance for ATHENA Free to Sink and Trim

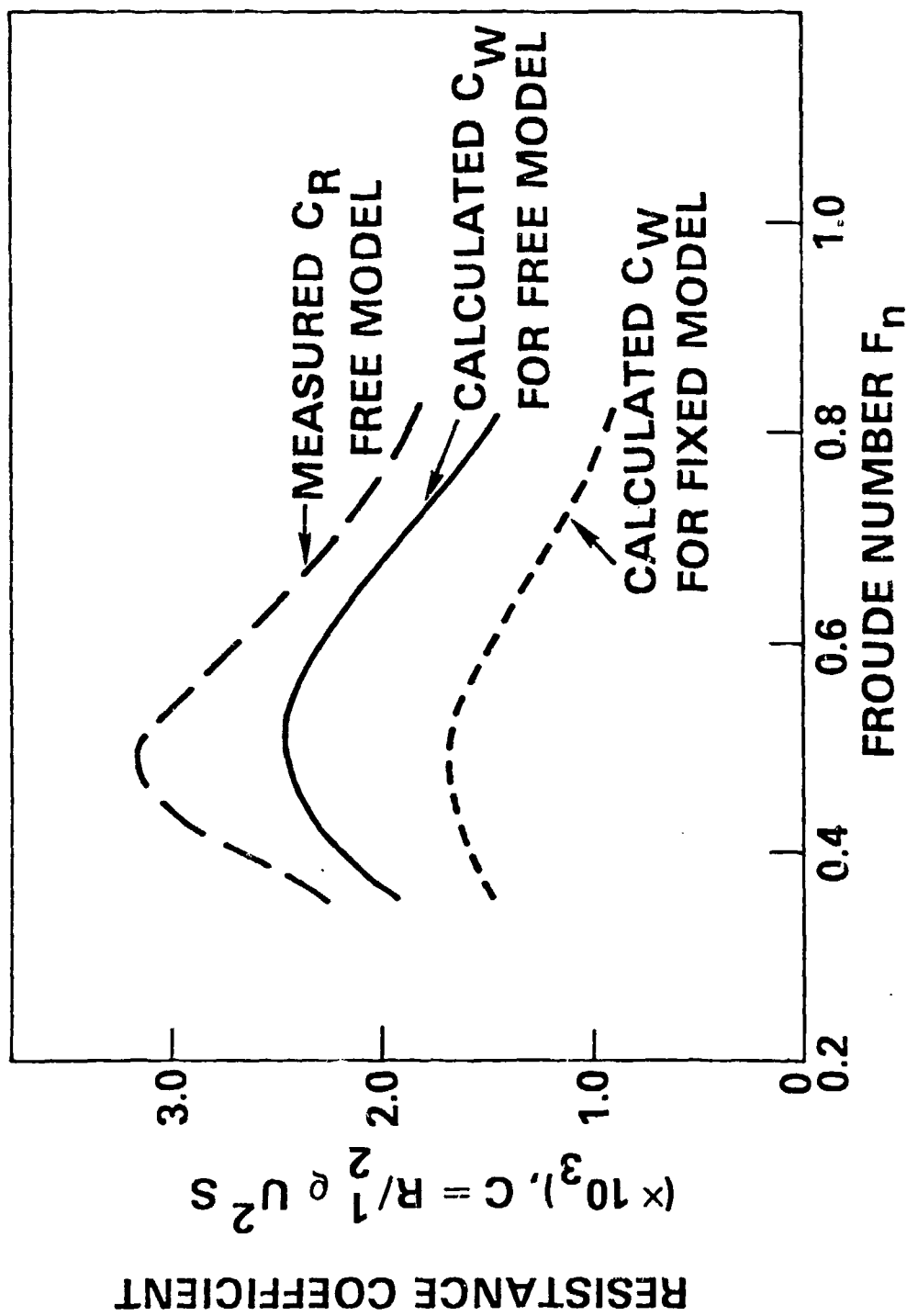


FIGURE 6 Calculated and Measured Resistance Coefficient for ATHENA

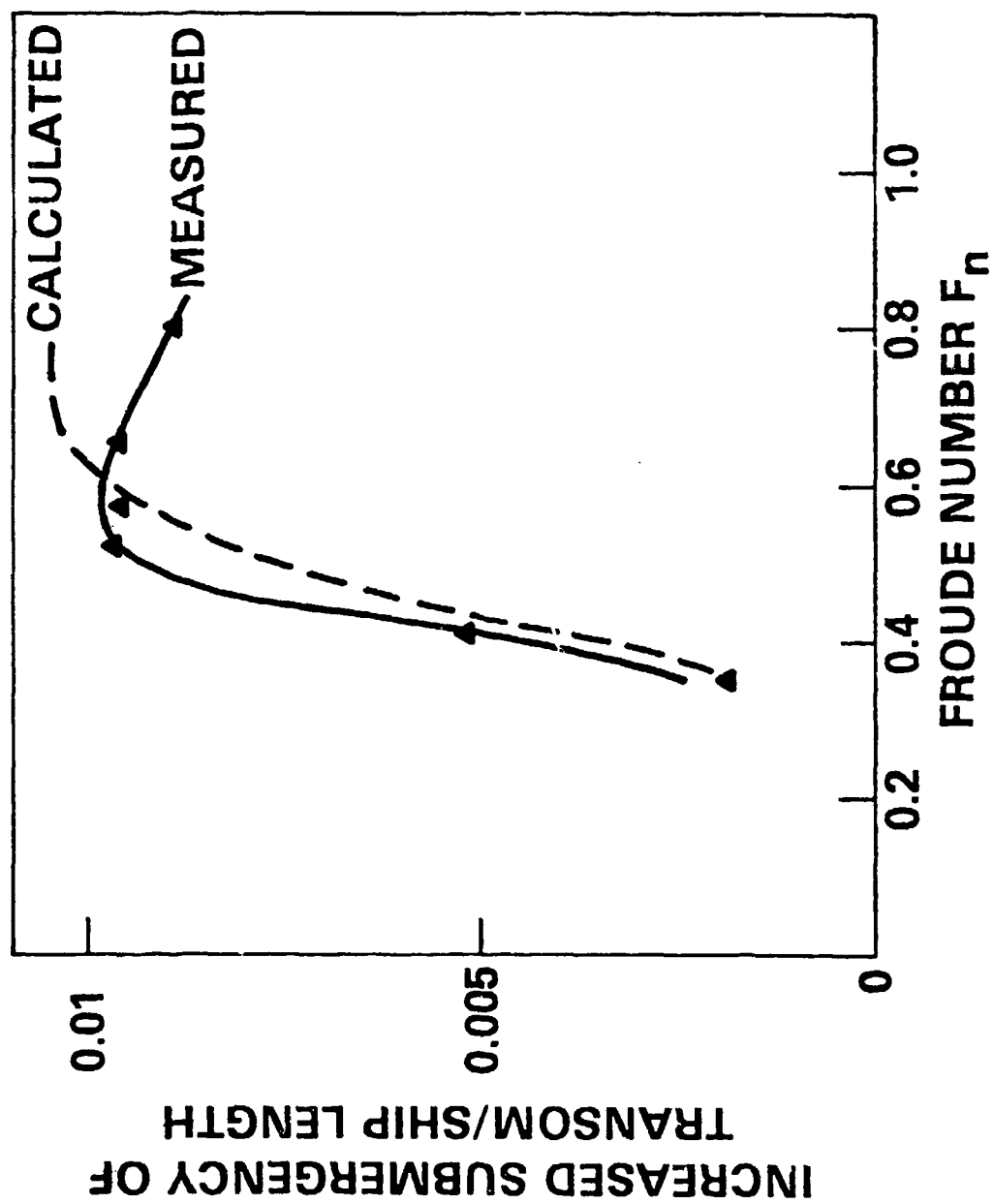


FIGURE 7 Calculated and Measured Increased Stern Submergency for ATHENA

Discussion

by K. Eggers
of paper by M. Chang

I feel that the transom stern correction for static pressure should consistently have included linearized dynamic pressure as well.

This would lead to just the same correction, but with opposite sign, probably even in better agreement with experiments.

Discussion

by C. M. Lee
of paper by M. Chang

Have you included the line integral term in your calculation?

Author's Reply

by M. Chang
to discussions by K. Eggers and by C. M. Lee

The line singularity has been the interest of many in recent years. With the source distribution method, the line singularity is source only, whereas with doublet distribution method the line singularities are both source and doublet. The source method thus implicitly includes the line singularity. It is different from the doublet distribution method in which an additional line source has to be added to the calculation explicitly.

The order of the resistance from the hull surface between the free surface and the still waterline is considered as a higher order force in the present approach. And, it is the basis for the estimation of the hydrostatic force from the transom below the still waterline only.

WAVE-RESISTANCE CALCULATION FOR WIGLEY, S-201 AND SERIES 60 HULLS

Kuniharu NAKATAKE, Akio TOSHIMA and Ryusuke YAMAZAKI
(Kyushu University, Fukuoka, Japan)

We adopt three kinds of numerical methods for the wave-resistance calculation. At first we give short descriptions of the methods.

[METHOD 1] Low Speed Theory Making Use of Mapping Procedures

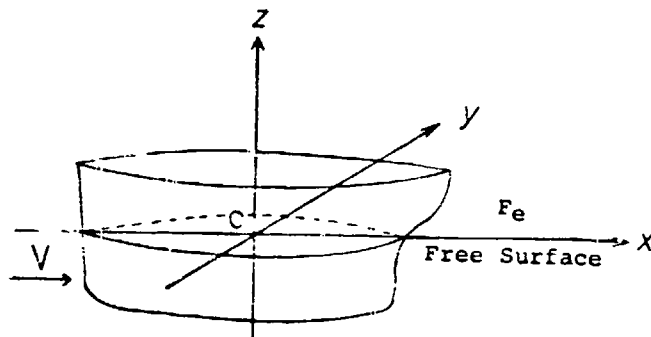


Fig. 1 Coordinate System

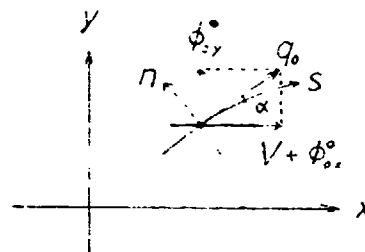


Fig. 2 Components of
Basic Flow

As an improvement of the low speed theory, this method [1] was proposed to take into consideration the effect of the local non-uniform flow around a ship in the expression of the wave-resistance. The wave-resistance expression R_w becomes as follows [vide. Fig. 1 and Fig. 2],

$$R_w = \frac{\rho}{2\pi} k_0^2 \int_{-\pi/2}^{\pi/2} |B(k_0 \sec^2 \theta, \theta)|^2 \sec^3 \theta d\theta, \quad (1)$$

where

$$B(k, \theta) = - \iint_{-\infty}^{\infty} D(x, y) V^2 q_0^{-2} e^{-ikV^2(\xi \cos \theta + \eta \sin \theta)} dx dy, \quad (2)$$

$$D(x, y) = \frac{\partial}{\partial x} \{ \zeta_0 (V + \phi_{0x}) \} + \frac{\partial}{\partial y} (\zeta_0 \phi_{0y}) \quad \text{on } F_e, \quad k_0 = g/V^2. \quad (3)$$

ϕ_0 and ζ_0 express the velocity potential of the double body flow and the wave elevation due to ϕ_0 , respectively. The coordinates ξ and η express the effect of non-uniform flow, and are obtained approximately as

$$\xi = \int_0^x \left[\frac{q_0^2}{\cos \alpha} \right]_{\text{along streamline}} dx, \quad \eta = \int_{y_0(x)}^y \left[\frac{q_0^2}{\cos \alpha} \right]_{\text{along equipotential line}} dy, \quad (4)$$

where $y_0(x)$ is the half breadth of a ship at the load water line, and q_0 and α are expressed as

$$q_0^2 = (V + \phi_{0x})^2 + \phi_{0y}^2, \quad \alpha = \tan^{-1} \left\{ \phi_{0y} / (V + \phi_{0x}) \right\}. \quad (5)$$

[METHOD 2] Baba's Low Speed Theory [2]

Usual low speed theory is derived from the above-described theory under some assumptions. In this case, the function $B(k, \theta)$ is defined as

$$B(k, \theta) = - \frac{k_0 \sec^2 \theta}{k} \iint_{-\infty}^{\infty} D(x, y) e^{-ik(x \cos \theta + y \sin \theta)} dx dy. \quad (6)$$

[METHOD 3] Guevel's Theory [3]

Since this theory corresponds to the case where the function $D(x, y)$ is linearized as

$$D(x, y) = - \frac{1}{k_0} [\phi_{0xx}]_{z=0}, \quad (7)$$

the function $B(k, \theta)$ is defined as

$$B(k, \theta) = \frac{1}{k \cos^2 \theta} \iint_{-\infty}^{\infty} [\phi_{0xx}]_{z=0} e^{-ik(x \cos \theta + y \sin \theta)} dx dy. \quad (8)$$

Calculation Method of $B(k, \theta)$ and $D(x, y)$

$B(k, \theta)$ is generally obtained by the surface integral over the stillwater surface F_e . And F_e is divided into a lot of small meshes along streamlines and equipotential lines. These streamlines and equipotential lines are obtained by Runge-Kutta-Gill method using 180(25×15) hull surface sources except S-201 hull. In case of S-201, they are obtained by using the given center plane source distribution.

$D(x, y)$ is expressed as

$$D(x, y) = \frac{\partial A}{\partial x} + \frac{\partial B}{\partial y} \quad \text{on } F_e, \quad (9)$$

where

$$A = \zeta_0 (V + \phi_{0x}^{\circ}) , \quad B = \zeta_0 \phi_{0y}^{\circ} .$$

In order to avoid the errors due to numerical differentiation, we use the following easy calculation method of $D(x,y)$. The integral of $D(x,y)$ over each small mesh becomes as

$$\iint_{\text{mesh}} D(x,y) dx dy = \iint_{\text{mesh}} \left(\frac{\partial A}{\partial x} + \frac{\partial B}{\partial y} \right) dx dy = \oint (A dx - B dy). \quad (10)$$

Letting the coordinates of four corner points of the small mesh be (i,j) , $(i,j+1)$, $(i+1,j+1)$ and $(i+1,j)$, and assuming that the functions A and B change linearly along the perimeter of the mesh, we have

$$D(x,y) \doteq \bar{H} / 2\Delta A, \quad (11)$$

where ΔA is the area of the mesh and

$$\begin{aligned} \bar{H} = & \{ y(i+1,j+1) - y(i,j) \} \{ A(i,j+1) - A(i+1,j) \} + \{ y(i+1,j) - y(i,j+1) \} \{ A(i+1,j+1) - A(i,j) \} \\ & - \{ x(i+1,j+1) - x(i,j) \} \{ B(i,j+1) - B(i+1,j) \} - \{ x(i+1,j) - x(i,j+1) \} \{ B(i+1,j+1) - B(i,j) \} \end{aligned}$$

The validity of Eq.(11) was checked for the lens-shaped ship with infinite draft and the semi-submerged sphere[1].

Next we show some calculation results for Wigley, S-201 and Series 60 hulls.

WIGLEY Hull

Fig. 3, Fig. 4 and Fig. 5 show the mesh division, the mapped coordinates (ξ,η) and the curves of $D(x,y)/(V^3/g)$, respectively. Table 1 shows the resistance coefficient C calculated by the three methods. These curves are compared with other curves in Fig. 6. There is not much difference between them in the range $F_n < 0.35$.

INUID S-201 Hull

Table 2 and Fig. 7 show the resistance coefficient C and their curves, respectively. METHOD 1 gives generally bigger values than other methods.

SERIES 60 Hull

In this case, the obtained hull source distributions do not represent well the shape of the load water plane especially near the stern. This seems to be due to inclined frame lines near the load water line. Therefore we calculate the function $B(k, \theta)$ on the water plane at $z = -0.03H$. But the streamline on the hull does not close well at the stern yet. Table 3 and Fig. 8 show the resistance coefficient and their curves, respectively. In the range of $F_n < 0.25$, the curves by the three methods seem to agree considerably well with the experimental wave-resistance curve.

REFERENCES

- [1] Yamazaki, R., Nakatake, K. and Nakamura, M., Low Speed Wave-Resistance Theory Making Use of Strained Coordinates, International Joint Research Report (1978)
- [2] Baba, E., Wave Resistance of Ships in Low Speed, Mitsubishi Tech. Bulletin No. 109 (1976)
- [3] Guevel, P., Vaussy, P. and Kobus, J.M., The Distribution of Singularities Kinematically Equivalent to a Moving Hull in the Presence of a Free Surface, Int. Ship. Prog., Vol.21 (1974)

Table 1 Resistance Coefficient
of WIGLEY Hull

Fn	METHOD 1	METHOD 2	METHOD 3
0.15	0.284	0.265	0.298
0.16	0.258	0.217	0.236
0.17	0.229	0.260	0.233
0.18	0.501	0.477	0.451
0.19	0.307	0.302	0.267
0.20	0.656	0.567	0.563
0.21	0.557	0.588	0.458
0.22	0.484	0.403	0.399
0.23	0.941	0.787	0.791
0.24	1.105	1.032	0.859
0.25	0.798	0.773	0.569
0.26	0.668	0.561	0.522
0.27	1.012	0.776	0.878
0.28	1.553	1.242	1.322
0.29	1.921	1.606	1.527
0.30	1.967	1.685	1.427
0.31	1.755	1.517	1.160
0.32	1.463	1.239	0.898
0.33	1.223	0.987	0.763
0.34	1.104	0.839	0.796
0.35	1.131	0.817	0.977
0.36	1.306	0.911	1.268
0.37	1.527	1.089	1.605
0.38	1.800	1.308	1.951
0.39	2.089	1.526	2.257
0.40	2.341	1.746	2.517
0.41	2.584	1.950	2.736
0.42	2.817	2.122	2.906
0.43	2.981	2.252	3.019
0.44	3.107	2.351	3.086
0.45	3.255	2.432	3.123
0.46	3.335	2.492	3.138
0.47	3.373	2.526	3.128
0.48	3.398	2.541	3.104

Table 2 Resistance Coefficient
of INUID S-201 Hull

Fn	METHOD 1	METHOD 2	METHOD 3
0.15	0.708	0.389	0.687
0.16	0.706	0.396	0.661
0.17	0.771	0.718	0.700
0.18	1.784	1.041	1.457
0.19	1.058	0.779	0.821
0.20	2.335	1.227	1.822
0.21	2.314	1.679	1.518
0.22	1.669	0.925	1.230
0.23	3.355	1.743	2.617
0.24	4.488	2.825	2.973
0.25	3.547	2.363	1.980
0.26	2.621	1.484	1.656
0.27	3.260	1.594	2.700
0.29	6.562	3.779	4.913
0.30	7.116	4.283	4.699
0.31	6.745	4.090	3.936
0.33	4.982	2.707	2.481
0.35	4.113	1.850	2.682
0.37	4.814	2.192	4.313
0.39	6.085	3.143	6.030
0.41	7.511	4.095	6.976
0.43	8.798	5.018	7.794
0.45	9.652	5.588	7.863
0.48	10.622	6.180	7.876
0.51	10.953	6.314	7.320
0.54	11.136	6.307	6.795
0.57	11.097	6.126	6.342
0.60	10.807	5.814	5.560
0.63	10.624	5.440	4.706
0.66	10.425	5.250	4.491

Table 3 Resistance Coefficient
of SERIES 60 Hull

Fn	METHOD 1	METHOD 2	METHOD 3
0.10	0.061	0.057	0.096
0.11	0.062	0.062	0.089
0.12	0.058	0.052	0.075
0.13	0.046	0.044	0.066
0.14	0.042	0.069	0.094
0.15	0.066	0.080	0.098
0.16	0.084	0.078	0.100
0.17	0.063	0.051	0.059
0.18	0.083	0.083	0.085
0.19	0.109	0.100	0.106
0.20	0.227	0.200	0.174
0.21	0.160	0.115	0.106
0.22	0.145	0.124	0.098
0.23	0.173	0.194	0.137
0.24	0.169	0.182	0.225
0.25	0.399	0.362	0.543
0.26	0.956	0.931	1.044
0.27	1.511	1.589	1.387
0.28	1.724	1.934	1.360
0.29	1.561	1.843	1.037
0.30	1.194	1.460	0.718
0.31	0.945	1.080	0.638
0.32	0.959	0.908	0.925
0.33	1.285	1.032	1.562
0.34	1.892	1.443	2.401
0.35	2.673	2.039	3.304

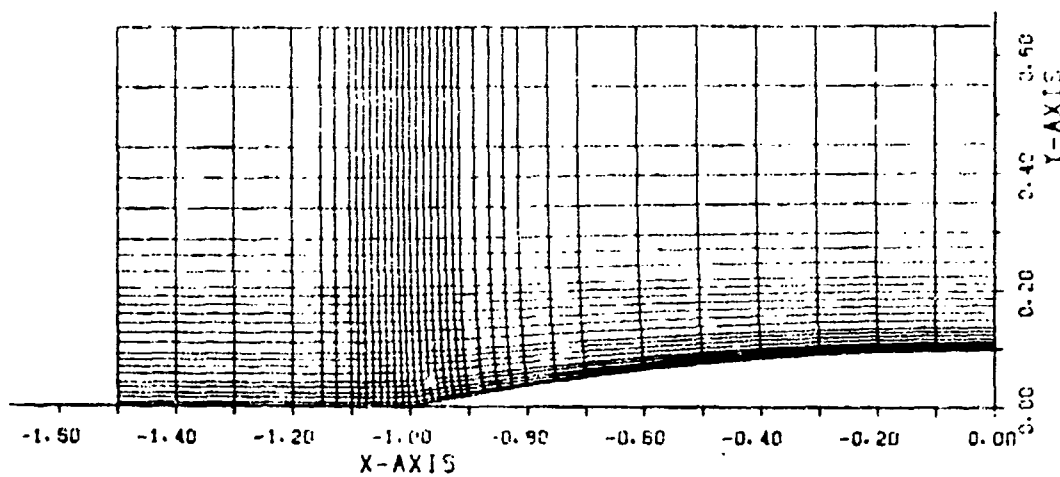


Fig. 3 Mesh division of WIGLEY Hull

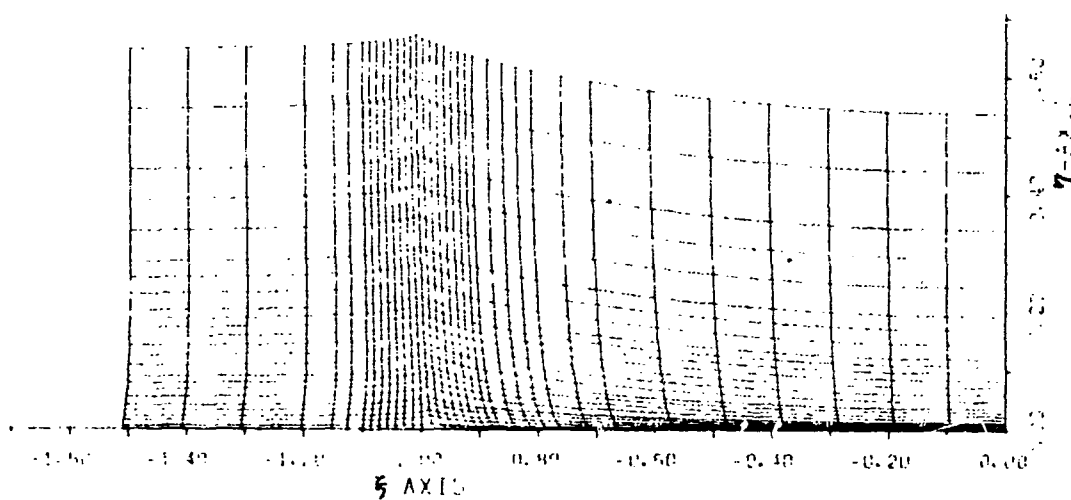


Fig. 4 Mapped coordinates of WIGLEY Hull

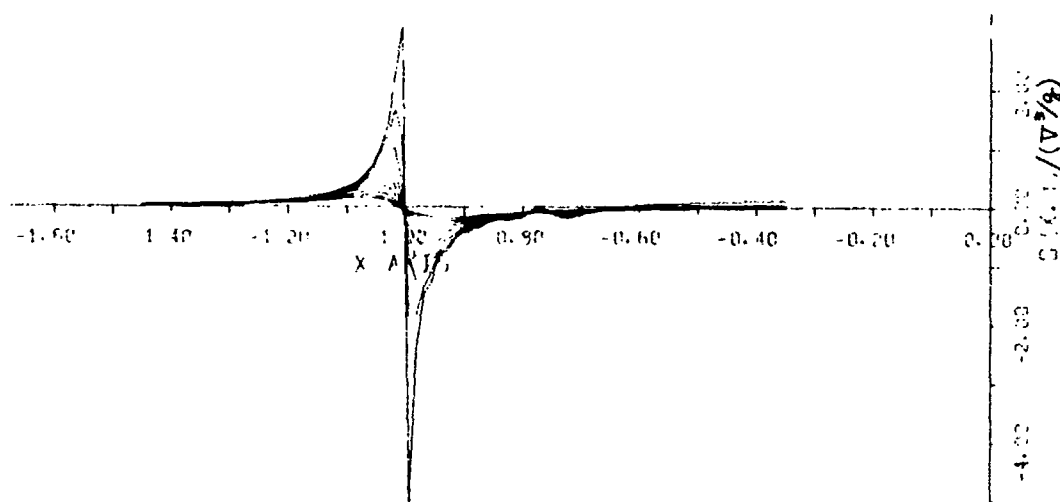


Fig. 5 Curves of $D(x,y)/(V^3/g)$ of WIGLEY Hull

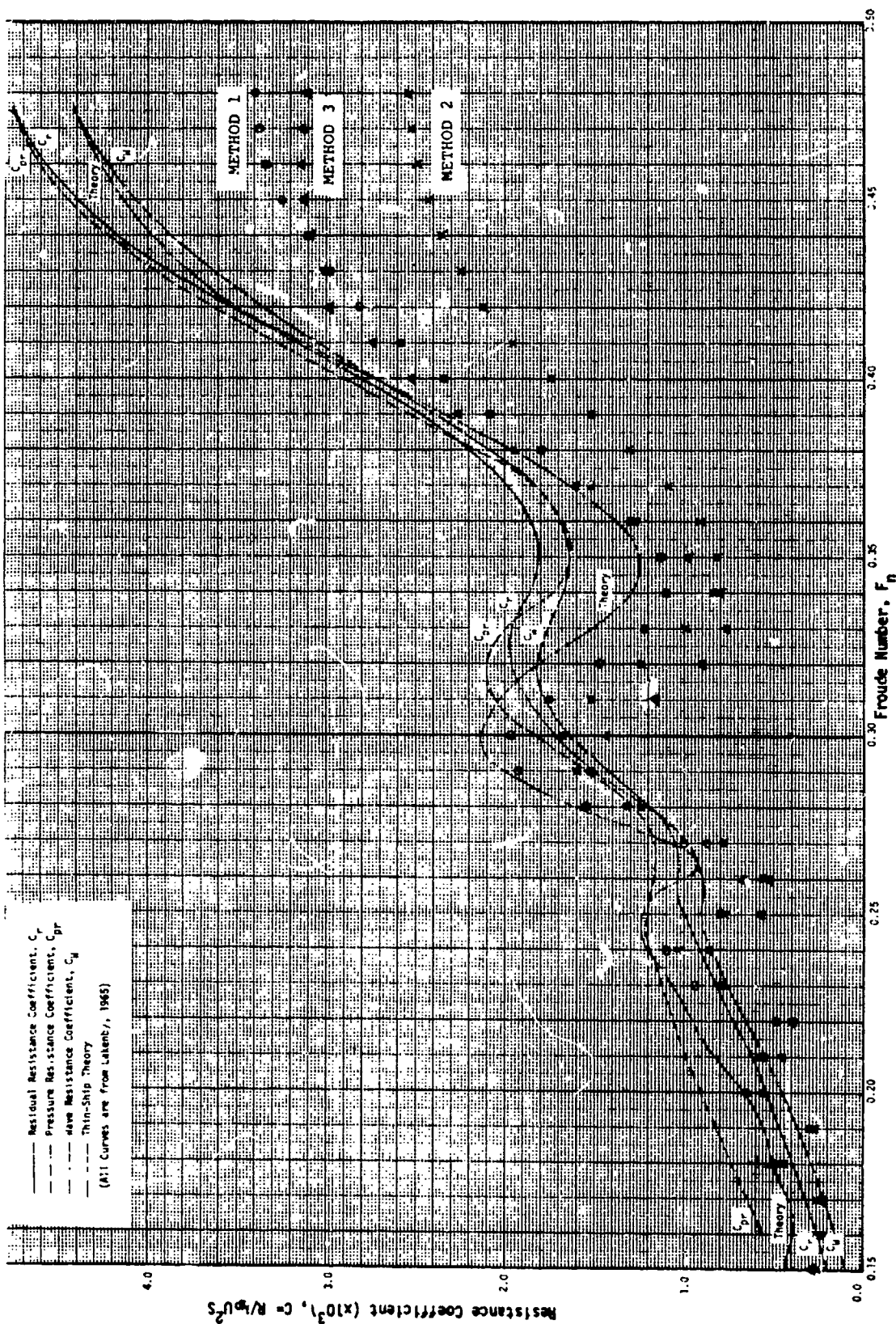


Fig. 6 Comparison of Resistance Curves for Wigley Hull

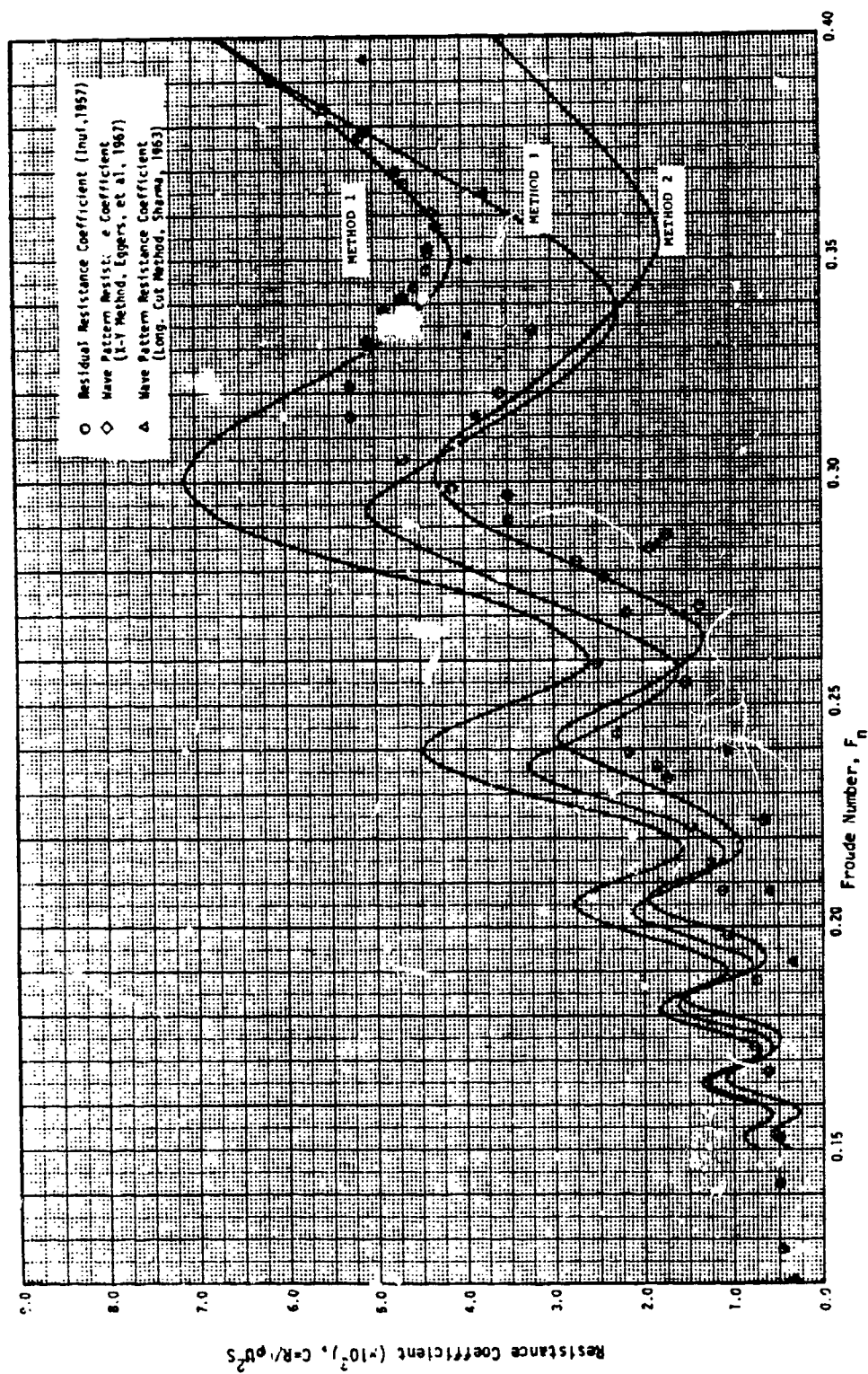


Fig. 7-1 Comparison of Resistance Curves for Inuid Hull, S-201

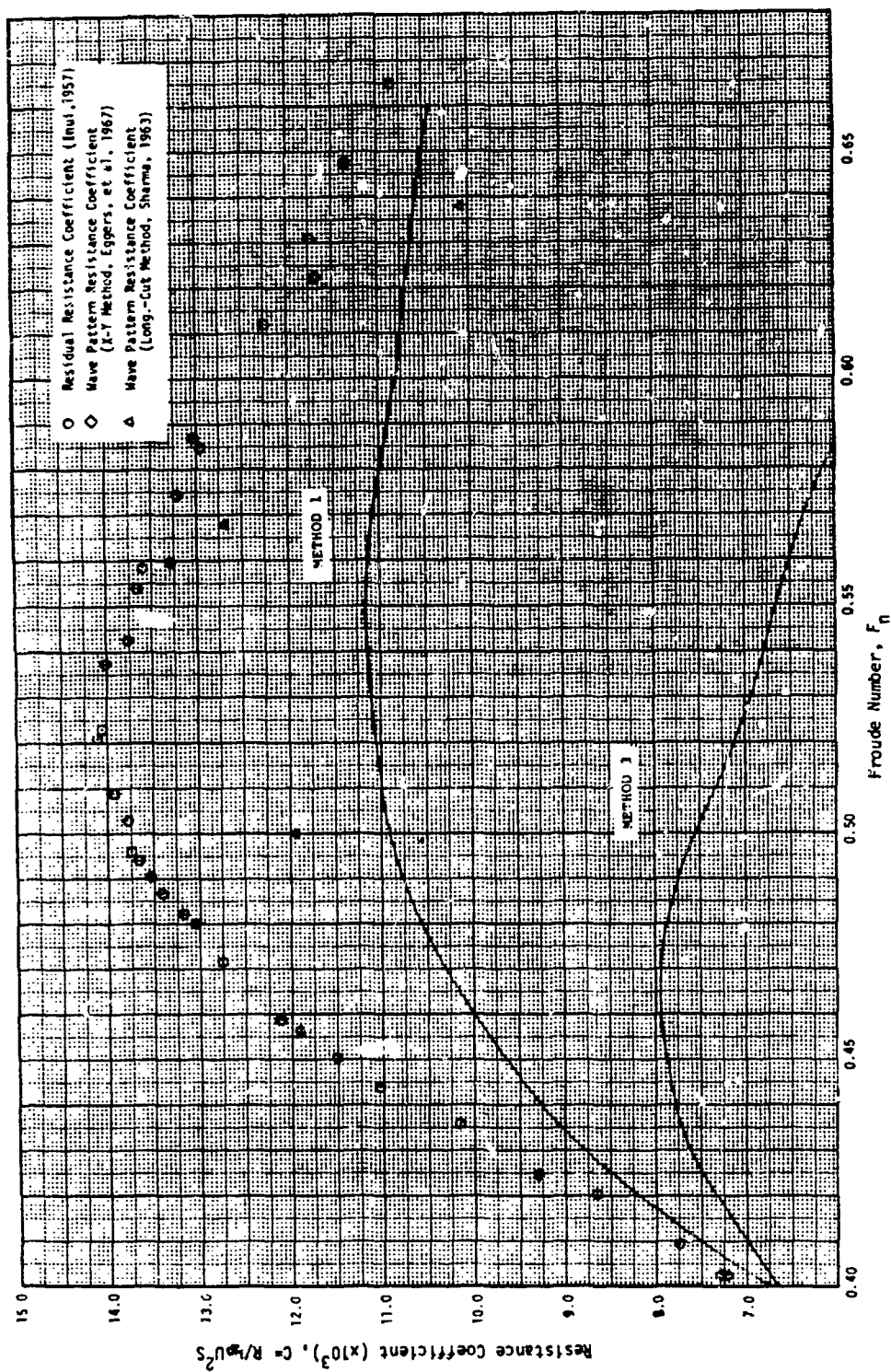


Fig. 7-2 Comparison of Resistance Curves for Inuid Hull, S-201

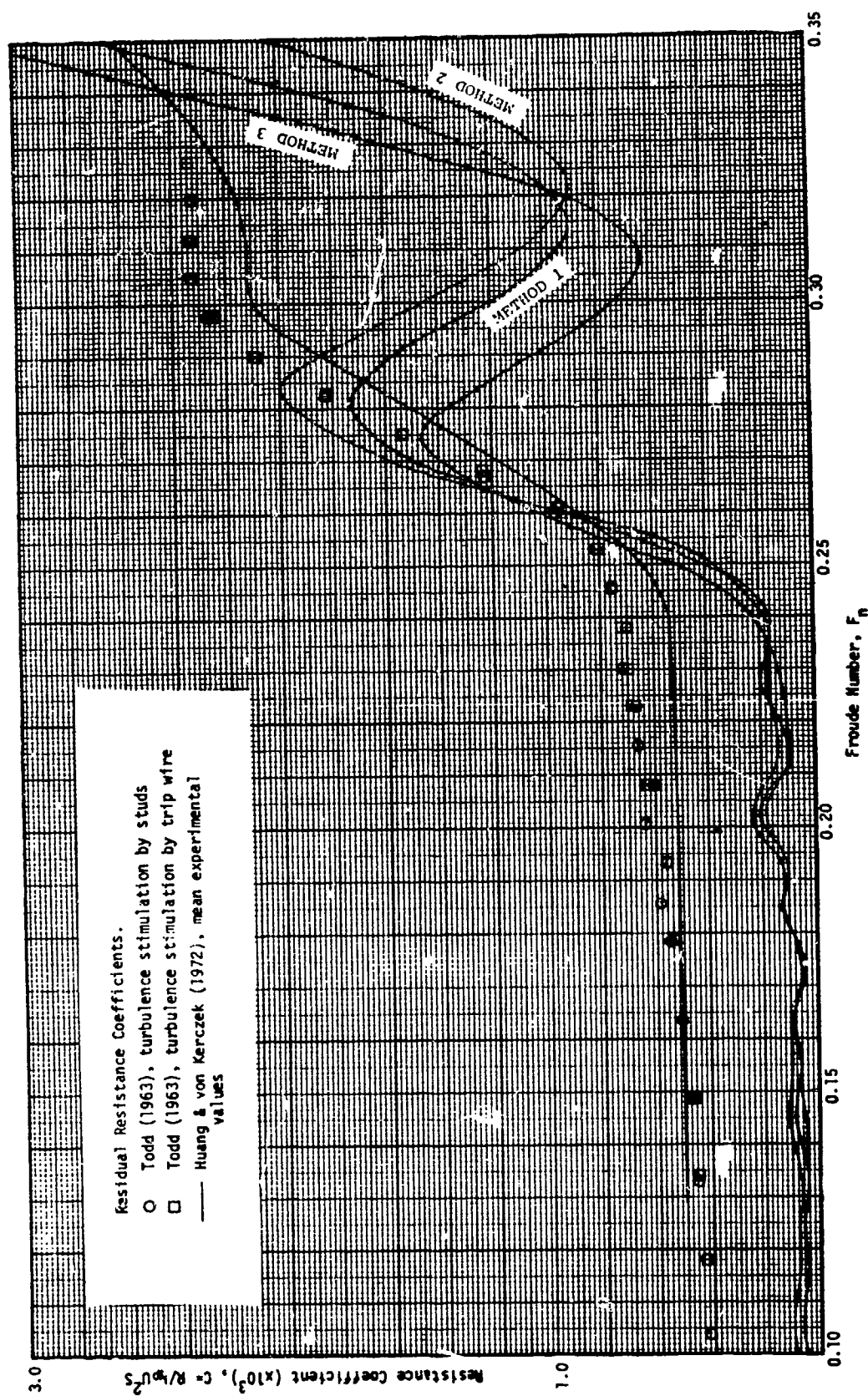


Fig. 8 Comparison of Resistance Curves for Series 60 Hull

FORMAT FOR TABULATED VALUES OF WAVE RESISTANCE
K. NAKATAKE/ Low Speed Theory Making Use of Mapping Procedures [METHOD 1]

WIGLEY		INUID S-201		SERIES 60	
F_n	C_w	F_n	C_w	F_n	C_w
0.15	0.284	0.15	0.708	0.10	0.061
0.16	0.258	0.16	0.706	0.11	0.062
0.17	0.229	0.17	0.771	0.12	0.058
0.18	0.501	0.18	1.784	0.13	0.046
0.19	0.307	0.19	1.058	0.14	0.042
0.20	0.656	0.20	2.335	0.15	0.066
0.21	0.557	0.21	2.314	0.16	0.084
0.22	0.484	0.22	1.669	0.17	0.063
0.23	0.941	0.23	3.355	0.18	0.083
0.24	1.105	0.24	4.488	0.19	0.109
0.25	0.798	0.25	3.547	0.20	0.227
0.26	0.668	0.26	2.621	0.21	0.160
0.27	1.012	0.27	3.260	0.22	0.145
0.28	1.553	0.29	6.562	0.23	0.173
0.29	1.921	0.30	7.116	0.24	0.169
0.30	1.967	0.31	6.745	0.25	0.399
0.31	1.755	0.33	4.982	0.26	0.956
0.32	1.463	0.35	4.113	0.27	1.511
0.33	1.223	0.37	4.814	0.28	1.724
0.34	1.104	0.39	6.086	0.29	1.561
0.35	1.131	0.41	7.515	0.30	1.194
0.36	1.306	0.43	8.798	0.31	0.945
0.37	1.527	0.45	9.652	0.32	0.959
0.38	1.800	0.48	10.622	0.33	1.285
0.39	2.089	0.51	10.953	0.34	1.892
0.40	2.341	0.54	11.136	0.35	2.673
0.41	2.584	0.57	11.097		
0.42	2.817	0.60	10.807		
0.43	2.981	0.63	10.624		
0.44	3.107	0.66	10.425		
0.45	3.255				
0.46	3.335				
0.47	3.373				
0.48	3.398				

FORMAT FOR TABULATED VALUES OF WAVE RESISTANCE
K. NAKATAKE/ Low Speed Theory (Surface Integral Method) [METHOD 2]

WIGLEY		INUID S-201		SERIES 60	
F_n	C_w	F_n	C_w	F_n	C_w
0.15	0.265	0.15	0.389	0.15	0.057
0.16	0.217	0.16	0.396	0.11	0.062
0.17	0.260	0.17	0.718	0.12	0.052
0.18	0.477	0.18	1.041	0.13	0.044
0.19	0.302	0.19	0.779	0.14	0.069
0.20	0.567	0.20	1.227	0.15	0.080
0.21	0.588	0.21	1.679	0.16	0.078
0.22	0.403	0.22	0.925	0.17	0.051
0.23	0.787	0.23	1.743	0.18	0.033
0.24	1.032	0.24	2.825	0.19	0.100
0.25	0.773	0.25	2.363	0.20	0.200
0.26	0.561	0.26	1.484	0.21	0.115
0.27	0.776	0.27	1.594	0.22	0.124
0.28	1.242	0.28	3.779	0.23	0.194
0.29	1.606	0.30	4.283	0.24	0.182
0.30	1.685	0.31	4.090	0.25	0.362
0.31	1.517	0.33	2.707	0.26	0.931
0.32	1.239	0.35	1.850	0.27	1.589
0.33	0.987	0.37	2.192	0.28	1.934
0.34	0.839	0.39	3.143	0.29	1.843
0.35	0.817	0.41	4.095	0.30	1.460
0.36	0.911	0.43	5.018	0.31	1.080
0.37	1.089	0.45	5.588	0.32	0.908
0.38	1.308	0.48	6.180	0.33	1.032
0.39	1.526	0.51	6.314	0.34	1.443
0.40	1.746	0.54	6.307	0.35	2.039
0.41	1.950	0.57	6.126		
0.42	2.122	0.60	5.814		
0.43	2.252	0.63	5.440		
0.44	2.351	0.66	5.250		
0.45	2.432				
0.46	2.492				
0.47	2.526				
0.48	2.541				

FORMAT FOR TABULATED VALUES OF WAVE RESISTANCE

K. NAKATAKE/ Guevel's Method [METHOD 3]

WIGLEY		INUID S-201		SERIES 60	
F_n	C_w	F_n	C_w	F_n	C_w
0.15	0.298	0.15	0.687	0.10	0.096
0.16	0.236	0.16	0.661	0.11	0.089
0.17	0.233	0.17	0.700	0.12	0.075
0.18	0.451	0.18	1.457	0.13	0.066
0.19	0.267	0.19	0.821	0.14	0.094
0.20	0.563	0.20	1.822	0.15	0.098
0.21	0.458	0.21	1.518	0.16	0.100
0.22	0.399	0.22	1.230	0.17	0.059
0.23	0.791	0.23	2.617	0.18	0.085
0.24	0.859	0.24	2.973	0.19	0.106
0.25	0.569	0.25	1.980	0.20	0.174
0.26	0.522	0.26	1.656	0.21	0.106
0.27	0.878	0.27	2.700	0.22	0.098
0.28	1.322	0.29	4.913	0.23	0.137
0.29	1.527	0.30	4.699	0.24	0.225
0.30	1.427	0.31	3.936	0.25	0.543
0.31	1.160	0.33	2.481	0.26	1.044
0.32	0.898	0.35	2.682	0.27	1.387
0.33	0.763	0.37	4.313	0.28	1.360
0.34	0.796	0.39	6.030	0.29	1.037
0.35	0.977	0.41	6.976	0.30	0.718
0.36	1.268	0.43	7.794	0.31	0.638
0.37	1.605	0.45	7.863	0.32	0.925
0.38	1.951	0.48	7.876	0.33	1.562
0.39	2.257	0.51	7.320	0.34	2.401
0.40	2.517	0.54	6.795	0.35	3.304
0.41	2.736	0.57	6.342		
0.42	2.906	0.60	5.560		
0.43	3.019	0.63	4.706		
0.44	3.086	0.66	4.491		
0.45	3.123				
0.46	3.138				
0.47	3.128				
0.48	3.104				

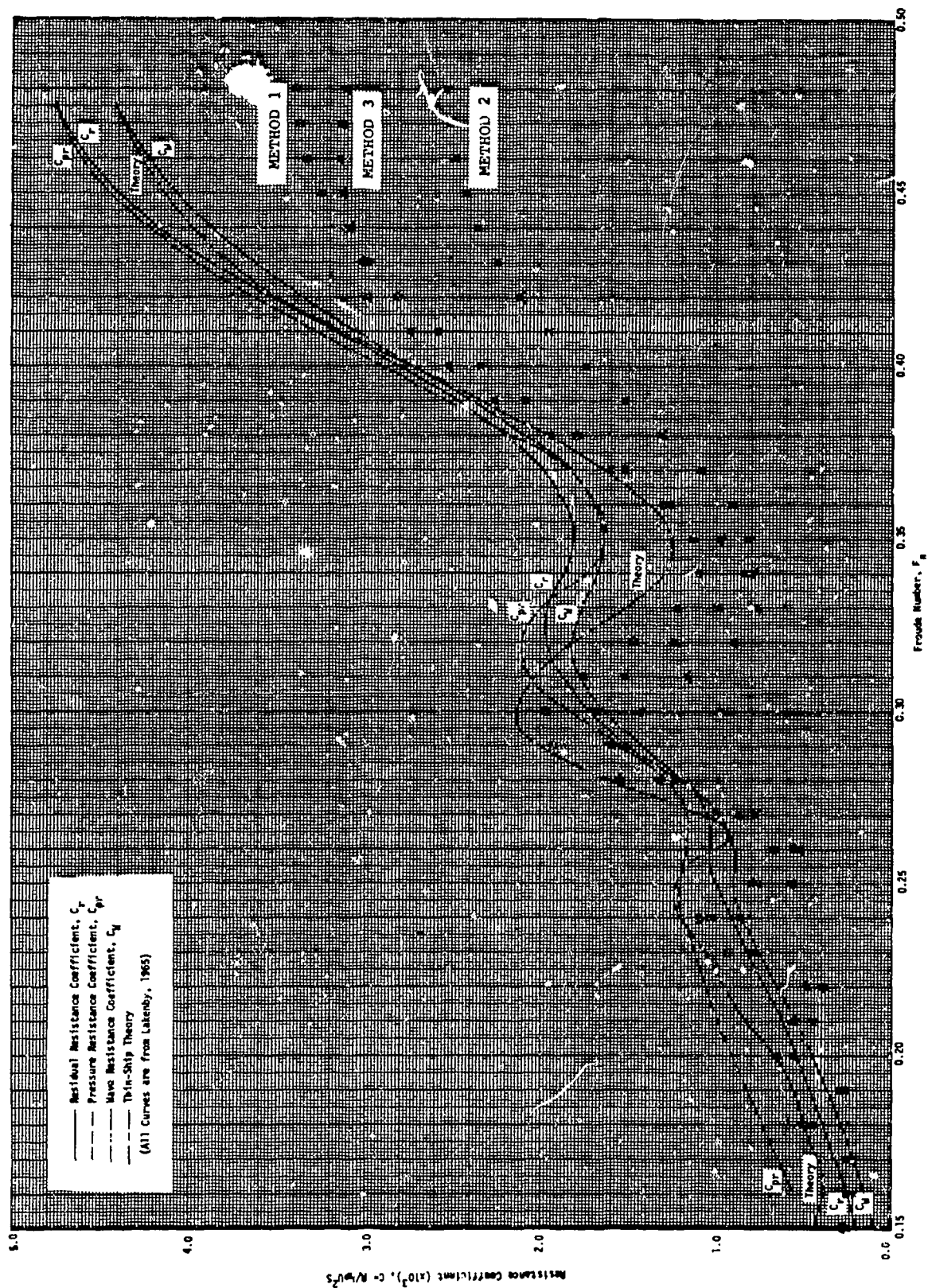


FIGURE 2.3 - Resistance Curves for Wigley Hull
2-4

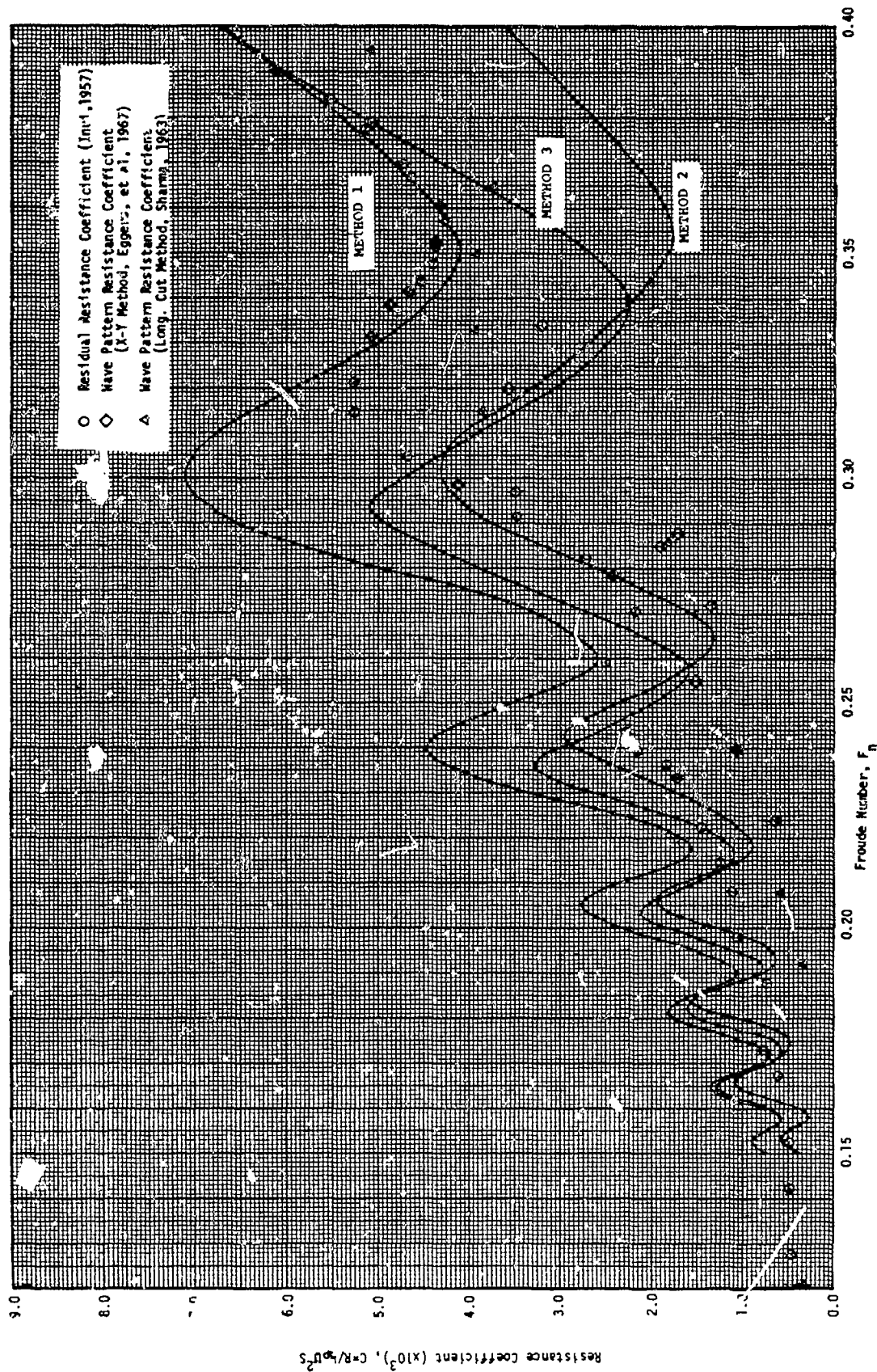


FIGURE 3.3 - Low-Speed Resistance Data, Inuid Hull 11, S-201

3-4

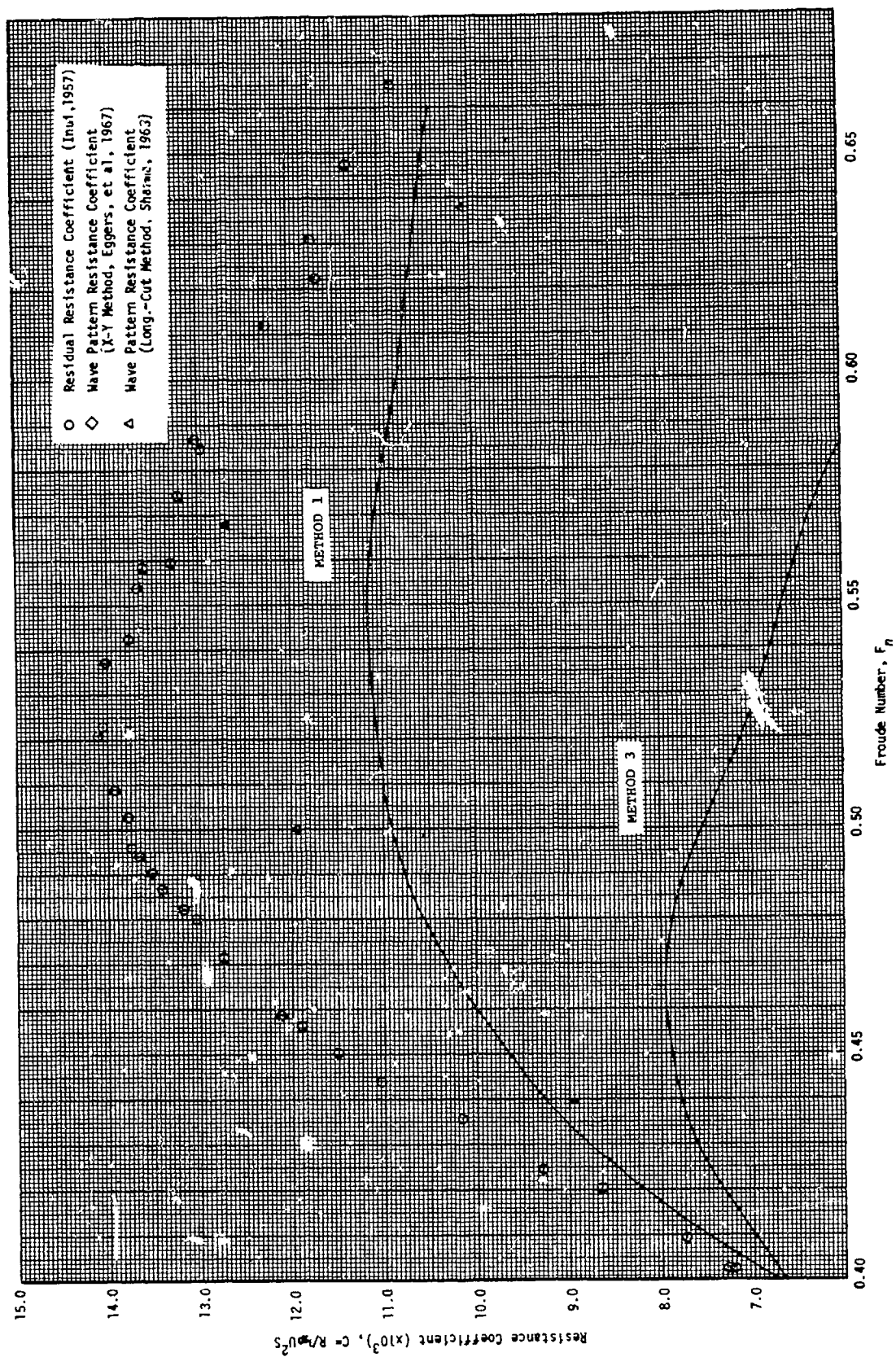


FIGURE 3.4 - High-Speed Resistance Data, Inuid Hull, S-201

3-5

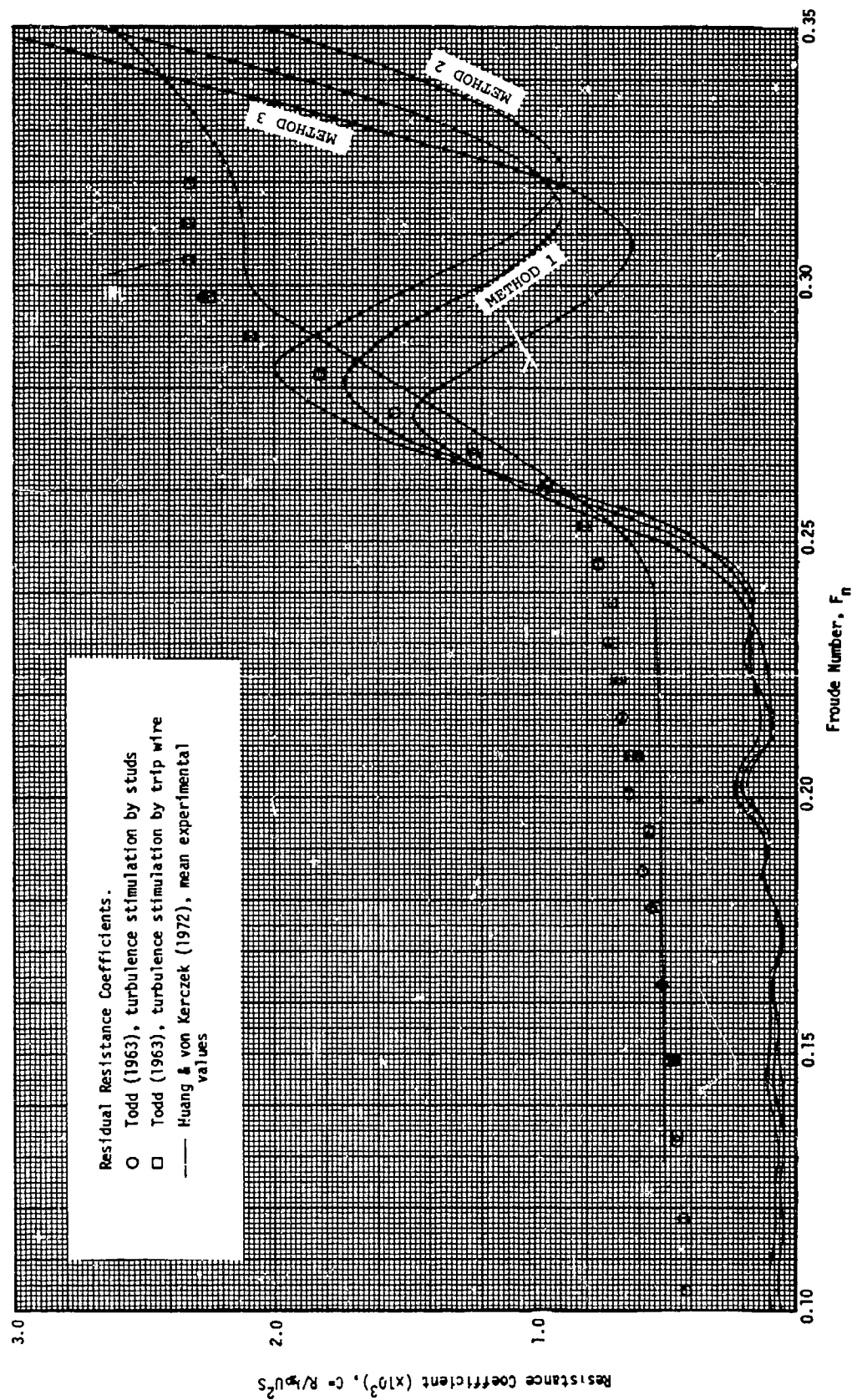


FIGURE 4.4 - Resistance Curves for Series 60, $C_B = 0.60$

CALCULATIONS WITH THE XYZ FREE SURFACE PROGRAM FOR FIVE SHIP MODELS

by Charles W. Dawson

David W. Taylor Naval Ship Research and Development Center

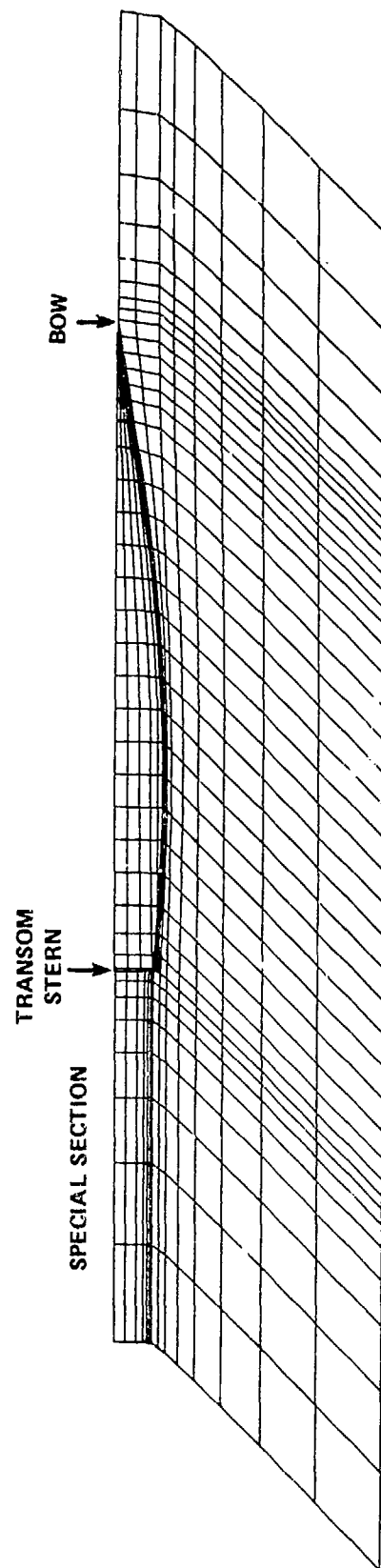
The XYZ FS Program

All five models specified for comparisons at the Workshop on Ship Wave Resistance were analyzed using the XYZ FS program. The basic part of the program has been described previously.¹ The solution is defined in terms of a Rankine source density distributed on the ship surface, on the image of the ship surface above the undisturbed free surface, and on a portion of the undisturbed free surface surrounding the ship. The free surface condition is linearized in terms of the double model solution and is applied at the undisturbed free surface. Both the ship surface boundary condition and the free surface condition are simultaneously satisfied by the solution.

Three additions to the XYZ FS program, since the 1977 International Conference on Numerical Ship Hydrodynamics, provide special calculations for transom sterns, for sinkage and trim and of a form factor.

If a ship has a transom stern, the transom is left open in the calculations and a special section of free surface panels is placed behind the transom. (See Figure 1.) Fluid from the source density on the hull passes through the transom and is absorbed by the free surface panels. Thus the flow separates from the hull at the edge of the transom. The source density on the panels next to the transom is determined so that the pressure at the edge of the transom is approximately zero (atmospheric).

Sinkage and trim are handled by first computing the flow with the ship fixed and then determining the vertical hydrodynamic forces. The ship is assumed to have vertical sides and the amounts of sinkage and trim needed to balance the vertical fluid dynamic forces are computed. If the change in position is large, the ship is then repositioned and the flow is recomputed. Additional iterations have been made in a few cases but have not improved the overall accuracy of the solutions since the convergence



MAIN SECTION OF FREE SURFACE

Figure 1 - Panel Arrangement for the Athena Showing the Local Part of the Free Surface with the Special Section behind the Transom

errors are less than other errors in the calculations.

A partial form factor K_p is computed from a simple formula that is a modification of an equation developed by Granville.² Some of the ideas for the modification were borrowed from the work of Hess.³ The modified formula is

$$K_p = \left[\frac{\iint (U/U_\infty)^{3.8} dS}{\iint dS} \right]^{0.856} - 1, \quad (1)$$

where the integration is over the ship's surface and U/U_∞ is the ratio of the local velocity to the free stream velocity.

A formula this simple cannot be expected to be very accurate and a study by White⁴ of a similar equation developed by Hess³ for axisymmetric bodies confirms the inaccuracy. However, the simplicity of the formula allows the partial form factor to be computed at each Froude number and the results have been useful.

Granville's work² showed that, for a ship with a cruiser stern, the total form factor is approximately twice the partial form factor. The difference is probably due to separation near the stern, generation of bilge vortices, and other three-dimensional effects. For a ship with a transom stern, the partial form factor should be closer to the total form factor since the separation of the stern is already accounted for. A coefficient of 1.5 was therefore chosen for use in calculations for the Athena.

The residual resistance coefficient is given by the following formula:

$$C_r = [(1 + \alpha K_p) S/S_0 - 1] C_f + C_w \quad (2)$$

where α is 1.5 for transom sterns and 2.0 for other sterns,

K_p is the partial form factor,

C_f is the 1957 ITTC friction coefficient,

C_w is the wave resistance coefficient, and

S/S_0 is the ratio of the wetted surface with sinkage and trim to the wetted surface with the ship fixed. The change in the wetted surface due to the wave profile is not included.

Panel Arrangements

Some features of the panel arrangements were the same for all five of the ship models. Eight rows of panels were used to represent the hull from the keel to the undisturbed free surface. The local region of the surface extended about $3/8$ of a ship length to the side and was represented by eight rows of panels. The panels were smaller near the bow and stern and also near the hull-free surface intersection than elsewhere.

The number of panels in a row and the extent of the free surface region ahead of and behind the ship varied as shown in Table 1. The Athena calculations also required a special region of free surface panels behind the transom. This region was as wide as the transom and extended $1/2$ ship length downstream. It was modeled with six rows of panels, with eight panels per row. Figure 1 shows the panels for the Athena as seen from below.

The HSVA Tanker was a special case. The maximum number of panels allowed by XYZ FS is 572. The low Froude numbers for the HSVA Tanker require better resolution than can be provided for the entire ship by 572 panels. Therefore, separate calculations were made for the bow and stern ends of the HSVA Tanker and the results were added together. The mid-section of the Tanker was left open so that, in effect, the bow and stern were the ends of two semi-infinite bodies.

TABLE 1 - PANEL ARRANGEMENTS

Ship	Panels per Row		Extent of Free Surface Ahead & Behind Ship in Ship Lengths
	Hull	Free Surface	
Early Wigley	26	36	$1/4$
Present Wigley	22	36	$3/8$
Inuid	24	40	$1/2$
Series 60	26	36	$1/4$
HSVA Tanker bow or stern	26	38	$1/4$
Athena	24	40	$1/2$

The values of the block coefficient C_B and the wetted surface coefficient C_S were computed from the panels for each ship. In Table 2, these values of C_B and C_S are compared with the values given in the Workshop instructions. The value of the wetted surface computed from the panel data was used in computing the resistance coefficients for all of the ship models.

TABLE 2 - COMPUTED AND "INSTRUCTION" VALUES OF THE BLOCK AND WETTED SURFACE COEFFICIENTS

Ship	C_B		C_S	
	Instructions	XYZ FS	Instructions	XYZ FS
Wigley	.444	.441	.661	.660
Inuid	.537	.526	.665	.663
Series 60	.600	.588	.710	.710
HSVA Tanker	.8503	.830	.8815	.883
Athena	.4775	.472	.6607	.651

Results

The computed values of the wave resistance coefficients are given in Table 3. When the models were repositioned for sinkage and trim, two values are given for the wave resistance coefficients.

The computed changes in the levels of the bow and stern for sinkage and trim are given in Table 4. Here a negative value means the model is lower than it was in the fixed position. Figures 2, 3, and 4 compare these results with experimental results for the Inuid, Series 60, and Athena models. Table 4 also gives the ratio of the area of the new wetted surface to the wetted area when the model was in the fixed position.

Table 5 gives the values of the quantities used in computing the residual resistance and the resulting residual resistance coefficients. Figures 5 through 9 compare these results with the experimental results.

Tables 6 through 9 give the computed wave profiles for the Wigley, Series 60, and Athena models. For the Athena, separate profiles are given for the model fixed and the model free to sink and trim. For the other ships, only one set of profiles is given. The model is free to sink and trim only at the higher Froude numbers where sinkage and trim are important.

Although the results of these calculations are generally very good, there are a few problem areas. The calculations for the Athena broke down completely for Froude numbers of 0.8 and 1.0. This result was expected since the length of the local region of the free surface (2 ship lengths) was less than the length of a two-dimensional wave, $2\pi F_n^2$, for Froude numbers greater than $1/\sqrt{\pi}$ (~ 0.564).

The calculations for the HSVA Tanker are also not satisfactory, in this case, because of inadequate resolution at low Froude numbers. This was also to be expected because the typical panel length near midship is 1/20 of the ship length. Thus, there are fewer than 5 panels per two-dimensional wave length for Froude numbers less than .2.

The results for the Inuid were a surprise. The computed wave resistance is too large, especially at the lower Froude numbers. The Inuid has an odd shape, but the results were still unexpected, and the reasons for the large values of wave resistance are not yet understood.

Arranging panels is still an art. Better resolution on the ship tends to give higher values for the wave resistance. Better representation of the free surface ahead of and behind the ship tends to give lower values for the wave resistance. The effect of different panel arrangements is shown by the difference in the earlier and present Wigley calculations; in this instance, the wave resistance changed by 10%. Clearly similar panel arrangements must be used when comparing different ship designs.

The computed values for sinkage agree quite well with the experimental values for the Series 60 and Inuid. The calculation of trim, however, is much less accurate than that of sinkage. The trim values computed for the Series 60 are fairly close to the experimental values for the higher Froude numbers ($F_n > .27$) but not for the lower Froude numbers.

The computation of trim for the Athena presents a problem. The hull is turned down next to the transom to reduce the amount of trim. The computed values of trim are reasonable for this type of ship but differ significantly from the experimental values. The ship line data do not give enough detail for the hull near the stern, and the discrepancy in the

trim may result from poor representation of this part of the hull.

The most gratifying result is the substantial effect of sinkage and trim on the resistance for Froude numbers greater than 0.3. This result was not expected but has now been confirmed by towing-tank experiments on the Athena carried out recently at DTNSRDC.

Although the computation of the form resistance is quite crude, the results compare well with experimental data. The form resistance as included in Equation (2) is a function of the Froude number and the Reynolds number. As a result the form resistance generally increases with Froude number but decreases with Reynolds number.

The previously reported wave resistance calculations¹ for the Series 60 model were in error. The corrected values for the wave resistance with the model fixed are much smaller than the earlier values. The corrected values, with the effects of sinkage, trim, and form resistance included, are quite good. (See Figure 7.)

Acknowledgment

This work was supported by the 6.2 Mathematical Sciences Research Program sponsored by the Naval Material Command (Task Area ZF 43411001, Program Element 62543N: Ships, Submarines, and Boats).

References

1. Dawson, C.W., "A Practical Computer Method for Solving Ship-Wave Problems," Proceedings of the Second International Conference on Numerical Ship Hydrodynamics, University of California, Berkeley (Sep 1977).
2. Granville, Paul S., "Partial Form Factors from Equivalent Bodies of Revolution for the Froude Method of Predicting Ship Resistance," First Ship Technology and Research (STAR) Symposium, The Society of Naval Architects and Marine Engineers, Washington, D.C. (Aug 1975).
3. Hess, John L., "On the Problem of Shaping an Axisymmetric Body to Obtain Low Drag at Large Reynolds Numbers," J. Ship Res., Vol. 20, No. 1 (May 1976).
4. White, Nadine M., "A Comparison Between a Simple Drag Formula and Experimental Drag Data for Bodies of Revolution," David W. Taylor Naval Ship Research and Development Center Report 77-0028 (Jan 1977).

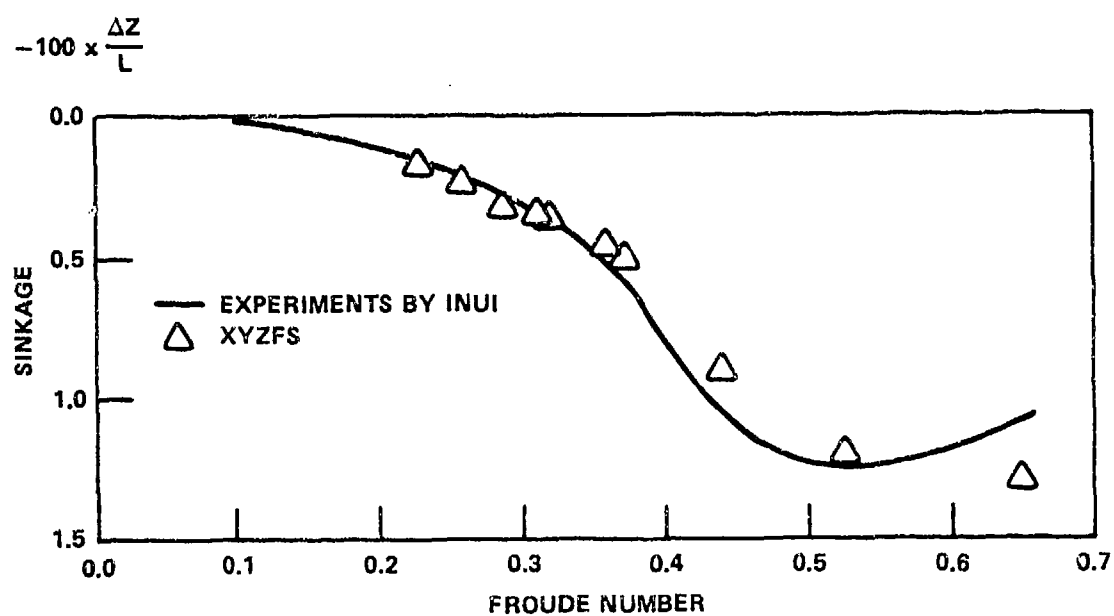


Figure 2 - Experimental and Computed Values for the Sinkage of the Inuid Model

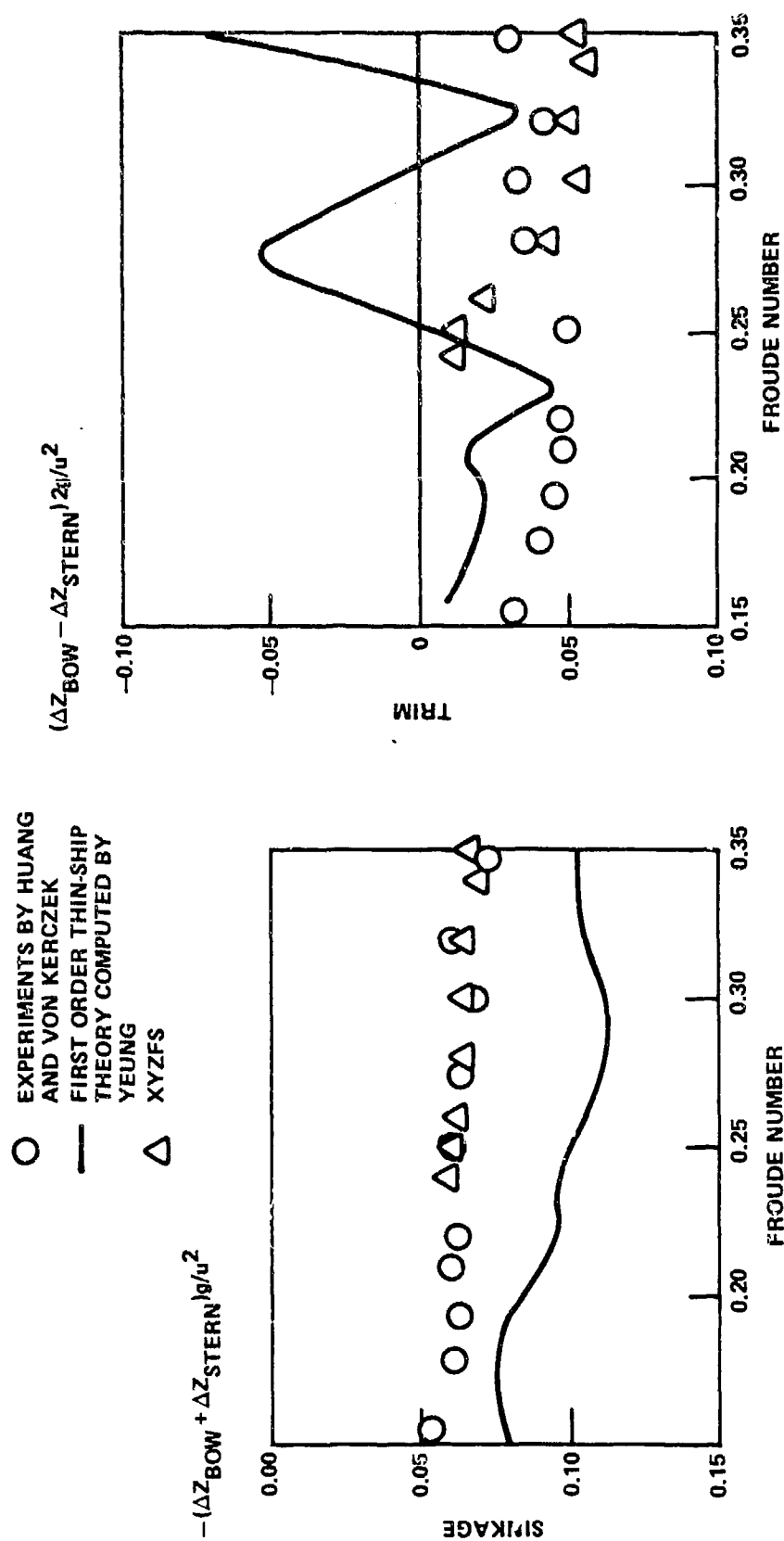


Figure 3 - Dimensionless Sinkage and Trim for the Series 60 Model

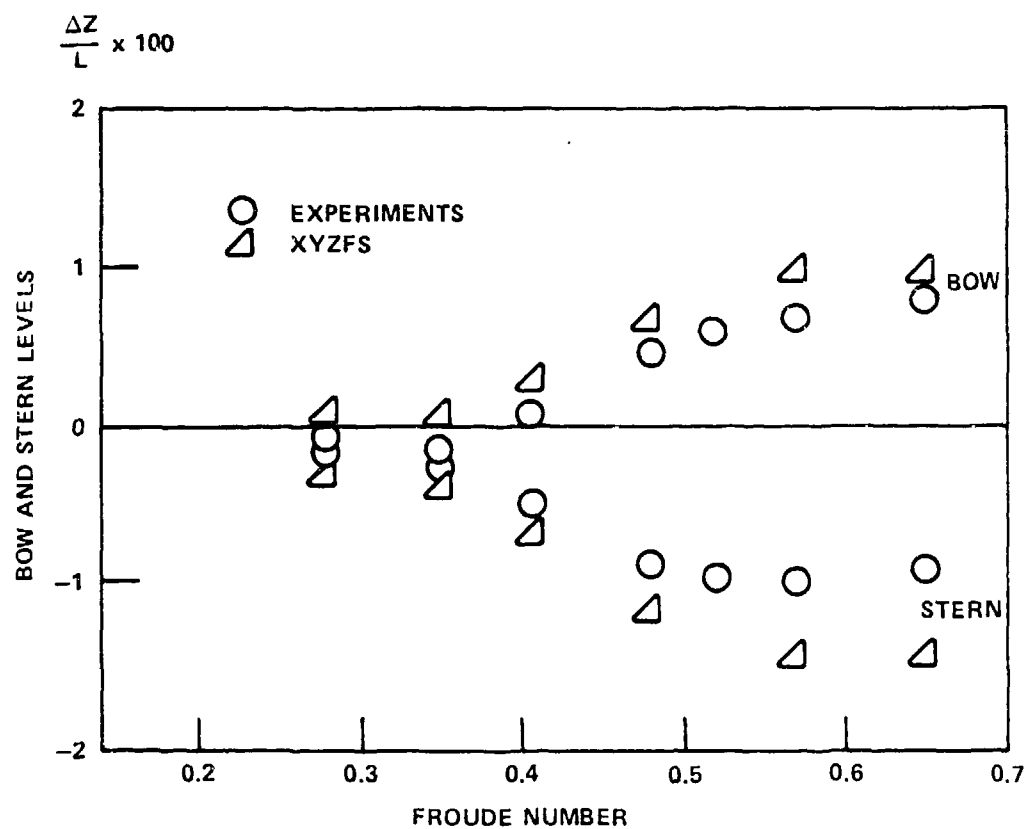


Figure 4 -- Changes in Bow and Stern Levels for the Athena Model

$$C \times 1000 = \frac{R}{\frac{1}{2} \rho u^2 S}$$

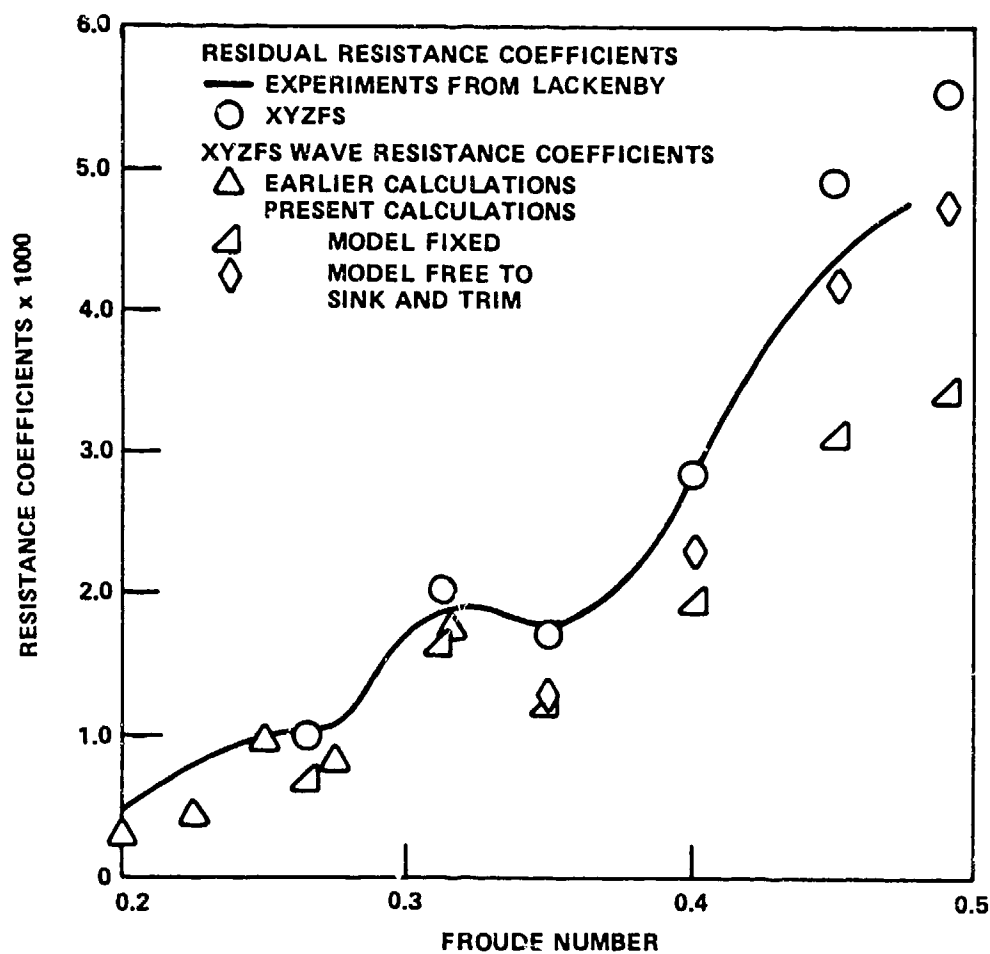


Figure 5 - Comparison of Resistance Coefficients for the Wigley Model

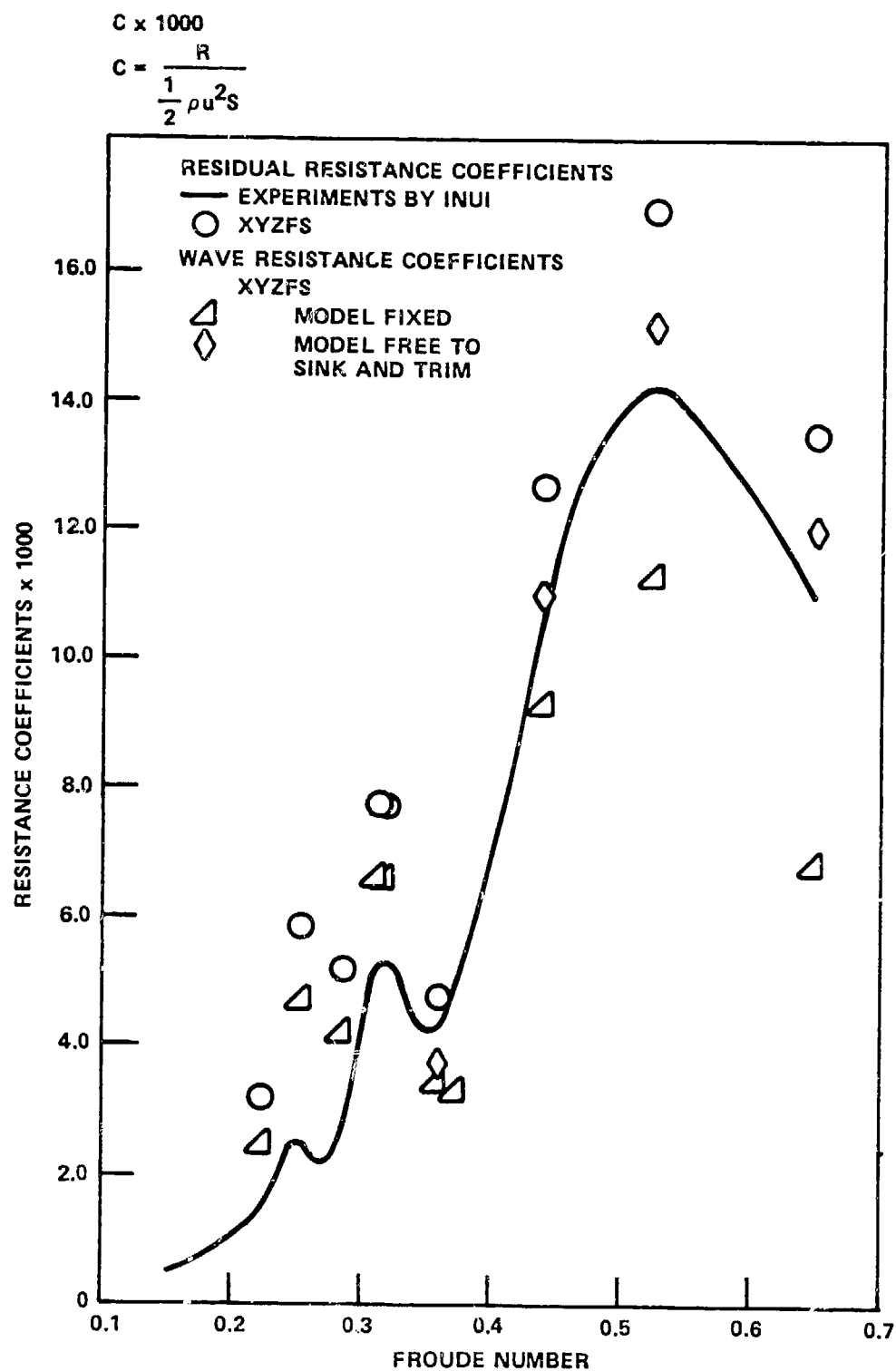


Figure 6 - Comparison of Resistance Coefficients for the Inuid Model

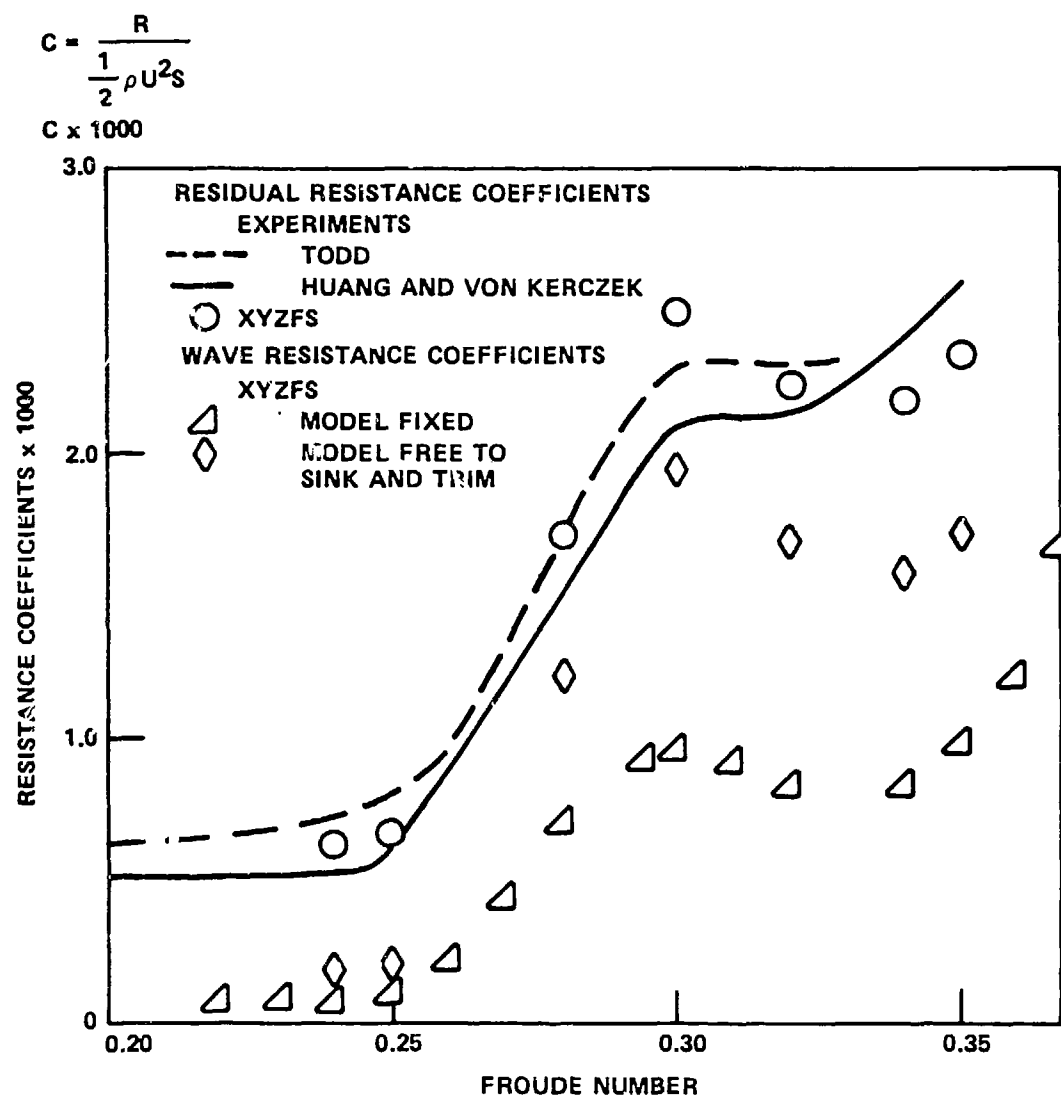


Figure 7 - Comparison of Resistance Coefficients for the Series 60 Model

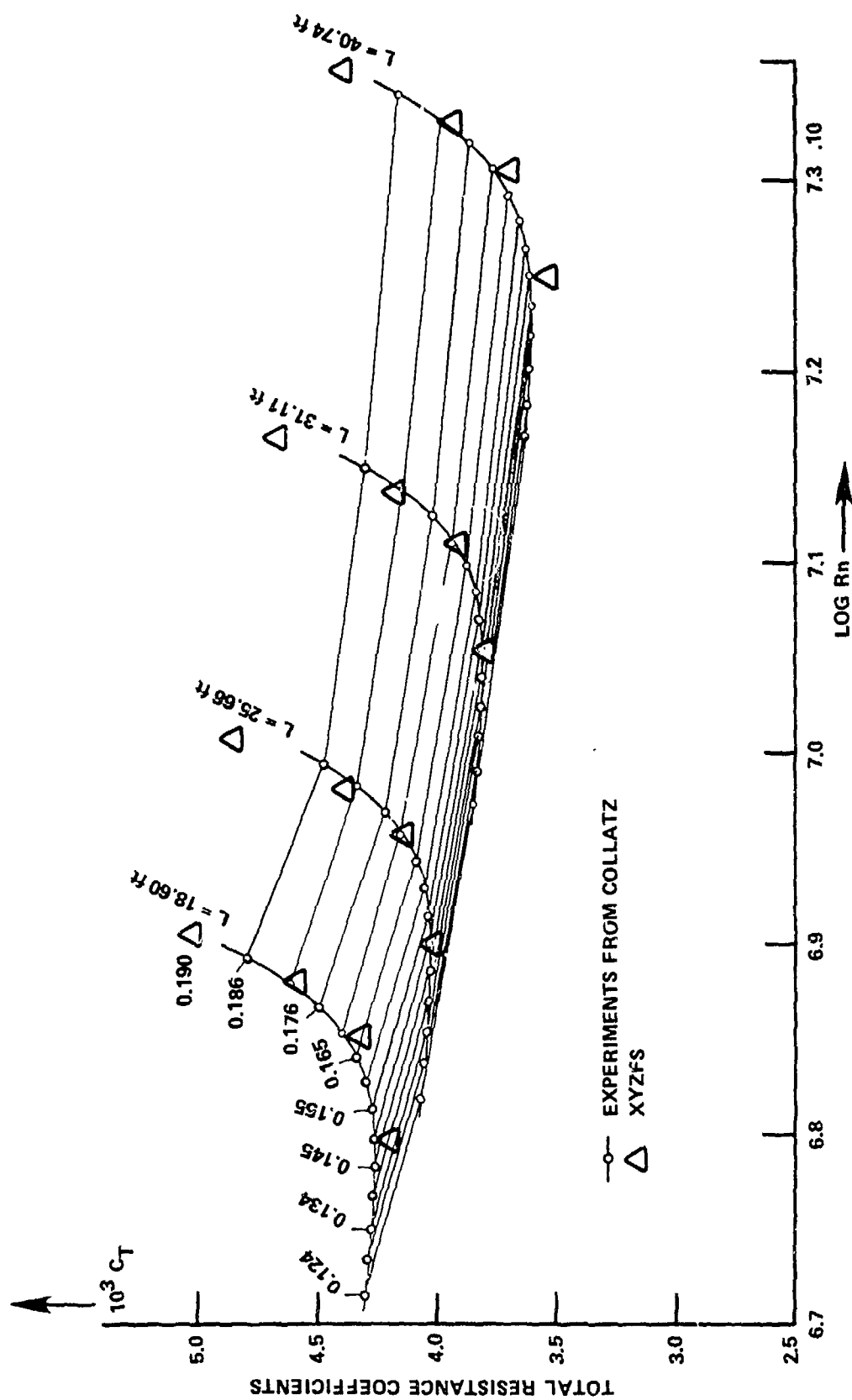


Figure 8 - Computed and Experimental Values of the Total Resistance for Four Models of the HSVA Tanker

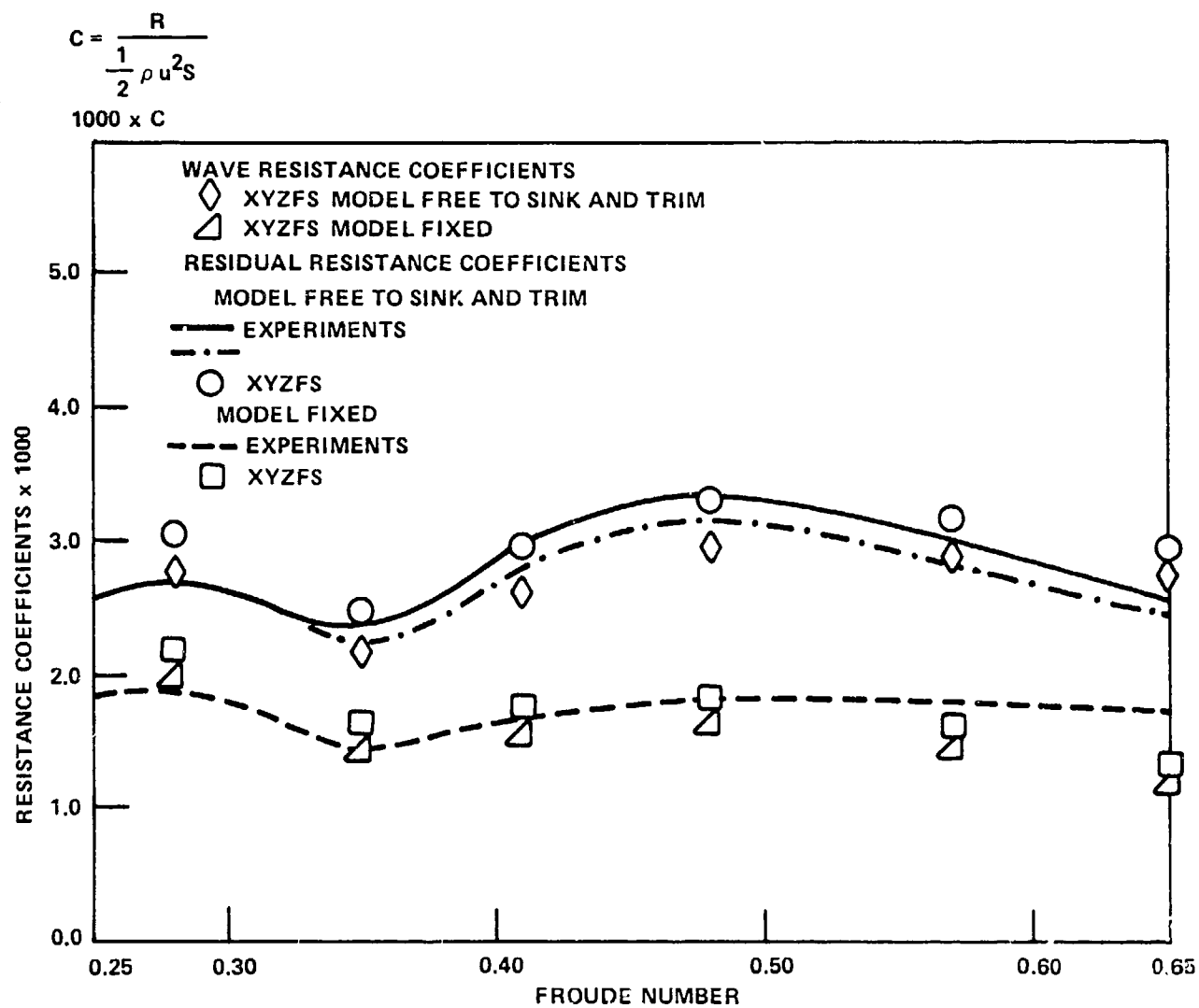


Figure 9 - Comparison of Resistance Coefficient for the Athena Model

TABLE 3 - COMPUTED WAVE RESISTANCE COEFFICIENTS

Earlier Calculations Wigley		Present Calculations Wigley		Inuid		HSVA Tanker	
F_n	$1000 \times C_w$	F_n	$1000 \times C_w$	F_n	$1000 \times C_w$	F_n	$1000 \times C_w$
Model	Fixed	Model		Model		Model	
		Fixed	Fixed	Fixed	Fixed	Fixed	Fixed
0.200	0.30	0.266	0.70	0.2255	2.23	0.15	0.07
0.225	0.43	0.313	1.66	0.255	4.76	0.17	0.25
0.250	0.97	0.350	1.23	0.287	4.10	0.18	0.54
0.275	0.82	0.402	1.94	0.311	6.63	0.19	1.02
0.316	1.79	0.452	3.13	0.319	6.60		
0.350	1.35	0.482	3.44	0.360	3.46		
		Model Free to Sink & Trim		0.371	3.30		
				0.440	9.30		
		0.350	1.31	0.525	11.31		
		0.402	2.31	0.650	6.81		
		0.452	4.21	Model Free to Sink & Trim			
		0.482	4.79				
				0.360	3.76		
				0.440	11.04		
				0.525	15.18		
				0.650	12.05		

TABLE 3 (Continued)

Series 60			Series 60			Athena			Athena		
F_n	$1000 \times C_w$		r_n	$1000 \times C_w$		F_n	$1000 \times C_w$		F_n	$1000 \times C_w$	
Model Fixed			Model Free to Sink & Trim			Model Fixed			Model Free to Sink & Trim		
0.220	0.09		0.240	0.19		0.28	1.98		0.28	2.78	
0.231	0.10		0.250	0.21		0.35	1.43		0.35	2.18	
0.240	0.09		0.280	1.23		0.41	1.54		0.41	2.62	
0.250	0.11		0.300	1.96		0.48	1.62		0.48	2.96	
0.260	0.13		0.320	1.70		0.57	1.44		0.57	2.89	
0.270	0.45		0.340	1.59		0.65	1.18		0.65	2.71	
0.280	0.72		0.350	1.73							
0.294	0.94										
0.300	0.96										
0.310	0.93										
0.320	0.85										
0.340	0.85										
0.350	1.01										
0.359	1.24										
0.3675	1.57										

TABLE 4 - COMPUTED CHANGES IN THE WETTED SURFACE
AND IN LEVELS OF THE BOW AND STERN

F_n	$100 \times \Delta Z/L$ Bow	$100 \times \Delta Z/L$ Stern	S/S_0
Wigley			
0.266	-0.15	-0.13	1.018
0.313	-0.16	-0.25	1.028
0.350	-0.23	-0.30	1.036
0.402	-0.05	-0.80	1.057
0.452	+0.29	-1.41	1.076
0.482	+0.46	-1.69	1.083
Inuid			
0.2255	-0.17	-0.17	1.016
0.255	-0.23	-0.23	1.022
0.287	-0.31	-0.31	1.029
0.311	-0.36	-0.35	1.034
0.319	-0.37	-0.36	1.035
0.360	-0.46	-0.45	1.043
0.371	-0.51	-0.50	1.047
0.440	-0.92	-0.87	1.085
0.525	-1.24	-1.14	1.113
0.650	-1.35	-1.23	1.122
Series 60			
0.24	-0.153	-0.185	1.021
0.25	-0.168	-0.205	1.023
0.26	-0.173	-0.242	1.025
0.28	-0.163	-0.336	1.030
0.30	-0.175	-0.412	1.035
0.32	-0.196	-0.450	1.039
0.34	-0.238	-0.556	1.047
0.35	-0.241	-0.558	1.048
Athena			
0.23	+0.103	-0.277	1.014
0.35	+0.095	-0.371	1.022
0.41	+0.304	-0.690	1.030
0.49	+0.662	-1.120	1.035
0.57	+0.963	-1.420	1.035
0.65	+0.958	-1.427	1.035

TABLE 5 - COMPUTATION OF RESIDUAL RESISTANCE COEFFICIENTS

F_n	K_p	S/S_0	$C_f \times 1000$	$C_w \times 1000$	$C_r \times 1000$
Wigley: 20 ft. Model					
0.266	0.044	1.018	2.88	.70	1.01
0.313	0.054	1.028	2.80	1.66	2.05
0.350	0.052	1.036	2.75	1.31	1.71
0.402	0.069	1.057	2.69	2.31	2.86
0.452	0.091	1.076	2.64	4.21	4.93
0.482	0.094	1.083	2.61	4.79	5.54
Inuid: 1.75 meter Model					
0.2255	0.108	1.016	4.14	2.23	3.20
0.255	0.121	1.022	4.01	4.76	5.84
0.287	0.118	1.029	3.91	4.10	5.16
0.311	0.126	1.034	3.85	6.63	7.76
0.319	0.123	1.035	3.83	6.60	7.71
0.360	0.112	1.043	3.74	3.76	4.79
0.440	0.173	1.085	3.60	11.04	12.70
0.525	0.180	1.113	3.48	15.18	16.97
0.650	0.141	1.122	3.35	12.05	13.52
Series 60: 20 ft. Model					
0.24	0.064	1.021	2.91	0.19	0.63
0.25	0.065	1.023	2.89	0.21	0.66
0.28	0.077	1.030	2.83	1.23	1.73
0.30	0.078	1.035	2.80	1.96	2.51
0.32	0.077	1.039	2.77	1.70	2.25
0.34	0.084	1.047	2.74	1.59	2.20
0.35	0.087	1.048	2.73	1.73	2.36
HSVA Tanker: 31.11 ft. Model					
0.15	0.127	1.0	2.93	0.07	0.81
0.17	0.131	1.0	2.87	0.25	1.00
0.18	0.134	1.0	2.84	0.54	1.30
0.19	0.138	1.0	2.82	1.02	1.80
HSVA Tanker: 18.6 ft. Model					
0.15	0.127	1.0	3.26	0.07	0.90
0.17	0.131	1.0	3.18	0.25	1.08
0.18	0.134	1.0	3.15	0.54	1.38
0.19	0.138	1.0	3.12	1.02	1.88

TABLE 5 - Continued

F_n	K_p	S/S_0	$C_f \times 1000$	$C_w \times 1000$	$C_r \times 1000$
Athena: 18.67 ft. Model, Model Fixed					
0.28	0.045	1.0	2.90	1.98	2.18
0.35	0.043	1.0	2.80	1.43	1.61
0.41	0.050	1.0	2.72	1.54	1.74
0.48	0.051	1.0	2.65	1.62	1.82
0.57	0.041	1.0	2.58	1.44	1.60
0.65	0.032	1.0	2.53	1.18	1.30
Athena: 18.67 ft. Model, Model Free to Sink and Trim					
0.28	0.050	1.014	2.90	2.78	3.04
0.35	0.050	1.022	2.80	2.18	2.46
0.41	0.060	1.030	2.72	2.62	2.95
0.48	0.059	1.035	2.65	2.96	3.30
0.57	0.047	1.035	2.58	2.89	3.17
0.65	0.032	1.035	2.53	2.71	2.92

TABLE 6 - WAVE PROFILES FOR THE WIGLEY MODEL

$x \backslash F_n$	0.266*	0.313*	0.350	0.402	0.452	0.482
1.0	Bow					
0.971	0.227	0.176	0.157	0.112	0.064	0.046
0.919	0.279	0.236	0.218	0.193	0.156	0.132
0.856	0.199	0.213	0.212	0.188	0.164	0.147
0.782	0.055	0.117	0.143	0.156	0.150	0.144
0.695	-0.056	0.019	0.053	0.075	0.082	0.084
0.599	-0.112	-0.050	-0.006	0.031	0.049	0.051
0.494	-0.113	-0.091	-0.057	-0.011	0.017	0.029
0.384	-0.075	-0.111	-0.095	-0.047	-0.015	-0.006
0.273	-0.032	-0.104	-0.116	-0.082	-0.039	-0.023
0.163	-0.008	-0.081	-0.112	-0.101	-0.071	-0.050
0.053	-0.010	-0.052	-0.102	-0.104	-0.088	-0.079
-0.058	-0.034	-0.023	-0.084	-0.111	-0.092	-0.088
-0.168	-0.062	-0.010	-0.057	-0.117	-0.106	-0.092
-0.278	-0.078	-0.014	-0.034	-0.105	-0.125	-0.109
-0.388	-0.073	-0.024	-0.023	-0.083	-0.132	-0.131
-0.499	-0.047	-0.037	-0.015	-0.066	-0.121	-0.140
-0.604	-0.016	-0.054	-0.007	-0.058	-0.104	-0.130
-0.700	0.006	-0.066	-0.004	-0.052	-0.099	-0.119
-0.786	0.010	-0.070	-0.009	-0.037	-0.106	-0.123
-0.861	0.014	-0.056	-0.012	-0.009	-0.091	-0.111
-0.924	-0.003	-0.060	-0.045	-0.005	-0.091	-0.109
-0.979	0.068	0.011	-0.027	0.002	-0.109	-0.141
-1.0	Stern					

*Model Fixed

TABLE 7 - WAVE PROFILES FOR THE SERIES 60 MODEL

$X \backslash F_n$	0.22*	0.25	0.28	0.30	0.32	0.35
1.0	Bow					
0.992	0.188	0.150	0.104	0.106	0.086	0.092
0.974	0.245	0.201	0.155	0.151	0.128	0.127
0.954	0.301	0.257	0.206	0.195	0.173	0.164
0.930	0.294	0.280	0.250	0.235	0.215	0.197
0.902	0.232	0.264	0.255	0.241	0.232	0.215
0.874	0.191	0.220	0.243	0.236	0.233	0.217
0.844	0.221	0.214	0.220	0.215	0.219	0.213
0.809	0.161	0.199	0.226	0.222	0.221	0.214
0.769	0.086	0.146	0.199	0.216	0.242	0.255
0.726	0.054	0.121	0.164	0.174	0.189	0.207
0.671	0.023	0.050	0.108	0.135	0.157	0.165
0.597	-0.012	-0.010	0.030	0.053	0.083	0.106
0.500	-0.044	-0.061	-0.039	-0.015	0.014	0.008
0.379	-0.071	-0.114	-0.144	-0.132	-0.112	-0.085
0.248	-0.111	-0.129	-0.179	-0.191	-0.191	-0.170
0.118	-0.122	-0.104	-0.150	-0.185	-0.207	-0.212
-0.011	-0.090	-0.062	-0.077	-0.121	-0.165	-0.206
-0.142	-0.064	-0.054	-0.021	-0.044	-0.086	-0.154
-0.271	-0.082	-0.097	-0.041	-0.020	-0.036	-0.101
-0.401	-0.110	-0.134	-0.113	-0.055	-0.0282	-0.073
-0.532	-0.091	-0.104	-0.157	-0.104	-0.042	-0.056
-0.666	0.007	-0.018	-0.115	-0.128	-0.065	-0.041
-0.785	0.099	0.105	0.066	-0.006	-0.004	+0.044
-0.870	0.176	0.154	0.225	0.154	0.116	+0.144
-0.935	0.201	0.219	0.280	0.235	0.183	0.199
-0.985	0.198	0.261	0.329	0.297	0.239	0.239
-1.0	Stern					

*Model Fixed

TABLE 8 - WAVE PROFILES FOR THE ATHENA
(Model Fixed)

$X \backslash F_n$	0.35	0.41	0.48	0.57
1.0	Bow			
0.972	0.047	0.033	0.026	0.021
0.922	0.112	0.079	0.050	0.037
0.874	0.135	0.115	0.091	0.069
0.824	0.137	0.124	0.098	0.080
0.774	0.069	0.108	0.114	0.096
0.724	0.022	0.046	0.072	0.084
0.642	0.053	0.041	0.039	0.039
0.550	0.040	0.050	0.047	0.038
0.450	-0.002	0.021	0.033	0.042
0.349	-0.017	-0.002	0.014	0.023
0.249	-0.027	-0.011	0.002	0.007
0.149	-0.037	-0.025	0.007	0.001
0.049	-0.040	-0.040	-0.023	-0.002
-0.051	-0.050	-0.051	-0.040	-0.020
-0.151	-0.056	-0.059	-0.051	-0.038
-0.251	-0.055	-0.071	-0.055	-0.054
-0.351	-0.047	-0.075	-0.068	-0.051
-0.452	-0.043	-0.069	-0.081	-0.050
-0.552	-0.032	-0.053	-0.081	-0.053
-0.652	-0.012	-0.037	-0.064	-0.066
-0.753	0.009	-0.018	-0.036	-0.068
-0.845	0.015	-0.001	-0.009	-0.052
-0.920	0.009	-0.008	-0.047	-0.030
-0.978	-0.008	-0.026	-0.072	-0.045
-1.0	Stern			

TABLE 9 - WAVE PROFILES FOR THE ATHENA
(Model Free to Sink and Trim)

$\frac{x}{F_n}$	0.35	0.41	0.48	0.57
1.0	Bow			
0.972	0.044	0.027	0.016	0.012
0.922	0.112	0.072	0.035	0.023
0.874	0.132	0.106	0.072	0.046
0.824	0.139	0.118	0.082	0.056
0.774	0.067	0.105	0.103	0.073
0.717	0.028	0.051	0.077	0.073
0.642	0.058	0.050	0.054	0.054
0.550	0.044	0.055	0.055	0.050
0.450	0.003	0.029	0.045	0.050
0.349	-0.012	0.008	0.030	0.038
0.249	-0.024	-0.002	0.018	0.029
0.149	-0.035	-0.017	0.006	0.017
0.049	-0.040	-0.034	-0.009	0.016
-0.051	-0.052	-0.049	-0.031	-0.003
-0.151	-0.059	-0.059	-0.045	-0.019
-0.251	-0.057	-0.072	-0.055	-0.042
-0.351	-0.051	-0.079	-0.064	-0.043
-0.452	-0.047	-0.077	-0.081	-0.050
-0.552	-0.038	-0.064	-0.089	-0.049
-0.652	-0.020	-0.052	-0.079	-0.066
-0.753	-0.001	-0.037	-0.061	-0.066
-0.845	0.003	-0.017	-0.064	-0.074
-0.920	-0.015	-0.050	-0.022	-0.063
-0.978	-0.048	-0.055	-0.002	-0.066
-1.0	Stern			

Calculation of Ship Wave Resistance with Special Reference to Sinkage

Katsuo SUZUKI
National Defense Academy

1. Introduction: The aim of the present paper is to develop Neumann-Kelvin problem (NK-problem) as a method of calculating the effect of the sinkage on the ship wave resistance.

The effects of sinkage and trim have been neglected because of their smallness. The sinkage is small, but the force of sinkage, which is calculated from the increment of the hydrostatic buoyancy caused by the sinkage, are known to be about ten times as large as the wave resistance. The wave resistance measured for the Wigley model with sinkage fixed is 10 to 20% less than the value with free sinkage.

It is important to consider the effect of the sinkage on the ship wave resistance^{1,2)}. But there were very few calculations^{3,4)} about sinkage or sinkage force. We are not aware of the relations between sinkage and wave resistance.

According to the previous study on the two-dimensional problem⁵⁾, it was found that the regular solution of the NK-problem including the line-integral term shows an abnormal flow, and for this reason the new source singularities should be added at the points of intersection between the body and the free surface. Their strength is approximately proportional to the sinkage and the solution with the singularities seems reasonable than that without.

In this paper, the extension to the three dimensional problem is performed.

2. Regular Neumann-Kelvin solution: Let the velocity potential be $\Phi = -x + \phi$, which is non-dimensionalized by the uniform velocity, U , and the ship length, L . The boundary conditions of the NK-problem are formulated as follows.⁶⁾

$$\Phi_{xx} + \kappa \Phi_z = 0 \quad \text{on } F \quad \dots (1)$$

$$\Phi_n = \partial \phi / \partial n \quad \text{on } H \quad \dots (2)$$

Here, F and H stand for the undisturbed water surface ($z = 0$) excluding the inside of the ship hull and the hull surface ($z < 0$) respectively. z is positive upwards and κ is the wave number. The NK-solution can be represented as follows.⁶⁾

$$\Phi(P) = \frac{1}{4\pi} \iint_H (\Phi_n(Q) - \Phi(Q) \frac{\partial}{\partial n_Q}) W(P, Q) dS_Q$$

$$-\frac{1}{4\pi\kappa} \oint_C (\phi_x(Q) - \phi(Q) \frac{\partial}{\partial x_0}) W(P, Q) dy_0 \quad \dots(3)$$

where $W(P, Q)$ is the wave source potential. The solution is written by the source alone as⁶⁾

$$\phi(P) = \frac{1}{4\pi} \iint_H \sigma(Q) W(P, Q) dS_Q - \frac{1}{4\pi\kappa} \oint_C \sigma(Q) \eta x_0 W(P, Q) dy_0. \quad \dots(4)$$

The second terms of the RHS of eqs. (3), (4) are the line-integral terms. When the ship is very thin, the line-integral term turns out higher order and negligible. However, the representations of eqs. (3), (4) are regular near the contour of intersection, C , between the undisturbed water surface and the hull surface only when accompanied by the line-integral term. Let us define the solutions (3), (4) as 'regular NK-solutions'.

The NK-problem is not consistent from the standpoints of perturbation method. It has two kinds of inconsistency. The above free surface condition (1) and the hull surface condition (2) are different in the order of magnitude. Furthermore, the hull surface condition is given precisely on the hull for $z < 0$ but it lacks the condition for $z > 0$. This inconsistency can be shown directly by the flux of water out of the undisturbed water surface. While the total flux of water out of the free surface vanishes in the consistent theory of thin ship⁷⁾, the flux of water, Q , is given by

$$Q = \iint_F \phi_z dx dy - \frac{1}{\kappa} \oint_C \phi_x dy - \oint_C \zeta dy \quad \dots(5)$$

which does not vanish in general for the regular NK-solution⁸⁾. Here, ζ stands for the wave elevation along the hull. It seems irrational that the flux, Q , flows out of the system which caused the unrealistic stream-lines in the two-dimensional regular NK-solution.⁵⁾

This disadvantage can not be removed by treating only the regular NK-solution. Hence, we introduce the singular NK-solution which is derived from the free surface condition of higher order. We consider additionally a condition of sheltering effect¹⁰⁾.

3. Singular NK-solution and sheltering effect: The singular NK-solution can be derived as a part of the particular solution satisfying the free surface condition of higher order. The higher-order free surface condition is written as follows.⁹⁾

$$\varphi_{sxx} + \kappa \varphi_{sz} = \frac{\partial}{\partial x} C_p(x, y) \quad \text{on } F \quad \dots(6)$$

where C_p is the pressure on F induced by the lower order solution. The particular solution of eq. (6) is given by

$$\varphi_s(x, y, z) = -\frac{1}{4\pi} \iint_F C_p(\xi, \eta) W_x(x, y, z; \xi, \eta, -0) d\xi d\eta$$

which is written by partial integration as follows.

$$\begin{aligned} \varphi_s(P) = & -\frac{1}{4\pi\kappa} \iint_F C_{p\xi}(Q) W(P, Q) d\xi_Q d\eta_Q \\ & + \frac{1}{4\pi\kappa} \oint_C C_p(Q) W(P, Q) d\eta_Q \end{aligned}$$

The first term of the RHS is to be neglected in the case of the NK-problem because $C_{p_x} = 0$ in the linearized free surface condition (1). Put $C_p = -n_x \sigma_L$, we have

$$\varphi_s(P) = -\frac{1}{4\pi\kappa} \oint_C \sigma_L(Q) n_{x_Q} W(P, Q) d\eta_Q \quad \dots(7)$$

The particular solution (7) of eq. (1), derived in the manner described above, may be thought to contain some effect of the free surface condition of higher order.

The solution (7) is regular for $z < 0$ except on C where the induced velocity in the normal direction of the hull has a jump by $1/2 \sigma_L$. Hence, if σ_L is given on C , it is possible to obtain a solution, which consists of the particular solution (7) and the regular solution (3) or (4), so as to satisfy the condition that the normal velocity vanishes on the hull $z < 0$. Let us call it the 'singular NK-solution', ϕ_h , which is written as follows.

$$\begin{aligned} \phi_h(P) = & \frac{1}{4\pi} \iint_F \sigma(Q) W(P, Q) dS_Q \\ & - \frac{1}{4\pi\kappa} \oint_C (\sigma(Q) + \sigma_L(Q)) n_{x_Q} W(P, Q) d\eta_Q \quad \dots(8) \end{aligned}$$

It is impossible to determine σ_L only by the mathematical condition since the solution (8) satisfies the homogeneous condition on the hull. Then, a physical condition is to be added so as to make up for the disadvantage of the regular NK-solution. The sheltering condition that no flow passes over the hull surface is essential to our problem.

It is not so easy rather than for the two-dimensional problem to describe the sheltering condition precisely for the three-dimensional NK-problem. In the present paper, following the two-dimensional sheltering condition⁵⁾, we adopt the condition that the wave elevation vanishes along the hull⁶⁾, i.e.

$$\zeta_c = \frac{1}{\kappa} \phi_{x_c} = 0 \quad \text{on } C. \quad \dots(9)$$

In fact the flux Q in eq. (5) vanishes.

Adding the singular solution to the regular solution so as to satisfy the sheltering condition, we obtain the 'NK-solution satisfying the sheltering condition', ϕ_0 . As described later ϕ_0 is considered to represent the flow around a ship with sinkage free.

4. Singular solution and sinkage: We investigate the relationship between the sinkage of a ship and a NK-solution that includes the singular solution but does not satisfy the sheltering condition.

Consider the singular NK-solution, ϕ_h , determined by the condition $\zeta_c = \text{const.} (\neq 0)$ on C. Then, eq. (5) indicates us that the water of $1 \cdot \zeta_c \cdot \Delta y$ flows in (out of, for $\zeta_c < 0$) the inside of the ship hull over the infinitesimal part of the contour C. Next, consider the stream-lines on the hull surface for the solution, ϕ_0 , satisfying the sheltering condition. When adding the singular solution, ϕ_h , ($\zeta_c \neq 0$) to ϕ_0 , the stream-lines may be near inside or outside the hull surface corresponding to the positive or negative ζ_c respectively. If ζ_c is very small, the slightly shifted stream-lines might be thought to correspond approximately to the hull surface sunken by $S = -\zeta_c$. The normal velocity on the shifted surface is written as

$$\phi_n(x, y, z-s) = \phi_n(x, y, z) - s \frac{\partial}{\partial z} \phi_n(x, y, z).$$

Because s is small, the hull surface condition holds even on the shifted surface.⁸⁾

Thence, the flow around the ship sunken by s may be described as

$$\Phi(x, y, z) = -x + \phi_0(x, y, z) + s \phi_h(x, y, z) \quad \dots (10)$$

where ϕ_0 stands for the NK-solution satisfying the sheltering condition and ϕ_h the singular solution for $s = 1$.

5. Wave resistance of ships with free sinkage: It can be deduced from eq. (10) that the pressure on the hull surface is written by a quadratic equation of s . The sinkage force C_z can be written by a quadratic form of s , too, because it is the pressure integration over the hull surface, that is

$$C_z = Z_2 s^2 + Z_1 s + Z_0. \quad \dots (11)$$

Similarly the wave resistance is written by

$$C_w = W_2 s^2 + W_1 s + W_0. \quad \dots (12)$$

The coefficients of the above equations can be determined by the values

of C_z or C_w calculated for three different values of s .

For the ship with free sinkage (fixed trim) the increment of buoyancy, $C_s = 2\kappa A_w s$, is to be in equilibrium with the sinkage force, that is

$$2\kappa A_w s = Z_2 s^2 + Z_1 s + Z_0 . \quad \dots (13)$$

Two roots, s_1, s_2 ($s_1 < s_2$) of eq.(13) turn out the sinkage of the ship with free sinkage. In the case when $Z_2 > 0$, the sinkage s_1 is the stable root. We can calculate the value of the wave resistance for the ship with free sinkage if s_1 is substituted to eq.(12).

6. Numerical examples: Wigley hull and Inuid (S-201) were chosen and the representation (4) was used for the calculation. Following Webster⁽¹⁾, the surface of source distribution is submerged inside the ship hull by $SM(<1)$. ($SM=0.8$ or 0.5 for Wigley hull, $SM=0.0$ for S-201) The surface is divided into 13 (in x -direction) \times 10 (in z -direction) triangular patches. The patches allow a linear variation of the source strength across them. We adopted a least squares method to solve the source distribution by expanding the solution to 8- or 10-terms Fourier series.

The source distributions for Wigley hull of the double-model solution, the regular NK-solution, the NK-solution satisfying the sheltering condition and the singular NK-solution are shown in figs. 1 to 4 respectively. Under certain circumstances small difference of source distribution causes a large effect on wave resistance calculation, so the source is to be calculated very precisely.

An example of source distribution for S-201 is shown in fig.5.

Wave profiles along Wigley hull (defined from the undisturbed water surface) are shown in fig.6. For the singular solution the values of ϕ_x at $z = -0$ were adopted.

The sinkage force for Wigley hull are compared with the experiments in fig.7. The sinkage force via the sinkage was calculated by using eq.(12) and its value for the state of free sinkage shown by the mark \odot was obtained through eq.(14). The mark \bullet shows the increments of buoyancy, C_s , which correspond from the left to the load conditions of full, 95%, 90%, 75% and 65% respectively. The mark \blacktriangle shows the sinkage force measured for the ship model with sinkage fixed at full load condition. The fairly good agreement between the measured C_s and C_z implies that the conversion of the sinkage to the sinkage force are adequate. The calculated values of the sinkage force show good agreement with the experimental results near the sinkage $s = 0$.

Accordingly, the evaluation of the sinkage is possible by the present method.

The sinkage and the equilibrium points for S-201 are shown in fig.8. In figs.9,10 good agreement between the experimental and the calculated sinkage are shown. The sinkage-force curves for Wigley hull are shown in fig.11.

The wave resistance for Wigley hull are shown in fig.12. The mark \odot shows the value of the state of free sinkage. The trend of the calculated values coincides with the experimental results near $s = 0$ though quantitative agreement is not so good. If calculated more precisely, the effect of the sinkage on the wave resistance for a ship with free sinkage might be estimated by the present method.

Fig.13 shows the pressure drag for S-201.

The wave resistance are shown in figs.14 to 16. We can not deduce a clear conclusion partly because the accuracy of calculation is not satisfactory and partly because the non-linear property of bow wave is strong.

Fig.17 shows the energy spectrum. The value of the diverging wave calculated by the singular solution becomes very large due to the contribution of the line integral term. When calculating the wave resistance we truncated it at such a angle that is determined by the temporal hypothesis on the wave-breaking.

The phase of the energy spectrum for the regular NK-solution shifts to the higher angle compared with the measured one. It is remarkable for the solution including the singular solution. We must consider the effect of the local non-uniformity of the flow⁽¹²⁾. Anyway, a certain degree of the effect of the sinkage on the wave spectrum might be obtained by the solution including singular solution.

7. Conclusions: Following conclusions are obtained although the numerical examination are still to be improved.

- 1) There exists a singular NK-solution that satisfies the homogeneous hull-surface condition if the singularity is admitted on the contour of intersection, C , between the hull surface and the undisturbed water surface.
- 2) The sheltering effect can be represented by the condition that the wave elevation, ζ_c , vanishes on C . Such a solution consists of the regular NK-solution and the singular NK-solution.
- 3) The effect of the sinkage is expressed by varying the value of ζ_c and the wave resistance of a ship with free sinkage can be calcu-

lated.

Acknowledgment

The author would like to thank Professor M.Bessho for his valuable guidance.

The author would also like to thank Professors T.Inui and H.Kajitani for their most valuable discussions.

Thanks are also due to Professor H.Miyata for enabling the author to perform the experiment at the towing tank of the University of Tokyo.

References

- 1) J.V.Wehausen, JSR 13 (1969)
- 2) F.Noblesse, JSR 19 (1975)
- 3) T.H.Havelock, ZAMM 19-4 (1939)
- 4) R.W.Yeung, JSR 16 (1972)
- 5) K.Suzuki, "On the Two-Dimensional Neumann-Kelvin Problem", unpublished (1978.7)
- 6) R.Brard, JSR 16 (1972)
- 7) T.Kitazawa, M.Takagi, ISWR.Kansai (1976)
- 8) M.Bessho, ISWR. Tokyo (1976)
- 9) H.Maruo, Fac.Eng.YNU (1966)
- 10) T.Inui et al, J.SNA.Japan 124 (1969)
- 11) W.C.Webster, JSR 19 (1975)
- 12) T.Inui, H.Kajitani, Schiffstechnik 24 (1977)

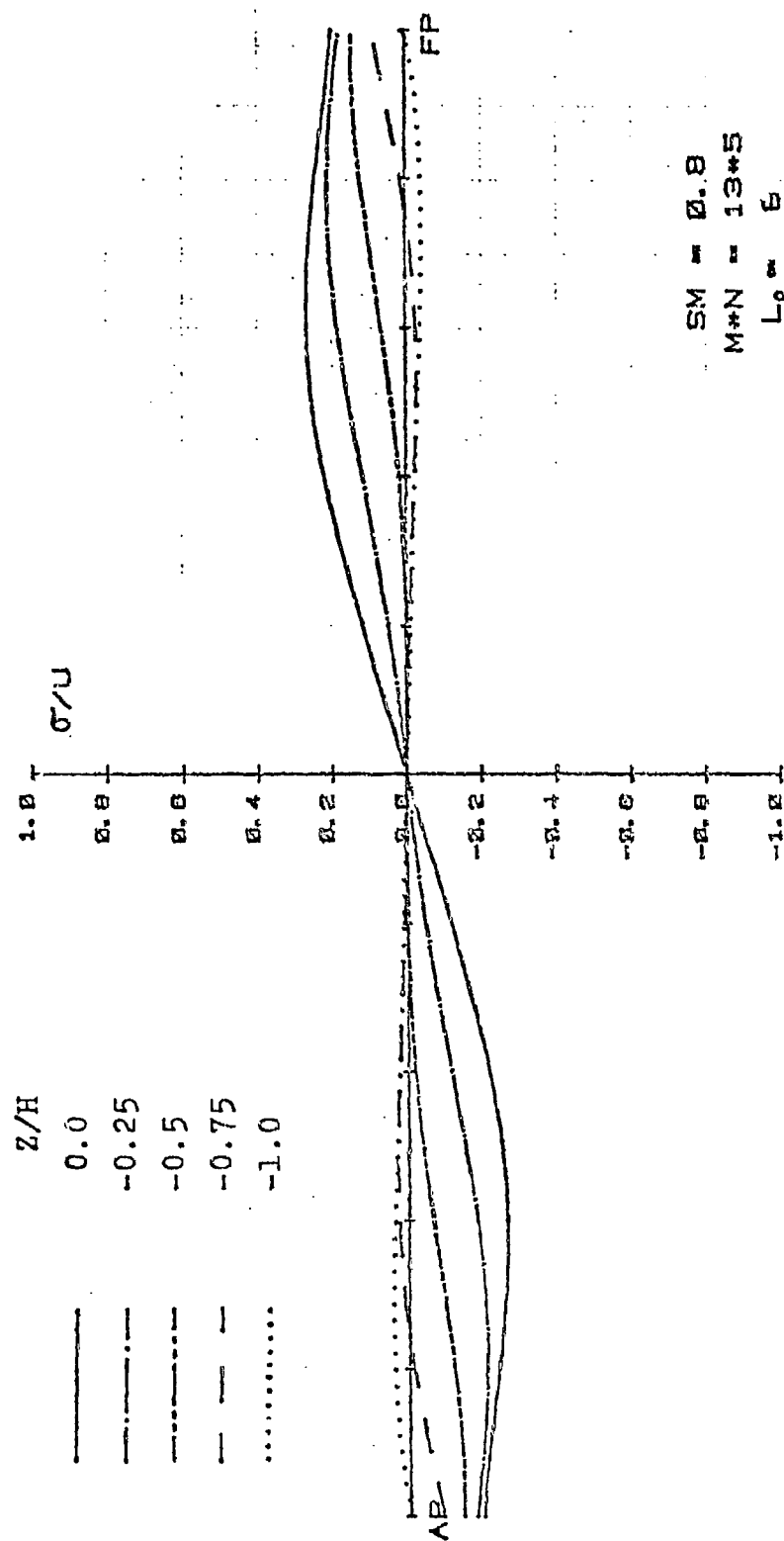


Fig. 1 Source Distribution (Wigley Hu1:Double Model)

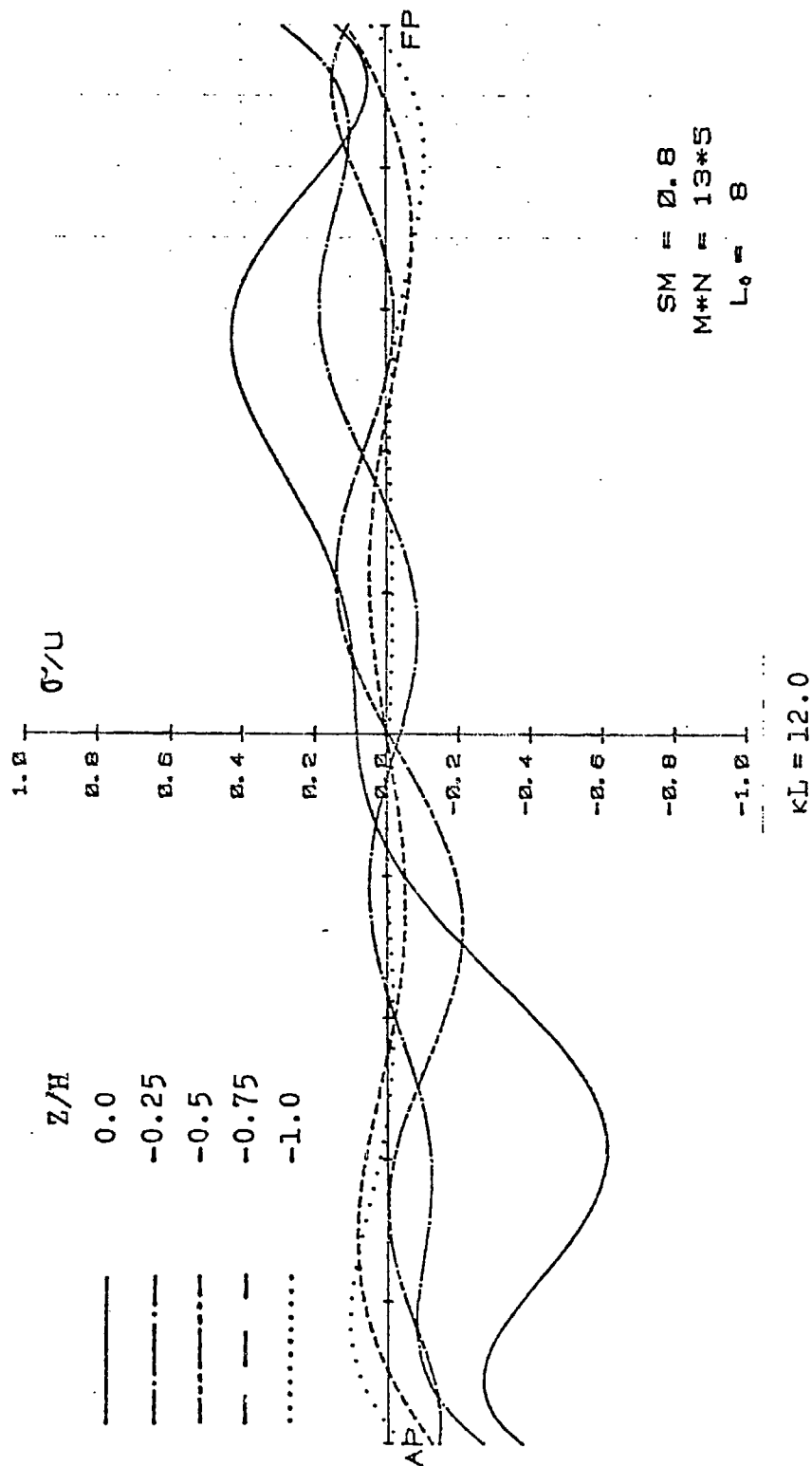
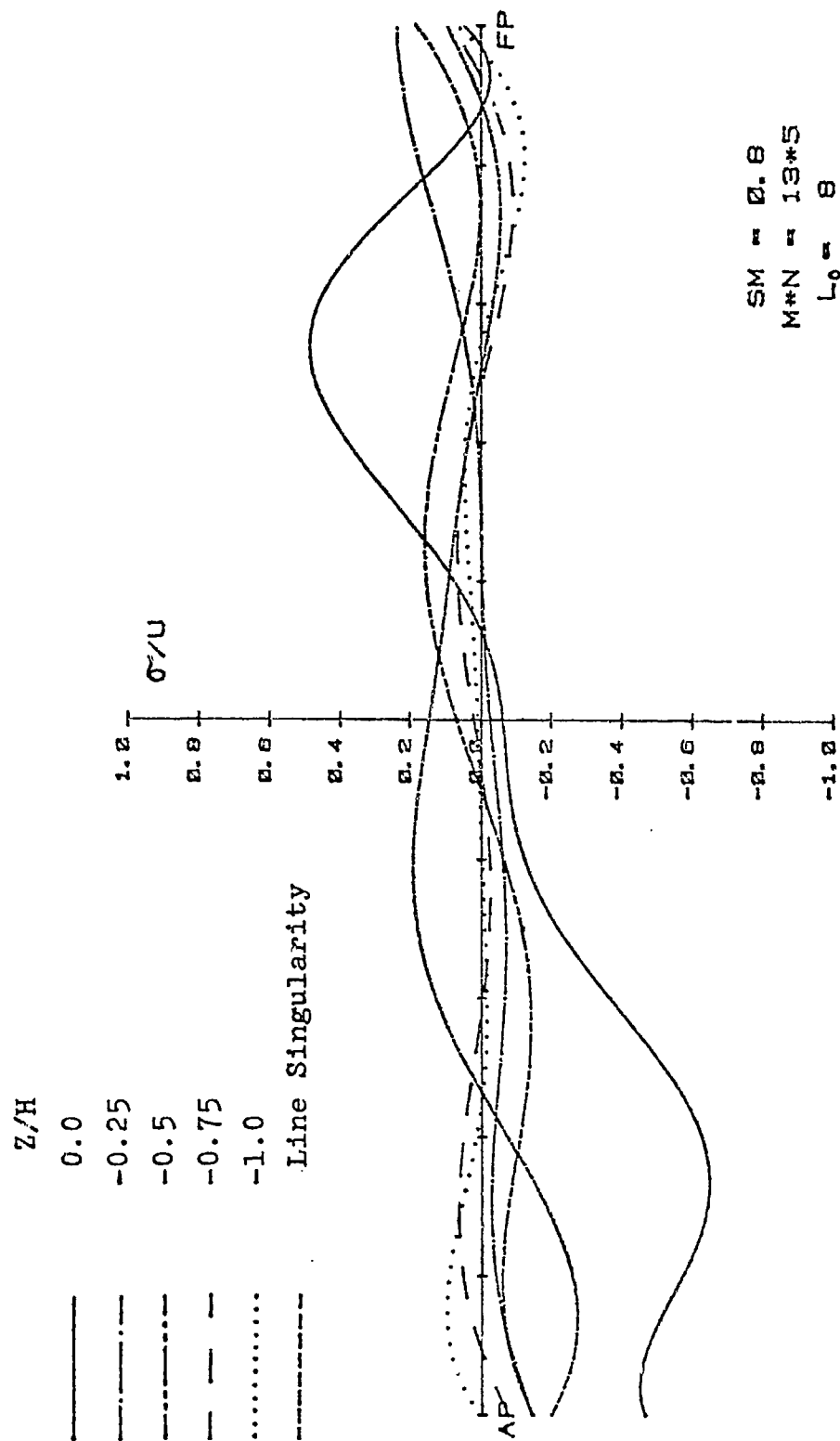
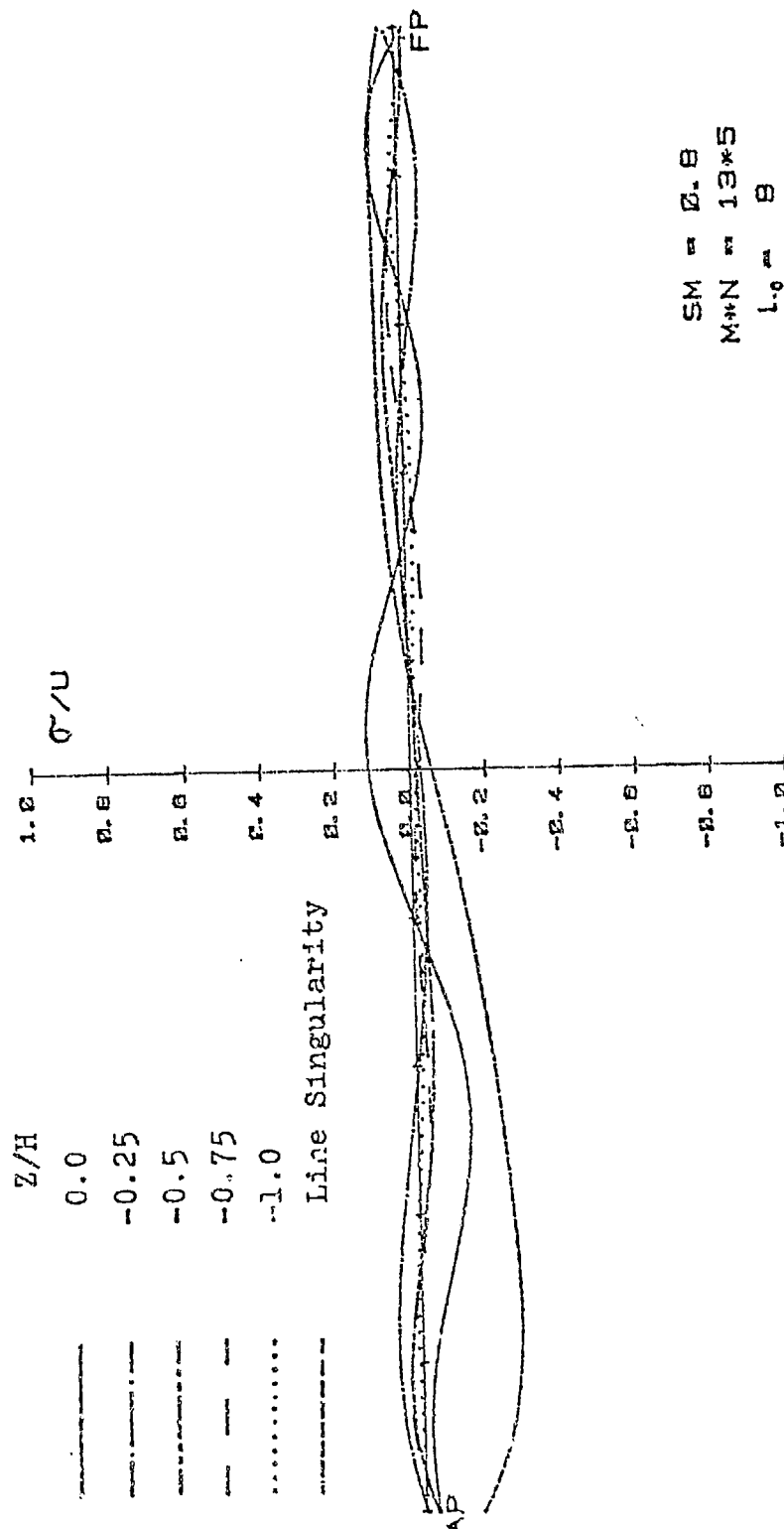


Fig.2 Source Distribution (Wigley Hull:regular NK-solution)



$\kappa L = 12.0$, $s/L = 0.0$

Fig. 3 Source Distribution (Wigley Hull: NK-sol. including singular sol., $\phi_{xc} = 0.0$)



$KL = 12.0$, $s/L = 0.42 \%$

Fig. 4 Source Distribution (Wigley Hull: singular NK-solution, $\phi_{\alpha_c} = -0.05$)

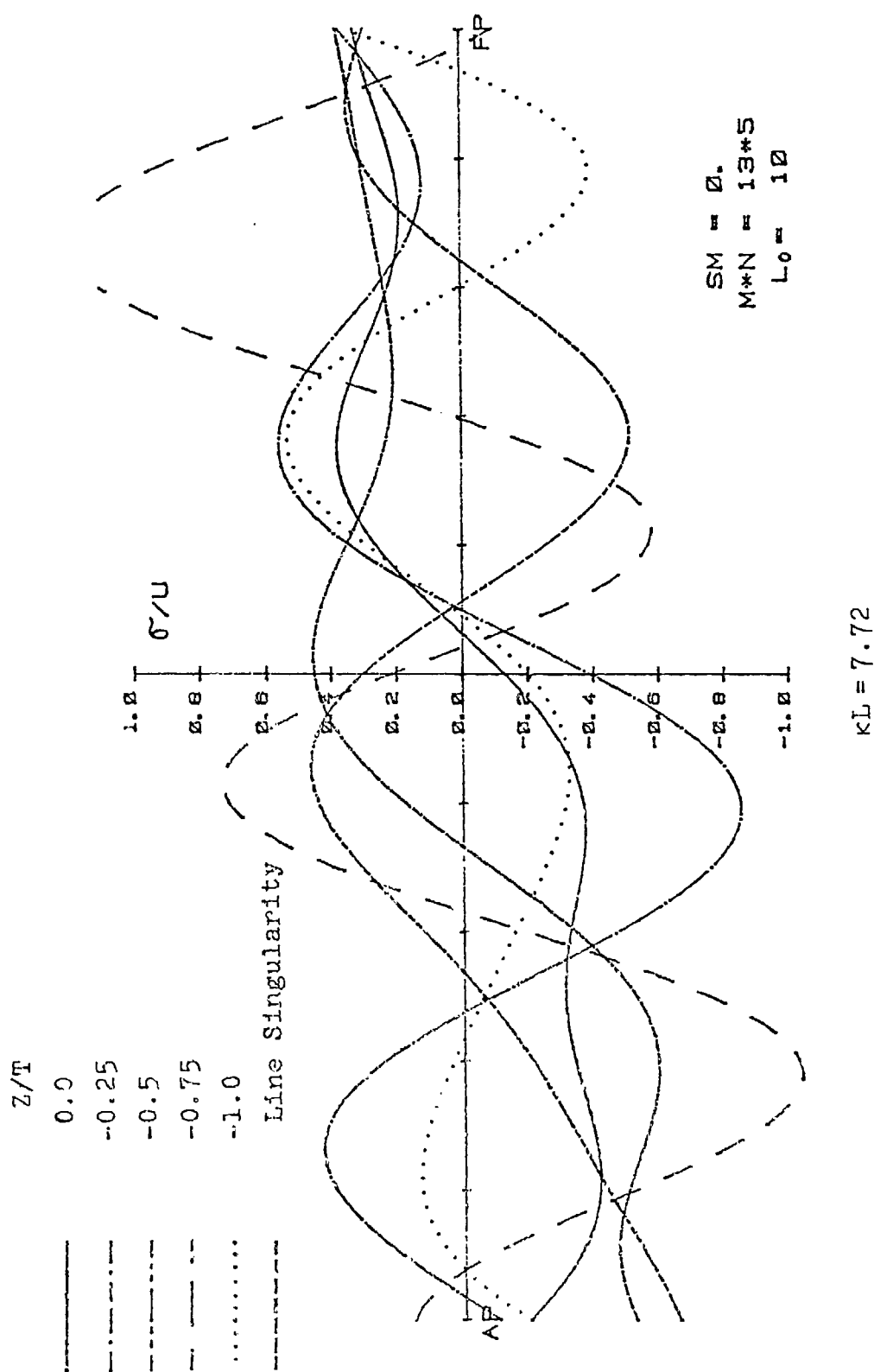


Fig. 5 Source Distribution (Inuid S-201, NK-sol. including singular sol., $\phi_{x_c} = 0.0$)

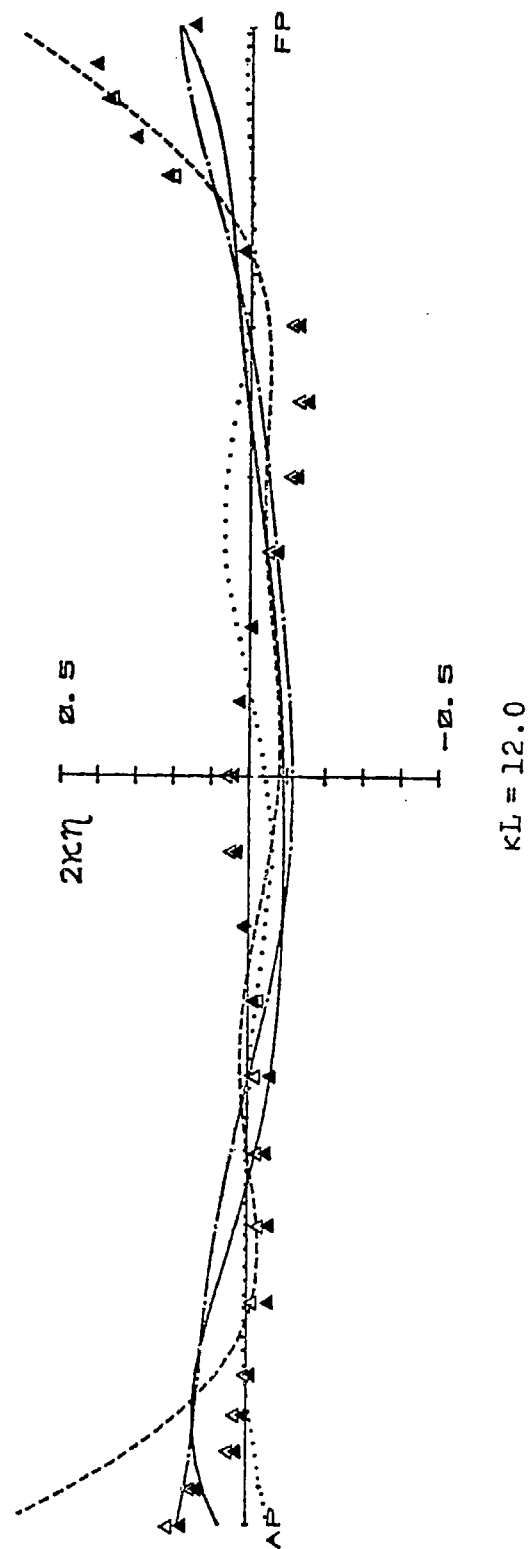


Fig. 6 Wave Elevation along Hull (Wigley)

- | | | |
|-----------------|-----------|---|
| EXP. | — | Fixed Sinkage ($S = 0$) |
| ▲ Free Sinkage | | To be added to the above curve ($S/L = 0.42\%$) |
| △ Fixed Sinkage | - · - · - | Regular NK-sol. |
| | ----- | Excluding L.W.T. |

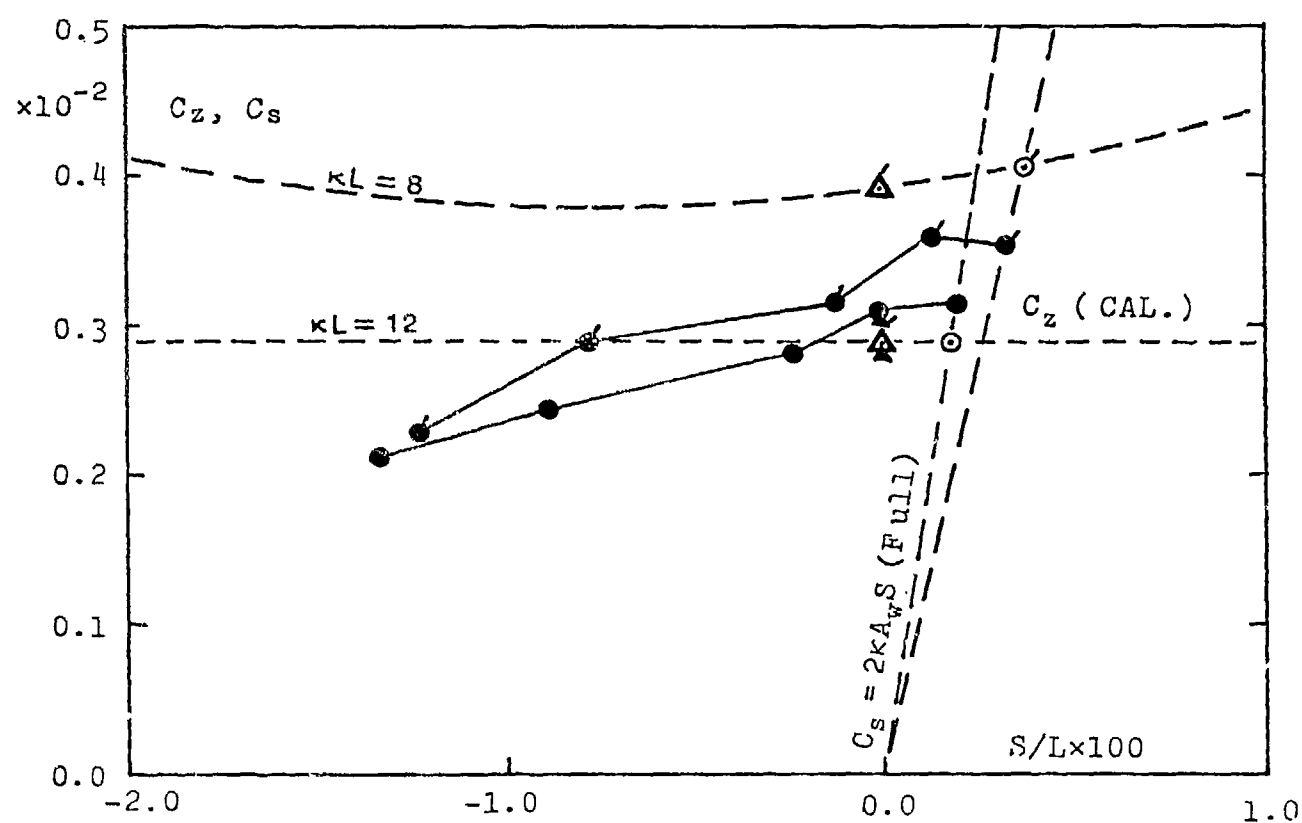


Fig. 7 Sinkage Force (Wigley Hull)

EXP.	$C_z (CAL.)$
● C_s (Free Sinkage)	○ Free Sinkage
▲ C_z (Fixed Sinkage)	△ Fixed Sinkage

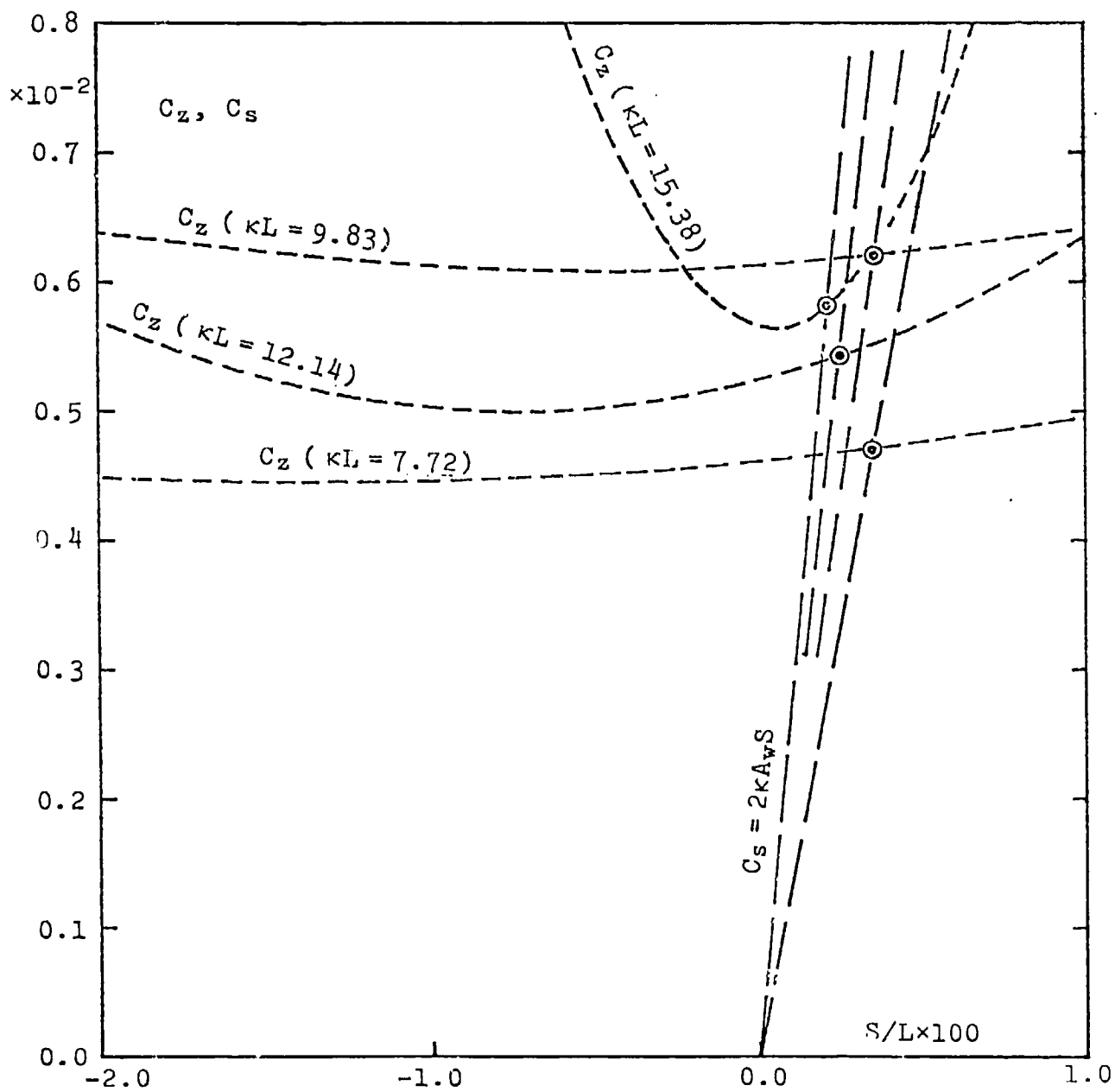


Fig. 8 Sinkage force (Inuid S-201)

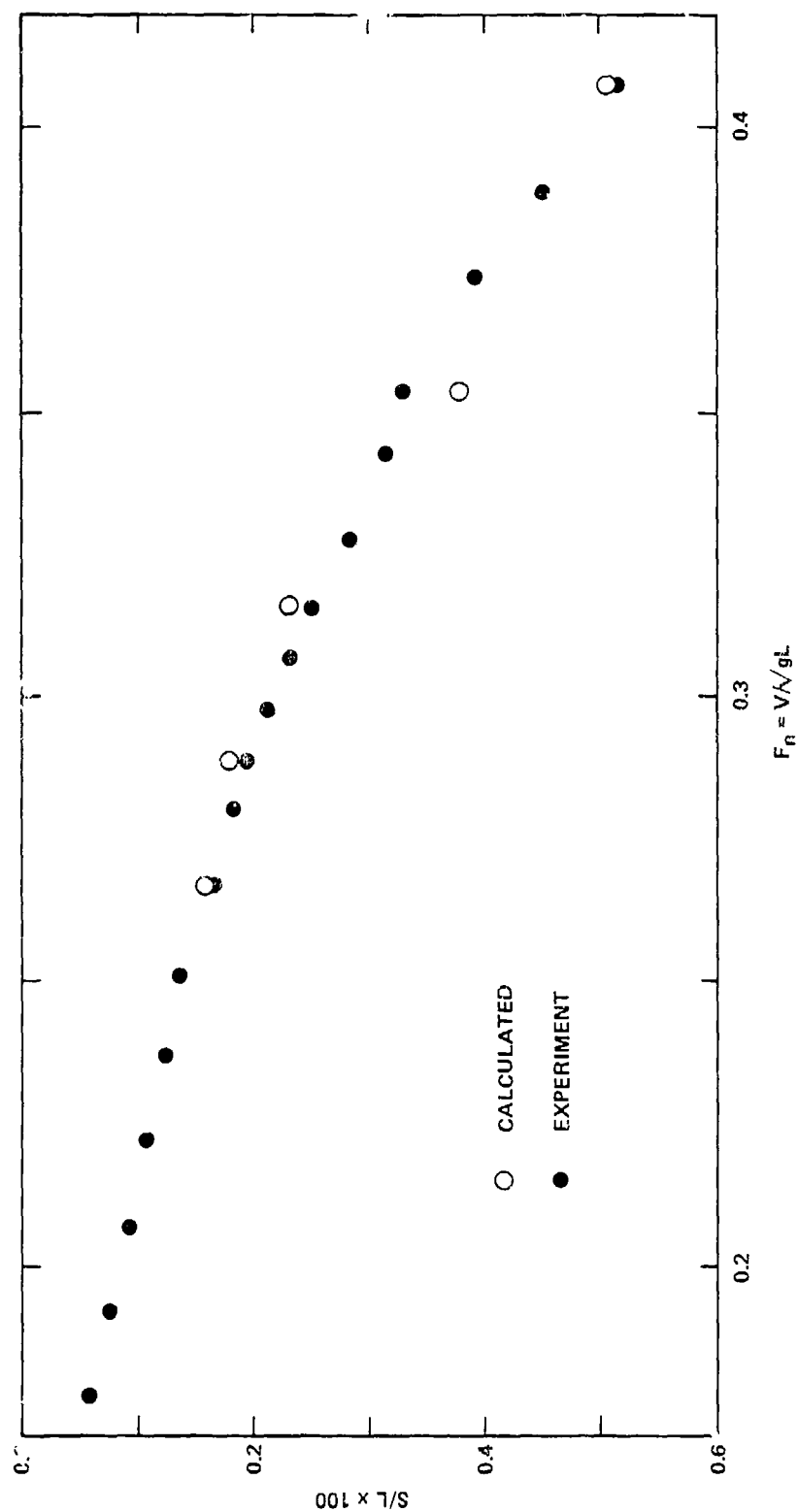


Figure 9 - Sinkage Curve for Wigley Hull

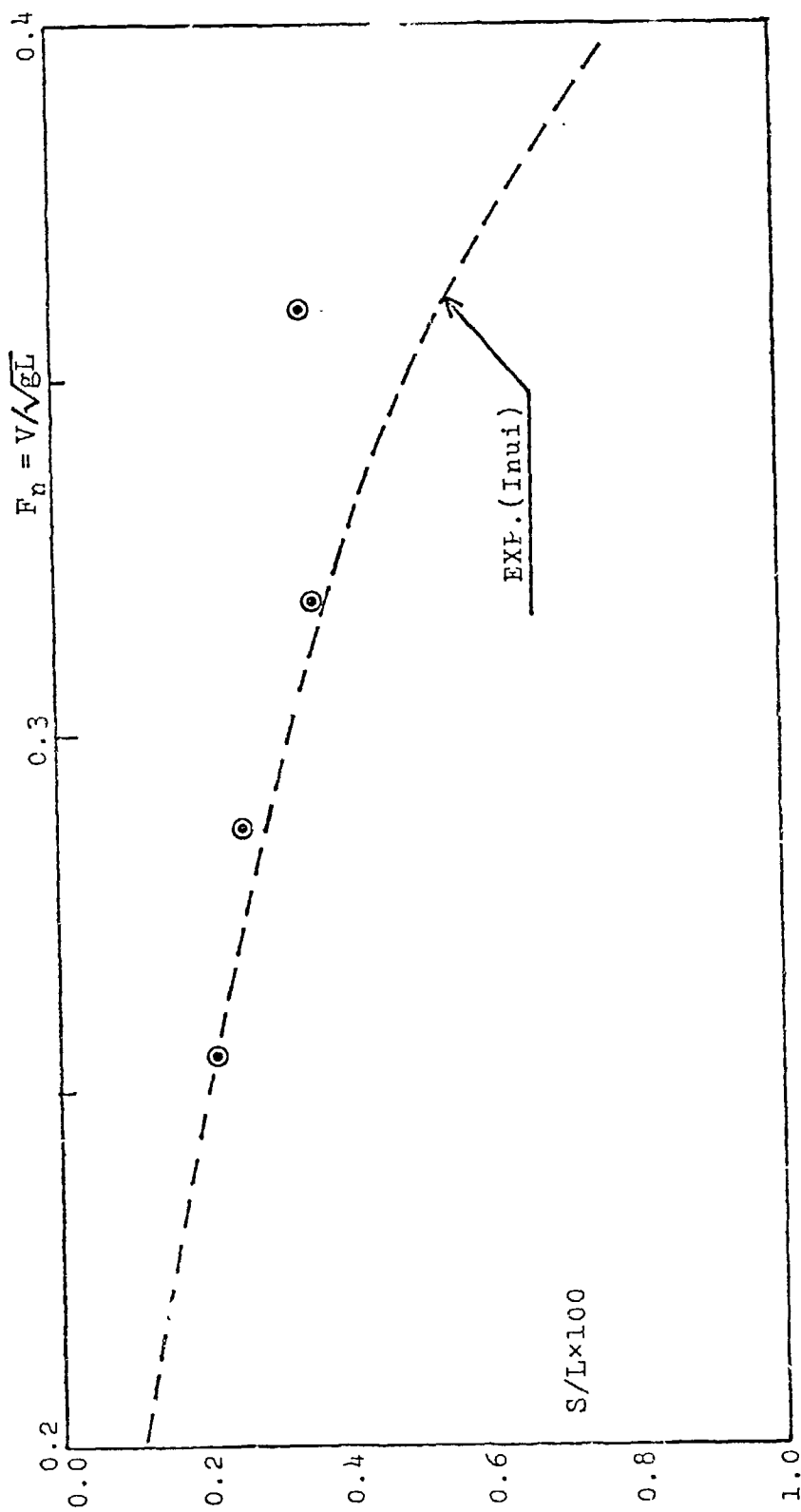


Fig.10 Sinkage Curve for Inuid S-201

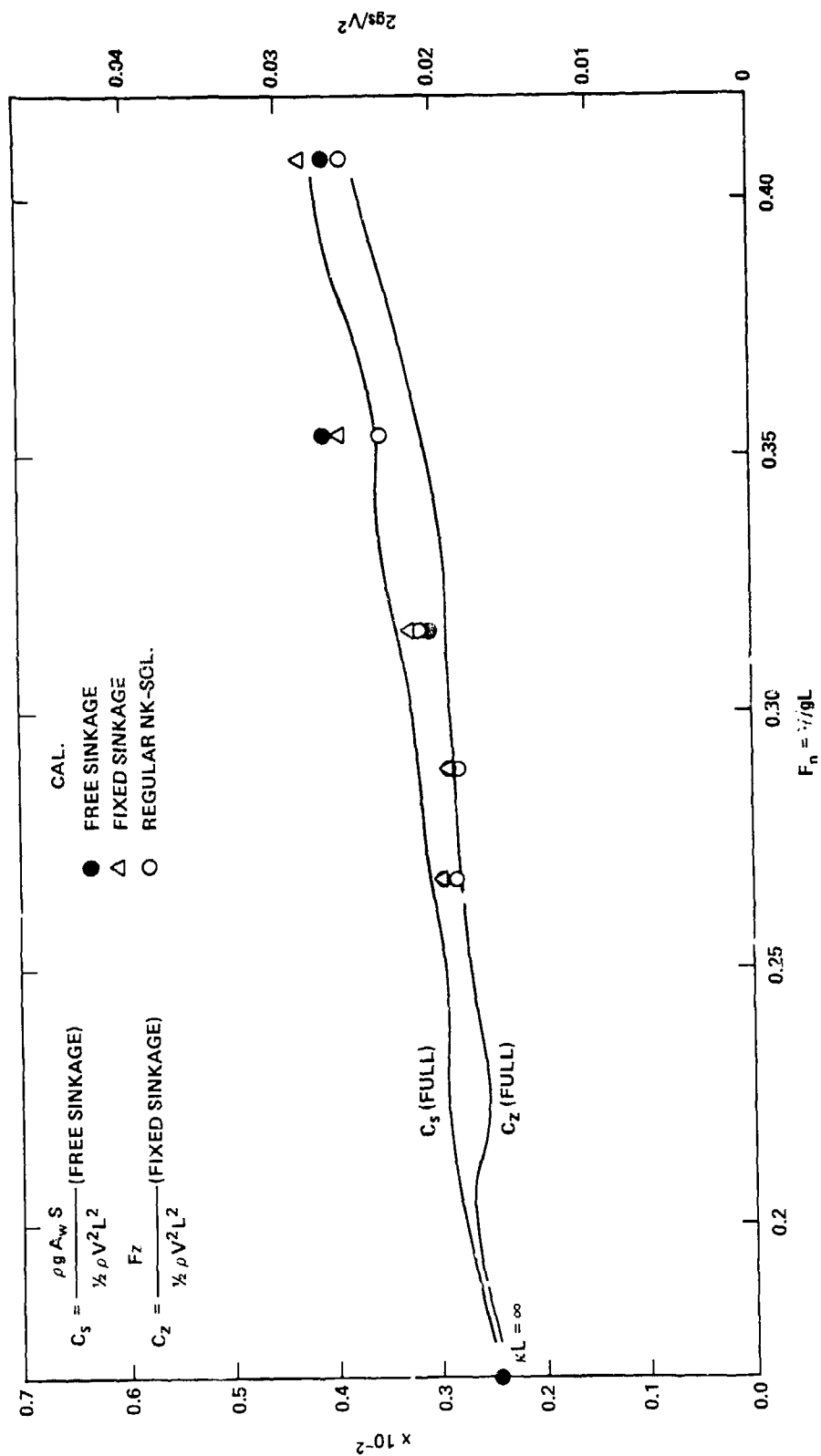


Figure 11 - Comparison of Sinkage Force (Wigley Hull)

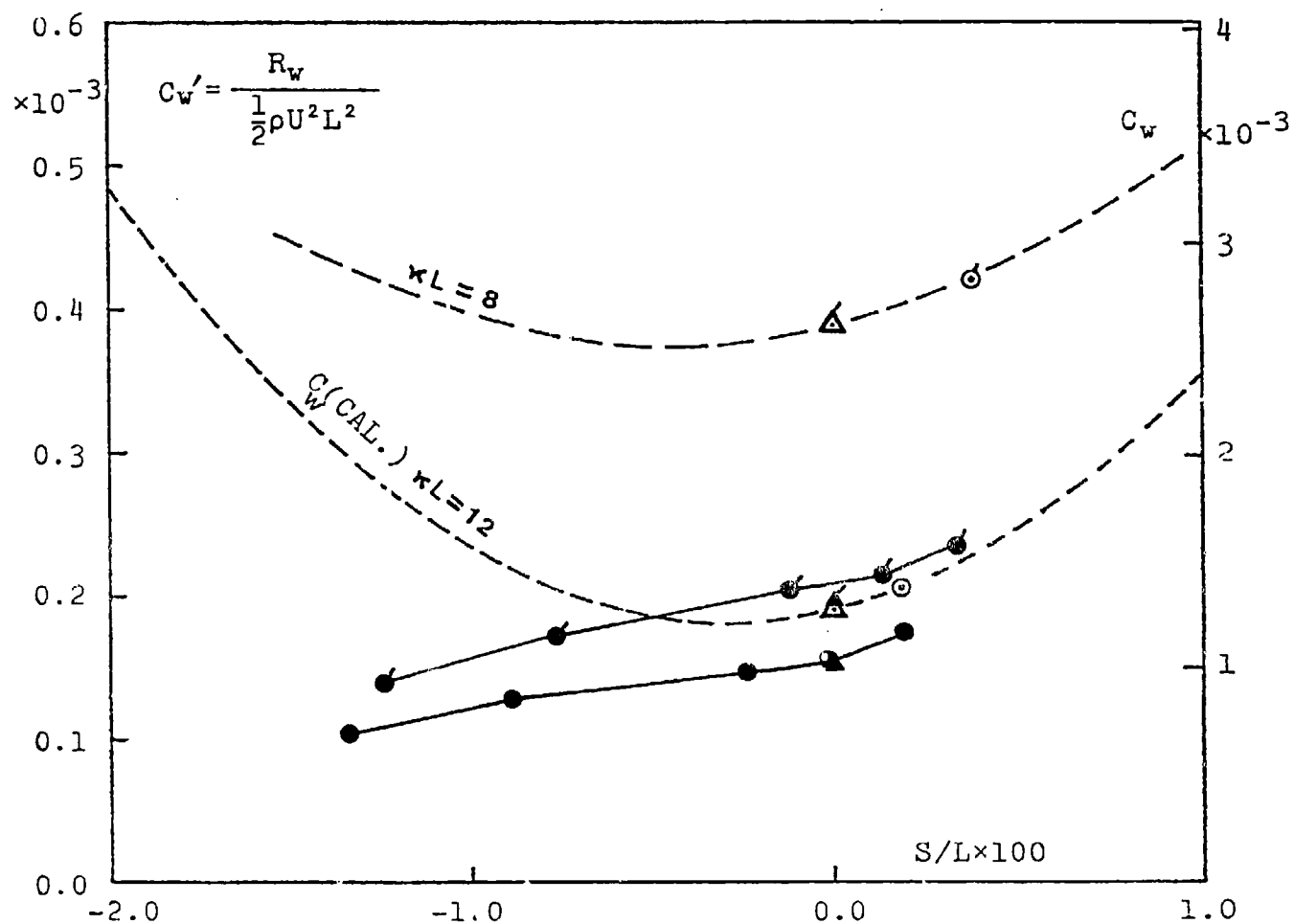


Fig.12 Wave Resistance (Wigley Hull).

C_w EXP.	C_w (CAL.)
● Free Sinkage	⊙ Free Sinkage
▲ Fixed Sinkage	△ Fixed Sinkage

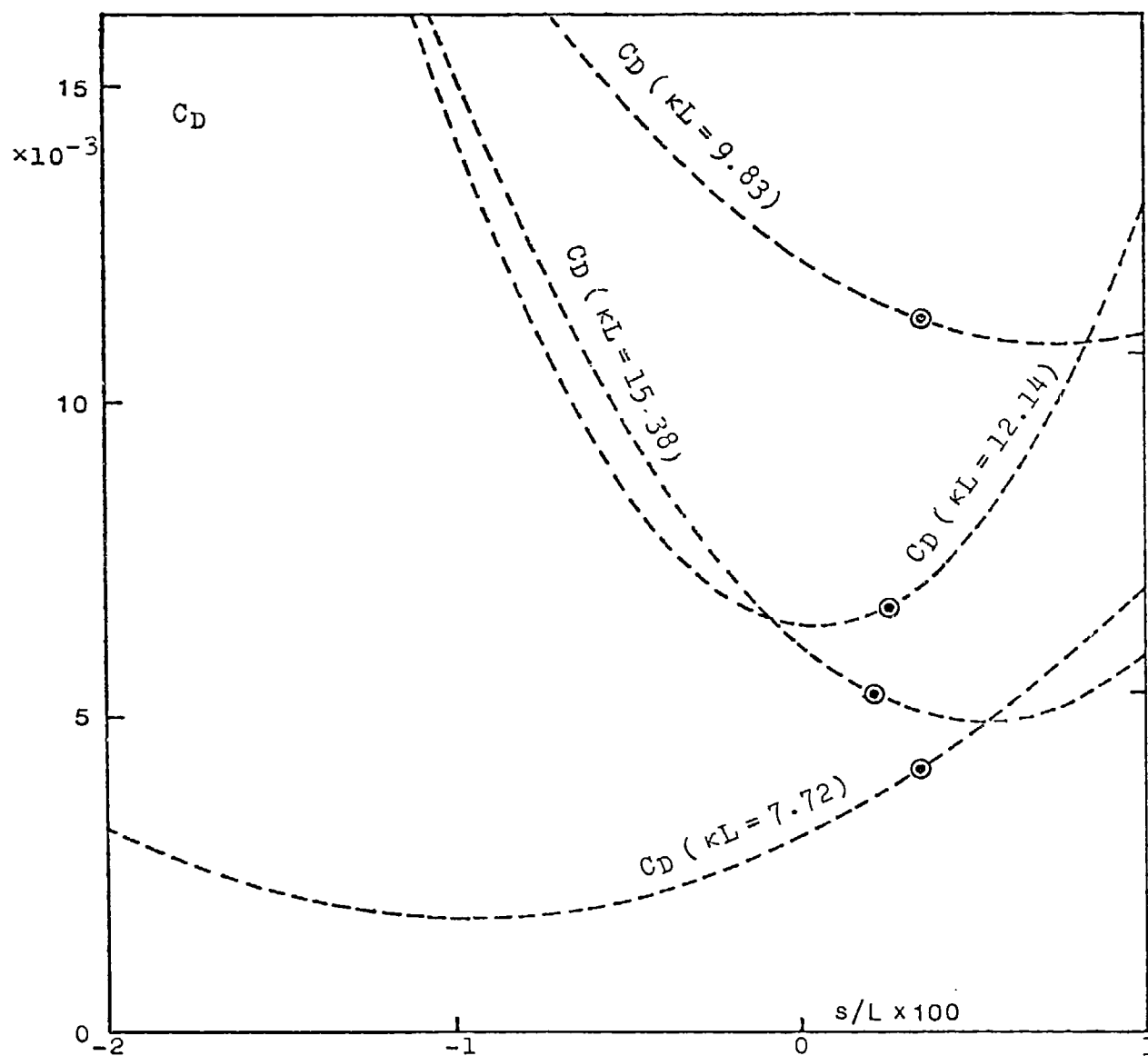


Fig. 13 Drag (Inuid S-201)

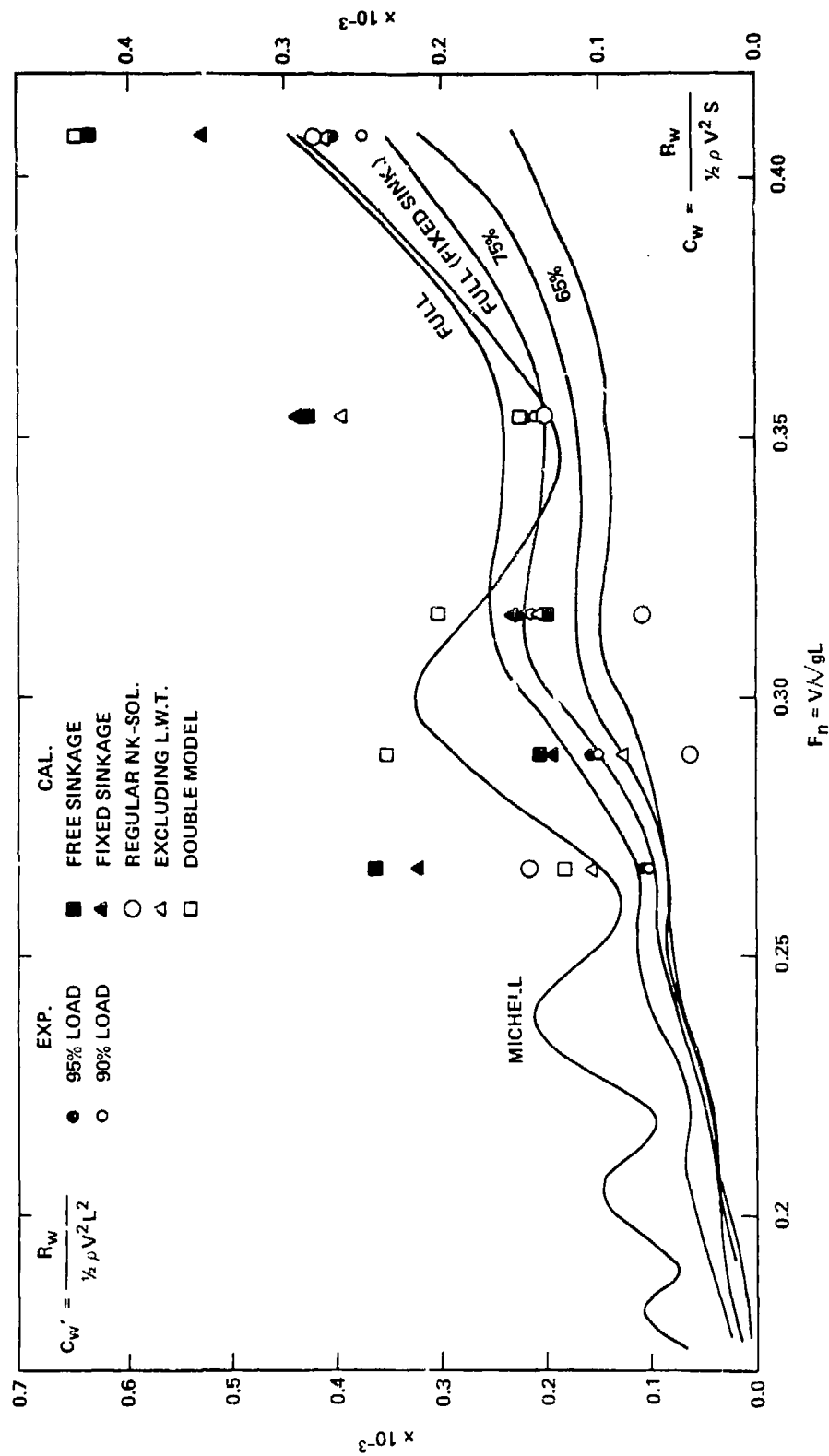


Figure 14 - Comparison of Wave Resistance (Wigley Hull)

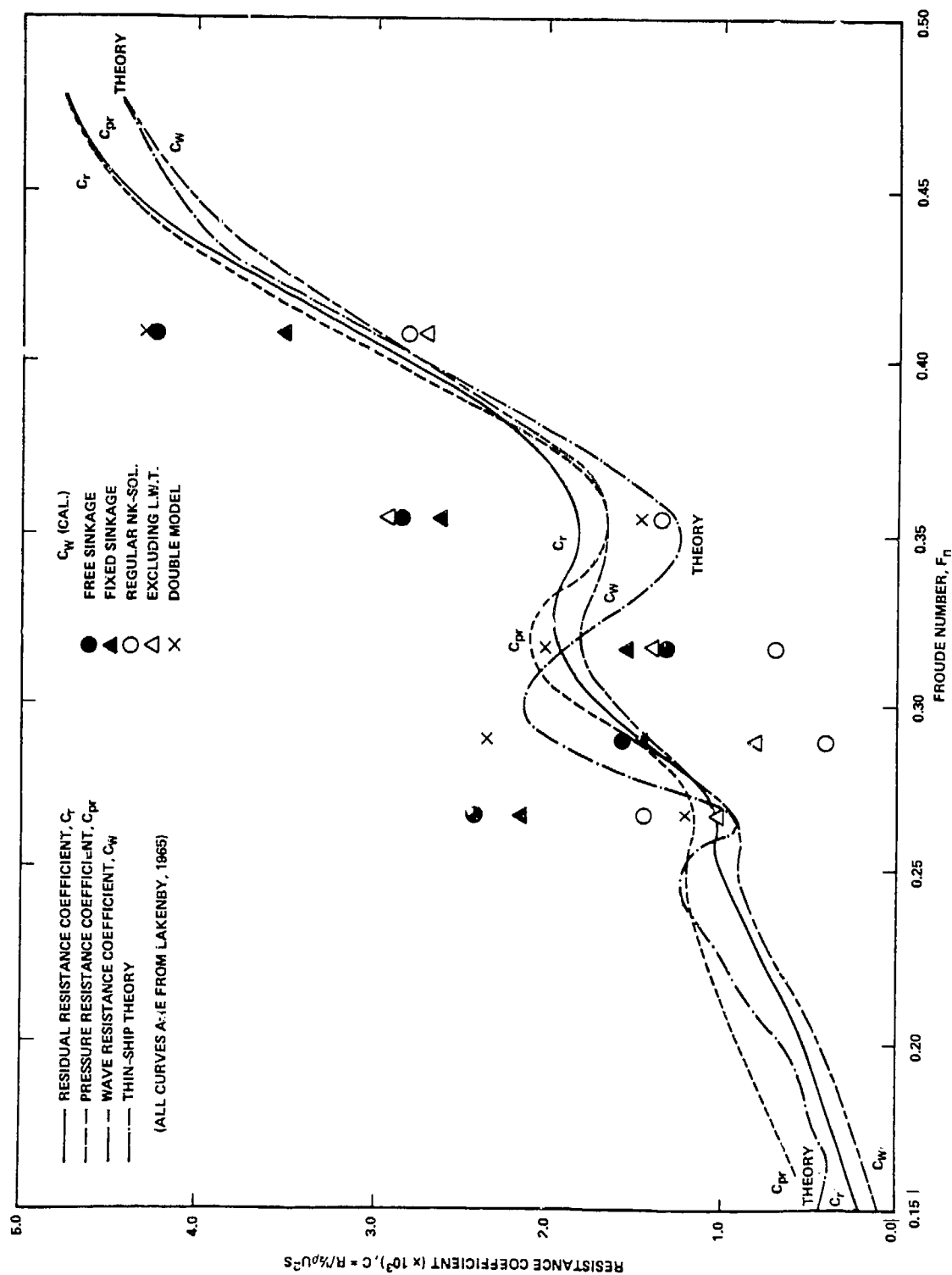


Figure 15 - Resistance Curves for Wigley Hull

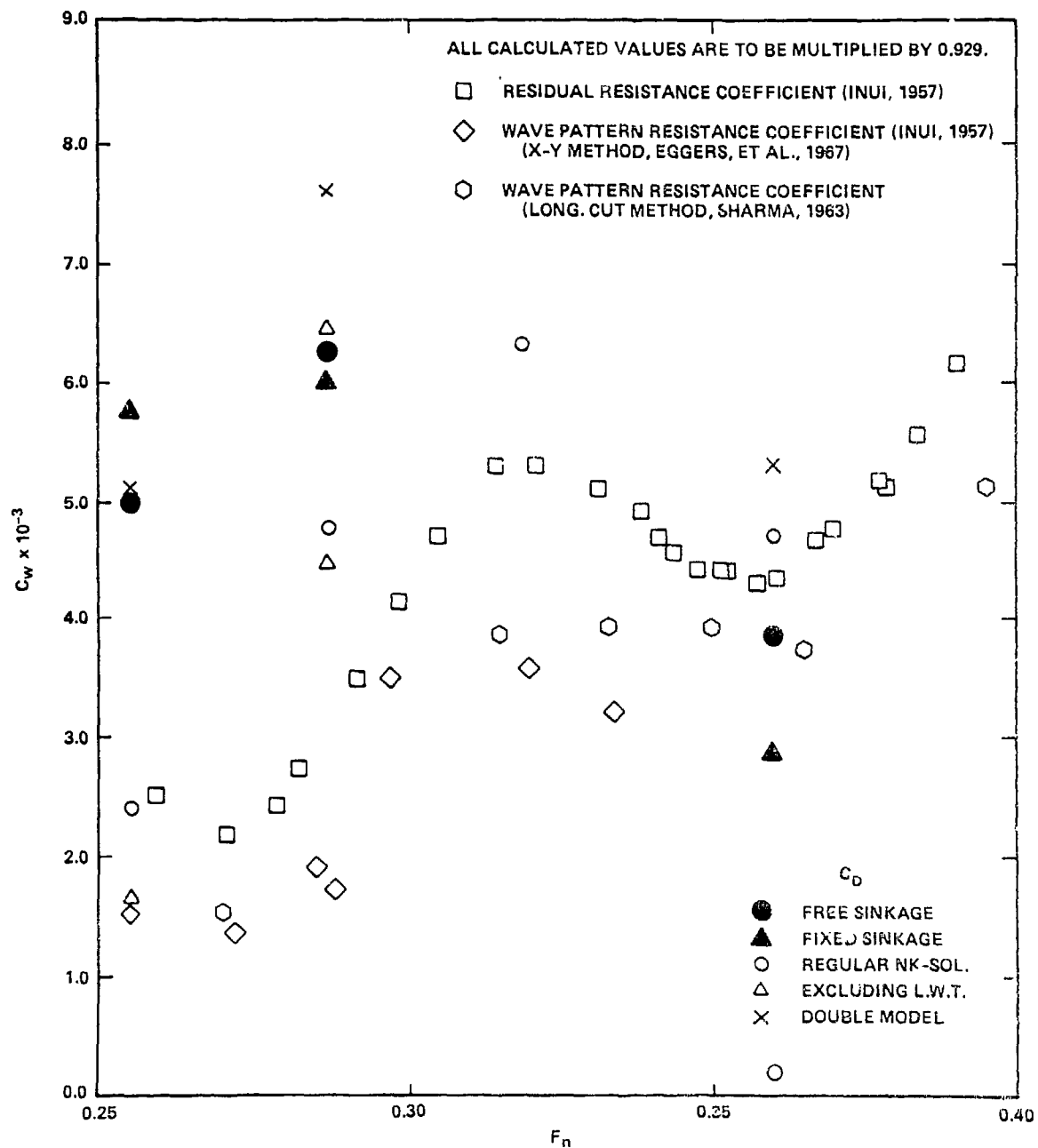


Figure 16 - Comparison of Wave Resistance (Inuid S-201)

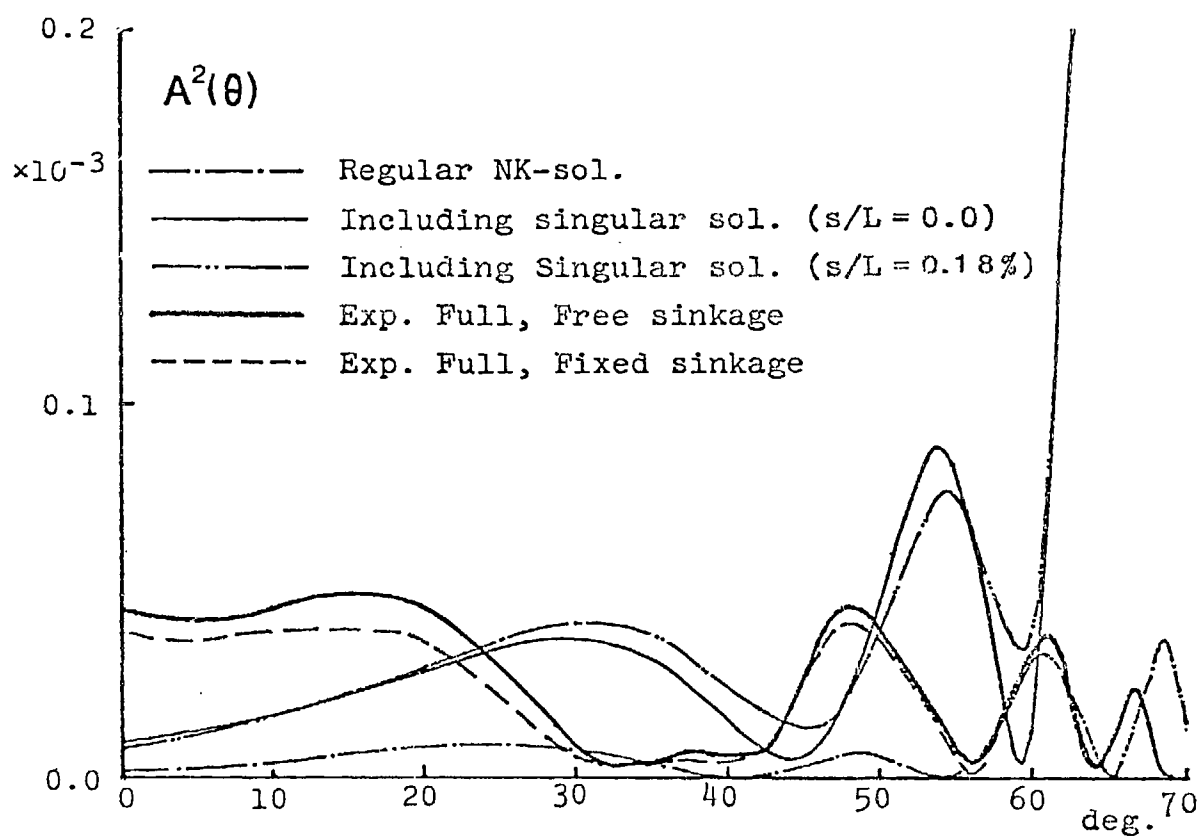


Fig.17 Energy Spectrum (Wigley, $\kappa L = 12.0$)

TABLE 1
FORMAT FOR TABULATED VALUES OF WAVE RESISTANCE

K.Suzuki / Neumann-Kelvin Prob.

WIGLEY	double model	excluding L.W.T.	regular NK-sol	including singular sol. $s/L = 0.0$	with free sinkage	sinkage	
Fn	$C_w \times 10^3$	$C_w \times 10^3$	$C_w \times 10^3$	$C_w \times 10^3$	$C_w \times 10^3$	$s/L \times 100$	
.267	1.204	1.028	1.445	2.144	2.408	0.16	
.289	1.924	1.789	0.479	1.492	1.372	0.18	
.316	2.011	1.378	0.699	1.539	1.317	0.23	
.354	1.479	2.897	1.351	2.621	2.837	0.38	
.408	4.291	2.702	2.796	3.502	4.231	0.51	

TABLE 2 FORMAT FOR TABULATED VALUES OF WAVE RESISTANCE

K. Suzuki / Neumann-Kelvin Prob.

INUID S-201	double model	regular NK-sol.	including singular sol. $s/L=0.0$	with free sinkage	sinkage	
F_n	$C_w \times 10^3$	$C_D \times 10^3$	$C_D \times 10^3$	$C_D \times 10^3$	$s/L \times 100$	
.255	4.71	0.24	5.29	4.60	0.20	
.287	7.20	4.40	5.55	5.80	0.23	
.319	6.38	6.77	10.61	9.76	0.33	
.360	4.91	0.20	2.67	3.59	0.32	

Computation of Wave-Resistance by Means of the Low
Speed Theory By H. Maruo, K. Suzuki
(Yokohama National University)

1. Formulation of the problem

By means of the application of Green's theorem in the lower half space with the Havelock source as the Green function, the velocity potential which satisfies the exact non-linear free surface condition is expressed as^{1) 2)}

$$\begin{aligned}\phi(P) = & -\frac{1}{4\pi} \iint_S [G(P, Q) \frac{\partial \phi(Q)}{\partial n_Q} - \phi(Q) \frac{\partial G(P, Q)}{\partial n_Q}] dS_Q \\ & + \frac{1}{4\pi\gamma_0} \int_{L_0} [G(P, Q) \frac{\partial \phi(Q)}{\partial x'} - \phi(Q) \frac{\partial G(P, Q)}{\partial x'}]_{z'=0} dy' \\ & - \frac{1}{4\pi\gamma_0} \iint_{\Sigma_0} \phi(x', y') G(P, Q)_{z'=0} dx' dy'\end{aligned}\quad (1)$$

where $P(x, y, z)$ is the field point, $Q(x', y', z')$ is a point on the hull surface S , or that on the contour L of the still waterline, or that on the horizontal plane $z = 0$ outside the hull surface, $G(P, Q)$ is the Havelock source potential and $\gamma_0 = g\ell/U^2$. $\phi(x', y')$ is a non linear factor defined by

$$\begin{aligned}\phi(x, y) = & \left[\frac{1}{2} \left(2 \frac{\partial}{\partial x} + u \frac{\partial}{\partial x} + v \frac{\partial}{\partial y} + w \frac{\partial}{\partial z} \right) (u^2 + v^2 + w^2) \right]_{z=\zeta} \\ & + \int_0^\zeta \left(\frac{\partial^2 u}{\partial x \partial z} + \gamma_0 \frac{\partial w}{\partial z} \right) dz\end{aligned}\quad (2)$$

ζ is the free surface elevation and all quantities are non-dimensionalized by ℓ and U . The asymptotic expression at a great distance is expressed as

$$\begin{aligned}\phi(P) \approx & 4\gamma_0 \text{Im} \int_{-\pi/2}^{\pi/2} H(\gamma_0 \sec^2 \theta, \theta) \exp[\gamma_0 z \sec^2 \theta + i\gamma_0 \sec \theta (x + y \tan \theta)] \\ & \cdot \sec^2 \theta d\theta\end{aligned}\quad (3)$$

where

$$\begin{aligned}H(k, \theta) = & -\frac{1}{4\pi} \iint_S \left(\frac{\partial \phi}{\partial n} - \phi \frac{\partial}{\partial n} \right) \exp[kz + ik(x \cos \theta + y \sin \theta)] dS \\ & + \frac{1}{4\pi\gamma_0} \int_{L_0} \left(\frac{\partial \phi}{\partial x} - ik \cos \theta \phi \right) \exp[i(x \cos \theta + y \sin \theta)] dy \\ & - \frac{1}{4\pi\gamma_0} \iint_{\Sigma_0} \phi(x, y) \exp[ik(x \cos \theta + y \sin \theta)] dx dy\end{aligned}\quad (4)$$

The wave-resistance is given by

$$R_w = 8\pi\rho U^2 \ell^2 \gamma_0^2 \int_{-\pi/2}^{\pi/2} |H(\gamma_0 \sec^2 \theta, \theta)|^2 \sec^3 \theta d\theta \quad (5)$$

On account of the basic assumption of low Froude numbers, the first approximation is obtained by the substitution of ϕ by the double body potential ϕ_0 . In this case, the non-linear factor takes the form like

$$\phi(x,y) = \frac{1}{2} \left[\left\{ (2+u_0) \frac{\partial}{\partial x} + v_0 \frac{\partial}{\partial y} \right\} (u_0^2 + v_0^2) + \left(\frac{\partial u_0}{\partial x} + \frac{\partial v_0}{\partial y} \right) (2u_0 + u_0^2 + v_0^2) \right]$$

where u_0, v_0 are disturbance velocities at $z = 0$ by the double body. If the hull surface is expressed by a source distribution of density $\sigma(x,y,z)$, the H-function takes the form like

$$\begin{aligned} H'(k, \theta) = & - \iint_S \sigma(x,y,z) \exp[kz + ik(x \cos \theta + y \sin \theta)] dS \\ & + \frac{1}{\gamma_0} \int_{L_0} \sigma(x,y,0) \exp[ik(x \cos \theta + y \sin \theta)] n_x dy \\ & - \frac{1}{4\pi\gamma_0} \iint_{\Sigma_0} \phi(x,y) \exp[ik(x \cos \theta + y \sin \theta)] dx dy \end{aligned} \quad (6)$$

2. Method of numerical computation

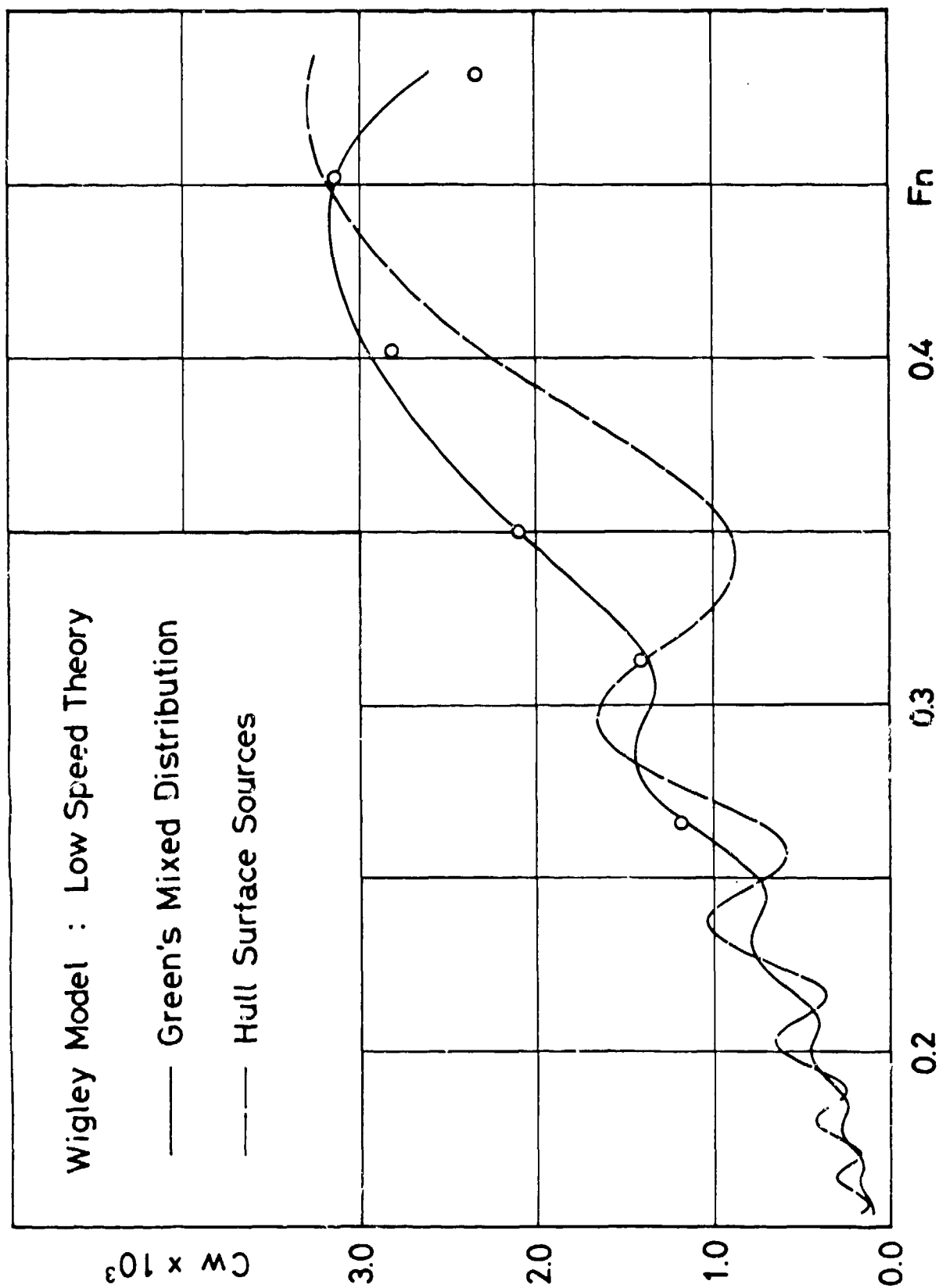
The source distribution on the double body and the velocities are determined by the method of Hess and Smith. Then the function $H'(\gamma_0 \sec^2 \theta, \theta)$ according to the definition (6) is calculated by the numerical integration. The wave-resistance is calculated by (4). In order to carry out the integration over S and Σ_0 , the hull surface is divided to 40 x 5 panels on each side and the horizontal plane is divided to 50 x 13 panels. If we employ Green's mixed distribution for the hull surface singularities, we have to evaluate the H-function defined by (4). However the following relation is useful for the calculation of $H(\gamma_0 \sec^2 \theta, \theta)$.

$$H(\gamma_0 \sec^2 \theta, \theta) = H'(\gamma_0 \sec^2 \theta, \theta) + \frac{1}{4\pi\gamma_0} \iint_{\Sigma_1} \frac{\partial u_0}{\partial x} \exp[ik(x \cos \theta + y \sin \theta)] dx dy \quad (7)$$

where Σ_1 is the horizontal plane $z = 0$ inside the hull.

References:

1. Maruo, H., Wave resistance of a ship with finite beam at low Froude numbers, Bulletin of Faculty of Eng., Yokohama National Univ. Vol.26 (1977)
2. Maruo, H., Wave resistance of a ship of finite beam predicted by the low speed theory, Journal of Soc. Naval Arch. Japan Vol. 142 (1977)
3. Kayo, Y., A note on the uniqueness of wave-making resistance when the double-body potential is used as the zero-order approximation, Trans. West Japan Soc. of Naval Arch. No.55(1978)



FORMAT FOR TABULATED VALUES OF WAV^e RESISTANCE

WIGLEY (hull surface sources)		Wigley (Green's mixed distribution)			
Fn	Cw x 10 ³	Fn	Cw x 10 ³		
0.266	1.19	0.266	0.75		
0.313	1.40	0.313	1.40		
0.350	2.10	0.350	1.92		
0.402	2.81	0.402	2.30		
0.452	3.14	0.452	3.19		
0.482	2.33	0.482	3.27		

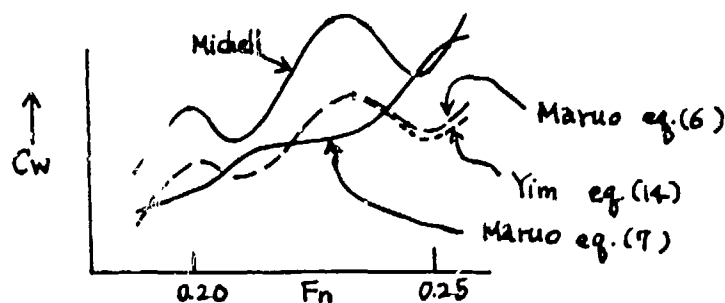
Discussion

by E. Baba

of papers by B. Yim and by H. Maruo

The wave resistance coefficient curve denoted by Maruo-Baba in Figure 2 of Dr. Yim's paper is cited from the paper by Maruo and Suzuki (reference (2)). In the calculation Maruo and Suzuki used the formula (6) of the Maruo paper of the present workshop. It is proved that this formula includes the contribution from the ϕ_{1xx} on the horizontal plane inside hull. On the other hand, Maruo's formula (7) does not include the contribution from ϕ_{1xx} inside hull since Maruo added the second term of (7). This term corresponds to Dr. Yim's correction term, the third term of Dr. Yim's equation (14).

The agreement of wave resistance curves of Dr. Yim and Maruo-Baba seems to indicate that the effect of ϕ_{1xx} inside hull is larger than any other nonlinear effects as concluded by Dr. Yim. From Figure 2 of Dr. Yim's paper we may understand that ϕ_{1xx} inside hull contributes to the reduction of the value of wave resistance in the whole speed range. On the other hand, in the paper by Maruo in the present workshop, a comparison of the calculated results based on the Maruo equations (6) and (7) is shown. The difference of the two curves corresponds to the contribution from ϕ_{1xx} inside hull. In Maruo's case the contribution of ϕ_{1xx} changes its sign with respect to Froude number. Therefore we may say that the trend of the contribution of ϕ_{1xx} inside hull with respect to Froude number is different from that of Dr. Yim's calculation. When we insert wave resistance curve by Michell theory in the Maruo figure, it is hard to conclude that the contribution of ϕ_{1xx} inside hull (Dr. Yim calls sheltering effect) is larger than any other nonlinear effects. This observation is inconsistent with the conclusion of Dr. Yim.



Author's Reply

by H. Maruo
to discussions by E. Baba

The so called sheltering effect seems to be formulated by the addition of the line integral on the one hand and the exclusion of the integral of ϕ_{1xx} inside the hull surface on the other hand. It is not clear that Yim's correction for the sheltering effect corresponds to which of the above two factors. At any rate, the discussion of the sheltering effect with the limitation of the thin ship theory is hard to become convincing.

Computations of Wave Resistance by the Low Speed Theory Imposing Accurate Hull Surface Condition

Takamune Kitazawa*
Hisashi Kajitani**

Summary

The velocity potential which satisfies both the nonlinear free surface condition and the hull surface condition is formulated by imposing accurate hull surface condition to the low speed wave resistance theory developed by Baba¹⁾ or Maruo²⁾. The wavy source distribution added to fulfill the hull surface condition is obtained numerically. The wave resistance, the hull side wave profiles and the velocities around the hull surface are evaluated. The results coincide fairly well with the measured in low speed, especially the humps and the hollows of the calculated wave resistance curves are remarkably reduced by considering the wavy source distribution on the hull surface, though its strength is one-order smaller than that of the double model source distribution.

Nomenclature

$A(\theta)$: amplitude function
$A^*(\theta) = A(\theta)\cos^{\frac{3}{2}}\theta$	
	: weighted amplitude function
$D(x,y)$: Kelvin source distribution on the free surface
F	: free surface of calm water
$F_n = U/\sqrt{gL}$	
	: Froude number
G	: Green's function (Havelock's wave source potential)
g	: acceleration of gravity
$K_0 = g/U^2$	
	: wave number

L	: intersection of plane F and S
L	: ship length
l	: half ship length
n	: outward normal
S	: hull surface
U	: velocity of the uniform stream
x,y,z	: Cartesian coordinate fixed to the ship
ρ	: density of water
ϕ	: wavy potential
ϕ_r	: basic double model potential
σ	: Kelvin source distribution on the hull surface

1. Introduction

Seeking of the hydrodynamical flow model which satisfies the nonlinear free surface condition and the hull surface condition is now on the way. The low speed wave resistance theory (L.S.T.) developed by Baba¹⁾ or Maruo²⁾ seems to be promising to predict the wave resistance of conventional ships, because it includes the nonlinear effect of the free surface condition, though the ship speed is confined to be low. Some successful results^{3),4)} are reported even in the case of full ships. The wave resistance curves calculated by L.S.T., however, have large humps and hollows^{4),5)}, if the computations are carried out by making use of only Kelvin sources over the free surface. The reason is that the interaction between the bow wave and the ship hull is not considered in L.S.T..

In this paper, a theory which includes the nonlinear effects of the

* Technical Research Institute, Hitachi Shipbuilding & Engineering Co., Ltd.

** Department of Naval Architecture, Faculty of Engineering, the University of Tokyo

boundary conditions is discussed by imposing more accurate hull surface condition to L.S.T.. The wavy potential which satisfies the boundary conditions in low speed is formulated and an iterative method to obtain the solution is shown. The first step solution is obtained numerically. The wave resistance, hull side wave profiles and velocities around the hull surface are evaluated by making use of the Kelvin sources distributed over the free surface and the hull surface. They are compared with the measured values to scrutinize the accuracy of the theory.

2. Formulation of the wavy potential

The Cartesian coordinate employed in this paper is shown in Fig.1. For the sake of brevity, the ship is considered to be constrained in the uniform stream.

Let us assume that the potential around a ship is expressed by the summation of two parts: the basic double model potential and the wavy potential.

$$\phi_{total} = \phi_r + \phi \quad (1)$$

Baba¹⁾ derived the free surface condition for the wavy potential on the assumption that the ship speed is low, which includes the nonlinear effect.

$$\begin{aligned} \text{[F]} \quad & \frac{1}{g} \left(\phi_{rx} \frac{\partial}{\partial x} + \phi_{ry} \frac{\partial}{\partial y} \right)^2 \phi + \phi_z \\ & = D(x, y) \quad \text{at } Z = 0 \end{aligned} \quad (2)$$

where

$$\begin{aligned} D(x, y) &= \frac{\partial}{\partial x} (\xi_r \phi_{rx}) + \frac{\partial}{\partial y} (\xi_r \phi_{ry}) \\ &\quad \text{at } Z = 0 \end{aligned} \quad (3)$$

$$\begin{aligned} \xi_r &= \frac{1}{2g} (U^2 - \phi_{rx}^2 - \phi_{ry}^2) \\ &\quad \text{at } Z = 0 \end{aligned} \quad (4)$$

The wavy potential must satisfy Laplace's equation, radiation condition and the hull surface condition.

$$\text{[L]} \quad \phi_{xx} + \phi_{yy} + \phi_{zz} = 0 \quad (5)$$

$$\begin{aligned} \text{[R]} \quad \phi &= \begin{cases} O(1/\sqrt{x^2 + y^2}) & \text{for } x \geq 0 \\ o(1/\sqrt{x^2 + y^2}) & \text{for } x < 0 \end{cases} \\ &\quad \text{as } |x| \rightarrow \infty \end{aligned} \quad (6)$$

$$\text{[H]} \quad \frac{\partial \phi}{\partial n} = 0 \quad \text{on } S \quad (7)$$

The velocity potential satisfying the boundary conditions is formulated based upon Green's theorem, where G is the Green's function which satisfies the linear free surface condition⁴⁾.

$$\begin{aligned} \phi &= - \frac{1}{4\pi} \iint_F DG dx dy \\ &\quad + \frac{1}{4\pi} \iint_S \phi G_n dS \\ &\quad - \frac{1}{4\pi K_o} \int_L (\phi G_x - G \phi_x) dy \\ &\quad + \frac{1}{4\pi g} \iint_F \left\{ \left(\phi_{rx} \frac{\partial}{\partial x} + \phi_{ry} \frac{\partial}{\partial y} \right)^2 \right. \\ &\quad \left. - U^2 \frac{\partial^2}{\partial x^2} \right\} \phi G dx dy \end{aligned} \quad (8)$$

where

$$G_{xx} + K_o G_z = 0 \quad \text{at } Z = 0 \quad (9)$$

ϕ can be expressed only by source distributions on the boundaries by assuming the linear free surface condition inside of the ship.

$$\phi = - \frac{1}{4\pi} \iint_F DG dx dy$$

$$\begin{aligned}
& + \frac{1}{4\pi} \iint_S \sigma G dS \\
& - \frac{1}{4\pi K_0} \int_L \sigma \frac{\partial x}{\partial n} G dy \\
& + \frac{1}{4\pi g} \iint_F \left\{ \left[\phi_{rx} \frac{\partial}{\partial x} + \phi_{ry} \frac{\partial}{\partial y} \right]^2 \right. \\
& \left. - U^2 \frac{\partial^2}{\partial x^2} \right\} \phi G dx dy \quad (10)
\end{aligned}$$

If the first term of the R.H.S. in eq.(10) could be considered to express the wave generation from the free surface, the second term shows the interaction between the wave and the ship hull. The third term indicates the so-called "line integral effect", while the fourth term expresses the effect of the local non-uniform flow to the wave propagation. In L.S.T. by Baba¹⁾ or Maruo²⁾, only the first term was taken into consideration.

3. Solution by the iterative method

The iterative method is required to determine the velocity potential. The first step solution ϕ_1 , which is written as follows,

$$\begin{aligned}
\phi_1 = & - \frac{1}{4\pi} \iint_F D C dx dy \\
& + \frac{1}{4\pi} \iint_S \sigma_1 G dS \\
& - \frac{1}{4\pi K_0} \int_L \sigma_1 \frac{\partial x}{\partial n} G dy \quad (11)
\end{aligned}$$

must satisfy the following conditions.

$$\begin{aligned}
[F_1] \quad \phi_{1xx} + K_0 \phi_{1z} &= D(x, y) \\
&\text{at } Z = 0 \quad (12)
\end{aligned}$$

$$[H_1] \quad \frac{\partial \phi_1}{\partial n} = 0 \quad \text{on } S \quad (13)$$

As the condition $[F_1]$ is automatically satisfied, ϕ_1 should be determined to fulfill the condition $[H_1]$, which is written as the following Fredholm's equation of the second kind.

$$\begin{aligned}
& - \frac{\sigma_1}{2} + \frac{1}{4\pi} \iint_S \sigma_1 \frac{\partial G}{\partial n_f} dS \\
& - \frac{1}{4\pi K_0} \int_L \sigma_1 \frac{\partial x}{\partial n} \frac{\partial G}{\partial n_f} dy \\
& = \frac{1}{4\pi} \iint_F D \frac{\partial G}{\partial n_f} dx dy \quad \text{on } S \quad (14)
\end{aligned}$$

where f means a field point

If the first step solution (ϕ_1) is obtained, the higher step (the k th) is written as follows, and it is determined by solving the following equation.

$$\begin{aligned}
\phi_k = & - \frac{1}{4\pi} \iint_F D G dx dy \\
& + \frac{1}{4\pi} \iint_S \sigma_k G dS \\
& - \frac{1}{4\pi K_0} \int_L \sigma_k \frac{\partial x}{\partial n} G dy \\
& + \frac{1}{4\pi g} \iint_F \left\{ \left[\phi_{k-1,rx} \frac{\partial}{\partial x} + \phi_{k-1,ry} \frac{\partial}{\partial y} \right]^2 \right. \\
& \left. - U^2 \frac{\partial^2}{\partial x^2} \right\} \phi_{k-1} G dx dy \quad (15)
\end{aligned}$$

$$\begin{aligned}
& - \frac{\sigma_k}{2} + \frac{1}{4\pi} \iint_S \sigma_k \frac{\partial G}{\partial n_f} dS \\
& - \frac{1}{4\pi K_0} \int_L \sigma_k \frac{\partial x}{\partial n} \frac{\partial G}{\partial n_f} dy \\
& = \frac{1}{4\pi} \iint_F \left(D - \frac{1}{g} \left\{ \left[\phi_{k-1,rx} \frac{\partial}{\partial x} + \phi_{k-1,ry} \frac{\partial}{\partial y} \right]^2 \right. \right. \\
& \left. \left. - U^2 \frac{\partial^2}{\partial x^2} \right\} \phi_{k-1} \right) dx dy \quad \text{on } S \quad (16)
\end{aligned}$$

In this way, the effect of the local non-uniform flow is included in the second and the higher solutions.

4. Numerical calculations

The higher step solutions are intractable for the enormous computing time. The first step solution still contains difficulty, because the numerical treatment is only available. Therefore, two simplifications are adopted to save the computing time. One is that only the fore body wavy source distribution is obtained, because the interaction between the bow wave and the fore body is dominant. The other is that the line source distribution in eq.(11) is neglected, because its effect is two orders smaller than that of the hull surface source distribution, which is discussed in Appendix 1.

The free surface is divided into 700 panels and the hull surface is divided into 320 panels. The calculations are performed according to the following procedures.

- (1) The hull surface Rankine source distribution which gives the double model flow is determined by the method developed by Hess and Smith⁶⁾.
- (2) The strength of the Kelvin source distribution on the free surface (D in eq.(10)) is calculated by making use of the Rankine source obtained at (1).
- (3) The wavy source distribution on the hull surface (σ_1 in eq.(11)) is determined by solving eq.(14).
- (4) Wave resistance, hull side wave profiles and velocities around the hull are calculated by making use of D and σ_1 .

The Havelock's wave source potential is calculated using exponential function as shown in Appendix 2. Calculations are performed for Wigley's model and M8. The arrangements of the hull surface panels are shown in Fig.2 and the free surface Kelvin source distributions are shown in Fig.3. Some examples of the wavy source distributions on the hull surface are shown in Fig.4, Fig.5 and Fig.6. The strength is one-order smaller

than that of the double model source distribution.

5. Comparison with the measured results

The measured and the calculated wave resistance is shown in Fig.7 and Fig.8. In the speed range lower than $F_n=0.25$, the results of the present theory coincide surprisingly well with those of the experiment, especially the humps and the hollows are less conspicuous than those of the low speed theory. Examples of amplitude functions and hull side wave profiles are shown in Fig.9 ~ 12. It is seen that better results are obtained by the present theory.

In order to scrutinize the accuracy of the velocity potential, the velocities around the hull surface are measured and compared with the calculated results (Fig.13 ~ 14). The agreement is fairly well in amplitude, but phase difference is observed, though the difference becomes smaller in the present analysis. The measured values seem to be pushed out to the transverse direction about half breadth of the ship. The main reason is that the effect of the local non-uniform flow on wave propagation, which is expressed by the fourth term of eq.(8), is not considered in the first step solution.

6. Conclusions

The conclusions obtained from these analyses are as follows.

- (1) The wavy potential which satisfies the nonlinear free surface condition and the hull surface condition is formulated by imposing more accurate hull surface condition to the low speed theory, and the first step solution is obtained numerically.
- (2) Wave resistance, hull side wave profiles and velocities around the hull surface are calculated. They agree well with the measured values in low speed ($F_n < 0.25$), especially the humps and the hollows of the wave resistance curves are

remarkably reduced by this improvement.
(3) Phase difference is observed between the calculated and the measured velocities. The measured values seem to be pushed out to the transverse direction about half breadth of the ship. The effect of the local non-uniform flow on wave propagation has to be taken into account to obtain more accurate results.

Acknowledgement

Dr. Matao Takagi (Hitachi Shipbuilding & Engineering Co., Ltd.) suggested the research to the authors and Mr. Yoshihiro Shimomura (Sumitomo Heavy Industries Co., Ltd.) assisted the authors with computations. They are gratefully acknowledged.

References

- 1) Baba, E., 'Wave Resistance of Ships in Low Speed', Mitsubishi Technical Bulletin, No.109, (1976).
- 2) Maruo, H., 'Wave Resistance of a Ship with Finite Beam at Low Froude Numbers', Bulletin of Faculty of Engineering, Yokohama National University, Vol.26, (1977).
- 3) Baba, E. and Hara, M., 'Numerical Evaluation of a Wave Resistance Theory', Second International Conference on Numerical Ship Hydrodynamics, Berkeley, (1977).
- 4) Kitazawa, T., and Tanaka, H., 'Wave Resistance of a Full Ship in Medium Speed', J. of the Kansai Society of Naval Architects, Japan, No.170, (1978).
- 5) Maruo, H. and Suzuki, K., 'Wave Resistance of a Ship of Finite Beam Predicted by the Low Speed Theory', J. of the Society of Naval Architects of Japan, No.142, (1977).
- 6) Hess, J.L. and Smith, A.M.O., 'Calculation of Nonlifting Potential Flow about Arbitrary Three-Dimensional Bodies', J.S.R., Vol.8, (1964).

Appendix 1 Effect of the line integral

The wavy potential of the first step is written as follows.

$$\begin{aligned}\phi_1 &= -\frac{1}{4\pi} \iint_F DGdx dy + \frac{1}{4\pi} \iint_S \sigma_1 GdS \\ &\quad - \frac{1}{4\pi K_0} \int_L \sigma_1 \frac{\partial x}{\partial n} G dy \\ &= -\frac{1}{4\pi} \iint_F DGdx dy + \frac{1}{4\pi} \iint_S \sigma_1 GdS \\ &\quad - \frac{1}{4\pi K_0} \int_L \sigma_1 G \frac{f_x^2}{1+f_x^2} dc \quad (A.1)\end{aligned}$$

where $y = f(x)$: equation of the hull surface at L.W.L..

C : the arc along the water line

If the order of f_x is ϵ , the contribution of the line integral is smaller than the second term by ϵ^2 times. In the case of Wigley's model and M8, the effect of the line integral is negligible.

Appendix 2 Numerical calculations of Green's function

Havelock's wave source potential is used as the Green's function and it is written by the following two formulae.

$$G^+(x, y, z; \xi, \eta, \zeta) = -\frac{1}{r_1} - \frac{1}{r_2} + H^+ \quad (A.2)$$

$$\begin{aligned}H^+ &= \frac{2}{\pi} \int_{-\frac{\pi}{2}}^{\frac{\pi}{2}} d\theta \int_0^\infty \frac{k \exp(k\bar{\omega}(\theta))}{k - K_0 \sec^2 \theta} dk \\ &\quad + 2K_0 i \int_{-\frac{\pi}{2}}^{\frac{\pi}{2}} \sec^2 \theta \\ &\quad \exp(K_0 \sec^2 \theta \bar{\omega}(\theta)) d\theta \quad (A.3)\end{aligned}$$

$$G(x, y, z; \xi, \eta, \zeta) = -\frac{1}{r_1} + \frac{1}{r_2} + H^- \quad (\text{A.4})$$

$$H^- = \frac{2}{\pi} \int_{-\frac{\pi}{2}}^{\frac{\pi}{2}} d\theta \int_0^{\infty} \frac{\exp(k \tilde{\omega}(\theta))}{k - K_0 \sec^2 \theta} dk + 2K_0 i \int_{-\frac{\pi}{2}}^{\frac{\pi}{2}} \sec^2 \theta \exp(K_0 \sec^2 \theta \tilde{\omega}(\theta)) d\theta \quad (\text{A.5})$$

where (x, y, z) : field point, (ξ, η, ζ) : singular point

$$r_1^2 = (x - \xi)^2 + (y - \eta)^2 + (z - \zeta)^2$$

$$r_2^2 = (x - \xi)^2 + (y - \eta)^2 + (z + \zeta)^2$$

$$\tilde{\omega}(\theta) = (z + \zeta) + i \{ (x - \xi) \cos \theta + (y - \eta) \sin \theta \}$$

Exponential function is introduced to calculate G numerically, for example H^- is written as follows.

$$H^- = -\frac{2K_0}{\pi} \int_{-\frac{\pi}{2}}^{\frac{\pi}{2}} \sec^2 \theta \exp(P(\theta)) \bar{E}_i(-P(\theta)) d\theta \quad (\text{A.6})$$

$$+ 2K_0 i \int_{-\frac{\pi}{2}}^{\frac{\pi}{2}} \sec^2 \theta \exp(P(\theta)) d\theta$$

$$= -\frac{2K_0}{\pi} \int_{-\frac{\pi}{2}}^{\frac{\pi}{2}} \sec^2 \theta \exp(P(\theta))$$

$$\{ \bar{E}_i(-P(\theta)) - \pi i \} d\theta \quad (\text{A.6})$$

$$\text{where } \bar{E}_i(-P) = \int_P^{\infty} \frac{\exp(-m)}{m} dm$$

$$: \text{Exponential function} \quad (\text{A.7})$$

$$P(\theta) = K_0 \sec^2 \theta / (z + \zeta) + i \{ (x - \xi) \cos \theta + (y - \eta) \sin \theta \}$$

The exponential function is calculated by the form of series expansions for small $|P(\theta)|$ and asymptotic expansions for large $|P(\theta)|$.

Appendix 3 Calculation of the wave resistance

The amplitude function and the wave resistance corresponding to eq.(11) is written as follows.

$$A(\theta) = -\frac{K_0}{\pi} \iint_F D \exp(q(\theta)) dx dy \sec^3 \theta + \frac{K_0}{\pi} \iint_S \sigma_1 \exp(q(\theta)) dS \sec^3 \theta - \frac{1}{4\pi} \int_L \sigma_1 \frac{\partial x}{\partial n} \exp(q(\theta)) dy \sec^3 \theta \quad (\text{A.8})$$

$$\text{where } q(\theta) = K_0 \sec^2 \theta \{ z - i(x \cos \theta + y \sin \theta) \}$$

$$C_w = R_w / \frac{1}{2} \rho U^2 L^2 = 2\pi \int_0^{\frac{\pi}{2}} \left| \frac{A(\theta)}{L} \right|^2 \cos^3 \theta d\theta = 2\pi \int_0^{\frac{\pi}{2}} \left| \frac{A^*(\theta)}{L} \right|^2 d\theta \quad (\text{A.9})$$

$$\text{where } A^*(\theta) = A(\theta) \cos^{\frac{3}{2}} \theta$$

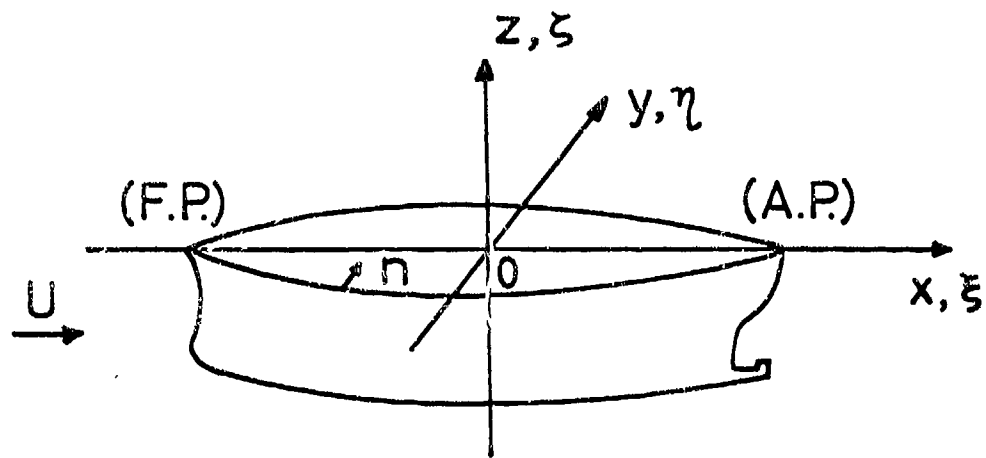


Fig.1 Coordinate System

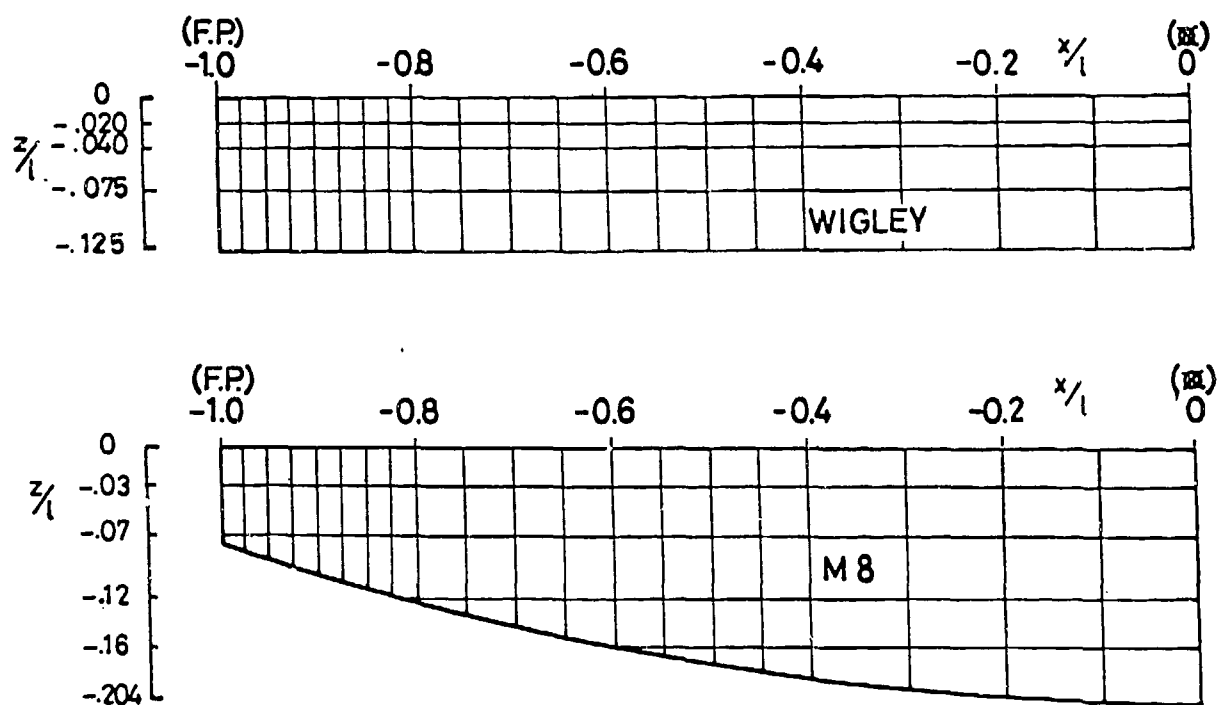


Fig. 2 Hull Surface Panel Array of "WIGLEY" & M8

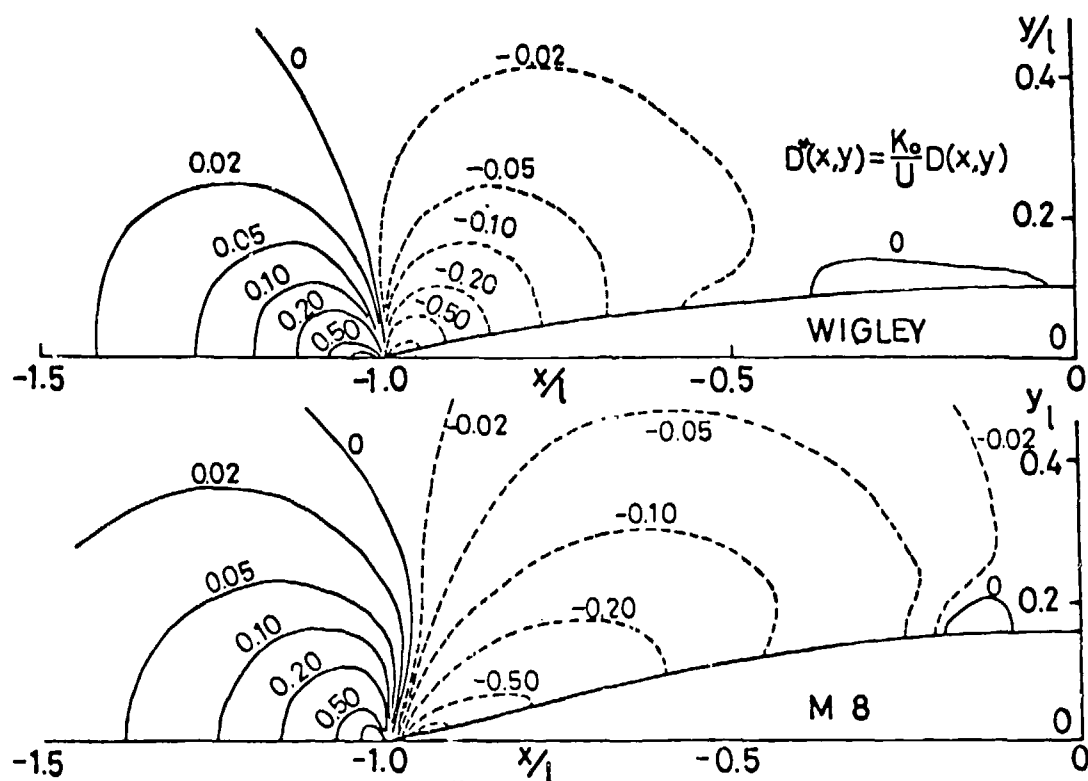


Fig. 3 Contour of $D^*(x,y)$ of WIGLEY & M8

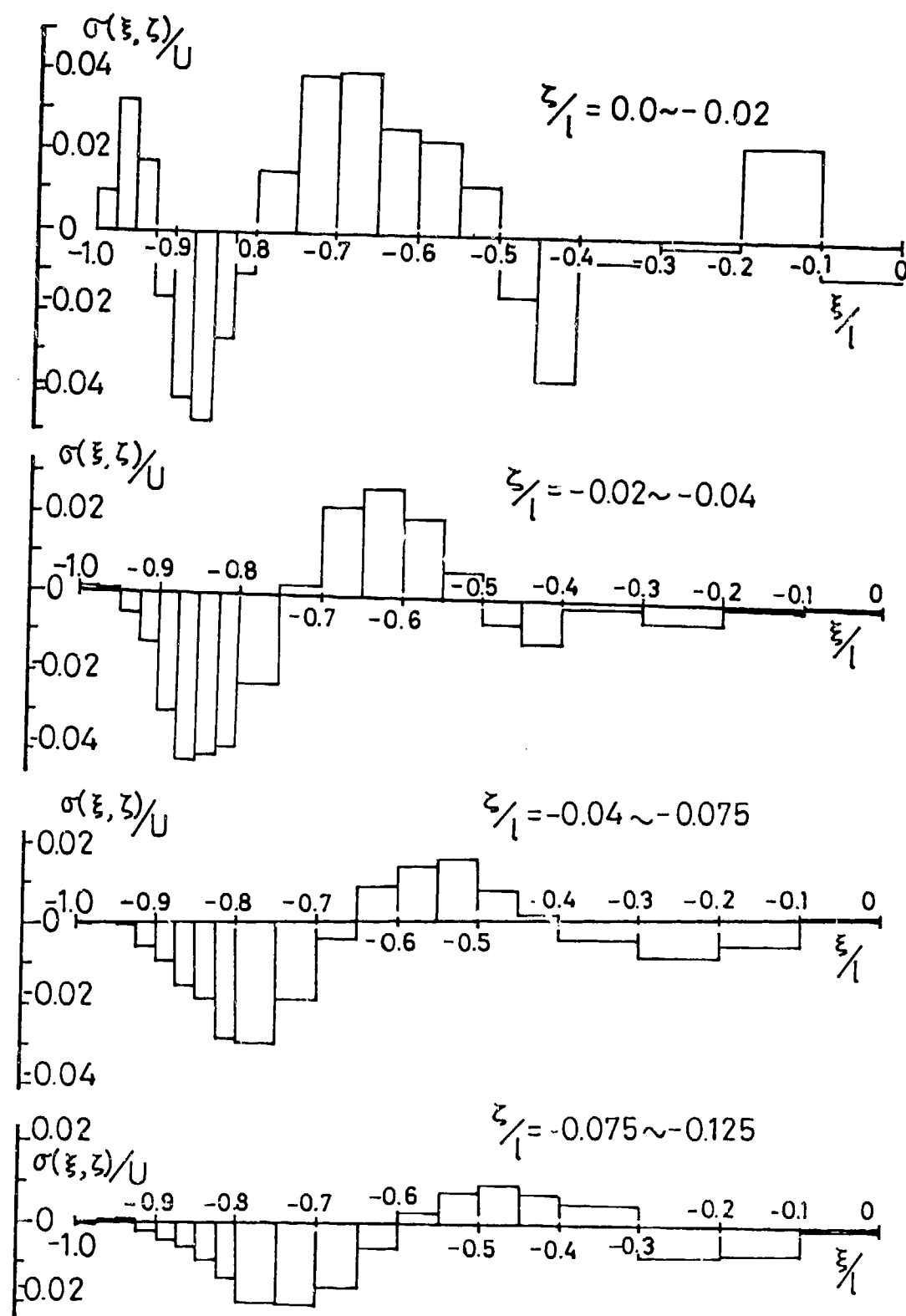


Fig. 4 Added Source on the Hull Surface
(WIGLEY $F_n = 0.2182$)

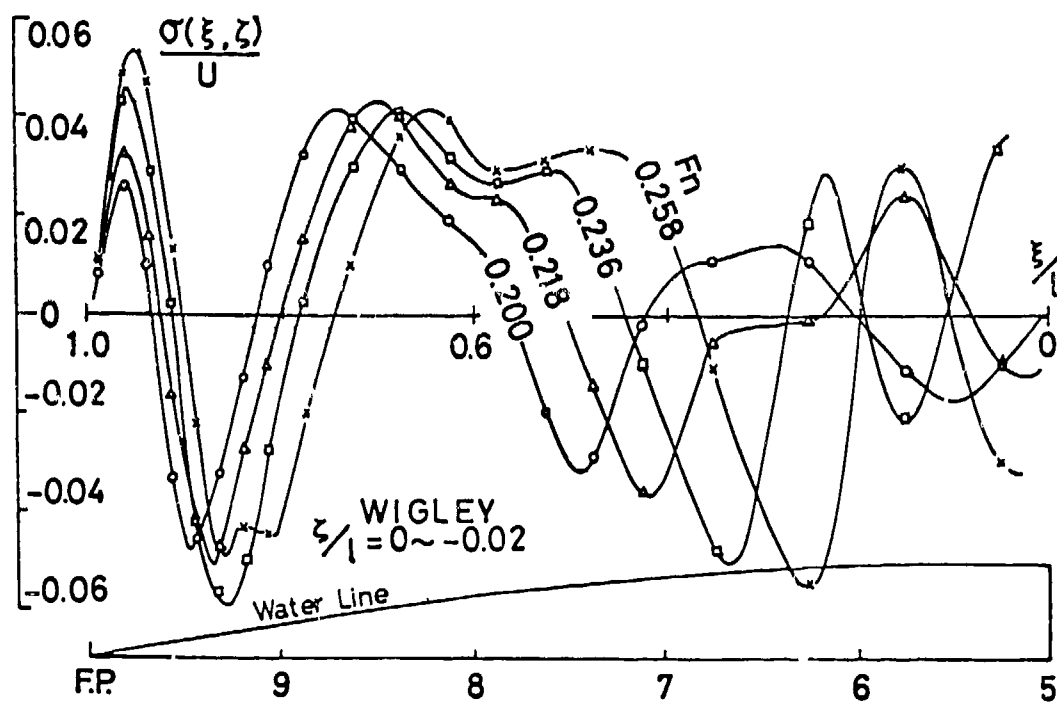


Fig. 5 Speed Dependence of Added Source

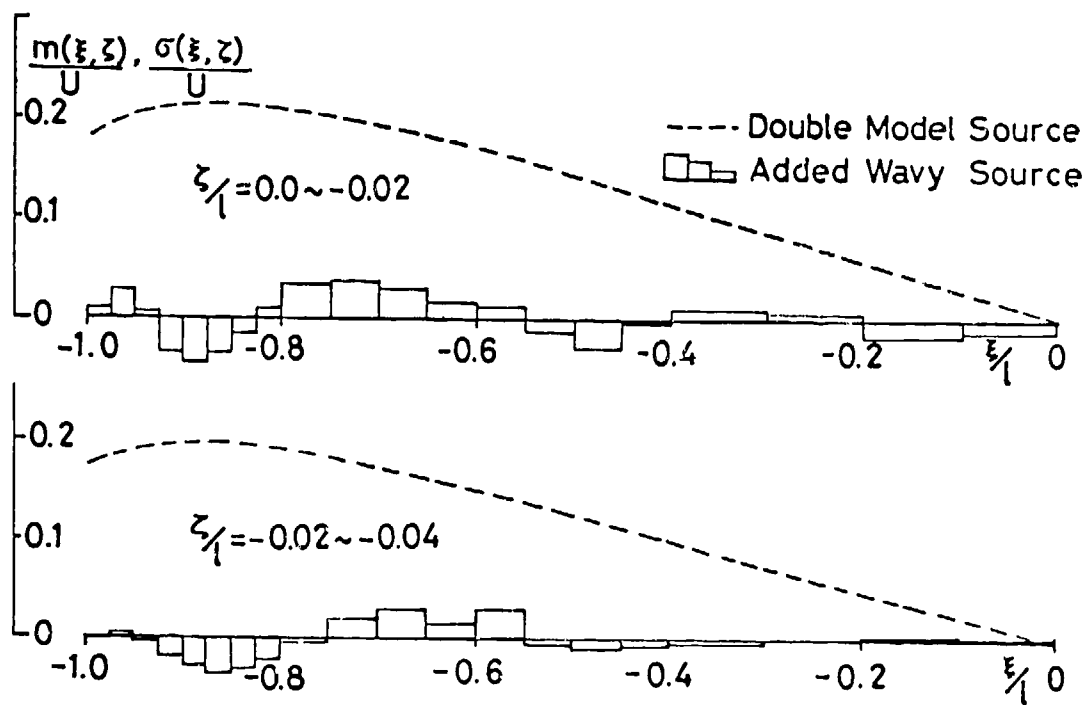


Fig. 6 Hull Source Distribution of WIGLEY ($Fn = 0.20$)

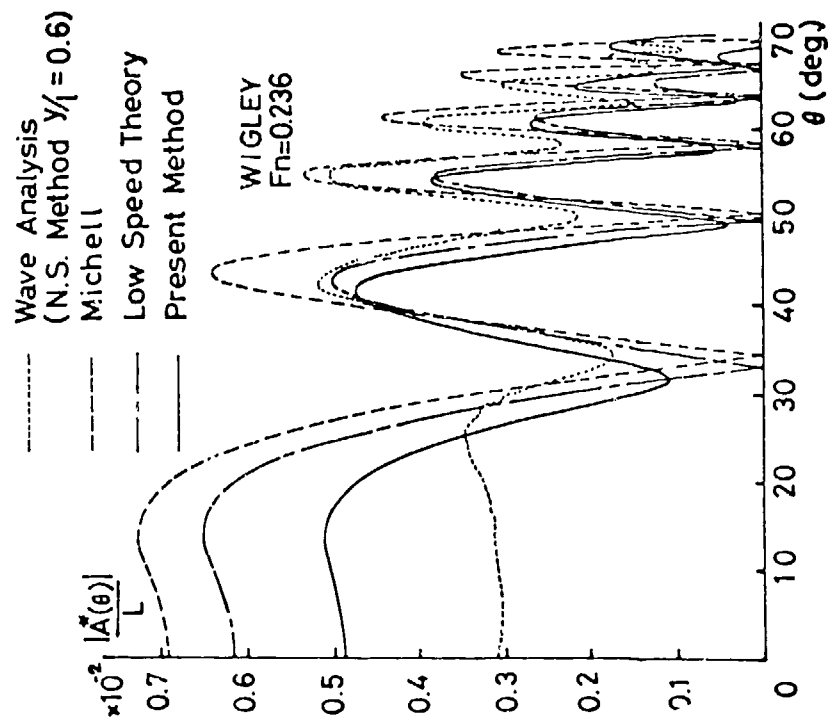


Fig. 7 Weighted Amplitude Function

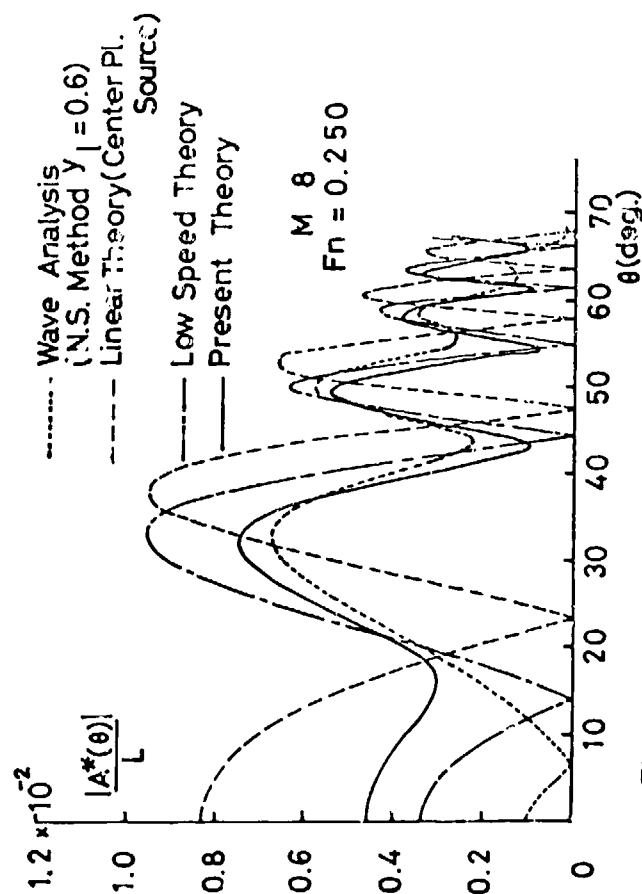


Fig. 8 Weighted Amplitude Function

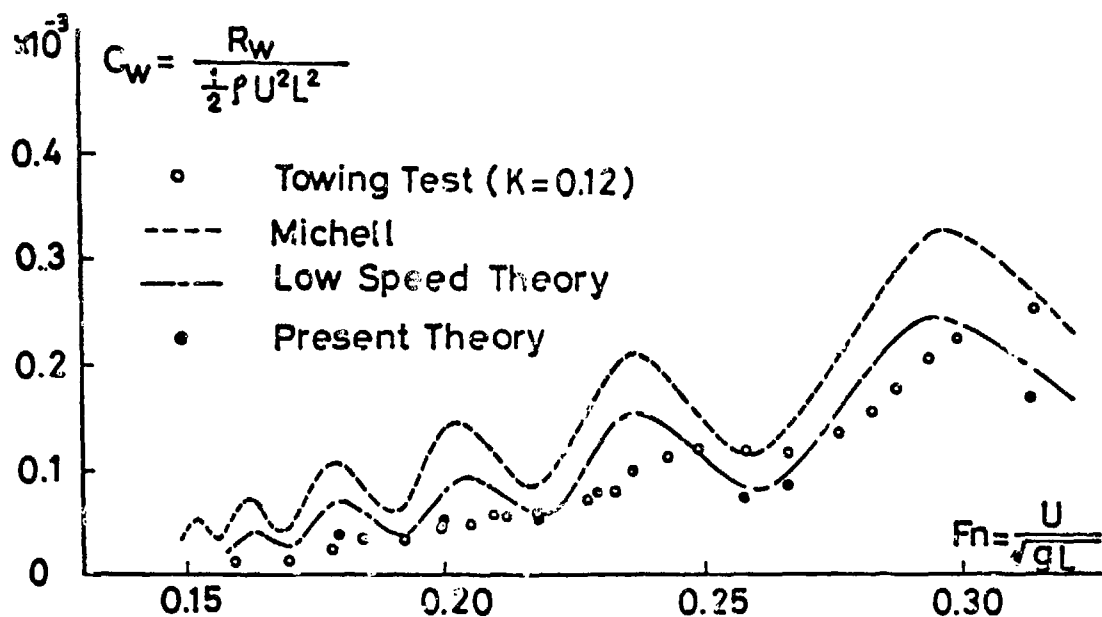


Fig. 9 Wave Making Resistance of WIGLEY

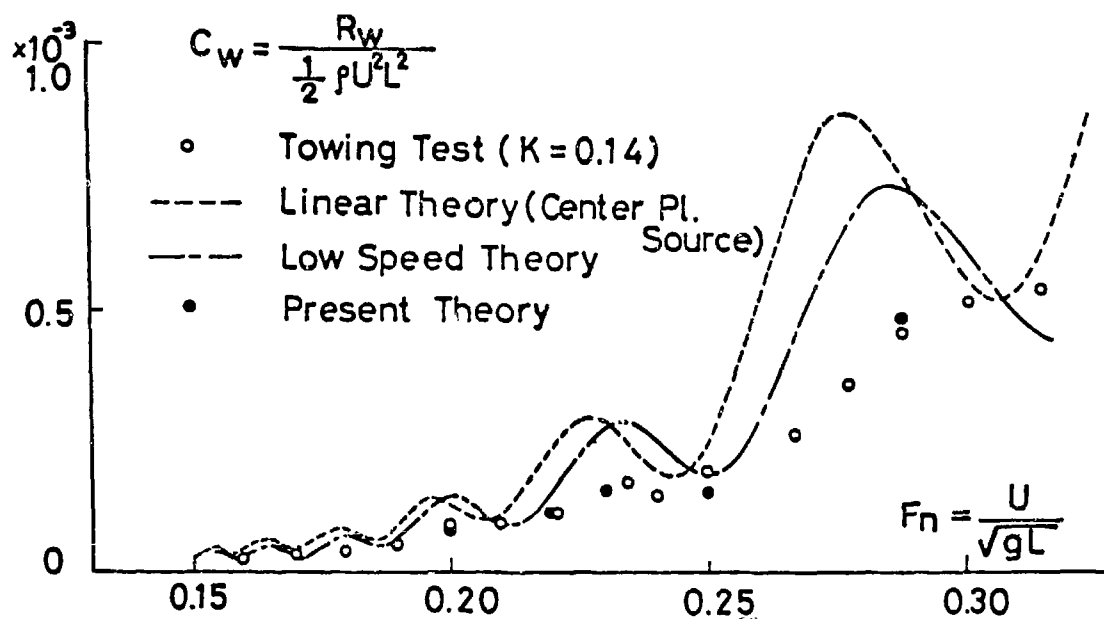


Fig. 10 Wave Making Resistance of M 8

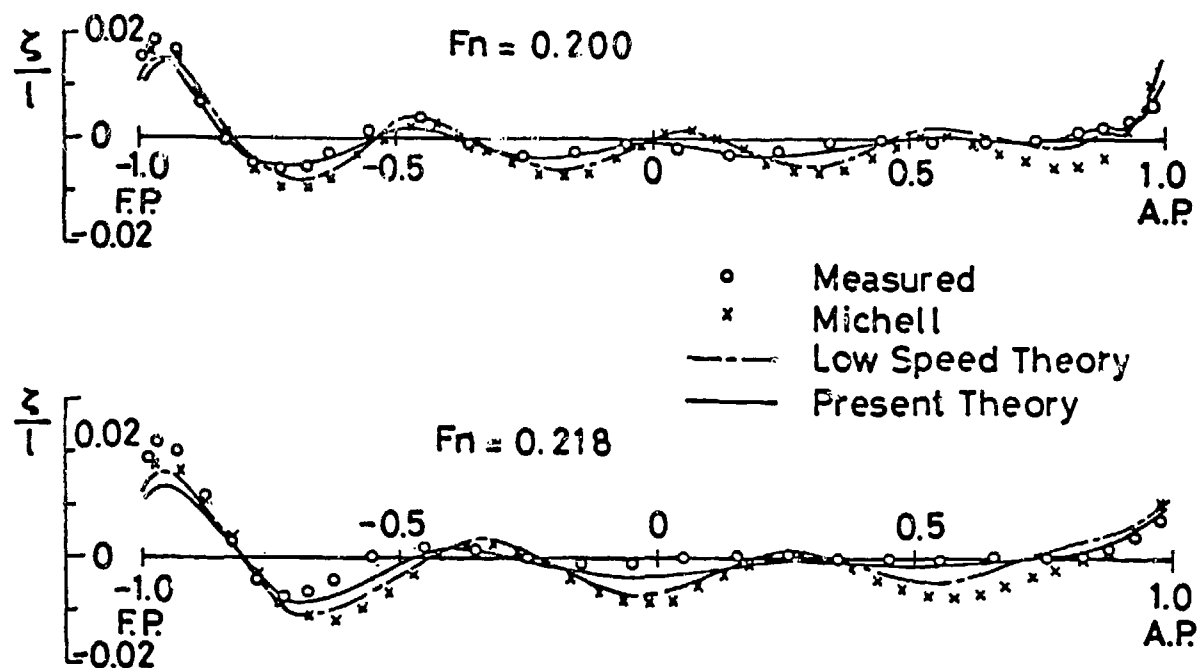


Fig.11 Hull Side Wave Profiles of WIGLEY

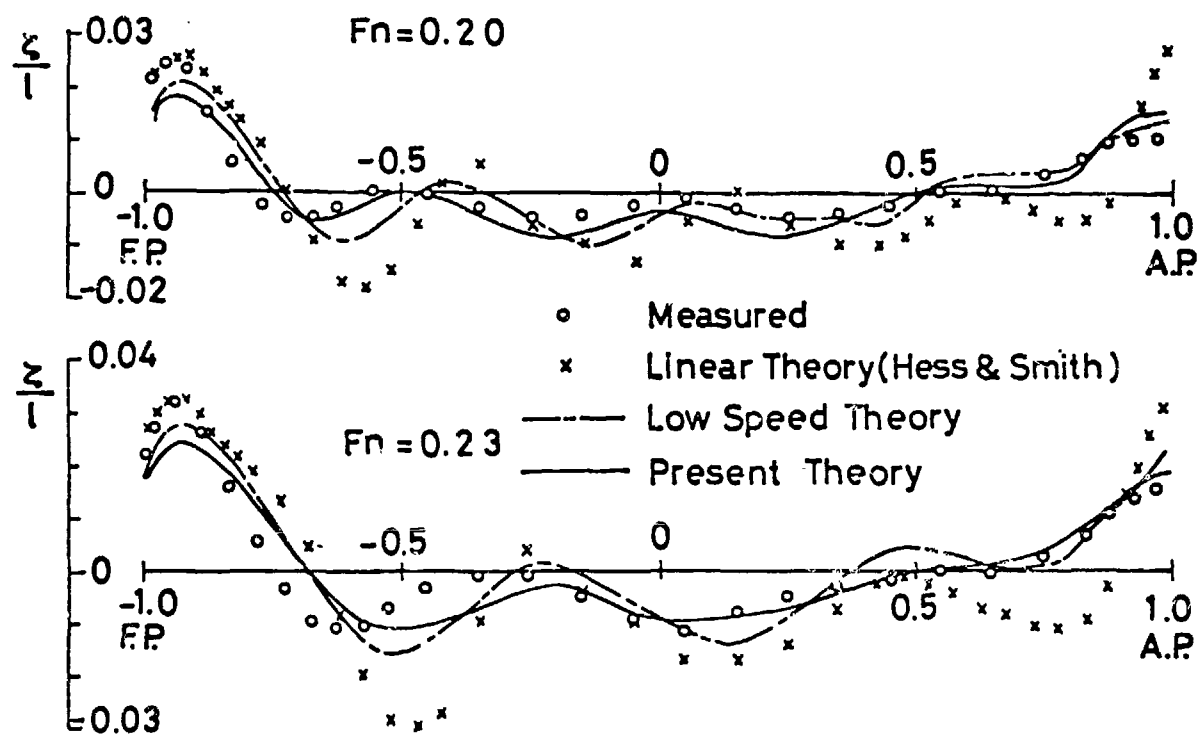


Fig.12 Hull Side Wave Profiles of M 8

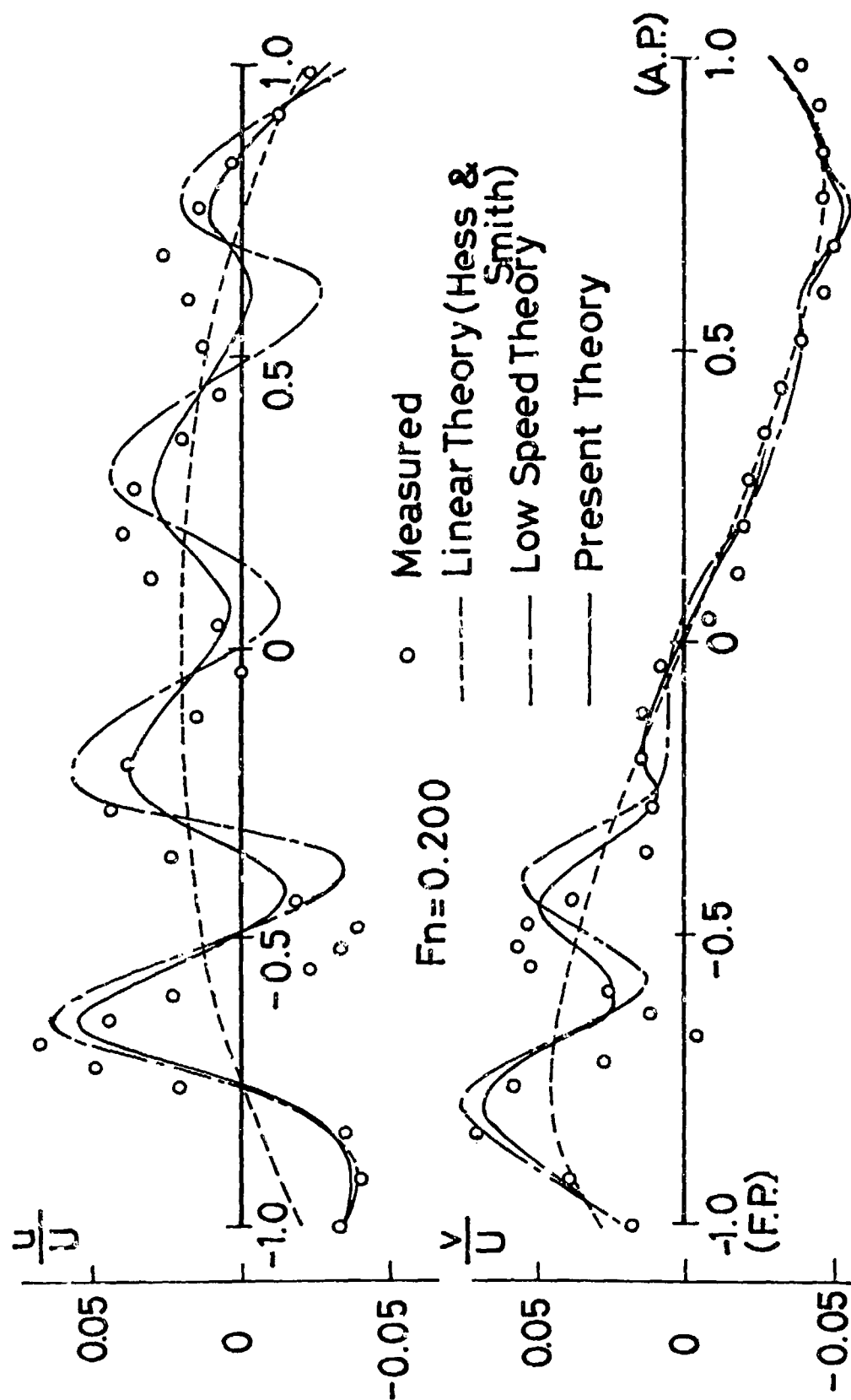
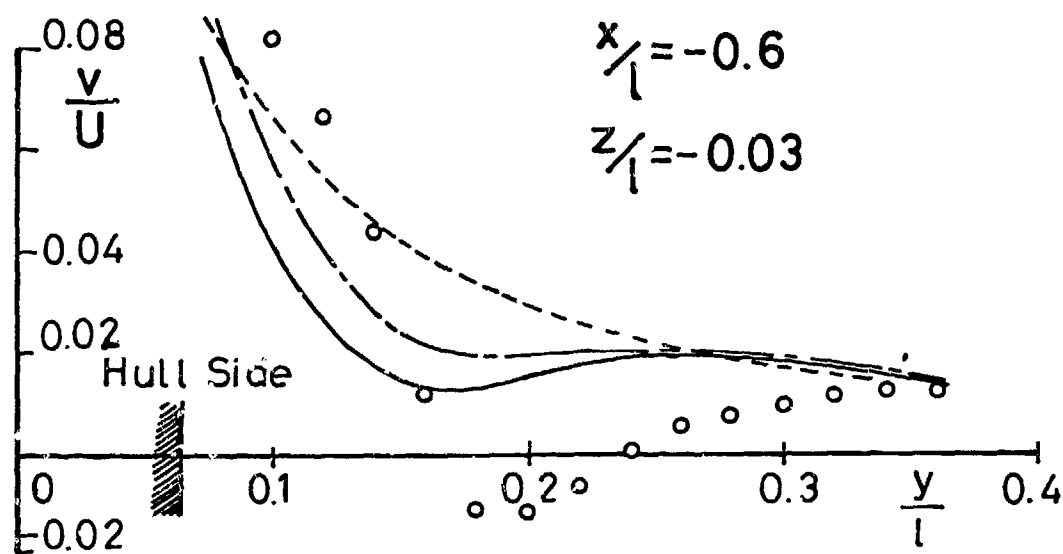


Fig. 13 Perturbation Velocity (u, v) of WIGLEY along Longl. Line $y/l = 0.15, z/l = -0.03$



• Measured

---- Double Model Component $F_n = 0.200$

-.-.- Low Speed Theory

— Present Theory

WIGLEY

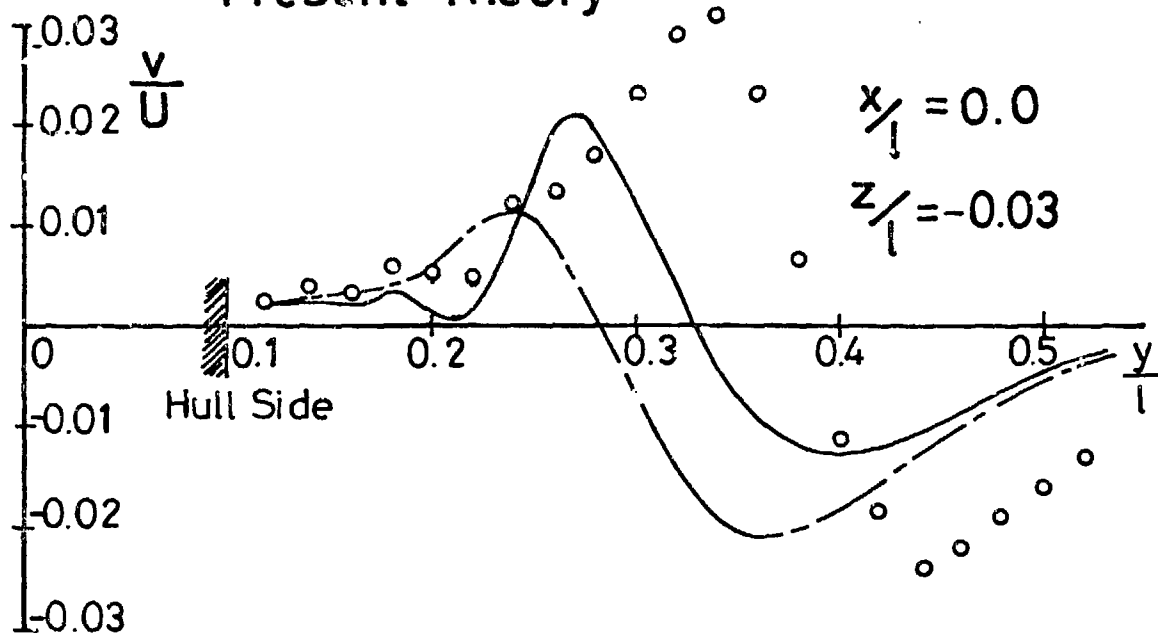


Fig. 14 Perturbation Velocity v
along Transv. Line

FORMAT FOR TABULATED VALUES OF WAVE RESISTANCE

T. Kitazawa / The Low Speed Theory Imposing Accurate Hull Surface Condition

Wigley Low Speed Theory		Wigley Present Theory		$CW = R_W / \frac{1}{2} \rho V^2 S$	
Fn	$CW \times 10^3$	Fn	$CW \times 10^3$		
0.200	0.55	0.200	0.37		
0.218	0.40	0.218	0.33		
0.236	0.99	0.236	0.68		
0.258	0.57	0.258	0.49		
0.266	0.69	0.266	0.57		
0.313	1.39	0.313	1.12		
0.350	0.74	0.350	0.72		
0.452	1.75	0.452	1.18		

FORMAT FOR TABULATED VALUE OF WAVE ELEVATION

T. Kitazawa / The Low Speed Theory Imposing Accurate Hull Surface Condition

Wigley / $Fn = 0.200$ Low Speed Theory		Wigley / $Fn = 0.200$ Present Theory		Wigley / $Fn = 0.218$ Low Speed Theory		Wigley / $Fn = 0.218$ Present Theory	
x/l	$\zeta(x)/l$	x/l	$\zeta(x)/l$	x/l	$\zeta(x)/l$	x/l	$\zeta(x)/l$
-1.0(FP)	0.0102	-1.0(FP)	0.0096	-1.0(FP)	0.0125	-1.0(FP)	0.0107
-0.95	0.0150	-0.95	0.0140	-0.95	0.0165	-0.95	0.0130
-0.9	0.0121	-0.9	0.0097	-0.9	0.0130	-0.9	0.0101
-0.85	0.0046	-0.85	0.0025	-0.85	0.0067	-0.85	0.0055
-0.8	-0.0034	-0.8	-0.0031	-0.8	-0.0014	-0.8	-0.0001
-0.7	-0.0072	-0.7	-0.0050	-0.7	-0.0108	-0.7	-0.0082
-0.6	-0.0051	-0.6	-0.0030	-0.6	-0.0083	-0.6	-0.0053
-0.5	0.0024	-0.5	0.0011	-0.5	-0.0034	-0.5	-0.0019
-0.4	0.0022	-0.4	0.0006	-0.4	0.0024	-0.4	0.0010
-0.3	-0.0028	-0.3	-0.0025	-0.3	0.0030	-0.3	0.0002
-0.2	-0.0054	-0.2	-0.0036	-0.2	-0.0012	-0.2	-0.0020
-0.1	-0.0059	-0.1	-0.0020	-0.1	-0.0052	-0.1	-0.0030
0.0	0.0001	0.0	-0.0008	0.0	-0.0060	0.0	-0.0034
0.1	0.0007	0.1	-0.0015	0.1	-0.0030	0.1	-0.0024
0.2	-0.0028	0.2	-0.0030	0.2	0.0007	0.2	-0.0012
0.3	-0.0045	0.3	-0.0027	0.3	0.0010	0.3	-0.0006
0.4	-0.0028	0.4	-0.0016	0.4	-0.0014	0.4	-0.0009
0.5	0.0013	0.5	-0.0001	0.5	-0.0038	0.5	-0.0014
0.6	0.0015	0.6	-0.0002	0.6	-0.0031	0.6	-0.0011
0.7	-0.0002	0.7	0.0000	0.7	0.0000	0.7	-0.0002
0.8	-0.0014	0.8	0.0009	0.8	0.0027	0.8	0.0014
0.9	0.0010	0.9	0.0023	0.9	0.0057	0.9	0.0049
1.0(AP)	0.0150	1.0(AP)	0.0120	1.0(AP)	0.0121	1.0(AP)	0.0106

FORMAT FOR TABULATED VALUES OF PERTURBATION VELOCITY
T. Kitazawa / The Low Speed Theory Imposing Accurate Hull Surface Condition

Wigley / Fn = 0.200 Low Speed Theory		Wigley / Fn = 0.200 Present Theory		Wigley / Fn = 0.200 Low Speed Theory		Wigley / Fn = 0.200 Present Theory	
$y/l = 0.15$ $z/l = -0.03$ x/l	$u(x)/U$	$y/l = 0.15$ $z/l = -0.03$ x/l	$u(x)/U$	$y/l = 0.15$ $z/l = -0.03$ x/l	$v(x)/U$	$y/l = 0.15$ $z/l = -0.03$ x/l	$v(y)/U$
-1.0	-0.0341	-1.0	-0.0330	-1.0	0.0206	-1.0	0.0209
-0.9	-0.0390	-0.9	-0.0366	-0.9	0.0484	-0.9	0.0467
-0.8	-0.0204	-0.8	-0.0196	-0.8	0.0703	-0.8	0.0666
-0.7	0.0282	-0.7	0.0320	-0.7	0.0541	-0.7	0.0535
-0.6	0.0566	-0.6	0.0468	-0.6	0.0156	-0.6	0.0240
-0.5	0.0058	-0.5	0.0048	-0.5	0.0520	-0.5	0.0404
-0.4	-0.0332	-0.4	-0.0125	-0.4	0.0548	-0.4	0.0415
-0.3	0.0154	-0.3	0.0222	-0.3	0.0232	-0.3	0.0156
-0.2	0.0568	-0.2	0.0364	-0.2	0.0063	-0.2	0.0146
-0.1	0.0389	-0.1	0.0253	-0.1	0.0061	-0.1	0.0092
0.0	-0.0012	0.0	0.0077	0.0	0.0029	0.0	0.0022
0.1	-0.0095	0.1	0.0080	0.1	-0.0040	0.1	-0.0072
0.2	0.0204	0.2	0.0223	0.2	-0.0173	0.2	-0.0185
0.3	0.0439	0.3	0.0283	0.3	-0.0294	0.3	-0.0257
0.4	0.0291	0.4	0.0203	0.4	-0.0336	0.4	-0.0327
0.5	-0.0052	0.5	0.0037	0.5	-0.0402	0.5	-0.0416
0.6	-0.0157	0.6	-0.0027	0.6	-0.0394	0.6	-0.0410
0.7	0.0057	0.7	0.0064	0.7	-0.0536	0.7	-0.0533
0.8	0.0201	0.8	0.0080	0.8	-0.0480	0.8	-0.0470
0.9	-0.0011	0.9	-0.0079	0.9	-0.0412	0.9	-0.0406
1.0	-0.0346	1.0	-0.0274	1.0	-0.0249	1.0	-0.0255

WAVE RESISTANCE COMPUTATIONS BY LOW SPEED THEORY

Eiichi Baba
Nagasaki Technical Institute
Mitsubishi Heavy Industries, Ltd.
1-1 Akunoura-machi
Nagasaki, Japan

METHOD OF COMPUTATION

A wave resistance formula in low speed has been proposed by Baba and Takekuma (1975) and Maruo (1976). In this report an asymptotic expression in the low speed limit of the above wave resistance formula is used. The details of the method of computation is shown in the paper by Baba and Hara (1977).

The asymptotic wave resistance coefficient is expressed as

$$C_w = \frac{R_w}{\frac{1}{2}\rho U^2 S} = 2\pi \frac{L^2}{S} \int_0^{\pi/2} \left| \frac{A(\theta)}{L} \right|^2 \cos^3 \theta d\theta,$$

where

$$\frac{A(\theta)}{L} = -i \frac{\sec^2 \theta}{2\pi} F_n^2 \int_0^{2\pi} d\beta F(\beta) \exp \left[i \frac{\sec^2 \theta}{2F_n^2} \psi(\beta, \theta) \right],$$

$$\psi(\beta, \theta) = \cos \beta \sin \theta + 2 \left(\frac{y}{L} \right) \sin \theta, \quad \frac{x}{L} = \frac{1}{2} \cos \beta,$$

$$F(\beta) = v p' - p w_z y', \quad p' = \frac{dp}{d\beta}, \quad y' = \frac{d}{d\beta} \left(\frac{y}{L} \right),$$

$$p = [1 - u^2 - v^2]_{z=0},$$

$$u = 1 + \frac{1}{U} \frac{\partial \phi}{\partial x}, \quad v = \frac{1}{U} \frac{\partial \phi}{\partial y}, \quad w_z = \frac{L}{U} \frac{\partial^2 \phi}{\partial z^2},$$

$\phi(x, y, z)$ is the perturbation velocity potential of a double body.

Editor's Note: For Inui S-201, $C_s = 0.618$ was used. However, in overview computer plot the correction was made.

The velocity components along the load waterline are calculated by Hess and Smith method (1964).

RESULTS OF COMPUTATIONS

Wave resistance of the following four ship forms were computed.

	No. of body surface elements
Wigley	300
S201	158
Series 60 $C_B=0.60$	146
HSVA Tanker	342

An example of arrangement of surface elements is shown in Fig.1. The computed values of p , v , w_z , p' , y' and $F(\beta)$ are tabulated in Tables 1 through 4. The calculated wave resistance coefficients are tabulated in Tables 5 and 6 and the wave resistance coefficient curves are shown in Figs.2 through 5. A comparison of wave amplitude of S201 is shown in Fig.6.

REFERENCES

1. Baba, E. and Takekuma, K., A study on free-surface flow around the bow of slowly moving full forms, Journal of The Society of Naval Architects of Japan, Vol.137, 1975.
2. Baba, E. and Hara, M., Numerical evaluation of a wave-resistance theory for slow ships, 2nd International Conference on Numerical Ship Hydrodynamics, Berkeley, 1977.
3. Hess, J. L. and Smith, A. M. O., Calculation of nonlifting potential flow about arbitrary three-dimensional bodies, Journal of Ship Research, Vol.8, No.2, 1964.
4. Maruo, H., Wave resistance of a ship with finite beam at low Froude numbers, Bulletin of the Faculty of Engineering, Yokohama National Univ., Vol.26, 1976.

Table 1

Wigley

NO.	π/L X	y/L Y	β BETA	p P	v U	ω_L UZ	$dt/d\beta$ P'	$d(\frac{1}{2})/d\beta$ Y'	$F(\beta)$ F(BETA)
1	.50000	.00000	.00000	1.0000	.00000	-1.5760	.00000	.14221-.03	.22412-.03
2	.49750	.50177-.03	.10004	.32377	-.15962	-2.0685	-8.5654	.98892-.02	1.3738
3	.49250	.14898-.02	.17342	.22816	-.16890	-2.4298	-1.1407	.16937-.01	.20205
4	.48625	.27136-.02	.23506	.16625	-.17340	-2.7669	-.87534	.23606-.01	.16218
5	.47875	.41619-.02	.29259	.12282	-.17520	-3.0836	-.9589	.27582-.01	.13237
6	.46250	.72371-.02	.38976	.04888-.01	-.17492	-3.3576	-.98528	.34944-.01	.09206-.01
7	.43750	.11730-.01	.50536	.24044-.01	-.16924	-3.5990	-.28713	.42031-.01	.52585-.01
8	.41250	.15981-.01	.60059	.18928-.02	-.16153	-4.1817	-.18265	.46363-.01	.29870-.01
9	.37500	.21914-.01	.72273	.12589-.01	-.14800	-4.3268	-.10542	.49116-.01	.12936-.01
10	.32500	.28901-.01	.86321	-.25274-.01	-.12931	-4.2651	-.75122-.01	.48740-.01	.44600-.02
11	.27500	.34893-.01	.98843	-.32987-.01	-.10992	-3.5780	-.53592-.01	.45438-.01	.71623-.04
12	.22500	.39887-.01	1.1040	-.38327-.01	-.90230-.01	-3.5038	-.40519-.01	.39810-.01	.16900-.02
13	.17500	.43883-.01	1.2132	-.42165-.01	-.70341-.01	-2.8794	-.30479-.01	.32505-.01	.18025-.02
14	.12500	.46881-.01	1.3181	-.44892-.01	-.50327-.01	-2.1391	-.21622-.01	.28006-.01	.12170-.02
15	.07500-.01	.48878-.01	1.4202	-.46665-.01	-.30233-.01	-1.3164	-.13000-.01	.14702-.01	-.51011-.03
16	.02500-.01	.49875-.01	1.5208	-.47540-.01	-.10093-.01	-.4434	-.43439-.02	.49955-.02	-.61680-.04
17	.00000	.50000-.01	1.5708	-.47649-.01	-.20687-.04	-.26375-.02	-.19370-.04	-.35366-.04	-.50190-.08
NO.	X	Y	BETA	P	U	UZ	P'	Y'	F(BETA)
1	.50000	-.37253-.08	3.1416	1.0000	.00000	1.5749	.00000	-.14353-.03	.22604-.03
2	.49750	.50144-.03	3.2416	.32382	-.15971	2.0666	-8.5650	-.98853-.02	1.3745
3	.49250	.14894-.02	3.3159	.22814	-.16897	2.4273	-1.1407	-.16936-.01	.20213
4	.48625	.27146-.02	3.3767	.16620	-.17346	2.7650	-.87549	-.22772-.01	.16233
5	.47875	.41624-.02	3.4342	.12274	-.17524	3.0817	-.69635	-.28352-.01	.13276
6	.46250	.72388-.02	3.5314	.04827-.01	-.17493	3.5365	-.8502	-.35704-.01	.09029-.01
7	.43750	.11732-.01	3.6470	.25992-.01	-.16924	3.9484	-.27709	.42914-.01	.52652-.01
8	.41250	.15982-.01	3.7422	.18483-.02	-.16152	4.1813	-.18261	.48035-.01	.29867-.01
9	.37500	.21913-.01	3.8643	.12620-.01	-.14808	4.3268	-.10536	.49116-.01	.12920-.01
10	.32500	.28901-.01	4.0048	-.25299-.01	-.12929	4.2651	-.75978-.01	.48741-.01	.44476-.02
11	.27500	.34892-.01	4.1300	.33007-.01	-.10991	3.9779	-.53560-.01	.45439-.01	.70318-.04
12	.22500	.39887-.01	4.2456	.38344-.01	-.90207-.01	3.5038	-.40486-.01	.39810-.01	.16963-.02
13	.17500	.43883-.01	4.3548	.43179-.01	-.70316-.01	2.8794	-.30447-.01	.32505-.01	.18068-.02
14	.12500	.46881-.01	4.4597	.49002-.01	-.50209-.01	2.1391	-.21584-.01	.28006-.01	.12200-.02
15	.07500-.01	.48878-.01	4.5618	.46671-.01	-.30203-.01	1.3163	-.13960-.01	.14701-.01	-.51170-.03
16	.02500-.01	.49875-.01	4.6624	.46742-.01	-.10062-.01	.4430	-.43040-.02	.49947-.02	-.62186-.04
17	.00000	.50000-.01	4.7124	-.47649-.01	-.20687-.04	-.26375-.02	-.19370-.04	-.36089-.04	-.39231-.08

Table 2

S201

NO.	X	Y	BETA	P	U	UZ	P'	V'	F(BETA)
1	.50000	.00000	.00000	.76657	-.34069	-2.0691	.00000	.87667-02	.13842-01
2	.49750	.16798-02	.10004	.55939	-.33168	-2.7946	-2.1549	.24855-01	.75102
3	.48500	.72367-02	.24557	.23738	-.31857	-3.8499	-1.6101	.47320-01	.57212
4	.46250	.15352-01	.38976	.68634-01	-.29649	-4.0474	-.94817	.60959-01	.29811
5	.43750	.22253-01	.50536	-.20391-01	-.24857	-3.1633	-.50870	.58758-01	.11861
6	.41250	.27864-01	.60060	-.48208-01	-.20208	-2.5637	-.16374	.57987-01	.25908-01
7	.37500	.34402-01	.72272	-.48951-01	-.15824	-1.9117	-.20320-01	.51311-01	-.15255-02
8	.32500	.41504-01	.86321	-.54598-01	-.13298	-1.6385	-.74623-01	.49629-01	.54754-02
9	.27499	.47678-01	.98845	-.67092-01	-.11593	-1.5731	-.99091-01	.47458-01	.63896-02
10	.22500	.52753-01	1.1040	-.78559-01	-.91853-01	-.2697	-.83444-01	.39629-01	.36949-02
11	.17500	.56535-01	1.2132	-.86044-01	-.65825-01	-.70622	-.40395-01	.29434-01	.87041-03
12	.12500	.59010-01	1.3181	-.87444-01	-.42067-01	-.52754	-.75719-02	.18851-01	.11881-02
13	.74991-01	.60684-01	1.4202	-.84590-01	-.24391-01	-.70467	.16954-01	.12825-01	-.74405-03
14	.25006-01	.61388-01	1.5208	-.83973-01	-.67817-02	-.58207-02	.30807-02	.24373-02	-.21976-04
15	.00000	.61450-01	1.5708	-.83997-01	-.48069-03	-.35441-01	-.26794-05	.00000	-.12880-08

NO.	X	Y	BETA	P	U	UZ	P'	V'	F(BETA)
1	.50000	.74506-02	3.1416	.76652	-.34076	2.0694	.00000	-.87667-02	.13843-01
2	.49750	.16798-02	3.2416	.55932	-.33172	2.7947	-2.1550	-.24855-01	.75312
3	.48500	.72367-02	3.3872	.23732	-.31856	3.8499	-1.6601	-.47320-01	.57208
4	.46250	.15352-01	3.5314	.68651-01	-.29646	4.0471	-.94817	.60959-01	.29803
5	.43750	.22253-01	3.6470	-.20418-01	-.24053	3.1629	-.50867	.58758-01	.11855
6	.41250	.27864-01	3.7422	-.48314-01	-.20203	2.5632	-.16365	.57987-01	.25883-01
7	.37500	.34402-01	3.8643	-.48061-01	-.15820	1.9608	-.20881-01	.51311-01	-.15321-02
8	.32500	.41504-01	4.0048	-.54705-01	-.13294	1.6380	-.74598-01	.49629-01	.54701-02
9	.27499	.47678-01	4.1300	-.67095-01	-.11459	1.5225	-.99372-01	.47458-01	.63850-02
10	.22500	.52753-01	4.2456	-.78560-01	-.91815-01	1.2691	-.83435-01	.39629-01	.36826-02
11	.17500	.56535-01	4.3548	-.86045-01	-.65787-01	.70667	-.40394-01	.29434-01	.87017-03
12	.12500	.59010-01	4.4597	-.87445-01	-.42030-01	.52700	.75723-02	.18851-01	.11870-02
13	.74991-01	.60684-01	4.5618	-.84591-01	-.24353-01	.30411	.16958-01	.12825-01	.74591-03
14	.25006-01	.61388-01	4.6624	-.83973-01	-.67444-02	.52666-02	.30668-02	.24373-02	-.21784-04
15	.00000	.61450-01	4.7124	-.83997-01	-.48069-03	.35441-01	.26859-05	-.18026-08	-.12966-08

Table 3

Series 60, $C_B=0.60$

NO.	X	Y	BETA	P	U	UZ	P'	Y'	F(BETA)
1	.56260	-.65453-06	.00000	.45591	-.28310-01	-5.0683	.00000	.37801-02	.87345-02
2	.48768	-.41012-02	.23242	.32219	-.12862	-21.400	-.60119	.33103-01	.30557
3	.47539	-.77175-02	.31503	.26551	-.17238	-28.200	-.90087	.45607-01	.49626
4	.46396	-.11109-01	.38201	.19166	-.17215	-21.300	-.88890	.55780-01	.38074
5	.44633	-.16466-01	.46756	.14060	-.15858	-18.400	-.50422	.69116-01	.25876
6	.42185	-.24121-01	.56667	.10126	-.16464	-22.200	-.40413	.83595-01	.25445
7	.39732	-.31628-01	.65237	.66094-01	-.16384	-19.200	-.39373	.80654-01	.17828
8	.36126	-.41715-01	.76335	.24778-01	-.16541	-23.700	-.36587	.86948-01	.10548
9	.31377	-.52093-01	.89498	-.22380-01	-.15559	-15.800	-.32532	.69147-01	.26492-01
10	.26336	-.59058-01	1.0161	-.58099-01	-.12508	-8.3000	-.24874	.45730-01	.93078-02
11	.21378	-.62802-01	1.1290	-.81318-01	-.85415-01	-2.8000	-.16192	.23015-01	.85899-02
12	.16396	-.64652-01	1.2367	-.94270-01	-.44700-01	.40000	-.30123-01	.11950-01	.17962-02
13	.11464	-.65414-01	1.3395	-.85255-01	-.13255-01	.70000	-.10788	.38895-02	-.11970-02
14	.65458-01	-.65560-01	1.4395	-.72672-01	-.80142-05	.41814	-.11182	.00000	-.89617-06
15	.16288-01	-.65560-01	1.5382	-.66177-01	-.12247-04	.11677	-.30768-01	.24061-11	.37682-06
16	.00000	-.65560-01	1.5708	-.68216-01	-.13737-04	.21098-01	-.94509-01	.19860-08	.12982-05

NO.	X	Y	BETA	P	U	UZ	P'	Y'	F(BETA)
1	.50000	.37253-08	3.1416	.23913	-.11589	.27719	.00000	-.30105-03	.19255-04
2	.48709	-.17677-02	3.3693	.16770	-.11885	1.7048	-.31366	-.15224-01	.41630-01
3	.46312	-.03367-02	3.5281	.11790	-.12930	2.7000	-.16697	-.25812-01	.28295-01
4	.43854	-.84875-02	3.6427	.11108	-.14384	3.6000	-.70170-01	-.37316-01	.24945-01
5	.41395	-.12627-01	3.7370	.10363	-.16550	4.8000	-.17333	-.50974-01	.53695-01
6	.37702	-.20235-01	3.8582	.67949-01	-.15664	7.2000	-.25777	-.71387-01	.85615-01
7	.32787	-.31400-01	3.9972	.37571-01	-.21021	9.4000	-.27773	-.85867-01	.87735-01
8	.27273	-.42267-01	4.1211	-.32837-02	-.19876	8.1000	-.36290	-.86083-01	.69840-01
9	.22264	-.51434-01	4.2352	-.47844-01	-.16933	5.7000	-.35744	-.72663-01	.40710-01
10	.18043	-.58198-01	4.3432	-.83083-01	-.12177	3.1000	-.24423	-.52731-01	.16159-01
11	.13124	-.62719-01	4.4468	-.10023	-.78613-01	1.2000	-.72737-01	-.34011-01	.16275-02
12	.82054-01	-.65048-01	4.5475	-.98471-01	-.30801-01	.22377	-.10943	-.13775-01	.36630-02
13	.32883-01	-.65560-01	4.6466	-.78675-01	-.6883-04	-.16642	.17525	.59020-08	.29587-05
14	.00000	-.65560-01	4.7124	-.68218-01	-.13737-04	.21098-01	.94509-01	.00000	.12982-05

Table 4

HSVA Tanker

NO.	X	Y	BETA	P	U	UZ	P'	Y'	F(BETA)
1	.50000	-.36159-05	.00000	.58632	-.27531-01	-.26.662	.00000	.28918-01	.32700
2	.49619	.50526-02	.12354	.48633	-.10441	-.22.739	-.80938	.60938-01	.76017
3	.48730	.13301-01	.22510	.40413	-.16760	-.19.822	-.72531	.89936-01	.83470
4	.47603	.21284-01	.31088	.32060	-.19540	-.17.390	-.75555	.96552-01	.73254
5	.46495	.28445-01	.38154	.28172	-.22479	-.15.041	-.85002	.10422	.69194
6	.45193	.34527-01	.44209	.21080	-.24360	-.13.600	-.85260	.99743-01	.49365
7	.43980	.40133-01	.49577	.26238	-.26238	-.12.166	-.89377	.10504	.47183
8	.42770	.44946-01	.54449	.12331	-.25908	-.9.9371	-.1.1478	.94120-01	.41271
9	.40925	.50940-01	.60957	.60148-01	-.25268	-.8.3269	-.96822	.88580-01	.28344
10	.38560	.57674-01	.69008	-.17576-01	-.23132	-.6.1147	-.77829	.77270-01	.17173
11	.35035	.64461-01	.79442	-.73482-01	-.17303	-.2.0979	-.44200	.53975-01	.68158-01
12	.30008	.69706-01	.92509	-.11588	-.10206	.87223	-.17225	.28426-01	.20453-01
13	.25190	.72149-01	1.0428	-.12002	-.51269-01	1.1924	-.75382-01	.14331-01	-.18139-02
14	.20331	.73248-01	1.1521	-.10453	-.20192-01	.56553	.23322	.61872-02	-.43571-02
15	.15420	.73490-01	1.2560	-.70859-01	-.22697-02	.15202	.26351	-.24206-10	-.59584-03
16	.10630	.73490-01	1.3566	-.45742-01	-.78348-03	.26572-01	.17920	-.16353-10	-.13962-03
17	.57782-01	.73490-01	1.4556	-.35146-01	-.35353-03	.76239-03	.87002-01	-.87610-11	-.31076-04
18	.92285-02	.73490-01	1.5522	-.27468-01	-.17693-03	-.13814-02	.41559-01	.13882-11	-.73985-05
19	.00000	.73490-01	1.5708	-.23751-01	-.15174-03	-.16159-02	.35410-01	.11788-08	-.53730-05

NO.	X	Y	BETA	P	U	UZ	P'	Y'	F(BETA)
1	.50000	.74506-08	3.1416	.00000	.17373-02	5.8448	.00000	-.13150	.76858
2	.49697	-.14452-01	3.2518	.85376	-.31584	10.902	-.3.346	-.13088	2.3096
3	.49091	-.25683-01	3.3326	.45099	-.54893	14.718	-.4.035	-.13066	3.0862
4	.48181	-.34942-01	3.4121	.20146	-.56316	13.604	-.2.8161	-.11943	1.9139
5	.46868	-.44171-01	3.4916	.32240-02	-.51592	11.314	-.2.0566	-.11252	1.0651
6	.45757	-.51304-01	3.5566	-.10686	-.46819	9.6366	-.1.4231	-.10584	.55728
7	.43939	-.59470-01	3.6321	-.19579	-.37434	5.7477	-.1.0133	-.90106-01	.26027
8	.41514	-.66931-01	3.7322	-.22337	-.26519	3.2124	-.65945	-.66930-01	-.1.1384
9	.39008	-.71237-01	3.8149	-.31787	-.15189	.76715	.13157	-.38383-01	-.29343-01
10	.36562	-.73077-01	3.8893	-.27173	-.58151-01	.24544	.89206	-.14312-01	-.52827-01
11	.33924	-.73490-01	3.9903	-.14313	-.46185-02	.16613	.95453	-.75309-08	-.44163-03
12	.28173	-.73490-01	4.1138	-.71111-01	-.10364-02	.11725	.39990	-.89256-08	-.41446-03
13	.23323	-.73490-01	4.2271	-.45700-01	-.39735-03	.53255-01	.16384	-.10077-07	-.64706-04
14	.18473	-.73490-01	4.3340	-.34511-01	-.18201-03	.23250-01	.78875-01	-.54946-08	-.14210-04
15	.13622	-.73490-01	4.4365	-.29127-01	-.72243-04	.10119-01	.37284-01	-.58323-08	-.26935-05
16	.87719-01	-.73490-01	4.5360	-.26880-01	-.28577-05	.26722-02	.10442-01	-.00000	-.26509-07
17	.38215-01	-.73490-01	4.6339	-.27024-01	.75471-04	-.13875-02	-.12613-01	-.61845-08	-.06703-06
18	.00000	-.73490-01	4.7124	-.23751-01	.15174-03	-.16159-02	-.35410-01	-.73103-08	-.53729-05

FORMAT FOR TABULATED VALUES OF WAVE RESISTANCE

E. Baba/Low speed theory Table 5

Wigley			Wigley		S201		S201	
Fn	Cw	Fn	Cw	Fn	Cw	Fn	Cw	
0.10	0.20668-4	0.20	0.59412-3	0.12	0.41411-4	0.27	2.8857-3	
0.11	0.32194-4	0.205	0.62666-3	0.13	0.58518-4	0.28	3.9579-3	
0.12	0.50656-4	0.21	0.59771-3	0.14	0.10646-3	0.287	4.5654-3	
0.13	0.62862-4	0.215	0.61698-3	0.15	0.16036-3	0.29	4.7643-3	
0.135	0.82498-4	0.22	0.73053-3	0.16	0.22027-3	0.30	5.0546-3	
0.14	0.10383-3	0.23	1.1266-3	0.17	0.23843-3	0.31	5.0862-3	
0.145	0.10567-3	0.24	1.2835-3	0.18	0.43230-3	0.319	5.0603-3	
0.15	0.14724-3	0.25	1.2358-3	0.19	0.44205-3	0.32	5.0602-3	
0.155	0.14852-3	0.26	1.4341-3	0.20	0.78410-3	0.33	5.3283-3	
0.16	0.18292-3	0.266	2.0142-3	0.21	0.72959-3	0.34	6.1967-3	
0.165	0.23076-3	0.27	2.0245-3	0.22	0.99722-3	0.35	7.5247-3	
0.17	0.21620-3	0.313	4.3372-3	0.23	1.5737-3	0.36	9.4249-3	
0.175	0.28158-3	0.350	5.9480-3	0.24	1.7062-3	0.44	31.652-3	
0.18	0.35694-3	0.402	15.865-3	0.25	1.6129-3	0.525	45.835-3	
0.185	0.34495-3	0.452	25.860-3	0.255	1.7051-3	0.650	79.124-3	
0.19	0.35559-3			0.26	1.9663-3			
0.195	0.46856-3							

FORMAT FOR TABULATED VALUES OF WAVE RESISTANCE

E. Baba/Low speed theory Table 6

Series 60, $C_B=0.60$		Series 60, $C_B=0.60$		HSVA Tanker			
F _n	C _w	F _n	C _w	F _n	C _w		
0.10	0.11325-5	0.26	0.63726-3	0.12	0.15351-3		
0.11	0.23286-5	0.27	0.78674-3	0.125	0.19765-3		
0.12	0.41980-5	0.28	0.90945-3	0.13	0.21558-3		
0.13	0.72848-5	0.29	1.0221-3	0.135	0.25019-3		
0.14	0.11975-4	0.30	1.2130-3	0.14	0.39036-3		
0.15	0.18605-4	0.31	1.4277-3	0.145	0.36452-3		
0.16	0.28066-4	0.32	1.7399-3	0.15	0.58849-3		
0.17	0.40406-4	0.33	2.1555-3	0.155	0.52900-3		
0.18	0.60232-4	0.34	2.6904-3	0.16	0.83161-3		
0.19	0.85932-4	0.35	3.2938-3	0.165	0.90082-3		
0.20	0.12080-3			0.17	0.89494-3		
0.21	0.16578-3			0.175	1.3994-3		
0.22	0.22239-3			0.18	1.6031-3		
0.23	0.28020-3			0.185	1.4253-3		
0.24	0.35915-3			0.19	1.7316-3		
0.25	0.50454-3						

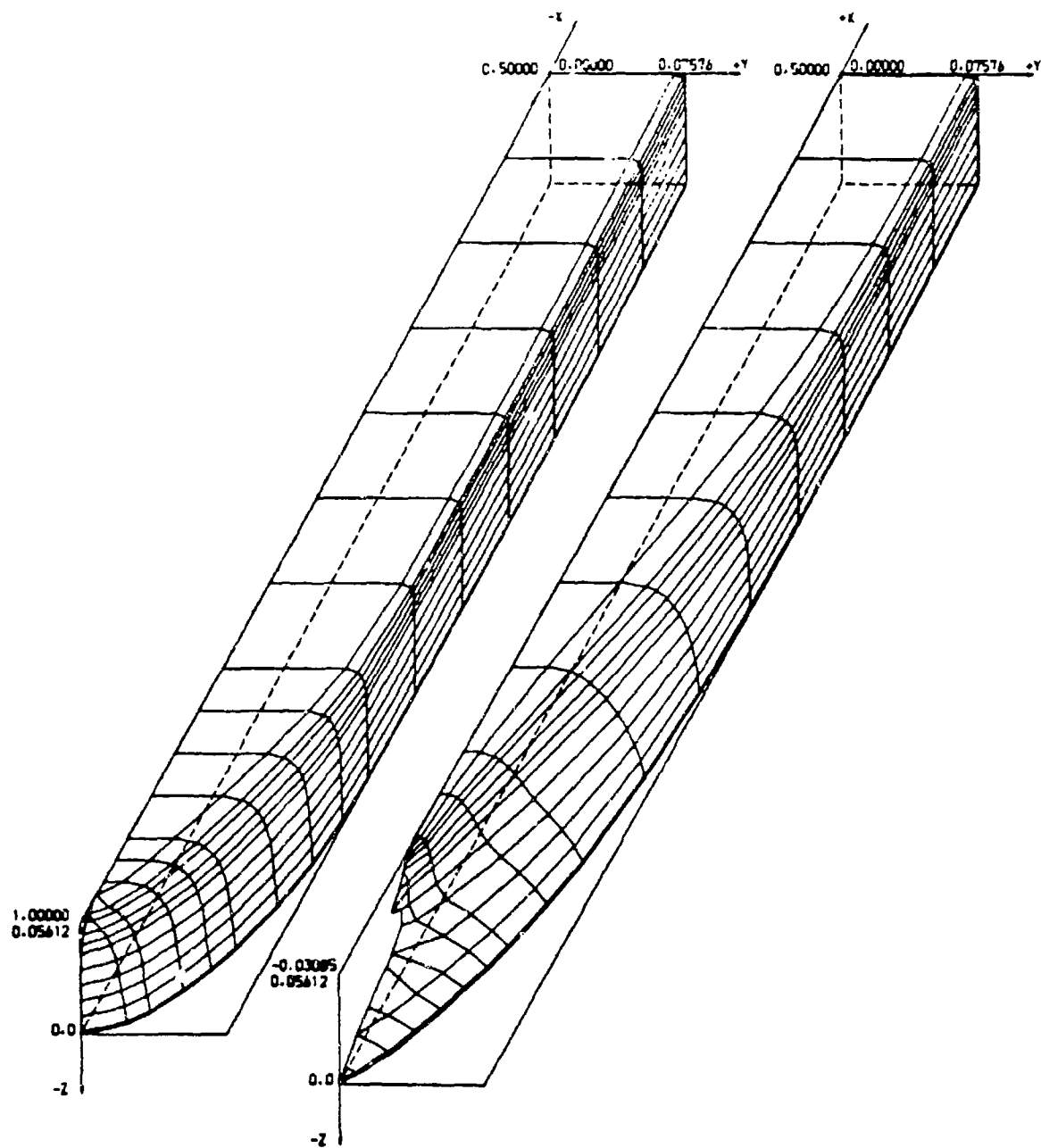


Fig. 1 Arrangement of surface elements
of HSVA Tanker

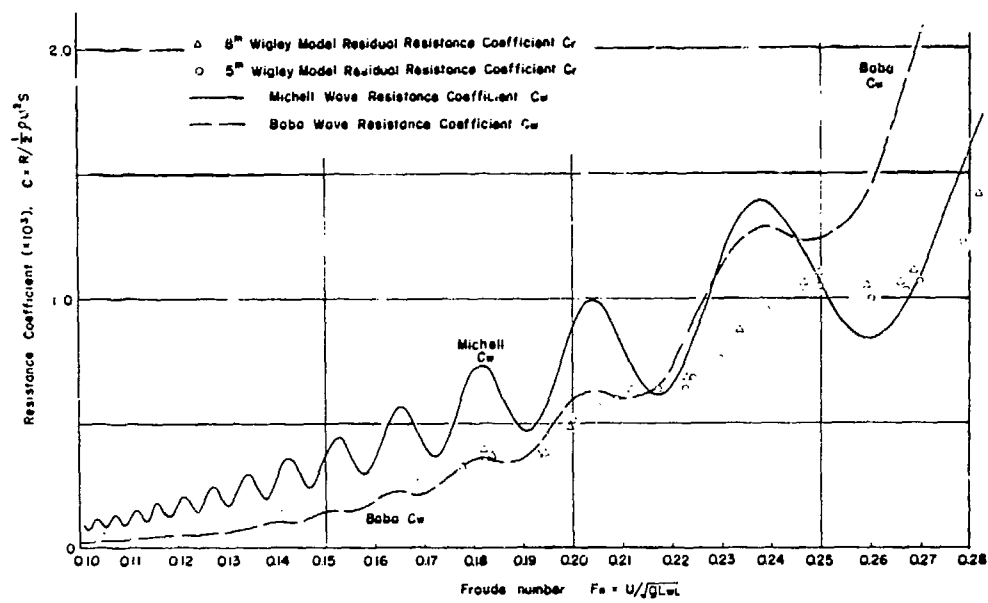


Fig 2 Comparison of resistance coefficient of Wigley Hull

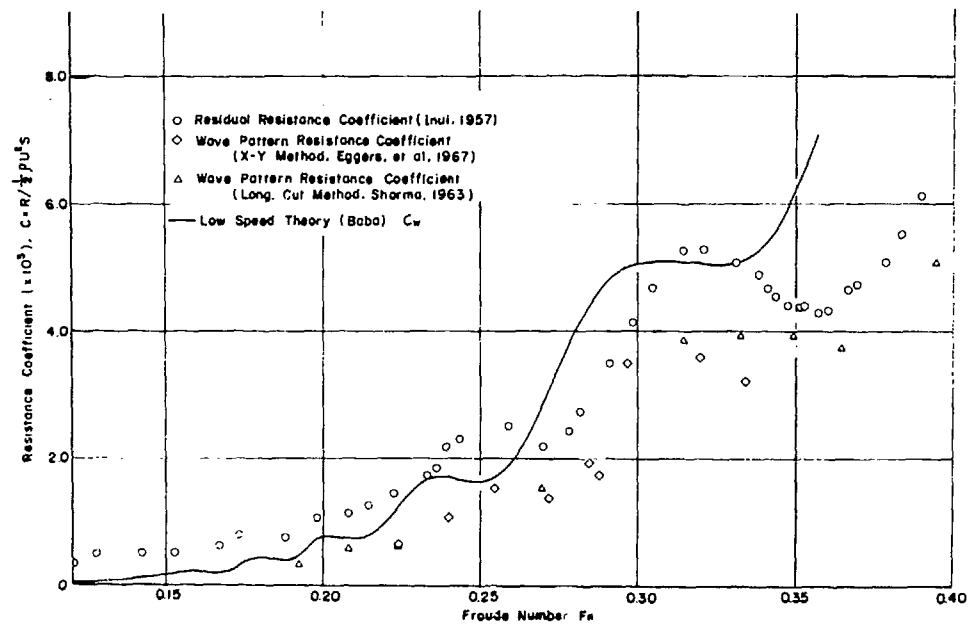


Fig 3 Comparison of resistance coefficient of S-201

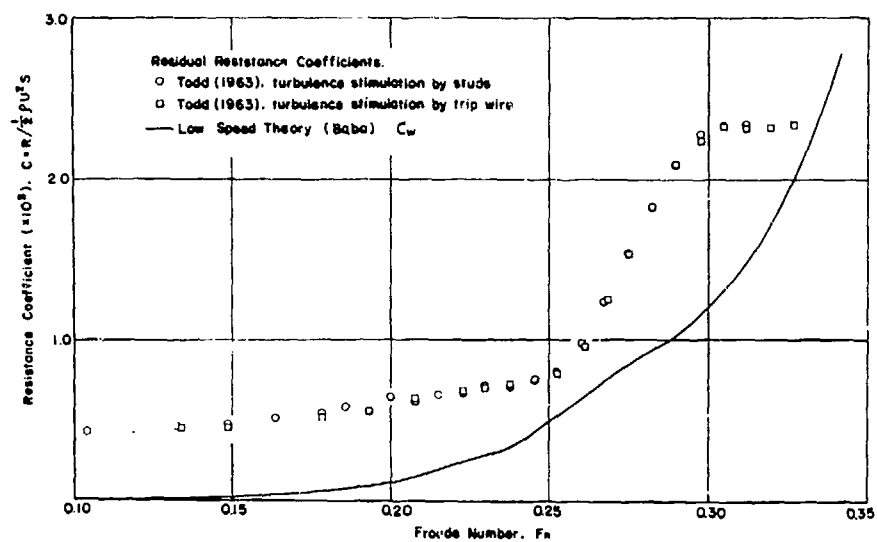


Fig. 4 Comparison of resistance coefficient of Series 60. $C_B = 0.60$

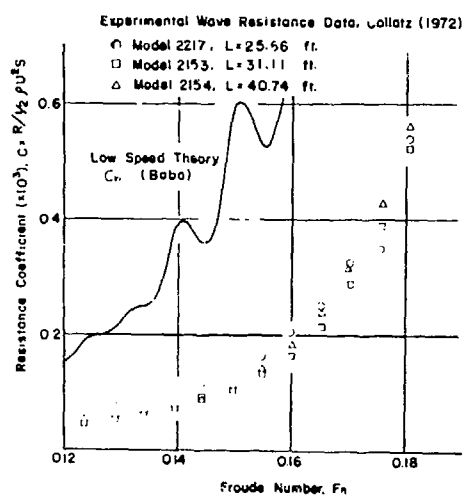


Fig 5 Comparison of resistance coefficient of HSVA Tanker

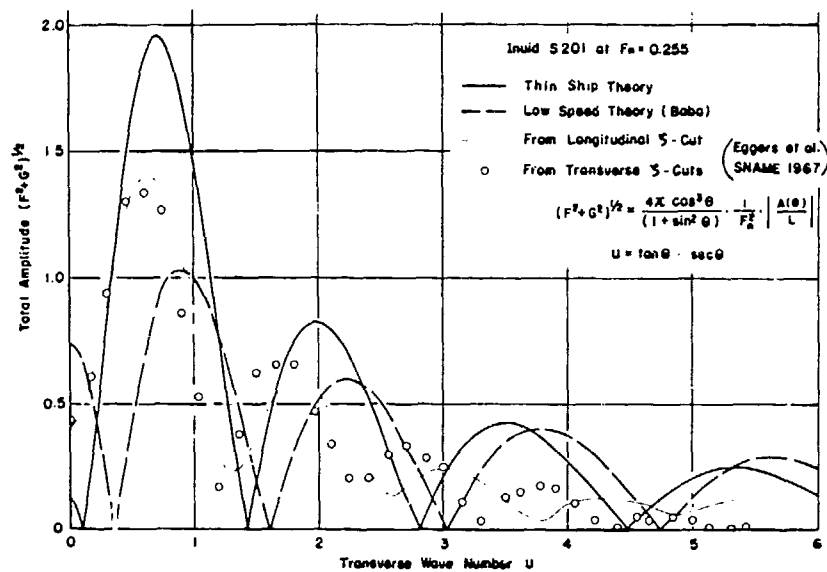


Fig. 6 Comparison of wave amplitude of S-201

SIMPLE CALCULATION OF SHELTERING EFFECT ON WAVE RESISTANCE OF LOW SPEED SHIPS

by

B. Yim

INTRODUCTION

Since the operating speed of ships is commonly in the range of Froude number less than 0.3, the low Froude number approximation of the wave resistance naturally draws interest. In the low speed range investigated here, the sheltering effect accounts for the influence of the ship beam at the water surface, creating and reflecting water waves. In 1966, the author suggested that the importance of this influence could be visualized in terms of a linear ship potential represented by a pressure distribution on the free surface induced by a double model source distribution.¹ In this case, the pressure distribution within the ship could be anything if it was distributed symmetrically with respect to the ship center plane, although the representation equivalent to Michell's solution is the pressure distribution due to the double model. The influence of the pressure distribution within the ship on Michell's solution is shown to be quite large. If the pressure within the ship is eliminated, the potential is shown to be an approximation to the case of low Froude number starting with the double model potential in the Green formula. The wave resistance calculated by Sretten's wave resistance formula for the Wigley model is shown to be very close to that computed by Maruo² using Baba's³ equations. The wave resistance of Inui's parabolic ship,⁴ Inuid S201, is also computed.

CORRECTED MICHELL'S WAVE RESISTANCE

If we use a rectangular Cartesian coordinate system 0-xyz with the origin 0 at the intersection of the ship bow and the mean free surface, and consider a ship surface represented by

$$y = \pm f(x, z) \quad (1)$$

then the linear source distribution is given by

$$\sigma = \frac{1}{2\pi} f_x \quad (2)$$

and the linear potential φ can be represented by

$$\varphi(x, y, z) = \frac{1}{2\pi} \iint_{y=0} f_x G dx dz \quad (3)$$

where G is the so-called Kelvin's Green function.⁵

$$G = G_1 + G_2 \quad (4)$$

$$G_1 = \frac{1}{r} + \frac{1}{r'}$$

$$r = \{ (x-x_1)^2 + (y-y_1)^2 + (z-z_1)^2 \}^{-\frac{1}{2}} \quad (5)$$

$$r' = \{ (x-x_1)^2 + (y-y_1)^2 + (z+z_1)^2 \}^{-\frac{1}{2}} \quad (6)$$

The Michell's wave resistance is given by

$$\frac{R}{\frac{1}{2}\rho U^2 L^2} = 2 \iint_{y=0} f_x \varphi_x dx dz \quad (7)$$

where we represent φ by

$$\varphi = \varphi_1 + \varphi_2 \quad (8)$$

with φ_1 defined as the double-model velocity potential, or

$$\varphi_1 = \frac{1}{2\pi} \iint_{Y=0} f_x G_1 dx, dz, \quad (9)$$

Then, the linearized free surface boundary condition on $z = 0$

$$\varphi_{xx} + k \varphi_z = 0 \quad (10)$$

where

$$k = \frac{gL}{U^2} \quad (11)$$

can be written as

$$\varphi_{2xx} + k \varphi_{2z} = -\varphi_{1xx} \quad \text{on } z=0 \quad (12)$$

Using the free surface condition (12) in Green's formula for φ_2 , we obtain⁴

$$\varphi_2 = -\frac{1}{4\pi k} \iint_{Z=0} \varphi_{1xx} G dx, dy, \quad (13)$$

Equation (8) with equations (9) and (13) provide a linear solution equivalent to equation (3), satisfying the same Laplace equation with the same boundary conditions on the free surface $Z = 0$ and the center plane $Y = 0$. Both formulations should give the same value as Michell's wave resistance. Equation (3) is represented by Kelvin's source distribution on the center plane while Equation (8) is represented by the combination of the double model Rankine source distribution on the center plane and Kelvin's source distribution on the free surface. The double model Rankine source distribution satisfies the body boundary condition on the center plane but not the free surface condition on $Z = 0$. Therefore, to satisfy the free surface condition, the Kelvin source distribution on the plane $Z = 0$ is needed. When we build a model Inuid by plotting the streamlines of a double model for a given source distribution, the double model potential is the solution for the Inuid at zero Froude number. When the Froude number is increased slightly, the free surface boundary condition is satisfied by equation (13) just considering the part of free surface S_F external to the hull. That is, Kelvin

sources inside the ship on $Z = 0$ are not needed. It is of interest to determine the influence of extra Kelvin sources inside the hull on Michell's wave resistance. This effect is the sheltering effect which is the effect of finite beam at the free surface. We may write

$$\varphi_c = \varphi_i - \frac{1}{4\pi k} \iint_{Z=0} \varphi_{i,xx} G dx dy + \frac{1}{4\pi h} \int_{-1}^1 \int_{-1}^1 \varphi_{i,xy} G dx dy, \quad (14)$$

where the last term is the correction term for the linear solution caused by elimination of the Kelvin sources inside the ship on $z = 0$.

In fact, it was proved that φ_c in equation (14) is an approximation of the potential represented by Green's formula

$$\varphi = \frac{1}{4\pi} \iint (\varphi G_{xx} - \varphi_{xx} G) ds + \frac{1}{4\pi h} \int_{-1}^1 (\varphi_x G - \varphi G_x) dy$$

when φ on the right-hand side is replaced by the double model potential φ_i .

The wave resistance is calculated from Sretensky's formula,⁷

$$\frac{R}{\frac{1}{2} \rho U^3 L^2} = \frac{16\pi^2 k}{W} \sum_{m=0}^{\infty} \varepsilon_m \frac{1 + \sqrt{1 + \left(\frac{4\pi m}{kW}\right)^2}}{\sqrt{1 + \left(\frac{4\pi m}{kW}\right)^2}} (P^2 + Q^2)$$

where

$$P + iQ = \iint \sigma(s) \exp\{kb(zb + ix) + i2\pi y \frac{m}{W}\} ds$$

$$b = \left[\frac{1}{2} + \frac{1}{2} \left\{ 1 + \left(\frac{4\pi m}{kW} \right)^2 \right\}^{\frac{1}{2}} \right]^{\frac{1}{2}}$$

WL = Width of the towing tank

$$\varepsilon_0 = 1 \quad \varepsilon_m = 2 \quad \text{for } m \geq 1$$

S = Domain of source distribution

σ = Source strength

NUMERICAL EXAMPLES AND DISCUSSIONS

We consider a correction of Michell's wave resistance for parabolic hulls,

$$y = \pm f(x)$$

$$\sigma_c = \frac{1}{2\pi} \frac{df}{dx} = -\frac{B}{L\pi} (2x-1) \quad \text{in } 0 < x < 1, y=0, 0 < z < -T/L$$

Inuid S201 and S101 are models made from the plotted streamlines with the above source distribution when $B/L = 0.2$, and 0.1 with $T/L = 0.01$ respectively. The computed values of both Michell and the corrected wave resistance for models S201 and S101 with the above source σ_c are shown in Figure 1. While not in close agreement with the experimental results, the corrected wave resistances are in better agreement with experimental values than Michell's wave resistance.

A slight variation from Inuid hulls is the Wigley hull whose source strength distribution is given by

$$\sigma_c = -\frac{B}{L\pi} (2x-1) \left\{ 1 - \left(\frac{zL}{T} \right)^2 \right\}$$

Values of both the Michell and corrected wave resistance are shown in Figure 2 together with the results obtained by Baba³ and Maruo² for the case of $B/L = 0.1$ and $T/L = 0.625$. The corrected wave resistance is almost the same as that calculated by Maruo^{2,3} using a complicated method which considers the nonlinear effect of the boundary condition for the double model representation. If the beam-length ratio is made unusually large, the difference between Maruo's and the present results may become large. However, the present comparison shows that the sheltering effect can be more important than any other nonlinear effects.

Although the corrected wave resistance is clearly shown to be a better approximation for low values of Froude number, it is not shown here how high a Froude number can be adequately treated by the corrected wave resistance theory. Because of the simplicity of the calculation method, further research may be fruitful. It is possible that the hump and hollow of the wave resistance curve may only be smoothed out by considering the boundary layer effect, without which the matching of theory and experiment may be hopeless.

REFERENCES

1. Yim, B., "Singularities on the Free Surface and Higher Order Wave Height far Behind a Parabolic Ship," Hydronautics, Inc. Technical Report 503-2, p. 16, (1966).
2. Maruo, H. and K. Suzuki, "Wave Resistance of a Ship of Finite Beam Predicted by the Low Speed Theory," JSNAJ, Vol. 142 (1977).
3. Baba, E. and M. Hara, "Numerical Evaluation of Wave Resistance Theory for Slow Ships," Proceedings of the Second International Conference on Numerical Ship Hydrodynamics, University of California, Berkeley (1977), pp. 17-29.
4. Inui, T., "Study of Wave-Making Resistance of Ships," SNAJ 60th Anniversary Series, Vol. 2 (1957).
5. Yim, B., "Simple Calculation of Sheltering Effect on Ship-Wave Resistance and Bulbous Bow Design," to be published, (1979).
6. Suzuki, K., "The Representations of the Velocity Potential in the Theory of Wave Resistance of Ships," The Memoirs of the Defense Academy, Vol. 15, No. 3 (1976).
7. Sretensky, L.N., "On the Wave-Making Resistance of a Moving Pressure Distribution in a Canal," Schiffstechnik, Vol. 9 (Jan 1962).

Wave Resistance Coefficient $C_w = \frac{R}{1/2\rho U^2}$ Due to Wigley Model and Inuid S201

C_{wc} = Corrected Wave Resistance

C_{wm} = from Michell's Source

F_n	Wigley			Inui (S201)		
	C_{wc}	C_{wm}	C_{wc}	C_{wm}	C_{wc}	C_{wm}
0.150	0.2599 -03	0.3131 -03	0.7951 -03	0.1141 -02		
0.1625	0.3566 -03	0.4352 -03	0.1092 -03	0.1621 -02		
0.1750	0.3222 -03	0.4024 -03	0.9637 -03	0.1508 -02		
0.1875	0.3766 -03	0.4822 -03	0.1236 -02	0.1832 -02		
0.2000	0.6679 -03	0.8277 -03	0.2113 -02	0.3223 -02		
0.2125	0.5089 -03	0.6080 -03	0.1535 -02	0.2569 -02		
0.225	0.6405 -03	0.8210 -03	0.1985 -02	0.3204 -02		
0.2375	0.1033 -02	0.1331 -02	0.3248 -02	0.5311 -02		
0.2500	0.7356 -03	0.1004 -02	0.2147 -02	0.3992 -02		
0.2625	0.5881 -03	0.8055 -03	0.1696 -02	0.3186 -02		
0.275	0.9763 -03	0.1266 -02	0.3060 -02	0.5123 -02		
0.2875	0.1424 -02	0.1864 -02	0.4476 -02	0.7626 -02		
0.3000	0.1528 -02	0.2079 -02	0.4637 -02	0.8530 -02		

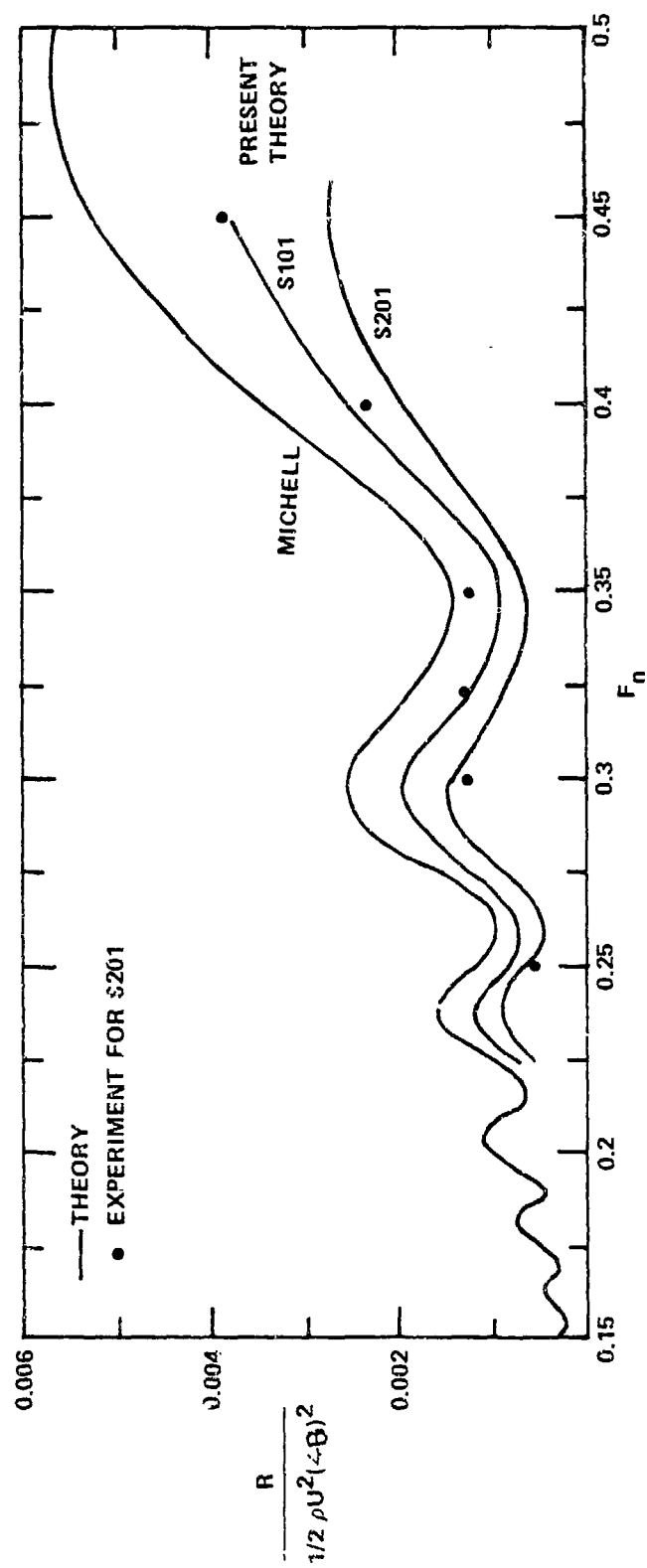


Figure 1 - Wave Resistance of Parabolic Ships S101 and S201

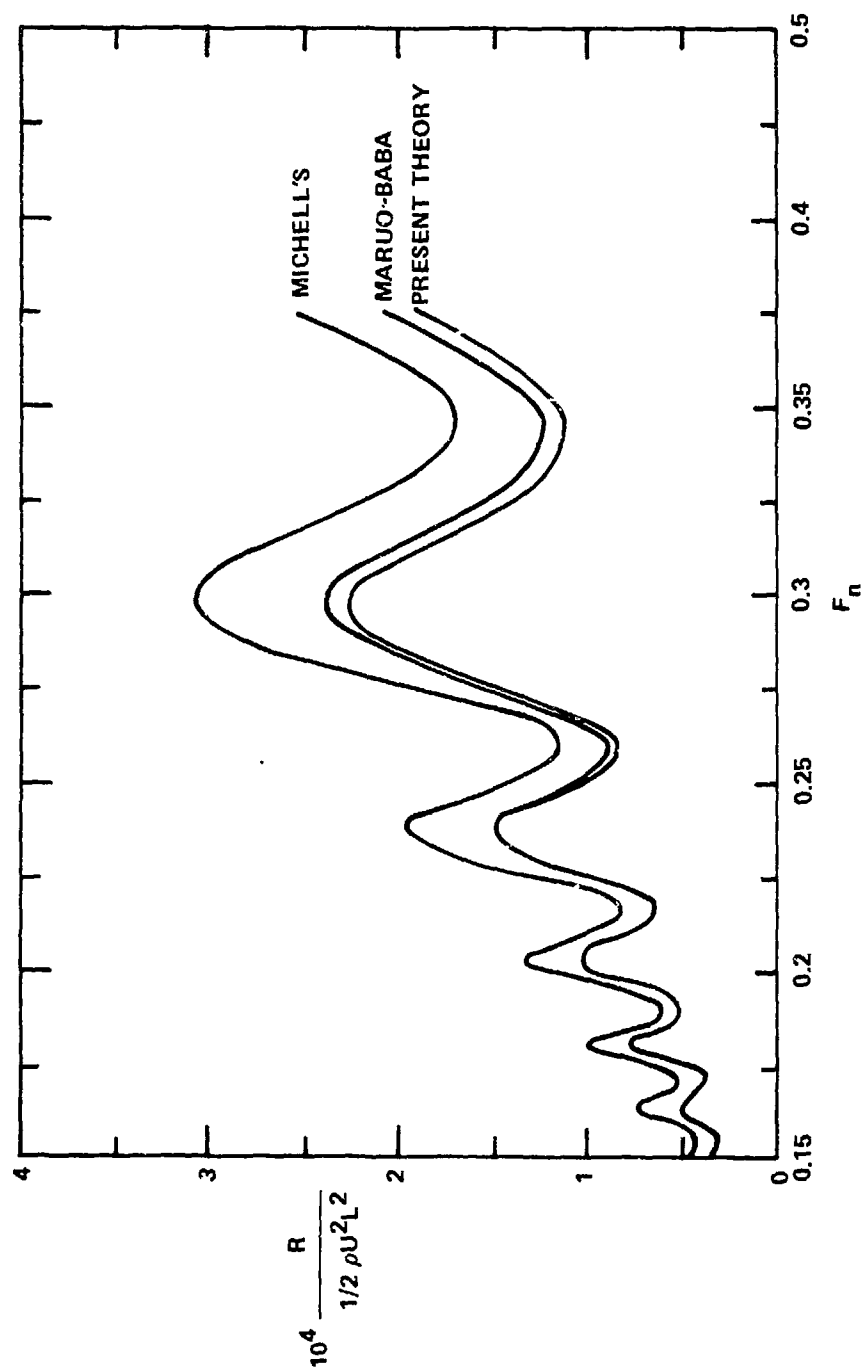


Figure 2 - Wave Resistance of Wigley Model, $B/L = 0.1$, $\frac{T}{L} = 0.0625$

Discussion

by E. Baba of paper by B. Yim
(See the Discussions of Paper by H. Maruo)

Author's Reply

by B. Yim
to discussions by E. Baba

I appreciate Dr. Baba's interest in my report and his recognition of the fact that my calculation agrees well with the Maruo-Baba result, which was carefully calculated from an exact integration of Dr. Baba's formula by Professor Maruo. The same result is shown not only in the Maruo-Suzuki paper (reference 2) but also in the Mori and Kitazawa-Kajitani papers in the present workshop. By using an asymptotic expansion of the same integral mentioned previously, Dr. Baba has obtained a result which is claimed to match better with experimental data. An asymptotic expansion of an integral is a crude approximation to the value of the integral. Especially, it seems to be very crude in the case of ship wave theory. Even if the approximation agrees better with the experimental results than the original integral does, I can not find any reason to justify that the approximation is better than the original value of the integral. If one recognizes the fact that my simple calculation agrees well with the Maruo-Baba semi-nonlinear result, he has to agree with the following statement: "The sheltering effect is almost enough to correct Michell's theory." That is, unless the ship is very thick, the nonlinear effect considered in Baba's low-speed ship theory beyond the sheltering effect is not necessary to correct Michell's wave resistance."

Second-order wave resistance and related topics

K. Eggers

A. Comments on analysis

Consistent second-order theory provides three additive improvements δR^H , δR^L , and δR^F to the resistance from linear theory, i.e. derived from first order flow $\nabla\phi$:

δR^H takes care of quadratic pressure terms, evaluates linear pressure closer to the hull and includes linear pressure from a correction flow $\nabla\phi^H$ generated from some source distribution σ^H on the longitudinal centerplane;

δR^L represents the action of linearized pressure on the area between $z = 0$ and the first-order wave profile $z = \zeta(x,0)$;

δR^F incorporates pressure from a flow $\nabla\phi^F$ generated from a singularity distribution $d(x,y)$ on the horizontal plane $z = 0$.

It is common to all these three correction terms (at least for ships with fore-and-aft symmetry, this being no significant restriction) that they can be expressed essentially in terms of first-order flow components near the hull. As long as one is not aiming at calculations of wave profiles, there is no need for evaluation of a first-order velocity potential nor for evaluation of $\nabla\phi^H$ and $\nabla\phi^F$. The corrections remain meaningful even if first-order flow is not necessarily from Michell's theory.

It should be observed in particular that for any flow model satisfying the linearized free surface condition only (e.g. for the Neumann-Kelvin flow), the term δR^L † represents one half of the excess of resistance from pressure integration over the hull including first-order wave profile against that from far-field momentum flux [1]. (It should be mentioned here that such type of discrepancy, first detected by Gadd [2] in his computations,

† More precisely: the line integral

$$- \int \frac{\zeta^2}{2} dy$$

around the water line with dy positive at the stern.

is apparent in flow models of slow ship theory as well, as far as Laplace's equation is violated [3]).

With the hull surface given as $y = \pm f(x, z)$ for $-\ell \leq x \leq \ell$, $-H \leq z \leq 0$, the explicit analytical expressions for δR^H , δR^L , and δR^F are

$$\begin{aligned} \delta R^H &= \rho \int_{-H}^0 \int_{-\ell}^{\ell} f_x \{ (\phi_x^2(x, 0, z) + \phi_y^2 + \phi_z^2) - 2Uf\phi_{xy} \} dx dz - \rho \int_{-H}^0 \int_{-\ell}^{\ell} U f_x \phi_x^H dx dz \\ &= -\rho \int_{-H}^0 \int_{-\ell}^{\ell} \sigma^H(x, z) \phi_x(x, 0, z) dx dz - 2\rho \int_{-\ell}^{\ell} f(x, 0) \phi_x(x, 0, 0) \phi_z(x, 0, 0) dx \\ &\quad - \rho \int_{-H}^0 \int_{-\ell}^{\ell} \sigma^H(x, z) \phi_x(-x, 0, z) dx dz, \end{aligned}$$

with

$$\sigma^H(x, z) = 2 \left((f\phi_x)_x + (f\phi_z)_z \right),$$

(cf. equations (C.24) - (C.26) of [4] and equation (16) of [1])

$$\delta R^L = -\frac{\rho}{k} \int_{-\ell}^{\ell} f_x(x, 0) \phi_x^2(x, 0, 0) dx = -\frac{\rho g}{2} \int_{-\ell}^{\ell} f_x \zeta^2 dx,$$

if ζ stands for the linearized wave elevation (the quantity δR^L is termed R^{profile} in [1]),

$$\begin{aligned} \delta R^F &= -2\rho \int_{-H}^0 \int_{-\ell}^{\ell} U f_x \phi_x^F dx dz = -\rho \int_{-\infty}^{\infty} \int_{-\infty}^{\infty} d(x, y) \phi_x(-x, -y, 0) dx dy \\ &= -\frac{\rho}{U} \int_{-\infty}^{\infty} \int_{-\infty}^{\infty} (\phi_x^2(x, y, 0) + \phi_y^2 + \phi_z^2) \phi_z(-x, -y, 0) dx dy, \end{aligned}$$

since

$$d(x, y) = \frac{1}{kU} \{ (\phi_x^2(x, y, 0) + \phi_y^2 + \phi_z^2)_x - \frac{1}{k} \phi_x (\phi_{xx} + k\phi_z)_z \}.$$

One may observe that under the linearized free-surface condition the line integral of δR^H is equal to δR^L !

If expressed as percentages of first-order wave resistance, all these three correction terms depend on the beam/length ratio in a strictly lin-

ear manner unless flow components are evaluated on the hull rather than on the longitudinal centerplane (so far, no significant improvements of resistance prediction could be observed as a benefit for digression from the path of consistency).

B. Numerical evaluations

For investigation of basic properties of second-order wave resistance, the computer program developed covers mathematical hull forms only. We could thus participate in the workshop calculations only for the Wigley model and for the Inuid S-201, and in the latter case only accepting the Inuid hypothesis which replaces the associated Michell ship with rectangular frames and parabolic water lines by the zero F_n double body generated by the underlying source distribution. The program can only handle centerplane source distributions of polynomial type. Its scope hence cannot cover the influence of trim, which seems to be significant for the Wigley model at high F_n . The effect of sinkage for the Inuid could be approximated by increasing the draft, as the frames are nearly vertical in the water plane area. However, the calculations do not really provide a test on efficiency of second-order wave resistance theory, which for this hull form would require a different source distribution for first-order flow and hence for the correction terms (note that the Inuid beam/length ratio is 0.1229, whereas for the Michell hull it would be 0.2!)

If nevertheless second-order calculations are presented here, it is first of all in order to display information on magnitude and character of the resistance component due to non-linear free-surface terms and of the discrepancy between far-field and hull-pressure resistance which arises if such nonlinearities are neglected.

Calculations for δR^H were described in [1]. For δR^L it was convenient to check numerical accuracy through comparison with the line integral term of δR^H . Integration over the plane $z=0$ was restricted to a rhombe shaped region bounded by a Kelvin angle with apex slightly ahead of the bow and an inverted one with apex slightly behind the stern. We observed strong positive contributions from x near the midship section which are nearly bal-

anced by negative contributions from the ends. The integrand has much better decay than that for a Kochin function for free-surface singularities, as it is of *third* power in flow components and a factor from behind the ship is always combined with a factor from ahead.

C. Complementary investigations on mapping procedures

For the Wigley model we had calculated the distorted wave pattern in comparison with the original wave pattern from linear theory ($F_n = 0.316$). More information on theory and numerical results may be found in [4].

The influence of mapping on wave profile along the hull is shown in another figure.

D. Wave resistance calculations for a ship under constant acceleration

The theory of instationary wave resistance of thin ships is well documented, but numerical evaluations are scarce.

W. Grollius in Duisburg, Germany, has treated the case of a ship with parabolic water lines and rectangular frames - which corresponds to the Inuid S-201 source distribution - for various constant accelerations $a = \epsilon g$ with ϵ ranging from 0.003 up to 0.1. The time integration can be carried out in closed form in this case. Calculations become difficult with low F_n and/or low ϵ , the stationary Michell resistance is approached with decreasing ϵ and *increasing* F_n .

If we apply the Inuid concept to this source distribution, i.e. if we think of the body as generated therefrom, it is pertinent to apply Lagally's formula for time dependent flow. The resistance expression then differs by a term representing action of the instationary pressure component $\rho \phi_t$ if use is made of an exact body boundary condition and if surface piercing is neglected. The difference term again tends to zero with high F_n and low ϵ .

We present two typical curves for the cases $\epsilon = 0.05$ and $\epsilon = 0.003$.

The work of Grollius has not yet been published, and I am obliged to him for letting me present these data.

References

- [1] Eggers,K., Choi,H.S. : On the calculation of stationary ship flow components
Proc. 1st Int. Conf. Num. Ship Hydrodyn., 1975, 649-672
- [2] Gadd,G. : A method for calculating the flow over ship hulls
TRINA 112 (1970), 335-345; disc., 345-351
- [3] Eggers,K. : On the basis of slow ship theory
Int. Joint Research "Study on local non-linear effects in ship waves"
Report 1978 (T. Inui, ed.), 649-672
- [4] Eggers,K., Gamst,A. : An evaluation of mapping procedures for the stationary ship wave problem
Schiffstechnik 26 (1979), 125-170

FORMAT FOR TABULATED VALUES OF WAVE RESISTANCE

INUID S-201

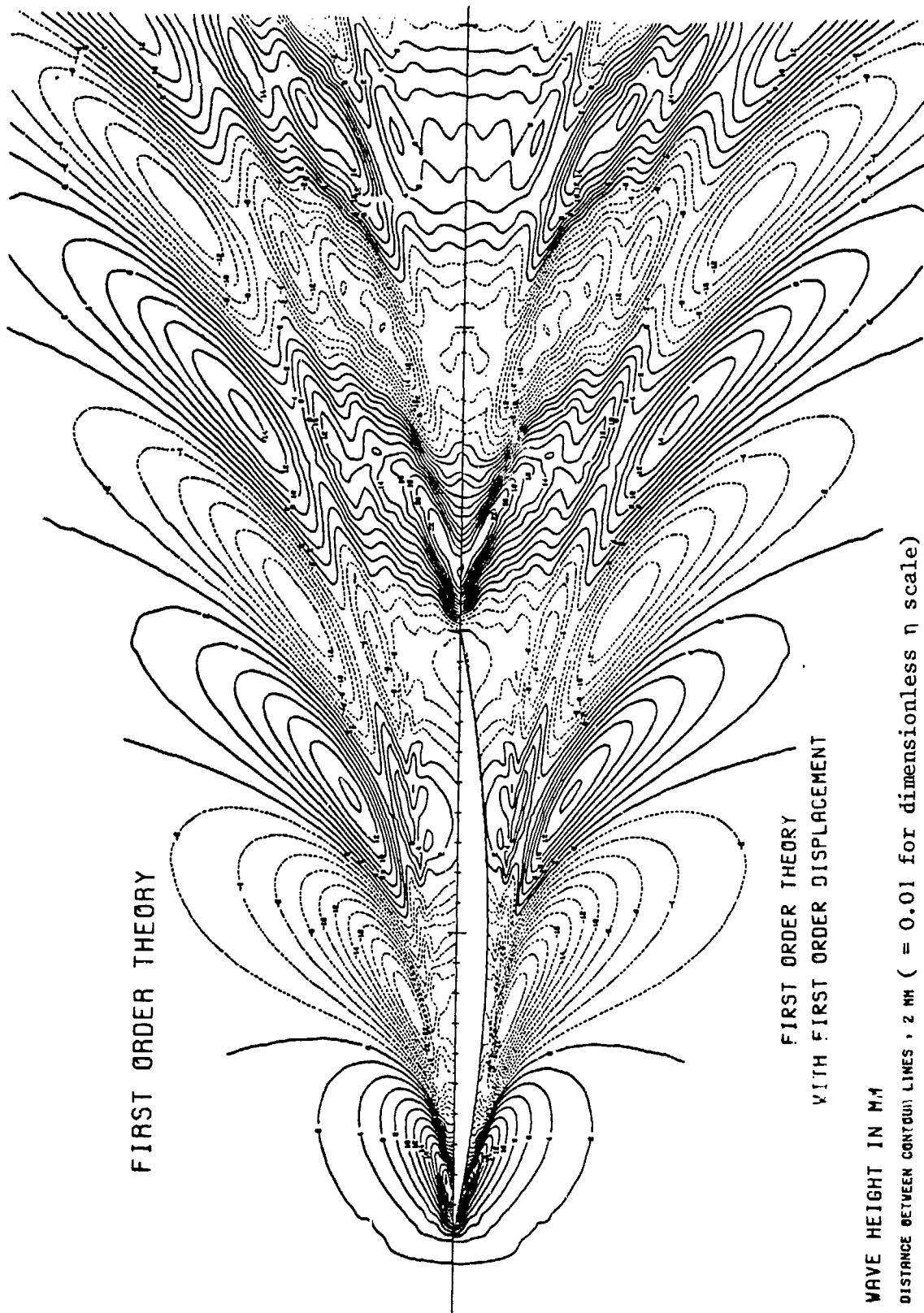
Fn	Percentage corrections to linear resistance (under Inuid assumption)				Corrections to C_w from linear theory			
	from δR^L	from δR^F	from change of sinkage		from δR^L	from δR^F	from change of sinkage	total correction
0.255	16.5 %	- 11.0 %	0.1 %		0.540	- 0.351	0.032	0.221
0.287	7.9 %	- 0.3 %	0.2 %		0.589	- 0.022	0.015	0.582
0.319	10.0 %	- 14.1 %	3.9 %		0.542	- 0.926	0.256	- 0.128
0.360	14.7 %	- 14.2 %	4.0 %		0.754	- 0.741	0.208	0.221
0.440	- 0.5 %	- 3.9 %	14.6 %		- 0.774	0.601	2.269	2.096
0.525	- 3.6 %	17.0 %	16.7 %		- 0.624	2.961	2.920	5.252
0.650	- 5.0 %	44.2 %	12.5 %		- 0.491	4.370	1.234	5.113

FORMAT FOR TABULATED VALUES OF WAVE RESISTANCE

WIGLEY HULL

Fn	Percentage corrections to linear resistance			$10^3 \times C_W$		
	from δR^H	from δR^L	from δR^F	first order	2nd order [†]	
0.266	- 25.4 %	18.0 %	- 3.8 %	1.01	0.896	
0.313	7.2 %	8.0 %	0.16 %	1.91	2.195	
0.350	18.0 %	17.0 %	- 7.0 %	1.24	1.59	
0.402	7.6 %	3.6 %	- 2.3 %	2.09	2.28	
0.452	- 1.3 %	- 2.2 %	- 1.8 %	4.193	3.942	
0.482	1.3 %	- 2.0 %	7.1 %	4.476	4.85	
					† Without correction for trim.	

FIRST ORDER THEORY



FIRST ORDER THEORY
WITH FIRST ORDER DISPLACEMENT

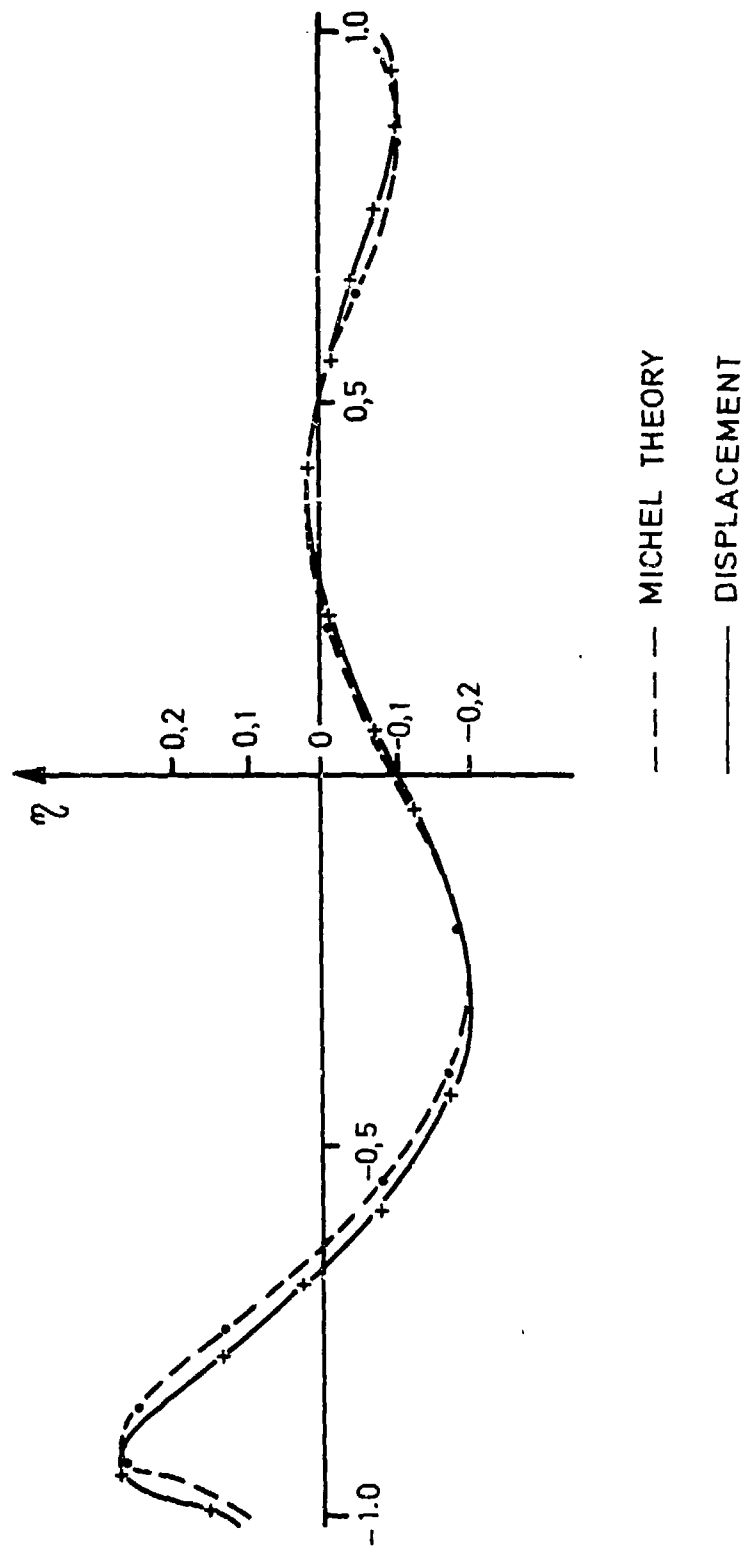
WAVE HEIGHT IN MM

DISTANCE BETWEEN CONTOUR LINES = 2 MM (= 0.01 for dimensionless η scale)

WAVE PATTERN WIGLEY MODEL (S) AT FN = 0.316

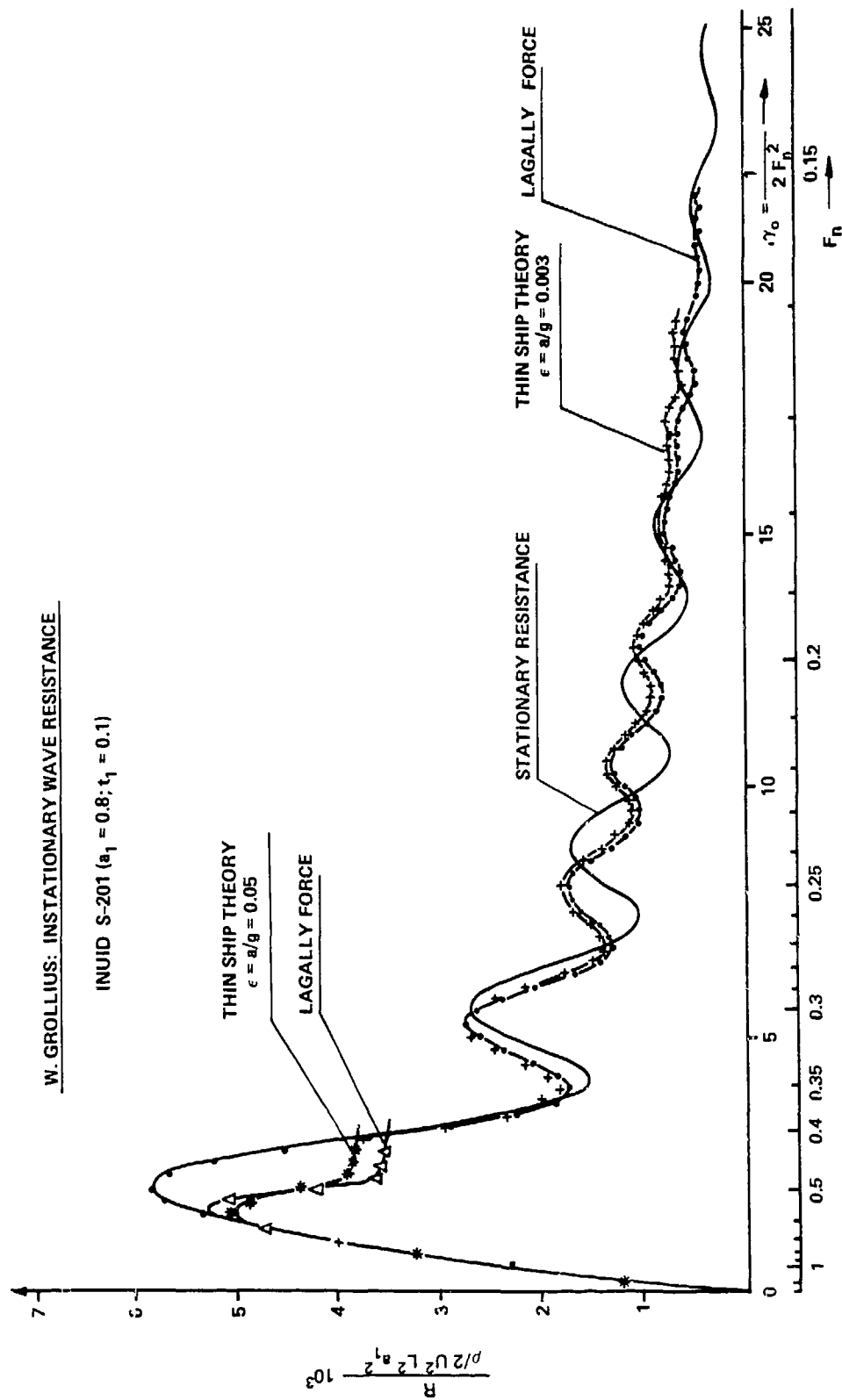
WAVE PROFILE
OF WIGLEY MODEL

$F_n = .316$



W. GROLLIUS: INSTATIONARY WAVE RESISTANCE

INUID S-201 ($a_1 = 0.8$; $t_1 = 0.1$)



Additional Calculations for the Test Cases at the
Workshop on Ship Wave Resistance

J. Kux

At the time this workshop was announced it was expected that the selected hull forms would also be used as test cases for the boundary layer workshop. Meanwhile this has been announced and only hull form (iv) Hoffmann Tanker has been included. Nevertheless at that time we started geometrical and potential theoretic calculations for all five cases. This information might be of interest for future work in wave resistance calculation too.

The idea was to present the five cases with the surface of the hull divided in a similar way into panels to achieve a comparable accuracy in all cases. As a result listings of the obtained source strengths, velocity magnitudes on the hull surface and pressure coefficients as well as curvature parameters were to be made available. Charts of isolines for the pressure coefficient, the potential streamlines, the mean curvature and the Gaussian curvature on the surface as projected onto the coordinate planes would complete the data. In order to obtain a rough estimate of the thickening of the hull due to the boundary layer a calculation along potential streamlines with a simple integral two-dimensional boundary layer method was envisaged.

The boundary layer calculation has not yet been started. The other mentioned points of this program have meanwhile been almost completed. Everybody interested in these data is invited to contact us to obtain the information.

WAVE RESISTANCE OF THE WIGLEY AND INUI HULL FORMS PREDICTED
BY TWO SIMPLE SLENDER-SHIP WAVE-RESISTANCE FORMULAS

by

P. Koch and F. Noblesse

Massachusetts Institute of Technology

Abstract

The wave resistance coefficients of the Wigley and Inui hull forms have been evaluated on the basis of two simple explicit slender-ship wave resistance formulas, namely the formula proposed by Hogner in 1932 and a modified-Hogner formula including a line integral around the ship waterline.

The general Neumann-Kelvin theory

The two above-mentioned wave-resistance formulas correspond to the simplest (and crudest) approximations in a hierarchy of slender-ship iterative approximations obtained in the general Neumann-Kelvin theory developed in [1,2,3]. This theory thus is briefly summarized here for clarity. As it is most well known, the wave resistance, R , of a ship can be determined from the classical Havelock wave-resistance formula

$$R/\rho U^2 L^2 = (1/2\pi F^4) \int_{-\infty}^{\infty} |K(t)|^2 (1+t^2)^{1/2} dt, \quad (1)$$

where ρ is the density of water, U and L are the speed and the length, respectively, of the ship, $F \equiv U/(gL)^{1/2}$ is the Froude number, and $K(t)$ is the Kochin free-wave spectrum function, which essentially gives the amplitudes of the elementary plane-wave components of the ship-wave pattern at angles $\theta = \tan^{-1} t$ from the direction of motion of the ship.

The Kochin free-wave spectrum function $K(t)$ is given by the following well-known formula:

$$K(t) = \int_h E_v da - F^2 \oint_c E_v^2 u d\ell + \int_h \phi E_n da + F^2 \oint_c [E(\gamma \phi_c + \delta \phi_d) - \phi E_x] u d\ell + \int_{\sigma} E_o dx dy, \quad (2)$$

where the significance of the various previously-undefined symbols is explained below. The function $E \equiv E(t; \vec{x}, F)$ is defined as

$$E \equiv \exp[zF^{-2}(1+t^2) - i(xF^{-2} + yF^{-2}t)(1+t^2)^{1/2}] \quad (2a)$$

The symbols h, c , and σ represent the portion of the ship hull surface below the plane $z=0$ of the undisturbed free surface, the intersection curve of the hull surface with the plane $z=0$, and the portion of the plane $z=0$ outside the ship, respectively. The symbol da represents the differential element of area of the hull surface h , and $d\ell$ is the differential element of arc length of the waterline c . The symbols v, μ, γ , and δ are defined as $v \equiv \vec{n} \cdot \vec{i}$, $\mu \equiv \vec{n}_0 \cdot \vec{i}$, $\gamma \equiv \vec{c} \cdot \vec{i}$, and $\delta \equiv \vec{d} \cdot \vec{i}$, where \vec{i} is the unit vector parallel to the velocity of the ship and pointing towards the ship stern, \vec{n} is the unit vector normal to the hull surface h and pointing inside the ship, \vec{n}_0 is the unit normal vector to the waterline c in the plane $z=0$ and pointing inside c , \vec{c} is the unit tangent vector to c oriented in the counter-clockwise sense, and $\vec{d} \equiv \vec{n} \times \vec{c}$ is the unit vector tangent to h orthogonal to both \vec{n} and \vec{c} and pointing downwards. The symbols $h, c, \sigma, i, \vec{n}, \vec{n}_0, \vec{c}$, and \vec{d} are shown in the definition sketch. The function $\phi \equiv \phi(\vec{x})$ is the velocity potential of the flow caused by the ship. The notation E_n, E_x, ϕ_c , and ϕ_d means $\partial E / \partial n \equiv \nabla E \cdot \vec{n}$, $\partial E / \partial x$, $\partial \phi / \partial c$, and $\partial \phi / \partial d$, respectively. Finally, the free-surface flux q is associated with the nonlinear terms in the free-surface boundary condition, and is given by

$$q = \left[\phi_z + F^2 \left\{ \phi_{xx} + (|\nabla \phi|^2)_x + \frac{1}{2} \nabla \phi \cdot \nabla |\nabla \phi|^2 \right\} \right]_{z = -F^2(\phi_x + \frac{1}{2} |\nabla \phi|^2)} - \left[\phi_z + F^2 \phi_{xx} \right]_{z = 0}.$$

The velocity potential ϕ which formula (2) requires on the hull surface $h+c$ and in the neighbourhood of the free-surface plane $z=0$, can be determined (in principle at least) by solving the integral equation

$$\begin{aligned} \phi_* = & \int_h G v da - F^2 \oint_c G v^2 \mu d\ell + \int_h (\phi - \phi_*) G_n da + \\ & + F^2 \oint_c [G(\gamma \phi_c + \delta \phi_d) - (\phi - \phi_*) G_x] \mu d\ell + \int_\sigma G q dx dy, \end{aligned} \quad (3)$$

where the significance of the previously-undefined symbols is explained below. The symbol ϕ_* is meant for $\phi(\vec{\xi})$, where $\vec{\xi}$ is an arbitrary "field point" on the hull surface $h+c$, on the undisturbed free surface σ , or in the solution domain bounded by $h+c+\sigma$, while ϕ is meant for $\phi(\vec{x})$, as in formula (2), where \vec{x} is the "point of integration" in the various integrals in the integral equation (3). The function $G \equiv G(\vec{\xi}, \vec{x})$ is

equation (3) is the Green function associated with the linearized free-surface boundary condition, and given in [4,5].

The Havelock wave-resistance formula (1), formula (2) for the Kochin free-wave spectrum function and the integral equation (3) for the velocity potential are the three basic equations upon which the general Neumann-Kelvin theory presented in [1,2,3] is based. While a direct numerical solution of the integral equation (3) may not be possible, an iterative method of solution can be used. Specifically, a sequence of iterative approximations $\phi^{(0)}$, $\phi^{(1)}$, $\phi^{(2)}$...can readily be defined (in principle at least) by choosing an initial approximation $\phi^{(0)}$ and by using the straightforward recurrence formula obtained by replacing the potential ϕ on the right and left sides of equation (3) by $\phi^{(n)}$ and $\phi^{(n+1)}$, respectively, with $n \geq 0$. A corresponding sequence of approximations $K^{(n)}$ and $R^{(n)}$ to the Kochin function $K(t)$ and the wave resistance R are then readily defined by replacing ϕ by $\phi^{(n)}$ and K by $K^{(n)}$ in formulas (2) and (1), respectively. Various choices for the initial approximation $\phi^{(0)}$ in the integral equation (3) immediately come to mind. The simplest choice consists in merely taking $\phi^{(0)} \equiv 0$. The hierarchy of iterative approximations $\phi^{(n)}$, $K^{(n)}$, $R^{(n)}$ associated with this choice of initial approximation may be regarded as a hierarchy of slender-ship approximations, which indeed provide a generalization of the classical hierarchy of thin-ship perturbation approximations, as is shown explicitly in [1,2]. Another natural choice for the initial approximation $\phi^{(0)}$ is the zero-Froude-number (double-ship) potential, which generates a sequence of low-Froude-number approximations. The low-Froude-number wave-resistance formulas of Guevel [6], Kayo [7], Baba [8], and Maruo [9] indeed correspond to the first approximation in this hierarchy of low-Froude-number approximations, as is shown explicitly in [3], where the second approximation is also given explicitly. Finally, a sequence of low-Froude-number slender-ship approximations is obtained in [3] by selecting $\phi^{(0)}$ as the slender-ship approximation to the zero-Froude-number potential.

The Hogner and modified-Hogner wave-resistance formulas

The simplest wave-resistance formula is the zeroth-order slender-ship approximation defined by the Havelock formula (1) and formula (2) in which

the unknown potential ϕ is simply taken as equal to zero, as may be justified (to some extent at least) for a sufficiently slender ship form. The resulting approximation is given by

$$K^{(0)}(t) = \int_h E v da - F^2 \oint_c E v^2 \mu d\ell, \quad (4)$$

where E is given by formula (2a). The integral equation (3) thus is merely ignored in this approximation, and formulas (1) and (4) provide a particularly simple expression for the wave resistance explicitly in terms of the speed, dimension, and shape of the ship. The first term on the right side of formula (4), that is the surface integral over the ship hull surface h , is actually identical to the approximation, K_H say, proposed by Hogner [10] in 1932:

$$K_H(t) = \int_h E v da, \quad (4a)$$

so that formula (4) may be regarded as a modified-Hogner approximation including a line integral around the ship waterline.

The numerical calculations of Chen [11] and Triantafyllou [12] have shown that differences between the values of the wave resistance predicted by the Michell, Hogner, and modified-Hogner formulas can be quite significant. In particular, the waterline integral in formula (4) is specially important for blunt ship forms (for which $|v|$ and $|\mu|$ is not small at the stern or/and bow), for ship forms with small draft, and in the low-speed limit. The drastic reduction in the value of the wave resistance brought about by the waterline integral at low Froude numbers is particularly striking. As a matter of fact, it is proved in [2] that the hull integral and the waterline integral are asymptotically equivalent in the low-Froude number limit $F \rightarrow 0$ [even though, for a thin ship--of small beam/length ratio β say--the hull and waterline integrals are $O(\beta)$ and $O(\beta^3)$, respectively].

Results for the Wigley and Inui hull forms

The large effect of the waterline integral is apparent also from the figures at the end of this paper presenting the results of calculations for the Wigley and Inui hull forms based on the Hogner formula (4a) and the zeroth (modified-Hogner) approximation (4), which are identified by the symbols H and O respectively (the curve identified by the symbol M

in the figure for the Wigley hull is the Michell wave resistance). These calculations show that for (relatively) high Froude numbers, say for $F \geq .31$ for the Wigley hull and for $F \geq .32$ for the Inui hull, the Hogner wave-resistance curve is in surprisingly good agreement with experimental measurements, while inclusion of the waterline integral appears to underpredict the wave resistance in this relatively high-Froude-number range. On the other hand, for relatively low values of the Froude number, say for $F \leq .31$ or $F \leq .32$ for the Wigley and Hogner hulls, respectively, the waterline integral appears to have an obvious beneficial effect. In fact, for moderately low values of the Froude number, say for $.21 \leq F \leq .31$ and for $.21 \leq F \leq .32$ for the Wigley and Inui hulls, respectively, the zeroth-order slender-ship (modified-Hogner) approximation may be seen to be in fairly good agreement with experimental measurements. The observable agreement between experimental measurements and the Hogner approximation in the fairly-high-Froude-number range (for $F \geq .31$ or $.32$), and the modified-Hogner approximation in the moderately-low-Froude-number range (for $.21 \leq F \leq .31$ or $.32$), is in fact somewhat remarkable in view of the extreme simplicity of these wave-resistance formulas and of the relative crudeness of the assumptions upon which they are based. Calculations for the three other (real-ship) hull forms considered in this Workshop are currently being performed by the first author; the results of these calculations should be instructive.

References

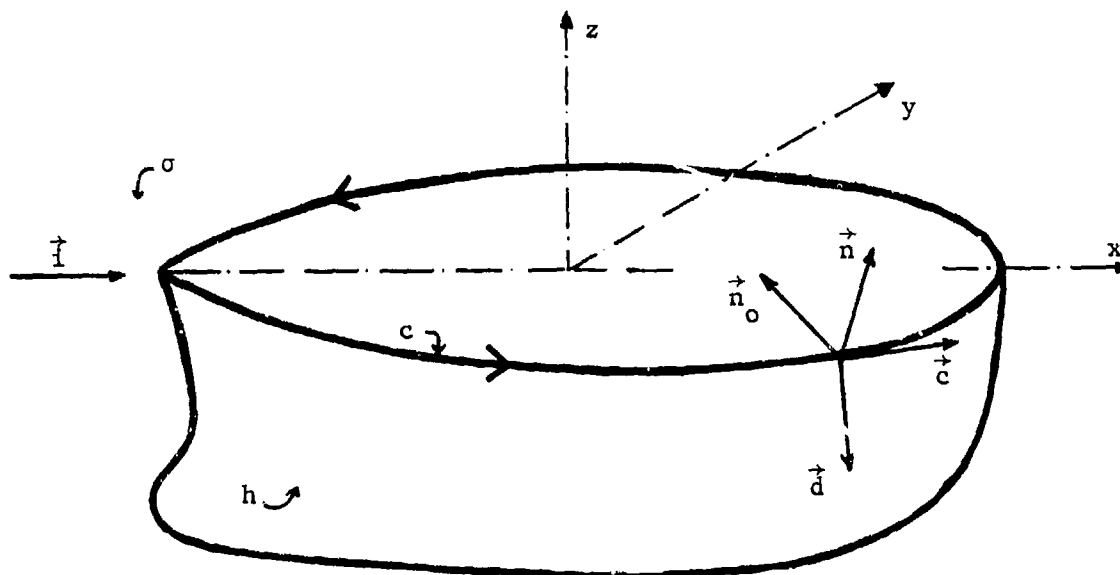
1. Noblesse F., "Potential Theory of Steady Motion of Ships, Parts 1 and 2", Massachusetts Institute of Technology, Department of Ocean Engineering Report No. 78-4, Sept. 1978, 43 pp.
2. Noblesse F., "Potential Theory of Steady Motion of Ships, Part 3: Wave Resistance", Massachusetts Institute of Technology, Department of Ocean Engineering Report No. 78-5, Nov. 1978, 26 pp.
3. Noblesse F., "Potential Theory of Steady Motion of Ships, Part 4: Low-Froude-Number Approximations", Massachusetts Institute of Technology, Department of Ocean Engineering Report No. 79-1, May 1979, 40 pp.
4. Noblesse F., "Alternative Expressions for the Green Function of the Theory of Ship Wave Resistance", Massachusetts Institute of Technology Sea Grant College Program, Report No. MITSG 79-23, Sept. 1979, 41 pp.
5. Noblesse F., "On the Fundamental Function in the Theory of Steady Motion of Ships", Journal of Ship Research, Vol.22, No. 4 Dec. 1978, pp. 212-215.
6. Guevel P., Vaussy P., and Kobus J.M., "The Distribution of Singularities Kinematically Equivalent to a Moving Hull in the Presence of a

- Free Surface", International Shipbuilding Progress, Vol. 21, 1974, pp. 311-324.
7. Kayo Y., "A Note on the Uniqueness of Wave-Making Resistance when the Double-Body Potential is Used as the Zero-Order Approximation", Transactions of the West-Japan Society of Naval Architects, No. 55, March 1978, pp. 1-11.
 8. Baba E., "Wave Resistance of Ships in Low Speed", Mitsubishi Technical Bulletin No. 109, August 1976, 20 pp.
 9. Maruo H., "Wave Resistance of a Ship with Finite Beam at Low Froude Numbers", Bulletin of the Faculty of Engineering, Yokohama National University, Vol. 26, March 1977, pp. 59-75.
 10. Hogner E., "Eine Interpolationsformel für den Wellenwiderstand von Schiffen", Jahrbuch der Schiffbautechnischen Gesellschaft, Vol. 33, 1932, pp. 452-456.
 11. Chen, C.Y., "Evaluation of a New Wave-Resistance Formula for a Wedge-Like Ship-Bow Form", Massachusetts Institute of Technology, Department of Ocean Engineering, M.S. Thesis, Jan. 1979, 50 pp.
 12. Triantafyllou G., "Investigation of a Simple Ship-Wave Resistance Formula", Massachusetts Institute of Technology, Department of Ocean Engineering, M.S. Thesis in preparation.

Acknowledgments

The numerical calculations reported in this study were performed as part of the MIT Sea Grant College Program with support from the Henry L. and Grace Doherty Foundation, and from the Office of Sea Grant in the National Oceanic and Atmospheric Administration, U.S. Department of Commerce.

Definition Sketch



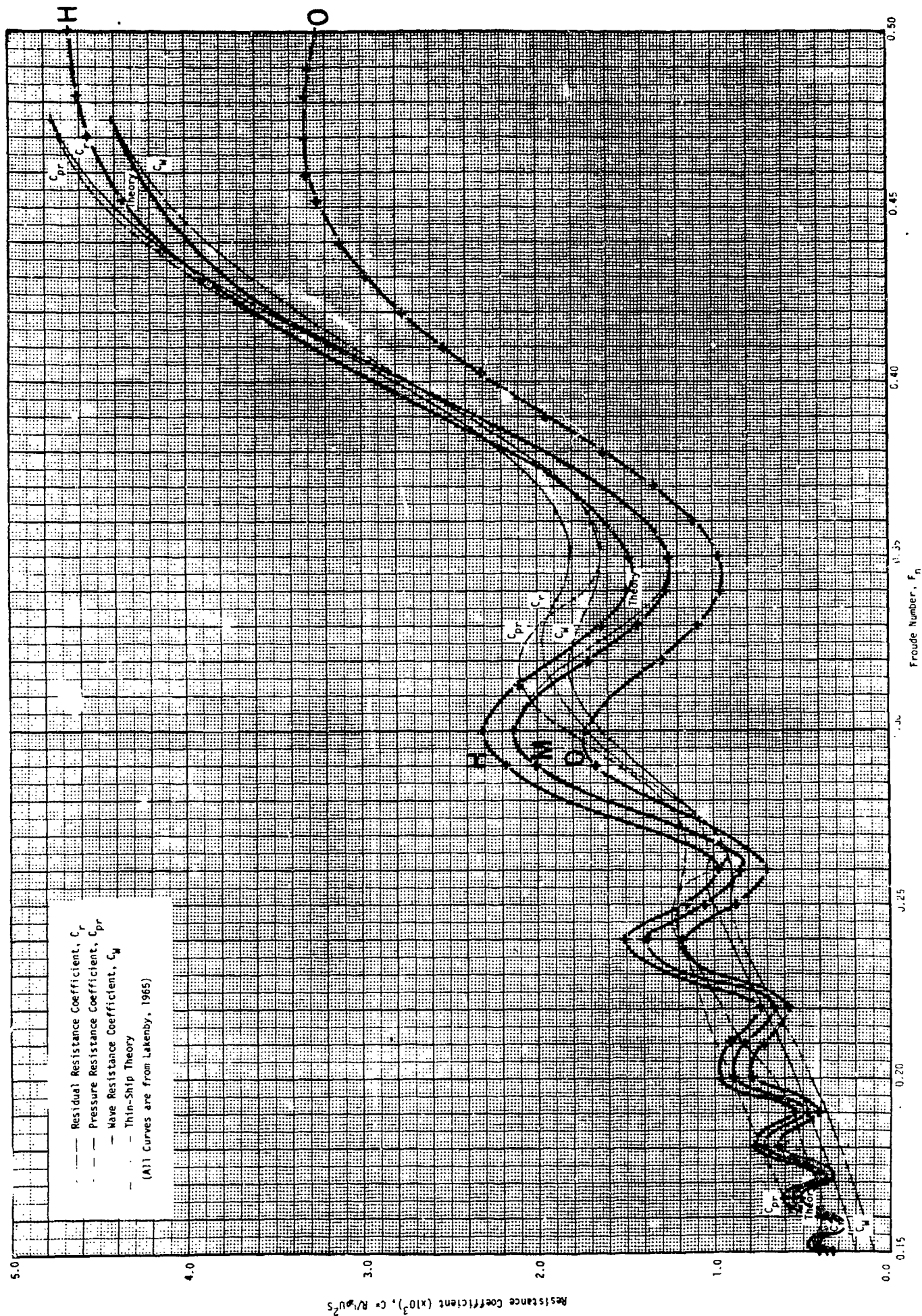


FIGURE 2.3 - Resistance Curves for Wigley Hull

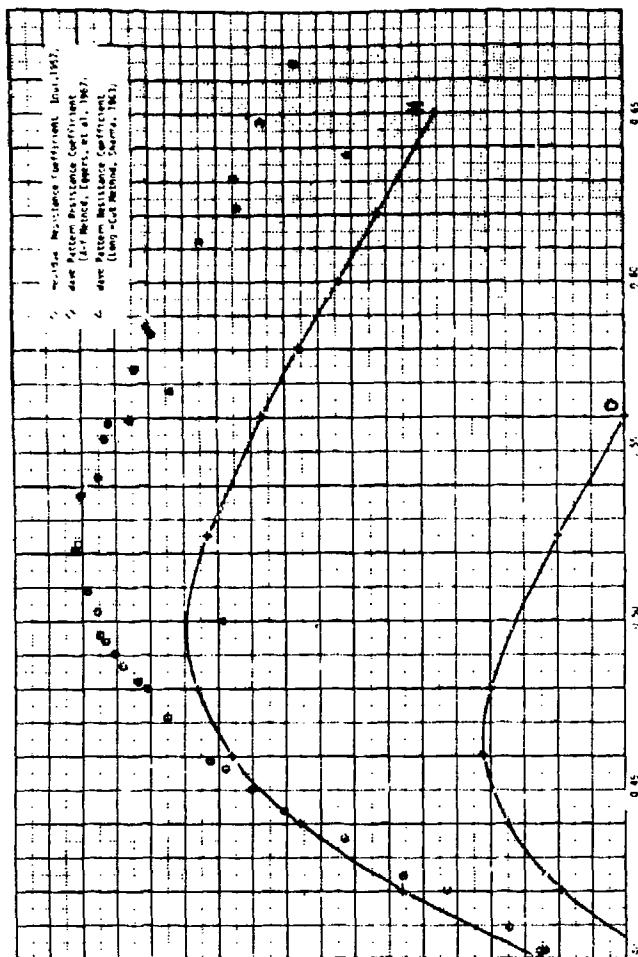


FIGURE 3 - Inund Wall Resistance Coefficient

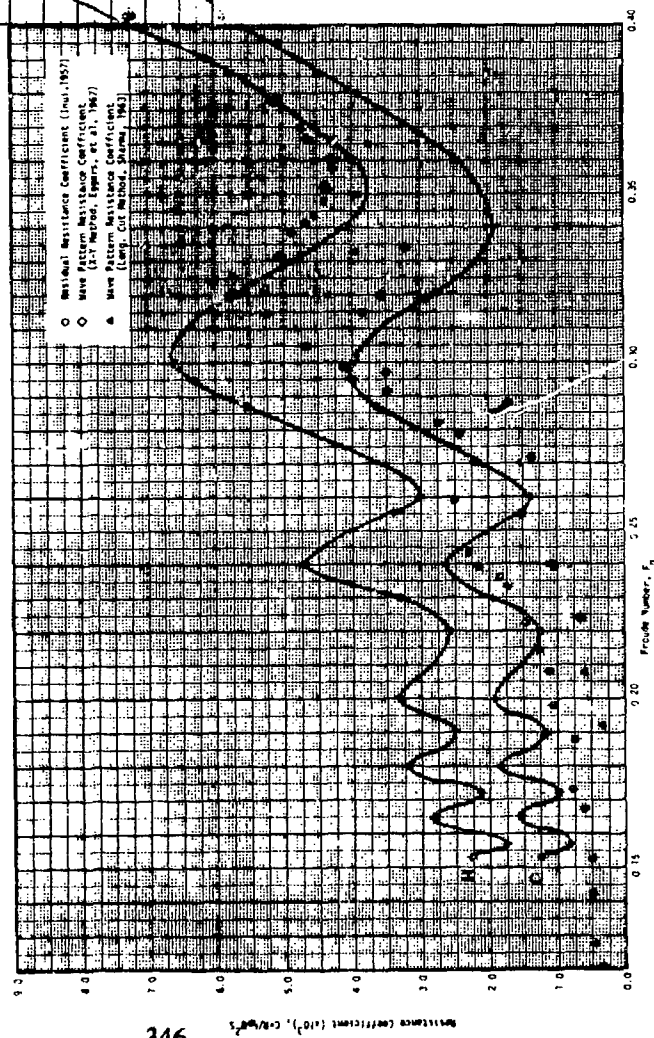


FIGURE 3 - Inund Wall Resistance Coefficient

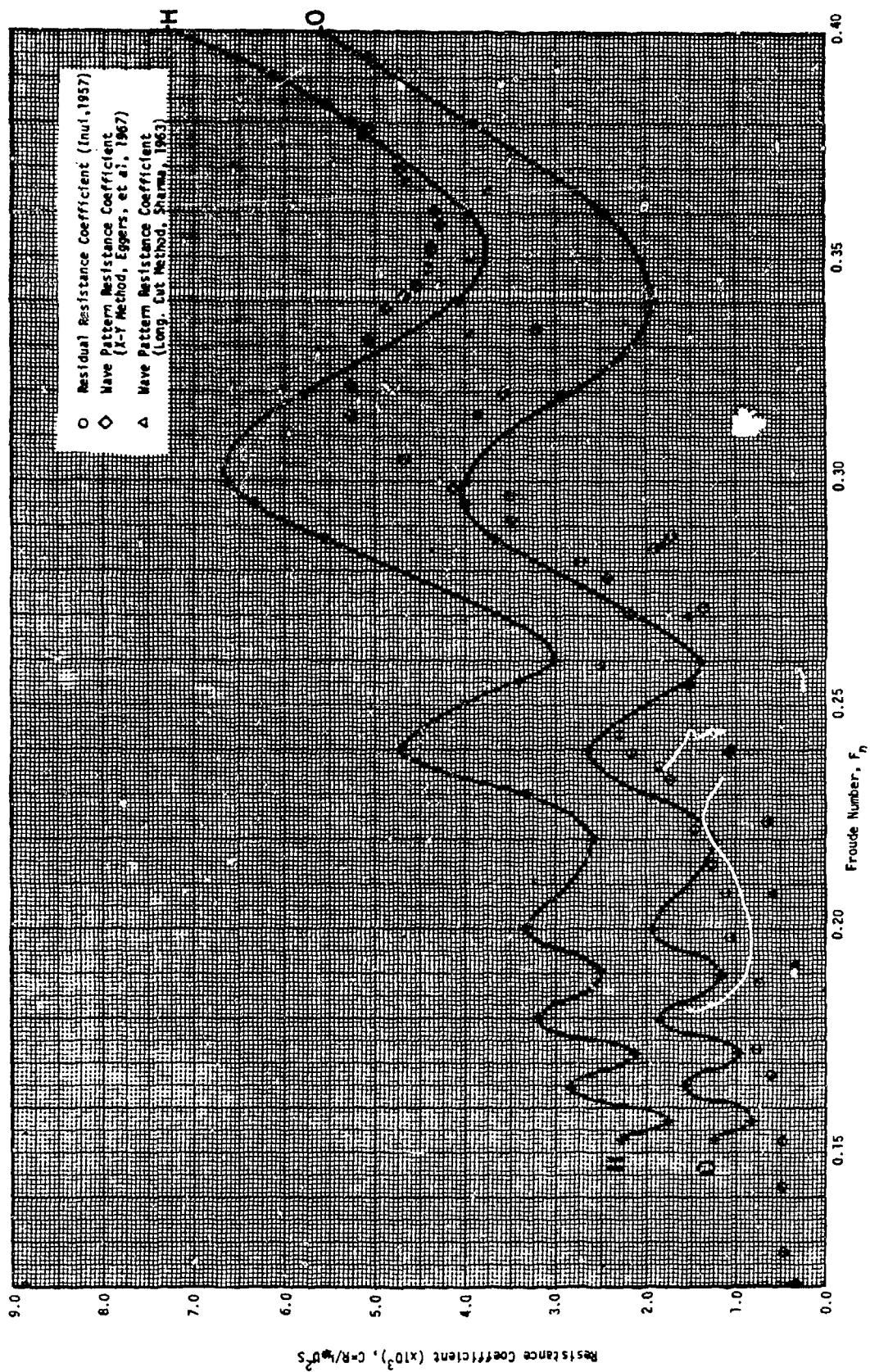


FIGURE 3.3 - Low-Speed Resistance Data, Inuid Hull, S-201

3-4

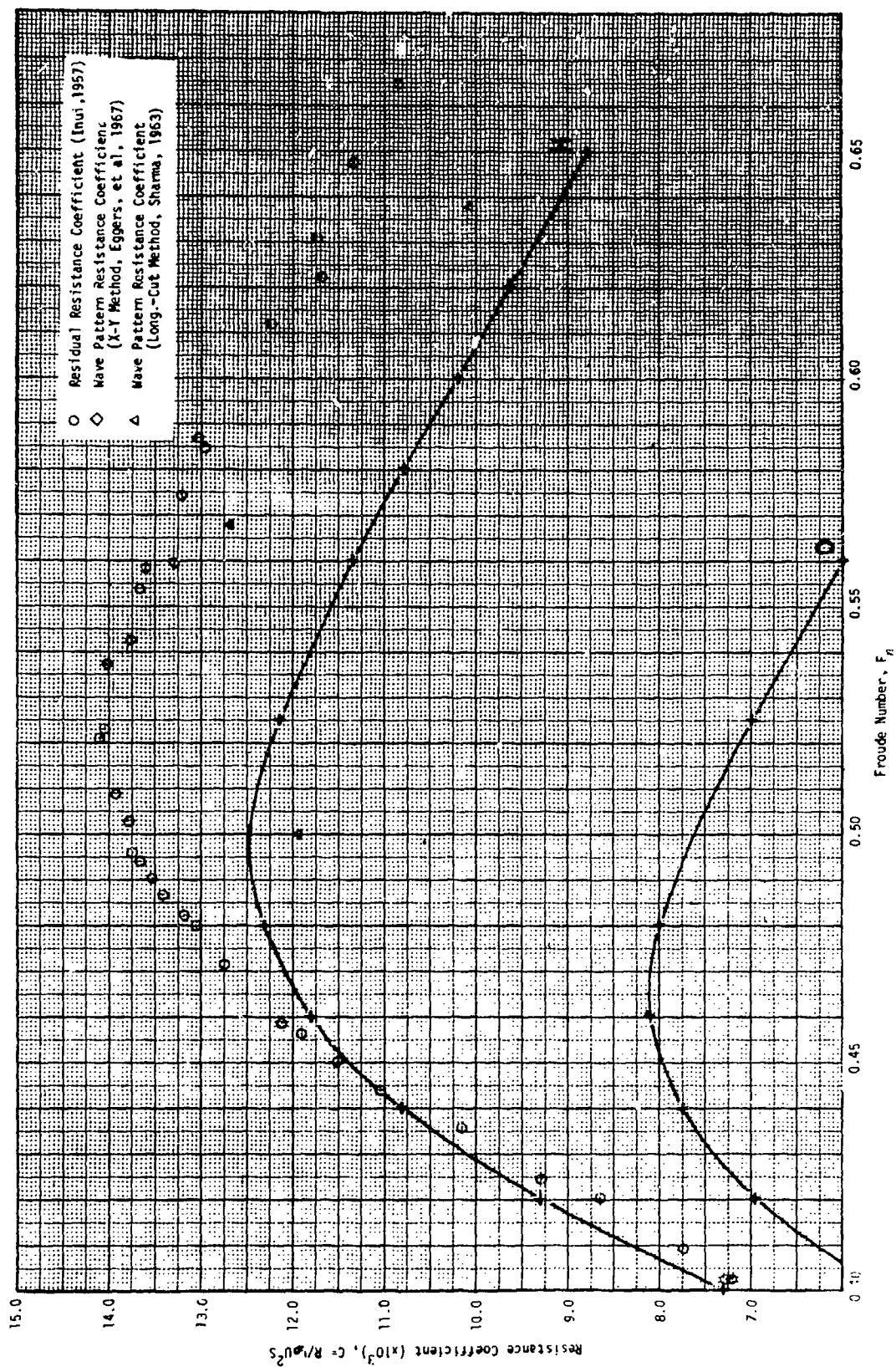


FIGURE 3.4 - High-Speed Resistance Data, Inuid Hull, S-201

Wave resistance coefficient of the Wigley model
given by Michell's and Hogner's wave resistance formulas

WIGLEY: MICHELL		WIGLEY: MICHELL		WIGLEY: HOGNER		WIGLEY: HOGNER	
F_N	$C_R \times 10^3$	F_N	$C_R \times 10^3$	F_N	$C_R \times 10^3$	F_N	$C_R \times 10^3$
0.150	0.361	0.250	1.065	0.150	0.390	0.300	2.311
0.152	0.442	0.260	0.847	0.155	0.422	0.313	2.098
0.155	0.380	0.270	1.092	0.157	0.345	0.330	1.638
0.157	0.307	0.280	1.603	0.160	0.380	0.340	1.477
0.160	0.348	0.290	2.016	0.166	0.598	0.350	1.472
0.163	0.512	0.300	2.142	0.170	0.464	0.360	1.602
0.166	0.558	0.310	1.995	0.175	0.488	0.402	3.036
0.168	0.491	0.320	1.711	0.180	0.774	0.430	3.907
0.170	0.407	0.330	1.432	0.185	0.695	0.452	4.360
0.172	0.369	0.340	1.263	0.190	0.536	0.470	4.550
0.175	0.454	0.350	1.245	0.200	0.962	0.482	4.618
0.177	0.570	0.360	1.378	0.210	0.908	0.500	4.661
0.180	0.715	0.370	1.634	0.220	0.741		
0.185	0.652	0.380	1.968	0.230	1.248		
0.190	0.475	0.390	2.344	0.240	1.494		
0.200	0.886	0.400	2.730	0.250	1.171		
0.210	0.832	0.410	3.095	0.260	0.978		
0.220	0.653	0.430	3.718	0.266	1.077		
0.230	1.166	0.440	3.957	0.290	2.169		
0.240	1.386	0.450	4.146				

Wave resistance coefficient of the Wigley model
given by the zeroth-order slender-ship approximation

WIGLEY: 0 TH APPROX.		WIGLEY: 0 TH APPROX.		WIGLEY: 0 TH APPROX.	
F_N	$C_R \times 10^3$	F_N	$C_R \times 10^3$	F_N	$C_R \times 10^3$
0.150	0.323	0.240	1.177	0.430	2.967
0.153	0.401	0.250	0.874	0.440	3.117
0.155	0.347	0.260	0.708	0.452	3.242
0.157	0.275	0.266	0.792	0.460	3.294
0.160	0.306	0.280	1.344	0.470	3.323
0.163	0.474	0.290	1.657	0.482	3.319
0.166	0.496	0.300	1.723	0.490	3.296
0.168	0.427	0.313	1.486	0.500	3.249
0.170	0.372	0.320	1.301	0.510	3.186
0.172	0.330	0.330	1.077	0.520	3.110
0.175	0.391	0.340	0.959		
0.177	0.498	0.350	0.973		
0.180	0.641	0.360	1.109		
0.185	0.563	0.370	1.339		
0.190	0.417	0.380	1.625		
0.200	0.787	0.390	1.955		
0.210	0.718	0.402	2.319		
0.220	0.566	0.410	2.533		
0.230	0.997	0.420	2.772		

Wave resistance coefficient of the Inui model
given by the Hogner and the zeroth approximations

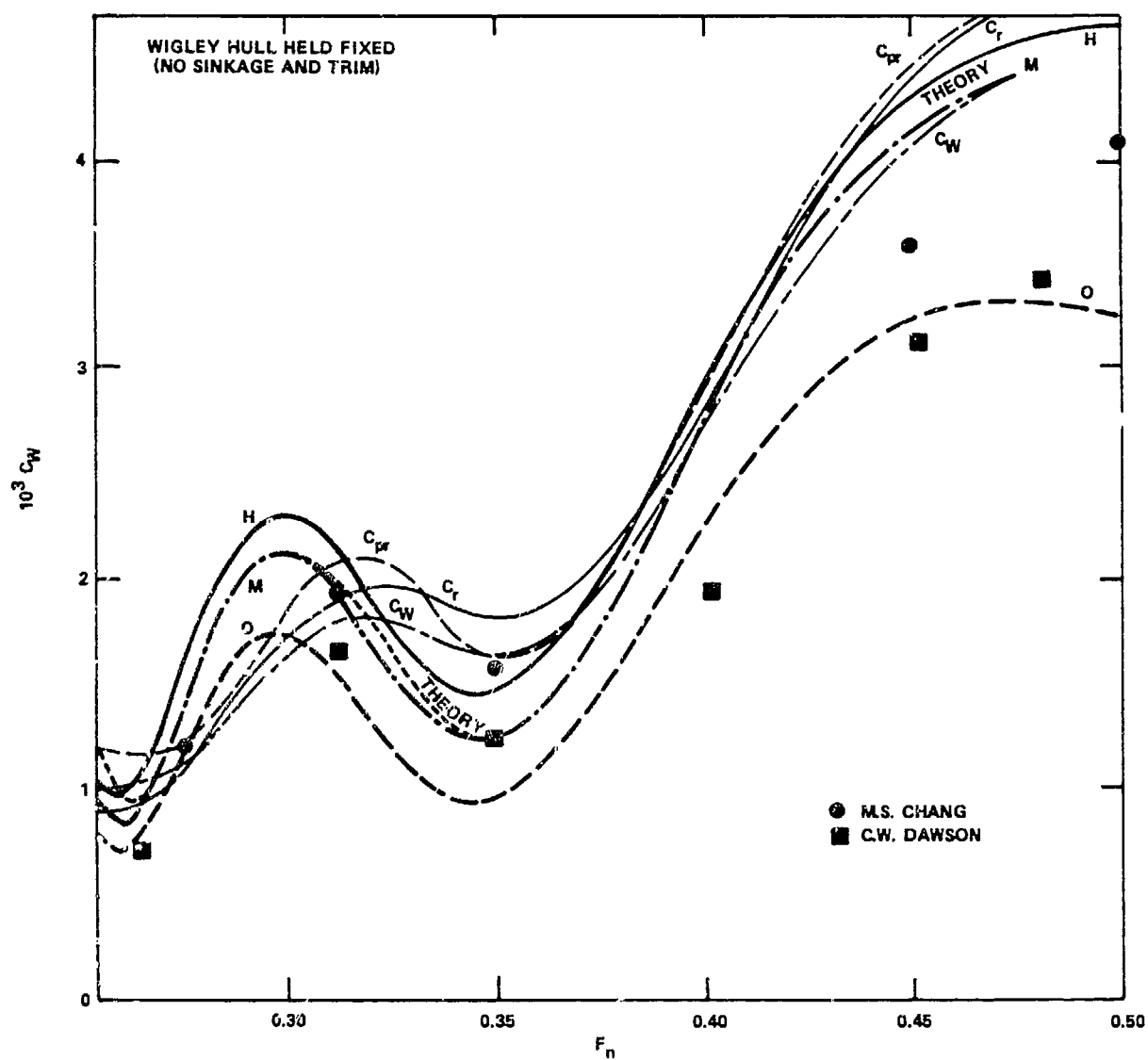
INUI: HOGNER		INUI: HOGNER		INUI: 0 TH APPROX.		INUI: 0 TH APPROX.	
F_N	$C_R \times 10^3$	F_N	$C_R \times 10^3$	F_N	$C_R \times 10^3$	F_N	$C_R \times 10^3$
0.153	2.269	0.380	5.233	0.153	1.248	0.380	3.889
0.157	1.760	0.400	7.289	0.157	0.828	0.400	5.602
0.166	2.840	0.420	9.237	0.166	1.564	0.420	6.946
0.172	2.128	0.440	10.767	0.172	1.009	0.440	7.744
0.180	3.210	0.460	11.797	0.180	1.856	0.460	8.093
0.190	2.492	0.480	12.292	0.190	1.170	0.480	7.983
0.200	3.324	0.525	12.135	0.200	1.928	0.525	7.013
0.220	2.606	0.560	11.342	0.220	1.240	0.560	5.930
0.230	3.324	0.580	10.795	0.230	1.928	0.580	5.379
0.240	4.708	0.600	10.211	0.240	2.635	0.600	4.789
0.255	3.409	0.620	9.637	0.255	1.527	0.620	4.182
0.260	3.026	0.650	8.780	0.260	1.403	0.650	3.356
0.287	5.549	0.800	5.484	0.287	3.667	0.800	1.013
0.295	6.330	1.000	3.056	0.295	4.008	1.000	0.808
0.300	6.565	1.200	1.701	0.300	3.999	1.200	2.720
0.319	5.769	1.273	1.330	0.319	2.931	1.273	3.022
0.320	5.647	1.414	0.801	0.320	2.830		
0.340	4.110			0.340	1.935		
0.360	3.945			0.360	2.424		

Note* on the paper "Wave Resistance of the Wigley and Inui Hull Forms Predicted by Two Simple Slender-ship Wave-resistance Formulas" by P. Koch and F. Noblesse

In this paper, the discussion of the results predicted by the wave resistance formula of Hogner (1932) and the "zeroth-order slender-ship wave-resistance formula" (also referred to as the "modified-Hogner formula") was based on the assumption that the given experimental measurements had been obtained for rigidly-held ship models, in which neither sinkage nor trim was allowed. It became apparent at the Workshop, however, that this assumption was incorrect, i.e. the given experimental measurements correspond to unrestricted ship models free to heave and trim. This erroneous assumption regarding the conditions in which the experimental measurements were obtained renders the discussion of the theoretical predictions given in the paper inadequate.

The attached figure displays the numerical results of M.S. Chang and C.W. Dawson, for the Wigley model held fixed (without sinkage and trim), together with the curves, identified by the symbols H, M, and O, corresponding to the Hogner (H), Michell (M), and zeroth-order slender-ship (O) approximations. It can be noted that the results of Dawson and Chang, which generally appear to be in fairly good agreement with experimental measurements, are closer to the modified-Hogner (O) than the Hogner curve (H); the results of Dawson in fact are rather close to the modified-Hogner curve (O). This would then seem to suggest that the waterline integral included in the modified Hogner formula has a beneficial effect not only at "low" Froude number, as was noted in the paper, but also at "high" Froude number (contrary to the conclusion previously stated in the paper). In other words, these results for the Wigley hull form suggest it is plausible that the "zeroth-order slender-ship wave resistance formula" may provide a more satisfactory basic slender-ship wave-resistance approximation than the Michell and Hogner formulas. To be sure, more calculations are necessary for fully assessing the zeroth-order slender-ship approximation (and the following first-order approximation).

Editor's Note: This has been submitted after the work shop.



Wave Resistance Calculations by the Low Speed Theory and Guilloton's Method

by Hideaki Miyata and Hisashi Kajitani
The University of Tokyo

In this paper, methods of calculating wave resistance by the low speed theory and Guilloton's method are briefly described, which have been computer-programmed as standard tools at the Experimental Tank of the University of Tokyo.

The remarkable discrepancies of wave resistance between theory and experiment do not all arise from the inadequacy of the conventional potential theories, but, they are considerably caused by the existence of nonlinear waves in the near-field of ships. In the last section, some results of experimental investigations on the nonlinear waves are introduced in short.

1. Low Speed Theory

Two methods of calculating wave resistance by the low speed theory are proposed, i.e., the line integral method and the surface integral method. Comparison of the two methods has been studied in reference 1). A typical result is shown in Fig.1. It is seen that the surface integral method provides preciser value of resistance. The difference between the two methods are rather small ; however, on usual hull forms of ships, this discrepancy tends to be enlarged because of the greater steepness of the disturbance velocity distribution in the neighborhood of the bow and stern. In general, arbitrariness of the calculated wave resistance makes us reluctant to utilize the line integral method. In fact, the surface integral method is adopted at our university.

Following Baba's formulation²⁾ the amplitude function is derived by integrating D-function over the free surface. D-function is obtained from the double model flow solution making use of Hess-Smith's method.

Editor's Note: For Inui S-201, $C_g = 0.618$ was used here, but the correction was made in the computer plots.

$$D(x,y) = \frac{\partial}{\partial x} \left[\eta_r(x,y) \phi_{rx}(x,y,0) \right] + \frac{\partial}{\partial y} \left[\eta_r(x,y) \phi_{ry}(x,y,0) \right] \quad (1)$$

$$\text{where} \quad \eta_r(x,y) = \frac{1}{2g} \left[U^2 - \phi_{rx}^2(x,y,0) - \phi_{ry}^2(x,y,0) \right] \quad (2)$$

This equation is modified into non-dimensional form as,

$$D(x,y) = -2 \left[v_x^2 \frac{\partial v_x}{\partial x'} + 2v_x v_y \frac{\partial v_y}{\partial x'} + v_y^2 \frac{\partial v_y}{\partial y'} + \frac{1}{2} \left(\frac{\partial v_x}{\partial x'} + \frac{\partial v_y}{\partial y'} \right) (v_x^2 + v_y^2 - 1) \right] F_n^2 U \quad (3)$$

v_x, v_y are straightly calculated by Hess-Smith's method and their derivatives are obtained from the derivative forms of the equations of v_x and v_y .

The undisturbed free surface that is the domain of integration is automatically divided into about 250 meshes for half part of a ship as is seen in Fig.1. The value of D is assumed to be constant over each mesh. With this number of division the numerical error that arise from the way of division is almost negligible.

The validity of the low speed theory have been examined on more than 10 ship models with extensive experiments⁶⁾. A part of the results is shown in Fig.3, which indicates unsatisfactory agreement. It is supposed that the application of this method must be restricted in a certain range of velocity and in some classes of hull forms, and that the fundamental defect of the linear theory cannot be remedied by this theory.

2. Guilloton's Method

A computer-program have been constructed according to Gadd's interpretation⁴⁾.

The singularity distributions on the center plane obtained by Michell's approximation are made use of as initial values. Iterative process in concern with equation (3) in reference 3) is carried out untill the value of wave resistance converges. The center plane of a ship is divided into about 200 meshes³⁾.

3. Calculated Results

Calculated results for Wigley model, Inuid S201 and Series 60 are shown in Fig.5. It is noted that the wave resistance by the low speed theory is grossly similar to that by Guilloton's method or Michell's approximation, although it ceases to be valid in high Froude number region ($F_n > 0.3$). Two modified linear theories applied here are essentially linear ones and they do not show satisfactory improvement having prominent humps and hollows in $F_n < 0.4$. The success with these methods will be confined within certain dimensions of hull in a restricted range of velocity.

4. Existence and Effects of Free Surface Shock Waves

Investigations on the characteristics of nonlinear waves in the near-field of ships and their effects on non-viscous resistance are under way, and some results are already presented in reference 5), 6) and 7).

The authors have experimentally verified the existence of a kind of shock wave in the near-field of ships, which satisfies the shock condition that shock waves in compressible fluid do and forms lines of discontinuity where fluid undergoes sudden change in velocity to the direction normal to the shock front. Fig.6 is a wave pattern picture of a simple model. Singular wave system in the near-field of the ship is evident. This wave system will remind us of shock waves around a body moving at supersonic speed in air, because the qualitative resemblance is prominent. A disturbance velocity distribution is shown in Fig.8, which was measured by a five-hole pitot tube on a surface below the disturbed free surface by 10mm. The line of discontinuity, where fluid velocity has abrupt change, is clearly shown. It is the most important property that the disturbance velocity vectors along the wave front are normal to the wave front, in other words, fluid does not experience change in velocity tangential to the wave front. These properties of waves in the near-field of ship are summarized as the existence of discontinuities and the fulfillment of the shock relation. These phenomena ^{are} ~~is~~ limited in a thin layer adjacent to the free surface and the authors named these waves as "Free Surface Shock Wave" in 1977.

It is a matter of nature in a sense, because the equations of motion of the fluid and the free surface boundary condition are nonlinear partial differential equations. Free surface deformation may not be

covered by the solutions of a elliptic partial differential equation.

The resistance by the free surface shock waves is approximately measured as momentum loss behind ships. A typical example of measured head loss distribution is present in Fig.8.

Oblique free surface shock waves and normal free surface shock waves are both observed, and normal free surface shock waves change into oblique ones with the increase of velocity, when the entrance angle is smaller than a certain value, as is shown in Fig.9.

Above described facts imply that dispersive waves and non-dispersive waves co-exist around ships. The problem of wave resistance come to be much more complex ; however, satisfactory progress in wave resistance calculations will not be achieved without sound clarification of these physical phenomena.

References

- 1) H. Kajitani, A. Fujii : Evaluation of Low Speed Theory by Waves and Wave Resistance Calculations of Simple Bodies, Research Report 1977 of the International Joint Research of Study on Local Non-Linear Effect in Ship Waves, edited at the University of Tokyo (1978)
- 2) E. Baba : Wave Breaking Resistance of Ships, International Seminar on Wave Resistance (1976)
- 3) G. E. Gadd : Wave Resistance Calculations by Guilloton's Method, T. of RINA 115 (1973)
- 4) Y. J. Lin, T. Inui, H. Kajitani and others : A Hull Form Improvement by Guilloton's Method, J. of the Kansai Society of Naval Architects, Japan, 172 (1979)
- 5) T. Inui, H. Kajitani, H. Miyata : Experimental Investigations on the Wave Making in the Near-Field of Ships, J. of Kansai Society of Naval Architects, Japan, 173 (1979), same paper is also in the Research Report 1978 of the International Joint Research of Study on Local Non-Linear Effect in Ship Waves edited by T. Inui (1979)
- 6) T. Inui, H. Kajitani, H. Miyata and others : Non-Linear Properties of Wave Making Resistance of Wide-Beam Ships, J. of the Society of Naval Architects of Japan, 146 (1979) (to be published)
- 7) H. Miyata, T. Inui, H. Kajitani : Free Surface Shock Waves around Ships and Their Effects on Ship Resistance, preparatory paper for the spring meeting of the Society of Naval Architects of Japan, which is to be held in May 1980, (1979)

All except 4) are written in English.

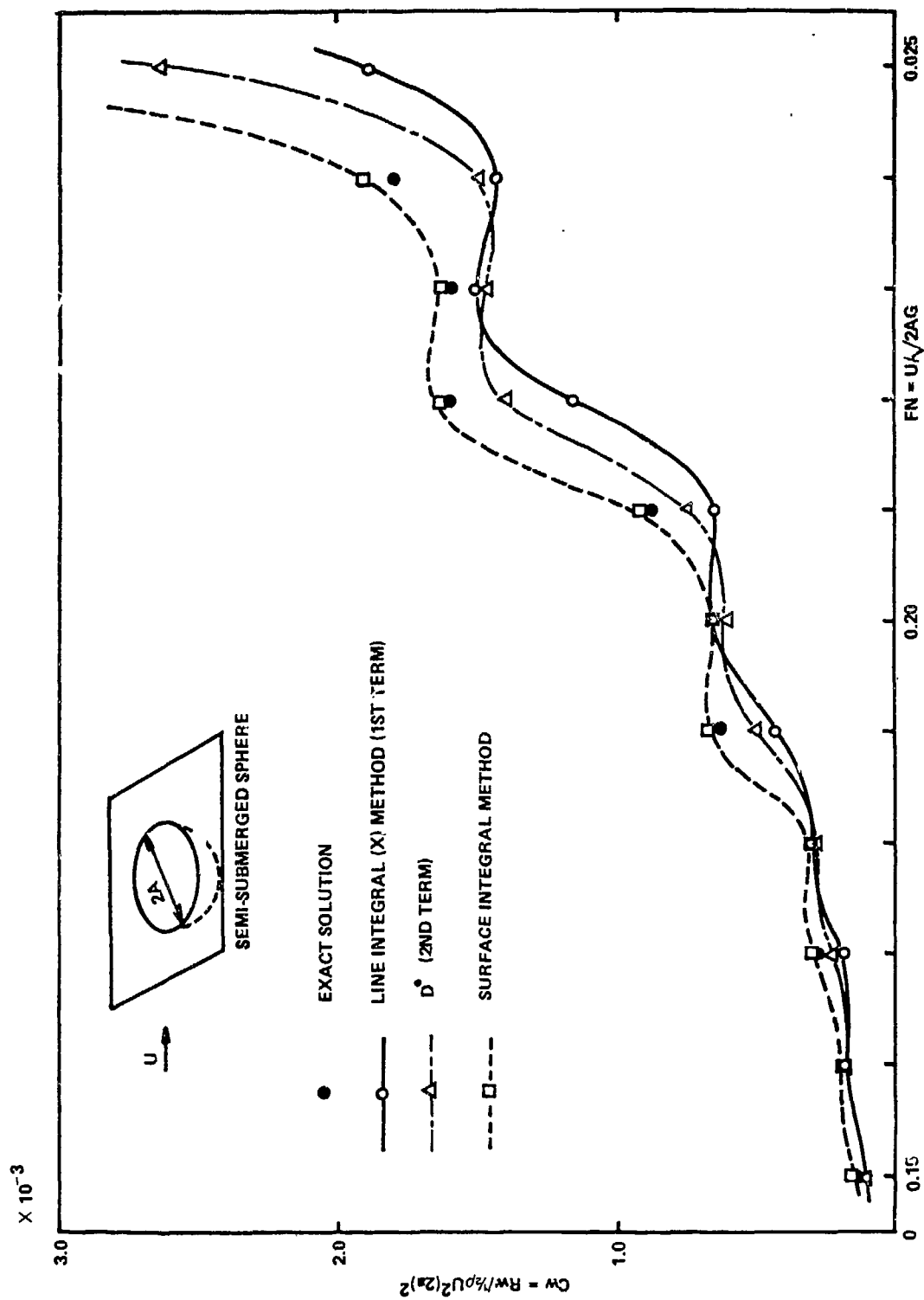


Figure 1 - Comparison of C_w Curves of a Semi-Submerged Sphere

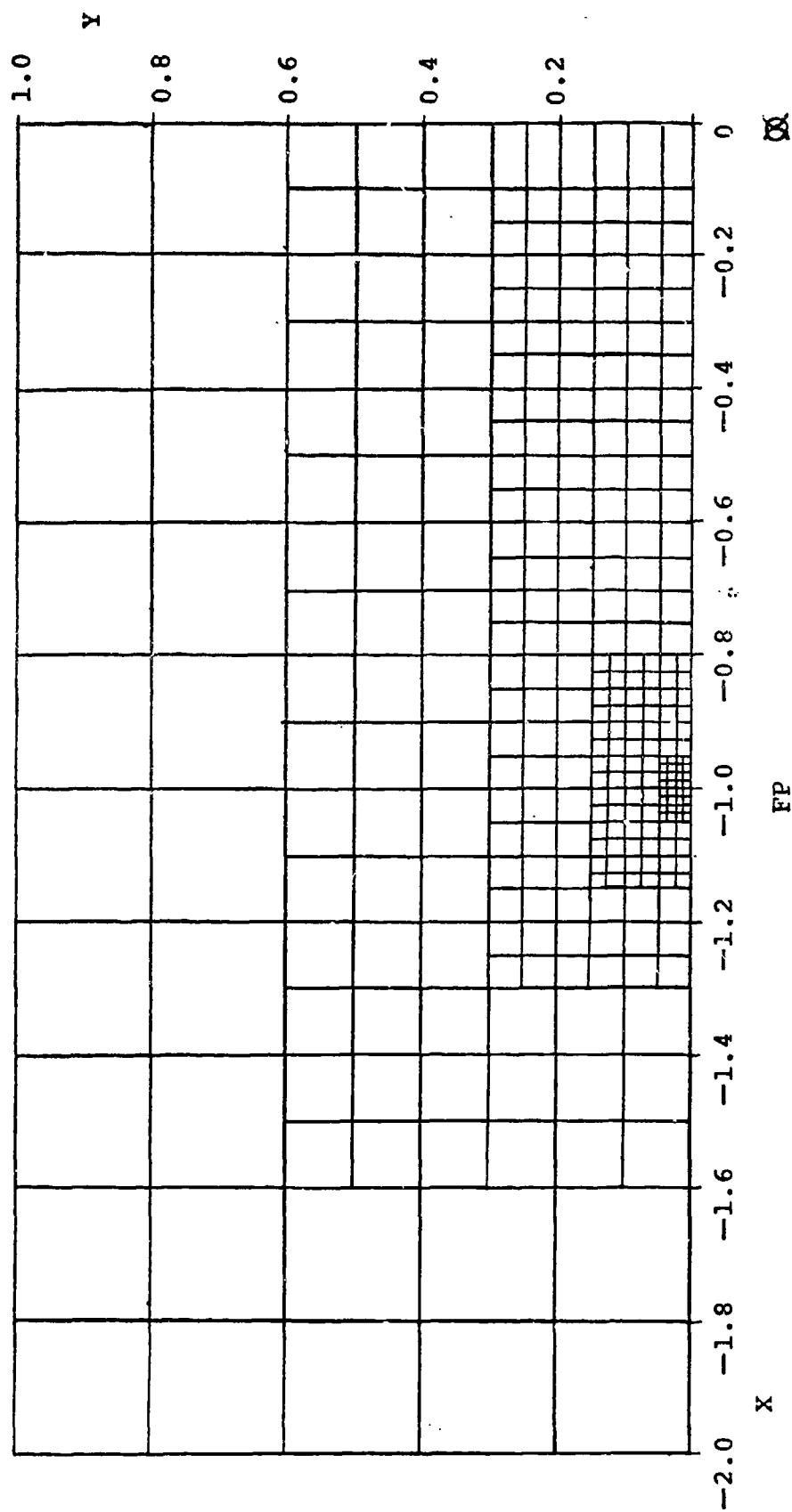


Fig. 2 PANEL DIVISION OF FREE SURFACE

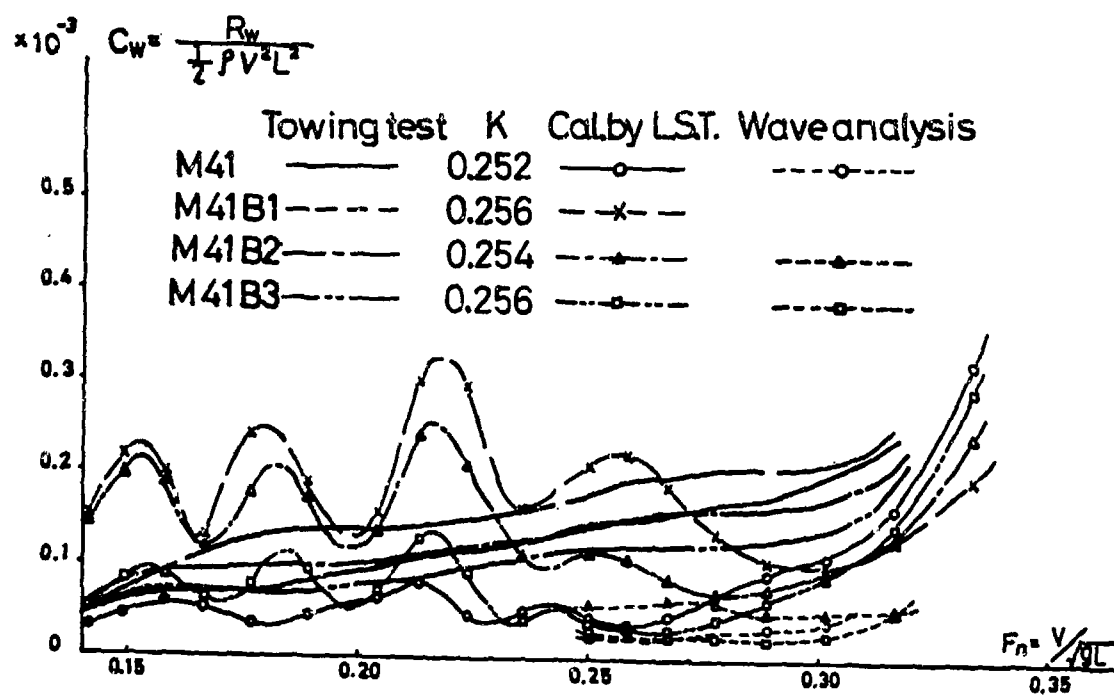


Fig. 3 C_w CURVES OF SERIES SHIPS ($L/B = 5.5$, $C_b = 0.54$)

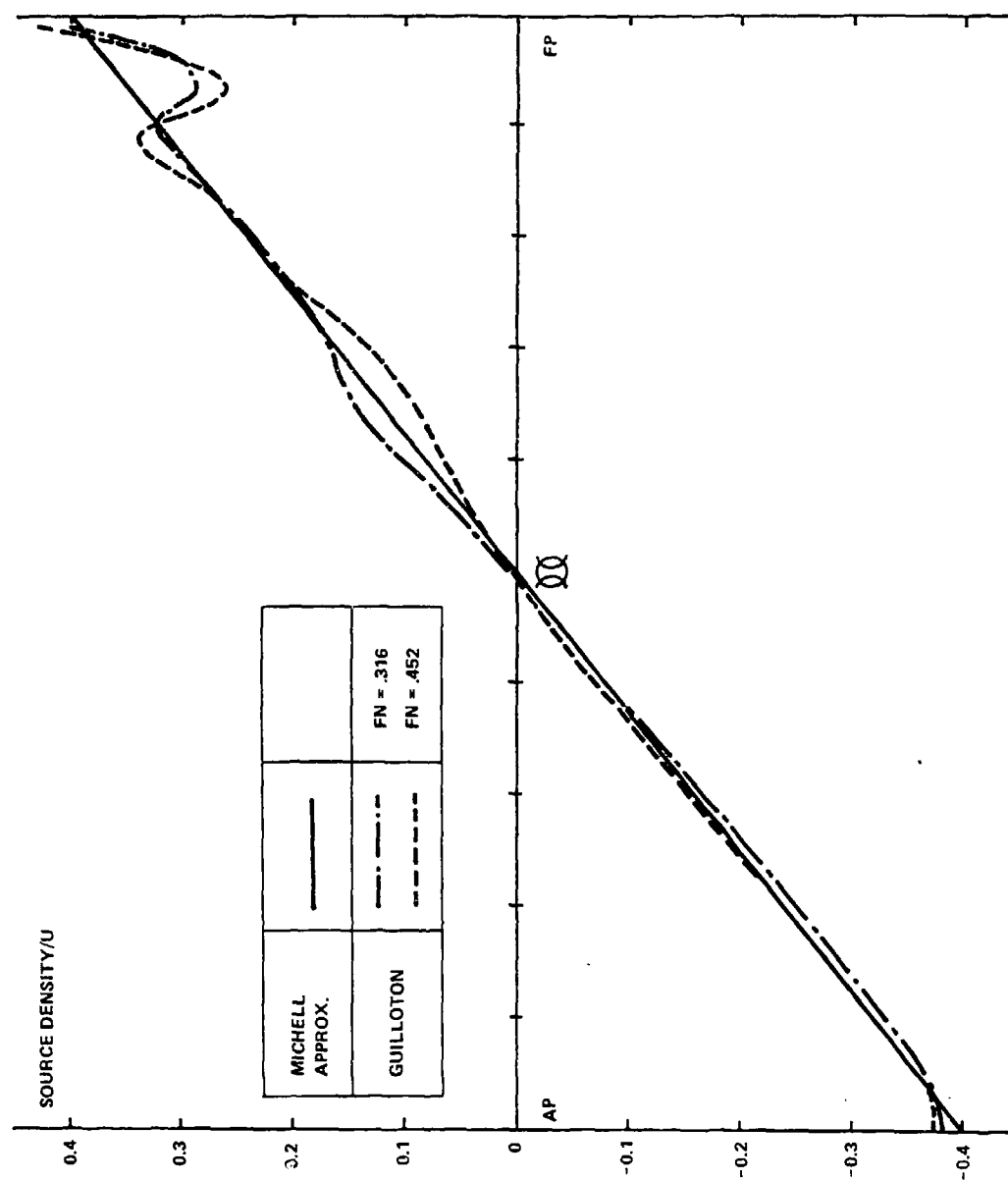


Figure 4 - Comparison of Source Distributions by Guilloton's Method

$C_w \times 10^3$

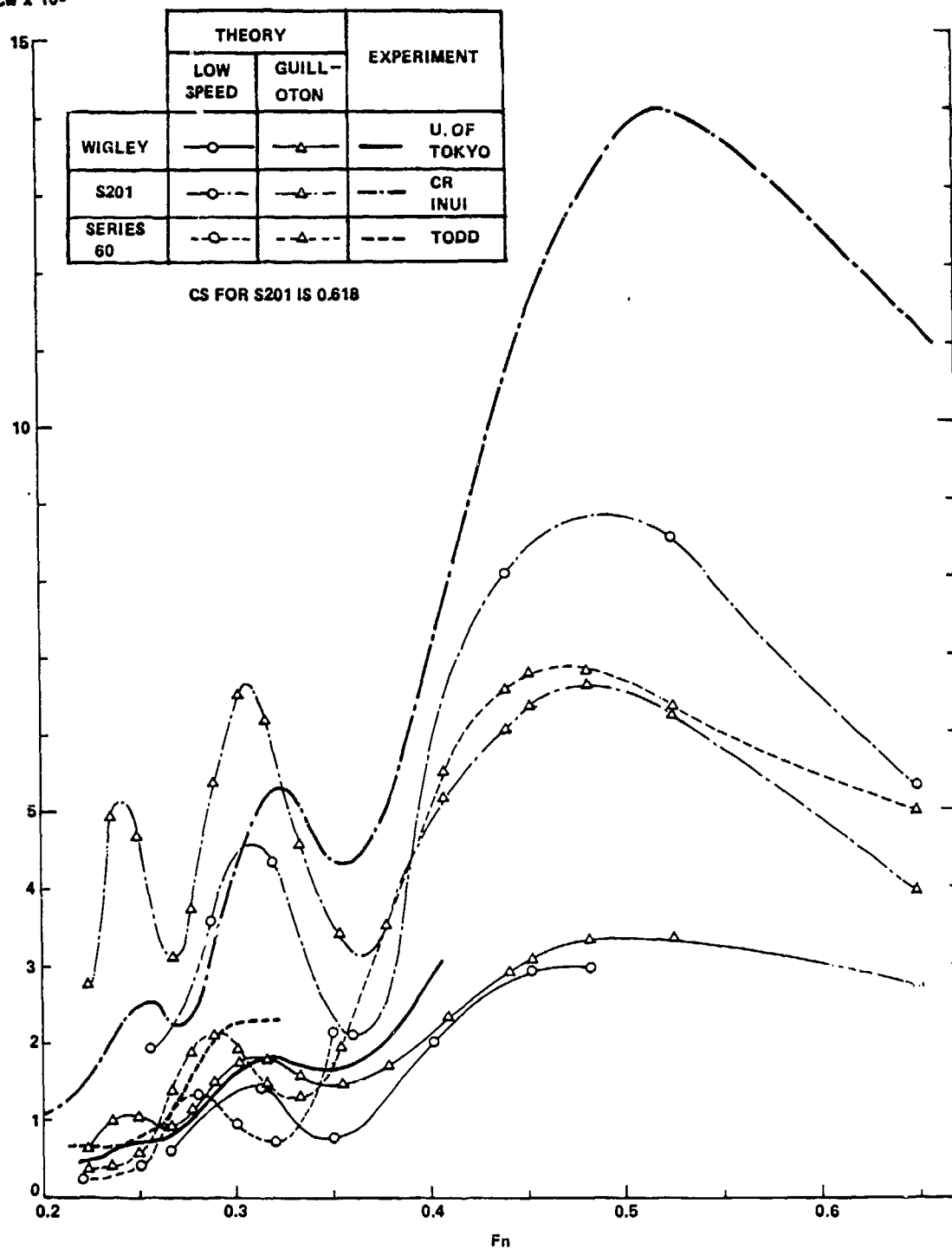


Figure 5 - C_w Curves

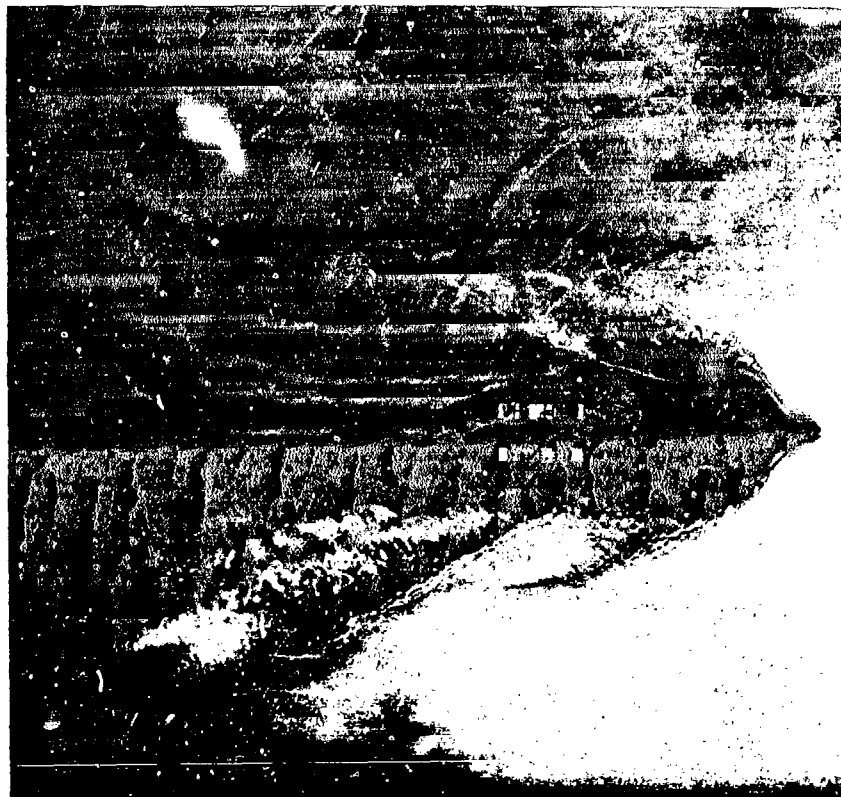


Figure 6 - Wave Pattern Picture of a Simple Model "WM2"
($L/B = 5.0$, $B/d = 8.0$, $Fn = 0.30$)

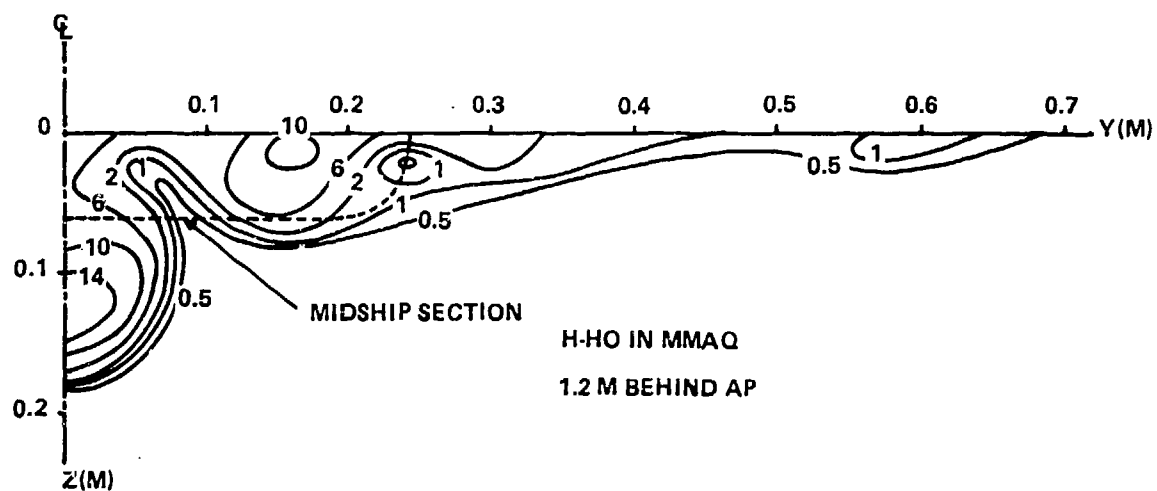


Figure 7 - Contour Lines of Momentum Loss Measured Far
Behind "WM2"

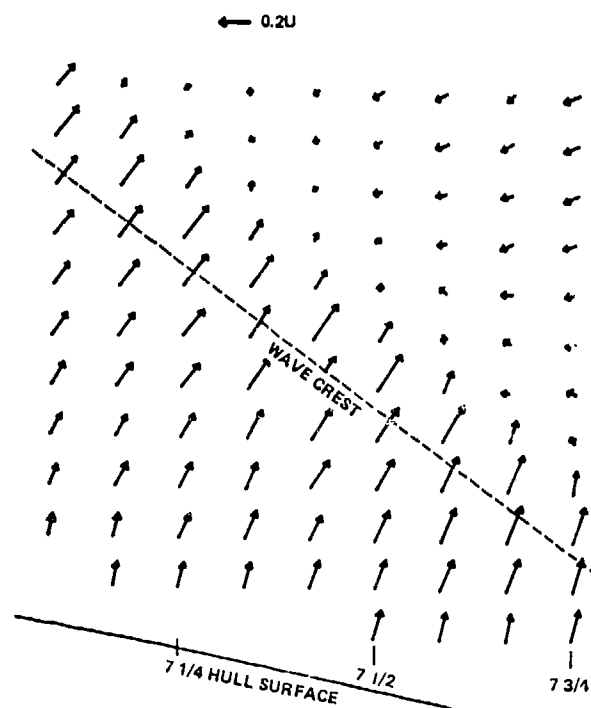


Figure 8 - Distribution of Horizontal Vectors of Disturbance Velocity (WM2)

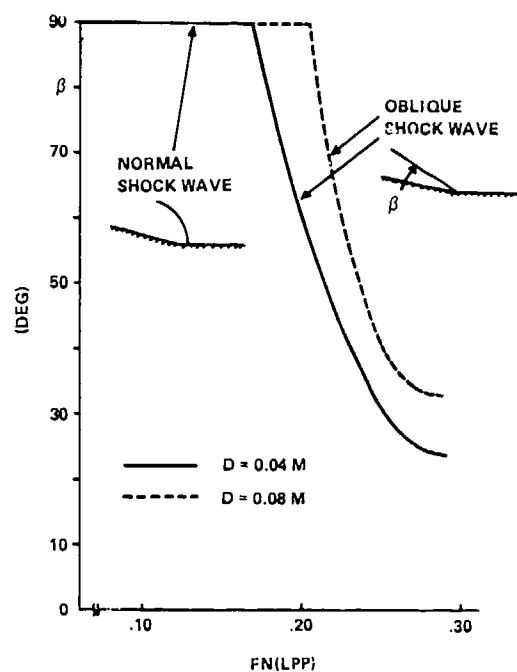


Figure 9 - Variation of the Shock Angle of the 2nd Free Surface Shock Wave on WM-B

FORMAT FOR TABULATED VALUES OF WAVE RESISTANCE

H. Miyata & H. Kajitani / Low Speed Theory

WIGLEY		INUI S201		SERIES 60	
Fn	Cw	Fn	Cw	Fn	Cw
0.266	0.605	0.255	1.939	0.220	0.223
0.313	1.425	0.287	3.595	0.250	0.411
0.350	0.780	0.319	4.346	0.280	1.327
0.402	2.010	0.360	2.102	0.300	0.957
0.452	2.932	0.440	8.093	0.320	0.740
0.482	2.979	0.525	8.529	0.350	2.137
		0.650	5.305		
			Cs=0.618		

FORMAT FOR TABULATED VALUES OF WAVE RESISTANCE

H. Miyata & H. Kajitani / Guilloton's Method

WIGLEY			INUI S201		SERIES 60	
Fn	Cw	Fn	Cw	Fn	Cw	
0.2236	0.652	0.2236	2.782	0.2236	0.393	
0.2357	1.002	0.2357	4.940	0.2357	0.405	
0.2500	1.042	0.2500	4.691	0.2500	0.569	
0.2673	0.928	0.2673	3.127	0.2673	1.368	
0.2774	1.157	0.2774	3.747	0.2774	1.890	
0.2887	1.495	0.2887	5.392	0.2887	2.119	
0.3015	1.748	0.3015	6.534	0.3015	1.932	
0.3162	1.782	0.3162	6.189	0.3162	1.503	
0.3333	1.567	0.3333	4.605	0.3333	1.327	
0.3536	1.459	0.3536	3.427	0.3536	1.961	
0.3780	1.708	0.3780	3.549	0.3780	3.552	
0.4082	2.347	0.4082	5.214	0.4082	5.554	
0.4400	2.932	0.4400	6.072	0.4400	6.617	
0.4520	3.093	0.4520	6.372	0.4520	6.810	
0.4820	3.335	0.4820	6.676	0.4820	6.828	
0.5250	3.362	0.5250	6.290	0.5250	6.352	
0.6500	2.770	0.6500	3.960	0.6500	4.979	
			Cs=0.618			

Discussion

by G. E. Gadd
of paper by H. Miyata and H. Kajitani

The photographs of "shock waves" were probably obtained for small models. I suggest that with larger models they might appear more like conventional breaking waves, and certainly, the total head losses shown in Figure 7 resemble those found behind breaking bow waves. Clearly, any fully adequate theory of wave resistance for such hull forms ought to include these effects. However, it is possible that a theory, which assumes potential flow, may still roughly predict residual resistance correctly by predicting the radiated undular waves to be larger than they really are.

Author's Reply

by H. Miyata

to discussions by G. E. Gadd

I would like to thank Dr. G. E. Gadd for his comments.

Wave breaking must follow wave making, and we have clarified that wave making itself is singular in the near-field and it satisfies shock relation. Wave breaking can be considered as one of the results of the occurrence of the free surface shock waves. Characteristics of the waves in the near-field described in our references 5), 6) and 7) show that our understanding is more general than that of wave breaking.

Breaking phenomena have considerable scale-effect and breaking cannot be observed for small models, as you point out. This fact also implies that breaking is not the essence of the nonlinear wave making properties of ships. The characteristics of the nonlinear waves, we call "free surface shock wave," are entirely different from those of linear dispersive waves; therefore, it will be impossible to predict wave resistance correctly by conventional methods.

Numerical Calculation of Second-Order Wave Resistance Using Lagrangian Coordinates

Y.S. Hong, DTNSRDC

I. Introduction

The wave resistance due to steady motion of a ship was formulated in Lagrangian coordinates by Wehausen (1). By introduction of an iteration scheme first order and second order solutions were obtained. At each iteration the domain of integration and a new hull function are obtained through a transformation of coordinates. The first-order solution becomes the classical thin ship result of Michell. For the second-order solution, a new hull function is obtained through tracing of streamlines. The second-order solution consists of two integrals: the first is a line integral along the stem and stern; the second is a double integral which is of the same form as Michell's integral, but with different integral domain and hull function.

II. Equations for the solutions

There are two coordinate systems. One is $O'x'y'z'$ which is attached to the ship; the other is $Oxyz$. These two systems coincide when the ship is at rest in its equilibrium position. Oy is positive vertically upwards, Ox is positive toward the stern and Oz is positive to starboard. We assume the ship moves at constant speed U in the negative x -direction. This is equivalent to keeping the ship fixed, but free to trim and sink, and letting the fluid flow in the positive x -direction with speed U . We now think of a streamline as a wire extending from $x = -\infty$ to $x = \infty$ and identify it by its y - and z -coordinates, β and γ , respectively, at $x = -\infty$. Then the trajectory of a particle can be expressed by

$$x = x(t, \beta, \gamma), \quad y = y(t, \beta, \gamma), \quad z = z(t, \beta, \gamma) \quad (1)$$

We use t , β and γ as the Lagrangian coordinates. Since at $x = -\infty$ there is a uniform flow with velocity $(U, 0, 0)$, equation (1) satisfies

$$\lim_{t \rightarrow -\infty} x_t(t, \beta, \gamma) = U, \quad \lim_{t \rightarrow -\infty} y_t(t, \beta, \gamma) = \lim_{t \rightarrow -\infty} z_t(t, \beta, \gamma) = 0 \quad (2)$$

For convenience we express (x, y, z) as follows:

$$x = \alpha + X(\alpha, \beta, \gamma), \quad y = \beta + Y(\alpha, \beta, \gamma), \quad z = \gamma + Z(\alpha, \beta, \gamma) \quad (3)$$

Where $\alpha = Ut$. The functions X , Y and Z in equation (3) must satisfy

$$\lim_{t \rightarrow -\infty} X(\alpha, \beta, \gamma) = \lim_{t \rightarrow -\infty} Y(\alpha, \beta, \gamma) = \lim_{t \rightarrow -\infty} Z(\alpha, \beta, \gamma) = 0 \quad (4)$$

from equation (2). By introducing the Lagrangian coordinates into the continuity equation, momentum equation and the boundary conditions at the free surface and the ship's surface, the solutions derived by Wehausen in reference (1) are as follows.

The first-order perturbation displacements:

$$X^{(1)}(\alpha, \beta, \gamma) = \frac{1}{2\pi} \iint_{S_0} G_\alpha(\alpha, \beta, \gamma; \alpha', \beta', 0) f(\alpha', \beta') d\alpha' d\beta' \quad (5)$$

$$Y^{(1)}(\alpha, \beta, \gamma) = \frac{1}{2\pi} \iint_{S_0} G_\beta(\alpha, \beta, \gamma; \alpha', \beta', 0) f(\alpha', \beta') d\alpha' d\beta' \quad (6)$$

$$Z^{(1)}(\alpha, \beta, \gamma) = \frac{1}{2\pi} \iint_{S_0} G_\gamma(\alpha, \beta, \gamma; \alpha', \beta', 0) f(\alpha', \beta') d\alpha' d\beta' \quad (7)$$

$$\begin{aligned} G(\alpha, \beta, \gamma; \alpha', \beta', \gamma') = & - [(\alpha - \alpha')^2 + (\beta - \beta')^2 + (\gamma - \gamma')^2]^{-\frac{1}{2}} \\ & + [(\alpha - \alpha')^2 + (\beta + \beta')^2 + (\gamma - \gamma')^2]^{-\frac{1}{2}} \\ & + \frac{4k_0}{\pi} \int_0^{\frac{\pi}{2}} d\theta \sec^2 \theta \int_0^\infty dk \exp[k(\beta + \beta')] \frac{\cos[k(\alpha - \alpha') \cos \theta] \cos[k(\gamma - \gamma') \sin \theta]}{k - k_0 \sec^2 \theta} \\ & + 4k_0 \int_0^{\frac{\pi}{2}} d\theta \sec^2 \theta \exp[k_0(\beta + \beta') \sec^2 \theta] \sin[k_0(\alpha - \alpha') \sec \theta] \cos[k_0(\gamma - \gamma') \sin \theta \sec \theta] \end{aligned} \quad (8)$$

where $k_0 = g/U^2$.

The first-order wave resistance:

$$T^{(1)} = 2\rho U^2 \iint_{S_0} f(\alpha, \beta) X_{\alpha\alpha}^{(1)}(\alpha, \beta, 0) d\alpha d\beta \quad (9)$$

The second-order perturbation displacements:

$$X_\alpha^{(2)}(\alpha, \beta, y) = \frac{1}{2\pi} \iint_{S_1} G(\alpha, \beta, y; \alpha', \beta', 0) f_{\alpha\alpha'}^{(1)}(\alpha', \beta') d\alpha' d\beta' \quad (10)$$

$$Y_\alpha^{(2)}(\alpha, \beta, y) = \frac{1}{2\pi} \iint_{S_1} G(\alpha, \beta, y; \alpha', \beta', 0) f_{\alpha\beta'}^{(1)}(\alpha', \beta') d\alpha' d\beta' \quad (11)$$

$$Z_\alpha^{(2)}(\alpha, \beta, y) = \frac{1}{2\pi} \iint_{S_1} G_y(\alpha, \beta, y; \alpha', \beta', 0) f_{\alpha'}^{(1)}(\alpha', \beta') d\alpha' d\beta' \quad (12)$$

The second-order wave resistance:

$$T^{(2)} = 2\rho U^2 \iint_{S_1} f^{(2)}(\alpha, \beta) X_{\alpha\alpha}^{(2)}(\alpha, \beta, 0) d\alpha d\beta \quad (13)$$

where $f^{(2)}(\alpha, \beta)$ is the second-order hull function and S_1 is the centerplane of $f^{(1)}(\alpha, \beta)$.

The transformation function for the hull is given by:

$$\begin{aligned} f^{(2)}(\alpha, \beta) &= f([\alpha + X^{(1)}(\alpha, \beta, 0)] \cos \varphi^{(1)} + [\beta - h^{(1)} + Y^{(1)}] \sin \varphi^{(1)}, \\ &\quad - [\alpha + X^{(1)}] \sin \varphi^{(1)} + [\beta - h^{(1)} + Y^{(1)}] \cos \varphi^{(1)}) \\ &= f(x_1', y_1') \end{aligned} \quad (14)$$

where

$$\begin{aligned} x_1' &= (\alpha + X^{(1)}) \cos \varphi^{(1)} + (\beta - h^{(1)} + Y^{(1)}) \sin \varphi^{(1)} \\ y_1' &= -(\alpha + X^{(1)}) \sin \varphi^{(1)} + (\beta - h^{(1)} + Y^{(1)}) \cos \varphi^{(1)} \end{aligned}$$

The sinkage (h) and trim (φ) are given by:

$$x_A' \varphi^{(1)} + h^{(1)} = \frac{2}{A} \int dx' f(x', 0) Y^{(1)}(x', 0, 0) \quad (15)$$

$$\frac{V}{A} H_p \varphi^{(1)} + x_A' h^{(1)} = \frac{2}{A} \int dx' f(x', 0) Y^{(1)}(x', 0, 0) \cdot x' \quad (16)$$

where A is the waterplane area, $(x_A', 0)$ its center of area, V the displaced volume, and H_p the longitudinal metacentric height. The details of derivation of equations (5) - (16) are given in reference (1).

By substitution of equations (5) and (8) into equation (9), the first-order wave resistance can be expressed as Michell's integral

$$T^{(1)} = -\frac{4}{\pi} \rho g k_0^2 \iint_{S_0} d\alpha d\beta \iint_{S_0} d\alpha' d\beta' f(\alpha, \beta) f(\alpha', \beta') \times \int_0^{\frac{\pi}{2}} d\theta \sec^5 \theta \exp[k_0(\beta + \beta') \sec \theta] \cos[k_0(\alpha - \alpha') \sec \theta] \quad (17)$$

If we assume $[f_\alpha(\alpha, \beta)]^2$ is small enough, then Guilloton's transformation in the x-direction is the same as the Lagrangian transformation. The transformation in the y-direction is along isobar lines in Guilloton's method. Guilloton's method does not take into account sinkage and trim. The details of this method are given in reference (2).

III. Numerical computations

The purpose of the first-order calculation is to provide the data that are needed for the transformation of the hull functions. In the first part of the computer program $X^{(1)}$, $Y^{(1)}$, $h^{(1)}$, $\phi^{(1)}$ and $T^{(1)}$ are calculated. With these values the transformation function, $f(\alpha, \beta)$, is calculated numerically. The second part of the computer program then computes $X_\alpha^{(2)}$ and $T^{(2)}$. When we are interested only in the wave resistance, the other second-order streamline displacements $Y_\alpha^{(2)}$ and $Z_\alpha^{(2)}$ are not computed. The complete details of the numerical procedures are given in reference (2).

The computed values of the first-order, second-order and Guilloton wave resistance are tabulated for the Inuid S201, Wigley, Series 60, $C_B = 0.6$, HSVA Tanker and Athena hulls in the following pages (Tables 1 and 2). The computed values of the second-order wave resistance for Wigley, Inuid and Series 60 hulls give poor agreement compared with the first-order results. The computed values are generally very low. At high Froude numbers the second-order results become negative for the Inuid hull. Between $F_n = 0.252$ and 0.282 the second-order results become negative for Series 60. The main reason for low or negative

value of the second-order wave resistance is the line integral (see equation (22) in reference (2)). The other reason might be that the centerplane of the second-order hull becomes too distorted through the hull transformation. The results of Guilloton's method show good agreement with the first-order results for Wigley and Inuid hulls, but the results for Series 60 have large discrepancies. While the hull function for Guilloton's method is obtained through the transformation along isobar lines which usually have smaller amplitude than the streamlines do, the results of Guilloton's method give better agreement than the second-order results. For low Froude numbers there is no appreciable difference between the streamlines and the isobar lines. Therefore, the results computed by these two methods are almost same.

For the HSVA Tanker and Athena hulls, only the first-order wave resistance has been computed. Because of the transom stern, the numerical computation of the transformed hull for Athena is not accurate. The computed values of the first-order wave resistance for the HSVA Tanker are surprisingly high due to the large value of block coefficient. Because this hull has a fairly long parallel middle body, the sink-source singularities are mainly distributed at bow and stern regions. Furthermore, the beam is far larger than the draft (beam-to-draft ratio is 2.7). The first-order theory can not be expected to compute wave resistance correctly for such a thick ship. In order to check the reason for the unreasonably high values of the first-order wave resistance for this model, numerical computations have been done for Model 4125 of reference (3). Weinblum et al compared Michell's wave resistance with the residual resistance for this model. This model is a thin plate with parallel middle body comprising half of the ship's length. The side walls are vertical. The results computed by the first-order, second-order, second-order without line integral term and Guilloton's theories of wave resistance are tabulated and compared with the residual resistance (Figure 1 and Table 3). The computed second-order wave resistances are quite different from the first-order, second-order without line integral term and Guilloton resistances.

This shows that the line-integral term is the main factor for low values of the second-order wave resistance. Furthermore, large values of the first-order wave resistance for the HSVA Tanker are caused by the fact that the hull is extremely flat. The parallel middle body does not have any effect on the wave resistance as long as the draft is large enough to approximate a thin ship.

Generally speaking, the computed values of the second-order wave resistance are less than the values computed by first-order theory or Guilloton's method. When a ship has a flat bottom such as Series 60, the wave resistance becomes negative even though the Froude number has a moderately low value. The main reason for the negative resistance in the second-order theory is caused by: first, the line integral and second, the centerplane of the second-order hull, $f^{(0)}(\alpha, \beta)$, becomes too distorted through the transformation.

All hulls examined here are rather more flat than thin. The beams are 1.25 - 2.5 times as large as the draft. In order to be thin, the draft must be larger than the beam. For a hull shape having a beam larger than the draft, the second-order wave resistance has given a bad prediction compared with the first-order result. To apply the present method effectively to the general hull shape, a modification in theory and numerical procedure is necessary.

IV. References

- 1 Wehausen, J.V., "Use of Lagrangian Coordinates for Ship Wave Resistance (First- and Second-Order Thin-Ship Theory)," Journal of Ship Research, Vol. 13, No. 1, March 1969, pp. 12 - 22.
- 2 Hong, Y.S., "Numerical Calculation of Second-Order Wave Resistance," Journal of Ship Research, Vol. 21, No. 2, June 1977, pp. 94 - 106.
- 3 Weinblum, G.P., Kendrick, J.J. and Todd, M.A., "Investigation of Wave Effects Produced by a Thin Body - TMB Model 4125," DTNSRDC Report 840, November 1952.

xxxx 1st order (thin ship theory)
 ++++ 2nd order
 □□□□ 2nd order without line integral
 oooo Michell's theory, Weinblum et al

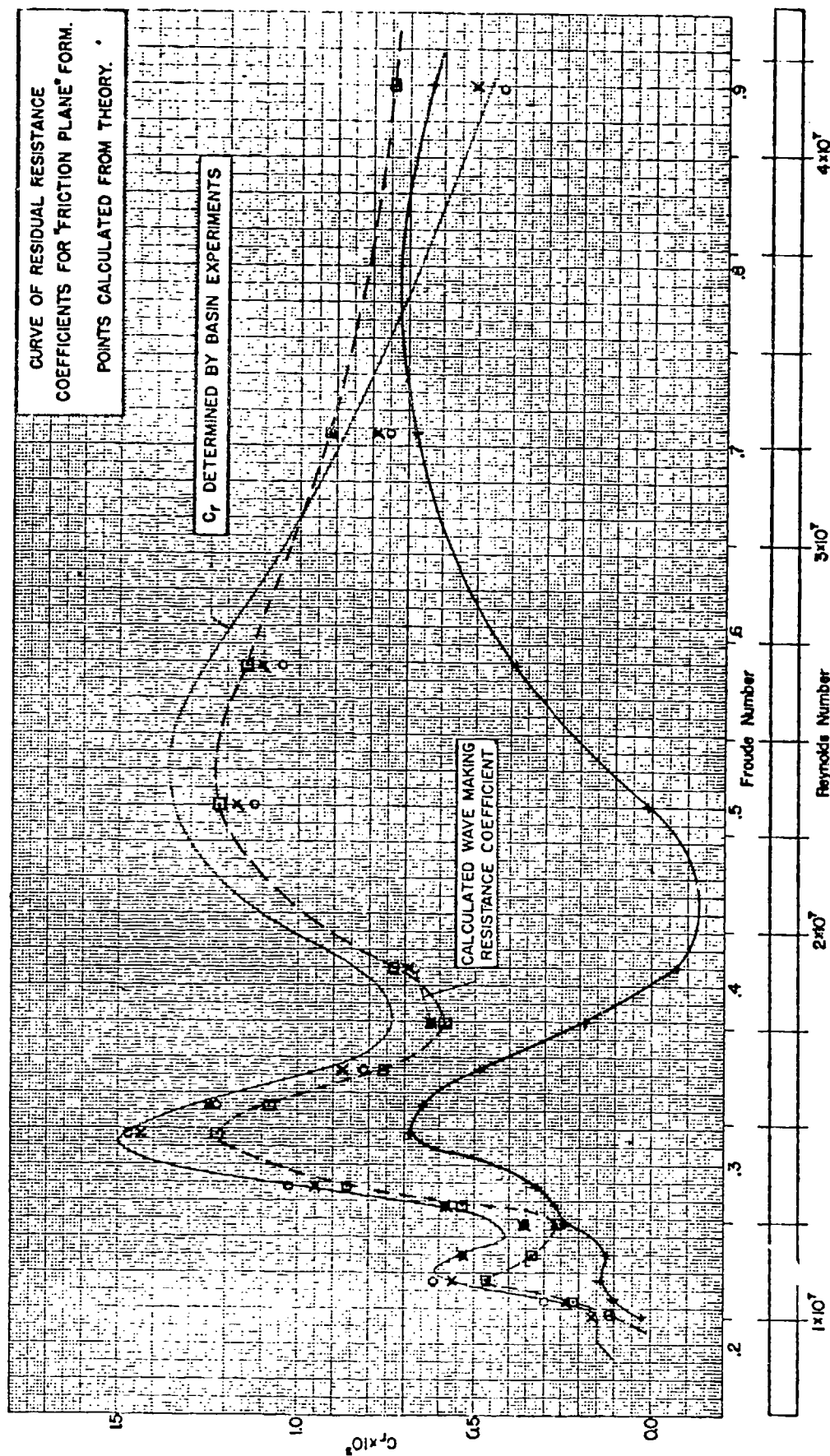


Figure1 - Comparison of Calculated and Observed Wave Resistance of Model 4125
 (Reference 3)

Table 1 Wave resistance of Wigley and Inuid hulls

Y.S.Hong/Lagrangian Coordinate Method

Wigley hull				Inuid hull			
F_n	1st order C_w	2nd order C_w	Guilloton C_w	F_n	1st order C_w	2nd order C_w	Guilloton C_w
0.266	0.901	0.465	0.862	0.255	3.402	1.542	1.652
0.313	1.858	0.857	1.910	0.287	5.521	0.820	-----
0.350	1.216	1.292	1.605	0.319	5.947	1.649	4.120
0.402	2.731	0.844	2.130	0.360	3.816	2.160	3.460
0.452	4.103	0.823	3.126	0.440	9.951	3.811	6.780
0.482	4.409	0.874	3.432	0.525	11.202	-1.244	8.861
	$\times 10^{-3}$	$\times 10^{-3}$	$\times 10^{-3}$	0.650	8.947	-254.4	-37.28
					$\times 10^{-3}$	$\times 10^{-3}$	$\times 10^{-3}$

Table 2 Wave resistance of Series 60, HSVA Tanker and Athena
Y.S.Hong/Lagrangian Coordinate Method

Series 60, $C_B = 0.60$				HSVA Tanker		Athena	
F_n	1st order C_w	2nd order C_w	Guilloton C_w	F_n	1st order C_w	F_n	1st order C_w
0.222	0.475	0.009	0.036	0.15	18.12	0.28	0.460
0.252	0.950	-0.365	-0.009	0.16	18.41	0.35	0.614
0.282	3.557	-0.044	1.469	0.17	22.18	0.41	1.70
0.302	3.107	1.126	2.025	0.18	23.72	0.48	2.09
0.323	2.234	2.507	1.512	0.19	22.15	0.65	1.48
0.353	3.472	0.475	1.505		$\times 10^{-3}$	0.80	1.65
	$\times 10^{-3}$	$\times 10^{-3}$	$\times 10^{-3}$			1.00	1.029
							$\times 10^{-3}$

Table 3 Wave resistance of TMB Model 4125
Y.S.Hong/Lagrangian Coordinate Method

F _n	TMB		Model 4125 (reference (3))		(3))	
	residual resistance C _r	1st order C _w	2nd order C _w	2nd order without l.i. C _w	Guilloton C _w	
0.215	0.15	0.169	0.025	0.106	0.104	
0.224	0.25	0.236	0.104	0.217	0.229	
0.235	0.56	0.559	0.139	0.462	0.478	
0.250	0.53	0.537	0.119	0.330	0.369	
0.267	0.43	0.347	0.242	0.262	0.307	
0.278	0.64	0.585	0.264	0.533	0.588	
0.288	0.99	0.946	0.322	0.854	0.894	
0.317	1.48	1.444	0.688	1.220	1.201	
0.332	1.30	1.252	0.648	1.076	1.040	
0.353	0.93	0.868	0.492	0.749	0.730	
0.380	0.74	0.616	0.183	0.579	0.566	
0.410	0.84	0.695	-0.071	0.729	0.692	
0.500	1.35	1.167	0.014	1.223	1.152	
0.578	1.26	1.105	0.385	1.147	1.118	
0.707	0.68	0.785	0.679	0.913	0.928	
0.900	0.47 x10 ⁻³	0.510 x10 ⁻³	0.635 x10 ⁻³	0.739 x10 ⁻³	0.843 x10 ⁻³	

Table 4 Wave elevation of Wigley hull
Y.S.Hong/Lagrangian Coordinate Method

Wigley hull		Wigley hull		Wigley hull		Wigley hull	
2x/L	$F_n=0.266$ $\eta(x)$	$F_n=0.313$ $\eta(x)$	$F_n=0.350$ $\eta(x)$	$F_n=0.402$ $\eta(x)$	$F_n=0.452$ $\eta(x)$	$F_n=0.482$ $\eta(x)$	2x/L
-1.0	0.096	0.070	0.056	0.042	0.033	0.028	-1.0
-0.9	0.301	0.252	0.221	0.187	0.157	0.142	-0.9
-0.8	0.156	0.185	0.181	0.163	0.144	0.137	-0.8
-0.7	-0.029	0.066	0.098	0.111	0.107	0.104	-0.7
-0.6	-0.163	-0.044	0.011	0.050	0.062	0.066	-0.6
-0.5	-0.218	-0.128	-0.062	-0.007	0.018	0.027	-0.5
-0.4	-0.195	-0.178	-0.119	-0.056	-0.021	-0.008	-0.4
-0.3	-0.122	-0.195	-0.157	-0.096	-0.055	-0.039	-0.3
-0.2	-0.038	-0.181	-0.179	-0.127	-0.084	-0.066	-0.2
-0.1	0.017	-0.145	-0.181	-0.148	-0.108	-0.089	-0.1
0.0	0.028	-0.096	-0.167	-0.163	-0.127	-0.109	0.0
0.1	-0.010	-0.047	-0.141	-0.167	-0.141	-0.124	0.1
0.2	-0.074	-0.012	-0.107	-0.163	-0.151	-0.136	0.2
0.3	-0.132	0.010	-0.072	-0.152	-0.156	-0.143	0.3
0.4	-0.159	0.007	-0.039	-0.134	-0.155	-0.148	0.4
0.5	-0.140	-0.013	-0.015	-0.112	-0.149	-0.149	0.5
0.6	-0.088	-0.045	0.003	-0.087	-0.139	-0.146	0.6
0.7	-0.027	-0.078	0.008	-0.062	-0.126	-0.139	0.7
0.8	0.021	-0.102	0.003	-0.037	-0.109	-0.130	0.8
0.9	0.043	-0.108	-0.006	-0.012	-0.089	-0.116	0.9
1.0	0.096	-0.048	0.016	0.032	-0.046	-0.081	1.0

Tabl 5 Wave elevation of Series 60

Y.S.Hing/Lagrangian Coordinate Method

Series 60		Series 60		Series 60		Series 60	
$2x/L$	$F_n=0.222$ $\eta(x)$	$F_n=0.252$ $\eta(x)$	$F_n=0.282$ $\eta(x)$	$F_n=0.302$ $\eta(x)$	$F_n=0.323$ $\eta(x)$	$F_n=C.353$ $\eta(x)$	$2x/L$
-1.0	0.109	0.089	0.073	0.064	0.057	0.048	-1.0
-0.9	0.315	0.288	0.254	0.235	0.214	0.191	-0.9
-0.8	0.194	0.243	0.253	0.250	0.242	0.226	-0.8
-0.7	0.003	0.104	0.165	0.186	0.199	0.205	-0.7
-0.6	-0.093	-0.027	0.057	0.097	0.129	0.156	-0.6
-0.5	-0.154	-0.165	-0.090	-0.037	0.010	0.059	-0.5
-0.4	-0.133	-0.232	-0.210	-0.166	-0.112	-0.049	-0.4
-0.3	-0.106	-0.229	-0.281	-0.262	-0.219	-0.154	-0.3
-0.2	-0.127	-0.168	-0.299	-0.319	-0.301	-0.246	-0.2
-0.1	-0.146	-0.110	-0.244	-0.304	-0.326	-0.300	-0.1
0.0	-0.156	-0.055	-0.152	-0.240	-0.301	-0.318	0.0
0.1	-0.107	-0.020	-0.034	-0.127	-0.218	-0.282	0.1
0.2	-0.062	-0.042	0.041	-0.020	-0.121	-0.221	0.2
0.3	-0.096	-0.138	0.016	0.015	-0.061	-0.178	0.3
0.4	-0.154	-0.226	-0.072	-0.007	-0.036	-0.146	0.4
0.5	-0.202	-0.263	-0.187	-0.075	-0.049	-0.132	0.5
0.6	-0.179	-0.210	-0.257	-0.139	-0.068	-0.110	0.6
0.7	-0.052	-0.055	-0.220	-0.144	-0.045	-0.045	0.7
0.8	0.072	0.092	-0.116	-0.112	-0.017	0.032	0.8
0.9	0.258	0.276	0.101	0.017	0.074	0.149	0.9
1.0	0.385	0.416	0.358	0.213	0.218	0.302	1.0

Discussion

by J. V. Wehausen
of paper by Y. Hong

Since I am the author of this evidently disastrous approximation, perhaps I may be permitted a few minutes to explain why, in my opinion, it has turned out so badly. In formulating the problem of flow about a ship in Lagrangian coordinates, a particular model of the flow was assumed that required a curve of stagnation points along the stem and the stern. Later on, in connection with another problem (v. Schiffstechnik, vol. 23 (1976), pp. 215-217), I became aware of the fact that curves of stagnation points are possible only under particular and rare circumstances associated with separability of Laplace's equation. It seems to me that the line integrals in my formulation must be a result of this faulty model. A correct treatment of the problem might be worth while, but would require a correct qualitative model of the flow about the hull as a starting point. I have not as yet been able to devise one that I find totally convincing. It is certainly a reasonable conjecture that a correct one would lead to the second-order approximation in Hong's paper without the stem and stern line integrals.

Wave Resistance of Double Model in Finite Depth and its Application to Hull Form Design

by

Hyochul Kim and J.C. Seo

Seoul National University
College of Engineering

Among various design parameters, wave resistance plays an important role on hull form design. Theoretical methods for a hull form with minimum wave resistance were developed by Inui^(1,2), Pien and others. In the above method, singularity distributions on prescribed surfaces are determined in the light of minimum wave-resistance condition. From the singularity distribution, hull forms are obtained by the streamline tracing method and their wave resistances are calculated by integrating the resistance components due to the singularities.

Theoretical hull form, however, can not be applied directly to a practical hull form. The main reason is the extruded bottom along the keel line. Therefore the hull form must be modified to have a flattened bottom. Normally, this modification is manually conducted with keeping both the shape of water plane and prismatic coefficient constant⁽³⁾.

Meanwhile if the depth of water is finite, the theoretical hull form is flattened by the effect of depth. This effect is due to image singularity distribution with respect to sea bed and free surface. Especially the geometrical change of hull form is remarkable for the depth of less than $0.2L$. This means that the wave resistance is no longer for the given hull but for the deformed one. Usually this range of water depth is out of practical application. However the geometrical characteristics can be utilized to develop a theoretical hull form with a flat bottom, which may be applied in deep water. This deformed hull form is developed by taking the sea bed merely as a fictitious plane.

For the Inui hull S201 and the deformed hull with flat bottom, the source densities on hull surfaces are determined by solving an integral equation^(4,5). Then the wave resistance in deep water are calculated. At the same time the wave resistance for the Inui hull S201 is evaluated using the original sources on center plane.

It is found out that the wave resistance in deep water does not significantly alter for the Froude number less than 0.35, even though a geometrical change at the bottom is remarkable. Comparing with the manual hull-form modification, flattening the bottom by the aid of the fictitious plane may be more rational for practical hull form design.

Velocity Potential for the Distributed Source

Assuming the fluid is incompressible, inviscid and its motion be irrotational, the induced fluid motion can be characterized by a velocity potential. In a laterally unbounded fluid with a free surface, the velocity potential of sources moving with a velocity U parallel to the negative X -axis is given by (6,7,8)

$$\phi = -\frac{1}{4\pi} \left[\left(\frac{1}{r_1} - \frac{1}{r_2} \right) \sigma dS - \frac{K_0}{\pi} \int \sigma dS \int_{-\pi}^{\pi} \sec^2 \theta d\theta \int_0^{\infty} \frac{\exp\{(z+z_0-iw)K\}}{K-K_0 \sec^2 \theta + i\mu \sec \theta} dK \right] \quad (1)$$

where

$$r_1 = (x-x_0)^2 + (y-y_0)^2 + (z-z_0)^2$$

$$r_2 = (x-x_0)^2 + (y-y_0)^2 + (z+z_0)^2$$

$$w = (x-x_0) \cos \theta + (y-y_0) \sin \theta$$

If the water depth is finite, the velocity potential is represented by (6,7)

$$\phi = -\frac{1}{4\pi} \left[\left(\frac{1}{r_1} + \frac{1}{r_2} \right) \sigma dS - \frac{1}{\pi} \int \sigma dS \int_{-\pi}^{\pi} d\theta \int_0^{\infty} \exp\{-K(iw+d)\} \times \frac{\cosh[K(d+z_0)](K+K_0 \sec^2 \theta + i\mu \sec \theta) \cosh[K(z+d)]}{\cosh(Kd) (K-K_0 \sec^2 \theta \tanh kd + i\mu \sec \theta)} dK \right] \quad (2)$$

where

$$r_1 = r_1$$

$$r_2 = (x-x_0)^2 + (y-y_0)^2 + (z+2d+z_0)^2$$

$$d = \text{Depth of water}$$

From eqs. (1) and (2), the wave resistance for deep water is expressed as (6,7,8,9)

$$R_w = \frac{\rho K_0^2}{\pi} \int_0^{\pi/2} (P^2 + Q^2) \sec^3 \theta d\theta \quad (3)$$

where

$$P+iQ = \int \sigma \exp\{K_0[i(x_0 \cos \theta + y_0 \sin \theta) \sec^2 \theta + z_0 \sec^2 \theta]\} dS$$

and for finite depth

$$R_w = \frac{\rho K_0}{\pi} \int_0^{\pi/2} \frac{(P_1^2 + Q_1^2) K \sec \theta}{\cosh^2(Kd) (1-K_0 d \sec^2 \theta \operatorname{sech}^2 Kd)} d\theta \quad (4)$$

where

$$P_1 + iQ_1 = \int \sigma \cos^2 [K(d+z)] \exp[iK(x_0 \cos \theta + y_0 \sin \theta)] dS$$

$$K = \text{Positive root of } K - K_0 \sec^2 \theta \tanh Kd = 0$$

$$\theta_0 = \begin{cases} \cos^{-1} \sqrt{gd/U^2} & \text{if } U^2 > gd \\ 0 & \text{if } U^2 \leq gd \end{cases}$$

Calculation of wave resistance

Distributing sources at center plane ($-l \leq x \leq l$, $y=0$, $-0.1l \leq z \leq 0$) with density as below, we can define Inui hull S201(2).

$$\sigma = -0.8 \frac{x}{l} \quad (5)$$

where

$$l = 0.5 L$$

The wave resistance at deep water or finite depth can be obtained by substituting eq. (5) into eq. (3) or (4). Corresponding hull form can be shaped out by the streamline tracing method under the double model approximation.

On the other hand the hull form can be represented by distributing singularities directly on the hull surface^(4,5). As well known this method requires a great computing time and storage. To perform it effectively Kan⁽¹⁰⁾ utilized the slender-body approximation and derived the following integral equation in cylindrical coordinate

$$P(x, \theta) = -2U_\infty + \frac{1}{2\pi} \int_0^\pi P(x; \theta') \bar{K}(x; \theta, \theta') d\theta' \quad (6)$$

where

$$P = \sigma \cdot F, \quad F = \sqrt{1 + R_x^2 + (R_\theta/R)^2}, \quad R_x = \frac{\partial R}{\partial x}, \quad R_\theta = \frac{\partial R}{\partial \theta}, \quad U_\infty = -U R_x/F$$

$$\bar{K}(x; \theta, \theta') = 2R' \left[\left\{ R' \cos(\theta - \theta') - R + R' \sin(\theta - \theta') \cdot \frac{R_\theta}{R} \right\} \frac{1}{R_M} + \left\{ R' \cos(\theta + \theta') - R + R' \sin(\theta + \theta') \cdot \frac{R_\theta}{R} \right\} \frac{1}{R_P} \right]$$

$$R_M = R^2 + R'^2 - 2RR' \cos(\theta - \theta'), \quad R_P = R^2 + R'^2 - 2RR' \cos(\theta + \theta')$$

From this equation the source density on hull surface is to be determined numerically, where ordinary offset data are used. This process is carried out by a small computer.

Numerical Results

For the Inui model S201 the wave resistance is calculated for various water depths as Inui did⁽²⁾. The results are shown in Fig. 1 as solid lines. In this calculation the source distribution defined in eq. (5) has been used. Also the hull forms corresponding to the water depths are shown in Fig. 2.

Among them the source densities on the hull surface for the models as shown in Fig. 2a and 2d are calculated by the Kan's method with 135 data points. Their wave resistances are represented in Fig. 1 as dotted lines.

The same process is conducted for the Wigley model with 240 offset data. The wave resistance thus obtained is plotted in Fig. 3.

Discussion

As mentioned previously, the hull forms corresponding to the water depth of greater than $0.2L$ are almost the same as the original hull form in infinite depth. As it can be immediately noticed in Fig. 2, the traced hull form in shallower cases has a remarkably flattened bottom. This geometrical characteristics may be utilized to practical hull form design. As long as wave resistance is concerned, this geometrical change does not affect when the Froude number is less than 0.35 (cf. Fig. 1).

Because of this fact the wave resistance of the modified hull form can be approximated by that of the original hull up to a moderate ship speed. Thus we can easily arrive at a hull form with a flat bottom which has minimum wave resistance.

This concept is exemplified to the Pienoid (Fig. 4a and 4b) to demonstrate its applicability to hull form design. The Pienoid in Fig. 4a was studied by Cho⁽³⁾ under the minimum wave-resistance condition. The Pienoid in Fig. 4b was modified according to this concept. For both cases the wave resistances in deep water are calculated and their results are plotted in Fig. 4c. The wave resistance of the latter is slightly increased compared to that of the former. However its magnitude is negligible in the common sense of engineering practice.

Concluding Remarks

The wave resistance in finite depth can be calculated as in the case of infinite water depth. In the case of finite depth the geometrical change in hull bottom is more meaningful for practical hull form design. This is mainly due to the effect of water depth. Taking the sea bed merely as a fictitious plane, a hull form of practical use can be developed theoretically. The wave resistance of

the hull thus obtained in deep water may be approximated by that of the extruded original hull form. A more reliable result is obtained by solving an integral equation. In this case an increase in computing time and effort is inevitable. Meanwhile improvement in numerical results is negligibly small. It is therefore recommended to use the wave resistance of the original hull for the modified hull form.

Further researches both in theory and experiment are necessary before this concept is put into practical application.

References

- (1) Inui, T. and Kajitani, H., "Hull Form Design, It's Practice and Theoretical Background", International Seminar on Theoretical Wave Resistance, Tokyo, Japan, 1976
- (2) Inui, T., "Study on Wavemaking Resistance of Ships", 60th Anniv. Series, Society of Naval Architects of Japan, Vol.2, 1957
- (3) Kyu Jong Cho and Sung Wan Hong, "A Study on Source Generated Ships of Minimum Wave Resistance", Journal of the Society of Naval Architects of Korea, Vol.7, No.2, 1970
- (4) Hess, J.L and Smith, A.M.O., "Calculation of Non-Lifting Potential Flow about Arbitrary Three Dimensional Bodies", Journal of Ship Research, Vol.8, No.2, 1964
- (5) Breslin, J.P. and King Eng. "Calculation of the Wave Resistance of a Ship Represented by Sources Distributed over the Hull Surface", International Seminar on Theoretical Wave Resistance, Ann Arbor, 1963
- (6) Kostyukov, A.A., "Theory of Waves and Wave Resistance", Effective Communications Inc., Iowa City, 1968
- (7) Lunde, J.K., "On the Linearized Theory of Wave Resistance for Displacement Ship in Steady and Accelerated Motion", Transaction of the Society of Naval Architects and Marine Engineers, Vol.59, 1951
- (8) Havelock, T.H., "The Theory of Wave Resistance", Proceedings of the Royal Society of London, Series A. Vol.138, No.835, 1932
- (9) Havelock, T.H., "The Calculation of Wave Resistance", Ibid., Vol.144, No.85, 1934
- (10) Kan, M., "Calculation of Non-Lifting Potential Flow about Ship Hulls", Selected Papers from the Journal of the Society of Naval Architects of Japan, Vol.2, 1972

- (11) Wigley, W.C.S., "Calculated and Measured Wave Resistance of Series of Forms", Transaction of the Royal Institution of Naval Architects, Vol.84, 1942
- (12) Yim B., "Some Considerations in Wave Resistance for Linearized Ships on the Deep Sea", Journal of the Society of Naval Architects of Korea, Vol.4, No.1, 1967

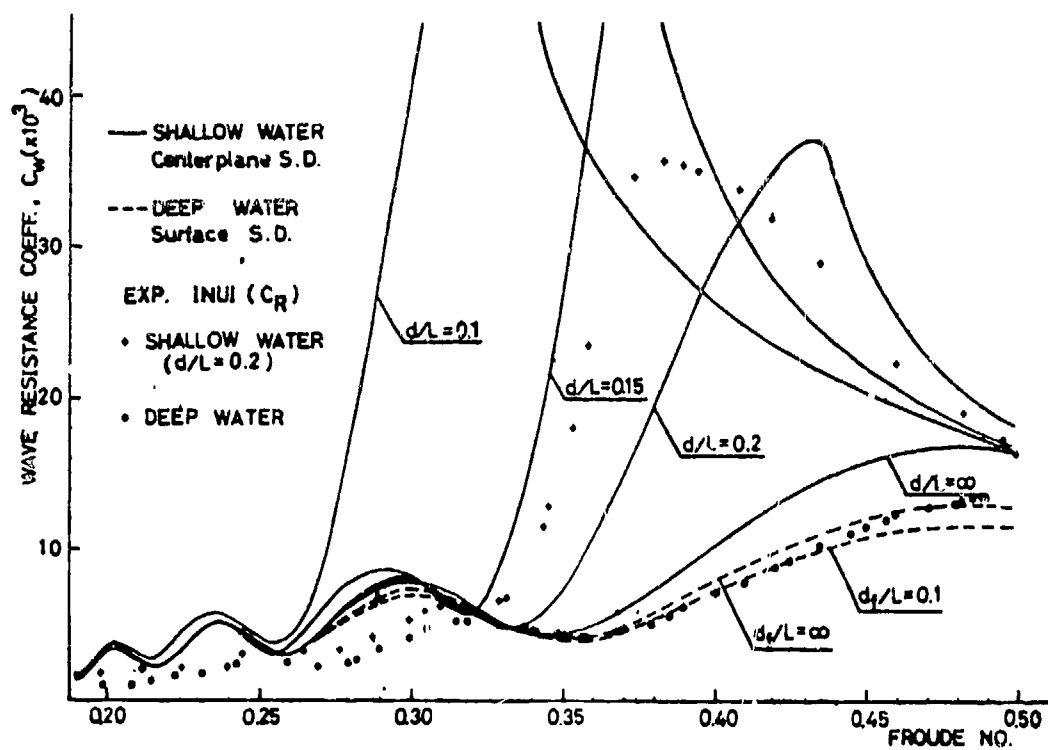


FIG. 1 WAVE RESISTANCE CURVES, INUID MODEL

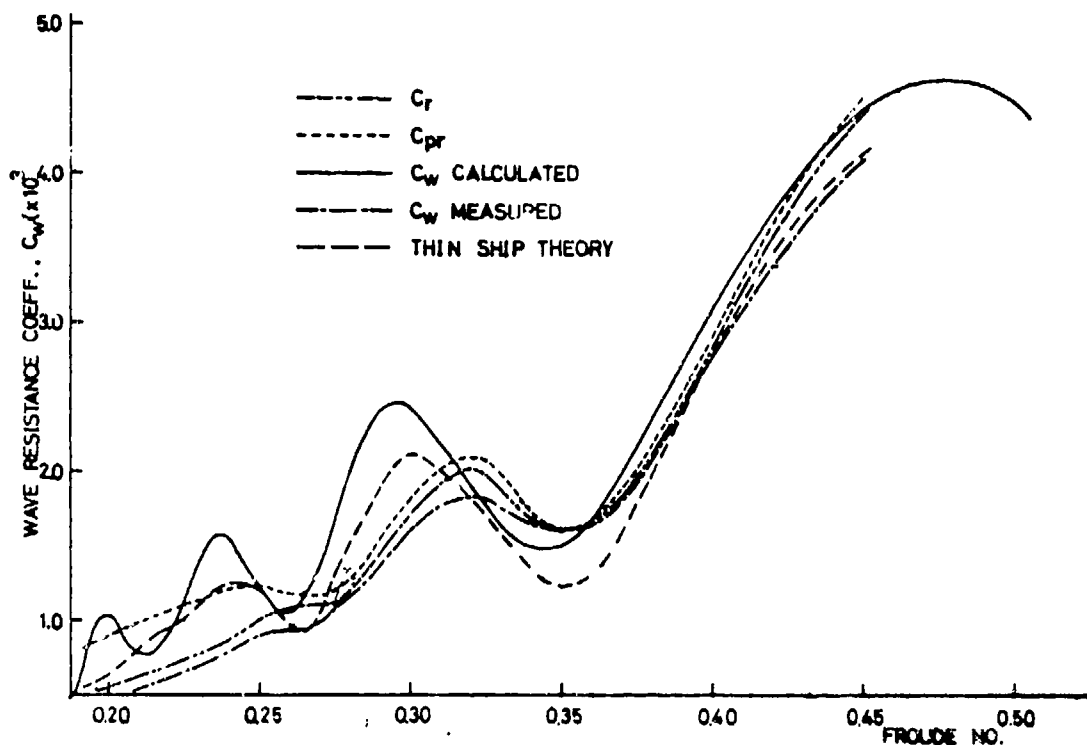


FIG. 2 WAVE RESISTANCE CURVE, WIGLEY MODEL

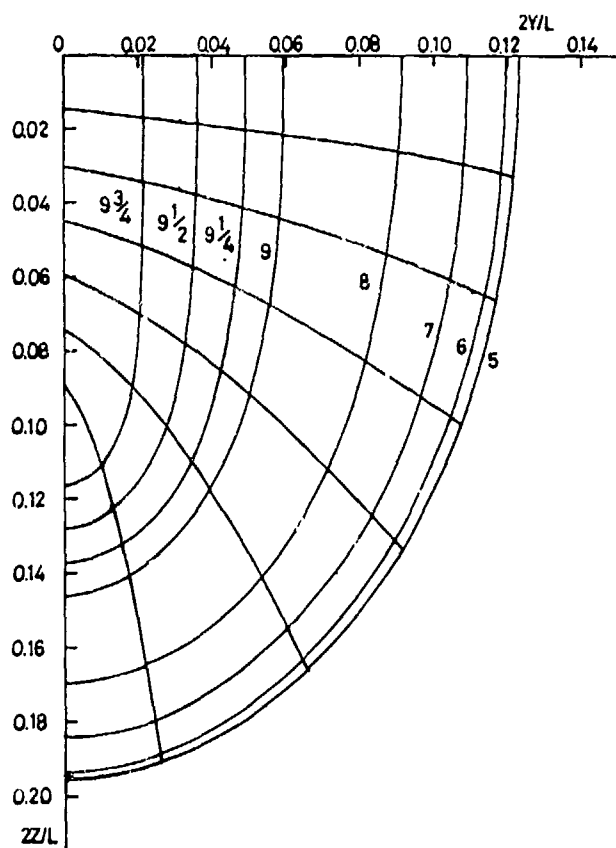


FIG. 2a BODY PLAN, INUID MODEL ($d/L=\infty$)

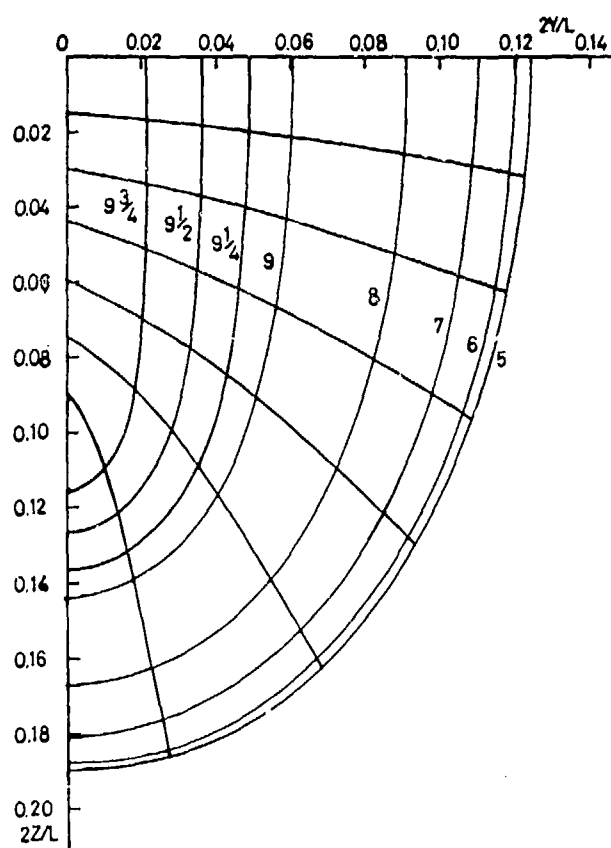


FIG. 2b BODY PLAN, INUID MODEL ($d/L=0.2$)

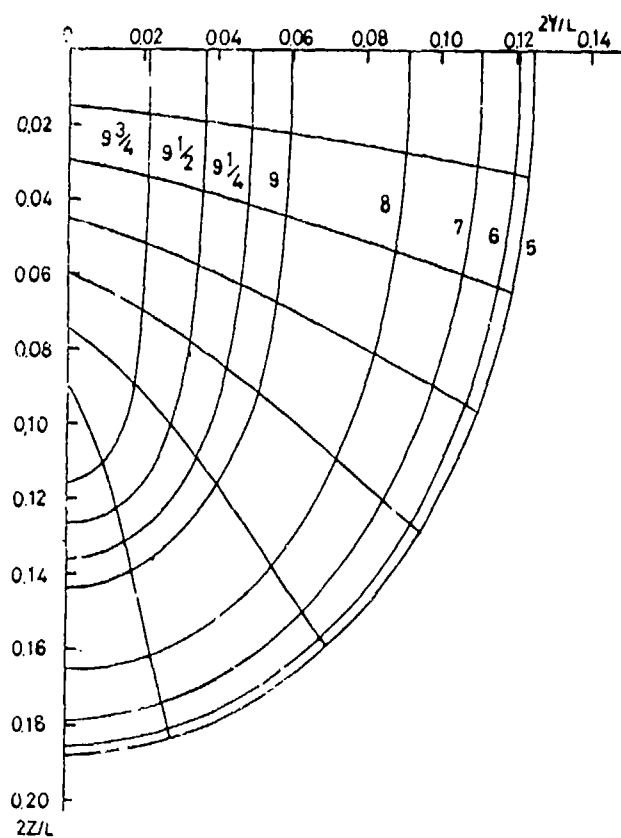


FIG. 2c BODY PLAN, INUID MODEL ($d/L=0.15$)

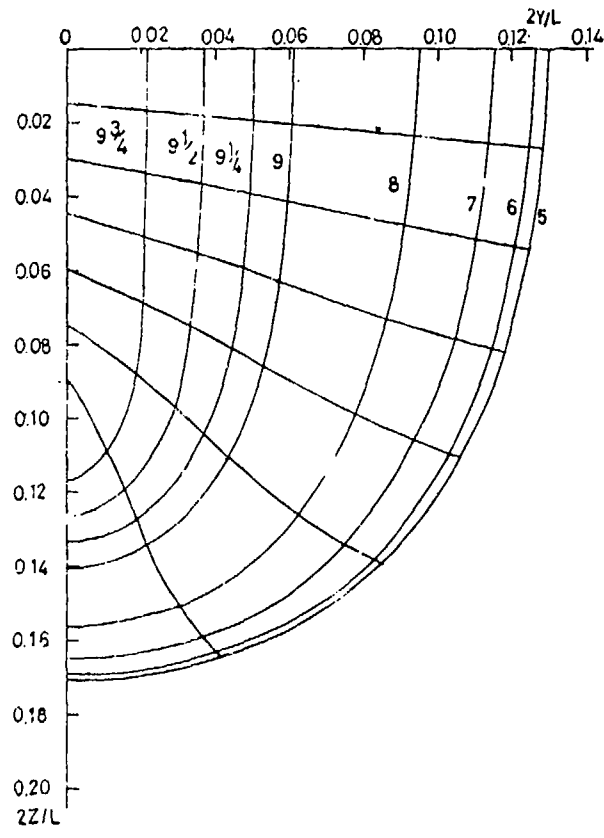


FIG. 2d BODY PLAN, INUID MODEL ($d/L=0.1$)

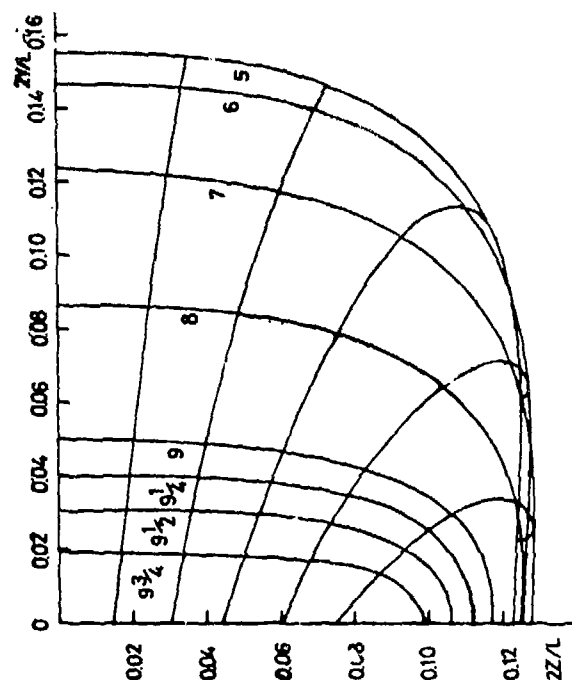


FIG. 4b BODY PLAN, PIENOID (d/L = 0.06)

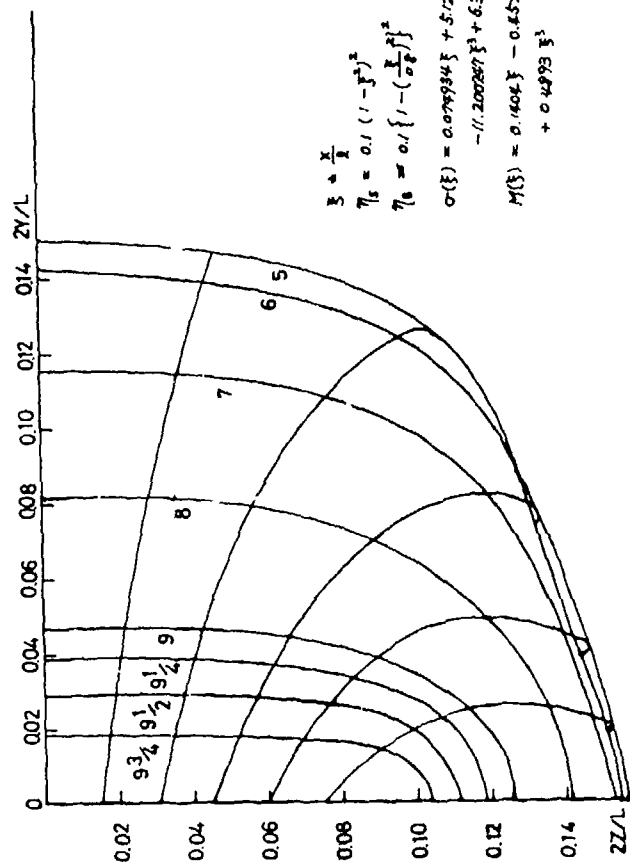


FIG. 4a BODY PLAN, PI-NOID (d/L = ∞)

$$\begin{aligned} \xi &= \frac{x}{L} \\ \eta &= 0.1 (1 - \xi^2)^2 \\ \gamma &= 0.1 \left\{ 1 - \left(\frac{\xi}{0.8} \right)^2 \right\}^2 \\ \sigma(\xi) &= 0.074934 \xi + 5.127134 \xi^2 \\ &\quad - 11.200267 \xi^3 + 6.397521 \xi^4 \\ M(\xi) &= 0.1404 \xi - 0.4528 \xi^2 \\ &\quad + 0.4293 \xi^3 \end{aligned}$$

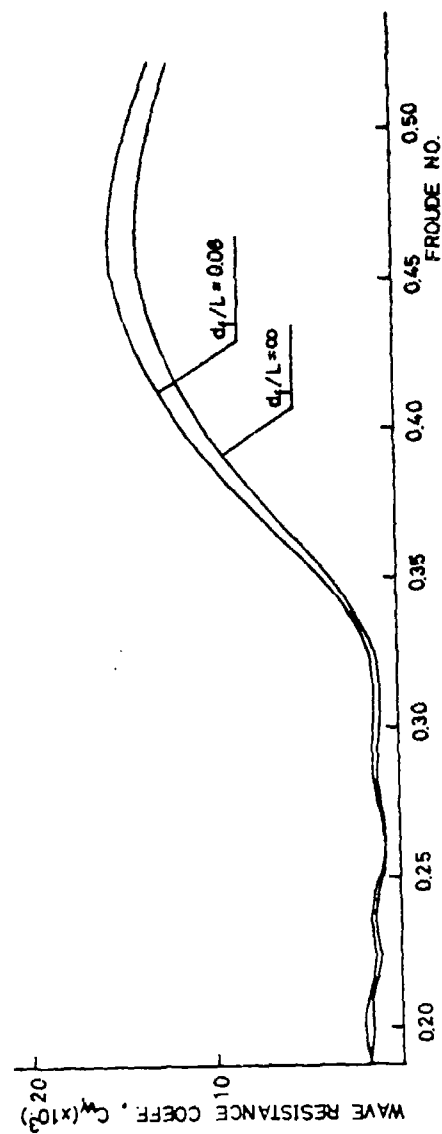


FIG. 4c WAVE RESISTANCE CURVES, PIENOID MODEL

Inuid S-201
 Hyochul Kim / Double Model Approach / Shallow water wave resistance /
 Source distribution on center plane

FORMAT FOR TABULATED VALUE OF WAVE ELEVATION

d/L = ∞		d/L = 0.2		d/L = 0.15		d/L = 0.1	
F _n	C _w	F _n	C _w	F _n	C _w	F _n	C _w
0.196	2.318	0.20	3.156	0.20	3.185	0.20	3.536
0.224	2.836	0.225	3.149	0.225	5.309	0.225	4.822
0.25	3.840	0.25	3.812	0.25	3.681	0.25	4.180
0.277	5.387	0.275	5.331	0.275	6.787	0.275	11.650
0.302	7.984	0.30	8.306	0.30	8.225	0.30	40.132
<u>0.319</u>	6.416	<u>0.319</u>	6.033	<u>0.319</u>	5.777	<u>0.319</u>	81.654
0.324	5.795	0.325	5.372	0.325	6.681	0.325	63.897
0.343	4.431	0.35	6.990	0.35	25.684	0.35	40.451
<u>0.36</u>	4.937	<u>0.36</u>	10.083	<u>0.36</u>	38.448	<u>0.36</u>	36.260
0.375	6.610	0.375	16.649	0.375	55.170	0.375	31.786
0.4	10.178	0.40	28.645	0.40	35.585	0.40	26.611
0.425	13.474	0.425	36.237	0.425	26.561	0.425	23.115
<u>0.44</u>	15.033	<u>0.44</u>	35.685	<u>0.44</u>	23.710	<u>0.44</u>	21.571

FORMAT FOR TABULATED VALUE OF WAVE ELEVATION

$d/L = \infty$		$d/L = 0.2$		$d/L = 0.15$		$d/L = 0.1$	
F_n	C_w	F_n	C_w	F_n	C_w	F_n	C_w
0.45	15.815	0.45	29.528	0.45	22.236	0.45	20.658
0.475	16.813	0.475	22.097	0.475	19.271	0.475	18.529
0.50	16.790	0.50	18.498	0.50	16.935	0.50	15.076
<u>0.525</u>	16.325	<u>0.525</u>	16.183	<u>0.525</u>	15.188	<u>0.525</u>	15.076
0.55	15.758	0.55	14.665	0.55	13.971	0.55	13.976

Inuid S-201
 Hyochul Kim / Double model approach / Deep water wave resistance /
 Source Distribution on Hull Surface

FORMAT FOR TABULATED VALUES OF WAVE RESISTANCE

$df/L = \infty$		$df/L = 0.1$		$df/L = \infty$		$df/L = 0.1$	
F_n	C_w	F_n	C_w	F_n	C_w	F_n	C_w
0.20	3.750	0.20	3.993	0.45	12.017	0.45	10.800
0.225	3.208	0.225	3.422	0.475	12.933	0.475	11.631
0.25	4.203	0.25	4.512	0.50	12.955	0.50	11.631
0.275	4.527	0.275	4.351	<u>0.525</u>	12.409	<u>0.525</u>	11.100
0.30	7.388	0.30	7.013	0.55	11.678	0.55	10.414
<u>0.319</u>	6.240	<u>0.319</u>	6.038				
0.325	5.615	0.325	5.467				
0.35	4.136	0.35	4.046				
<u>0.36</u>	4.252	<u>0.36</u>	4.090				
0.375	5.264	0.375	4.932				
0.40	7.943	0.40	7.263				
0.425	10.282	0.425	9.269				
<u>0.44</u>	11.404	<u>0.44</u>	10.250				

* df stands for depth to fictitious bottom

FORMAT FOR TABULATED VALUE OF WAVE ELEVATION

Wigley Model / Double Model Approach / Deep water wave resistance /
 Hyochul Kim / Source distribution on hull surface

Wigley Hull		Wigley Hull					
F_n	C_w	F_n	C_w				
0.20	1.043	<u>0.452</u>	4.479				
0.225	1.124	0.475	4.643				
0.25	1.218	0.50	4.524				
<u>0.266</u>	1.197	0.55	4.084				
0.275	1.579						
0.30	2.440						
<u>0.313</u>	2.134						
0.325	1.774						
<u>0.35</u>	1.495						
0.375	2.166						
0.40	3.083						
0.425	3.871						
0.45	4.449						

A Finite Element Method For Ship Wave Resistance Computations

A. Oomen
Netherlands Ship Model Basin

THEORY

The solution method to compute the velocity potential is based on the method described in 1. for the flow in turbo machines and 2. for two-dimensional free surface flows. I will explain the method briefly for the three-dimensional free surface flow.

First, I assume that the flow is free of rotation and that the fluid is incompressible and frictionless. Under these conditions, we may assume the existence of a velocity potential.

The mathematical equations for the fluid motion are then, in curvilinear coordinates:

1. In the computation domain the velocity potential ϕ must fulfil the Laplace equation:

$$\frac{1}{\sqrt{g}} \frac{\partial}{\partial x^i} (\sqrt{g} g^{ij} \frac{\partial \phi}{\partial x^j}) = 0$$

2. At the boundaries of the region the kinematical boundary condition must be fulfilled:

$$\frac{1}{\sqrt{g^{ii}}} g^{ji} \frac{\partial \phi}{\partial x^i} = f^j$$

3. At the free surface the dynamical boundary condition must be fulfilled:

$$\tilde{g}\eta(x^1, x^2) + \frac{1}{2} (g^{ij} \frac{\partial \phi}{\partial x^i} \frac{\partial \phi}{\partial x^j}) + \frac{p}{\rho} = c$$

where: $i, j = 1(1)3$
 g^{ij} = metric tensor quantity
 \tilde{g} = gravitational acceleration
 η = unknown surface elevation
 ρ = mass density
 x^1, x^2, x^3 = curvilinear coordinate

The curvilinear coordinates are chosen such that the boundaries coincide with planes $x^1 = \text{constant}$. Now that we have a mathematical formulation of the problem, we want to compute a solution. To do this, we first make it a little bit easier and split the problem into two parts. First we assume that the position of the free surface is known and that it a fixed boundary. Then we have a Neumann problem which can be solved. After the solution of this problem we will correct the position of the free surface and so on until the position of the free surface does not change anymore.

The Neumann Problem.

How can we solve the Neumann problem ? Because we have a three-dimensional case we may expect that we will get a tremendous number of equations to solve when we use a finite element technique. That is why we try to reduce the three-dimensional problem to a few two-dimensional problems. We can do this by dividing the computational region into a set of sub-regions separated from each other by planes $x^3 = \text{constant}$. If we make the assumption that the potential may be approximated by an interpolation polynomial in the x^3 -direction that agrees with the real potential value and its derivatives in x^3 -direction at the intersection planes, we get as unknowns the potential value and its derivatives in x^3 -direction on a set of two-dimensional planes. In fact 3 to 5 intersection planes will be enough for approximating the real potential when we use as interpolation polynomial a spline function (of third degree) with continuous second derivative at the planes between two sub-regions. For $N-1$ regions we get for the $2N$ unknowns: N equations from the Laplace equation, $N-2$ equations from the prescribed continuous second derivative and 2 equations from the kinematical condition, one at the fixed surface and one at the bottom. Applying the collocation method we state that the Laplace equation has to be satisfied at the intersection planes. If we want to solve the system by

a finite element method, we can approximate the solution by

$$\phi^j(x^1, x^2) = \sum_{s=1}^M a_s^j p^s(x^1, x^2) \quad \text{and}$$

$$\phi_{x^3}(x^1, x^2) = \sum_{s=1}^M b_s^j p^s(x^1, x^2)$$

where $p^s(x^1, x^2)$ is a set of linearly independent functions. The Galerkin method now implies that, when we substitute this approximation into the Laplace equation and the boundary conditions the residue of the system must be perpendicular to this set of functions.

This gives the integral equation:

$$\iint_{\Omega} L_1(\phi^1, \dots, \phi^N, \phi_{x^3}^1, \dots, \phi_{x^3}^N) p^s dx^1 dx^2 + \int_M \alpha_{ij} ((n^k \phi, k)^j - f^j) p^s d\eta = 0$$

with $i, j = 1(1)N$ and $s = 1(1)M$.

The divergence theorem gives a similar integral equation so that the difference of these two integral equations gives an equation without second derivative terms.

In conclusion we may reduce the system to a diagonally dominant system if the angles between the x^1, x^2 and x^3 coordinate lines are large enough (greater than 45 degrees) and then the number of unknowns can also be reduced from $2N$ to N by eigenvalue and eigenvector computation of the dominant terms.

The resulting matrix equation can then be solved by iterative solution of the equation for one plane at a time. So we have reduced the three-dimensional problem to a set of coupled two-dimensional problems.

Surface Correction

After the computation of the Neumann velocity potential we want to compute a better position of the free surface. So now we have to take into account all the equations, also the dynamical surface condition. In general, the velocity potential from the Neumann problem will not satisfy this dynamical condition. That is why we introduce a disturbance potential. If we assume that the disturbance potential is small compared with the Neumann potential, we get by linearization the following equations for the disturbance potential ϕ .

1. $\Delta\phi = 0$ Laplace equation
2. $\frac{\partial\phi}{\partial n} = 0$ fixed boundaries + inflow boundary
3. $\frac{\partial\eta}{\partial x} \frac{\partial\phi}{\partial x} (+\frac{\partial\eta}{\partial y} \frac{\partial\phi}{\partial y}) = \frac{\partial\phi}{\partial z}$ free surface
4. $\tilde{g}\eta + \frac{\partial\phi}{\partial x} \frac{\partial\eta}{\partial x} (+\frac{\partial\phi}{\partial y} \frac{\partial\eta}{\partial y} + \frac{\partial\phi}{\partial z} \frac{\partial\phi}{\partial z}) = \frac{1}{2}(U_0^2 - V^2)$

with U_0 = inflow velocity, V = local velocity.

Now we may assume that in a small element $(\Delta x, \Delta y)$ the disturbance potential has the form:

$$\phi = (A_0 + A_1x + A_2x^2 + A_3x^3 + B_1y + B_2y^2 + B_3y^3 + C_1xy + C_2x^2y + C_3xy^2 + \dots) \times \cosh(\alpha(z+H)) / \cosh(\alpha H)$$

so that $\frac{\partial\phi}{\partial n} = 0$ at the bottom.

$$\text{and } \eta = a_0 + a_1x + a_2x^2 + b_1y + b_2y^2 + C_1xy + \dots$$

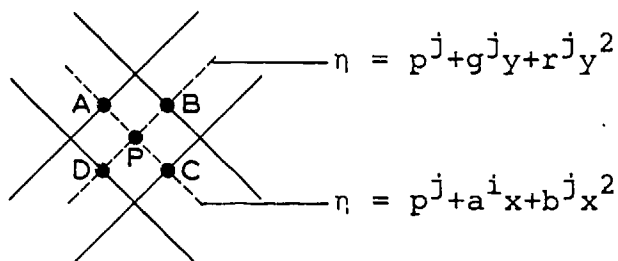
When we put these approximations into the equations and require that the sum of the terms of equal powers in x and y must be zero, this leads to the equations:

1. $\alpha^2 = \tanh(\alpha H) (C+1) / V^2$
2. $b_2 = C a_2$

$$3. \frac{2(C+1)}{\alpha^2} a_2 = -a_0 + \frac{1}{2}(U_0^2 - v^2)/\tilde{g}$$

where C is connected with the wave velocity: $C = \tan^2 \theta$ and wave velocity $= U_0 \cos \theta$.

If we approximate the surface correction by a spline function in x and y direction



We can solve the system for one Δx station when in the point A the values of η and $\frac{\partial \eta}{\partial x}$ are given, and in the points B/D continuity of η and $\frac{\partial \eta}{\partial y} + 2$ boundary-conditions are given

$$\text{and } b^j = (-p^j + \frac{1}{2}(U_0^2 - v^2)/\tilde{g})\alpha^2/2(C+1)$$

$$\text{and } r^j = Cb^j$$

With these conditions the new position of the free surface can be computed in this Δx region and so on to the outflow boundary.

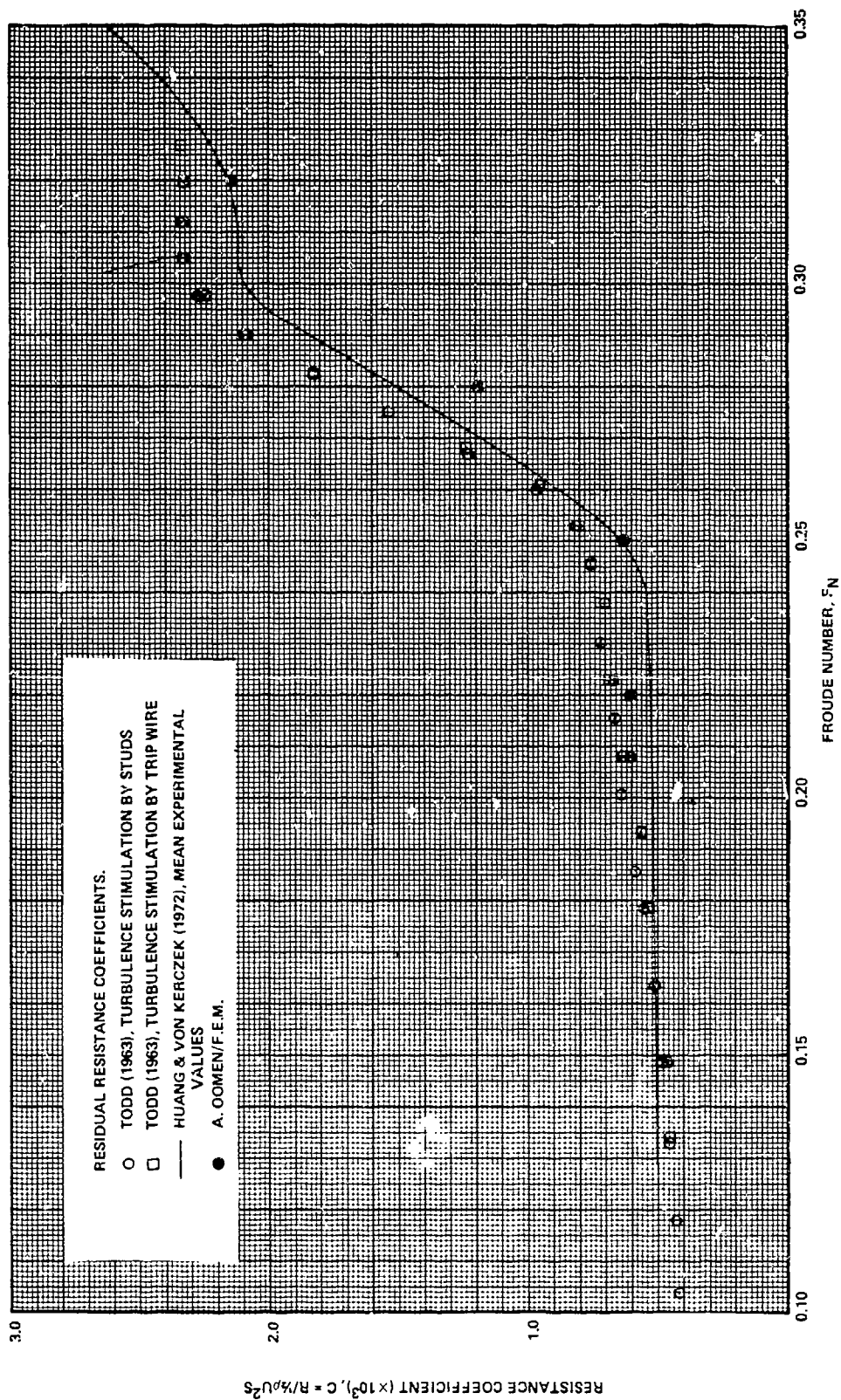
Literature.

1. A three-dimensional method for the calculation of flow in turbo-machines using finite elements on a blade-to-blade surface of revolution. C. Korving, Delftse Universitaire Pers.
2. The wave resistance for flow problems with a free surface. C. Korving and A.J. Hermans, 2nd Intern. Conference on Num. Ship Hydr. 1978.

Computations.

Computations have been made up to now only for the series 60 at the recommended Froude numbers. The number of elements I have used is quite small, for a computational region of $0 \leq B_c/L_{pp} \leq 0.75$, $-5 \leq L_c/L_{pp} \leq 2.0$ and $-0.5 \leq H_c/L_{pp} \leq \text{free surface}$.

I have used 17 points in breadth direction, 51 points in length direction and 3 points in depth direction. This has been done for time reasons and to keep the metric tensor quantities g^{ij} for $i \neq j$ small. With this number of points the real ship-hull is very roughly represented in the computations so the wave elevations near the ship hull cannot be acceptable. The wave resistance coefficient, however, seems to be quite reasonable.



FORMAT FOR TABULATED VALUES OF WAVE RESISTANCE

Serie 60							
F_n	C_w						
.22	.102						
.25	.132						
.28	.69						
.32	1.64						

FORMAT FOR TABULATED VALUE OF WAVE ELEVATION

A. Oomen / F.E.M.

Serie 60/Fn=.22		Serie 60/Fn=.25		Serie 60/Fn=.28		Serie 60/Fn=.32	
x/L	$\eta(x)$	x/L	$\eta(x)$	x/L	$\eta(x)$	x/L	$\eta(x)$
-1.1	.34	-1.1	.41	-1.1	.43	-1.1	.48
-1	.14	-1	.31	-1	.35	-1	.53
-.9	-.16	-.9	-.06	-.9	.03	-.9	.31
-.8	-.47	-.8	-.46	-.8	-.34	-.8	-.10
-.7	-.28	-.7	-.50	-.7	-.51	-.7	-.36
-.6	.04	-.6	-.31	-.6	-.54	-.6	-.55
-.5	.06	-.5	-.11	-.5	-.41	-.5	-.62
-.4	.04	-.4	.08	-.4	-.23	-.4	-.59
-.3	-.08	-.3	.04	-.3	-.10	-.3	-.54
-.2	-.20	-.2	-.06	-.2	-.03	-.2	-.44
-.1	-.18	-.1	-.11	-.1	+.03	-.1	-.34
0	-.12	0	-.14	0	+.01	+0	-.23
.1	-.08	.1	-.19	.1	-.06	.1	-.14
.2	-.12	.2	-.22	.2	-.15	.2	-.09
.3	-.16	.3	-.22	.3	-.24	.3	-.04
.4	-.20	.4	-.17	.4	-.28	.4	-.02
.5	-.14	.5	-.11	.5	-.26	.5	-.02
.6	-.04	.6	.06	.6	-.13	.6	0
.7	.10	.7	.28	.7	+.05	.7	.07
.8	.14	.8	.24	.8	+.14	.8	.01
.9	-.02	.9	.03	.9	+.11	.9	-.08
1.0	+.02	1.0	-.17	1.0	+.03	1.0	-.20

Discussion

by K. J. Bai
of paper by A. Oomen

1) From my own experience, the radiation condition upstream and downstream in a numerical method like yours is the most difficult to treat. If you used a Neumann condition (specifying assumed normal velocity profile) on both upstream and downstream truncation boundaries, you would obtain an unwanted parasitic solution, which is the homogeneous solution embedded in your solution. How do you treat this?

2) In your paper, you assumed $\phi = (A_0 + A_1 X + A_2 X^2 + \dots) \cosh(\alpha(z + H)) / \cosh \alpha H$ in the global coordinates. I think that this is not a proper representation of the z -dependency because in the near field, where the finite element method is applied, the z -dependency of the velocity potential does not behave entirely as $\cosh \alpha(z + H)$. If we represent the near field solution by eigenfunction expansions, we should have infinite discrete eigenfunctions, for instance, $\cos m_i(z + H)$ ($i = 1, 2, \dots$) for the two-dimensional case. Here the m_i are the real roots of

$$\frac{U^2}{g} m_i = \tan m_i H, \quad i = 1, 2, 3, \dots$$

Discussion

by F. Chan
of paper by A. Oomen

The free surface wave pattern in steady state is not known a priori and its solution is coupled with the solution of the Laplace equation for interior points. How do you construct your finite elements such that the free surface boundary conditions are applied exactly at the free surface?

Author's Reply

by A. Oomen

to discussion by K. J. Bai

1) At the upstream truncated boundary a uniform inflow is assumed. At the downstream truncated boundary a kind of damping of the waves is introduced, over at least half a wave length, which makes the outflow uniform.

2) The z dependency of the potential solution is given by a spline for the Neumann potential solution and only for the disturbance potential it is assumed that the z dependency is given by the mentioned formula. If the value of x is computed iteratively for each element it may approximate the z dependency of the small disturbance potential quite well.

Author's Reply

by A. Oomen

to discussion by F. Chan

The finite elements are constructed for each iteration such that they follow the position of the assumed or, for later iterations, computed free surface. So during each iteration new finite elements are chosen. However, by using curvilinear coordinates each nodal point keeps the same curvilinear coordinates but the metric tensor quantities are different for each iteration.

By using curvilinear coordinates the boundary conditions are applied exactly for each iteration because the nodal points are exactly at the free surface and the boundaries of the iteration. With the position of the free surface also the position of the intersection planes changes.

WAVE RESISTANCE IN A RESTRICTED WATER BY THE LOCALIZED FINITE-ELEMENT METHOD

Kwang June Bai

David W. Taylor Naval Ship Research and Development Center

Computations of the wave resistance of a ship moving along the centerline of a towing tank at a constant speed are made by the localized finite-element method developed by the present author (Bai, 1975, 1977, 1978). In earlier work of the author, a test of the new method was made by applying it to a simple ship hull geometry in a canal or towing tank having a relatively small rectangular cross section. One may expect that the method can be applied, in principle, to a problem simulating unbounded water by simply allowing the canal width and depth to become very large in the computation. On the other hand, the efficiency of the numerical method may suffer when applied to the case of unbounded water.

The present investigation tests the efficiency as well as the accuracy of the finite-element method when applied to more realistic ship hull forms and towing tank conditions. Numerical computations have been made for four ship hull forms in towing tanks of a few different sizes. Specifically, the Wigley parabolic hull, the Inuid S-201, the Series 60, and the high-speed ATHENA model were chosen for computations. For some ship models, the computations were made for two different sizes of towing tanks, one being represented by coarse-mesh finite-element subdivisions and the other being represented by fine-mesh subdivisions; the total number of nodes in the fine mesh subdivision is roughly double that in the coarse mesh subdivision.

Both the exact and the linearized boundary conditions are tested for the ship hull boundary condition; the linearized free-surface condition is used throughout this work. The description of the localized finite-element method is left out since one can find the details in Bai (1975, 1977, 1978). The trim and sinkage have not been taken into account in the present computations.

Typical ship hull and towing-tank boundaries are given in Figure 1. The width and depth of the tank are denoted by W and D , respectively, as

shown in Figure 1. Due to the symmetry of the flow with respect to the vertical plane, $z = 0$, the actual numerical computation was made for only half of the fluid domain, i.e. $0 < z < W/2$. After truncating the fluid domain for $|x| > x_T$, where $x_T \cong 0.7 L$, the reduced localized finite-element domain defined by $|x| < x_T$, $0 > y > -D$, and $0 < z < W/2$, is subdivided into eight-point linear four-sided elements (like a cube). In the present study, two different finite-element subdivisions were used, i.e., the coarse finite-element subdivisions have a total of 1496 nodes with 1120 elements and the fine finite-element subdivisions have a total of 2730 nodes with 2160 elements. The nodal points along the x-, y-, and z-axes are, respectively, 17, 8, and 11 for the coarse meshes and 21, 10, and 13 for the fine meshes. On the ship hull boundary, for both the exact or linearized body boundary conditions, 11 nodes lie length-wise along the ship and 4 nodes lie draft-wise along the ship for the coarse subdivision; 13 nodes and 5 nodes, respectively, were used in the fine subdivision.

Numerical Results and Discussions

In the present numerical method, we obtain the velocity potentials everywhere in the fluid domain. Note that the velocity potential in the truncated fluid domain is also obtained by the eigenfunction expansions of which coefficients are obtained as part of the solution. From the computed velocity potential, one can compute easily all of the velocity field in the entire fluid domain as well as the free-surface profiles. One can also obtain the blockage effect based on the approximate theory of Bai (1979). However, in the present study, we present mainly the wave resistance. In the following, we will describe each ship hull model considered here.

(1) Wigley Parabolic Hull

Both exact and linearized ship hull boundary conditions were used for a small tank of $W/L = 0.76125$, and $D/L = 0.444$, and also for a large tank of $W/L = D/L = 1.25$. The wave resistance coefficients were computed for Froude numbers of 0.35, 0.40, 0.43, and 0.45 using the coarse meshes and for Froude numbers of 0.35, 0.402, 0.452, and 0.482 using

the fine meshes. The results are given in Table 1 and Figure 2. Comparison between the present results obtained using the fine meshes in the large tank and the theoretical results given by Lackenby (1965) for infinite water depth, both based on the thin-ship approximation, shows fairly good agreement for Froude numbers greater than 0.35, the finite element predictions being less than 10 percent than the predictions of thin-ship theory. The slight deviations may be caused by the present 'finer meshes' not being fine enough to obtain good resolution particularly at the lowest values of Froude number considered (i.e., $F_n = 0.35$) and also by the present 'larger tank' not being large enough to ignore blockage effects at the higher values of Froude number considered (i.e., $F_n = 0.45$). It is of interest to note that the computed wave resistance coefficients in the larger tank obtained by using either the exact or the linearized ship hull condition are somewhat lower than those given for thin-ship theory by Lackenby for the infinite water depth. Figure 2 also shows that the blockage effect on the computed values of wave resistance is not negligible for the small tank. The wave resistance coefficient in the smaller tank is slightly higher when the exact body boundary condition is satisfied for the Froude numbers studied here whereas the opposite is true for the larger tank at values of Froude numbers greater than 0.40. The computed spread in hump and hollow values of wave resistance coefficients for $0.35 \leq F_n \leq 0.48$ is smallest when the exact hull boundary condition is satisfied in the larger tank.

(2) Inuid S-201

For the Inuid S-201, both the coarse and fine meshes were used for the linearized ship hull boundary condition. Froude numbers of 0.5, 0.55, and 0.60 were treated for the coarse meshes and Froude numbers of 0.319, 0.36, 0.44, 0.525, and 0.65 were treated for the fine meshes. For the coarse meshes, $W/L = 0.5$ and $D/L = 0.4$ and for the fine meshes, $W/L = D/L = 1.0$. The results are given in Table 2 and Figure 3. The results for the large towing tank case with fine meshes agrees reasonably well with the experimental data. However, the predictions for the small tank case with coarse meshes show considerably higher values of wave resistance than measured values in the infinite water depth case.

(3) Series 60

For this model, the exact as well as the linearized body boundary conditions were satisfied using coarse meshes with $W/L = 1$ and $D/L = 0.5$. Fine meshes were used for $W/L = 1$ and $D/L = 1$ with the linearized body boundary condition. The results are given in Table 3 and Figure 4. It is of interest to note that all three sets of numerical results have a pronounced hollow and hump whereas the mean experimental values of the residual resistance do not.

(4) High-Speed-Hull ATHENA Model

ATHENA has the largest beam/length ratio of the four models examined here. The numerical computation of wave resistance for this far-from-the-ship model using the linearized body boundary condition was done mainly to determine how bad the thin-ship approach is. For this model, computations were made for Froude numbers of 0.41, 0.48, 0.65, 0.80 with $W/L = 2$ and $D/L = 2$, using the fine meshes and the linearized body boundary condition. In the present numerical computation, the physical offsets of the hull at Station 20 are replaced by all zeroes; i.e., treating stern as a wedge. The numerical results are given in Table 4 and Figure 5. Figure 5 shows that the use of the seemingly-very-crude-approximation (i.e., the use of linearized body boundary condition applied on the centerplane) is not too bad. The comparison between the present results and the measured residual resistance in Figure 5 suggests that the brute-force application of the thin-ship approach to a high-speed transom-stern ship like the ATHENA model may provide some useful information about wave resistance.

REFERENCES

- K.J. Bai, 1975, "A Localized Fined-Element Method for Steady, Two-Dimensional Free-Surface Flow Problems," Proc. First Int. Conf. Numerical Ship Hydrodynamics, held at the NBS, Edited by Schot and Salvesen, Sponsored by the David W. Taylor Naval Ship R&D Center, Bethesda, Maryland.

- K.J. Bai, 1977, "A Localized Finite-Element Method for Steady Three Dimensional Free-Surface Flow Problems," Proc. Second International Conf., Numerical Ship Hydrodynamics, held at the University of California, Berkeley, Calif., Sponsored by the David W. Taylor Naval Ship R&D Center, Bethesda, Maryland.
- K.J. Bai, 1978, "A Localized Finite-Element Method for Two-Dimensional Steady Potential Flows with a Free Surface," Journal of Ship Research, Vol. 22, No. 4, pp. 216-230.
- K.J. Bai, 1979, "Blockage Correction with a Free Surface," Journal of Fluid Mechanics, Vol. 94, Pt. 3, pp. 433-452.

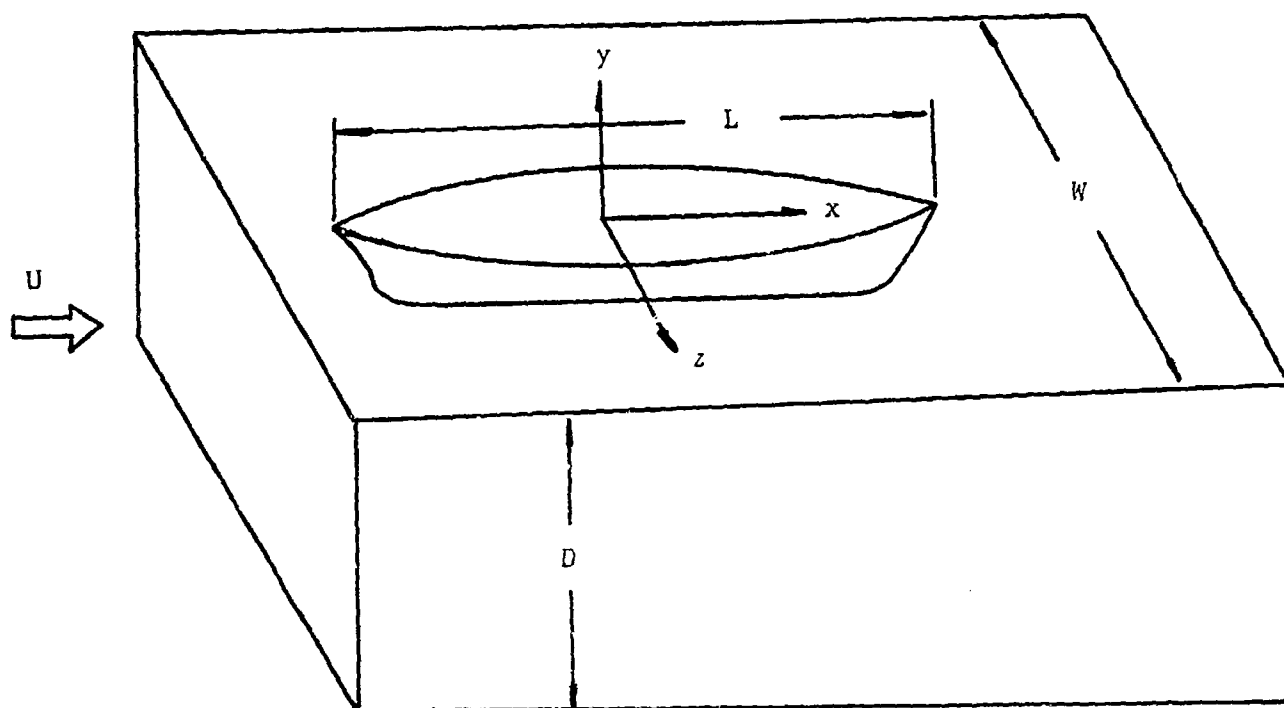


Figure 1. Boundary Configurations of Towing Tank Test

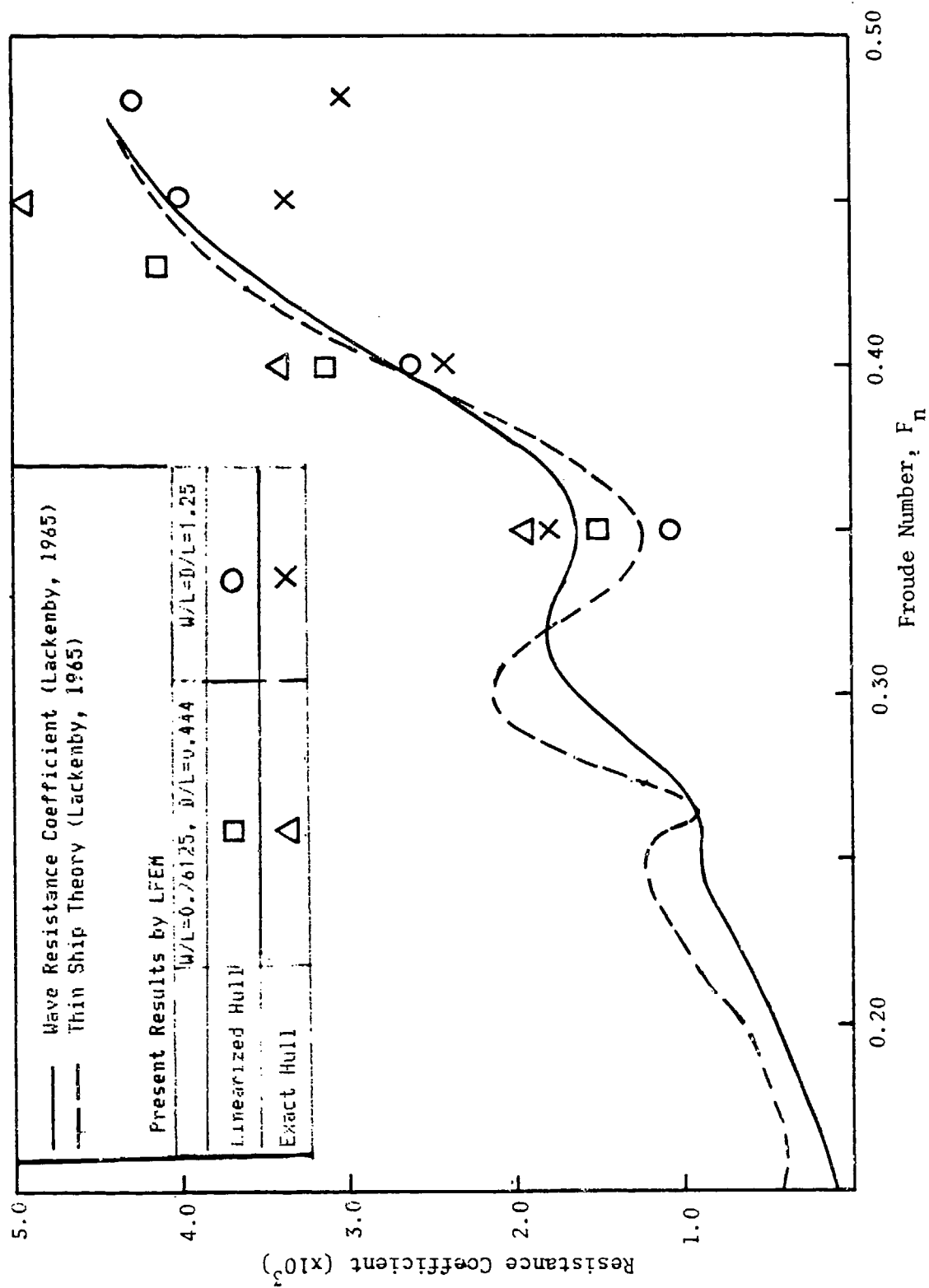


Figure 2. Resistance Curves for Wigley Hull

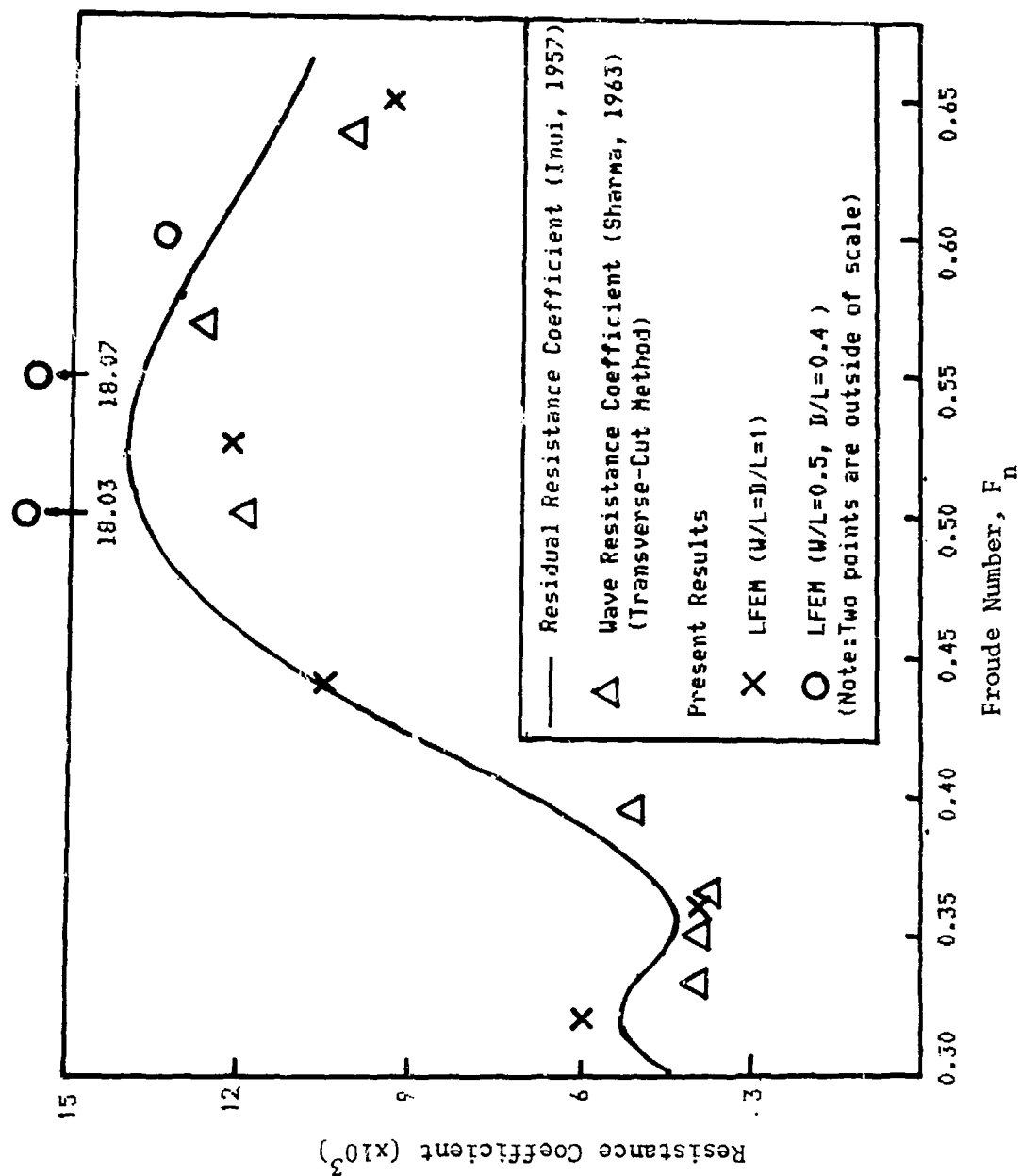


Figure 3. Resistance Curves for Inuid S-201

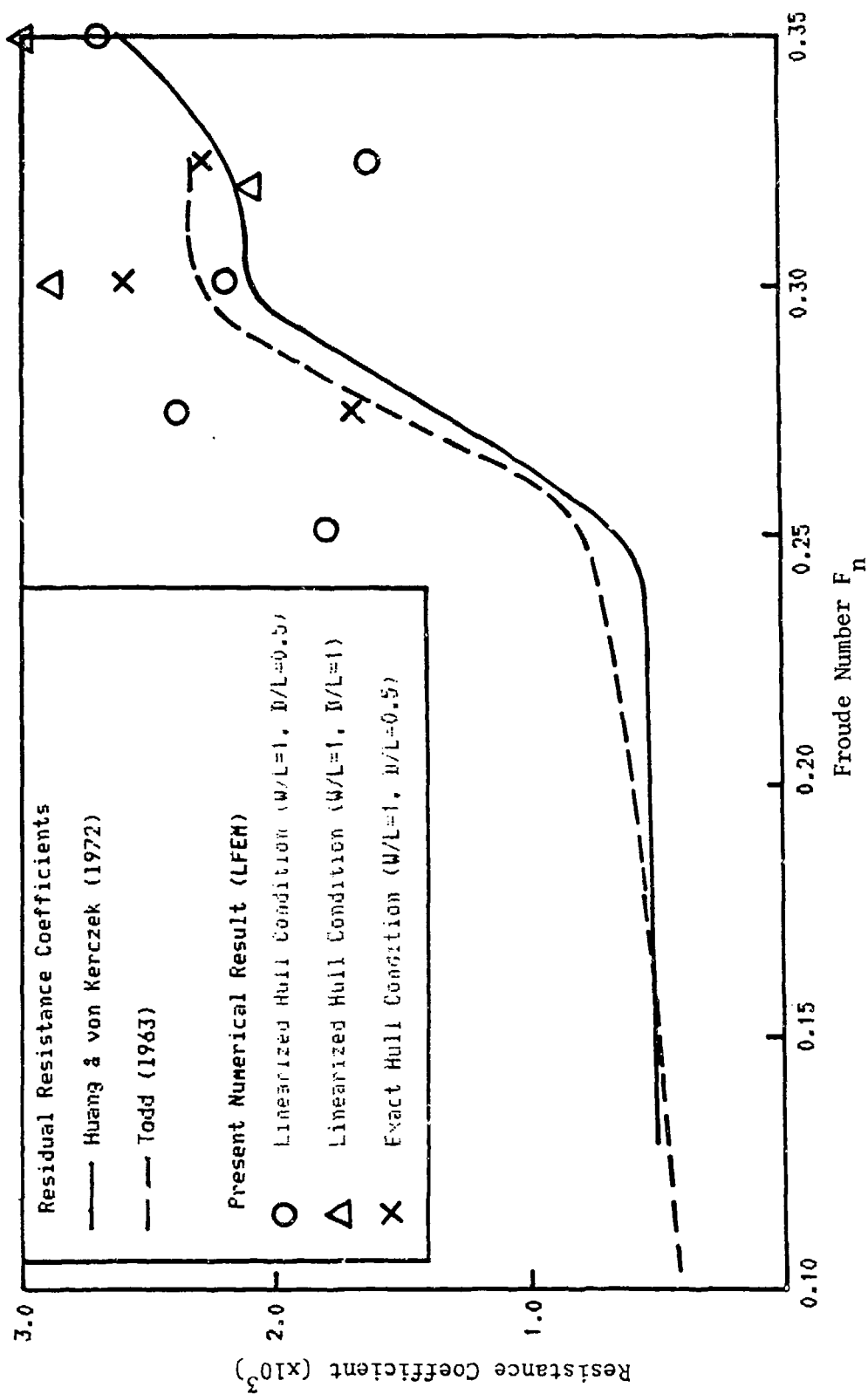


Figure 4. Resistance Curves for Series 60, $C_B=0.60$

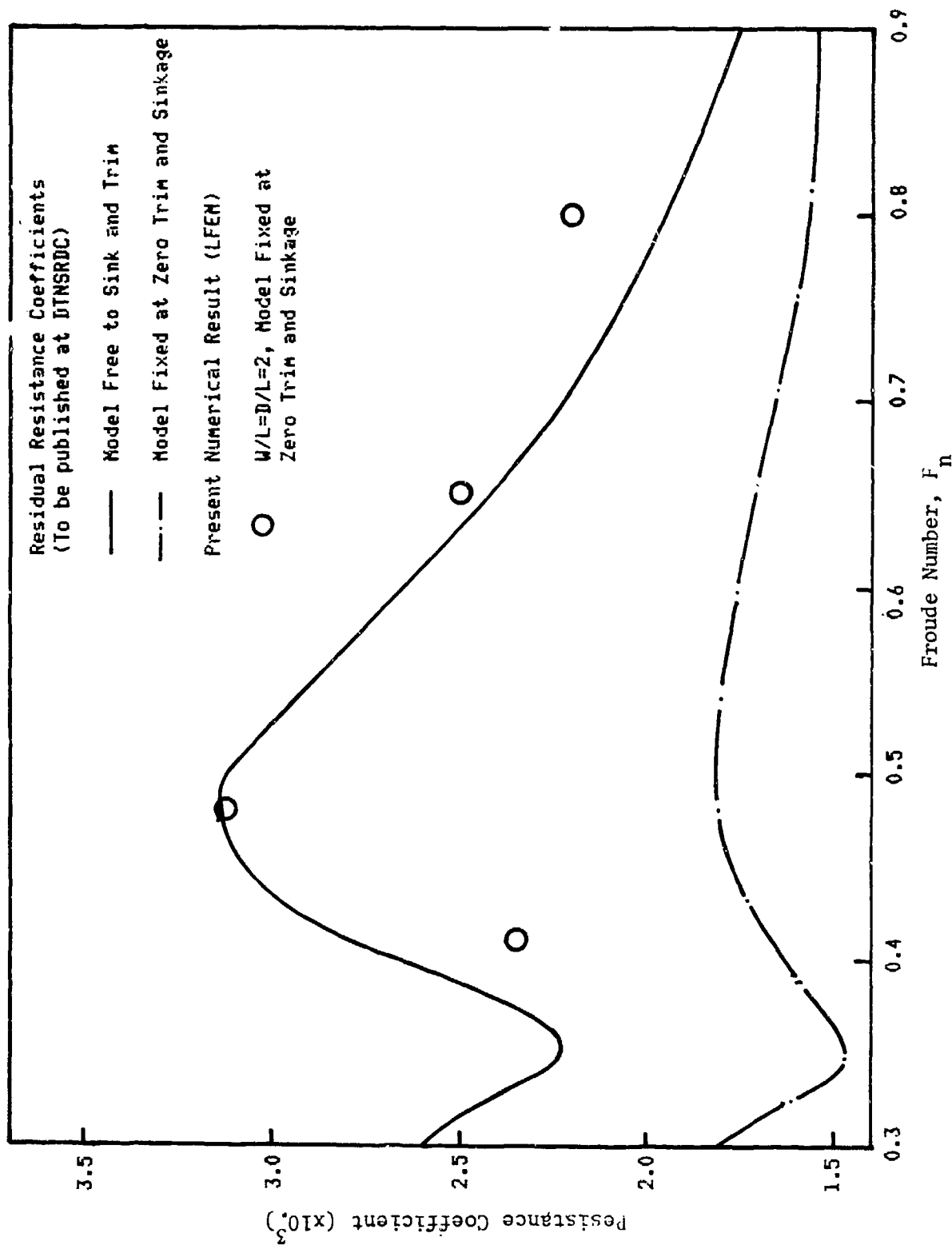


Figure 5. Wave Resistance Curve for the High-Speed Hull, Athena

Table 1. TABULATED VALUES OF WAVE RESISTANCE FOR WIGLEY HULL.

K. J. Bai / Localized Finite Element Method

W/L=0.76125, D/L=0.444				W/L=D/L=1.25			
Wigley/Thinship		Wigley/Exact		Wigley/Thinship		Wigley/Exact	
F_n	$C_W \times 10^3$	F_n	$C_W \times 10^3$	F_n	$C_W \times 10^3$	F_n	$C_W \times 10^3$
0.35	1.50		1.94	0.35	1.079		1.818
0.40	3.14		3.40	0.402	2.617		2.431
0.43	4.14		-	0.452	3.980		3.179
0.45	-		4.92	0.482	4.287		3.093

Table 2. TABULATED VALUES OF WAVE RESISTANCE FOR INUI HULL S-201.

K. J. Bai / Localized Finite Element Method

W/L=0.5, D/L=0.4				W/L=D/L=1			
Inui/Thinship		Inui/Thinship		Inui/Thinship		Inui/Thinship	
F_n	$C_W \times 10^3$	F_n	$C_W \times 10^3$	F_n	$C_W \times 10^3$	F_n	$C_W \times 10^3$
0.50	18.03	0.319	5.99				
0.55	18.07	0.36	7.95				
0.60	13.47	0.44	10.54				
		0.525	12.19				
		0.65	9.38				

Table 3. TABULATED VALUES OF WAVE RESISTANCE FOR SERIES 60.
K. J. Bai / Localized Finite Element Method

W/L=1, D/L=0.5			W/L=D/L=1		
Series 60/Thinship		Series 60/Exact Hull		Series 60/Thinship	
F_n	$C_w \times 10^3$	F_n	$C_w \times 10^3$	F_n	$C_w \times 10^3$
0.251	1.46		-	0.30	2.91
0.275	2.42		1.75	0.32	2.15
0.28	2.58		-	0.35	3.10
0.301	2.20		2.63		
0.325	1.67		2.28		
0.35	2.69		-		

Table 4. TABULATED VALUES OF WAVE RESISTANCE FOR ATHENA MODEL.
K. J. Bai / Localized Finite Element Method

W/L=D/L=2					
Athena/Thinship					
F_n	$C_w \times 10^3$				
0.41	2.352				
0.48	3.143				
0.65	2.505				
0.80	2.201				

Discussion

by K. Nakatake
of paper by K. J. Bai

Your results of wave-resistance seem to be fine.

How about the wave elevation along the hull surface?

Author's Reply

by K. J. Bai
to discussions by K. Nakatake

In my method I obtain the velocity potential everywhere in the fluid. At present I do not compute the wave profiles in my computer output, even though it is easy to build in. However, once I did calculate the wave profile along Series 60 by hand from the velocity potential obtained. My wave profile agreed fairly well with the experimental measurement in the forebody region; however, the agreement was not very good near the stern. Presumably, this disagreement near the stern is partly due to the fact that I took only ten free wave terms in this particular computation.

NONLINEAR CALCULATIONS OF THREE-DIMENSIONAL POTENTIAL FLOW ABOUT A SHIP*

Robert K.-C. Chan and Frank W.-K. Chan
JAYCOR
Del Mar, California, U.S.A.

Introduction

A finite-difference solution procedure has been developed for calculating three-dimensional potential flows, both transient and steady, about a floating body of a wide range of hull shapes. The complete set of nonlinear free-surface conditions is applied to the exact position of the free surface. Also, appropriate boundary conditions are imposed at the correct location of the hull surface. Thus, the only approximations consist of the potential flow assumption and the discretization of the governing equations by finite difference.

Major computational problems in this and many other approaches include the treatment of geometry, unphysical wave reflections from the boundaries of computational domain, stability and accuracy of the finite-difference schemes and efficiency of the algorithm. The geometry problem has been resolved by employing a three-dimensional body-fitted coordinate system^[1] which permits rigorous application of correct boundary conditions at the precise location of the boundary. The spurious wave reflection is practically eliminated by a novel radiative condition^[2], while the computational stability and accuracy are successfully achieved by using the newly

*This work was sponsored by the Office of Naval Research under Contract N00014-76-C-0455.

developed BET technique^[3]. The bulk of computation time is consumed in solving the three-dimensional Laplace's equation. By using a powerful new technique of direct solver, one can economically compute flows with high resolution.

Because of the generality of the present method, the computer code provides a very useful tool for investigating the detailed dynamics of the flow about a ship. For example, the geometry of a tanker hull can be easily set up and the flow field calculated. Some insight will be obtained concerning the nature of the stagnation point at the bow, as well as the quantitative determination of the role of nonlinearity in the bow wave region. Furthermore, the code can be employed to assess the validity of certain assumptions often made in other approaches, e.g., localized bow wave calculations as if they were independent of the flow pattern at the rear part of the ship. Another interesting application of the method is to investigate the sensitivity of wave drag to changes in the hull shape. This information will help guide experimental research on hull designs.

Theoretical Discussions

Three major difficulties can be indentified when calculating three-dimensional flows about a ship by finite difference. These are:

- a. Wave reflections due to finite computation region.
- b. Stability and accuracy of the finite difference schemes.
- c. Complications due to geometries; i.e., body shape and free surface.

Due to limitation in computer storage, one has to use a body-fixed frame of reference to maximize resolution near the

ship. In this reference frame, the ship appears to be stationary in a running stream. Numerically, this situation created two problems. The first problem concerns boundary conditions at the "open-boundary", where the flow or waves are allowed to leave the computation region. Improper treatment of this type of boundary usually results in undesirable reflections.

The second problem associated with streaming flow is that the advection terms in the free surface conditions require careful construction of finite difference representation. Many conventional explicit schemes, such as the first-order, forward-time, central-space difference, have been tried and found unstable. Other schemes, like the first-order upwind differencing, are too dissipative for our purpose, because the potential flow is nondissipative. Detailed descriptions of the nature and the attendant problems of various advection schemes can be found in Reference 4. The main problem with geometry is the fact that, to simulate properly the finite-amplitude aspects of the physical problem, correct boundary conditions must be applied at the exact positions of the body surface and at the free surface.

During the last three years, considerable progress has been made in all these three areas of difficulties. To be specific, Orlanski's^[2] technique for implementing Sommerfeld radiation condition has been modified for a nondissipative system and we are now able to reduce wave reflections to a negligible degree. A new, upwind-centered difference scheme, which is a second-order version of the BET (Balanced Expansion Technique) method^[3], is used to solve the time-dependent free-surface conditions, without introducing artificial viscosity. And, as to the problems of geometry, a body-fitted, but fixed coordinate system describes the interior of the flow

field, while a second system, moving with the free surface, is employed to implement the free surface conditions.

The method developed was first applied^[5] to the forward motion of a shiplike body, the shape of which was specified by a single-valued function $y = f(x,z)$, where y is the distance of the hull from the ship's center plane or the x - z plane. The class of body shapes was therefore limited to those representable by $f(x,z)$, with a sharp-edged keel.

To extend the method to body shapes without the restriction of sharp-edged keel, a different coordinate system must be used. Stated simply, a spherical polar coordinate system is deformed, i.e., stretched in the radial direction, such that the new coordinate surfaces conform to the physical surfaces, e.g., the hull surface and the free surface. Referring to Figure 1, the bulk of the flow field can be described by a fixed mesh which conforms to the body surface (labeled as "lower region" in the figure), except for a relatively small "upper region" in which a time-dependent curvilinear mesh is employed to handle the free surface as well as the body surface conditions.

Let the ship hull be described by the single-valued function

$$r' = f(\theta', \psi') \quad (1)$$

where (r', θ', ψ') are the spherical coordinates with origin at point 0 in Figure 1. We use ψ' to denote the angle as shown in Figure 2 to avoid confusion with the velocity potential ϕ . The origin is suitably located inside the body and placed at some distance below the mean level of the free surface. To generate a body-fitted coordinate system, we make the following coordinate transformation

$$r = r' - f(\theta', \psi')$$

$$\theta = \theta' \quad (2)$$

$$\psi = \psi'$$

The surface $r=0$ coincides with the hull surface, and the plane $\theta=\pi/2$ separates the upper region from the lower one. As shown in Figure 1, the mesh points on and below the plane $\theta=\pi/2$ are fixed in space relative to the ship. The mesh points at the free surface, however, move with the free surface, and the region between the free surface and the plane $\theta=\pi/2$ is subdivided into equally spaced subregions; e.g., between points 1 and 2 in Figure 1 (point 2 is fixed but point 1 is allowed to slide up and down along the mesh line $r = \text{constant}$). This arrangement allows one to resolve the flow near the intersection of the free surface and body most effectively. By using the coordinate transformation (2), one can obtain suitable forms for the Laplace equation $\nabla^2 \phi = 0$ and the surface boundary conditions. The resulting system of differential equations are solved by a suitable finite difference technique.

The extended method has been applied to flow about a semi-submerged sphere. For the Froude number $F_r = U/\sqrt{gr} = 0.2$, the wave drag was found to be $C_w = 0.53 \times 10^{-4}$ which compares well with the theory of Baba and Hara. Figure 3 shows the steady-state contours of the free surface elevation around the sphere. The heavy solid lines represent elevations above the initially undisturbed water surface, while the dotted lines are for the portion of the free surface lying below the undisturbed level. As the contour plot shows, there is a crest both at the bow and at the stern, while a trough is located approximately half way between them. The same method is now used to compute the flow about a Hoffman tanker and the

associated wave resistance. The development of the surface waves is shown in Figures 4 and 5. Similar to the case of semi-submerged sphere, the ship was started from rest. Figure 4 shows the contours of the surface elevation during the acceleration, while Figure 5 shows the wave pattern in steady state.

References

1. Thames, F. C., et al., "Numerical Solutions for Viscous and Potential Flow about Arbitrary Two-Dimensional Bodies using Body-Fitted Coordinate Systems", Journal of Comp. Physics, 24, 1977.
2. Orlanski, I., "A Simple Boundary Condition for Unbounded Hyperbolic Flows", Journal of Comp. Physics, 21, 1976.
3. Chan, R. K.-C., "A Balanced Expansion Technique for Constructing Accurate Finite Difference Advection Schemes", International Journal for Numerical Methods in Engineering, 12, 1131-1150, 1978.
4. Roache, P. J., Computational Fluid Dynamics, Hermosa Publishers, Albuquerque, New Mexico, 1976.
5. Chan, R. K.-C., "Finite Difference Simulation of the Planar Motion of a Ship", Proceedings of the Second International Conference on Numerical Ship Hydrodynamics, Berkeley, California, 1977.

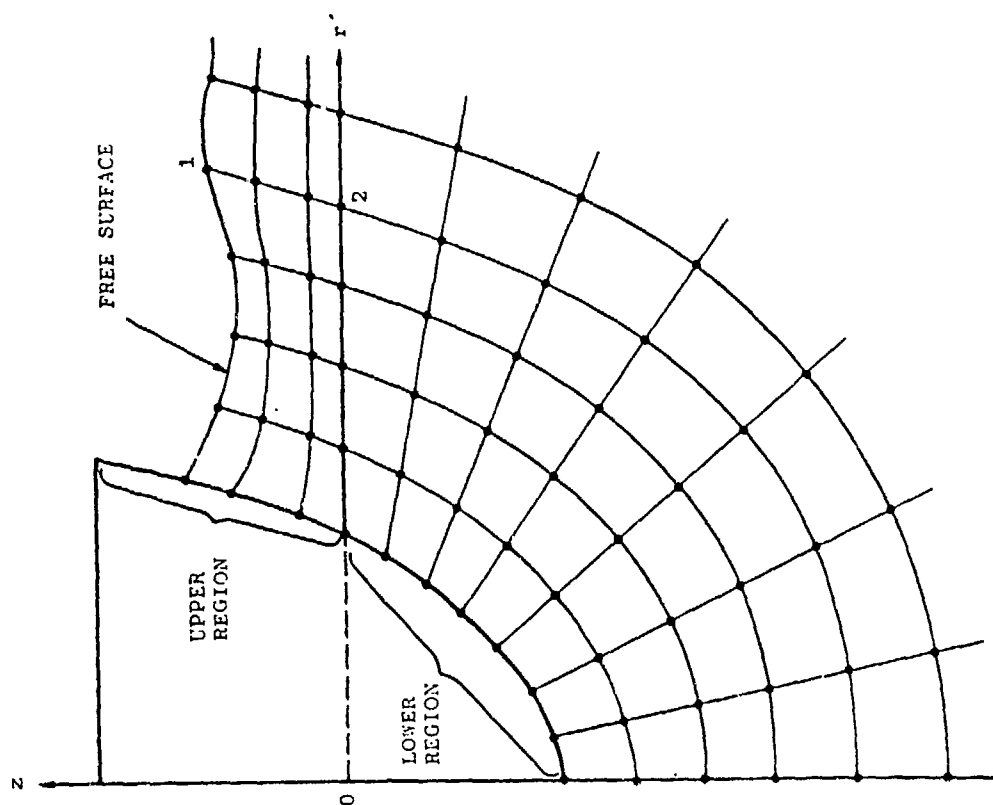


Figure 1. Composite Mesh System

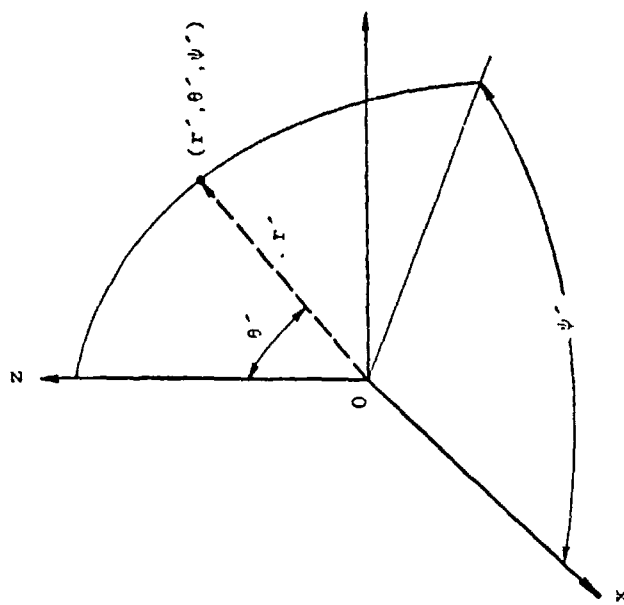


Figure 2. Spherical Coordinate System

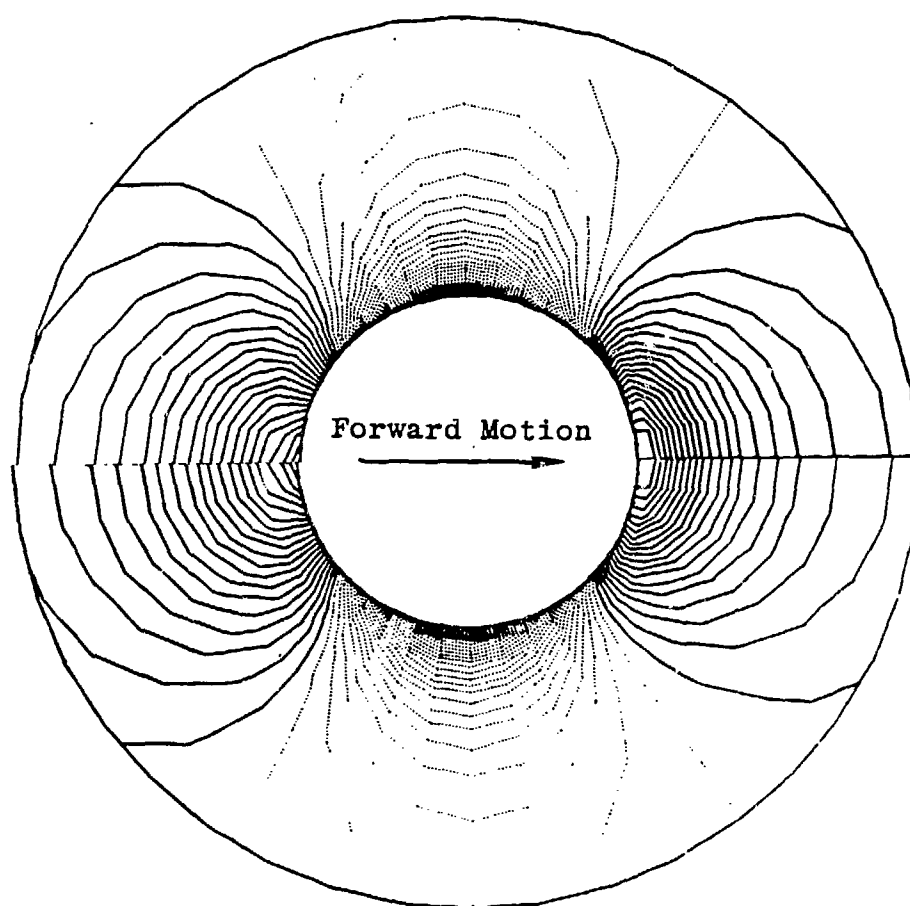


Figure 3. Steady-state free surface contours around a semi-submerged sphere ($U/\sqrt{gr} = 0.2$)

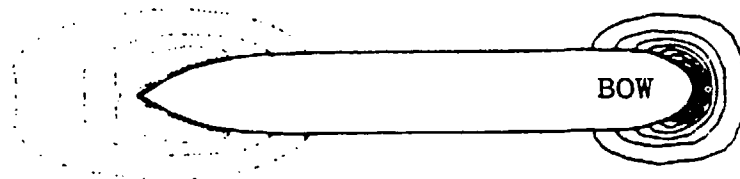


Figure 4. Free surface contours about a Hoffman tanker during acceleration.

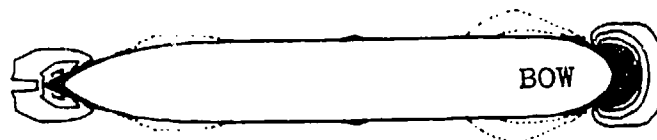


Figure 5. Steady-state free surface contours about a Hoffman tanker ($F_n = 0.13$)

FORMAT FOR TABULATED VALUE OF WAVE ELEVATION

R. K.-C. Chan and F. W. Chan/Nonlinear Finite Difference

Hoffman Tanker $F_n = 0.13$		Hoffman Tanker $F_n = 0.14$		Hoffman Tanker $F_n = 0.15$		Hoffman Tanker $F_n = 0.16$	
x/L	n/L	x/L	n/L	x/L	n/L	x/L	n/L
-0.01	0.00856	-0.01	0.00995	-0.01	0.0114	-0.01	0.0160
0.00	0.00753	0.00	0.00886	0.00	0.0103	0.00	0.0121
0.01	0.00419	0.01	0.00523	0.01	0.0064	0.01	0.0062
0.03	0.00068	0.03	0.00090	0.03	0.0013	0.03	0.0002
0.05	-0.00086	0.05	-0.00100	0.05	-0.0011	0.05	-0.0022
0.08	-0.00231	0.08	-0.00279	0.08	-0.0032	0.08	-0.0042
0.09	-0.00137	0.09	-0.00169	0.09	-0.0021	0.09	-0.0026
0.13	-0.00120	0.13	-0.00139	0.13	-0.0016	0.13	-0.0018
0.19	-0.00111	0.19	-0.00129	0.19	-0.0015	0.19	-0.0016
0.24	-0.00077	0.24	-0.00090	0.24	-0.0010	0.24	-0.0011
0.29	-0.00026	0.29	-0.00030	0.29	-0.0005	0.29	-0.0005
0.32	0.00000	0.32	0.00000	0.32	0.0000	0.32	0.0000
0.35	-0.00000	0.35	-0.00000	-0.35	-0.0000	0.35	-0.0000
0.39	-0.00017	0.39	-0.00020	0.39	-0.0001	0.39	-0.0002
0.42	-0.00009	0.42	-0.00010	0.42	-0.0001	0.42	-0.0002
0.45	0.00026	0.45	0.00030	0.45	0.0003	0.45	0.0003
0.48	0.00068	0.48	0.00080	0.48	0.0009	0.48	0.0010
0.51	0.00051	0.51	0.00060	0.51	0.0007	0.51	0.0008

FORMAT FOR TABULATED VALUE OF WAVE ELEVATION

R. K.-C. Chan and F. W. Chan/Nonlinear Finite Difference

Hoffman Tanker $F_n = 0.13$		Hoffman Tanker $F_n = 0.14$		Hoffman Tanker $F_n = 0.15$		Hoffman Tanker $F_n = 0.16$	
x/L	n/L	x/L	n/L	x/L	n/L	x/L	n/L
0.55	0.00009	-0.55	0.00010	0.55	0.0002	0.55	0.0002
0.58	-0.00000	0.58	-0.00000	0.58	-0.0000	0.58	-0.0000
0.61	-0.00009	0.61	-0.00010	0.61	-0.0001	0.61	-0.0002
0.66	-0.00017	0.66	-0.00020	0.66	-0.0002	0.66	-0.0002
0.71	-0.00043	0.71	-0.00040	0.71	-0.0005	0.71	-0.0005
0.80	-0.00077	0.80	-0.00080	0.80	-0.0009	0.80	-0.0010
0.85	-0.00077	0.85	-0.00080	0.85	-0.0009	0.85	-0.0011
0.90	-0.00051	0.90	-0.00060	0.90	-0.0007	0.90	-0.0008
0.94	0.00009	0.94	0.00000	0.94	0.0000	0.94	0.0000
0.98	0.00163	0.98	0.00179	0.98	0.0019	0.98	0.0021
1.02	0.00394	1.02	0.00438	1.02	0.0048	1.02	0.0054
1.04	0.00847	1.04	0.00985	1.04	0.0114	1.04	0.0128

FORMAT FOR TABULATED VALUES OF WAVE RESISTANCE

R. K.-C. Chan and F. W. Chan/Nonlinear Finite Difference

Hoffman Tanker						
F_n	C_w					
0.13	0.559×10^{-4}					
0.14	0.652×10^{-4}					
0.15	0.760×10^{-4}					
0.16	0.895×10^{-4}					

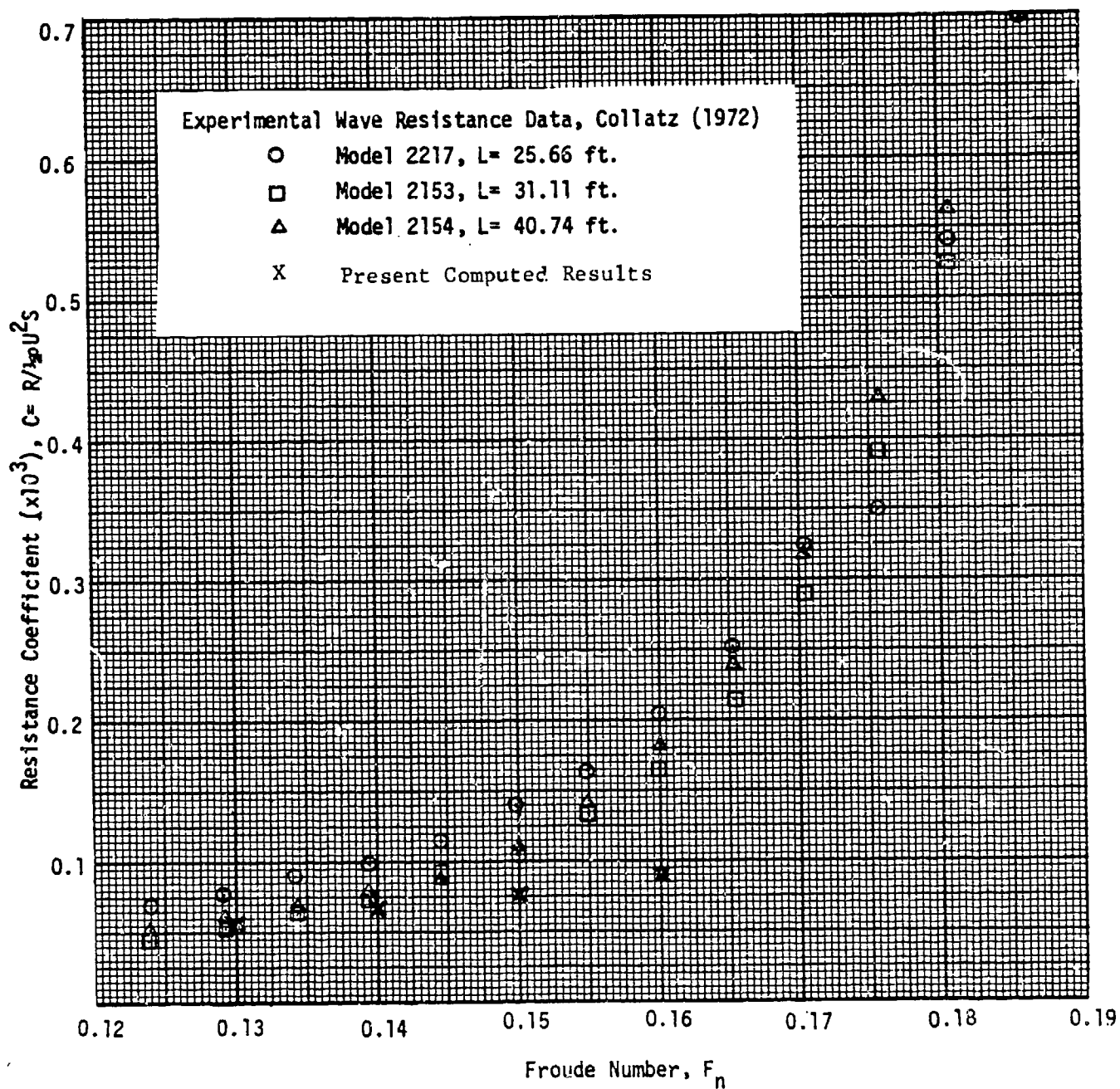


FIGURE 5.4 - Resistance Data for the Hoffman Tanker

Discussion

by C. M. Lee
of paper by R. Chan and F. Chan

Since your method can treat the transient problem, I suppose that the computation time involved can be significant. Could you tell us the amount of computation time required for a Froude number?

Author's Reply

by R. Chan and F. Chan
to discussions by C. M. Lee

For the Hoffman tanker, we used a spatial resolution of $15 \times 20 \times 30$ mesh points to cover one-half of the flow field. For a given Froude number in the range of $0.13 \leq F_n \leq 0.16$, it takes approximately 250 seconds of cpu on a CDC 7600 system to obtain steady-state solutions if one begins the calculation with the ship at rest and gradually accelerates to a final speed. Using the computer at the Lawrence Berkeley Laboratory, the actual cost is about \$80 per run at regular rates, or \$20 per run at reduced weekend rates. The cost of computation can be greatly reduced if one runs through the whole series of Froude numbers starting from the steady-state solution of an adjacent Froude number, instead of starting from rest each time.

THE GUILLOTON'S METHOD

P. Guével G. Delhommeau and J.P. Cordonnier

The analysis of the GUILLOTON's method gives two independent parts :

- The wedge method which is a practical solution of MICHELL problem for a given hull
- The GUILLOTON's transformation which gives, from the solution of MICHELL problem, a new hull shape for which the boundary conditions are better satisfied.

THE MICHELL PROBLEM

A ship hull with a longitudinal plane of symmetry is moving in an incompressible perfect fluid with an horizontal constant speed. We assume that there is a velocity potential in the domain outside the hull. The linearised free-surface condition is written on the plane of the undisturbed free-surface. Assuming that the hull is very slender, the gliding condition is written on the longitudinal plane of symmetry.

The notations are the following ones : the axis Oz is vertical downwards, ϕ is the absolute potential written in the moving system of coordinates, $y = \eta(x, z)$ is the hull description whose speed is V_0 . We set $\frac{\partial \eta}{\partial x} = f(x, z)$.

Potential expression

This problem was solved by MICHELL in 1898. Taking care of the non-radiation condition at forward infinity, we get for the potential :

$$\begin{aligned}
\phi(x, y, z) = & \frac{2V_0}{\pi^2} \int_0^\infty dm \int_0^\infty dn \int_{-\infty}^{+\infty} d\alpha \int_0^\infty d\beta f(\alpha, \beta) \cos(nz - \varepsilon) \cos(n\beta - \varepsilon) \\
& \cos m(\alpha - x) \frac{e^{-|y|} \sqrt{m^2 + n^2}}{\sqrt{m^2 + n^2}} \\
& + \frac{2V_0^3}{\rho g} \int_0^\infty \frac{dm}{V_0^2} \int_{-\infty}^{+\infty} d\alpha \int_0^\infty d\beta f(\alpha, \beta) \sin \left[m(\alpha - x) - m|y| \sqrt{\frac{m^2 V_0^4}{g^2} - 1} \right] m e^{\frac{-m^2 V_0^2}{g} (z + \beta)} \\
& \frac{1}{\sqrt{\frac{m^2 V_0^4}{g^2} - 1}} \\
& + \frac{2V_0^2}{\rho g} \int_0^\infty \frac{dm}{V_0^2} \int_{-\infty}^{+\infty} d\alpha \int_0^\infty d\beta f(\alpha, \beta) \cos m(\alpha - x) e^{\frac{-m^2 V_0^2}{g} (z + \beta)} m e^{\frac{-m|y| \sqrt{1 - \frac{m^2 V_0^4}{g^2}}}{\sqrt{1 - \frac{m^2 V_0^4}{g^2}}}}
\end{aligned}$$

with $\operatorname{tg} \varepsilon = - \frac{V_0^2}{g} \frac{m}{n}$

Isobars and wave making resistance

Differentiating the potential expression, we get the isobars equations : $\zeta(x, y; z_0) = - \frac{V_0}{g} \frac{\partial \phi}{\partial x} \Big|_{z=z_0}$

The wave making resistance is obtained by integrating the pressures along the hull :

$$R = 2\rho g \iint_{S_P} \zeta(x, 0; z) \, dn \, dz$$

where S_P is the domain bounded by the hull projection on the vertical plane.

THE METHOD OF WEDGES

The principle of the method of wedges is to decompose the hull into elementary elements, the "wedges", for which we know how to compute the isobars by integrating the MICHELL equation.

The functions H

The functions H defined by $\zeta = 2k \frac{v_o^2}{g} H$, where k is a coefficient depending on the hull geometry, were tabulated by GUILLOTON. The calculations were made with $\frac{v_o^2}{g} = 2.5$ meters.

Example of computation

Since the functions H are tabulated for $\frac{v_o^2}{g} = 2.5$ meters, the size of the computational model is obtained by a FROUDE similitude :
 $\frac{v^2}{gL_R} \Big|_{\text{real}} = \frac{v_o^2}{gL_m} \Big|_{\text{model}}$ that is $L_m = \frac{2.5g}{v^2} L_R$. The spacing between wedges is constant, the number of wedges used to represent the ship hull is a decreasing function of the speed.

Practically, the use of wedges leads to the following approximations :

- the stem and the stern are represented with steps
- the hull sections are polygonal contours
- the waterlines are represented by parabolic lines of constant length.

Calculation of the resistance

The isobars are calculated by integrating the influence of each wedge in each point. Then the wave making resistance can be determined by a double integration of the MICHELL equation.

THE GUILLOTON TRANSFORMATION

The GUILLOTON transformation consists in determining, from a "linearised" hull for which the MICHELL problem is solved, a "real" hull defined by the following equations :

$$X = x + \int_0^x \left[\sqrt{\frac{1 - \frac{2g}{v_o^2} \zeta}{1 + \left(\frac{\partial \eta}{\partial x}\right)^2 + \left(\frac{\partial \zeta}{\partial x}\right)^2}} - 1 \right] dx$$

$$Y = \eta(x, z)$$

$$Z = z + \zeta(x, z)$$

Properties

- The wave making resistance is not affected by this transformation
- The linearised free surface condition and the gliding condition over the real hull are satisfied with a better accuracy than in the MICHELL problem.
- The LAPLACE equation is now : $\frac{v^2}{v_o^2} \frac{\partial^2 \phi}{\partial x^2} + \frac{\partial^2 \phi}{\partial y^2} + \frac{\partial^2 \phi}{\partial z^2} = 0$ with $v = |\text{grad } \phi|$; this expression is not far from $\Delta \phi = 0$
- This transformation, refining the mathematical model of the wave resistance problem, is not any more valid when the stem angle of the hull becomes too wide.

Practical setting

We do not know the "linearised" hull giving the expected real ship. We then begin by choosing the hull to be computed as linearised one and we determine the corresponding real one. This real hull is compared to the hull to be computed and we modify the widths of the linearised hull in consequence. The wave making resistance is computed from the isobars on the real hull. From the new linearised hull, we find a new real hull and this is made until the wave making resistance becomes a constant within one per cent from a computation to the following.

RESULTS

WIGLEY hull

The results are good for FROUDE numbers up to 0.4. Beyond this value, the wave making resistance is under estimated. We have to note that, on the one hand, the computer program does not take care of the hull trim and sinkage and, on the other hand, at those speeds, the hull representation by wedges is very rough.

INUID S 201

Up to a FROUDE number of 0.5, the shape of the computed wave making resistance curve is similar to the experimental one, bumps and hollows are in good position. Beyond this FROUDE number of 0.5, the

remark made for the WIGLEY hull is still valid.

Series 60

The computed points are quite good up to a FROUDE number of 0.3. However, we find a hollow in the wave making resistance curve for $F_n = 0.32$ which does not appear in the experimental results. We must note that the experimental and the computed wave elevations along the hull are not any more similar beyond $F_n = 0.3$. This can be due to fluid flow detachments at the stern which cannot be studied with GUILLOTON method.

Hoffman Tanker

This hull has a too wide angle of stem to be computed by the GUILLOTON method, such as we use it. The iterative procedure does not converge.

BIBLIOGRAPHY

- R. GUILLOTON
"Contribution à l'étude des carènes minces" Juin 1939
Thèses de Doctorat ès Sciences, Presses Universitaires de France
- R. GUILLOTON
"Potential theory of wave resistance of ships, with tables for its calculation"
Transactions S.N.A.M.E. Vol. 59 - 1951
- R. GUILLOTON
"Compléments sur le potentiel linéarisé avec surface libre appliqué à l'étude des carènes"
A.T.M.A. - Paris 1956
- R. GUILLOTON
"L'étude théorique du bateau en fluide parfait"
A.T.M.A. Paris 1964
- R. GUILLOTON
"La Pratique du calcul des isobares sur une carène linéarisée"
A.T.M.A. Paris 1965

FORMAT FOR TABULATED VALUES OF WAVE RESISTANCE

P. Guével / Guilloton method

WIGLEY		INUID S 201		SERIES 60	
F_n	C_w	F_n	C_w	F_n	C_w
0.266	$1.15 \cdot 10^{-3}$	0.255	$3.64 \cdot 10^{-3}$	0.220	$0.59 \cdot 10^{-3}$
0.313	$1.88 \cdot 10^{-3}$	0.287	$6.36 \cdot 10^{-3}$	0.250	$0.72 \cdot 10^{-3}$
0.350	$1.86 \cdot 10^{-3}$	0.319	$6.39 \cdot 10^{-3}$	0.280	$1.80 \cdot 10^{-3}$
0.402	$2.44 \cdot 10^{-3}$	0.360	$5.38 \cdot 10^{-3}$	0.300	$1.95 \cdot 10^{-3}$
0.452	$3.19 \cdot 10^{-3}$	0.440	$1.09 \cdot 10^{-2}$	0.320	$1.63 \cdot 10^{-3}$
0.482	$3.40 \cdot 10^{-3}$	0.525	$1.19 \cdot 10^{-2}$	0.350	$2.90 \cdot 10^{-3}$
		0.650	$9.13 \cdot 10^{-3}$		

FORMAT FOR TABULATED VALUE OF WAVE ELEVATION

P. Guével / Guilloton method

Wigley / Fn = 0.266		Wigley / Fn = 0.313		Wigley / Fn = 0.350		Wigley / Fn = 0.402	
x/L	$\eta(x)$	x/L	$\eta(x)$	x/L	$\eta(x)$	x/L	$\eta(x)$
-1.	0.088	-1.	0.066	-1.	0.054	-1.	0.040
-0.94	0.290	-0.91	0.249	-0.88	0.221	-0.85	0.183
-0.88	0.242	-0.83	0.186	-0.78	0.148	-0.70	0.098
-0.82	0.129	-0.74	0.067	-0.66	0.026	-0.55	-0.014
-0.75	-0.006	-0.64	-0.055	-0.54	-0.085	-0.38	-0.101
-0.60	-0.170	-0.54	-0.139	-0.413	-0.148	-0.21	-0.141
-0.52	-0.190	-0.44	-0.165	-0.282	-0.150	-0.03	-0.130
-0.45	-0.149	-0.33	-0.162	-0.151	-0.139	0.13	-0.119
-0.37	-0.110	-0.22	-0.117	-0.02	-0.103	0.30	-0.094
-0.30	-0.054	-0.12	-0.084	0.106	-0.079	0.47	-0.078
-0.16	-0.006	-0.02	-0.051	0.232	-0.053	0.64	-0.057
-0.01	-0.028	0.08	-0.033	0.36	-0.041	0.80	-0.034
0.130	-0.076	0.18	-0.025	0.48	-0.029	0.96	-0.001
0.28	-0.102	0.28	-0.029	0.60	-0.030	1.02	0.033
0.43	-0.090	0.38	-0.038	0.728	-0.031		
0.58	-0.056	0.48	-0.053	0.851	-0.024		
0.72	-0.015	0.58	-0.067	0.97	-0.006		
0.78	-0.0077	0.68	-0.078	1.01	0.021		
0.86	-0.005	0.78	-0.078				

FORMAT FOR TABULATED VALUE OF WAVE ELEVATION

P. Guével / Guilloton method

Wigley / Fn = 0.266 cont'd		Wigley / Fn = 0.313 cont'd		Wigley Fn = 0.452		Wigley Fn = 0.482	
x/L	$\eta(x)$	x/L	$\eta(x)$	x/L	$\eta(x)$	x/L	$\eta(x)$
0.92	0.023	0.88	-0.054	-1	0.032	-1	0.027
0.99	0.080	0.98	-0.006	-0.81	0.154	-0.78	0.136
1.01	0.105	1.02	0.034	-0.62	0.057	-0.56	0.037
				-0.42	-0.046	-0.33	-0.056
				-0.20	-0.108	-0.09	-0.109
				0.01	-0.130	0.16	-0.123
				0.228	-0.113	0.40	-0.102
				0.44	-0.109	0.64	-0.095
				0.66	-0.094	0.88	-0.080
				0.86	-0.056	1.02	-0.032
				1.03	-0.001		

FORMAT FOR TABULATED VALUE OF WAVE ELEVATION

P. Guével / Guilloton method

Inuid S201 / Fn = 0.255		Inuid S201 / Fn = 0.287		Inuid S201 / Fn = 0.319		Inuid S201 / Fn = 0.360	
x/L	$\eta(x)$	x/L	$\eta(x)$	x/L	$\eta(x)$	x/L	$\eta(x)$
-1.	0.209	-1.	0.168	-1.	0.140	-1.	0.111
-0.954	0.592	-0.939	0.520	-0.921	0.468	-0.895	0.402
-0.911	0.457	-0.880	0.377	-0.844	0.301	-0.790	0.213
-0.861	0.226	-0.812	0.157	-0.756	0.080	-0.672	0.018
-0.735	-0.218	-0.734	-0.069	-0.547	-0.244	-0.541	-0.127
-0.663	-0.319	-0.648	-0.235	-0.434	-0.290	-0.401	-0.247
-0.589	-0.362	-0.462	-0.305	-0.318	-0.307	-0.255	-0.288
-0.514	-0.313	-0.368	-0.289	-0.203	-0.257	-0.109	-0.281
-0.441	-0.253	-0.276	-0.230	-0.091	-0.195	0.036	-0.219
-0.302	-0.067	-0.187	-0.140	0.018	-0.108	0.177	-0.160
-0.236	0.001	-0.101	-0.066	0.123	-0.046	0.314	-0.088
-0.172	0.034	0.017	0.000	0.226	-0.005	0.447	-0.051
-0.043	-0.005	0.063	0.023	0.328	-0.004	0.579	-0.029
0.091	-0.143	0.146	0.007	0.430	-0.034	0.710	-0.052
0.161	-0.205	0.229	-0.039	0.534	-0.069	0.841	-0.073
0.233	-0.245	0.314	-0.110	0.639	-0.113	0.971	-0.058
0.306	-0.244	0.402	-0.176	0.746	-0.172	1.026	0.006
0.449	-0.166	0.498	-0.220	0.855	-0.201		
0.517	-0.106	0.588	-0.231	0.961	-0.163		

FORMAT FOR TABULATED VALUE OF WAVE ELEVATION

P. Guével / Guilloton method

cont ^d Inuid S201 / Fn = 0.255		cont ^d Inuid S201 / Fn = 0.287		cont ^d Inuid S201 / Fn = 0.319	
x/L	$\eta(x)$	x/L	$\eta(x)$	x/L	$\eta(x)$
0.584	-0.023	0.672	-0.201	1.032	-0.040
0.648	0.024	0.761	-0.179		
0.712	0.033	0.847	-0.127		
0.775	-0.008	0.931	-0.092		
0.841	-0.055	1.010	0.038		
0.906	-0.106	1.033	0.147		
0.971	-0.108				
1.020	0.032				

FORMAT FOR TABULATED VALUE OF WAVE ELEVATION

P. Guével / Guilloton method

Inuid S201 / Fn = 0.440		Inuid S201 / Fn = 0.525		Inuid S201 / Fn = 0.650	
x/L	$\eta(x)$	x/L	$\eta(x)$	x/L	$\eta(x)$
-1.	0.073	-1.	0.048	-1.	0.028
-0.833	0.304	-0.751	0.218	-0.602	0.130
-0.665	0.106	-0.498	0.029	-0.194	-0.035
-0.477	-0.067	-0.220	-0.119	0.244	-0.163
-0.274	-0.173	0.075	-0.193	0.699	-0.199
-0.062	-0.236	0.377	-0.226	1.033	-0.119
0.153	-0.234	0.679	-0.210		
0.367	-0.220	0.972	-0.155		
0.578	-0.176	1.048	-0.114		
0.784	-0.161				
0.984	-0.098				
1.051	-0.024				

FORMAT FOR TABULATED VALUE OF WAVE ELEVATION

P. Guével / Guilloton method

Serie 60 / Fn = 0.22		Serie 60 / Fn = 0.25		Serie 60 / Fn = 0.28		Serie 60 / Fn = 0.30	
x/L	$\eta(x)$	x/L	$\eta(x)$	x/L	$\eta(x)$	x/L	$\eta(x)$
-1	0.108	-1	0.091	-1	0.074	-1	0.066
-0.96	0.288	-0.94	0.269	-0.93	0.245	-0.92	0.234
-0.92	0.274	-0.89	0.251	-0.86	0.238	-0.84	0.230
-0.88	0.233	-0.84	0.219	-0.80	0.212	-0.77	0.202
-0.80	0.124	-0.79	0.166	-0.73	0.157	-0.69	0.143
-0.70	0.022	-0.67	0.031	-0.66	0.084	-0.605	0.059
-0.61	-0.52	-0.61	-0.037	-0.51	-0.097	-0.52	-0.043
-0.51	-0.083	-0.48	-0.141	-0.43	-0.166	-0.43	-0.143
-0.41	-0.108	-0.36	-0.173	-0.34	-0.230	-0.33	-0.221
-0.31	-0.146	-0.29	-0.173	-0.17	-0.266	-0.24	-0.287
-0.21	-0.181	-0.22	-0.18	-0.08	-0.238	-0.13	-0.300
-0.11	-0.200	-0.15	-0.173	0	-0.176	-0.03	-0.266
-0.00	-0.141	-0.09	-0.162	0.08	-0.087	0.06	-0.189
0.09	-0.066	0.04	-0.098	0.16	-0.040	0.16	-0.120
0.19	-0.055	0.11	-0.068	0.24	-0.021	0.25	-0.047
0.29	-0.147	0.17	-0.072	0.32	-0.067	0.34	-0.040
0.40	-0.227	0.23	-0.103	0.40	-0.137	0.43	-0.058
0.50	-0.177	0.36	-0.207	0.48	-0.187	0.52	-0.093
0.60	-0.066	0.43	-0.216	0.56	-0.186	0.61	-0.107

FORMAT FOR TABULATED VALUE OF WAVE ELEVATION

P. Guével / Guilloton method

Serie 60 / Fn = 0.22 Cont'd		Serie 60 / Fn = 0.25 cont'd		Serie 60 / Fn = 0.28 cont'd		Serie 60 / Fn = 0.30 cont'd	
x/L	$\eta(x)$	x/L	$\eta(x)$	x/L	$\eta(x)$	x/L	$\eta(x)$
0.69	-0.003	0.50	-0.165	0.66	-0.137	0.70	-0.069
0.79	0.062	0.63	-0.054	0.72	-0.058	0.79	-0.009
0.83	0.086	0.75	0.045	0.802	+0.008	0.88	0.024
0.87	0.101	0.81	0.088	0.88	0.081	0.96	0.088
0.92	0.110	0.86	0.111	0.94	0.148	0.99	0.196
0.96	0.142	0.92	0.093	0.99	0.287		
0.99	0.271	0.97	0.160				
		0.99	0.228				

FORMAT FOR TABULATED VALUE OF WAVE ELEVATION

P. Guével / Guilloton method

Serie 60 / Fn = 0.32		Serie 60 / Fn = 0.35		Serie 60 / Fn = 0.32 cont'd	
x/L	$\eta(x)$	x/L	$\eta(x)$	x/L	$\eta(x)$
-1	0.060	-1	0.050	0.93	0.077
-0.91	0.228	-0.89	0.214	0.99	0.189
-0.82	0.229	-0.78	0.222		
-0.73	0.189	-0.68	0.168		
-0.64	0.111	-0.57	0.073		
-0.55	0.013	-0.45	-0.041		
-0.45	-0.094	-0.33	-0.156		
-0.34	-0.198	-0.19	-0.257		
-0.23	-0.266	-0.06	-0.310		
-0.12	-0.300	+0.08	-0.307		
-0.00	-0.281	0.21	-0.249		
0.11	-0.231	0.35	-0.207		
0.22	-0.137	0.48	-0.116		
0.33	-0.091	0.60	-0.032		
0.43	-0.047	0.72	0.055		
0.53	-0.038	0.83	0.077		
0.63	-0.026	0.94	0.103		
0.73	-0.004	0.991	0.224		
0.83	0.022				

Discussion

by G. E. Gadd
of paper by Guevel, et al.

Do the authors find any difficulties with convergence near the keel of a hull form with a flat bottom? Again, for a ship with a bulbous bow, isobars might cross over one another since the dynamic pressure at the side of the bulb might be considerably less than at some points at lesser depth. Would this invalidate the method?

Author's Reply

by Guevel, et al.
to discussions by G. E. Gadd

When the GUILLOTON's transformation is applied to hulls with flat bottom, the "linearised" model is computed with some difficulties: the width corrections near the bottom of the hull can become very large. This is a reason why we chose as a convergence criterion the fact that the pressure remains a constant on each waterline. In spite of this precaution, the convergence is not always warranted for hulls with flat bottom, low draft and more generally in cases where the bottom contributes greatly in the wave resistance.

This method cannot be used for hulls with bulbous bow for two reasons:

-- It is difficult to discretise spheric surfaces with parabolic elements for the waterlines and polygonal contours for the sections. It is not possible to compute with enough accuracy the wave resistance of such hulls by the wedge method.

-- The GUILLOTON's transformation described in paper /1/ is not any more valid for bows presenting a too wide angle. We have made trials just "to see," they gave unstable results (without converging) and the wave resistance was less than zero!

/1/ L'étude théorique du bateau en fluide parfait, ATMA Paris 1964

The Calculation of Ship Wave Resistance Using a Surface Source Distribution

Bruce H. Adee

Department of Mechanical Engineering
University of Washington, Seattle

ABSTRACT

A surface singularity distribution technique is applied to the problem of computing the inviscid fluid flow about a ship's hull. By computing the far field disturbance of the ensemble of sources moving through the fluid, wave resistance is also obtained. Results for the Series 60, block coefficient 0.60 hull are presented for various Froude numbers.

INTRODUCTION

The surface source distribution method for computing the fluid flow about a ship's hull was developed to provide a completely theoretical scheme for predicting the fluid flow using only the offsets of the hull. No empirical corrections are used in the formulation and solution of the boundary-value problem for the velocity potential.

The original goal in applying this scheme was to provide a series of computer programs which would yield:

- (1) the individual source strengths associated with the surface source distribution,
- (2) the velocity distribution at discrete points on the hull surface,
- (3) the hull surface streamlines, including the free-surface elevation,
- (4) the development of the three-dimensional boundary layer using the hull surface streamlines as input.

To provide a further verification of the validity of the programs as well as important results, a computation of wave resistance was added to the original goals. Once the source strengths have been obtained, wave resistance may be determined using only a relatively small amount of additional computer time.

Unfortunately, the numerical procedures used in determining the inviscid fluid flow require extensive amounts of computer time. Thus, the calculations performed to date have been limited almost exclusively to the Series 60, block coefficient 0.60 hull. Because of severe constraints on the available computer time, it was only possible to extend the calculations to include a few more Froude numbers rather than to other hulls used in the workshop.

THE SURFACE SOURCE DISTRIBUTION METHOD

This method for computing the inviscid fluid flow about a ship's hull is discussed in detail in previous papers [1,2,3]. An overview of the important points is included here to provide a foundation for the numerical results.

An inconsistent mathematical approach has been adopted in formulating the boundary-value problem for the velocity potential. While a linearized free-surface boundary condition is retained, the hull-surface boundary condition is satisfied on the actual hull surface rather than on the centerplane. In addition, the contribution of a line integral at the waterline which appears under this formulation has been ignored.

To solve the boundary-value problem, the source distribution is represented by a source density function times a Green function integrated over the wetted surface when the ship is at rest. The Green function is chosen so that the velocity potential satisfies the Laplace equation and all the boundary conditions except the hull-surface boundary condition. Satisfaction of the hull-surface boundary condition then determines the source-density function.

Surface Platelets

From the table of offsets for a ship, the first computer program divides the hull into flat-plate elements. Four points from the offset table are used to form each element. The normal is determined by taking the cross product of the two vectors connecting diagonally opposed corners. The platelet is completely determined by assuming that a point located by taking the average of the four corner coordinates lies on the platelet. This point is also taken as the control point where the hull-surface boundary condition is satisfied.

Source Density Function and Source Strength

The source density function is assumed to be constant over each individual platelet even though the hull-surface boundary condition is satisfied only at the control point. A "Kelvin" or "Havelock" source of unit strength is placed at each of the control points and the effect of each source at every control point on the hull is determined. Since the Green function must be evaluated more times than the square of the

number of control points, computer time is the most important limiting factor. Under the numerical schemes used at present, this places a practical limit of about 150 points on the number of platelets used to represent one side of the hull.

Once the matrix of Green function influence coefficients has been formed, the linear equation representing the hull-surface boundary condition is solved for the actual source strength by inverting the influence coefficient matrix. The fluid velocity at the control points is then obtained by matrix multiplication.

WAVE RESISTANCE

At this point in the calculation procedure a known distribution of discrete source points is moving into the undisturbed fluid at constant velocity. The wave resistance for this ensemble of sources is computed by determining their effect on surface elevation in the far field. This again requires the evaluation of a matrix of influence coefficients related to the disturbance of each individual source.

SERIES 60, BLOCK COEFFICIENT 0.60

Results of the wave resistance calculations are presented in Table 1, where the hull is approximated by 100 sources. The table includes calculations published previously and those done specifically for this workshop. (Froude number throughout is based on the waterline length.)

Table 1. Wave resistance coefficient for the series 60, block coefficient 0.60 hull using 100 source points

F_n	C_W
0.220	3.06×10^{-3}
0.257	0.43×10^{-3}
0.280	2.18×10^{-3}
0.300	2.78×10^{-3}
0.320	2.64×10^{-3}
0.342	2.10×10^{-3}

Comparative calculations for this hull have shown that there is considerable difference in the wave resistance coefficient when less than 100 sources are used. For two of the above Froude numbers calculations were made using 144 sources. Compared to the 100 source calculations, there is negligible difference.

Free-surface elevation may be found using the free-surface boundary condition. For these calculations the velocity potential is not available for points at the undisturbed waterline. Under the assumption that the source density is constant over each platelet, the potential at the control point nearest the free surface is used to evaluate the wave profile along the hull. An improvement in these calculations might be achieved by establishing a thin layer of platelets near the free surface. Unfortunately this adds considerably to computation costs and has not been attempted to date.

Predicted free-surface elevations along the hull are given in Table 2. These are presented in the nondimensional form

$$\eta(x) = \frac{2 \phi_x(x, -b, z)}{V}$$

where

$\phi_x(x, -b, z)$ = derivative with respect to x of the velocity potential at a control point a distance b below the free surface,

V = forward speed.

Table 2. Nondimensional free surface elevation for the series 60, block coefficient 0.60 hull using 100 source points

	$F_n=0.220$	$F_n=0.257$	$F_n=0.280$	$F_n=0.320$	$F_n=0.342$
x/L_{BP}^*	$\eta(x)$	$\eta(x)$	$\eta(x)$	$\eta(x)$	$\eta(x)$
0.475	0.214	0.1560	0.136	0.09930	0.0840
0.425	0.217	0.2090	0.199	0.16400	0.1450
0.375	0.148	0.1850	0.197	0.19100	0.1870
0.325	0.092	0.1320	0.154	0.18000	0.1850
0.275	0.016	0.0519	0.083	0.13300	0.1450
0.225	0.045	-0.0436	-0.143	0.05130	0.0793
0.175	-0.084	-0.1500	-0.134	-0.06400	-0.0202
0.125	-0.056	-0.1110	-0.148	-0.16300	-0.1390
0.075	-0.123	-0.1850	-0.146	-0.13600	-0.1440
0.025	-0.124	-0.1130	-0.174	-0.16000	-0.1430
-0.025	-0.106	-0.0599	-0.104	-0.16400	-0.1630
-0.075	-0.019	-0.0295	-0.041	-0.14400	-0.1580
-0.125	-0.052	-0.0245	-0.012	-0.08940	-0.1370
-0.175	-0.123	-0.0854	-0.021	-0.06210	-0.1070
-0.225	-0.198	-0.1240	-0.089	-0.03820	-0.0836
-0.275	-0.052	-0.1420	-0.115	-0.01280	-0.0458
-0.325	0.112	-0.1150	-0.143	-0.00337	-0.0216
-0.375	0.017	0.0430	-0.110	0.00393	0.0268
-0.425	0.247	0.2620	-0.118	-0.13100	0.0231
-0.475	0.357	0.4620	-0.054	-0.10200	-0.0168

Computer time required to perform the calculation is given in Table 3.

*Editor's Note: FP and AP are $x/L_{pp} = 0.5$ and -0.5 , respectively, in this paper.

Table 3. Computer time required for source strength and wave resistance calculations

<u>Froude Number</u>	<u>Source Strengths</u>	<u>Wave Resistance</u>
0.220	2.47 hours	0.36 hours
0.257	3.21	
0.280	3.51	0.87
0.300	3.54	
0.320	3.55	0.87
0.342	4.71	

CONCLUSION

For the higher Froude numbers above 0.25, the results are as good as previous wave resistance estimates using a centerplane source distribution. In fact, the large "bump" in wave resistance predicted by centerplane source distribution techniques in the region of Froude number equal to 0.3 is lessened considerably by the surface source distribution method.

Unfortunately the widespread application of this technique for testing is still severely restricted by the cost of performing the calculations. Three and four hours of computer time for each speed are excessive and could be significantly reduced by using several quadrature techniques which have become available.

Lack of time prevented a complete investigation of why the computation seems to "blow up" at the lower Froude number (0.22). In the numerical evaluation of the Green function spacing between ordinates and the point of truncation for the infinite integrals is controlled by a series of logical control routines. These algorithms were determined by conducting a large number of numerical experiments to find the correct values of ordinate spacing and truncation point to achieve accuracy. All of these experiments were performed for Froude numbers of 0.257 and higher. Further testing for lower Froude numbers may indicate that the logical control routines should be improved for lower Froude numbers. Another indication that this is possible is the reduction in computer time required for the calculation at lower Froude numbers. Here one

would expect more balance because as Froude number decreases the intergrand oscillates more slowly, but the exponential portion also decreases more slowly.

The surface source distribution method for computing fluid flow about a ship's hull continues to hold the promise of reasonable results. The efficiency of the calculation must be increased and it must be applied to many situations to improve the logical control portion of the program.

REFERENCES

1. Adee, B. H., "Calculation of the Streamlines About a Ship Assuming a Linearized Free-Surface Boundary Condition," Journal of Ship Research, Vol. 17, No. 3, Sept. 1973, pp. 140-146.
2. Adee, B. H., "Fluid Flow Around a Ship's Hull," Proceedings First International Conference on Numerical Ship Hydrodynamics, 20-22 October 1975, pp. 435-454.
3. Adee, B. H., "Wave-Making and Frictional Resistance for Practical Ship Forms," International Seminar on Wave Resistance, February 1976, pp. 333-340.

Discussion

**by G.E. Gadd
of paper by B. Adee**

Although the resistance prediction at $F_n = 0.22$ is far too high, the hull wave profile at this speed looks quite reasonable. Is it possible that there has been some computational error in the calculation of resistance?

WAVE RESISTANCE COMPUTATION BY NUMERICAL FAR FIELD WAVE SURVEY DATA

Sander Calisal
U.S. Naval Academy

ABSTRACT

Experimental wave survey methods give a wave spectrum which provides an insight into the calculations of wave resistance. As the experimental wave spectrum is relatively easy to obtain, a numerical wave survey method appears to offer a better comparison of experimental and numerical calculations. The present program can be extended to a higher order study.

INTRODUCTION

The wave resistance of ship-models can be directly calculated by wave survey methods. As these methods are based on energy flow or momentum equations and do not contain Froude's hypothesis directly, they are expected to give a better measurement of wave resistance. The measurements involved in wave survey methods are also relatively simple compared to measurements of the pressure at the hull surface. These have led to an attempt to develop a computer program based on the computation of numerical wave data. A standard computer program which can handle such data can then be chained to the calculations. Wave survey methods require only the far field data, which can be computed relatively easily compared to near field data. Ursell's (1960) far field expansion procedure can be used to compute wave height or lateral wave slope data away from the ship hull. A library of singularities such as pressure, source, and dipole can be developed to calculate the ship's numerical wave data. It is also expected that a combination of such singularities will be sufficient to represent ships such as surface effect ships, planing hulls, etc.

Gadd (1973) reported that Guilloton's method, which assigns a new location to the source distribution given by linearized theory, improves the predictions of wave resistance. As this method is based on the distribution of singularities as well, the program can be extended for the application of Guilloton's method. The computer programs under development, based on wave survey methods, have the following advantages:

a - Numerical wave spectra can be compared to easily obtainable experimental ones.

b - Far field values can be computed relatively quickly, as there is no numerical integration to be performed.

c - Programming can be extended to include higher order formulations.

d - New ship forms can possibly be represented by a set of singularities.

REPRESENTATION OF SHIP GEOMETRY

Slender ship models such as the Wigley model and the Inuids can be well represented by Thin Ship Theory. To check the accuracy of calculations based on far field expansions, a source distribution based on thin ship theory is assumed to represent the model. The Wigley model and the Inuid 201 are represented by 120 sources. The horizontal location of the source is given by:

$$\bar{x} = \frac{\int_A \sigma(x,z) x dx}{\int_A \sigma(x,z) dx}, \quad (1-a)$$

and the vertical location by:

$$z = -\frac{1}{k_0} \ln \frac{\int_A \sigma(x,z) e^{-k_0 z} dz}{\int_A \sigma(x,z) dz} \quad (1-b)$$

where A is a projected area on the plane of symmetry of the model, and σ the source strength predicted by thin ship theory. To be consistent the wave resistance values obtained by this method should compare with the Mitchell integral values.

The formulas used in computation of far field wave height and wave slope values are:

$$\zeta(\theta, N) = \frac{8\pi m k_0}{c} \left[\cos(N\nu(\theta)) \frac{P_0(\theta)}{N^{1/3}} A_1(-N^{2/3}\nu(\theta)) \right. \\ \left. + \sin(N\nu(\theta)) \frac{Q_0(\theta)}{N^{2/3}} A_1(-N^{2/3}\mu(\theta)) \right]$$

and

$$\zeta_y(\theta, N) = \frac{8\pi m k_0}{c} \left[\cos(N\nu(\theta)) N^{-2/3} Q_0(\theta) A_1(-N^{2/3}\mu(\theta)) \right. \\ \left. - \sin(N\nu(\theta)) N^{-1/3} P_0(\theta) A_1(-N^{2/3}\nu(\theta)) \right]$$

where c is ship speed, m source strength, $k_0 = \frac{g}{c^2}$, $N = k_0 \sqrt{x^2 + y^2}$, $\theta = \tan^{-1} \left(\frac{y}{x} \right)$, A_1 and A_1' the Airy function and its derivative. Further details of the computations can be found in Calisal (1976).

The computer program used to compute wave resistance from the wave survey data was developed by Reed (1969) and was also reported by Ward (1976). Two wave resistance values, one based on wave height data and the other based on wave slope data are reported separately. The difference between these two values is observed to increase as the Froude number increases. This is believed to be due to the truncation corrections required for wave height data.

As this program generates only far field data, the wave profile around the ship hull is not given. Sample wave height, wave slope and wave spectra for the Series 60 are given in Figures 1-3. Further data on spectra can be supplied on request. The author regrets that the extension of the program to include Guilloton's method cannot be reported at present.

A further source of concern is the representation of viscous effects. Recent experiments by Calisal (1979) suggest that the model Reynolds number, as well as turbulence intensity affect wave resistance. These might be significant parameters in the representation of the stern of the ship.

RESULTS

The method of calculation outlined above was first used to obtain a wave spectrum corresponding to the source distribution computed by Adey (1975) for a Series 60 C_b 60 ship. Numerical wave profiles obtained by asymptotic expression formulas and the exact formulations and their corresponding spectra are compared. The wave resistance values obtained by this method are observed to be higher than those calculated by Adey.

The application of the program to the Wigley model resulted in wave resistance values comparable to Mitchell values. Computations based on wave slope data gave higher wave resistance values. The ship is represented by panels and the source strength corresponding to each panel is obtained by the appropriate integration of the source strength

distribution given by linear theory. Figure 4 shows a comparison of the calculated values and the theoretical curve. The agreement is good with one exception, namely, the value corresponding to Froude number $Fr = 0.32$. The computed numbers are observed to be smaller than the theoretical values.

The computations for Inuid 201 are based on the interpretation of source strength by Inui. Figure 5 shows the computed values and the digitized form of the curve reported in Eggers (1967). This curve is labelled as "Theoretical wave resistance calculated by the method of Inui" in the article referred to above. While the values computed for the lower Froude numbers agree very well with the theoretical curve; the ones at higher Froude numbers show a discrepancy.

For the computation corresponding to a series 60 $C_B = 60$, the ship is defined by 120 panels. The average slope at each waterline and the projected area on the center line plane are used for the estimation of source strength based on linearized theory. Figure 6 presents the Michell's integral curve labelled "Theory" as computed by Webster and an experimental curve obtained by Ward. Both of these curves are the digitized form of the curves given by Adey (1975). Even though the computed values and the Michell's integral curve show the same trend, the agreement is seen to decrease at higher Froude numbers. In all cases the wave resistance values based on wave slope data are observed to be larger than those based on wave height data computations. It seems that a better definition of ship geometry is the next step in the computations before extending the program to higher order calculations.

About 800 points are used in the definition of numerical wave height data. Fourier analysis techniques suggest that this number can be reduced by a factor of two. 1000 CPU units were required for the generation of wave height and wave slope data composed of 800 data points for one run representing a Series 60 model. The computations of wave resistance based on the numerical data required about 50 CPU units for the same model.

BIBLIOGRAPHY

1. Adee, B., Harvey, P., "An Analysis of Ship Resistance," Department of Mechanical Engineering, University of Washington, March 1975, pp 108.
2. Calisal, S. M., "A Calculation of the Free Wave Spectrum for a Ship," U. S. Naval Academy, Division of Engineering and Weapons Report No. EW-10-76, September 1976.
3. Calisal, S. N., "An Attempt to Detect the Importance of Turbulent Boundary Layer in Ship Wave Resistance," U. S. Naval Academy, Division of Engineering and Weapons Report No. EW-4-79, June 1979.
4. Eggers, K., Sharma, S. C., and Ward, L. W., (1967), "An Assessment of some Experimental Methods for Determining the Wavemaking Characteristics of a Ship Form," Trans, SNAME, Vol. 75, pp 112-157.
5. Gadd, G. E., "Wave Resistance Calculations by Guilloton's Method," Transactions of the Royal Institution of Naval Architects, Vol. 115, pp. 377-392, 1973.
6. Reed, A. M., Sharma, S. D., "Computer Programs for the Analysis of Longitudinal Ship Wave Surveys" University of Michigan, Nov. 1969.
7. Ursell, F., "On Kelvin Ship Wave Pattern," J. Fluid Mechanics, 1969.
8. Ward, L. W., Hooff, R. W., "The Effect of Probe Location on a Model Resistance Survey Along a Longitudinal Cut," Journal of Ship Research.

FORMAT FOR TABULATED VALUES OF WAVE RESISTANCE

WIGLEY		INUID		SERIES 60 CB = 60			
F_n	C_w by W.H. C_w by W.S.	F_n	C_w by W.H. C_w by W.S.	F_n	C_w by W.H. C_w by W.S.		
0.265	.930 .943	.319	6.385 6.558	0.22	.400 .440		
0.312	1.878 1.934	.360	4.895 4.854	0.25	1.402 1.485		
0.349	1.164 1.234	.440	14.617 16.578	0.28	3.268 3.471		
0.451	3.96 6.306	.525	13.11 15.33	0.32	1.948 2.110		

TABLE 1

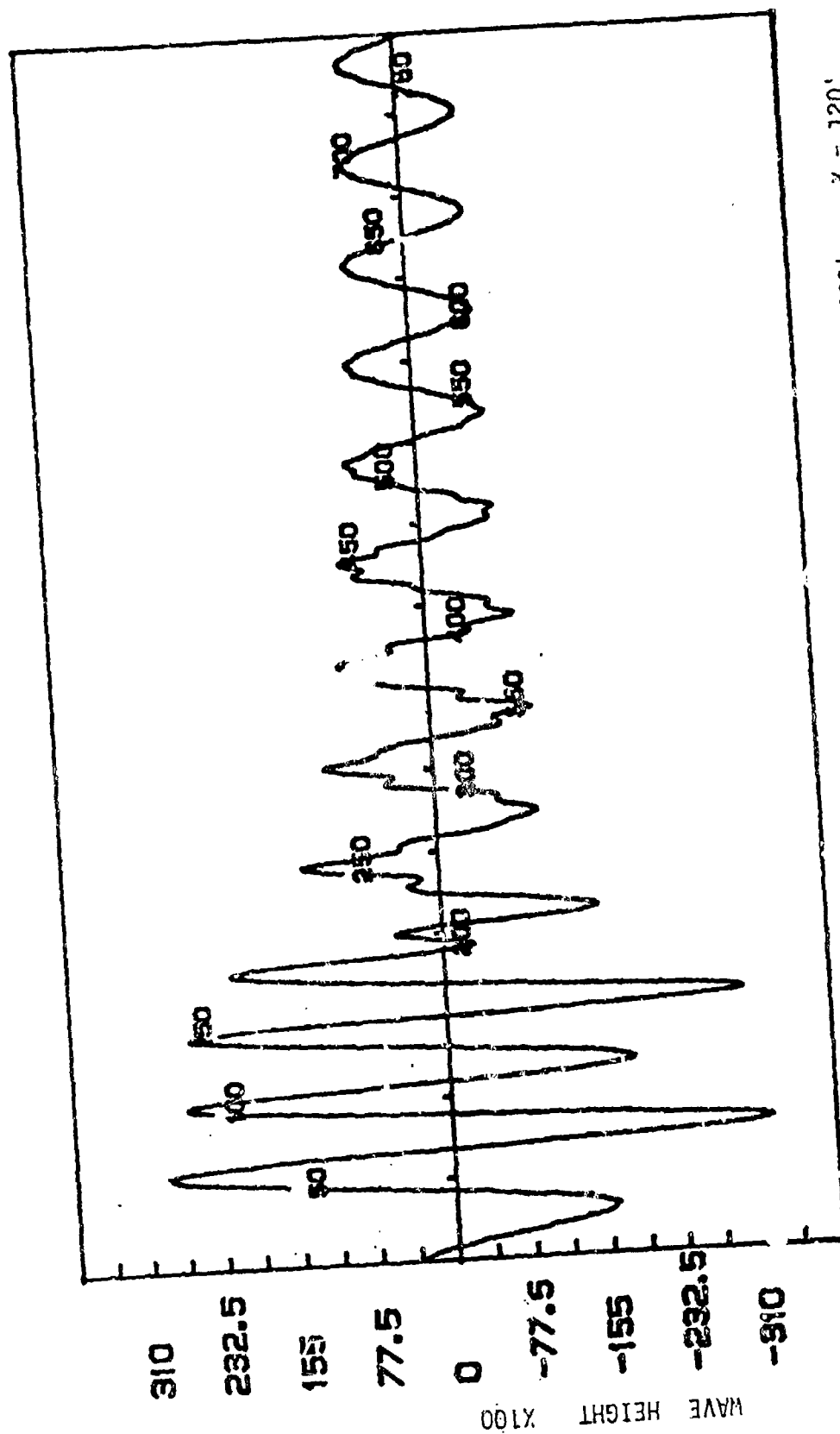
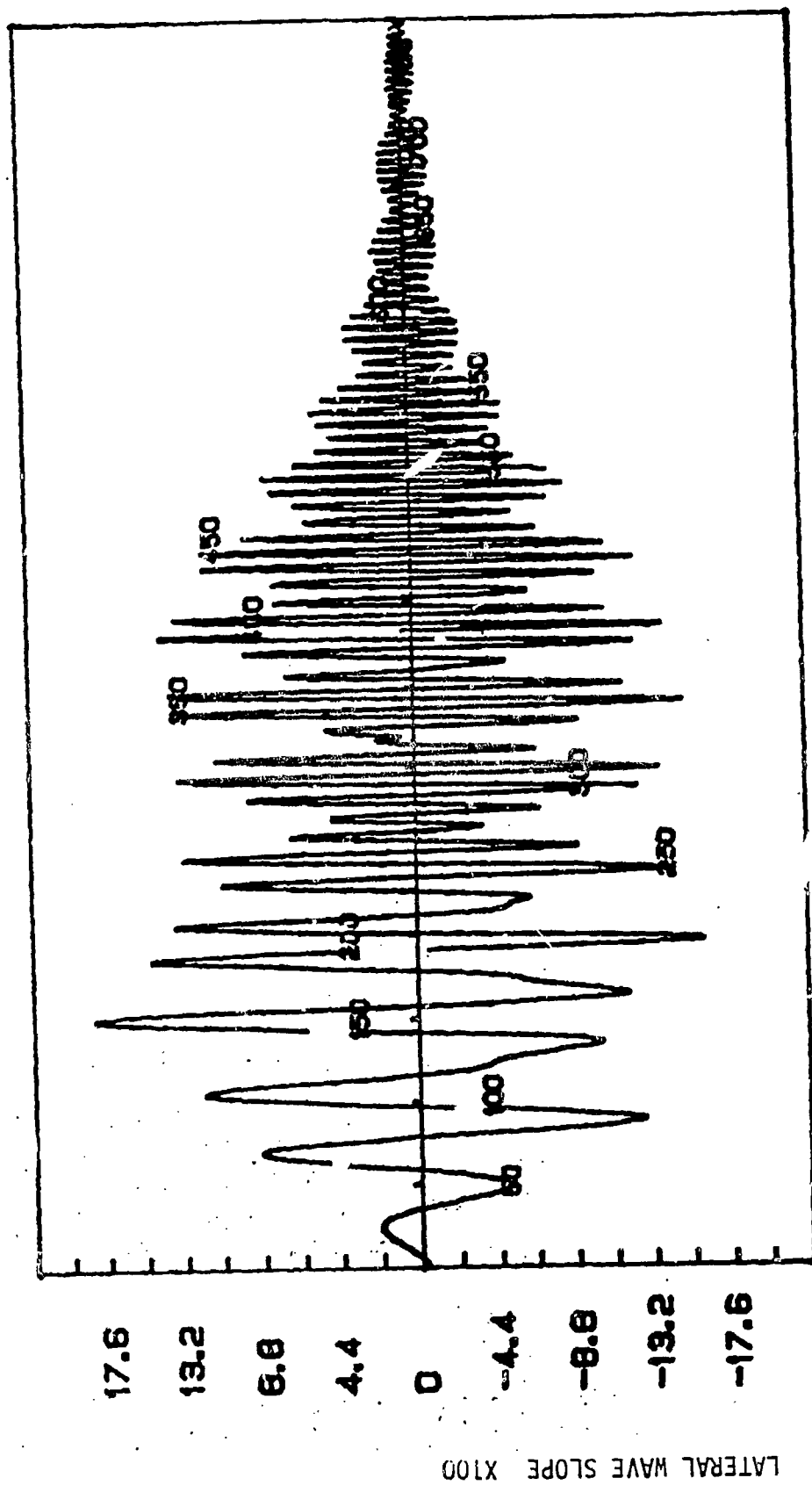


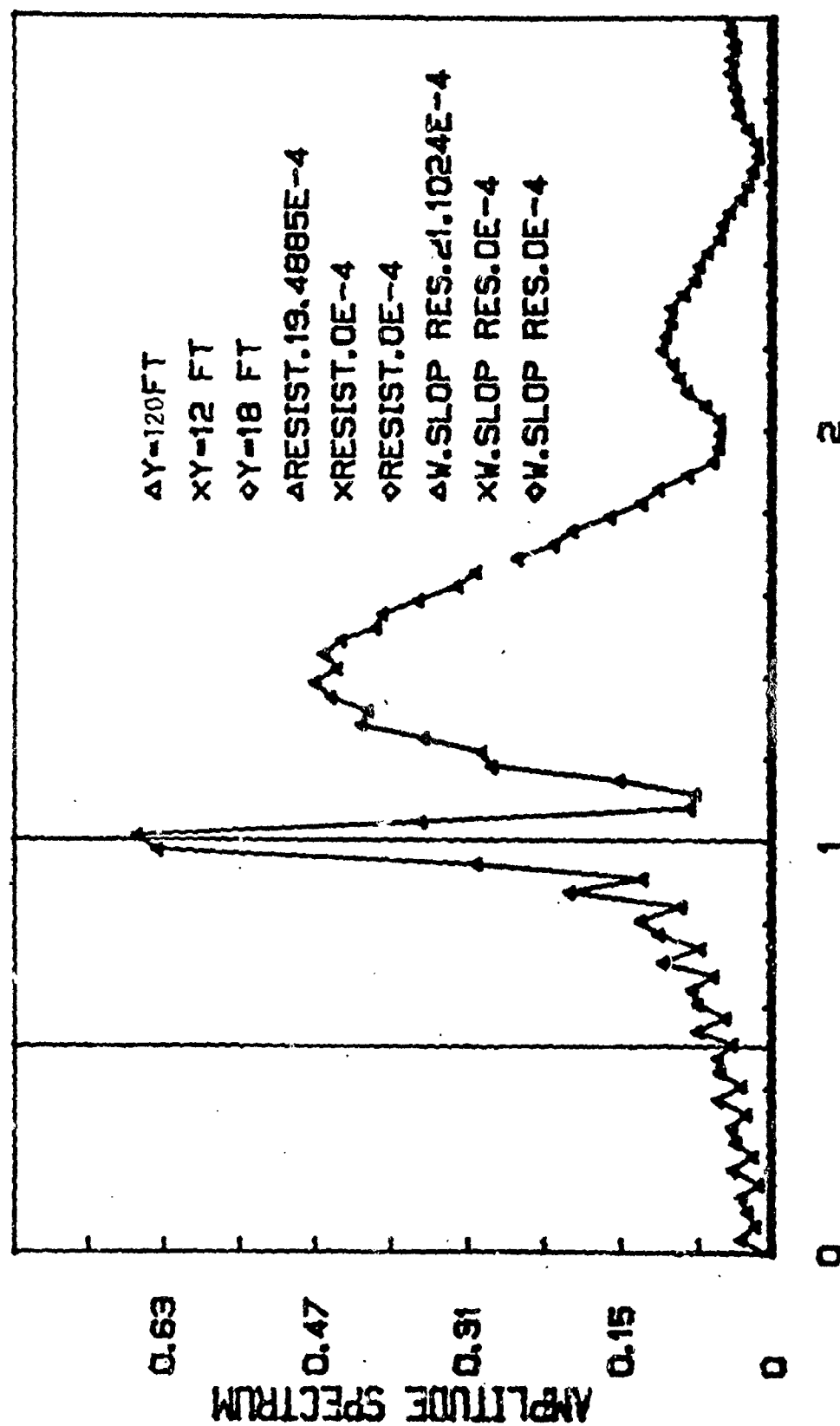
FIGURE 1



SERIES 60 CB 60 L = 400' Y = 120' FR = 0.32

Figure 2

SPECTRUM AT FROUDE NR=0.319



S VALUE SERIES 60 MODEL 104

Figure 3

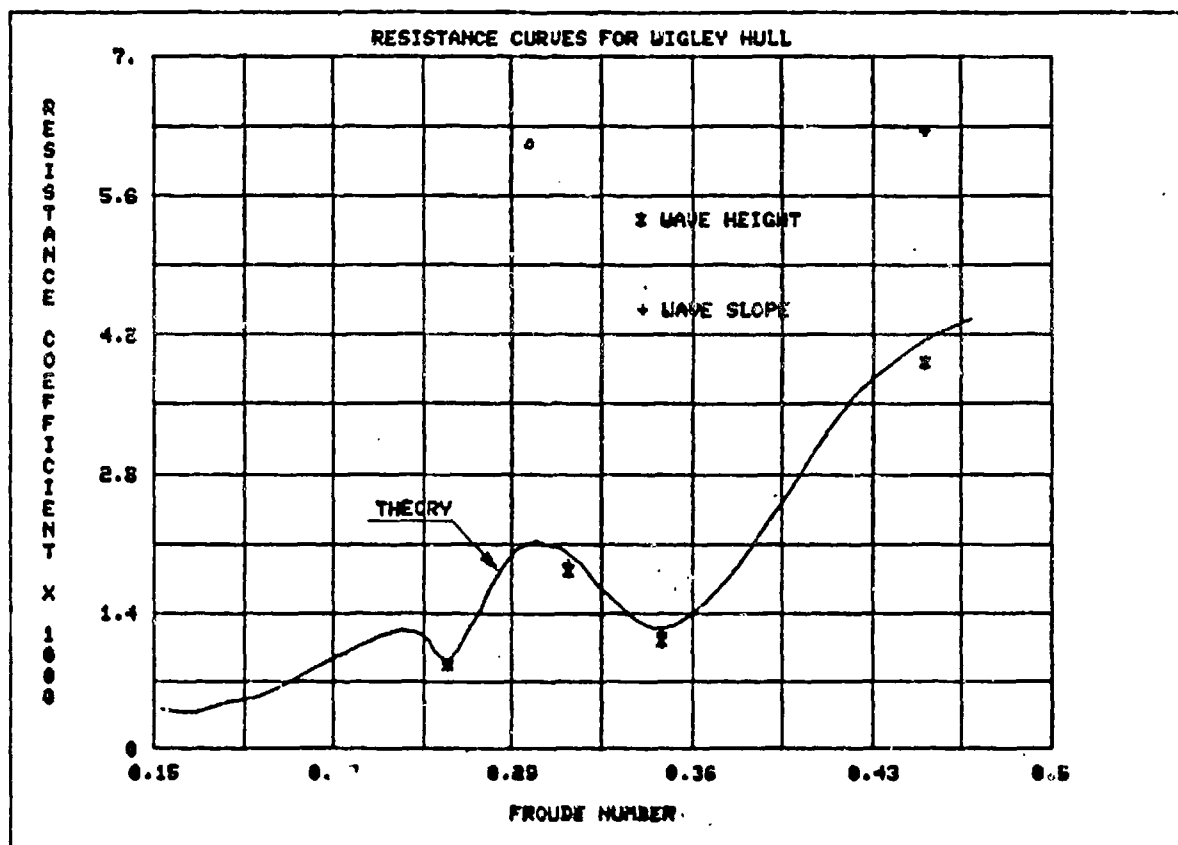


FIGURE 4

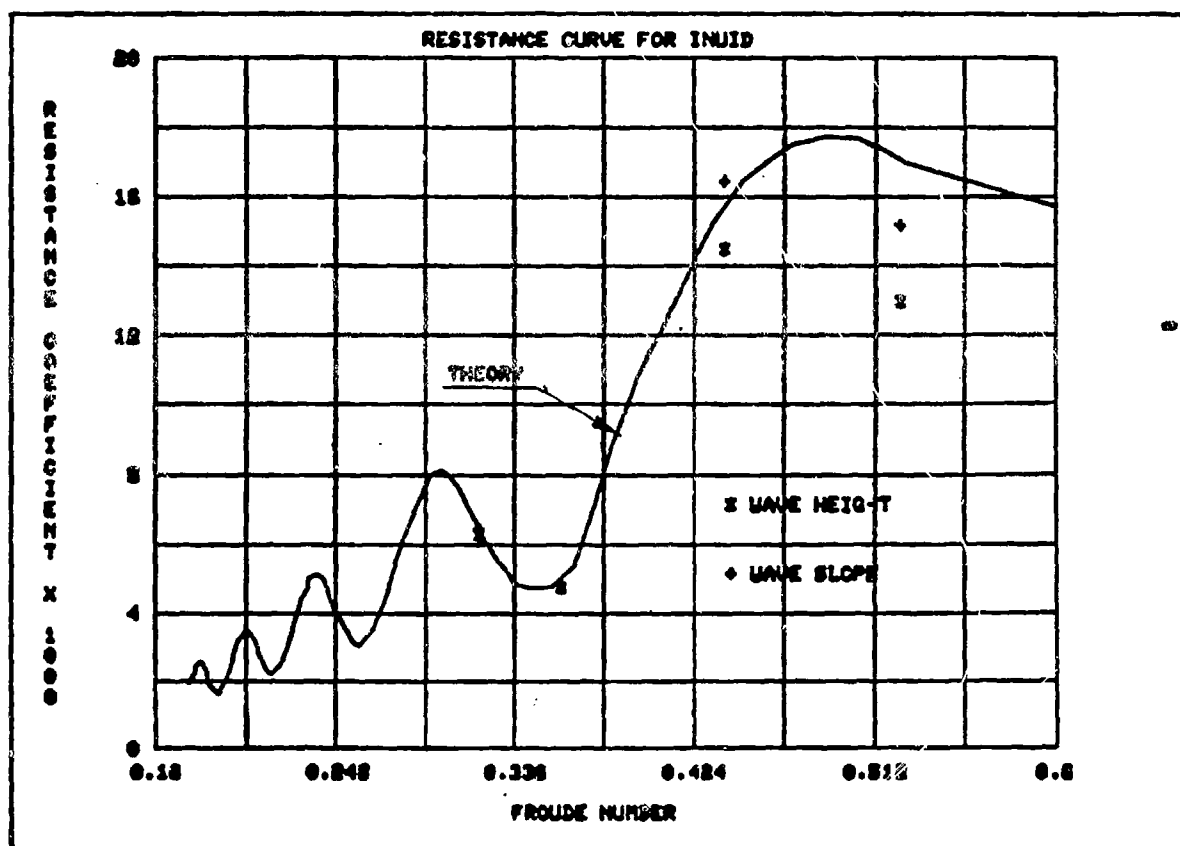


FIGURE 5

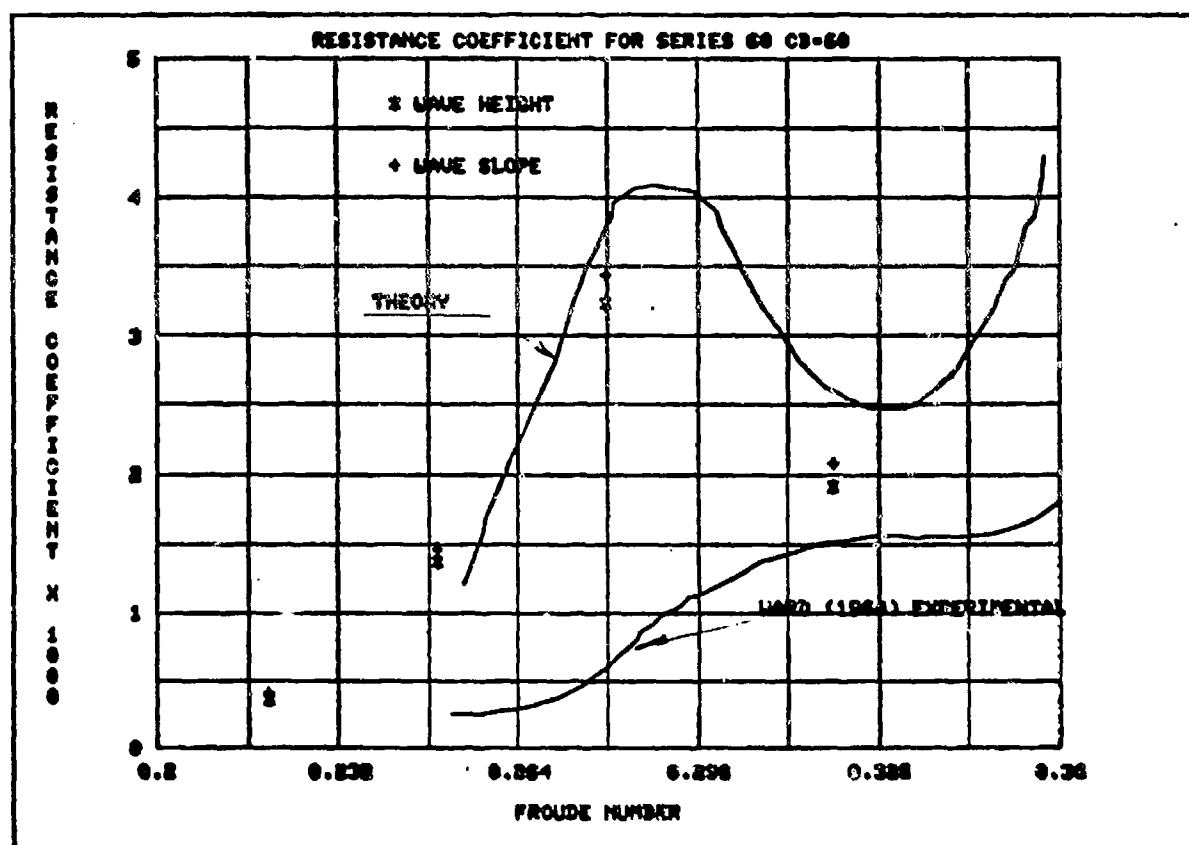


FIGURE 6

Calculation of Ship Wave Resistance Including
the Effects of Boundary Layer and Wake

Kazuhiro Mori
Kiroshima University

1. Introduction

The discrepancies between calculated wave-making resistance and experiments are being unveiled mainly from the non-linear potential theory. Calculated results are, however, always compared with experiments paying no attention to the viscous effects and they are sometimes underestimated when inviscid calculations have resulted in good agreements with experiments. On the other hand, the remaining discrepancies, if exist, are sometimes attributed to the neglect of the viscosity.

It seems to be worthwhile, for the further steps in the wave resistance theory, to make clear how far the neglect of viscosity is responsible for the existing discrepancies. For this purpose it is primarily important to predict the viscous effects based on the viscous flow theory. Unless, the yielded results are not general and not persuasive even if they compensate the gaps.

In the present paper, the effects of boundary layer and wake are entrained into the low speed theory (Baba 1976) according to the discussions in Mori(1979). Calculations are carried out for three models, the elliptic-waterplane model, say, EM-01, Wigley model and Inuid S-201 model. Their principal dimensions are shown in Table 1.

The calculated results do not compensate all of the discrepancies between the inviscid low speed theory and experiments; the stern wave reduction is realized but the phase shift of hump-hollow is not appreciated. This may be because the present scheme takes into account only the leading viscous effect term which can not yield significant phase modifica-

D 708222-MSC-119-01V2 W
ID 119 009

tions. Nevertheless, the viscous effects evaluated here will serve for further developments in the potential wave resistance theory.

2. Calculation of near wake flow

The separated near wake flow is calculated by the matched asymptotic expansion approximation (Mori-Doi 1978). EM-01 is exactly calculated while Wigley model and S-201 are calculated by its simplified method where the contributions from the retarding subregion are neglected (Mori 1980).

The ship-fixed cartesian coordinate is adopted throughout the present paper; the origin is at the midship on the still waterplane, x-axis is forward to F.P., y-axis portside and z-axis upward. All the quantities are made dimensionless by the half ship length $\ell (= L/2)$ and the ship speed U except especially specified. u , v and w are the velocity components of basic flow in x-, y- and z-directions respectively.

Calculated results of EM-01 are shown in Fig.1 compared with measured. The calculation is carried out 2-dimensionally while the measurements are carried out at the half draft with an end plate at the bottom. The calculated results show rather good agreements with experiments and they guarantee our application to the wave resistance prediction.

The velocity profiles of Wigley model and S-201 are shown in Fig.2 which are those on the free surface ($z = 0$) and will be used in the wave resistance prediction. The measured velocity profiles of the 3 m Wigley model are shown for reference which are measured at 0.01 beneath the free surface ($z = -0.01$) and whose Reynolds number, $R_n (= UL/\nu)$, is about 3.3×10^6 ; where ν is the kinematic viscosity coefficient.

In the present calculation, the separation positions are assumed at $x = 0.8$, 0.9 and 0.85 for EM-01, Wigley model and S-201 respectively. The calculations are carried out at the Froude numbers of 0.158 , 0.20 and 0.20 for EM-01, Wigley model and S-201 respectively, which correspond to $R_n = 1.29 \times 10^6$,

8.2×10^6 , 1.27×10^6 .

3. Calculation of wave-making resistance

According to the conclusion of Mori(1979), the viscosity in the ship boundary layer and wake plays a much more important role in the wave resistance than that in the free surface boundary layer and the wave resistance formula including the viscous effects is given as follows;

$$C_w = R_w / \frac{1}{2} \rho U^2 L^2 = \frac{\pi}{2} \int_0^{\frac{\pi}{2}} |c^*(\theta) + i s^*(\theta)|^2 d\theta \quad (1)$$

where C_w is the wave resistance coefficient, R_w is the wave resistance, ρ is the density, $\gamma_0 = gL/U^2$, g is the gravity acceleration and

$$c^*(\theta) + i s^*(\theta) = -\frac{\gamma_0}{\pi} \sec^{3/2} \theta \iint_{-\infty}^{\infty} D(\xi, \eta) e^{i\gamma_0 \sec^2 \theta (\xi \cos \theta + \eta \sin \theta)} d\xi d\eta \quad (2)$$

$$D(\xi, \eta) = -\frac{1}{\gamma_0} \left\{ u^2 \frac{\partial u}{\partial x} + uv \left(\frac{\partial u}{\partial x} + \frac{\partial u}{\partial y} \right) + v^2 \frac{\partial v}{\partial y} \right\} - \frac{\partial w}{\partial z} \left\{ \frac{1}{2\gamma_0} (1 - u^2 - v^2) - \delta H \right\} \quad (3)$$

Eqs.(1)-(3) are the same in form as the original formula of the low speed theory except Eq.(3) contains δH which is the head loss due to the viscosity. However, the velocity components, u , v and w are those of viscous flow. δH is given by

$$\gamma_0 \delta H = - \int_y^{y_0} u \frac{\partial v}{\partial x} dy + \frac{1}{2} u^2 \Big|_y^{y_0} \quad (4)$$

In the integration x should be kept constant; y_0 is the position where δH is almost zero. This formula has derived under the condition that the viscous decay is faster than that of the free wave.

Eq.(3) can be calculated by using the preceding results. For the velocity profiles of far behind in wake, similar velocity profiles are assumed; for $x \geq 1.3$, the velocity defect at $y=0$, $\Delta u (= 1 - u(x, 0))$, is assumed to be proportional to $x^{-2/3}$ while the breadth of wake to spread proportionally to $x^{1/2}$.

The calculated amplitude function of EM-01 is shown in Fig.3 and wave resistance coefficient curves are in Figs.4-6.

The results shown in Fig.3 tell us only changes in amplitude have been realized and non in wave number. They show also that the sine component decreases due to the stern wave attenuation and the cosine component appears because of the asymmetry. This means the viscous effects do not always make the wave resistance decrease; they, some cases, yield increments of the wave resistance.

The present results, shown in Figs.4-6, get closer to the experiments (we should remind here the present scheme is good for low speed range). However, the expected phase shifts in the hump-hollow are not realized, which is discussed later.

4. Discussions for the present results

By the momentum theorem, the total resistance coefficient, C_t , of a ship moving steadily forward is given by

$$C_t = C_v + C_w + C_{vw}, \quad (5)$$

where

$$C_v = \frac{\gamma_0}{2} \int_{-\infty}^{\infty} dy \int_{-\infty}^0 \partial H dz + \frac{1}{4} \int_{-\infty}^{\infty} dy \int_{-\infty}^0 \{-(1-u)^2 + v^2\} dz, \quad (6)$$

$$C_w = \frac{\gamma_0}{4} \int_{-\infty}^{\infty} \zeta^2 dy + \frac{1}{4} \int_{-\infty}^{\infty} dy \int_{-\infty}^0 \left\{ -\left(\frac{\partial \phi}{\partial x}\right)^2 + \left(\frac{\partial \phi}{\partial y}\right)^2 + \left(\frac{\partial \phi}{\partial z}\right)^2 \right\} dz, \quad (7)$$

$$C_{vw} = \frac{1}{2} \int_{-\infty}^{\infty} dy \int_{-\infty}^0 \left\{ (1-u) \frac{\partial \phi}{\partial x} + v \frac{\partial \phi}{\partial y} \right\} dz. \quad (8)$$

C_v , C_w and C_{vw} are the viscous resistance, the wave resistance and their interaction component coefficients respectively; they are all made non-dimensional by $1/2\rho U^2 L^2$; ζ is the wave elevation and ϕ is the velocity potential. C_w and C_{vw} are rewritten as follows;

$$\begin{aligned} C_w = C_{w0} - \frac{1}{4\pi^2} & \left[\int_{-\infty}^{\infty} dy \int_{-\infty}^{\xi_1} d\xi_1 \int_{-\infty}^{\infty} D(\xi_1, \eta_1) d\eta_1 \int_{-\infty}^{\xi_2} d\xi_2 \int_{-\infty}^{\infty} D(\xi_2, \eta_2) d\eta_2 \int_{-\frac{\pi}{2}}^{\frac{\pi}{2}} \sec^3 \theta_1 d\theta_1 \int_{-\frac{\pi}{2}}^{\frac{\pi}{2}} \sec^3 \theta_2 d\theta_2 \right. \\ & \cdot \left[\gamma_0^2 \cos(\gamma_0 \sec^2 \theta_1 \tilde{\omega}_1) \cos(\gamma_0 \sec^2 \theta_2 \tilde{\omega}_2) - \gamma_0^2 \cos(\gamma \sec^2 \theta_1 \tilde{\omega}_1) \cos(\gamma \sec^2 \theta_2 \tilde{\omega}_2) \right] \\ & + \iint_W dy dz \int_{-\infty}^{\xi_1} d\xi_1 \int_{-\infty}^{\infty} D(\xi_1, \eta_1) d\eta_1 \int_{-\infty}^{\xi_2} d\xi_2 \int_{-\infty}^{\infty} D(\xi_2, \eta_2) d\eta_2 \\ & \cdot \int_{-\frac{\pi}{2}}^{\frac{\pi}{2}} \sec^4 \theta_1 d\theta_1 \int_{-\frac{\pi}{2}}^{\frac{\pi}{2}} \sec^4 \theta_2 d\theta_2 e^{\gamma_0 (\sec^2 \theta_1 + \sec^2 \theta_2)} d\theta_2 \left[(\sin \theta_1 \sin \theta_2 - \cos \theta_1 \cos \theta_2) \right] \end{aligned}$$

$$\cdot \{ \gamma_0^4 \cos(\gamma_0 \sec^2 \theta_1 \bar{\omega}_1) \cos(\gamma_0 \sec^2 \theta_2 \bar{\omega}_2) - \gamma_0^4 \cos(\gamma \sec^2 \theta_1 \bar{\omega}_1) \cos(\gamma \sec^2 \theta_2 \bar{\omega}_2) \} \\ + \{ \gamma_0^4 \sin(\gamma_0 \sec^2 \theta_1 \bar{\omega}_1) \sin(\gamma_0 \sec^2 \theta_2 \bar{\omega}_2) - \gamma_0^4 \sin(\gamma \sec^2 \theta_1 \bar{\omega}_1) \sin(\gamma \sec^2 \theta_2 \bar{\omega}_2) \} \} \quad (9)$$

$$C_{vw} = \frac{\gamma_0^2}{2\pi} \iint_W du dy dz \int_{-\xi_0}^{\xi_0} d\xi \int_{-\infty}^{\infty} D(\xi, \eta) d\eta \int_{-\pi/2}^{\pi/2} \sec^3 \theta \cos(\gamma \sec^2 \theta \bar{\omega}) e^{\gamma_0 \sec^2 \theta} d\theta, \quad (10)$$

where C_{w0} is Eq. (1) itself, a is the wake breadth on the free surface, W is the wake section, and $\gamma_r = u^2 l/g$, $\bar{\omega}_i = (x - \xi_i) \cos \theta_i + (y - \eta_i) \sin \theta_i$ ($i=1, 2$ or without suffix).

The present formula, to give the wave resistance by Eqs. (1)-(4), means the neglect of the second term of Eq. (9) and C_{vw} , given by Eq. (10). This is quite valid if the control surface is chosen enough downstream where the basic flow has recovered to be the uniform velocity, i.e., $\gamma_r \rightarrow \gamma_0$. In this sense the present scheme is the same in orders of approximation as the low speed theory where the local velocity deformation from the uniform velocity is neglected on the control surface.

In the present viscous flow case, however, this approximation brings forth a contradiction; on choosing the control surface at such downstream where the viscous velocity defect can be safely neglected, the viscous resistance, given by Eq. (6), itself reduces to be non-contribution.

It may be concluded from the above consideration that though the neglect of the second term of Eq. (9) and C_{vw} is consistent from the stand point of the potential theory, such a choice of a control surface is not approved for the estimation of the viscous resistance. The full evaluation of Eqs. (9) and (10) would remove this contradiction and phase shifts of hump-hollow, unrealized here, may be expected also.

5. Concluding remarks

Though the full prediction of the viscous effects on the wave resistance is left for a future work, the first order of them are estimated. The mean lines of the wave resistance curves are better reproduced by the introduction of the

viscous effects. This implies that the viscous effects on the wave resistance is as important as the nonlinear terms in the potential theory and that the low speed theory is enough reliable for the prediction of the wave resistance under the inviscid assumption as far as low speed range is concerned.

Mr. H. Nishimoto, postgraduate student of Hiroshima University, is appreciated for his help in carrying out the calculation.

References

- Baba, E. Wave resistance of ships in low speed. Mitsubishi Tech. Bul. no.109 1976.
- Inui, T. Study on wavemaking resistance of ships. 60th Anniv. series, Soc. of Nav. Arch. of Japan, vol.2 1957.
- Mori, K., Doi, Y. Approximate prediction of flow field around ship stern by asymptotic expansion method. Jour. of Soc. of Nav. Arch. of Japan, vol.144 1978.
- Mori, K. Prediction of viscous effects on wave resistance of ship in framework of low speed theory. Mem. of the Faculty of Eng. of Hiroshima Univ. vol.7 no.1 1979.
- Mori, K. An assessment of theoretical methods for determining near wake flow and some applications to ship wake prediction. Mem. of the Faculty of Eng. of Hiroshima Univ. vol.8 1980 (to be published).
- Shearer, J.R., Cross, J.J. The experimental determination of the components of ship resistance for a mathematical model. Trans. of RINA vol.107 1965.

Table 1 Principal dimensions of used models

	L(m)	B/L	d/L	remarks
EM-01	2.000	0.2000	0.2500	2-D form with vertical frameline
Wigley model	6.096	0.1000	0.0625	
S-201	1.750	0.1229	0.0979	

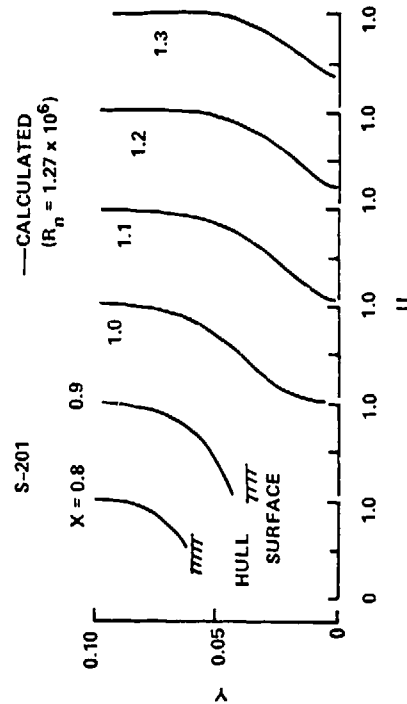
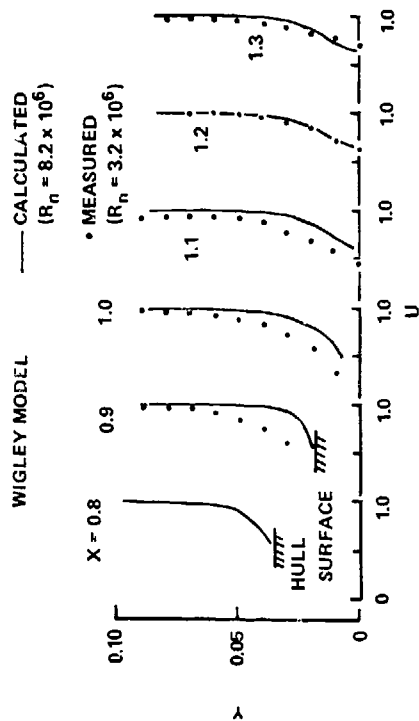
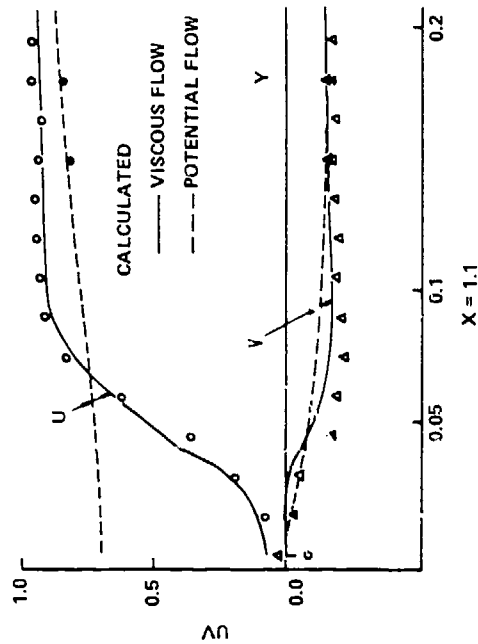
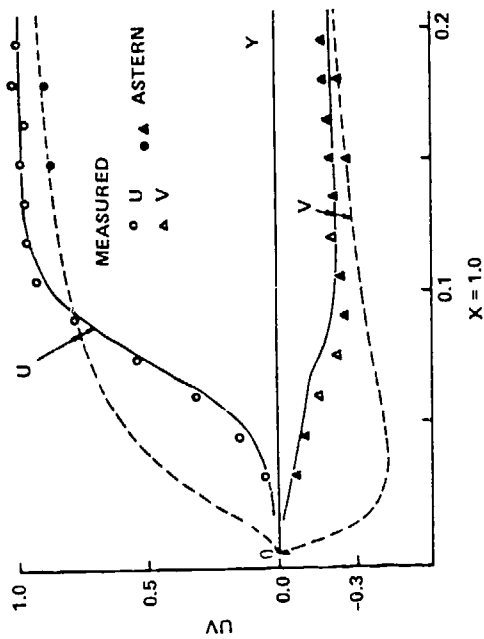


Figure 1 - Velocity Profiles in Near Wake of EM-01 ($R_n = 1.295 \times 10^6$)

Figure 2 - Velocity Profiles in Near Wake of Wigley Model and S-201

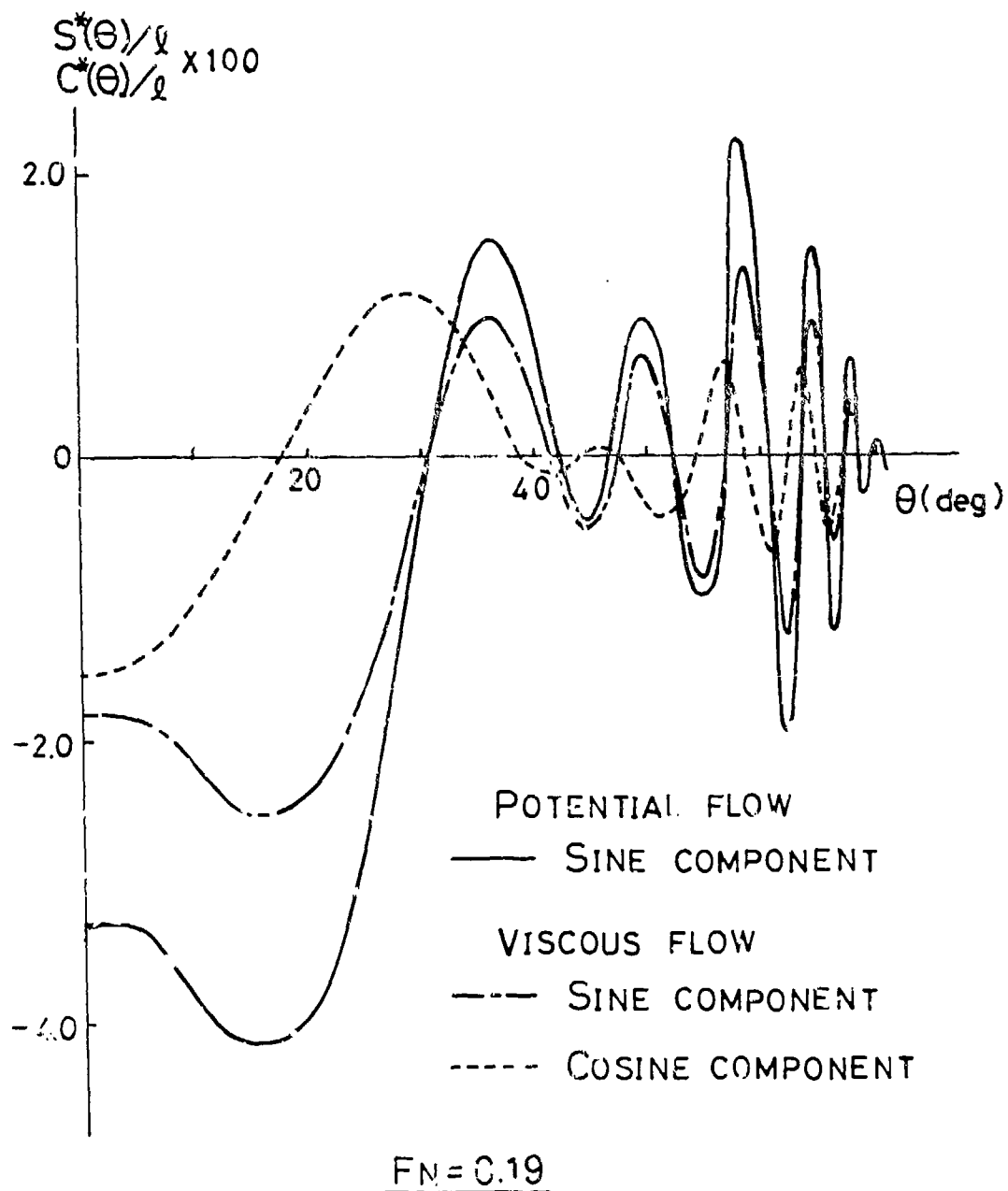


FIG. 3 AMPLITUDE FUNCTION OF EM-01

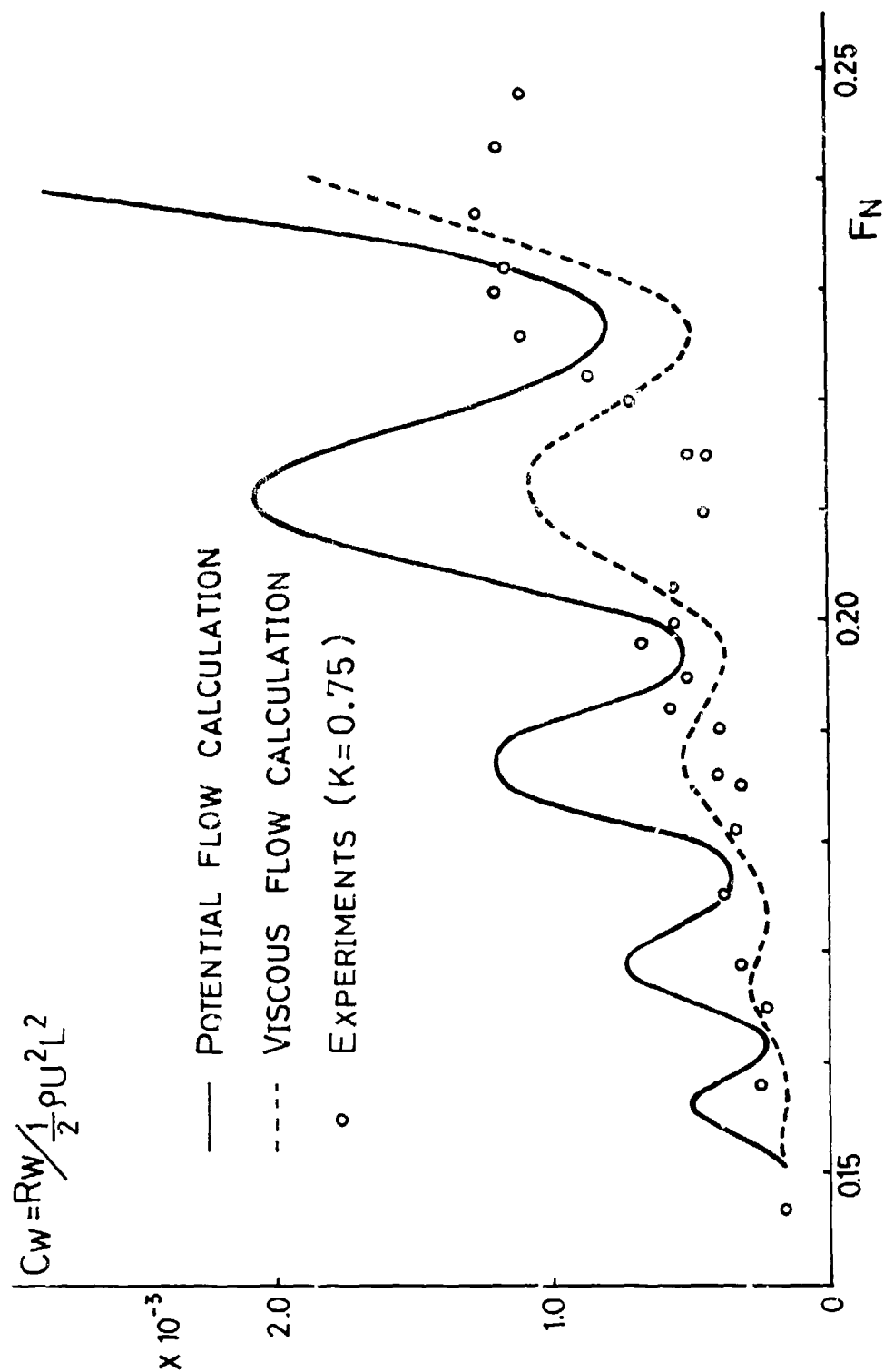


FIG. 4 WAVE MAKING RESISTANCE COEFFICIENT CURVE OF EM-01

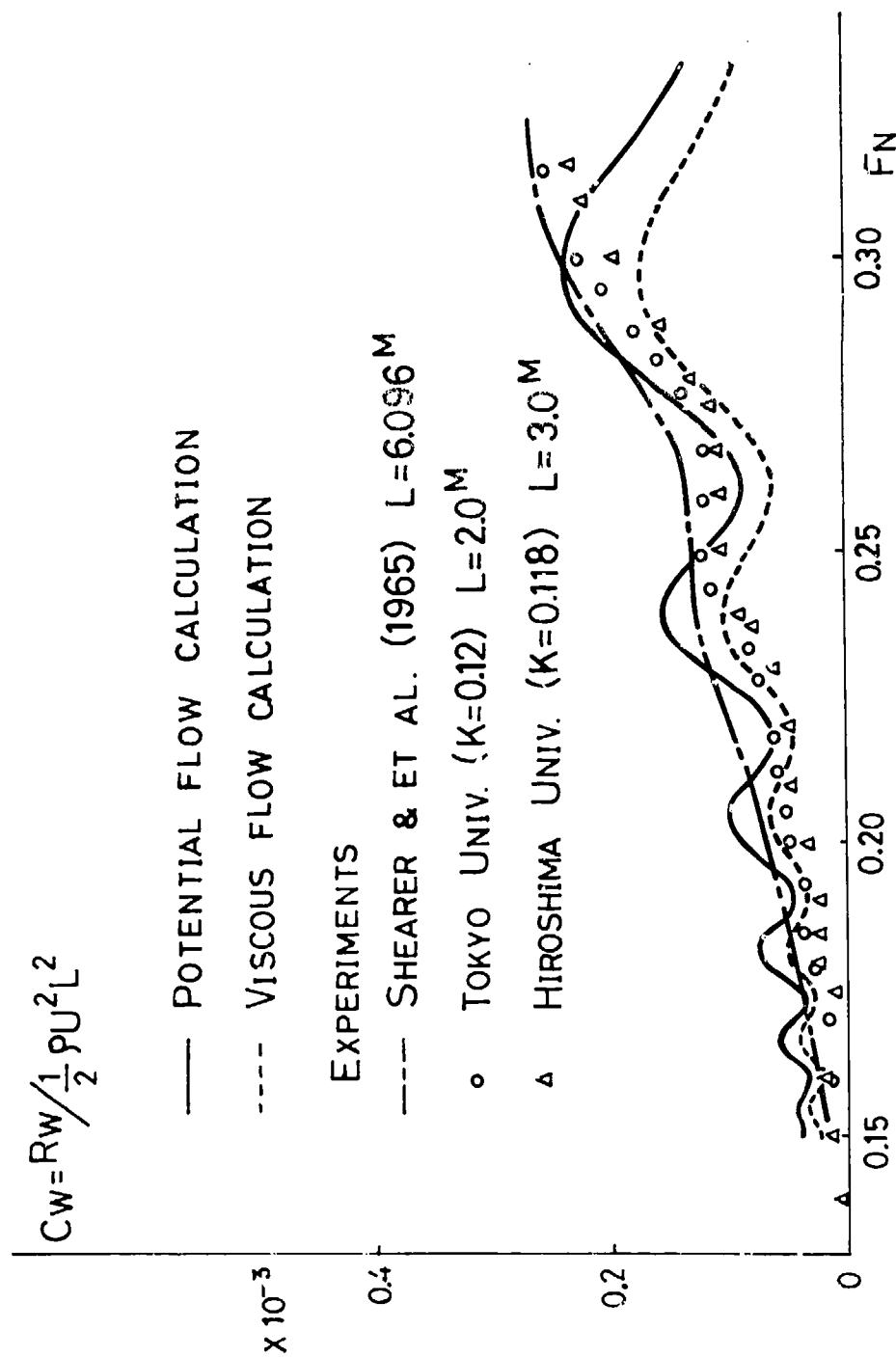


FIG. 5 WAVE MAKING RESISTANCE COEFFICIENT CURVE

OF WIGLEY MODEL

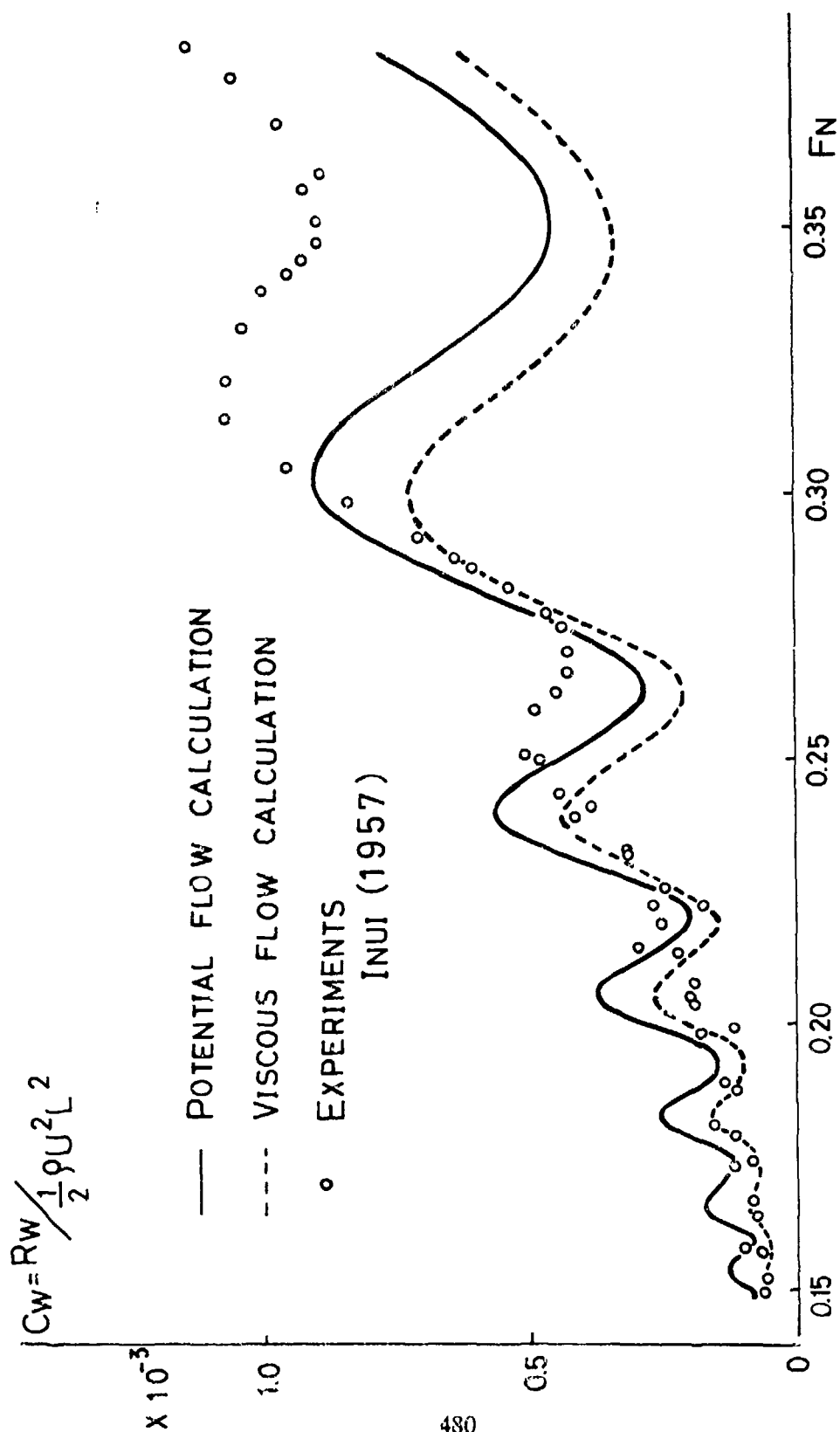


FIG. 6 WAVE MAKING RESISTANCE COEFFICIENT CURVE OF S-201

Table I Wave resistance coefficients of EM-01

F_n	$R_w / \frac{1}{2} \rho U^2 L^2 \times 10^3$	
	Potential Flow	Viscous Flow
0.150	0.1484	0.1457
0.160	0.2649	0.1745
0.170	0.7016	0.2561
0.180	0.4639	0.3561
0.190	1.0887	0.4991
0.200	0.6480	0.4535
0.210	2.0444	1.0537
0.220	1.2708	0.7206
0.230	0.9139	0.6783
0.240	3.0372	1.8478

Table II - Wave Resistance Coefficient of Wigley Model

F_n	$R_w / \frac{1}{2} \rho U^2 S \times 10^3$	
	Potential Flow	Viscous Flow
0.150	0.237	0.146
0.160	0.203	0.139
0.170	0.269	0.222
0.180	0.467	0.294
0.190	0.290	0.214
0.200	0.587	0.374
0.210	0.551	0.380
0.220	0.409	0.288
0.230	0.801	0.546
0.240	1.032	0.698
0.250	0.791	0.534
0.260	0.570	0.398
0.266	0.624	0.451
0.270	0.738	0.542
0.280	1.156	0.857
0.290	1.504	1.102
0.300	1.598	1.148
0.313	1.385	0.966
0.350	0.806	0.577
0.402	1.849	1.505
0.452	2.563	2.081
0.482	2.654	2.135

Table III - Wave Resistance Coefficient of S-201

F_n	$R_w / \frac{1}{2} \rho U^2 S \times 10^3$	
	Potential Flow	Viscous Flow
0.150	0.391	0.251
0.160	0.387	0.250
0.170	0.669	0.365
0.180	1.072	0.627
0.190	0.747	0.476
0.200	1.314	0.933
0.210	1.612	1.132
0.220	0.931	0.679
0.230	1.845	1.478
0.240	2.666	2.070
0.250	2.118	1.559
0.255	1.683	1.213
0.260	1.397	1.024
0.270	1.596	1.346
0.280	2.591	2.286
0.287	3.373	2.923
0.290	3.658	3.130
0.300	4.219	3.421
0.319	3.632	2.643
0.360	2.256	1.782
0.440	7.408	5.625
0.525	7.684	6.212
0.650	4.846	5.118

On Wave Making Resistance of the Model
Series 60 '4210 W' by Regression Analysis

by

Masahiro Yamaguchi
Ship Research Institute
Ministry of Transport
Japan

This paper described the results of estimation of the wave making resistance of the model Series 60 '4210 W' by use of the regression analysis technique.

Regression analysis technique has been used to analyse resistance and propulsion data of fishing boats, Series 60, B.S.R.A. Series, etc. The qualities of total resistance and viscous resistance of ship hulls, which are assumed to have the same displacement or the same length, have been expressed in equational terms, dependent on certain non-dimensional parameters of their dimensions and forms, while the qualities of wave making resistance have been analysed using the wave making resistance theories.

Tagano modified Michell's approximation and applied it to the regression analysis of wave making resistance. He expressed wave making resistance by the equation (1).

$$\begin{aligned} r_w &= \frac{R_w}{\rho U^2 V^{2/3}} \\ &= \frac{C_x^2}{\pi} \left(\frac{1}{C_b} \frac{B}{L} \frac{B}{H} \right)^{2/3} \left(1 - e^{-K_0 \frac{B}{L} \frac{H}{\theta}} \right)^2 (H_{00} f_0 f_0 + H_{01} f_0 f_1 + \dots + H_{nn} f_n f_n) \end{aligned} \quad (1)$$

where $f_i = A(x_i)/A_x$, $K_0 = g/U^2$ and H_{ij} are the regression coefficients.

Revised November 9, 1979.

Here we introduce a new coefficient "Wave Resistance Coefficient" C'_w as follows;

$$C'_w = r_w / \frac{C_x^2}{\pi} \left(\frac{1}{C_b} \frac{B}{L} \frac{B}{H} \right)^{2/3} \left(1 - e^{-K_d \frac{B}{L} \frac{H}{B}} \right)^2 \quad (2)$$

Then we get

$$C'_w = H_{00} f_0 f_0 + H_{01} f_0 f_1 + \dots + H_{nn} f_n f_n \quad (3)$$

If wave making resistance by expression of r_w is used in the regression analysis, the factor $\frac{C_x^2}{\pi} \left(\frac{1}{C_b} \frac{B}{L} \frac{B}{H} \right)^{2/3} \left(1 - e^{-K_d \frac{B}{L} \frac{H}{B}} \right)^2$ is considered as the weighting factor of "Wave Resistance Coefficient" C'_w .

The regression coefficients H_{ij} in the equation (3) are derived using the method of least squares, by differentiating the sums of squares of discrepancies between the measured and the calculated values of C'_w with respect to each coefficient, equating to zero, and solving the series of simultaneous equations generated.

The data used here cover the range of C_b from 0.4 to 0.8, L/B from 4 to 8 and B/H from 2.1 to 4.7, and include various kinds of ships such as liners, container ships, car ferries and car carriers except for oil tankers and bulk carriers over $C_b = 0.8$. Those data have been accumulated through commercial testings and analysed by Schoenherr's frictional resistance coefficients. The data are, therefore, re-analysed by the ITTC 1957 friction line before using the regression analysis.

The wave making resistance are obtained by the equation (4).

$$C_w = C_t - (1 + K_{ITTC}) \cdot C_{ITTC} \quad (4)$$

where

$$C_t = \frac{R_t}{\frac{1}{2} \rho U^2 S}$$

$$C_t = C_w + (1 + K) \cdot C_{f_0}$$

$$K_{ITTC} = (1 + K) \cdot \left[C_{f_0} / C_{ITTC} \right]_{F_n=0.1} - 1$$

- C_{ITTC} : form factor by C_{ITTC}
- K : form factor experimentally determined by C_{f_0}
- C_{ITTC} : the ITTC 1957 friction line
- C_{f_0} : Schoenherr's frictional resistance coefficient

The numbers of data are dependent on Froude numbers and more than 200 and less than 390. The values of $f_i = A(x_i) / A_x$ are chosen at 7 points of x_i , i.e., at S.S.No. 1, 3, 7, 8, 9, $9 \frac{1}{2}$ and F.P., while those of Tagano are at S.S.No. 1, $3 \frac{1}{2}$, $6 \frac{1}{2}$, 8, 9, $9 \frac{1}{2}$ and F.P. for finer ship hull forms of $0.55 < C_B < 0.65$. Figure 1 shows the results of the model Series 60 '4210 W'. The form factor $K_{ITTC} = 0.12$ is adopted for this model. The residual resistance coefficients $C_r = (C_w)_{regression} + K_{ITTC} \cdot C_{ITTC}$ are shown in the figure. The results show that there is some discrepancy in the range of F_n from 0.20 to 0.26 between the measured and the calculated residual resistance coefficients. The same regression equation for wave making resistance coefficient is also applied directly to residual resistance data, extending beyond theoretical reasonableness. The residual resistance coefficients directly obtained by the regression analysis, $(C_r)_{regression}$, are also shown in the figure. There is not clear discrepancy between the values of $C_r = (C_w)_{regression} + K_{ITTC} \cdot C_{ITTC}$ and $(C_r)_{regression}$.

The discrepancy between the measured and the calculated residual resistance will be caused by the particular difference in hull forms between the analysed ship data and the model '4210 W'. The models analysed by the present regression analysis have, in general, bulbous bows, and their frame

lines in the fore body are V-shaped, while the model '4210 W' has a normal bow and its frame line is U-shaped.

The regression analysis technique will successfully be applied to ship design in predicting resistance and performance of the ships. The basic data, however, to be analysed by the regression analysis, should carefully be treated and chosen for obtaining reasonable results in prediction. Unfortunately, the limited numbers of ship resistance data accumulated through the commercial testing in ordinary towing tanks have some unfavourable characteristics in hull forms and main particulars especially for general use of the total data in the regression analysis.

Reference:

H. Tagano, 'Study on the method to estimate the wave-making resistance of ships by statistical analysis', Journal of the Kansai Society of Naval Architects, No.147, March, 1973 (in Japanese).

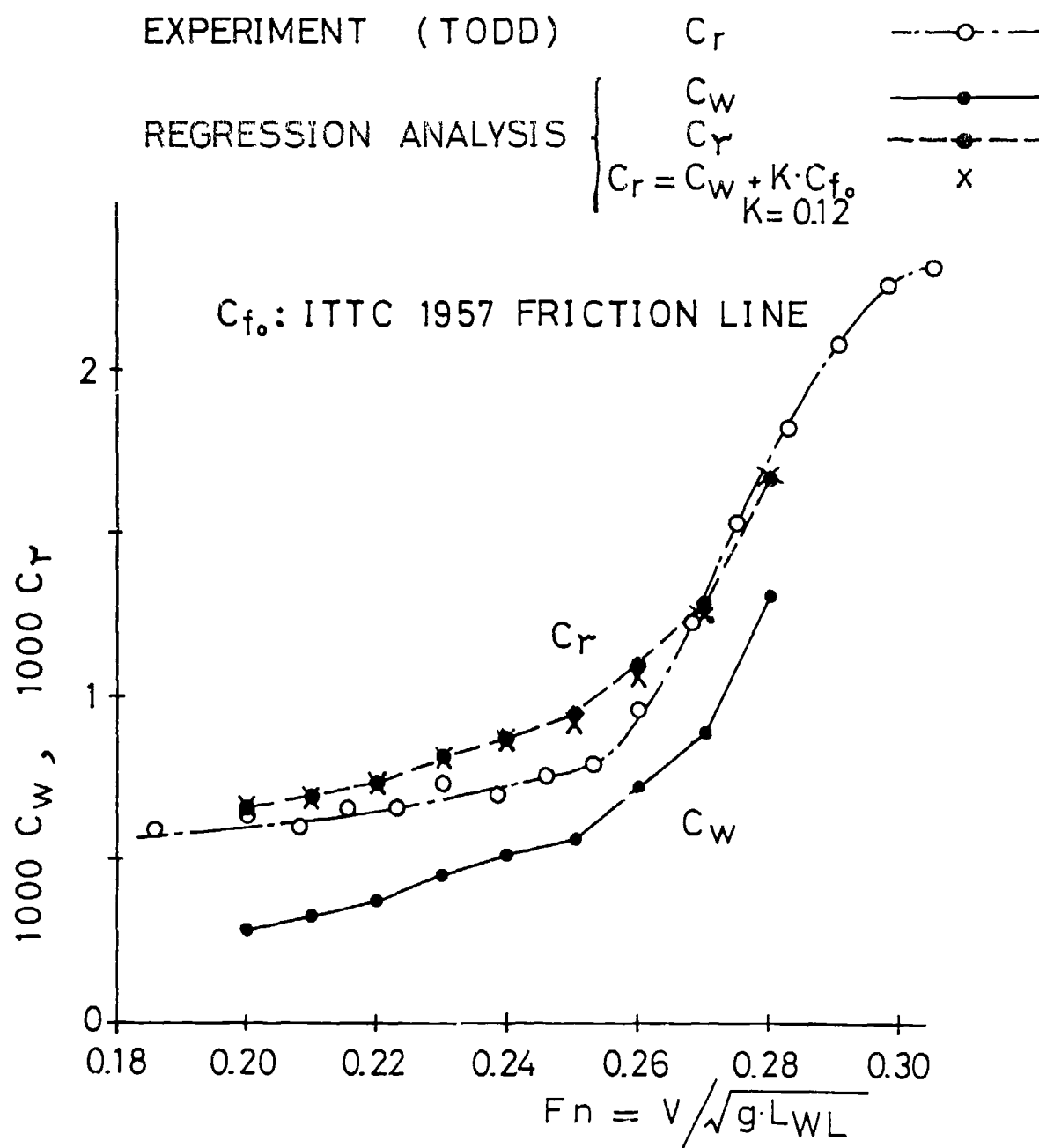


Figure 1 C_w and C_r

FORMAT FOR TABULATED VALUE OF WAVE AND RESIDUAL RESISTANCE

SERIES 60, 4210 W						
Fn	$C_w \times 10^3$	$C_p \times 10^3$ $C_w + (1+K)C$	$C_p \times 10^3$			
0.20	0.287	0.659	0.655			
0.21	0.327	0.696	0.695			
0.22	0.374	0.740	0.738			
0.23	0.454	0.817	0.821			
0.24	0.516	0.876	0.883			
0.25	0.577	0.935	0.951			
0.26	0.726	1.082	1.099			
0.27	0.896	1.249	1.288			
0.28	1.315	1.666	1.677			

APPENDIX
SUPPLEMENTARY CONTRIBUTIONS FOLLOWING WORKSHOP

In this Appendix ten papers are included which were originally presented at an in-depth study meeting held on May 16-18, 1980 in Shuzenji, Izu, Japan. These papers constitute a continuation of discussions held at the November Workshop.

On the Linearization of the Free Surface Condition

Takamune Kitazawa**

Summary

The exact free surface condition is expressed by a simple formula and its linearization is discussed on the assumption that the ship speed is low. Lagrangean coordinate is introduced to transform the condition into the form of the classical linearized condition and the method is compared with the classical linear theory and Guilloton's method.

Nomenclature

g	: acceleration of gravity
l	: unit length along the stream line
U	: velocity of the uniform stream
x, y, z	: Cartesian coordinate
x_0, y_0, z_0	: Lagrangean coordinate
α, β	: straining function
Φ	: total velocity potential
ϕ	: perturbation potential
ϕ_r	: double body potential
ϕ_w	: wavy potential
ξ	: wave height
ξ_r	: wave height calculated with double body velocity

** Technical Research Institute, Hitachi Shipbuilding & Engineering Co., Ltd., Osaka, Japan

1. Introduction

Since the exact free surface condition is highly nonlinear, linearizations are necessary to obtain the solution, if any approximate method is adopted. Even in cases purely numerical approaches are applied, the iterative procedures are mostly based on the linear solutions. The properties of the exact condition, however, should be scrutinized previous to the linearizations. Strictly speaking, the flow field analysis carried out by Inui et al.¹⁾ implies that the existence of a stable solution which satisfies the exact condition is doubtful.

In this paper, the exact free surface condition is derived into a explicit formula using the method like Dawson's²⁾ or Maruo's³⁾, and its properties are discussed. In the following step, a linearization is discussed on the assumption that the ship speed is low and Baba's⁴⁾ free surface condition in low speed range is derived. The transformation of the free surface condition into the form of the classical linearized condition is also discussed by introducing Lagrangean coordinate. The method is originally suggested by Wehausen⁵⁾ and Maruo⁹⁾, but it differs from them in some points.

2. Derivation of the exact free surface condition

Taking a Cartesian coordinate system fixed to the ship, where the origin lies on the undisturbed free surface and x-axis coincides with the direction of the uniform stream, the velocity potential needs to satisfy the pressure condition and the kinematical condition on the free surface:

$$[P] \quad \frac{1}{2} (\Phi_l^2 - U^2) + g\zeta = 0 \quad \text{at } z = \zeta \quad (1)$$

$$[K] \quad \Phi_l \zeta_l - \Phi_z = 0 \quad \text{at } z = \zeta, \quad (2)$$

where Φ is the total velocity potential including the uniform stream and l means the derivative along the stream line.

Substituting eq. (1) into eq. (2), the following condition is obtained.

$$\frac{1}{2} \Phi_l (\Phi_l^2)_l + g\Phi_z = 0 \quad \text{at } z = \zeta \quad (3)$$

Further, eq. (3) is written as follows.

$$\Phi_l^2 \Phi_{ll} + g \Phi_z = 0 \quad \text{at } z = \zeta \quad (4)$$

Eq. (3) and eq. (4) can be written by the following formulae in Cartesian coordinate.

$$\frac{1}{2} \left[\Phi_x \frac{\partial}{\partial x} + \Phi_y \frac{\partial}{\partial y} + \Phi_z \frac{\partial}{\partial z} \right] / (\Phi_x^2 + \Phi_y^2 + \Phi_z^2) + g \Phi_z = 0$$

$$\text{at } z = \zeta \quad (5)$$

$$\left[\Phi_x \frac{\partial}{\partial x} + \Phi_y \frac{\partial}{\partial y} + \Phi_z \frac{\partial}{\partial z} \right]^2 \Phi + g \Phi_z = 0 \quad \text{at } z = \zeta \quad (6)$$

Maruo³⁾ derived eq. (5) by the manipulations in Cartesian coordinate.

On the other hand, the classical linearized free surface condition is written as follows.

$$U^2 \Phi_{xx} + g \Phi_z = 0 \quad \text{at } z = 0 \quad (7)$$

Since eq. (7) characterizes the wave propagation on the uniform stream, eq. (4) is interpreted to describe the wave propagation on the local non-uniform flow.

3. Linearized condition for the wavy potential

As the exact condition is highly nonlinear and untractable, let us consider the linearization basing on the double body flow. In this approach, the total velocity potential is expressed by the summation of two parts:

$$\Phi = \phi_r + \phi_w, \quad (8)$$

where

ϕ_r : double body potential

ϕ_w : wavy potential

Substituting eq. (8) into eq. (4), the following formula is obtained.

$$(\phi_{rl} + \phi_{wl})^2(\phi_{rll} + \phi_{wll}) + g(\phi_{rz} + \phi_{wz}) = 0 \quad \text{at } z = \zeta \quad (9)$$

Eq. (9) can be linearized for ϕ_w in low speed by introducing Ogilvie's⁶⁾ assumption⁴⁾.

$$\begin{aligned} \phi_r &= O(U), & \phi_w &= O(U^5) \\ \zeta_r &= O(U^2), & \zeta_w &= O(U^4) \\ \frac{\partial}{\partial t} &= O(1), & \frac{\partial}{\partial z} &= O(1) \quad \text{when operating on } \phi_r \\ \frac{\partial}{\partial t} &= O(U^{-2}), & \frac{\partial}{\partial z} &= O(U^{-2}) \quad \text{when operating on } \phi_w \end{aligned} \quad (10)$$

According to the assumption, the order of each term of eq. (9) is as follows.

$$\begin{aligned} \frac{\phi_{rl}^2 \phi_{wll}}{[U^3]} + \frac{2\phi_{rl} \phi_{rll} \phi_{wl}}{[U^5]} + \frac{\phi_{wl}^2 \phi_{wll}}{[U^7]} + \frac{g\phi_{wz}}{[U^3]} &= -\frac{\phi_{rl}^2 \phi_{rll}}{[U^3]} - \frac{g\phi_{rz}}{[U^3]} \\ &\text{at } z = \zeta \end{aligned} \quad (11)$$

In the same way, the order of the wave elevation is examined.

$$\begin{aligned} \zeta &= \frac{1}{2g} [U^2 - (\phi_{rl} + \phi_{wl})^2] \\ &= \frac{1}{2g} \left(\frac{U^2}{[U^2]} - \frac{\phi_{rl}^2}{[U^2]} - \frac{2\phi_{rl} \phi_{wl}}{[U^4]} - \frac{\phi_{wl}^2}{[U^6]} \right) \quad \text{at } z = \zeta \end{aligned} \quad (12)$$

The lowest order terms of the free surface condition are

$$(\phi_{rl}^2 \phi_{wll} + g\phi_{wz})_{z=\zeta_r} = (-\phi_{rl}^2 \phi_{rll} - g\zeta_r \phi_{rzz})_{z=0} \quad (13)$$

and those of the wave elevation are written by the following formula.

$$\xi_r = \frac{1}{2g} (U^2 - \phi_{rl}^2) \quad \text{at } z = 0 \quad (14)$$

In Cartesian coordinate, eq. (13) is written as follows.

$$\begin{aligned} & (/\phi_{rx} \frac{\partial}{\partial x} + \phi_{ry} \frac{\partial}{\partial y} + \phi_{rz} \frac{\partial}{\partial z})^2 \phi_w + g \phi_{wz} \Big|_{z=\xi_r} \\ & = (-/\phi_{rx} \frac{\partial}{\partial x} + \phi_{ry} \frac{\partial}{\partial y})^2 \phi_r - g \xi_r \phi_{rzz} \Big|_{z=0} \end{aligned} \quad (15)$$

Assuming that eq. (15) holds on $z=0$ approximately, Baba's⁴⁾ free surface condition in low speed range is derived:

$$/\phi_{rx} \frac{\partial}{\partial x} + \phi_{ry} \frac{\partial}{\partial y})^2 \phi_w + g \phi_{wz} = g D(x, y) \quad \text{at } z = 0, \quad (16)$$

where

$$D(x, y) = \frac{\partial}{\partial x} (\xi_r \phi_{rx}) + \frac{\partial}{\partial y} (\xi_r \phi_{ry}) \quad \text{at } z = 0 \quad (17)$$

Dawson²⁾ adopted the following condition.

$$\phi_{rl}^2 \phi_{wll} + 2 \phi_{rl} \phi_{rll} \phi_{wl} + g \phi_{wz} = -\phi_{rl}^2 \phi_{rll} \quad \text{at } z = 0 \quad (18)$$

He took the second term of the l.s. of eq. (11) into account. The term may not be smaller than the other terms in higher speed range. He neglect the second term of the r.s. of eq. (11). The term is not necessarily smaller than the first term.

In eq. (16), wave propagation along Φ_z in eq. (6) is not considered as the higher order. It may effect the unstable phenomena and the wave breaking phenomena around the bow of full ships.

4. Transformation by introducing Lagrangean coordinate

Eq. (6) expresses the wave propagation on the local non-uniform flow and eq. (16) means the wave propagation over the double body flow. Introducing Lagrangean coordinate⁵⁾, they can be transformed into the form of the classical linearized condition.

Let (x, y) be the space fixed coordinate on $z=0$ and (x_0, y_0) be the corresponding point in the strained coordinate on $z_0=0$:

$$x = x_0 + \alpha(x_0, y_0) \quad (19)$$

$$y = y_0 + \beta(x_0, y_0) \quad (20)$$

where α and β are straining functions. Eq. (19) and eq. (20) yield the following relation.

$$\begin{aligned} U \frac{\partial}{\partial x_0} &= U \frac{\partial x}{\partial x_0} \frac{\partial}{\partial x} + U \frac{\partial y}{\partial x_0} \frac{\partial}{\partial y} \\ &= U \left(1 + \frac{\partial \alpha}{\partial x_0} \right) \frac{\partial}{\partial x} + U \frac{\partial \beta}{\partial x_0} \frac{\partial}{\partial y} \end{aligned} \quad (21)$$

If we adopt the straining functions which satisfy the equations:

$$U \left(1 + \frac{\partial \alpha}{\partial x_0} \right) = \phi_{rx} \quad (22)$$

$$U \frac{\partial \beta}{\partial x_0} = \phi_{ry} \quad (23)$$

the l.s. of eq. (16) can be transformed into the form of the classical linearized condition in the strained coordinate as follows.

$$U^2 \frac{\partial^2}{\partial x_0^2} \phi_w + g \phi_{wz_0} = g D_0(x_0, y_0) \quad \text{at } z_0 = 0 \quad (24)$$

From eq. (22) and eq. (23), α and β are determined by the following formulae.

$$\alpha(x_0, y_0) = \int_{-\infty}^{x_0} [\phi_{rx}(x, y)/U - 1] dx' \quad (25)$$

$$\beta(x_0, y_0) = \int_{-\infty}^{x_0} \phi_{ry}(x, y)/U dx' \quad (26)$$

They are coordinate strainings for Lagrangean coordinate and written in the space fixed coordinate as follows:

$$\alpha(x_0, y_0) = \int_{-\infty}^{x(x_0, y_0)} [1 - U/\phi_{rx}(x', y')] dx' \quad (27)$$

$$\beta(x_0, y_0) = \int_{-\infty}^{x(x_0, y_0)} \phi_{ry}(x', y')/\phi_{rx}(x', y') dx' , \quad (28)$$

where both are line integrals along the stream lines. $D_0(x_0, y_0)$ is determined on the condition that the amount of the source in a small particle does not change.

$$D_0(x_0, y_0) = D(x, y) / (1 + \frac{\partial \alpha}{\partial x_0} + \frac{\partial \beta}{\partial y_0} + \frac{\partial \alpha}{\partial x_0} \frac{\partial \beta}{\partial y_0} - \frac{\partial \alpha}{\partial y_0} \frac{\partial \beta}{\partial x_0}) \quad (29)$$

Yamazaki et al.⁷⁾ calculated the wave resistance of ships by a similar method to this approach, suggested by Maruo⁹⁾.

5. Comparison among the exact condition, the classical linearized condition and the condition of Guilloton's method

The exact condition is written by the following formula in the classical linear theory.

$$U^2 \phi_{xx} + g \phi_z = -U(\text{grad } \phi)_x^2 + \frac{U}{g} (U^2 \phi_{xx} + g \phi_z)_z \phi_x + O(\epsilon^3) \quad (30)$$

at $z = 0$

On the other hand, in Wehausen's⁵⁾ method of Lagrangean coordinate, it is written as follows.

$$U^2 \phi_{0x_0 x_0} + g \phi_{0z_0} = -\frac{U}{2} (\text{grad } \phi_0)_{x_0}^2 \quad \text{at } z_0 = 0 \quad (31)$$

In Guilloton's method interpreted by Gadd⁸⁾ almost the same coordinate strainings are utilized as those of Lagrangean coordinate. The terms in the r.s. of eq. (30) are neglected as the higher order in thin ship theory. In the same way, the r.s. of eq. (31) is neglected in Guilloton's method.

In Guilloton's method, physical quantities are assumed to be equal both in the space fixed coordinate and in Lagrangean coordinate. If velocity potential is assumed to be equal in both coordinates, the exact condition is written by the form of the classical linearized condition in Lagrangean coordinate:

$$U^2 \phi_{x_0 x_0} + g \phi_{z_0} = 0 \quad \text{at } z_0 = 0, \quad (32)$$

which is obtained by the same derivation discussed in section 4.

6. Concluding remarks

The exact free surface condition is derived in a simple formula and its properties are discussed. Baba's⁴⁾ free surface condition is derived from the formula and Lagrangean coordinate is introduced to transform it into the form of the classical linearized condition.

The exact free surface condition expresses the wave propagation on the local non-uniform flow. All the existing theories are approximate ones without or with some part of the effect of the local non-uniform flow. The region needs to be examined, where each theory has sufficient accuracy to estimate the wave resistance of ships, by numerical calculations, and experimental analyses of flow fields around ships.

References

- 1) Inui, T. et al. : Non-Linear Properties of Wave Making Resistance of Wide-Beam Ships, J. Soc. Nav. Arch. of Japan, Vol.146 (1979).
- 2) Dawson, C.W. : A Practical Computer Method for Solving Ship-wave Problems, Second Int. Conf. on Numerical Ship Hydrodynamics, Berkeley (1977).
- 3) Maruo, H. : Wave Resistance of a Ship with Finite Beam at Low Froude Numbers, Bulletin of Fac. of Eng., Yokohama National Univ., Vol.26 (1977).
- 4) Baba, E. and Takekuma, K. : A Study on Free-Surface Flow around Bow of Slowly Moving Full Forms, J. Soc. Nav. Arch. of Japan, Vol.137 (1975).
- 5) Wehausen, J.V. : Use of Lagrangean Coordinate for Ship Wave Resistance (First- and Second-Order Thin Ship Theory), J. Ship Research (1969).
- 6) Ogilvie, T.F. : Wave Resistance : The Low Speed Limit, Univ. of Michigan, Nav. Arch. and Mar. Eng., No.002 (1968).
- 7) Yamazaki, R. et al. : Low Speed Wave-Resistance Theory Making Use of Strained Coordinate, Research Report of Int. Joint Research (1978).
- 8) Gadd, G.E. : Wave Resistance Calculations by Guilloton's Method, Trans. RINA, Vol.115 (1973).
- 9) Maruo, H. : New Treatment for the Ship Wave Problem in Low Speed, JTTC 46th Meeting (1978), (unpublished paper written in Japanese).

ON THE DOUBLE-HULL LINEARIZED FREE SURFACE CONDITION

Kazuhiro Mori
Hiroshima University

According to Newman(1976), the double-hull linearized free surface condition is given as follows.

When the velocity potential ϕ is expressed in the form

$$\phi = U(\phi_0 + \phi_1) \quad , \quad (1)$$

the free surface condition is

$$\phi_{0z} + \phi_{1z} = -\frac{U^2}{2g} \nabla(\phi_0 + \phi_1) \cdot \nabla [(\nabla(\phi_0 + \phi_1))^2] \quad \Big|_{z=\zeta} \quad (2)$$

and

$$\zeta = -\frac{U^2}{2g} \{(\nabla(\phi_0 + \phi_1))^2 - 1\} \quad \Big|_{z=\zeta} \quad (3)$$

where ϕ_0 is the double-hull potential and U , g and ζ are ship speed, gravitational acceleration and wave elevation respectively. (x, y, z) is a Cartesian coordinate system fixed with respect to the ship. $z=0$ represents undisturbed plane of free-surface with z positive upward; $y=0$, the centerplane of the ship; and x positive toward the bow.

In consequence of Newman's consideration, the orders of expanded terms of Eq.(2) are as follows;

$$\begin{aligned} \phi_{0z} + \phi_{1z} = & \underbrace{-\varepsilon \nabla \phi_0 \cdot \nabla (\nabla \phi_0)^2}_{[\varepsilon]} - \underbrace{2\varepsilon \nabla \phi_0 \cdot \nabla (\nabla \phi_0 \cdot \nabla \phi_1)}_{[\varepsilon]} - \underbrace{\varepsilon \nabla \phi_1 \cdot \nabla (\nabla \phi_0)^2}_{[\varepsilon^2]} \\ & - \underbrace{\varepsilon \nabla \phi_0 \cdot \nabla (\nabla \phi_1)^2}_{[\varepsilon^2]} - \underbrace{2\varepsilon \nabla \phi_1 \cdot \nabla (\nabla \phi_0 \cdot \nabla \phi_1)}_{[\varepsilon^2]} - \underbrace{\varepsilon \nabla \phi_1 \cdot \nabla (\nabla \phi_1)^2}_{[\varepsilon^3]} \end{aligned} \quad (4)$$

where

$$\varepsilon = \frac{U^2}{2g} \quad (5)$$

The leading-order terms of Eq.(4) give

$$\frac{U^2}{g} (\phi_{0x}^2 \phi_{1xx} + 2 \phi_{0x} \phi_{0y} \phi_{1xy} + \phi_{0y}^2 \phi_{1yy}) + \phi_{1z} = D \quad \Big|_{z=0} \quad (6)$$

$$D = -\frac{U^2}{g} (\phi_{0x}^2 \phi_{0xx} + 2 \phi_{0x} \phi_{0y} \phi_{0xy} + \phi_{0y}^2 \phi_{0yy}) + \frac{U^2}{2g} \phi_{0zz} (1 - \phi_{0x}^2 - \phi_{0y}^2).$$

Eq.(6) is the same as the free surface condition proposed by Baba-Takekuma(1975) under the low speed assumption. Eq.(6) can be written in the streamline coordinate system which is consisting of double-hull streamlines and equi-potential lines;

$$\frac{U^2}{g} \phi_{0\Delta}^2 \phi_{1\Delta\Delta} + \phi_{1z} = -\frac{U^2}{g} \phi_{0\Delta}^2 \phi_{0\Delta\Delta} + \frac{U^2}{2g} \phi_{0zz} (1 - \phi_{0x}^2 - \phi_{0y}^2) \quad \Big|_{z=0} \quad (7)$$

where Δ is the distance along a streamline.

Regardlessly of the orders, when non-linear terms of ϕ_1 are neglected and Eq.(4) is applied on $z=0$, then Eq.(4) is

$$\phi_{1z} = -\frac{U^2}{2g} \nabla \phi_0 \cdot \nabla (\nabla \phi_0)^2 - \frac{U^2}{g} \nabla \phi_0 \cdot \nabla (\nabla \phi_0 \cdot \nabla \phi_1) - \frac{U^2}{2g} \nabla \phi_1 \cdot \nabla (\nabla \phi_0^2) \quad (8)$$

Eq.(8) can be written in a simple form in the streamline coordinate as follows;

$$\frac{U^2}{g} (\phi_{0\Delta}^2 \phi_{1\Delta})_{\Delta} + \phi_{1z} = -\frac{U^2}{g} \phi_{0\Delta}^2 \phi_{0\Delta\Delta} \quad (9)$$

Dawson used Eq.(9) as the free surface condition in his calculation. The first term of LHS of Eq.(9) can be written in another form by partial differentiations

$$\frac{U^2}{g} \phi_{0\Delta}^2 \phi_{1\Delta\Delta} + \frac{U^2}{g} (\phi_{0\Delta}^2)_{\Delta} \phi_{1\Delta} + \phi_{1z} = -\frac{U^2}{g} \phi_{0\Delta} \phi_{0\Delta\Delta} \quad (10)$$

And also it can be rewritten in another form in the Cartesian coordinate as follows;

$$\begin{aligned} \frac{U^2}{g} (\phi_{0x}^2 \phi_{1xx} + 2 \phi_{0x} \phi_{0y} \phi_{1xy} + \phi_{0y}^2 \phi_{1yy}) + \frac{2U^2}{g} \{ \phi_{1x} (\phi_{0x} \phi_{0xx} + \phi_{0y} \phi_{0xy}) + \phi_{1y} (\phi_{0x} \phi_{0xy} + \phi_{0y} \phi_{0yy}) \} \\ + \phi_{1z} = -\frac{U^2}{g} (\phi_{0x}^2 \phi_{0xx} + 2 \phi_{0x} \phi_{0y} \phi_{0xy} + \phi_{0y}^2 \phi_{0yy}) \end{aligned} \quad (11)$$

The second terms of LHS of Eqs.(10) and (11), which are not appearing in Eqs.(6) and (7), are higher order terms according to Baba-Newman's order assumption. They come partially from the second term and from the third term of Eq.(8). The second term of RHS of Eq.(7) is missing in Eq.(11). This is due to an easy putting of $z=0$ where the free surface condition is applied.

Yamazaki-Nakatake used another form of the double-hull linearized free surface condition in their calculation;

$$\frac{U^2}{g} (\phi_{0\Delta})^{-2} \phi_{1\xi\xi} + \phi_{1z} = D \quad (12)$$

Being ξ related to Δ by

$$\frac{\partial}{\partial \xi} = (\phi_{0\Delta})^2 \frac{\partial}{\partial \Delta} \quad (13)$$

Eq.(13) can be written as follows;

$$\frac{U^2}{g} (\phi_{0\Delta} \phi_{1\Delta})_{\Delta} + \phi_{1z} = D \quad (14)$$

LHS of Eq.(14) is the same as that of Eq.(9) which includes higher order terms, while RHS is the same as that of Eq.(7).

It is interesting that, though conditions used by Dawson and Yamazaki-Nakatake may be not consistent in a mathematical sense, as far as Baba-Newman's order assumption is appreciated, they yield rather reasonable wave resistance for wide speed range as a whole.

Baba, E., Takekuma, K.; A study on free-surface flow around bow of slowly moving full forms, J. of Soc. of Nav. Arch. of Japan, Vol.137 (1975).

Newman, J.N.; Linearized wave resistance theory, Proc. of Intern. seminar on wave resistance, The Soc. of Nav. Arch. of 76). Japan (1976).

On the free-surface conditions used by Nakatake et al.
and Dawson

Eiichi Baba
Nagasaki Technical Institute
Mitsubishi Heavy Industries, Ltd.

Calculation of wave resistance by Nakatake et al. is quasi-analytical while Dawson's is purely numerical. The free-surface condition used in the both methods is the so called double-hull linearized free-surface condition. The free-surface condition used by Nakatake et al. is slightly different from Dawson's. However, both methods give closer values of wave resistance for Wigley form and Inui S201 as shown in Fig.1 and Fig.2. On the other hand, a large difference is observed for Series 60 form as shown in Fig.3.

To get better understanding of the results of both methods a comparative study of the free-surface conditions used by Nakatake et al. and Dawson is made.

The free-surface condition used by Dawson is

$$\frac{\partial}{\partial \ell} \left(\Phi_{\ell}^2 \frac{\partial \phi'}{\partial \ell} \right) + g \frac{\partial \phi'}{\partial z} = - \Phi_{\ell}^2 \Phi_{\ell\ell}, \quad z = 0 \quad (1)$$

where Φ is the double-body potential, ϕ' wavy potential and ℓ is the variable along the streamline. The free-surface condition used by Nakatake et al. is derived by applying the coordinate transformation to the free-surface condition proposed by Baba and Takekuma(1975) for a ship in low speed:

$$\frac{\partial^2 \phi'}{\partial \xi^2} + g \frac{\partial \phi'}{\partial \zeta} = g q_0^2 D(\xi, \eta), \quad \zeta = 0 \quad (2)$$

Since there are following relations in the fomulation by Nakatake et al. in terms of the variables used by Dawson

$$q_0^2 = \Phi_{\ell}^2, \quad \partial/\partial \xi = \Phi_{\ell}^2 \partial/\partial \ell, \quad z = q_0^2 \zeta$$

The equation of Nakatake et al. is then found to be expressed by

$$\frac{\partial}{\partial \ell} \left(\phi_{\ell}^2 \frac{\partial \phi'}{\partial \ell} \right) + g \frac{\partial \phi'}{\partial z} = - \phi_{\ell}^2 \phi_{\ell\ell} - g \zeta_r \phi_{zz} \quad (3)$$

where

$$\zeta_r = [U^2 - \phi_{\ell}^2] / 2g$$

In the Dawson's equation the second term of the right-hand side of the equation (3) is dropped. Dawson applied the free-surface condition not on the double-body free-surface but on $z = 0$. The term $g \zeta_r \phi_{zz}$ then does not appear. This term is regarded as one of the leading order terms in the formulation of the free-surface condition by Baba and Takekuma (1975) and Newman (1976).

The present discussor found from the computational experiences of a variety of ship forms that the contribution of the term $g \zeta_r \phi_{zz}$ is dependent on the hull form. For hull forms such as Wigley form and S201 which have vertical framelines at the load waterline the contribution of the term $g \zeta_r \phi_{zz}$ in the evaluation of wave resistance is small. On the other hand, the contribution of this term is large for ship forms which have inclined framelines at the load waterline such as Series 60 form of the present workshop.

To show this difference clearly following comparisons are made. A function $F(\beta)$ used in Baba's report of the present workshop has a relation with the right-hand side of the equation (3):

$$\begin{aligned} F(\beta) &= v \frac{dp}{d\beta} - w_z p \frac{dy}{L d\beta} \\ &= - \frac{2}{g} \frac{dy}{L d\beta} \frac{1}{F_n^2 U} [\phi_{\ell}^2 \phi_{\ell\ell} + g \zeta_r \phi_{zz}] \end{aligned} \quad (4)$$

along the curve of the intersection between the body and the free-surface. In the Tables 3 through 5 of Baba's report we may find first the values of $F(\beta)$ defined by (4). Making use of the values of v and $dp/d\beta$ of the Tables we can also calculate $F(\beta)$ when eliminating the term $g \zeta_r \phi_{zz}$, i.e.

$$F(\beta) = v \frac{dp}{d\beta} = - \frac{2}{g} \frac{dy}{Ld\beta} \frac{1}{F_n^2 U} [\phi_{\ell}^2 \phi_{\ell\ell}] \quad (5)$$

Figs. 4, 5 and 6 show the comparison of $F(\beta)$ with and without the contribution of the term $g\zeta_r\phi_{zz}$.

For Wigley form and S201 the difference of $F(\beta)$ is small, while it is large for Series 60 form. Therefore it may be said that the free-surface condition is practically same for both methods when calculating wave resistance of Wigley form and S201. On the other hand, for Series 60 form the free-surface condition of Nakatake et al. differs slightly from Dawson's. Therefore the present discussor considers that one of the reasons for the difference of wave resistance observed for Series 60 form is attributed to the difference of the free-surface condition.

It may be also said that the term $g\zeta_r\phi_{zz}$ has a significant effect on the wave resistance calculation for conventional ship forms which usually have inclined framelines at the load waterline.

References

- Baba, E. and Takekuma, K., A study on free-surface flow around bow of slowly moving full forms, Journal of The Society of Naval Architects of Japan, Vol.137, 1975.
- Newman, J. N., Linearized Wave Resistance Theory, Proceedings of The International Seminar on Wave Resistance, Tokyo, 1976.

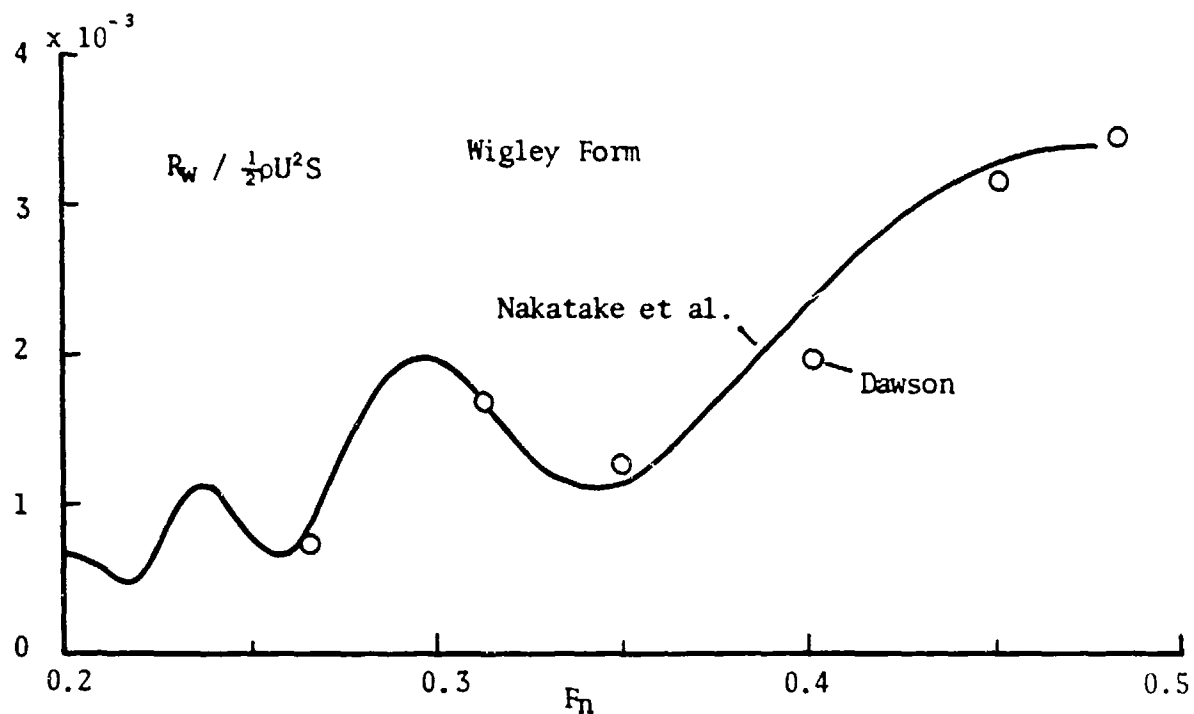


Fig.1 Comparison of calculated wave resistance for Wigley form

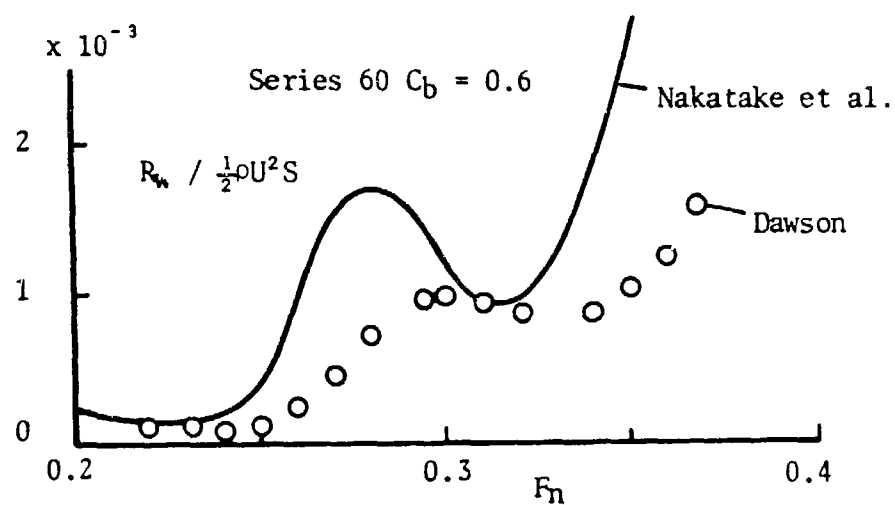


Fig.3 Comparison of calculated wave resistance for Series 60 $C_b = 0.6$

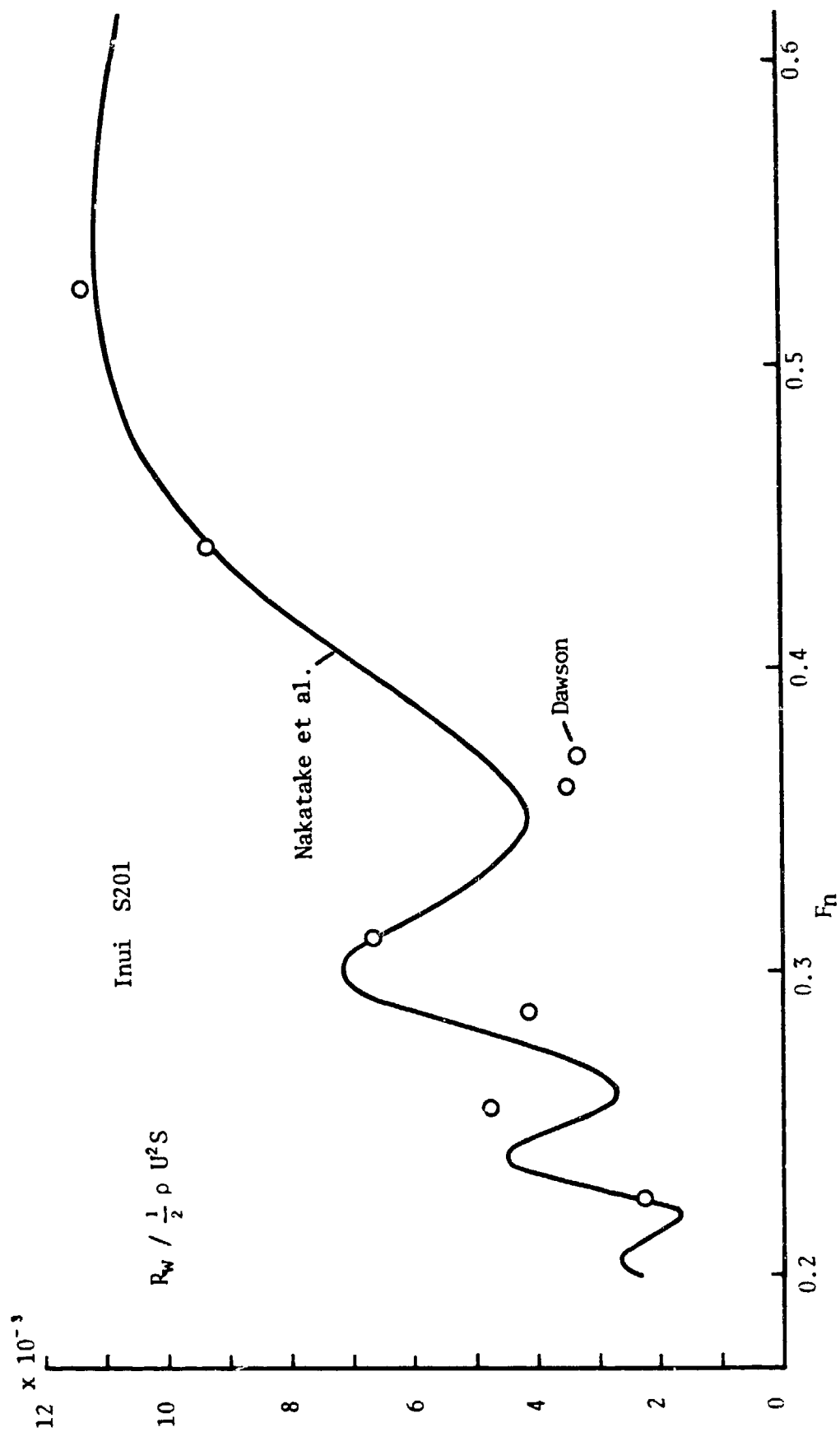


Fig.2 Comparison of calculated wave resistance for Inui S201

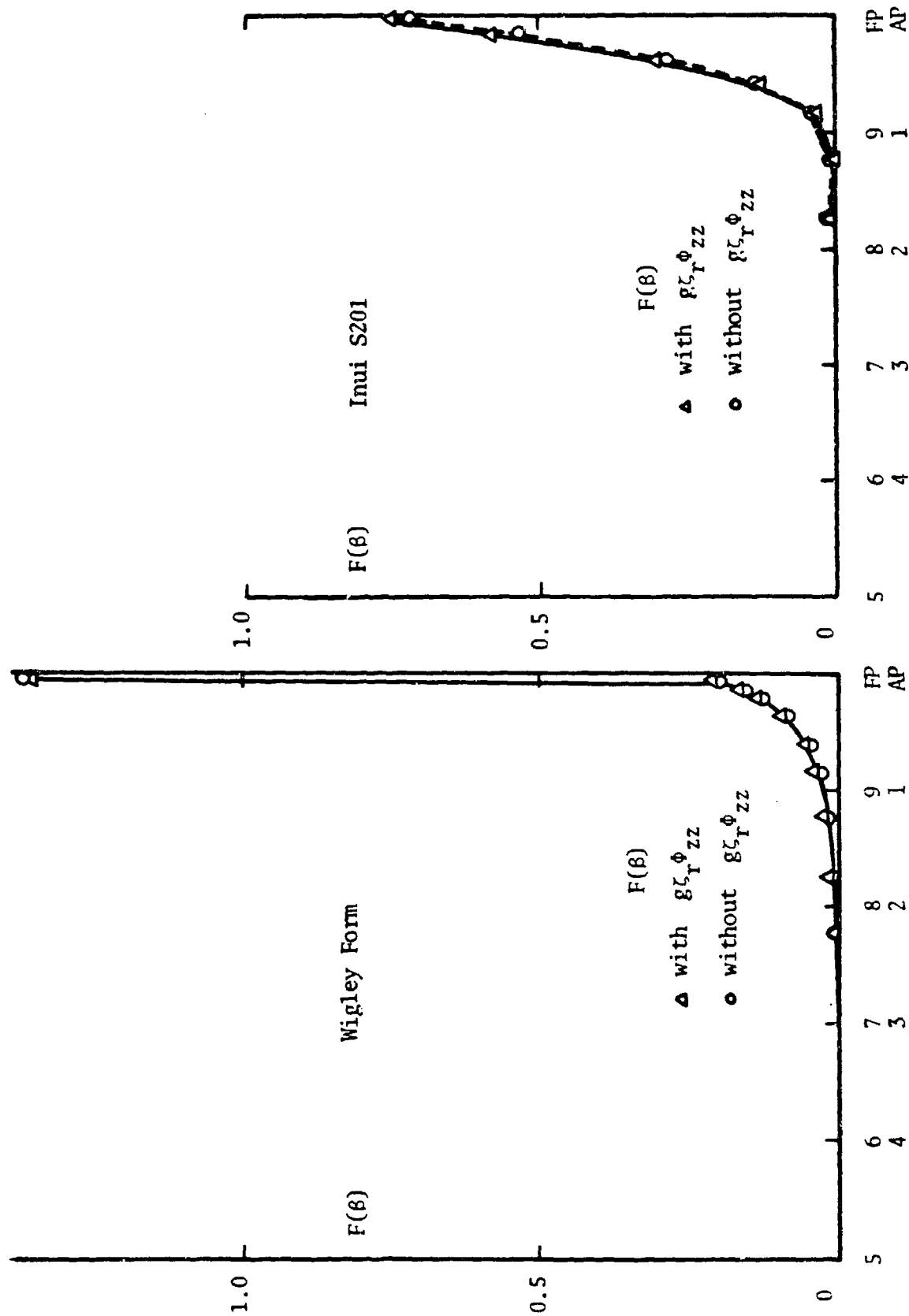


Fig.4 Comparison of $F(\beta)$ for Wigley form

Fig.5 Comparison of $F(\beta)$ for Inui S201

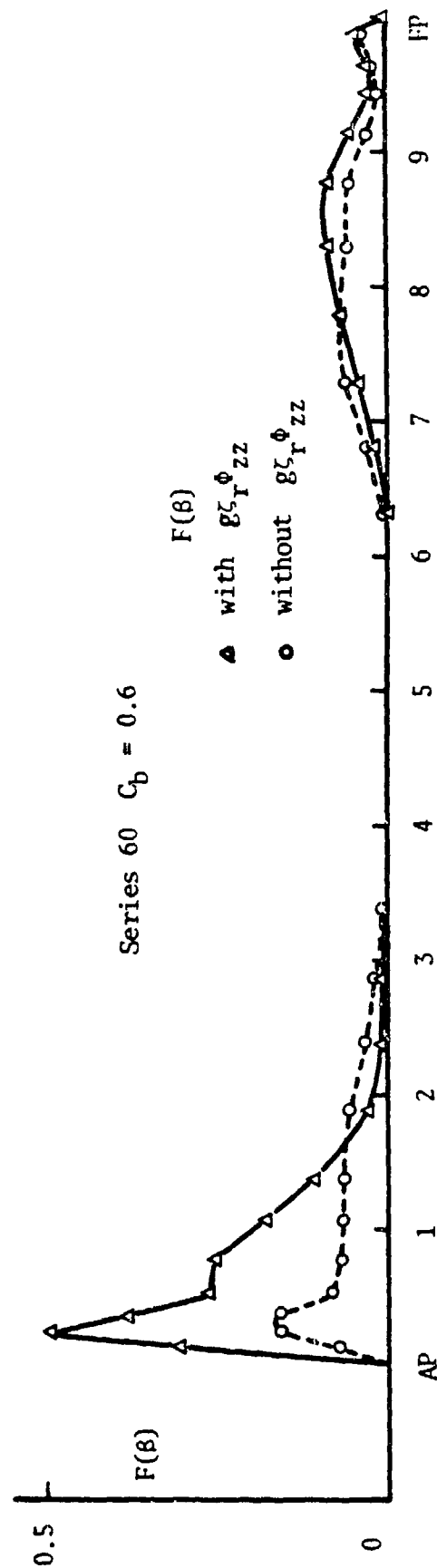


Fig.6 Comparison of $F(\beta)$ for Series 60 form

A note on the double model approximations

Katsuo Suzuki
National Defense Academy

If a solution in the N-K problem tends to a double model solution at low speed, the following double model approximation may be an approximation for the N-K solution,

$$\psi(P) = \frac{1}{4\pi} \iint_H (\phi_n(Q) - \phi \frac{\partial}{\partial n}) W(P, Q) dS_Q - \frac{1}{4\pi R} \oint_C (\phi_f - \phi \frac{\partial}{\partial f}) W dy, \quad \dots (1)$$

where ϕ is the double model solution and $W(P, Q)$ is a wave source potential, C the intersection of the hull surface H and the free surface F . Eq.(1) is rewritten in the form

$$\psi(P) = \phi(P) + \frac{1}{4\pi R} \iint_F \phi_{xz} W dx dz, \quad \dots (2)$$

the Kottchin function of which coincides with Guevel et al's (1974). When ϕ_{xz} in eq. (2) is replaced by $D(x, y)$ which is used in the low speed theory, the amplitude function of eq. (2) is equal to that in the low speed theory (Baba et al. 1975). Therefore the wave resistance of eq. (2) may also be an approximation to that of the low speed theory for fine ships. The wave spectrum of eq. (1) for the parabolic strut is shown in fig. 1, 2 (Double model with L.I.). The amplitude of the transverse wave region is reduced compared with the Michell approximation, while the diverging wave component is abnormally large. These properties may hold in the low speed theory. A method which includes implicitly the effect of line integral of making the transverse wave component decrease and which has the effect of decreasing the diverging wave component was presented (Suzuki 1978).

$$\psi_M(P) = \frac{1}{2\pi} \iint_{H_0} \phi_y(x, y, z) W(P, x, 0, z) dx dz \quad \dots (3)$$

The results calculated by the method are compared with the eq. (1) and low speed theory in Fig. 1 to 4 (Modified Michell approximation). Eq. (1) is calculated by Nakatake, Yim (for Inuid hull), Maruo et al. and the new methods similar to eq. (1), are used by Yim (for Wigley hull), Koch-Noblesse. Almost all these wave resistance curves give a fairly good agreement. As shown in fig. 1, 2, however, the agreement of the wave resistance curves

does not already give the equal wave spectrums. Especially it is noted that both the double model approximations and the low speed theory does not overcome the defect that the real part of the amplitude function of the Michell approximation vanishes for longitudinally symmetric ships. In order to study these facts we need to calculate and compare not only the wave resistance but the amplitude function.

References:

P.Guevel et al., ISP 21,1974

E.Baba et al., JSNA Japan 137, 1975

K.Suzuki, Sci. Eng. Defense Acad. 16-3,1978

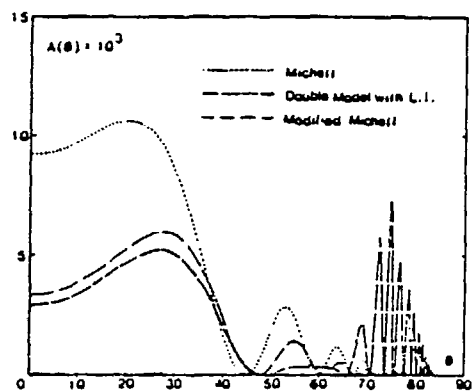


Fig. 1 Wave spectrum for parabolic strut ($B/L=0.2$, $Fn=0.302$)

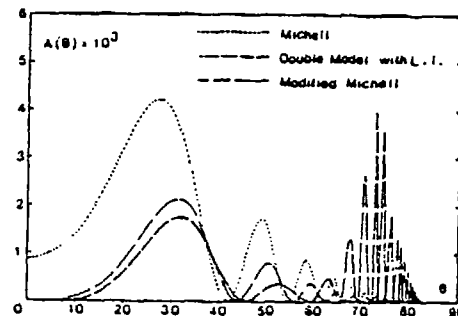


Fig. 2 Wave spectrum for parabolic strut ($B/L=0.2$, $Fn=0.248$)

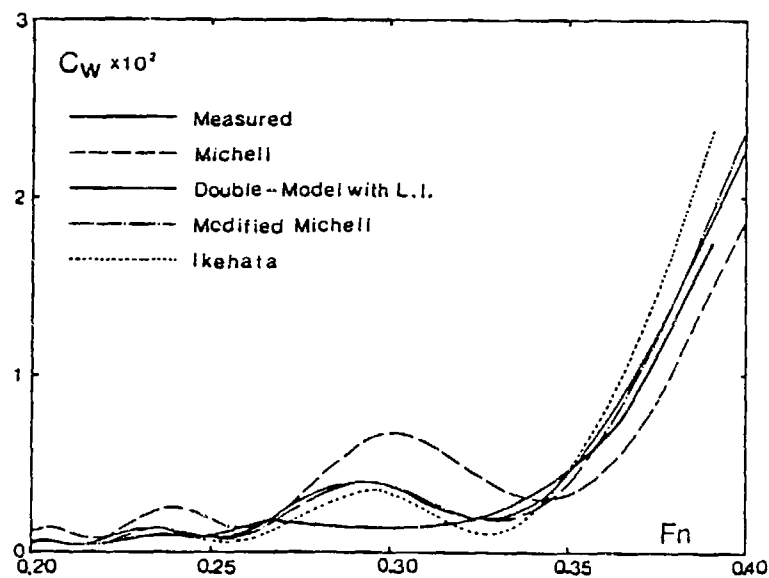


Fig. 3 Comparison of wave resistance for parabolic strut ($B/L=0.2$)

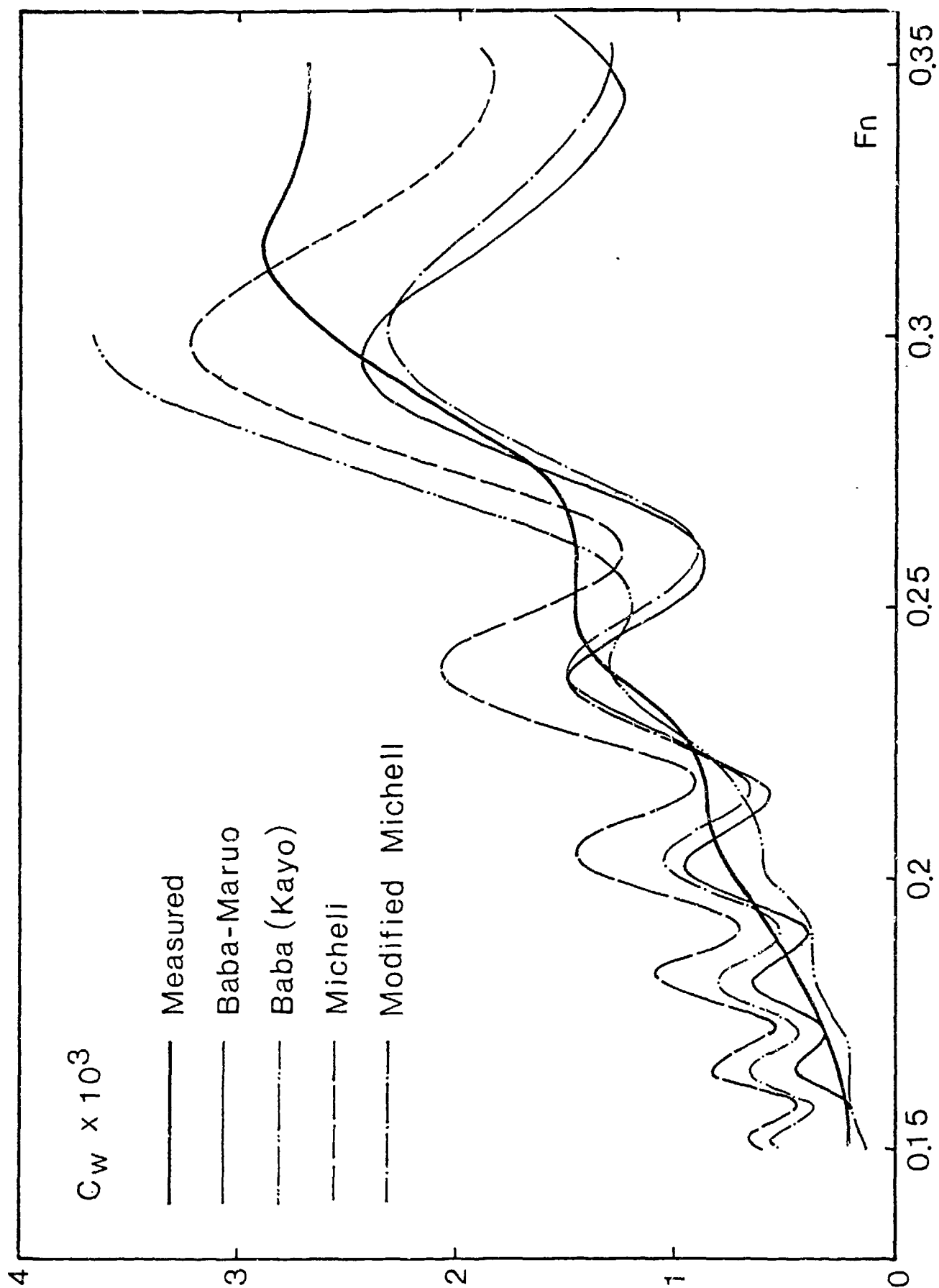


Fig. 4 Comparison of wave resistance for Wigley hull ($B/L=0.1$, $d/L=0.0625$)

A NOTE ON THE WATERLINE INTEGRAL AND THE THIN-SHIP APPROXIMATION

by

P. Koch and F. Noblesse

Massachusetts Institute of Technology

Abstract

In this brief note, several elementary (zeroth-order) slender-ship wave-resistance approximations are compared. Differences between these approximations reside in that the waterline integral is included, and the thin-ship approximation is used, in some of the approximations and not in the others. Differences between the wave resistance values predicted by these various approximations thus provide quantitative insight into the effects of neglecting the waterline integral and using the thin-ship approximation. Calculations are performed for two mathematical hull forms: the Wigley hull and a hull with a fine bow and a blunt stern. Neglect of the waterline integral and use of the thin-ship approximation yield moderate (although not negligible) differences in the value of the wave resistance for the Wigley hull, but differences for the hull with a blunt stern are extremely large.

The zeroth-order slender-ship wave-resistance formula

The zeroth-order slender-ship wave-resistance approximation corresponds to simply taking the velocity potential of the disturbance flow caused by the ship as zero, as is discussed in [1]. For a hull with port and starboard symmetry, the corresponding approximation to the Kochin free-wave spectrum function $K(t)$ takes the form

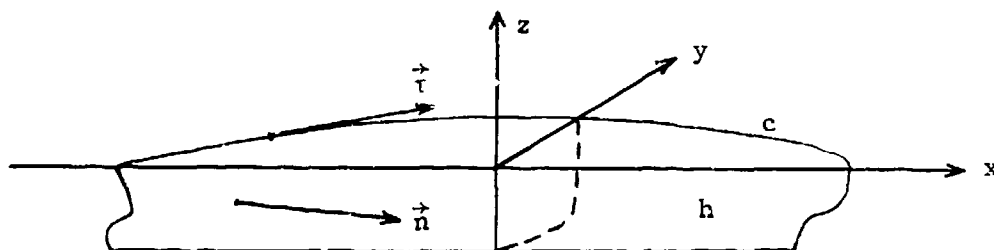
$$K(t) = \int_h E_{\mathbf{x}} d\mathbf{a} - F^2 \int_c E_{\mathbf{x}y}^2 d\ell, \quad (1)$$

where $E \equiv E(t; \vec{\mathbf{x}}, F^2)$ is the function

$$E \equiv \exp[zF^{-2}(1+t^2) - ixF^{-2}(1+t^2)^{1/2}] \cos[yF^{-2}t(1+t^2)^{1/2}] \quad (1a)$$

In the above formulas, $F \equiv U/(gL)^{1/2}$ is the Froude number, with $U \equiv$ the speed of the ship and $L \equiv$ a characteristic length (which may be taken as the length of the ship, for instance). In formula (1a), x, y , and z are

the nondimensional coordinates given by $\vec{x} \equiv \vec{X}/L$ (with $\vec{X} \equiv$ dimensional coordinates) and defined as in the definition sketch below (i.e. the undisturbed free surface is taken as the plane $z=0$, and the x axis is taken along the ship course, pointing towards the stern). In formula (1), h and c represent the starboard (positive) half of the portion of the hull surface below the plane $z=0$, and of the intersection curve of the hull surface with the plane $z=0$, respectively, as shown in the definition sketch.



The symbols da and $d\ell$ in formula (1) represent the differential elements of area and arc length of the hull surface h and waterline c , respectively. Finally, n_x is the x component of the unit vector \vec{n} normal to the hull h and pointing towards the interior of the ship, and τ_y is the y component of the unit vector $\vec{\tau}$ tangent to the waterline c and pointing towards the stern, as shown in the above definition sketch.

Formula (1) involves a surface integral over the hull surface h and a line integral along the waterline c . For the sake of easy reference, these two integrals will simply be referred to as the hull integral and the waterline integral, respectively. Neglect of the waterline integral in formula (1) yields the approximation of Hogner [2]. If, furthermore, y in formula (1a) is taken as zero, so that the term $\cos[yF^{-2}t(1+t^2)^{1/2}]$ can simply be ignored, Hogner's approximation becomes the classical Michell thin-ship approximation [3]. Another simple slender-ship approximation which can readily be obtained as a particular case of the zeroth-order approximation (1) is the approximation obtained by putting $y=0$ in formula (1a), while retaining the waterline integral in formula (1); this approximation was recently used by Yim [4]. In other words, the

approximations of Michell and Yim can be obtained from the Hogner and the zeroth-order approximations, respectively, by using the thin-ship approximation $y=0$ in formula (1a), and the Hogner and Michell approximations can be obtained by neglecting the waterline integral in the zeroth-order and the Yim approximations, respectively.

The wave resistance R can be determined from the Kochin free-wave spectrum function $K(t)$ by using the classical Havelock formula

$$r \equiv R/\rho U^2 L^2 = (4/\pi F^4) \int_0^\infty |K(t)|^2 (1+t^2)^{1/2} dt, \quad (2)$$

where ρ is the density of water. The wave-resistance values predicted by the four above-defined slender-ship approximations are compared in the following section, for two mathematical hull forms, with the view of gaining some quantitative insight into the effects of neglecting the waterline integral and using the thin-ship approximation.

Calculations for two mathematical hull forms

Figure 1 shows the results of calculations for the classical Wigley hull defined by the equation

$$y = .05(1-4x^2)(1-64z^2); \quad -.5 \leq x \leq .5, \quad -.125 \leq z \leq 0.$$

The differences between the Hogner (H) and the Michell (M) approximations, on the one hand, and between the zeroth-order (O) and the Yim (Y) approximations, on the other hand, may be seen to be fairly small. Furthermore, these differences are appreciably smaller than the differences between the Hogner (H) and the zeroth-order (O) approximations, on the one hand, and between the Michell (M) and the Yim (Y) approximations on the other hand. These results indicate that, on the one hand, the thin-ship approximation, which accounts for the differences between the curves H and M and between the curves O and Y, affects the wave resistance only slightly; more precisely, the thin-ship approximation appears to yield a slight decrease in the value of the wave resistance (the Michell curve is slightly below the Hogner curve; the Yim curve likewise is slightly below the zeroth-order curve). On the other hand, the waterline integral, which accounts for the differences between the curves H and O and between the curves M and Y, yields an appreciable reduction in the value of the wave resistance (the zeroth-order and the Yim curves are appreciably lower than the Hogner and

the Michell curves, respectively). While appreciable, these differences clearly remain moderate. Modest differences indeed were to be expected as a result of the fact that the Wigley hull is a fine-ended hull form; specifically, if we denote by β and δ the beam/length ratio and the draft/length ratio, respectively, of the Wigley hull ($\beta = .1$, $\delta = .125$), the terms n_x and τ_y in formula (1) may readily be shown to be of order β , and the hull integral and the waterline integral can be seen to be of order $\beta\delta$ and β^3 , respectively, so that the waterline integral is "an order of magnitude smaller" than the hull integral.

The waterline integral must however be expected to be of primordial importance in the case of blunt-ended hull forms, as the above "order of magnitude analysis" readily suggests. Indeed, the terms n_x and τ_y then are of order 1 at the ship stern or (and) bow (over a width y of order β), and the hull and waterline integrals in formula (1) are of order $\beta\delta$ and β , respectively, so that the waterline integral now is "an order of magnitude larger" than the hull integral. The primordial importance of the waterline integral in the case of a blunt hull form is also apparent from figure 2, which presents results of calculations for a hull form with a fine bow and a blunt stern. Specifically, this hull form is defined by the equations

$$y = b(x/a)(1-x/2a)\sin\gamma, \quad z = -d\cos\gamma; \quad 0 \leq x \leq a, \quad 0 \leq \gamma \leq \pi/2,$$

$$x = a + (1-a)\sin\alpha, \quad y = (b/2)\cos\alpha\sin\gamma, \quad z = -d\cos\gamma; \quad a \leq x \leq 1, \quad 0 \leq \alpha, \gamma \leq \pi/2.$$

The above-defined hull has elliptic framelines, and its waterline consists in a "fine" parabolic fore part ($0 \leq x \leq a$) joined to a "blunt" elliptic aft part ($a \leq x \leq 1$); the value of a is taken as $a = 1/(1+1/\sqrt{2}) \approx .586$, which yields a continuous curvature at the transition point $x=a$ between the parabolic and elliptic portions of the waterline. The values of the beam/length ratio b and of the draft/length ratio d are taken as $b=.15$ and $d=.05$. The various wave-resistance curves shown in figure 2 are now discussed.

The Hogner approximation (H) and the corresponding Michell thin-ship approximation (M) may be seen to be very close to each other, as in figure 1 (although the Michell curve here is very slightly above, rather than below, the Hogner curve). The zeroth-order approximation (O) and its corresponding Yim thin-ship approximation (Y), on the other hand, are very

far apart (more precisely, the Yim curve is much higher than the zeroth-order curve), which is at variance with the result shown in figure 1. The fact that the Yim curve (Y) is quite different (much higher) than the zeroth-order curve (0) mainly stems from the use of the thin-ship approximation in the waterline integral, rather than in the hull integral. Indeed, differences between the zeroth-order curve (0) and the curve (MW), which corresponds to the use of the thin-ship approximation in the hull integral alone (that is, the thin-ship approximation $y=0$ is not used in the waterline integral), remain moderate, although larger than the differences between the Hogner and Michell curves and increasing with decreasing Froude number. Furthermore, differences between the curve (W), which corresponds to the use of the waterline integral alone (that is, the hull integral is neglected) in formula (1), and its corresponding thin-ship approximation (W_0) are very large; more precisely, the curve (W_0) is much higher than the curve (W), and this may explain why the Yim curve (Y) is much higher than the curve (0). Comparison between the curves (W) and (H), and between the curves (W_0) and (M) also demonstrate the primordial importance of the waterline integral. It may finally be noted that (due to the waterline integral) the differences between the Michell approximation (M) and the zeroth-order approximation (0) are quite large. In particular, the Michell curve is lower than the zeroth-order curve for sufficiently high values of the Froude number (for $1/F^2 < 19.5$, i.e. for $F > .23$, approximately), while the opposite is true for sufficiently low speed (for $1/F^2 > 27.5$, i.e. for $F < .19$, approximately). An appreciable phase shift between the Michell and the zeroth-order curves may also be observed.

Concluding remarks

The order of magnitude analysis regarding the relative importance of the hull and the waterline integrals (and thus the conclusion that the waterline integral is an order of magnitude smaller or larger than the hull integral for a slender hull with fine or blunt ends, respectively) is based entirely upon "geometrical arguments", which evidently ignore any possible influence of the Froude number. One would however expect the relative importance of the hull and the waterline integrals in formula (1) to depend on the Froude number, as well as on the shape of the hull. Indeed, in the limit $F \rightarrow 0$, the hull and the waterline integrals can be proved

[1] to be asymptotically equivalent, which results in a drastic reduction in the wave resistance. This reduction in wave resistance at low Froude number may in fact be observed in figure 2, where the zeroth-order curve (0) is significantly below both the Hogner "hull-integral-alone" curve (H) and the "waterline-integral-alone" curve (W) for $1/F^2 > 28$, i.e. for $F < .19$. One must also expect the waterline integral to be primordial in the high-Froude-number limit. Indeed, formula (1a) shows that we have $E \sim 1$ as $F \rightarrow \infty$, so that formula (1) yields

$$K(t) \sim -F^2 \int_c \frac{n_x^2}{x^2 y} d\ell + \int_h n_x da \quad \text{as } F \rightarrow \infty ; t < \infty .$$

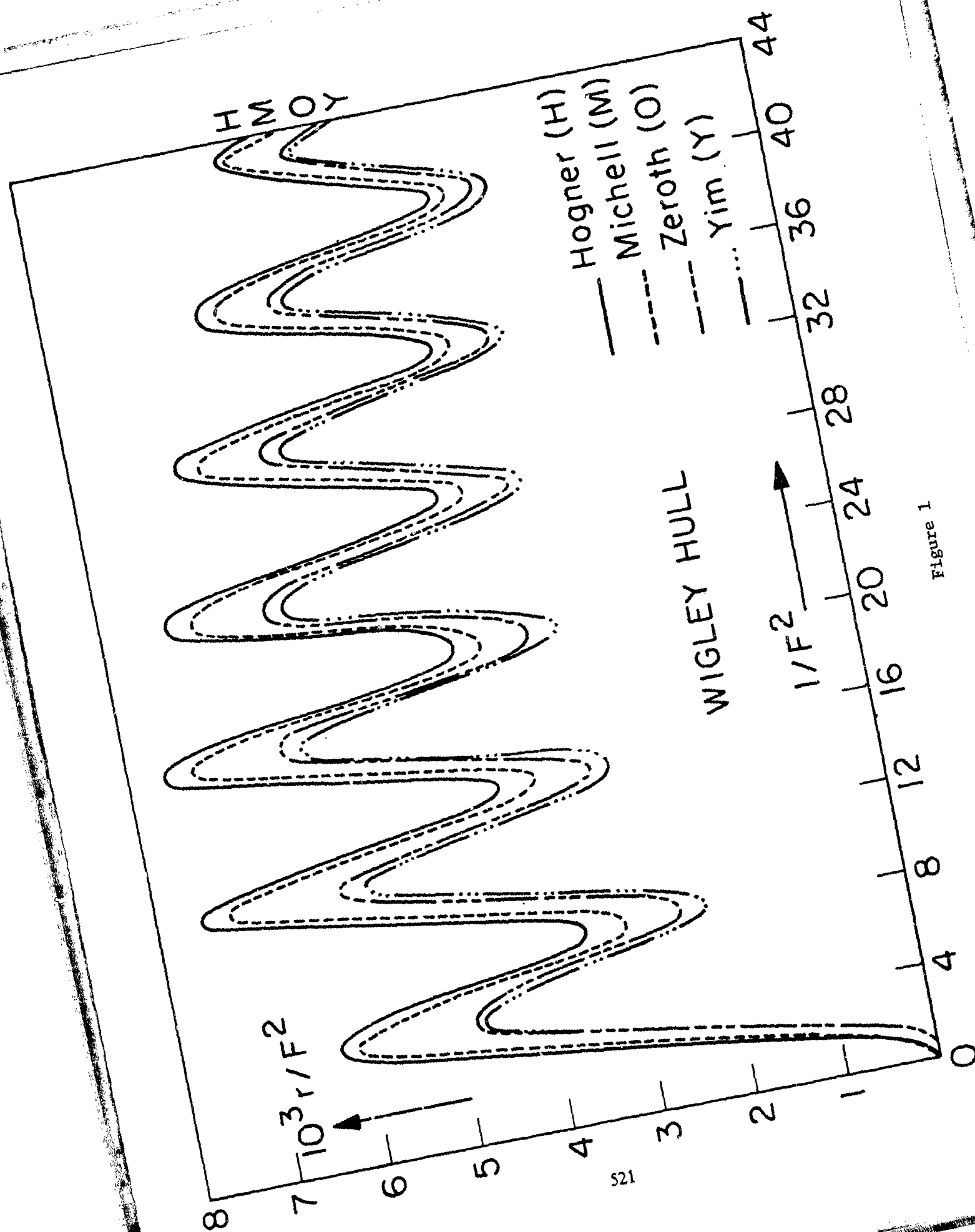
The hull integral in the above formula can readily be shown to be identically zero for any closed hull, while the waterline integral vanishes for a waterline with fore and aft symmetry. In summary, the waterline integral may be seen to be important for blunt ship forms, and in the low-and high-Froude-number limits.

Acknowledgments

The calculations reported in this note were performed as part of the MIT Sea Grant College Program with support from the Henry L. and Grace Doherty Foundation, and from the Office of Sea Grant in the National Oceanic and Atmospheric Administration, U.S. Department of Commerce.

References

1. Noblesse F. "Potential Theory of Steady Motion of Ships, Parts 1 & 2", MIT Dept of Ocean Eng. Rep. No. 78-4, Sep. 1978, 43 pp.
"Part 3: Wave Resistance", Rep. No. 78-5, Nov. 1978, 26 pp.
"Part 4: Low-Froude-Number Approximations", Rep. No. 79-1 May 1979, 40pp.
2. Hogner E. "Eine Interpolationsformel für den Wellenwiderstand von Schiffen", Jahrbuch der Schiffbautechnischen Gesellschaft, Vol. 33, 1932, pp. 452-456.
3. Michell J.H. "The Wave Resistance of a Ship", Philosophical Magazine, Series 5, Vol. 45, 1898, pp. 106-123.
4. Yim, B. "Simple Calculation of Sheltering Effect on Wave Resistance of Low Speed Ships", Workshop on Wave Resistance Computations, David Taylor Naval Ship Research and Development Center, Bethesda, Md., Nov. 1979.



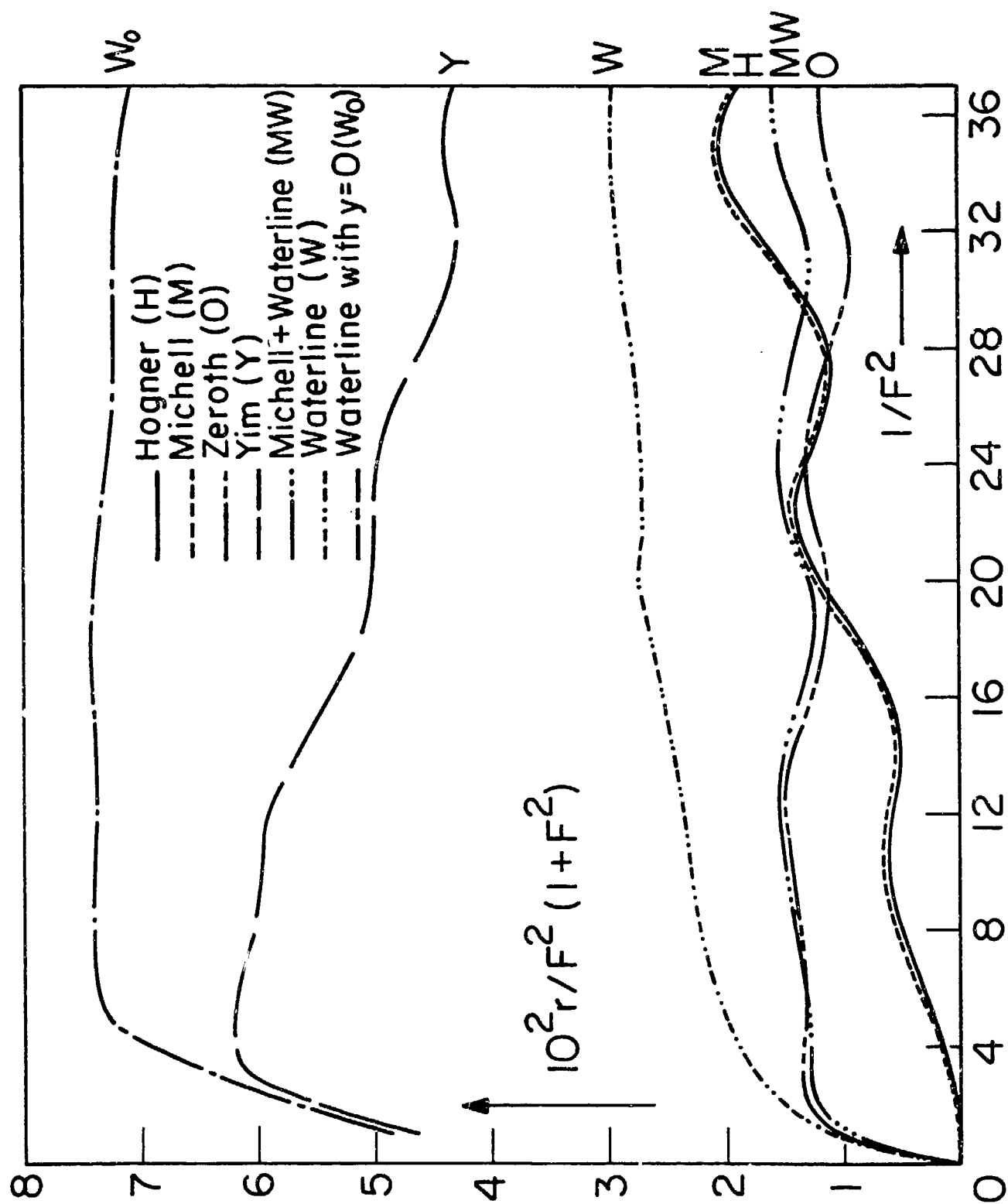


Figure 2

COMMENTS ON NUMERICAL SOLUTION OF
NEUMANN-KELVIN PROBLEM

by T. Tsutsumi

1. Chang and Tsutsumi computed the solution of Neumann-Kelvin problem numerically for Wigley hull form and for Series 60 hull form. They used the same method except Chang calculated the wave resistance from integration of pressure over the hull surface while Tsutsumi did it from the far-field wave spectrum. The results, however, did not show the same values [1].
2. We study a little more on the numerical solutions of Neumann-Kelvin problem here. Fig. 1 shows the calculated wave resistance for above two hull forms, comparing with several numerical results obtained from other linearized theories.
3. There is a close analogy between thin ship theory and Guevel's theory [2] when using double body sources, in respect of including the effect of waves inside the body. The numerical results of these theories confirm the concept.
4. Kayo-Guevel theory [3] excludes the effect of waves inside the body. So the difference of wave resistance between Tsutsumi (Double Body) and Nakatake (Method 3) in Fig. 1 can be due to the sheltering effect from the theoretical viewpoint. The effect seems to decrease the wave resistance and shift the phase of resistance curve toward the lower speed side.
5. The solution of Neumann-Kelvin problem satisfies the exact hull surface condition while the solution of Kayo-Guevel theory does not. Assuming that numerical errors do not occur for the solution of Neumann-Kelvin problem and comparing the results with Nakatake (Method 3) in Fig. 1, the effect of making the hull surface condition exact seems to increase the wave resistance and shift the phase of resistance curve toward the higher speed side.

6. Wave resistance R_w obtained from the far-field wave spectrum should correspond with the resistance R_p obtained from integration of pressure over the wetted hull surface. After the Workshop, we calculated both R_w and R_p for Wigley hull form at $F_n=0.288$ (See Fig. 1), by using the solution of Neumann-Kelvin problem. The difference between R_w and R_p is considerable contrary to our expectation. The cause of the discrepancy may be due to numerical errors especially in the calculation of the flow near the still water line. The errors are supposed to be more considerable for Series 60 hull form because of the non-vertical hull side at the water line. We are interested in the comparison of R_p and R_w in the case of Chang's calculation.

7. For evaluating numerical solutions in more detail, it may be considered to compare the calculated pressure distribution over the wetted hull surface with experiment, especially paying attention to the pressure near the free surface [4].

8. References

- [1] Mori, K. "Comments on Papers Presented at the Workshop on Wave Resistance Computations", 51th JTTC (1980).
- [2] Guevel, P, Vaussy, P. and Kobus, J.M. "The Distribution of Singularities Kinematically Equivalent to a Moving Hull in the Presence of a Free Surface", Int. Ship. Prog., Vol.21 (1974).
- [3] Kayo, Y. "A Note on the Uniqueness of Wave-Making Resistance When the Double-Body Potential is Used as the Zero-Order Approximation", Trans. of the West-Japan Soc. Nav. Arch., No.55 (1978).
- [4] Namimatsu, M. "A Measuring Method of Hull Pressure Resistance and Its Application", Jour. of Soc. Nav. Arch. of Japan, Vol.139 (1976).

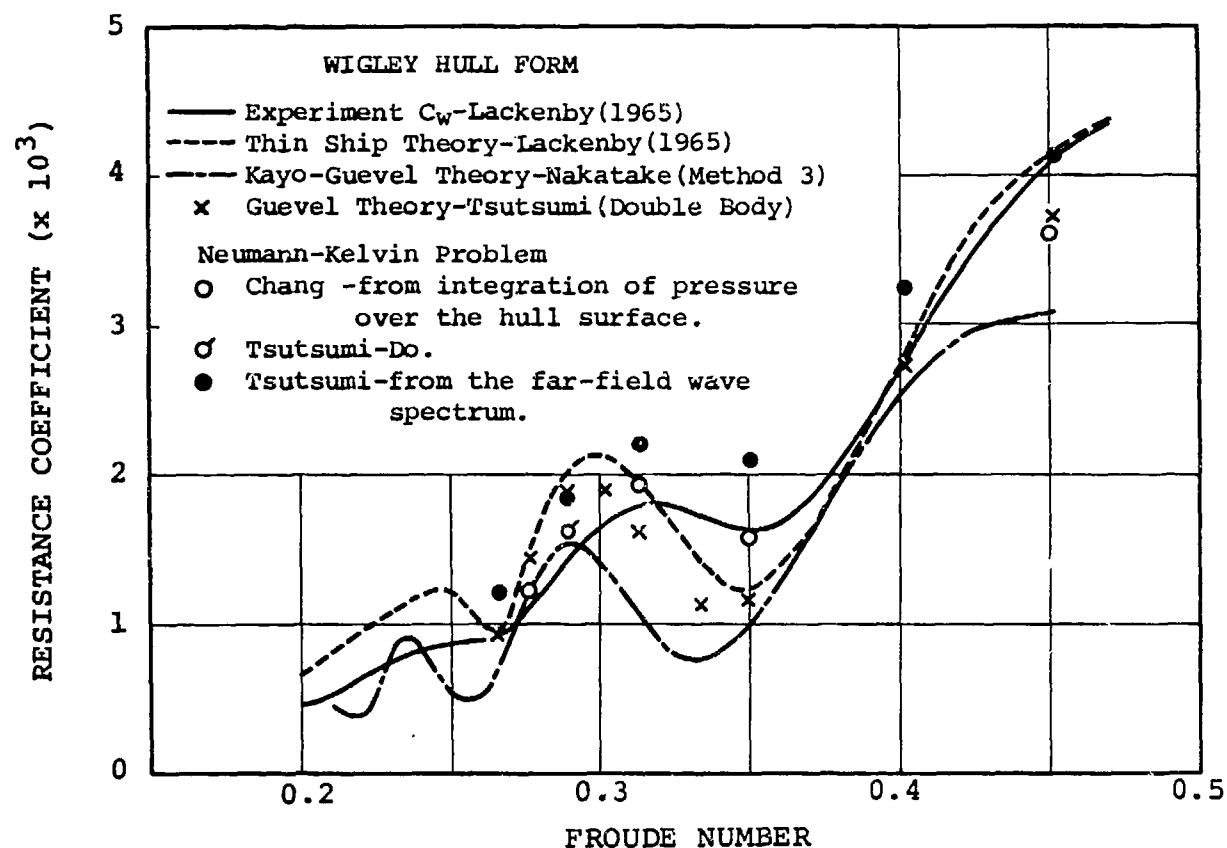
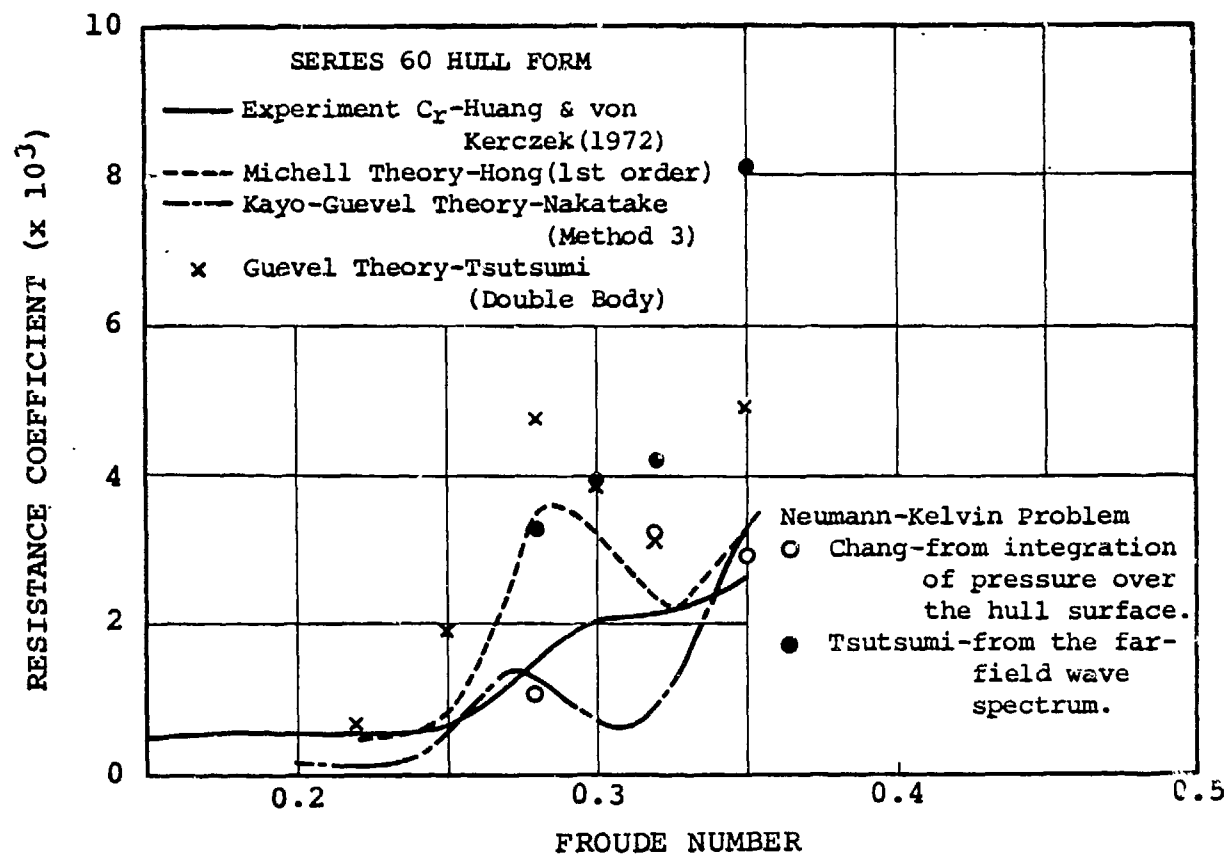


Fig. 1 Comparison of Wave Resistance

Klaus Eggers:

A Method for Assessing Numerical Solutions to a Neumann-Kelvin Problem.

It must be expected that differences between alternative approaches to the Neumann-Kelvin boundary value problem (such as source or doublet distributions with or without line integrals along the waterline C_0) will be reflected in the degree of irregularity of the flow components calculated in the vicinity of C_0 . Even if uniformly bounded near the main part of C_0 , their continuous limits may depend on the direction of approach towards C_0 [1]. Assuming that no such indeterminacy occurs, we can derive a simple integral expression for the difference between the resistance R_p obtained from integration of pressure over the hull surface S_0 below $z = 0$ plus a correction for the wave profile as an exactly quadratic functional of the calculated disturbance flow components and the resistance R_f , quadratic again, calculated from the far-field wave spectrum, i.e. representing an integral over the square of a Kochin function. In general there will be a finite difference between these two due to the inconsistency of having the free surface condition linearized. We shall re-derive in the sequel the expression for $R_p - R_f$, after indicating how the wave profile contribution has to be incorporated when calculating R_p .

Let ϕ stand for a solution to the N-K problem. Otherwise essentially using Newman's [2] terminology, we have shown elsewhere [3] that the expression

$$R_f = -\rho \left\{ \iint_S \{ (\nabla\phi \nabla\phi) / 2 \cdot n_x - \phi_x \phi_n \} dS + 1/2k_0 \oint_C \phi_x^2 dy \right\} \quad (1)$$

for any surface S enclosing the ship hull surface S_0 from below up to $z = 0$ where it intersects along a line C is independent from the choice of S as ϕ satisfies $\Delta\phi = 0$ and the linearized free surface condition. Eq.(1) corresponds to

$$R_f = -\rho \left\{ \iiint \{ \phi_y^2(x_s, y, z) + \phi_z^2 - \phi_x^2 \} / 2 \, dydz + 1/2k_0 \int \phi_x^2(x_s, y, 0) dy \right\} \quad (2)$$

if S degenerates to a transverse plane $x = x_s$ behind the ship. For the special case that S coincides with S_0 , we may insert $\phi_n = U n_x$ and obtain

$$R_f = -\rho \left\{ \iint_{S_0} \{ (\nabla\phi \nabla\phi) / 2 - U \phi_x n_x \} dS + 1/2k_0 \oint_{C_0} \phi_x^2 dy \right\} \quad (3)$$

Note that the double integral represents the action of pressure up to $z = 0$.

The second term, however, is *not* the pertinent correction to the pressure integral with regard to the linearized wave profile ! A careful analysis reveals that it just takes account of the *static* pressure component. The contribution of the linear part of dynamic pressure $\rho U \phi_x$, as represented in the surface integral, yields twice this quantity with reversed sign [4]!

Accordingly we have:

$$R_f - R_p = 1/k_0 \oint_C \phi_x^2 dy \quad (4)$$

where the line integral's orientation is such that dy is positive astern.

It was Gadd [5] who detected this discrepancy numerically and correctly attributed it to the neglect of non-linear free surface effect contrary to this author's claim. I have consequently given the name *Gadd's paradoxon* (English: paradox) to this phenomenon, which is resolved under use of a second-order free surface condition as shown in [4].

Recommendation:

For any numerical treatment of the Neumann-Kelvin problem (including those using finite elements !) both R_f and R_p should be calculated, and the difference should be compared with the r.h.s. of (4).

References :

- 1 Eggers, K.: Disc. to Bessho, M.: Line integral, uniqueness and diffraction of wave in the linearized theory. Proc. Int. Sem. on Wave Resistance Tokyo 1976 pp 401-404 (see also discussion to [2]).
- 2 Newman, J. N.: Linear wave resistance theory. Proc. Int. Sem. on Wave Resistance Tokyo 1976 pp 31-43, disc. 393-401.
- 3 Eggers, K., Gamst, A.: An evaluation of mapping procedures for the stationary ship wave problem. Schiffstechnik 26 (1979) Appendix C pp 150-156. See also: Study on non-linear local effects in ship waves, Report 1978 (edited by T. Inui) pp 84-93.
- 4 Eggers, K.: On the role of line integrals for the improvement of wave resistance calculations. Proc. 14th ITTC Ottawa 1975, contribution to the report of the Resistance Committee pp 259-265.
- 5 Gadd, G. E.: A method for calculating the flow over ship hulls. TRINA 112 (1970) pp 335-345, disc. 345.351.

Note: In our analysis (eq.(1) and (3) in particular) we have considered the case of the ship advancing in + x direction with speed U , the normal vector \vec{n} is pointing towards the ship and line integrals are in clockwise direction.

Klaus Eggers:

Must the Water Plane Area be excluded when Singularities on the Undisturbed Free Surface are considered ?

It is generally accepted now that the inconsistent Neumann-Kelvin problem admits an infinity of essentially different solutions if we accept the principle that we may use singularity distributions generating the flow around the associated double body integrated with the weight of the Havelock source potential G (see e.g. [1], [2], [3], [4]). After a study by Guevel and others [5], it was Kayo [6] who re-analysed the problem again and demonstrated that ambivalence still persisted. Kayo derived an integral equation for the wavy potential ϕ supplementing the double body potential ϕ_r^e in his eq. (28) :

$$\phi = \iint_{S_s} \phi G_n dS - 1/k_o \oint_C (\phi G_\xi - G \phi_\xi) d\eta + 1/k_o \iint_{S_f} \phi_{r\xi\xi}^e G d\xi d\eta \quad (1)$$

and he suggested to take the inhomogeneous part of (1) (i.e. the term not containing ϕ) as the unique first approximation, i.e. he set

$$\phi = 1/k_o \iint \phi_{r\xi\xi}^e G d\xi d\eta \quad (2)$$

The present writer favors an alternative first approximation. He proposes to extend the definition of $\phi_{r\xi\xi}^e$ across the water line C , given analytically through an equation $|\eta| = f(\xi)$, in a continuous manner through

$$\phi_{r\xi\xi}^i(\xi, \eta) = \phi_{r\xi\xi}^e(\xi, f(\xi)) \quad (3)$$

and to have the integration extended over the entire undisturbed free surface in (2). This would have favorable consequences for the decay of the generalised Kochin function (H_3 in Kayo's eq. (33)), i.e. of the wave spectrum, with wave angle θ approaching $\pi/2$. It is certainly true that even with Kayo's (33)

$$H_3 = - 1/k_o \iint \phi_{r\xi\xi}^e E(\xi, \eta, 0) d\xi d\eta \quad (4)$$

the integrals for free wave elevation and wave resistance (just) converge. However, inclusion of (3) as integrand of (2) would lead to

$$H_3 = + 1/k_o \iint \phi_{r\xi\xi\eta}^e E(\xi, \eta, 0) d\xi d\eta \{i \cos^2 \theta / (k_o \sin \theta)\} \quad (5)$$

The higher derivative of the double body potential (with source influence function like $1/r$) does not lead to numerical difficulties but rather to an

improved rate of decay of the integrand in (4) away from the hull (note that in both (4) and (5) the water plane area is considered as excluded from the range of surface integration). Making use of the oddness of the function $\phi_{r\xi\xi\eta}^e$ with regard to η for a ship with sidewise symmetry, it can be shown easily that the zero of $\sin\theta$ with θ approaching zero in the denominator of (5) is compensated by a zero in the integral over

$$E(\xi, \eta, 0) = \exp\{-ik_0 \sec^2\theta(\xi\cos\theta + \eta\sin\theta)\} \quad (6)$$

We should observe that changing from (4) to (5) does affect the asymptotic rate of growth of the associated wave resistance by a factor k_0^{-2} within a small Froude number expansion.-

Our suggestion

$$\phi = 1/k_0 \iint \{\phi_{r\xi\xi}^e + \phi_{r\xi\xi}^i\} G \, d\xi d\eta \quad (7)$$

with integration over the entire plane $z = 0$ (with one summand vanishing in either subarea) is certainly as unique as Kayo's suggestion (2), where the water plane area is excluded from integration. Why should the latter one be preferred in spite of its discontinuous character?

There seems to exist a deeply rooted belief in our community that for solving Fredholm type integral equations by iteration it is optimal in whatever sense (if not even obligatory) to have the inhomogeneous part as the first approximation. Certainly, for slender bodies of revolution, it happens that for body surface source distributions the inhomogeneous term in the relevant integral equation as evaluated by Hess and Smith [7] does already provide the proper solution (i.e. twice the normal velocity) in the sense of strip theory for the case of *transverse* motion. However, for longitudinal motion, half this value makes a far better first guess!

Let us digress to a formal analysis of the underlying very general problem. Consider an integral equation:

$$f(x) + \int K(x, x') f(x') \, dx' = h(x) \quad (8)$$

where $f(x)$ is the unknown function, $h(x)$ is the inhomogeneous term and $K(x, x')$ is the Kernel function. Let now $g(x)$ stand for *any* function which admits a representation

$$g(x) = \int K(x, x') \tilde{g}(x') \, dx' \quad (9)$$

Then the equivalent integral equation for the function $f^*(x) = f(x) - \tilde{g}(x)$

$$f^*(x) + \int K(x, x') f^*(x') dx' = h(x) - \tilde{g}(x) + g(x) \quad (10)$$

leads to the initial approximation $h(x) - g(x)$ for $f(x)$ of (9) if the r.h.s. of (10) is considered the appropriate first iteration to determine f^* !

Recommendation: All computations using free surface singularity distributions from double body flow information (Neumann-Kelvin type as well as those taking account of free surface non-linearity and using distributions connected with Baba's $D(x, y)$) should be repeated with the singularity distribution extrapolated constant in crosswise direction into the water plane area. It is expected that the resulting flow components near the ship's water line will display less irregularity, in accord with Gadd's numerical experience [8]. In any case the associated wave spectra will display a more realistic behavior in the divergent wave range.

For eq.(27) of the preceeding contribution we have tacitly assumed that the horizontal flow components have the same continuous limit when C is approached from different directions. If not expecting wave breaking concentrated along C , the most regular flow model should be preferred.

References:

- [1] Kotik, J.; Mangulis, V.: Comparison of two approximate dipole distributions for a lenticular cylinder in semi infinite fluid. J. Math. Phys. 41 (1962) pp. 280-290.
- [2] Eggers, K.: Disc. to: Sharma, S.D.: Zur Problematik der Aufteilung des Schiffswiderstandes in zähigkeits- und wellenbedingte Anteile. Jahrb. STG 59 (1965) pp. 505-506.
- [3] Eggers, K.: Disc. to: Pien, P.C.: The application of wavemaking resistance theory to the design of ship hulls with low total resistance. 5th Symposium ONR Bergen (1964) p. 185.
- [4] Kotik, J.; Morgan, R.: The uniqueness problem for wave resistance calculated from singularity distributions which are exact at zero Froude number. J. Ship Research 13 (1969) pp. 61-68.
- [5] Guevel, P.; Vaussy, P., and Kobus, J.M.: The distribution of singularities kinematically equivalent to a moving hull in the presence of a free surface. Int. Shipbuildg. Progress 21 (1974) pp. 311-329.
- [6] Kayo, Y.: A note on the uniqueness of wave making resistance when the double body potential is used as the zero-order approximation. J. Cos. Nav. Arch. West Japan 1978.
- [7] Hess, J.L.; Smith, A.M.O.: Calculation of non-lifting potential flow around three-dimensional bodies. Journ. Ship Research 8 (1964) pp. 22-44.
- [8] Gadd, G.E.: Wave theory applied to practical hull forms. Proc. Intern. Seminar on Wave Resistance Tokyo (1976) pp. 149-158.

CONTRIBUTION TO THE DEPTH STUDY ON WAVE RESISTANCE

Robert K.-C. Chan and Frank W.-K. Chan
JAYCOR; Del Mar, California

Professor Mori suggested that we make some comments on the numerical techniques used in our method and compare them with those of Gadd and Dawson. In his commentary report of the Workshop on Wave Resistance Computations,⁽¹⁾ Professor Mori explains the essence of our method and the Rankine source method very well. Here, we would like to inject some ideas which we hope will stimulate further discussions at the Continued Workshop on Wave Resistance.

Our direct method is similar to the Rankine source method in that the boundary condition at the hull surface is exactly satisfied, and that, as in Gadd's approach, the nonlinear free surface conditions can be easily applied. One advantage of the Rankine source method is that the unknown potential needs to be computed only on the hull surface and on the free surface, while our direct method requires the solution for the internal values of the potential also. However, the Rankine source method is applicable only if the flow is potential, while the direct method can be applied to non-potential flows equally well. Most of the papers presented at the Workshop, including ours, are based on the potential flow theory, with the exception of Professor Mori, who gave an estimate of the effect of boundary layer and wake on wave resistance, and Professors Miyata and Kajitani, who pointed out the importance of including the "free surface shock waves" in analysis. Using the general coordinate transformation developed in our work, we will be able to investigate various interesting problems in the future. The first extension of our present method is to use the shallow-water type approximation for the "upper region" (Fig. 1 in our paper presented at the Washington workshop) to allow the formation of shock waves at the free surface, while keeping the potential flow in the "lower region." This modification would allow simulation of breaking waves and other related phenomena. The next extension will be to use Navier-Stokes equations, with appropriate models for turbulence in the boundary

layer and in the wake, so that more interactions of significant physical parameters can be included. At present, however, we just like to see how much we can learn from more exact solutions of the potential flow.

Another major difference between our approach and the Rankine source method is that we solve an initial-value problem, while Gadd and Dawson solve steady-state, boundary-value problems. This difference has an important effect on the treatment of boundary conditions at the "open boundaries," i.e., where the computational mesh ends. In a steady-state formulation, the open boundary conditions are not available, while in a transient approach one can use the approximation of Orlanski⁽²⁾ to propagate the waves out of the computational region. Even if there is any doubt to the applicability of Orlanski's method to multi-dimensional problems, in a transient method we can always use a mesh large enough so that wave reflection from the mesh boundary does not happen before the flow around the ship and the associated resistance reach the steady state. We feel that it is important to clarify the effect of open boundary treatment on the solution in the steady-state Rankine source methods.

Both Gadd's method and our direct method are capable of computations employing the full nonlinear free surface conditions. However, the nonlinearity can lead to steepening of waves near the ship and some waves may even break, which is in sharp contrast to the linear solutions for which the waves will never turn into shocks. In our calculations of the HSVA tanker, the bow wave starts to steepen and become unstable at $F_n = 0.16$. Upon his return to Hamburg from the Washington workshop, Professor Eggers called Dr. Collatz of HSVA and found there had been considerable wave breaking and instability when the tanker model was in steady forward motion during experiments.⁽³⁾ This brings up a very interesting point. That is, one can not obtain strongly nonlinear solutions unless the equations are modified to handle the shock waves properly. Without this modification, one can perform the transient calculation only up to the point when the wave starts to break. The same limitation applies to nonlinear steady-state methods in flow regimes where shock waves exist. In Gadd's computations of HSVA, Froude numbers as high as 0.19 were carried out. We wonder how his nonlinear calculation would behave if the bow wave became unstable. From his paper we could not determine whether his nonlinear free

surface conditions are applied at the exact position of the free surface or at the undisturbed surface. Also, to satisfy the nonlinear free surface conditions, how many iterations does it take typically and what is the convergence criterion? The other question we have is why does Gadd need axial source distribution while Dawson does not?

Gadd presented tabulated wave elevations for the HSVA tanker in his paper, which is compared with our result in Fig. 1 for $F_n = 0.15$. Other than the fact that the two profiles appear similar to each other, with some small variations on the sides of the ship which do not really contribute to the wave drag, we can not determine which calculation is more accurate unless a comparison is made with experimental measurements. Nevertheless, one observation is perhaps worth mentioning: the maximum wave elevation at the bow, η_{\max} , should be 1.0 from the Bernoulli equation. Our η_{\max} was 1.013, with a 1% error which is consistent with the error allowed by our convergence criterion used in the numerical procedure. Gadd, however, reported $\eta_{\max} = 0.752$ at $x/L = -0.49375$. Of course, this value of η may not correspond precisely to the location of the bow.

In concluding our discussions, we feel it is important to say a few words about the potential value of the direct methods and their relationship to other approaches. Direct methods, if carefully implemented, can include many physical phenomena which are simply beyond the power of the simpler analytical approaches. Direct methods, like experiments, can produce a wealth of information about the flow field which can be used to design new concepts or improve existing assumptions in many current theories. For example, our calculation shows that the stagnation point for an HSVA tanker is located at the bow below the undisturbed free surface by a distance equal to about 4% of the draft at midship. This suggests that, except for a thin layer near the free surface, the flow field of a double hull is probably a good approximation for some types of flows, which agrees with many experimental measurements. As far as the thin surface layer is concerned, assumptions such as the double-hull linearization can be examined by using the detailed data produced in direct simulations. Although direct methods are much more expensive to use than the more classical approaches, they constitute a class of very powerful tools capable of bringing new dimensions into the field of ship wave research.

REFERENCES

1. Mori, K., "Comments on Papers Presented at the Workshop on Wave Resistance Computations," Hiroshima University, 1980.
2. Orlanski, I., "A Simple Boundary Condition for Unbounded Hyperbolic Flows," Journal of Comp. Physics, 21, 1976.
3. Eggers, K., Private Communication, December 4, 1979.

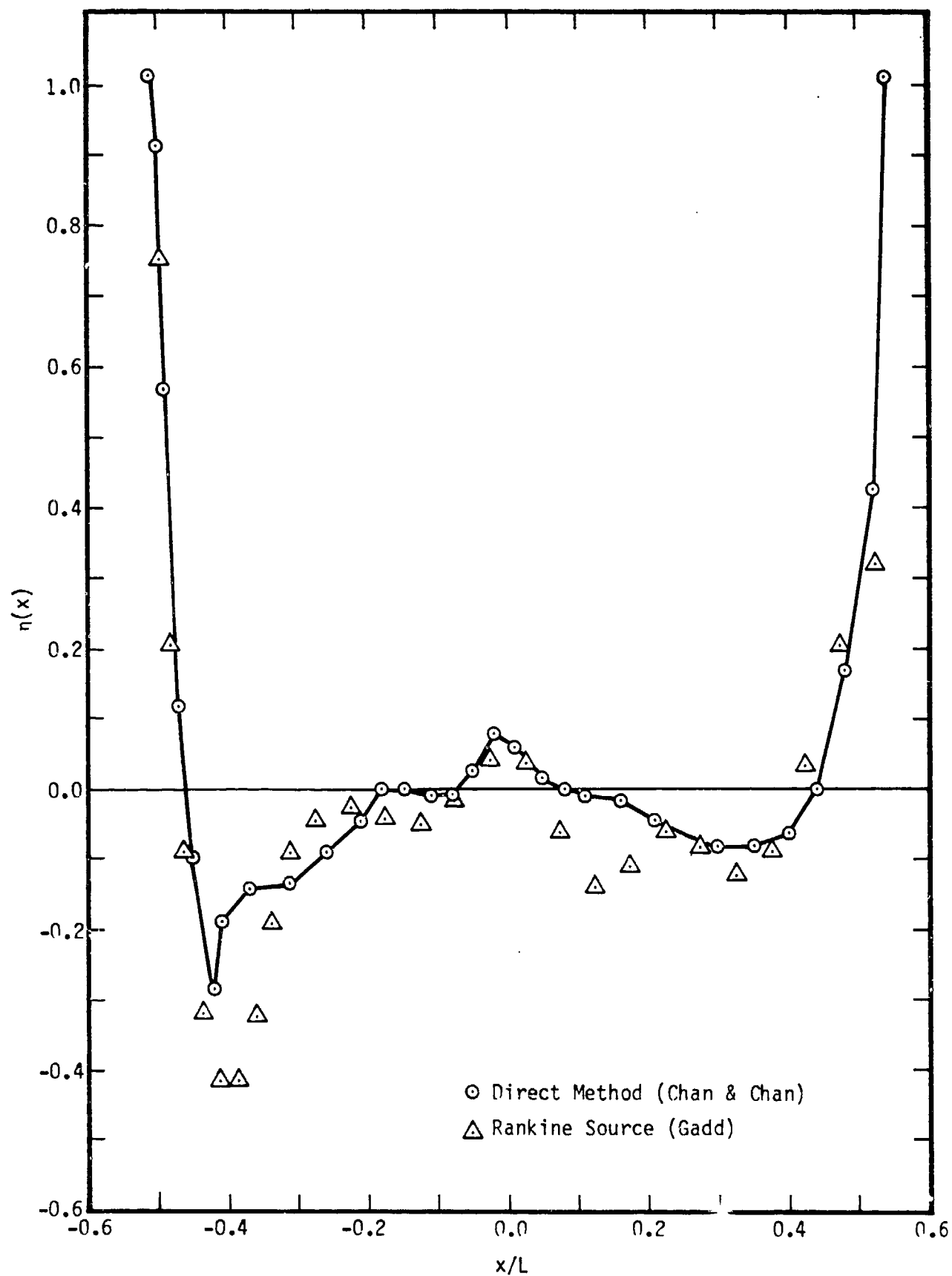


Fig. 1. Comparison of Wave Elevation along the Waterline of an HSVA ($F_n = 0.15$)

Discussion

by K. NAKATAKE

of papers by C.W. Dawson, C.E. Gadd, K.J. Bai, A.C.W.J. Oomen and
R.C. Chan & W.K. Chan

These papers are very impressive to me, because they do not use Havelock source potential as a basic tool. I would like to express my sincere appreciation for their endeavors.

Dr. Dawson shows that the effect of trim and sinkage on wave-resistance can not be neglected in the range of high Froude number. His results are good. But eight rows of the hull panels do not seem to be sufficient in order to represent the double flow around Series 60 hull at the still water surface.

Dr. Gadd introduced newly "passive" panels and point Kelvin sources. These sources are used only for the velocity field on the "passive" panels. They may be also used in order to satisfy the downstream radiation condition as Dr. Bai's eigenfunctions. How to arrange the "active" and "passive" panels may have direct effects on wave-resistance.

Dr. Bai uses the linearized and the exact hull boundary conditions. Is the CPU time decreased considerably when the linearized one is used? It will make easier to compare the results calculated by using the exact one for Inuid and ATHENA hulls with residual resistance of these hulls. In the purely numerical method, I think, the number of simplifications should be as small as possible.

Mr. Oomen shows reasonable wave-resistance coefficients and unacceptable wave elevations near Series 60 hull. Increase of sub-regions may improve the wave elevations. How is the radiation condition satisfied? I wish his method will be applied to Inuid, Wigley hulls and the detailed paper will be published.

Drs. R. Chan & F. Chan showed very impressive picture of the wave patterns around HSVA tanker. Wave profiles and wave-resistance seem to be very reasonable. Their method, I hope, will be also applied to Inuid, Wigley and Series 60 hulls.

WORKSHOP PARTICIPANTS

ADEE, BRUCE H., University of Washington, Seattle, Washington, USA
BABA, EIICHI, Mitsubishi Heavy Industries, Nagasaki, Japan
BAI, KWANG JUNE, DTNSRDC, Bethesda, Maryland, USA
BARTELS, FRITZ, DTNSRDC, Bethesda, Maryland, USA
BRESLIN, JOHN P., Stevens Institute of Technology, Hoboken, New Jersey, USA
CALISAL, SANDER M., U.S. Naval Academy, Annapolis, Maryland, USA
CHAN, FRANK W.-K., JAYCOR, Del Mar, California, USA
CHAN, ROBERT K. C., JAYCOR, Del Mar, California, USA
CHANG, MING SHUN, DTNSRDC, Bethesda, Maryland, USA
COOPER, RALPH D., Office of Naval Research, Arlington, Virginia, USA
CORDONNIER, JEAN-PIERRE V., ENSM, Nantes, France
CUMMINS, WILLIAM E., DTNSRDC, Bethesda, Maryland, USA
DAWSON, CHARLES W., DTNSRDC, Bethesda, Maryland, USA
EGGERS, KLAUS, Hamburg University, Hamburg, West Germany
GADD, GEORGE E., National Maritime Institute, Feltham, Middlesex, England
HAUSSLING, HENRY J., DTNSRDC, Bethesda, Maryland, USA
HONG, YOUNG S., DTNSRDC, Bethesda, Maryland, USA
HUANG, THOMAS T., DTNSRDC, Bethesda, Maryland, USA
JENKINS, DOUGLAS S., DTNSRDC, Bethesda, Maryland, USA
KAJITANI, HISASHI, University of Tokyo, Tokyo, Japan
KIM, HYOCHUL, Seoul National University, Seoul, Korea
KIM, YOON-HO, DTNSRDC, Bethesda, Maryland, USA
LANDWEBER, LOUIS, University of Iowa, Iowa City, Iowa, USA
LEE CHOUNG M., DTNSRDC, Bethesda, Maryland, USA
LIBBY, JULIANNA, DTNSRDC, Bethesda, Maryland, USA
LIN, WEN C., DTNSRDC, Bethesda, Maryland, USA
LUGT, HANS J., DTNSRDC, Bethesda, Maryland, USA
MARUO, HAJIME, Yokohama National University, Yokohama, Japan
McCARTHY, JUSTIN H., DTNSRDC, Bethesda, Maryland, USA
MIYATA, HIDEAKI, University of Tokyo, Tokyo, Japan
MORGAN, WILLIAM B., DTNSRDC, Bethesda, Maryland, USA